



Simplified Shear Design of Structural Concrete Members: Appendixes

DETAILS

0 pages | | PAPERBACK

ISBN 978-0-309-43237-5 | DOI 10.17226/22070

AUTHORS

BUY THIS BOOK

FIND RELATED TITLES

Visit the National Academies Press at NAP.edu and login or register to get:

- Access to free PDF downloads of thousands of scientific reports
- 10% off the price of print titles
- Email or social media notifications of new titles related to your interests
- Special offers and discounts



Distribution, posting, or copying of this PDF is strictly prohibited without written permission of the National Academies Press. (Request Permission) Unless otherwise indicated, all materials in this PDF are copyrighted by the National Academy of Sciences.

**NCHRP Web-Only Document 78 (Project 12-61): Contractor's Final Report--
Appendixes**

Simplified Shear Design of Structural Concrete Members Appendixes

Prepared for:
National Cooperative Highway Research Program

TRANSPORTATION RESEARCH BOARD
OF THE NATIONAL ACADEMIES

Submitted by:
**Neil M. Hawkins, Daniel A. Kuchma, Robert F. Mast,
M. Lee Marsh, and Karl-Heinz Reineck**
**University of Illinois
Urbana, Illinois**

July 2005

ACKNOWLEDGMENT

This work was sponsored by the American Association of State Highway and Transportation Officials (AASHTO), in cooperation with the Federal Highway Administration, and was conducted in the National Cooperative Highway Research Program (NCHRP), which is administered by the Transportation Research Board (TRB) of the National Academies.

DISCLAIMER

The opinion and conclusions expressed or implied in the report are those of the research agency. They are not necessarily those of the TRB, the National Research Council, AASHTO, or the U.S. Government.

This report has not been edited by TRB.

THE NATIONAL ACADEMIES

Advisers to the Nation on Science, Engineering, and Medicine

The **National Academy of Sciences** is a private, nonprofit, self-perpetuating society of distinguished scholars engaged in scientific and engineering research, dedicated to the furtherance of science and technology and to their use for the general welfare. On the authority of the charter granted to it by the Congress in 1863, the Academy has a mandate that requires it to advise the federal government on scientific and technical matters. Dr. Ralph J. Cicerone is president of the National Academy of Sciences.

The **National Academy of Engineering** was established in 1964, under the charter of the National Academy of Sciences, as a parallel organization of outstanding engineers. It is autonomous in its administration and in the selection of its members, sharing with the National Academy of Sciences the responsibility for advising the federal government. The National Academy of Engineering also sponsors engineering programs aimed at meeting national needs, encourages education and research, and recognizes the superior achievements of engineers. Dr. William A. Wulf is president of the National Academy of Engineering.

The **Institute of Medicine** was established in 1970 by the National Academy of Sciences to secure the services of eminent members of appropriate professions in the examination of policy matters pertaining to the health of the public. The Institute acts under the responsibility given to the National Academy of Sciences by its congressional charter to be an adviser to the federal government and, on its own initiative, to identify issues of medical care, research, and education. Dr. Harvey V. Fineberg is president of the Institute of Medicine.

The **National Research Council** was organized by the National Academy of Sciences in 1916 to associate the broad community of science and technology with the Academy's purposes of furthering knowledge and advising the federal government. Functioning in accordance with general policies determined by the Academy, the Council has become the principal operating agency of both the National Academy of Sciences and the National Academy of Engineering in providing services to the government, the public, and the scientific and engineering communities. The Council is administered jointly by both the Academies and the Institute of Medicine. Dr. Ralph J. Cicerone and Dr. William A. Wulf are chair and vice chair, respectively, of the National Research Council.

The **Transportation Research Board** is a division of the National Research Council, which serves the National Academy of Sciences and the National Academy of Engineering. The Board's mission is to promote innovation and progress in transportation through research. In an objective and interdisciplinary setting, the Board facilitates the sharing of information on transportation practice and policy by researchers and practitioners; stimulates research and offers research management services that promote technical excellence; provides expert advice on transportation policy and programs; and disseminates research results broadly and encourages their implementation. The Board's varied activities annually engage more than 5,000 engineers, scientists, and other transportation researchers and practitioners from the public and private sectors and academia, all of whom contribute their expertise in the public interest. The program is supported by state transportation departments, federal agencies including the component administrations of the U.S. Department of Transportation, and other organizations and individuals interested in the development of transportation.

www.TRB.org

www.national-academies.org

Appendix A: Models for Shear Behavior

A.1 Introduction

A.1.1 The Problem of Shear Transfer

A flexural member supports loads by internal moments and shear forces. Classical beam theory, in which plane sections are assumed to remain plane, provides an accurate, simple, and effective model for designing a member to resist bending in combination with axial forces. The simplicity and rationality of beam theory can be kept even after cracking for several reasons. The first reason is that flexural cracks form perpendicular to the axis of bending so that the traditional “plane sections remain plane” assumption is valid. The second reason is the weakness of concrete in tension, so that tensile stresses can be effectively neglected at a crack. The third reason is that flexural failure occurs at the maximum moment location so that consideration of conditions at the maximum moment section is sufficient for flexural design.

Shear failure is initiated by inclined cracks caused not only by shear force but also by shear force in combination with moments and axial loads. The shear failure load depends on numerous factors such as the dimensions, geometry, loading and structural properties of members. Because shear cracks are inclined and the shear failure load depends on a large number of factors, shear design—unlike flexural design—must consider the response of a finite length of the member, (B-region), rather than the response of a single section. Due to the complications of shear behavior and the difficulties of shear design, the shear behavior and shear strength of members have been major areas of research in reinforced and prestressed concrete structures for decades. This chapter provides information on mechanisms of shear transfer, influencing parameters, shear failure modes, and various key approaches to analyzing shear behavior.

A.1.2 Shear Transfer Actions and Mechanisms

Shear transfer actions and mechanisms in concrete beams are complex and difficult to clearly identify. Complex stress redistributions occur after cracking, and those redistributions have been shown to be influenced by many factors. Different researchers impose different levels of relative importance to the basic mechanisms of shear transfer. Fig. A-1 shows the basic mechanisms of shear transfer that are now generally accepted in the research community. In 1973 the ASCE-ACI Committee 426 and, again in 1998, its current counterpart the ASCE-ACI Committee 445, reported five important shear transfer actions for beams with shear reinforcement: shear in the uncracked compression zone of the beam; interface shear transfer due to aggregate interlock or surface roughness along inclined cracks; dowel action of the longitudinal reinforcement; residual tensile stresses across inclined cracks; and shear transfer of the shear reinforcement. Each of these actions is depicted in Fig. A-2 and is more fully described below.

Shear in the Uncracked Concrete Zone: The uncracked compression zone contributes to shear resistance in a cracked concrete member (i.e. a beam or a slab). The magnitude of that shear resistance is limited by the depth of the compression zone. Consequently, in a relatively slender beam without axial compression, the shear contribution by the uncracked compression zone becomes relatively small due to the small depth of the compression zone.

Interface shear transfer: Local roughness in the crack plane provides resistance against slip and thus there is shear transfer across shear cracks. The contribution of interface shear transfer to shear strength is a function of the crack width and aggregate size. Thus, the magnitude decreases as the crack width increases and as the aggregate size decreases. Consequently, this component is also called “aggregate interlock”. However, it is now considered more appropriate to use the terminology “interface shear transfer” or “friction” since this action still exists even if crack propagation occurs through the aggregate as it does in high strength concrete where the matrix is of a similar strength to the aggregates. The relatively smooth crack plane in high strength concrete can reduce interface shear transfer compared to the rough crack plane of normal strength concrete.

Dowel Action: When a crack forms across longitudinal bars, the dowelling action of the longitudinal bars provides a resisting shear force. The contribution of dowel action to shear resistance is a function of the amount of concrete cover beneath the longitudinal bars and the degree to which vertical displacements of those bars at the inclined crack are restrained by transverse reinforcement. Typically, little dowel action can be provided by reinforcement that is near the tension face of a member without transverse reinforcement because that action is then limited by the tensile strength of the concrete.

Residual Tensile Stresses: In concrete tensile stresses can be transmitted directly across cracks because small pieces of concrete bridge the crack. As shown in Fig. A-3, even when concrete is cracked and loaded in uniaxial tension, it can transmit tensile stresses until crack widths reach 0.06 mm to 0.16 mm. Due to the presence of these tensile stresses the cracked concrete, in the vicinity of the tips of inclined and flexural cracks, can also carry shear stresses that add to the shear capacity of the concrete. When the crack opening is small, the resistance provided by residual tensile stresses is significant. However, in a large member, the contribution of crack tip tensile stresses to shear resistance is less significant due to the large crack widths that occur before failure in such members.

Shear Reinforcement: In members with shear reinforcement, a large portion of the shear is carried by the shear reinforcement after diagonal cracking occurs. The contribution of shear reinforcement to shear resistance is typically modeled either with a 45 degree truss plus a concrete term, or a variable angle truss without a concrete term. Shear reinforcement also provides a certain level of restraint against the growth of inclined cracks and thus helps to ensure a more ductile behavior. Finally, shear reinforcement provides dowelling resistance to shear displacements along the inclined crack. For these reasons, the presence of shear reinforcement changes the relative contributions of the different shear resisting mechanisms. The minimum amount of shear reinforcement required to affect such changes becomes important and that minimum amount is taken as a function of the concrete strength in most major design codes. Such is the case in both the AASHTO Standard and LRFD specifications.

Longitudinal reinforcement, bent up at 30 degrees or more to the longitudinal axis of the beam, extended across the web and anchored on the compression side, was used effectively for many years as shear reinforcement in reinforced concrete beams. Therefore, in the early years of prestressed concrete construction, it was believed that draped prestressing tendons would also be effective in all situations as shear reinforcement. However, University of Illinois tests (Bulletin 493) demonstrated that such reinforcement was effective only in delaying shear cracks formed in the web due to

principal tensile stresses. Draping the prestressing tendons did not delay the formation of inclined cracks that developed out of flexural cracks. Thus, in the ACI 318 Code, and in the AASHTO Standard Specifications, the term for the vertical component of the prestressing force appears only in expressions for the shear strength for web-shear cracking and does not appear in either the expressions for the shear strength for flexure-shear cracking or the shear strength contributed by shear reinforcement.

In addition to the shear transfer actions mentioned above, arch action is a dominant shear transfer mechanism in deep members. This is because as members become deeper, a larger portion of the shear is transmitted directly to the support by an inclined strut.

A.1.3 Significant Parameters for Members without Transverse Reinforcement

Several parameters have been identified as significantly influencing the relative contributions of the different shear resistance mechanisms and thus the ultimate shear capacity. The influence of the most dominant mechanisms is described in the following in accordance with the findings of the state-of-the-art reports by ASCE-ACI Committee 426 (1973) and ASCE-ACI Committee 445 (1998).

Concrete Strength: As concrete strength increases, the shear strength also increases. Some researchers believe that concrete compressive strength has a large influence on the shear resistance while others believe that concrete tensile strength has a greater influence than compressive strength on shear strength. The concrete contribution to shear, in ACI 318-02, for example, is regarded as being that due to diagonal cracking shear, and therefore dependent on the tensile strength of the concrete. The concrete compressive strength, f'_c , is generally used to estimate the tensile strength because direct tension tests are difficult to conduct, require interpretation of the results, and usually show more scatter than compression test results. In most major design codes, the shear strength of a member is taken as directly proportional to $(f'_c)^{0.25}$ or $(f'_c)^{0.33}$ or $(f'_c)^{0.5}$. Those power values indicate that the concrete tensile strength is being used as the governing parameter.

Recent test results have illustrated that the presumed effect of concrete tensile strength on shear capacity is strongly influenced by the characteristics of the tests conducted to examine the effect. Fig. A-4 presents results from several beam test series that show very different trends. The ACI 318-02 shear design approach in which the shear strength is taken as proportional to the square root of f'_c is also shown in the same figure. The shear failure stresses of the beams tested by Moody et al. (1954) increase as the concrete compressive strength increases. ACI 318-02 is shown to provide a reasonable estimate of the influence of f'_c for these beams which were small, heavily reinforced, and cast with low-to-medium-strength concrete. Similarly, the ACI provision is only slightly unconservative for the moderately reinforced and mid-sized members that were tested by Yoon and Cook (1996). However, Collins, Angelakos, Kuchma et al. (1999, 2001) did not find a similar increase in shear strength with concrete strength for their tests of larger, more lightly reinforced beams, and cast with high strength concretes with a small maximum aggregate size. The explanation offered by some researchers for why the shear stress at failure does not increase as greatly, or not at all, with increasing concrete compressive strength is that the smoother shear cracks in high-strength concrete members reduce the effectiveness of the interface shear transfer mechanism.

Size Effect: The shear strength of reinforced and prestressed beams without shear reinforcement decreases as the member depth increases; this is called the “size effect” in shear. Both the tests by Kani on size effect in 1967, and the tests by Shioya et al. (1989), effectively demonstrated this effect. Shioya et al. tested beams with depths ranging from 4 to 120 inches (102 mm to 3.0 m), Fig. A-5. The shear stress at failure of the largest beam was only about one-third of that of the smallest beam, and the ultimate shear stress of the largest beam was less than one half of the value calculated using ACI 318-02.

In 1956, several US Air Force warehouse beams collapsed under a shear force less than one half of the ACI design value, as indicated in Fig. A-5. The depth of these beams was 36 inches (914 mm). Investigators examining these failures conducted experiments with one-third scale models of the warehouse beams at the Portland Cement Association (PCA) and the failure strengths for those model beams are also shown in Fig. A-5. Due to the much higher failure strength of the PCA test beams than that of the warehouse beams, the investigators concluded that axial tensile stresses due to shrinkage restraints by columns were the primary cause for the low failure strengths. However, it seems more reasonable to explain the results in terms of the size effect in shear.

In models used to account for the size effect in shear, some researchers (Bazant and Kim, 1984) explain the size effect by fracture mechanics and suggest that the large amount of energy that is released in the cracking of large members leads to the faster propagation of inclined cracks and lower shear failure stresses. Other researchers, like Collins and Kuchma (1998) and Reineck (1990, 1991), explain the size effect as due to a reduction in interface shear transfer due to the larger crack widths that occur in larger members.

Shear Span to Depth Ratio: The shear span is the distance, a , between a support and a point of concentrated load. As the shear span to depth ratio (a/d) decreases, the shear strength increases. Many empirical formulas for calculating shear strength include an a/d ratio to account for the influence of this parameter. The increase in strength is significant in members with a/d ratios less than about 2.5 to 3.0, because a significant portion of the shear may be transmitted directly to the support by an inclined strut. This mechanism is frequently referred to as arch action and the magnitude of the direct load transfer increases with decreasing a/d -ratios. For deep members and the ends of beams, it is therefore more appropriate to use strut-and-tie models than sectional design approaches.

The key characteristic of the a/d -ratio is obvious for simple beams subject to point loads. The term relates the maximum moment and the maximum shear force, since $M_{\max} = V_{\max} \times a$ and thus the moment to shear force ratio is $M_{\max} / V_{\max} d = a/d$. For distributed loading this term is also significant, as has already been pointed out by Kani (1964, 1967), and it gives $M_{\max} / V_{\max} d = l / 4d$, which means that “ a ” is the distance to the resultant of the loads in one half of the span. Therefore, the a/d -ratio characterizes the slenderness of a simple beam and the value influences the relationships between the different shear transfer actions. The value, a , also relates the flexural and shear capacities, i.e. the shear force at flexural failure can be calculated by dividing by “ a ” or the moment at mid-span corresponding to shear failure can be calculated by multiplying by “ a ”.

Longitudinal Reinforcement Ratio: For the same magnitude of loading, as the longitudinal reinforcement ratio decreases, flexural stresses and strains increase. Thus, crack widths increase and the shear strength is lowered. Further, as the longitudinal reinforcement ratio decreases, dowel action decreases. It has also been reported that for members having longitudinal bars distributed over their

height crack spacings are smaller and that improves shear strength significantly (Collins and Kuchma, 1999).

Axial Force: When members are subjected to axial tension, the shear strengths of such members decrease. Since axial tension makes the crack angle steeper over almost the full depth of the member, longitudinal reinforcement needs to be provided in both the top and bottom of the member. Once appropriate amounts of longitudinal reinforcement are provided, the failure of such members may occur in a relatively ductile manner. By contrast, axial compression increases the depth of the uncracked compression zone, decreases the width of the shear cracks, and thus the interface shear transfer is increased. All of these factors lead to an increase in shear capacity with increase in axial compression. However, for members subjected to significant axial compression, brittle failures are common.

Other Significant Parameters: In a simply supported member, high shear and high moment do not coexist. Thus, in high shear regions of such members, the effect of moment is relatively small. However, in a continuous beam, the negative moment region is subject to both high shear and high moment and, thus, the effect of moment can be significant. Further, in a negative moment region, the compression and tension sides are reversed over those in a positive moment region. Consequently, the size of the uncracked compressive zone in the negative moment regions of a T-beam differs from that for the positive moment region because there is no longer a wide slab in compression.

When a member is supported on the bottom and loads are applied on the top, applied forces can be transmitted directly to the supports through inclined struts. However, when the member is supported on the bottom and loaded on the bottom, or supported from the top and loaded from the top, those struts cannot form. The member may have a lower shear capacity than that of a beam supported on the bottom and loaded on the top.

A.1.4 Shear Failures of Members without Transverse Reinforcement

Shear failures of members without transverse reinforcement depend on several factors as discussed in this section. Shear failures are initiated by inclined cracks, and these cracks are typically divided into two types, i.e., web-shear cracks and flexure-shear cracks as shown in Fig. A-6. More detailed explanations of these two types of inclined cracks are provided in Appendix B.

Kani (1964) conducted a very large experimental study on shear and reported relationships between the beam capacity and the a/d ratio. “Kani’s Valley of Shear Failures” is presented in Fig. A-7 (McGregor, 1988). Kani tested a large number of rectangular beams without shear reinforcement and having various a/d ratios, while the rest of the beam details remained the same, as shown in Fig. A-7(a). The moment and shear at inclined cracking and failure were observed to be as shown in Fig. A-7(b). The flexural capacity, M_n , is the horizontal line while the shaded area represents the reduction in flexural strength due to shear. From this figure, beams can be classified into four types depending on their a/d ratio: very short, short, slender, and very slender beams. Fig. A-7(c) can be obtained by dividing the moment in Fig. A-7(b) by the shear span, “ a ”, since the moment is $M = V \times a$ for beams with two point loads. Kani also tested beams subjected to uniformly distributed load and used the a/d ratio as a quarter of the span length, i.e., $L/4$.

The shear failure modes of beams without shear reinforcement were also discussed by ASCE-ACI Committee 426 (1973). They also classified beam types by their a/d -ratios. The failure modes of simply supported rectangular beams without shear reinforcement were described as follows;

- a) In very slender beams ($a/d > 6$), the members will likely fail in flexure even before the formation of inclined cracks.
- b) In slender beams ($2.5 < a/d < 6$), some of the flexural cracks grow and may become flexure-shear cracks. The diagonal cracks may continue to propagate towards the top and bottom of the beam and cause yield of the tension steel (Fig. A-8). The beam may split into two pieces at failure. This is called as *diagonal tension failure*.
- c) In short beams ($1 < a/d < 2.5$), a diagonal crack may propagate along the tension steel causing splitting between the concrete and the longitudinal bars (Fig.A-9(a)). This is called a *shear-tension failure*. The diagonal crack may propagate toward the top of the beam resulting in crushing of the compression zone. This is called a *shear-compression failure* (Fig.A-9(b)).
- d) In very short beams ($a/d < 1$), inclined cracks occur along the line between load and reaction. Thus, most of the shear force is transferred by arch action with a structural system as shown in Fig. A-10. *Anchorage failure* of the tension steel may occur at the end of a tension tie. *Bearing failure* may occur by the crushing of concrete above a support. *Flexural failure* is also possible due to the yielding of the tension steel or crushing of the compression zone. *Tension failure of the "arch-rib"* near the top of an edge may occur due to the eccentricity of the thrust of the compressive stresses in the inclined strut. *Compression strut failure* is also possible by crushing of the web along the line of the crack.

The failures of I-shaped beams are somewhat different from those of rectangular beams because the shear stresses in the webs are much higher than in rectangular beams. Web-crushing failures are the most common failure mode for I-beams, as shown in Fig. A-11, although all the failure modes described previously for rectangular beams are also possible for I-beams.

A.1.5 Shear Failures of Members with Transverse Reinforcement and Significant Parameters

If a member contains transverse reinforcement (or shear reinforcement) then, after the appearance of the first inclined crack, the behavior changes considerably from that for a beam without transverse reinforcement. Depending on the amount of the transverse reinforcement more inclined cracks may develop until the stirrups yield. After yielding of the stirrups the load may also increase due to flatter inclined struts crossing the cracks. That action is possible due to interface shear or friction along the crack faces. While failure is then initiated by the break-down of the interface shear, the primary cause is still the yielding of the stirrups so that the final failure is relatively ductile.

For large amounts of transverse reinforcement the concrete in the inclined struts may fail, the so-called "web-crushing" failure. This failure mode is very likely in thin webbed members such as the I-beams shown in Fig. A-11.

The main parameter affecting the behavior and failure mode of webs is the amount of the transverse reinforcement. For that mode, apart from interface shear and some shear transfer in the

compression zone, the shear transfer actions discussed previously for beams without shear reinforcement do not play a dominant role. For these reasons, the terms for the shear strength provided by the concrete are differentiated as follows:

- V_{ct} for members without transverse reinforcement, in order to indicate that the failure is governed by the concrete tensile strength, and
- V_c for members with transverse reinforcement.

Axial compression influences the shear capacity of members with transverse reinforcement because the depth of the uncracked compression zone increases. However, axial compression also influences the behaviour in the web: shear crack widths decrease, and crack angles decrease, so that the angle of diagonal compression is flattened and this change increases the effectiveness of the shear reinforcement.

Concrete strength influences the transfer of forces across cracks, because for high strength concrete, the inclined cracks may run through the aggregates and thus interface shear transfer is reduced.

The **size effect** plays only a minor role for members with transverse reinforcement because the crack widths are mainly controlled by the transverse reinforcement.

A.2 Shear Strength Models

A.2.1 Overview

The truss model was widely used to understand the shear behavior of reinforced concrete beams with transverse reinforcement in the early 1900's. Ritter (1899) developed a 45° truss model for the analysis of the post-cracking behavior of a reinforced concrete beam and Mörsch (1920, 1922) refined that 45° truss model. Mörsch also used the flexure-shear crack to derive the shear stress distribution for a reinforced concrete beam, i.e., $\tau = \frac{V}{b_w jd}$. This stress has for many years been called

the “nominal” shear stress. In 1907, Withey introduced the 45° truss model into American literature. Withey reported that the 45° truss model gave a conservative result when compared to experimental test results, a statement that was confirmed by Talbot (1909). In the USA in the late 1950's the 45° truss model was also adopted for prestressed concrete based on the work reported in University of Illinois Engineering Experiment Station Bulletin 493. That bulletin reported that while the 45° model provided conservative results compared to experimental results, its use was recommended because “the design procedure should be no more complicated than would be justified by the certainty of the theory and the economy of the end result”.

In 1950s and 1960s, a large amount of experimental research was conducted to study the contribution of aggregate interlock and dowel action on shear resistance. Zwoyer and Siess (1954), Bresler and Pister (1958), Guralnick (1959), and Walther (1962) studied the stress conditions in the concrete above flexural cracks of beams without transverse reinforcement, assuming that all shear would be carried in the flexural compression zone. In 1964, Kani introduced the “comb” model in which the concrete between the flexural cracks is considered as the teeth of the comb and uncracked concrete above the flexural cracks as the backbone of the comb. After studying the large amount of

available experimental results, the ACI-ASCE shear committee (1962) recommended the use of an empirical expression for the shear stress at inclined cracking as the shear failure load. That expression first appeared in the 1963 ACI 318 Code and is still present in ACI 318-02 as Equation 11-5. That expression is:

$$v_{cr} = 1.9\sqrt{f'_c} + 2500\rho_w \frac{Vd}{M} \leq 3.5\sqrt{f'_c} \text{ (psi)}$$

In the 1950s and 1960s extensive work at the University of Illinois (Bulletin 493) and at the PCA resulted in the development of the shear strength provisions for prestressed concrete beams that continue to be incorporated into ACI 318-02 and the AASHTO Standard Specification. While the model used for the shear strength provided by the transverse reinforcement was the same as that for reinforced concrete beams, the models used for the shear at inclined cracking differed considerably from those for reinforced concrete beams

Fenwick and Paulay (1968) suggested that shear resistance carried by the compression zone is only about 25% of the total shear and that “aggregate interlock” and dowel forces carried the remainder of the shear. In 1964, Kupfer took a step forward for members with transverse reinforcement by predicting the strut angle using minimum energy principles, and Baumann (1972) further pursued this concept, presenting dimensioning diagrams for plate elements with reinforcement in two and three directions.

Inspired by Baumann’s work, and also by Wagner’s tension field theory (1929), Collins and Mitchell (1981) developed the compression field theory (CFT) where equilibrium conditions, compatibility conditions, and constitutive relationships are considered for shear stress conditions. The CFT assumes that the direction of the inclined compression field, (i.e. the strut angle and the crack angle), and the principal compressive stress coincide, similar to the assumptions of Kupfer and Baumann. The model is a pure truss and the cracked concrete carries no shear.

Thürlimann et al. (1983) and Nielsen (1984) introduced plasticity methods for predicting shear strength.

In 1986, Vecchio and Collins proposed the modified compression field theory (MCFT). That theory modifies the CFT by considering the contribution of the concrete in tension. The MCFT provides a behavioral model for predicting the complete load-deformation response in shear.

From 1992 through 1995, Hsu et al. developed the rotating-angle softened-truss model (RA-STM) and the fixed-angle softened truss model (FA-STM). While the RA-STM assumes that the direction of both principal stress and strain coincide, the FA-STM considers that after cracking, the direction of the principal stress in the concrete struts does not coincide with the direction of the crack. Unlike the MCFT where the stress conditions at a crack are checked, both the RA-STM and FA-STM reduce the average strength of the reinforcement to account for the local stress effects at a crack. Both the MCFT and FA-STM predict similar strengths in most cases.

Descriptions of several of the more important models for determining the behavior in shear of beams with shear reinforcement are presented in the next five sections.

A.2.2 45° Truss Model

Truss models were widely used to understand the shear behavior of reinforced concrete beams in the early 1900's. Ritter (1899) was the first to use a 45° truss model for the analysis of the post-cracking behavior of a reinforced concrete beam. In his model, diagonal concrete struts were considered to be the diagonal members of the truss, the stirrups were the vertical members of the truss, the longitudinal reinforcement served as the bottom chord of the truss, and the flexural compression zone served as the top chord of the truss. In 1902 Mörsch improved this model by assuming that the diagonal struts extended across more than one stirrup. The tensile stresses in cracked concrete were neglected in this model and diagonal compression stresses were assumed to remain at 45° after the concrete cracked.

Equilibrium equations for this model, assuming an angle of diagonal compression of $\theta = 45^\circ$, are shown in Fig. A-12. For a uniform distribution of shear stresses in the effective web area, $b_w jd$, the vertical component of the diagonal compressive force must be balanced by the applied shear:

$$f_2 = \frac{2V}{b_w jd} \quad (\text{A-1})$$

The horizontal component of the diagonal compressive force also must be balanced by the tension in longitudinal reinforcement:

$$N_v = V \quad (\text{A-2})$$

From Fig. A-12, the vertical component of the diagonal compression force must be balanced by the tension in the stirrups over the length $jd \cdot \cot 45^\circ = jd$:

$$\frac{A_v f_v}{s} = \frac{V}{jd} \quad (\text{A-3})$$

Eq. (A-3) is used to design the required amount of stirrups. Eq. (A-1) is used to check the compressive stresses in the concrete and this determines the upper limit of the shear force or capacity.

In the middle of the 1960's the 45° truss model was re-examined because it gives overly conservative results for predictions of the shear strength of members with shear reinforcement. The model lowers the effectiveness of the stirrups and, consequently, efforts were directed towards predicting the actual strut angle, which may be flatter than the angle of the inclined cracks.

A.2.3 Variable-Angle Truss Model

The variable-angle truss model is a version of the 45° truss model modified by assuming flatter strut angles, $\theta \leq 45^\circ$. In this model, the three equilibrium equations can be derived in the same manner as for the 45° truss model. The equilibrium conditions for this model are shown in Fig. A-13 and Eqs. A-4(a), (b), and (c):

$$f_2 = \frac{V}{b_w j d} \frac{1}{\sin \theta \cos \theta} = \frac{V}{b_w j d} (\tan \theta + \cot \theta) \quad (\text{A-4a})$$

$$N_v = V \cot \theta \quad (\text{A-4b})$$

$$\frac{A_v f_v}{s} = \frac{V}{j d} \tan \theta \quad (\text{A-4c})$$

However, these three equilibrium equations are not sufficient to solve member forces, because there are four unknowns; the principal compressive stress, f_2 ; the tension in the longitudinal direction, N_v ; the stresses in the shear reinforcement, f_v ; and the strut angle or inclination of the principal compressive stresses, θ .

There have been different approaches to solve for the strut angle. In 1964, Kupfer used minimum energy principles to determine the crack angle θ while assuming linear elastic behavior of both reinforcement and concrete. Baumann (1972) continued this work, which was later taken up by Collins and Vecchio in their compression field theory. The traditional truss model assumes that the stirrups yield (i.e., $f_v = f_y$) and $\theta = 45^\circ$, and uses Eq. (A-4c). Plasticity methods assume yielding of the stirrups (i.e., $f_x = f_v = f_y$) and that the maximum compressive stress, f_2 , is attained. Such methods result in lower limits for the angle θ .

A.2.4 Compression Field Theory

The compression field theory uses the same approach for equilibrium conditions as described in the variable-angle truss model. Eqs. A-4 (a), (b), and (c) can be expressed respectively in terms of the stresses as shown below. These equilibrium equations can also be derived from Fig. A-14(a and b):

$$f_2 = v(\tan \theta + \cot \theta) \quad (\text{A-5a})$$

$$\rho_x f_{sx} = v \cot \theta \quad (\text{A-5b})$$

$$\rho_v f_{sv} = v \tan \theta \quad (\text{A-5c})$$

For determining the crack angle, θ , in the variable-angle truss model, Wagner (1929) contributed an important fundamental concept in his “tension field theory”. In his shear design of thin “stressed-skin” aircraft, he assumed shear was carried by a diagonal tension field after buckling of the thin metal web. Then, he considered the deformations of the system by assuming that the angles of inclination of the diagonal tensile stresses would coincide with the angles of the inclination of the principal tensile strains.

Similar to Wagner’s tension field theory model, the compression field theory model developed by Collins and Mitchell utilizes the deformations for reinforced concrete by assuming that a diagonal compression field carries shear after cracking. The compatibility conditions used in the compression field theory can be derived from Mohr’s circle for strains as shown in Fig. A-14(c and d).

From Fig. A-14(c and d), the relation between θ and the strains can be expressed as follows:

$$\tan 2\theta = \frac{\gamma_{xy}}{\varepsilon_y - \varepsilon_x} \quad (\text{A-6})$$

Since $\tan 2\theta = 2 \tan \theta / (1 - \tan^2 \theta)$, Eq. (A-6) can be expressed as:

$$\tan \theta = \frac{1}{\gamma_{xy}} \left(\varepsilon_x - \varepsilon_y \pm \sqrt{(\varepsilon_y - \varepsilon_x)^2 + \gamma_{xy}^2} \right) \quad (\text{A-7})$$

From Fig. A-14(c and d), the relation between θ and the strains can also be expressed as:

$$\sin 2\theta = \frac{\gamma_{xy}}{\sqrt{(\varepsilon_y - \varepsilon_x)^2 + \gamma_{xy}^2}} = \frac{\gamma_{xy}}{2R} \quad (\text{A-8})$$

where $R = \frac{\varepsilon_x + \varepsilon_y}{2} - \varepsilon_2$. Therefore, the relationship between the strains is:

$$\sqrt{(\varepsilon_y - \varepsilon_x)^2 + \gamma_{xy}^2} = \varepsilon_x + \varepsilon_y - 2\varepsilon_2 \quad (\text{A-9})$$

From Eqs. A-7 and A-9, the relation between θ and the strains can be simplified as:

$$\tan \theta = \frac{2}{\gamma_{xy}} (\varepsilon_x - \varepsilon_2) \quad (\text{A-10})$$

Thus,
$$\gamma_{xy} = 2(\varepsilon_x - \varepsilon_2) \cot \theta \quad (\text{A-11})$$

From Eq. (A-9), the following expression can be formed:

$$\left(\frac{\gamma_{xy}}{2} \right)^2 = (\varepsilon_x - \varepsilon_2)(\varepsilon_y - \varepsilon_2) \quad (\text{A-12})$$

From Eqs. A-10, A-11, and A-12, the following expression can be derived:

$$\tan^2 \theta = \frac{\varepsilon_x - \varepsilon_2}{\varepsilon_y - \varepsilon_2} \quad (\text{A-13})$$

Eq. (A-13) is Wagner's and Baumann's compatibility equation, which can be applied in cracked concrete using average strains. From Eq. (A-13), the influence of θ on strains is readily apparent. For steep crack angles, the longitudinal strain is high and for flat crack angles, the transverse strain is high.

As shown in Fig. A-14(e), the stress-strain relationships for both longitudinal and transverse reinforcement were assumed as bilinear for the CFT. Stress-strain relationships for cracked concrete in compression were proposed by Collins (1978), based on experimental test results, as follows:

$$f_2 = \left(\frac{f_c'}{\varepsilon_c'} \right) \varepsilon_2 \leq f_{2\max} = \frac{3.6f_c'}{1 + 2(\varepsilon_1 + \varepsilon_2)/\varepsilon_c'} \quad (\text{A-14})$$

where ε_c' = strain corresponding to f_c' in a cylinder test.

In this equation, the softening of the compressive strength in cracked concrete is expressed in terms of the principal tensile strain, ε_1 . The principal tensile strain, ε_1 , can be derived from Fig. A-14(d) and Eq. (A-14) as:

$$\varepsilon_1 = \varepsilon_x + \varepsilon_y - \varepsilon_2 = \varepsilon_x + (\varepsilon_x - \varepsilon_2) \cot^2 \theta \quad (\text{A-15})$$

From Eq. (A-15), the longitudinal strain, ε_x , can be expressed as:

$$\varepsilon_x = (\varepsilon_1 \tan^2 \theta + \varepsilon_2) / (1 + \tan^2 \theta) \quad (\text{A-16})$$

A similar expression for ε_y can be derived from Eqs. A-15 and A-16 as:

$$\varepsilon_y = (\varepsilon_1 + \varepsilon_2 \tan^2 \theta) / (1 + \tan^2 \theta) \quad (\text{A-17})$$

Once the compression field theory was developed, the governing stress-strain relationships were studied by researchers in a large series of experiments. The result from a typical test (Vecchio and Collins, 1982) is shown in Fig. A-15. Based on the experimental findings, Eq. (A-14) was refined by Vecchio and Collins in 1986 to be as follows:

$$f_2 = f_{2\max} \left[2 \left(\frac{\varepsilon_2}{\varepsilon_c'} \right) - \left(\frac{\varepsilon_2}{\varepsilon_c'} \right)^2 \right] \quad (\text{A-18})$$

where $\frac{f_{2\max}}{f_c'} = \frac{1}{0.8 + 170\varepsilon_1} \leq 1.0$. This relationship is shown in Fig. A-14(f) and can also be visualized in terms of both ε_1 and ε_2 as shown in Fig. A-16.

Because the compression theory provides the equilibrium conditions, compatibility conditions, and constitutive relationships for both reinforcement and cracked concrete, it can predict shear behavior for any load level as well as the shear strength of members. However, since the compression field theory neglects the tensile stresses in cracked concrete, it gives conservative results for the shear behavior of members, meaning that it underestimates both the shear stiffness and the shear strength.

A.2.5 Modified Compression Field Theory

The tensile stresses in cracked concrete provide significant shear resistance. The modified compression field theory (MCFT) accounts for the influence of tensile stresses on the post-cracking shear behavior. The equilibrium equations for the MCFT can be derived in a similar manner to those for CFT with a concrete tensile stress term added. For the conditions shown in Fig. A-17 (a and b), equilibrium equations are:

$$\rho_x f_{sx} = v \cot \theta - f_1 \quad (\text{A-19a})$$

$$\rho_v f_{sy} = v \tan \theta - f_1 \quad (\text{A-19b})$$

$$f_2 = v(\tan \theta + \cot \theta) - f_1 \quad (\text{A-19c})$$

Conditions are expressed in terms of average stresses. The average principal tensile stress after cracking, f_1 , was suggested by Collins and Mitchell (1991) to be as follows:

$$f_1 = \frac{f_{cr}}{1 + \sqrt{500\varepsilon_1}} \quad (\text{psi}) \quad (\text{A-20})$$

where f_{cr} is taken as $4\sqrt{f'_c}$. It can be seen, as shown in Fig. A-17(j), that the average principal stress decreases as the average principal strain increases. On a local level, however, stresses vary and differ from the values calculated from Eqs. A-19 and A-20. The failure of the member can be governed by either average stresses or local stresses at a crack. Therefore, the conditions at a crack also need to be checked.

At a crack, the concrete tensile stresses decrease to zero and thus the tensile stresses in the reinforcement increase significantly. Assuming that cracks are parallel, the equilibrium conditions at a crack can be found from Fig. A-17 (c and d):

$$\text{Longitudinal direction: } f_{sxcr} \rho_x (A_{cr} \sin \theta) - (v_{ci} \cos \theta) A_{cr} - v (A_{cr} \cos \theta) = 0 \quad (\text{A-21a})$$

$$\text{Transverse direction: } f_{syrcr} \rho_v (A_{cr} \cos \theta) + (v_{ci} \sin \theta) A_{cr} - v (A_{cr} \sin \theta) = 0 \quad (\text{A-21b})$$

where A_{cr} = area of crack plane, and v_{ci} = interface shear stress at a crack (see Eq. A-23). Therefore, Eqs. A-21(a) and (b) become as follows:

$$\rho_x f_{sxcr} = v \cot \theta + v_{ci} \cot \theta \quad (\text{A-22a})$$

$$\rho_v f_{syrcr} = v \tan \theta - v_{ci} \tan \theta \quad (\text{A-22b})$$

From Eqs. A-22(a) and (b) it is apparent that as v_{ci} at a crack increases, the stress in the longitudinal reinforcement increases but the stress in the transverse reinforcement decreases. The shear stresses that can be transmitted across a crack, v_{ci} , can be expressed as a function of crack

width. A limit on v_{ci} was proposed by Vecchio and Collins (1986), based on the experimental data of Walraven (1981), and simplified by Bhide and Collins (1989), as follows:

$$v_{ci} \leq \frac{2.16\sqrt{f'_c}}{0.3 + \frac{24w}{a + 0.63}} \quad (\text{psi and in}) \quad (\text{A-23})$$

Fig. A-17(k) shows the normalized magnitude of the allowable shear stress on a crack in the case that the maximum aggregate size is 0.75 inch. In the Eq. (A-23), the crack width, w , can be obtained as the average crack spacing multiplied by the principal tensile strain, as shown in Fig. A-17(g). Thus,

$$w = \varepsilon_1 s_{m\theta} \quad (\text{A-24})$$

where the average crack spacing, $s_{m\theta}$ is taken as:

$$s_{m\theta} = 1 / \left(\frac{\sin \theta}{s_{mx}} + \frac{\cos \theta}{s_{my}} \right) \quad (\text{A-25})$$

In Eq. (A-25), s_{mx} and s_{my} are the estimated crack spacings in the longitudinal and vertical directions, respectively. The expression for these estimated crack spacings are taken from the CEB-FIP Code (1978) and, for uniform tensile strain, these expressions become:

$$s_{mx} = 2 \left(c_x + \frac{s_x}{10} \right) + 0.25k_1 \frac{d_{bx}}{\rho_x} \quad (\text{A-26a})$$

$$s_{my} = 2 \left(c_y + \frac{s_y}{10} \right) + 0.25k_1 \frac{d_{by}}{\rho_y} \quad (\text{A-26b})$$

where

c_x, c_y : distance between midsection and longitudinal and transverse reinforcement, respectively.

s_x, s_y : spacing of longitudinal and transverse reinforcement, respectively

k_1 : coefficient for bond characteristics of bars (0.4 for deformed bars, 0.8 for plain bars)

d_{bx}, d_{by} : bar diameter of longitudinal and transverse reinforcement, respectively.

In a typical member, the average strain in the stirrups exceeds the yield strain under high load and, then, Eqs. A-19(b) and A-22(b) must be equivalent. Thus,

$$f_1 \leq v_{ci} \tan \theta = \frac{2.16\sqrt{f'_c}}{0.3 + \frac{24w}{a + 0.63}} \tan \theta \quad (\text{psi and in}) \quad (\text{A-27})$$

Eq. (A-27) limits the average principal tensile stress in cracked concrete so that possible failure of the aggregate interlock mechanism can be taken into account in the MCFT.

Both the CFT and MCFT can predict the shear behavior of members with shear reinforcement for all loading histories. However, the CFT predicts no shear strength for those members without shear reinforcement as it neglects the contribution of the tensile stress carried by cracked concrete. The MCFT can predict shear behavior even for those members without shear reinforcement because it accounts for the tensile stresses carried by cracked concrete.

A.2.6 Rotating-Angle Softened-Truss Model and Fixed-Angle Softened-Truss Model

Two models, the Rotating-Angle Softened-Truss Model (RA-STM) and the Fixed-Angle Softened-Truss Model, have been developed by Hsu and his researchers (Hsu 1988, 1993; Belarbi and Hsu 1991, 1994, 1995; Pang and Hsu 1992, 1995; 1996). These methods utilize equilibrium, compatibility and stress-strain relationships for softened concrete.

A.2.6.1 Rotating-Angle Softened-Truss Model (RA-STM)

This model assumes that the crack angle in post-cracking concrete coincides with the principal stress and strain directions. Since the crack angle in typical elements decreases as the shear increases, this model is called the Rotating-Angle Softened-Truss Model.

The average stresses in the reinforced concrete element shown in Fig. A-18(a) can be expressed as sum of the stresses in the concrete (Fig. A-18b, c) and the stresses in the steel (Fig. A-18d). Two coordinate systems are used as shown in Fig. A-18(e); the ℓ and t axes represent the longitudinal and transverse directions, respectively, while d and r represent the principal compressive and tensile directions with an angle, θ , from the ℓ axis, respectively.

Equilibrium equations can be derived by superposing the stresses in the concrete and the stresses in the steel bars and assuming that the steel bars resist axial stresses only. The resultant equations are:

$$\sigma_\ell = \sigma_d \cos^2 \theta + \sigma_r \sin^2 \theta + \rho_\ell f_\ell \quad (\text{A-28a})$$

$$\sigma_t = \sigma_d \sin^2 \theta + \sigma_r \cos^2 \theta + \rho_t f_t \quad (\text{A-28b})$$

$$\tau_{\ell t} = (\sigma_d - \sigma_r) \sin \theta \cos \theta \quad (\text{A-28c})$$

where σ_ℓ , σ_t , $\tau_{\ell t}$ = normal and shear stresses in each direction in ℓ - t coordinate, σ_d , σ_r = principal stresses in the d and r directions, respectively, ρ_ℓ , ρ_t = reinforcement ratios in the ℓ and t directions, respectively, and f_ℓ , f_t = steel stresses in the ℓ and t directions, respectively.

Compatibility relationships can be derived from Mohr's strain circle. These relationships can simply be obtained from the Eqs. A-28(a), (b), and (c) by replacing σ_ℓ by ε_ℓ , σ_t by ε_t , σ_d by ε_d , σ_r by ε_r , and τ_{tt} by $\gamma_{tt}/2$. Then, the compatibility equations become:

$$\varepsilon_\ell = \varepsilon_d \cos^2 \theta + \varepsilon_r \sin^2 \theta \quad (\text{A-29a})$$

$$\varepsilon_t = \varepsilon_d \sin^2 \theta + \varepsilon_r \cos^2 \theta \quad (\text{A-29b})$$

$$\gamma_{tt} = 2(\varepsilon_d - \varepsilon_r) \sin \theta \cos \theta \quad (\text{A-29c})$$

Belarbi and Hsu (1995) suggested stress-strain relationships to account for concrete softening that are similar to those of MCFT but somewhat more complex:

$$\sigma_d = \zeta_{\infty} f'_c \left[2 \left(\frac{\varepsilon_d}{\zeta_{\infty} \varepsilon'_c} \right) - \left(\frac{\varepsilon_d}{\zeta_{\infty} \varepsilon'_c} \right)^2 \right] \quad \text{if } \frac{\varepsilon_d}{\zeta_{\infty} \varepsilon'_c} \leq 1 \quad (\text{A-30a})$$

$$\sigma_d = \zeta_{\infty} f'_c \left[1 - \left(\frac{\varepsilon_d / \zeta_{\infty} \varepsilon'_c - 1}{2 / \zeta_{\infty} - 1} \right)^2 \right] \quad \text{if } \frac{\varepsilon_d}{\zeta_{\infty} \varepsilon'_c} > 1 \quad (\text{A-30b})$$

where for "proportional loading"

$$\zeta_{\infty} = \frac{0.9}{\sqrt{1 + 400\varepsilon_r}} \quad \text{and} \quad \zeta_{\infty} = \frac{1}{\sqrt{1 + 500\varepsilon_r}} \quad (\text{A-30c})$$

for "sequential loading"

$$\zeta_{\infty} = \frac{0.9}{\sqrt{1 + 250\varepsilon_r}} \quad \text{and} \quad \zeta_{\infty} = 1 \quad (\text{A-30d})$$

The predictions from Eq. (A-30) give very similar results to those from Eq. (A-18) in the Compression Field Theory (CFT).

Belarbi and Hsu (1994) also suggested that the average stress-strain relationship of concrete in tension after cracking was as follows:

$$\sigma_d = \frac{f_{cr}}{(12,500\varepsilon_r)^{0.4}} \quad (\text{psi}) \quad \text{when } \varepsilon_r > 0.00008 \quad (\text{A-31})$$

where f_{cr} , the cracking stress of concrete, is taken as $3.75\sqrt{f'_c}$ (in psi).

The principal tensile stress, σ_d , predicted by Eq. (A-31), decreases more rapidly with increasing principal tensile strain, ε_r , than the stress predicted by Eq. (A-20) as used in the MCFT.

Unlike the MCFT, where local stress conditions are checked to account for transmissibility of stresses at a crack, the RA-STM accounts for local yielding of steel bars by using an adjusted average stress-strain curve for mild steel bars embedded in concrete. As shown in Fig. A-18(I), average yield stresses for embedded bars are smaller than the average yield stresses of bare bars. The relationships are:

$$f_s = E_s \varepsilon_s \text{ if } \varepsilon_s \leq \varepsilon_n \quad (\text{A-32a})$$

$$f_s = f_y \left[(0.91 - 2B) + (0.02 + 0.25B) \frac{E_s}{f_y} \varepsilon_s \right] \left[1 - \frac{2 - \phi / 45}{1,000\rho} \right] \text{ if } \varepsilon_s > \varepsilon_n \quad (\text{A-32b})$$

$$\text{where } \varepsilon_n = \frac{f_y}{E_s} (0.93 - 2B) \left[1 - \frac{2 - \phi / 45}{1,000\rho} \right], \quad B = \left(\frac{f_{cr}}{f_y} \right)^{1.5} / \rho, \text{ and } \phi = \text{the initial crack angle.}$$

The shear strength predictions by the RA-STM are similar to those predicted by the MCFT for members with low amounts of reinforcement but are somewhat lower than those of the MCFT for members with large amounts of reinforcement. The RA-STM model does not account for the concrete contribution to shear due to the assumption that the crack angle coincides with the principal stress direction in cracked concrete, resulting in a vanishing of shear stresses along cracks. To account for the concrete contribution to shear, the Fixed Angle Softened Truss Model (FA-STM) was developed by Hsu and his researchers.

A.2.6.2 Fixed-Angle Softened-Truss Model (FA-STM)

Unlike the RA-STM which considers the reorientation of the crack angle in post-cracking behavior, the FA-STM assumes that the initial crack angle remains constant. For this reason the model is called the Fixed-Angle Softened-Truss Model (FA-STM). Pang and Hsu (1995) recommended that the FA-STM, rather than the RA-STM, be used for cases where the crack angle changes by more than 12 degrees after initial cracking.

The two coordinate systems used in this model are shown in Fig. A-18(g); The 1-2 coordinate system represents the principal tensile and compressive directions for an initial crack angle, ϕ , from the ℓ axis, with the direction of the latter dependent on the principal concrete stress direction just prior to cracking (Fig. A-18h).

The equilibrium and compatibility equations for the FA-STM can be derived from the transformation of stresses and strains into the two coordinate systems as follows:

Equilibrium equations:

$$\sigma_\ell = \sigma_2^c \cos^2 \phi + \sigma_1^c \sin^2 \phi + \tau_{21}^c 2 \sin \phi \cos \phi + \rho_\ell f_\ell \quad (\text{A-33a})$$

$$\sigma_t = \sigma_2^c \sin^2 \phi + \sigma_1^c \cos^2 \phi - \tau_{21}^c 2 \sin \phi \cos \phi + \rho_t f_t \quad (\text{A-33b})$$

$$\tau_{\ell t} = (-\sigma_2^c + \sigma_1^c) \sin \phi \cos \phi + \tau_{21}^c (\cos^2 \phi - \sin^2 \phi) \quad (\text{A-33c})$$

where σ_ℓ , σ_t , $\tau_{\ell t}$ are the normal and shear stresses in each direction in the ℓ - t coordinate system (positive for tension), σ_2^c , σ_1^c are the average normal stresses of the concrete in the 2 and 1 directions, respectively, τ_{21}^c is the average shear stress in the concrete in the 2-1 coordinate system and ϕ is the angle of the initial inclined cracks.

Compatibility relationships are:

$$\varepsilon_\ell = \varepsilon_2 \cos^2 \phi + \varepsilon_1 \sin^2 \phi + \gamma_{21} \sin \phi \cos \phi \quad (\text{A-34a})$$

$$\varepsilon_t = \varepsilon_2 \sin^2 \phi + \varepsilon_1 \cos^2 \phi - \gamma_{21} \sin \phi \cos \phi \quad (\text{A-34a})$$

$$\gamma_{\ell t} = 2(-\varepsilon_2 + \varepsilon_1) \sin \phi \cos \phi + \gamma_{21} (\cos^2 \phi - \sin^2 \phi) \quad (\text{A-34c})$$

where the ε_2 , ε_1 = average normal strain in the directions 2 and 1, respectively, and γ_{21} = average shear strain in the 2-1 coordinate.

Note that the principal compressive direction in the concrete after cracking does not coincide with the crack angle, and thus, $\theta \neq \phi$.

The shear resistance of an element subjected to pure shear has been derived by Pang and Hsu (1996) as:

$$\tau_{\ell t} = \frac{(\tau_{21}^c)^2 + (\sigma_1^c)^2 + (\rho_\ell f_\ell + \rho_t f_t) \sigma_1^c}{2\sqrt{\rho_\ell f_\ell \rho_t f_t}} + \sqrt{\rho_\ell f_\ell \rho_t f_t} \quad (\text{A-35})$$

The first term is the “concrete contribution”, V_c , and the second term is the “steel contribution”, V_s . When the steel stresses reach their local yield stresses, f_y'' , at cracks, the local tensile strength of the concrete, σ_1^c , must be zero and Eq. (A-35) becomes:

$$\tau_{\ell t} = \frac{(\tau_{21}^c)^2}{2\sqrt{\rho_\ell f_{\ell y}'' \rho_t f_{t y}''}} + \sqrt{\rho_\ell f_{\ell y}'' \rho_t f_{t y}''} \quad (\text{A-36})$$

where $f_y'' = f_y \left[1 - \frac{2 - \phi / 45 \text{ deg}}{1,000 \rho} \right]$ and f_y'' becomes $f_{\ell y}''$ or $f_{t y}''$ for the longitudinal reinforcement and transverse reinforcement, respectively.

If the crack angle coincides with the d -r coordinates, the concrete shear stress term, τ_{21}^c , vanishes and Eq. (A-36) gives:

$$\tau_{tt} = \sqrt{\rho_\ell f_{ly}'' \rho_t f_{ty}''} \quad (\text{A-37})$$

which does not involve a “concrete contribution” term, V_c .

It should be noted that the first terms in both Eqs. A-35 and A-36 become infinite when no transverse reinforcement exists and thus those expressions cannot predict a concrete contribution to shear resistance for such members. Further, the assumption that the crack angle remains parallel to the principal direction of the applied stresses is true only when the amounts of longitudinal and transverse reinforcement are equal. In most practical cases, however, those amounts are different and the shear crack angles depend on the principal strain direction.

A.2.7 Truss Model with Crack Friction

A.2.7.1 Introduction

The failure of concrete members or structures in shear is mostly determined by the formation of inclined cracks, one of which opens widely due to excessive strains in the reinforcements crossing one of those cracks. The opening of that crack eventually leads to crushing of the concrete on the compression face of the member and sometimes to non-ductile behavior because yielding of the reinforcement does not occur before failure of the member. Therefore it is understandable that designers have always first looked for the weakest sections along such cracks and determined the amount of reinforcement required there.

For shear design, an intensive observation of the shear cracking and failure of beams led Morsch (1909, 1922) to regard the concrete between the inclined cracks as struts of a truss (Fig. A-19). Morsch looked at the equilibrium along the failure surface in the B-region, (beam region), initially by means of graphic statics. The same approach was later used by Lessig (1959), who proposed skew, spatial failure surfaces for reinforced concrete beams subjected to torsion, and to torsion combined with shear forces and bending moments.

The ASCE-ACI Committee 426 in their State-of-the-Art Report on Shear (1973) was also guided by the concept of looking at failure mechanisms. They extensively reviewed the different shear failure modes and the possible actions and mechanisms for shear transfer at cracks. Generally, "failure mechanism approaches" are not restricted to the kinematic theory of plasticity, but are approaches characterized by the modeling of the actual failure surface in a member, or the critical crack and the localized crushing of the concrete compression zone. In this sense, failure mechanism approaches have a common feature with fracture mechanics approaches, where the localization of the failure zone, either in tension or compression, plays the major role in the failure concept.

For shear it is important to note that rarely are all the shear transfer actions modeled in the theories presented in the foregoing sections. Despite the fact that a failure mechanism approach is used, it may well be that a lower bound estimate of the failure load is attained, as for any other non-linear analysis, if safe assumptions for the material characteristics and shear transfer actions are made.

The “truss model with crack friction” for members with transverse reinforcement is such a failure mechanism approach and is a “discrete” approach with respect to cracking. It is based on the research of dei Poli et al. (1987, 1990), Gambarova (1979), Kirmair (1985/87), Kupfer and his coworkers Mang, Bulicek, Moosecker and Karavesyrouglou (1979, 1983, 1991), Bulicek (1993) and Reineck (1990, 1991, 1995). The shape and the geometry (inclination) of the crack and the spacing of the cracks are modeled. Therefore, this approach is, in principle, different to smeared approaches based on truss analogies or compression field theories.

The shear design method “truss model with crack friction” was implemented as a shear design procedure in the 1999 FIP Recommendations “Practical Design of Structural Concrete” and is explained in this section. The method is also used for shear design in the new German code DIN 1045-1 (2001), which is presented in Section B.1.8. The background for this method is explained more extensively by Reineck (1995, 1998) and also described in Chapter 3.4 of the ASCE-ACI 445 report (1998).

A.2.7.2 Equilibrium

The shear design method “truss model with crack friction” starts from the fundamental free-body diagram shown in Fig. A-20. That diagram is obtained by separating the member along an inclined crack in the B-region of a structural concrete member with transverse reinforcement. The approach is similar to that of Morsch and shown in Fig. A-19. The forces acting on the free body are the forces at the end support, the chord forces, the forces in the stirrups and the friction forces along the crack, as shown in Fig. A-20b.

In Fig. A-20 the dowel force in the longitudinal reinforcement is neglected, even though that force plays a role in members without transverse reinforcement. Furthermore, for simplicity, as shown in Fig. A-20 the chords are assumed to be parallel to the axis of the member so that there are no vertical components of an inclined compression chord or an inclined tension chord of the truss. That condition means that a different model is necessary in the “disturbed region” (D-region) of the beam near the support because the compression chord must descend towards the support if that support is located beneath the beam as shown in Fig. A-20.

The basic requirement for shear design is:

$$V_{Rd} \geq V_{Sd} \quad (\text{A-38})$$

where: V_{Sd} = shear force at about a distance $z \cot\theta$ from the face of the support.

The basic equation for the shear resistance follows directly from vertical equilibrium:

$$V_{Rd} = V_{swd} + V_{fd} + V_{pd} + V_{ccd} \quad (\text{A-39})$$

where: V_{swd} = shear force carried by the stirrups across the crack

V_{fd} = vertical component of the friction forces at the crack (Fig. A-20b)

V_{pd} = vertical component of the force in the prestressing tendon, and

V_{ccd} = vertical component of the force in an inclined compression chord.

From Eqs. A-38 and A-39, the design shear force for the web of a structural concrete member is defined as:

$$V_{Sd,web} = V_{Sd} - V_{pd} - V_{ccd} \quad (\text{A-40})$$

Therefore, the web must provide the following resisting shear force:

$$V_{Rd,web} = V_{swd} + V_{fd} \geq V_{Sd,web} \quad (A-41)$$

The shear force component V_{swd} carried by the vertical stirrups across the inclined crack at the ultimate capacity is given by:

$$V_{swd} = (A_{sw}/s_w) f_{ywd} z \cot\beta_r \quad (A-42)$$

where: A_{sw} = area of transverse reinforcement

s_w = stirrup spacing in the longitudinal direction

f_{ywd} = design yield strength of transverse reinforcement

z = internal lever arm, and

β_r = crack angle

The shear force component V_{sw} is known at any load level, (and not at the ultimate capacity only), if the shear force component V_f due to friction is known, in addition to the amount of transverse reinforcement and the crack angle. The force V_f is the vertical component of the combined friction forces T_f and N_f across the inclined crack in the web, as shown in Fig. A-20(b). Normally only a part of the force T_f combines with N_f to provide an inclined compressive force, but additionally a component without axial stresses exists on the crack surface. The shear force component V_f due to friction represents the "concrete contribution" appearing in many codes such as ACI 318, as explained later.

A.2.7.3 Inclination and Spacing of Inclined Cracks

The crack inclination, as well as the crack spacing, must be assumed based either on tests or determination by a non-linear analysis. The angle of the inclined cracks is normally assumed at 45° for a reinforced concrete member. However, Kupfer and Moosecker (1979) have also pointed out, that the angle could be up to 5° flatter, due to a reduced modulus of elasticity caused by micro-cracking. Flatter angles occur for prestressed concrete members or for members with axial compression, and steeper angles occur for members with axial tension. For such members, the angle of the principal compressive stress at the neutral axis for the uncracked state is commonly assumed as the crack angle.

The spacing of the inclined cracks is mainly determined by the amount of reinforcement and relevant formulas have been proposed by Gambarova et al. (1979, 1991), dei Poli et al. (1987, 1990) and Kirmair (1985/87), amongst others.

A.2.7.4 Constitutive Laws for Crack Friction

Any approach, like the "truss model with crack friction", relies on constitutive laws for the transfer of forces across cracks by friction or interface shear. This shear transfer mechanism is clearly defined in the works of Fenwick and Paulay (1968), Taylor (1972, 1974) and others. However, only a few tests and no theories were available initially for formulating reliable constitutive laws. This situation has changed considerably through the research of the last 20 years by Hamadi (1976), Walraven (1980), Walraven and Reinhardt (1981), Gambarova (1979), Daschner (1980), Nissen (1987), and Tassios and Vintzeleou (1987) in Europe, White and Gergeley and Mattock and Hawkins in the USA (Section 11.7 of ACI 318-02), and Okamura in Japan(JSCE 1986). An extensive state-of-

the-art report on interface shear has been provided by Gambarova and di Prisco (1991). The constitutive law proposed by Walraven (1980) is often used by others because it describes not only the shear stress-slip relationship for different crack widths but also the associated normal stresses.

A.2.7.5 Shear Force Component V_f due to Crack Friction

The shear force component V_f in Eqs. A-39 and A-40, that is transferred by friction across the crack, depends on the available slip and the crack width. These displacements have to be calculated in order to determine the strains in the chords and in the web. In return, the displacements and the strains must be compatible with the forces in the model according to the constitutive laws for the shear force components. The variation in the force V_f is plotted in Fig. A-21. Its value depends on the magnitude of the shear, on the strain conditions in the member, on the longitudinal strain ε_x in the middle of the web, and on the crack spacing, in addition to the assumed friction law. However, for simplicity a constant value V_f may be assumed for code purposes, as indicated in Fig. A-21(a). Because the web area is reinforced by the stirrups, the value for V_f is influenced to a minor extent only by size effects and the longitudinal reinforcement ratio.

The practical result for shear design is a constant value for the shear V_f . In the 1999 FIP Recommendations the following value was specified for V_f , along with the crack angle, for reinforced concrete members without axial forces:

$$V_{fd} = 0.070 (b_w z f_{cwd}) \quad (\text{A-43a})$$

$$\cot\beta_r = 1.20 \quad \text{i.e. } \beta_r \approx 40^\circ \quad (\text{A-43b})$$

The results of Eqs. A-41, A-42 and A-43 are plotted in the simple, non-dimensional design diagram, Fig. A-22, which is well known and used in many codes. The crack friction governs the design for low and medium shear stress values and only for a small range of very high shears, is the strength of the compression struts f_{cwd} reached. That value is characterized by the quarter circle in Fig. A-22.

For low shear stresses or low reinforcement ratios, ρ_w , the strength is limited by the minimum reinforcement ratios $\rho_{w,\min}$ specified in codes, and the corresponding values $\omega_{w,\min}$ therefore represent the lower limit for applying Eq. (A-43). For members without transverse reinforcement that capacity is far lower than the value for V_f . Clearly this result means that V_{fi} is completely different to the ultimate shear force V_{ct} for members without transverse reinforcement.

The approach “truss model with crack friction” can consider the influence of axial forces as well as prestress. Flatter cracks occur and V_f is reduced as consequence of the negative longitudinal strain, ε_x . The influence of the crack inclination is very pronounced as shown in Figs. A-20(b) and A-21(b). For cracks flatter than about 30° , the shear force component V_f no longer plays any role and the struts are parallel to the cracks. In the 1996 FIP Recommendations, the following relationships are proposed for members with axial compression or prestress, and the practical results are shown in Fig. A-23.

$$\cot\beta_r = 1.20 - 0.2 \sigma_{xd} / f_{ctm} \quad (\text{A-44a})$$

$$V_{fd} = 0.10 (1 - \cot\beta_r / 4) (b_w z f_{cwd}) \geq 0 \quad (\text{A-44b})$$

where: $\sigma_{xd} = N_{Sd} / A_c =$ axial stress [(-) in compression]

$f_{cwd} = 0.80 f_{lcd} =$ compressive strength of inclined struts

In the case of axial tension, the cracks may be steeper than 45° and the strain ε_x is positive. In the FIP Recommendations the following relations are given for members with axial tension:

$$\cot\beta_r = 1.20 - 0.9 \sigma_{xd} / f_{ctm} \geq 0 \quad (\text{A-45a})$$

$$V_{fd} = 0.10 (1 - 0.36 / \cot\beta_r) (b_w z f_{cwd}) \geq 0 \quad (\text{A-45b})$$

The influence of axial tension is quite noticeable, because the value $V_{fd} = 0$ is already reached at a value of $\sigma_{xd} = 0.933 f_{ctm}$ and a crack angle of about 70° , corresponding to a value $\cot\beta_r = 0.36$. This result leads to high stirrup amounts. The approach may be on the safe side because the crack angle is evaluated on basis of the uncracked state, rather than the cracked state. Unfortunately, there are too few tests with which to compare predictions and propose a better relationship.

The shear force component V_f in DIN 1045-1 was made dependent on the concrete strength and its value decreases with increasing strength. Values are given in Section B.1.8.

A.2.7.6 The Truss - Model

When the shear force component V_f is known, all the forces are defined at the crack or failure surface, so that the state of stress in the struts between the cracks is also known. Obviously the solid concrete between the cracks is the strut of a truss formed together with the stirrups (Fig. A-24a). This was the action that Mörsh utilized in his truss analogy (see Fig. A-19). The frictional forces cause a biaxial state of stress as shown in the Fig. A-24(b) with a principal compression field at a flatter inclination than that of the cracks, and a tension field perpendicular to it.

For high shear forces the minor principal stress turns into compression because the normal stresses due to friction prevail. However, these compressive stresses are so small, that they are usually neglected. Then, only the truss of Fig. A-24(a) remains with an uniaxial compression field. That result is the model normally used for theory of plasticity analyses.

The minor principal stress is tension for small shear forces, so that the state of stress can be represented by the two truss models shown in Fig. A-25. The usual truss model, with uniaxial compression struts inclined at the angle θ in Fig. A-25(a), is superimposed on a truss with compression struts in the same direction and concrete ties perpendicular to the struts (Fig. A-25b). Then there are two load paths for shear transfer, as defined by Schlaich, Schäfer and Jennewein (1987) and as also shown earlier by Reineck (1982), and with different explanations by Lipski (1971, 1972) and by Vecchio and Collins (1986) in their "modified compression field theory". The model in Fig. A-25(b) is the same as that proposed by Reineck (1990, 1991) for members without transverse reinforcement, so that the transition from members with, to members without, transverse reinforcement is consistently covered.

For simplicity only the truss with a uniaxial compression field is modeled, because it is applicable for both the intermediate and high shear stress ranges, $v_d = \tau_{Rd} / f_{cwd}$. With the shear force components V_{sw} and V_f defined by the equations given above, the angle θ of the inclined struts in the web may be derived as follows:

$$\cot\theta = \frac{\cot\beta_r}{\left(1 - \frac{V_{fd}}{V_{Sd,web}}\right)} \quad (\text{A-46a})$$

$$\text{or} \quad \cot \theta = \frac{V_{Sd,web}}{\left(\frac{A_{Sw,web}}{s_w} \right) f_{ywd} z} \quad (\text{A-46b})$$

$$\text{with} \quad V_{Rd,web} = V_{swd} + V_{fd} \geq V_{Sd,web}$$

This means that the angle θ varies with the magnitude of the applied shear force, i.e. the angle θ increases with increasing applied shear force $V_{Sd,web}$.

The upper limit of the resistant shear force may then be derived from the truss analogy as follows:

$$V_{Rd,web,max} = b_w z f_{cwd} \sin \theta \cos \theta = b_w z f_{cwd} / (\cot \theta + \tan \theta) \quad (\text{A-47a})$$

For $\theta = 45^\circ$ and $f_{cwd} = 0.80 f_{1cd}$ ($\nu = 0.80$) the highest value is reached with

$$V_{Rd,web,max} = 0.5 b_w z f_{cwd} = 0.4 b_w z f_{1cd} \quad (\text{A-47b})$$

However, this check is rarely required, because it is only relevant in a small range of very high shear stresses, as can be seen from Figs. A-22 and A-23. For example, for reinforced concrete beams web compression failures occur only for values of $\nu_d > 0.472$.

A.2.7.7 Strength of Concrete between Cracks

The concrete between the cracks is uncracked and forms the strut. However, apart from the compressive stresses due to the truss action there are also transverse tensions in the struts due to the friction stresses and due to the forces induced by the bonded stirrups. This action leads to a reduction in strength compared to the uniaxial compressive strength allowed in compression chords, which is $f_{1c} = 0.95 f_c$ (not considering any reduction for a rectangular stress block).

Additional reasons for such a reduction in strength of the inclined struts are the smaller effective width of the strut, (rough crack surfaces), and the disturbances caused by the crossing stirrups. Consequently it was found by Schlaich and Schäfer (1983), Schäfer, Schelling and Kuchler (1990), Eibl and Neuroth (1988) and Kollegger and Mehlhorn (1990) that the following value may be assumed for the concrete strength of the struts:

$$f_{cwu} = 0.80 f_{1c} \quad (\text{A-48})$$

where f_{1c} = uniaxial compressive strength of concrete, (strength of slender prism).

This strength has a relatively high value compared to the lower values proposed elsewhere as so-called “effective strengths” e.g. $\nu f_{1c} = 0.60 f_c$ or $0.50 f_c$ as used in the theory of plasticity. This result illustrates that these lower effective strengths are meant also to cover insufficient transfer of forces across the cracks by friction. The practical outcome of the foregoing higher value for the compressive strength is that, for high ratios of transverse reinforcement, the capacities are far higher for the variable truss angle method in the EC 2 than for the theory of plasticity, Reineck (1991, 1999).

A.2.7.8 Concluding Remarks on Truss-Model with Crack Friction

The “truss-model with crack friction” is a failure mechanism approach, where the expected failure cracks are considered discretely. The possible transfer of forces over the crack due to friction

or interface shear is modeled explicitly. The approach gives directly the shear capacity and the required amount of transverse reinforcement. The contribution of friction across the cracks provides a physical explanation of the “concrete term V_c ” as used in US Codes as the vertical component V_f of the forces transferred across the crack. For practical design it can be assumed that this shear force component V_f is independent of the applied shear force V_u . This assumption yields, for a reinforced concrete beam, the diagram of Fig. A-22, which is similar to proposals that use a concrete contribution V_c , like the approach proposed by Leonhardt (1965, 1977), the approach in the EC 2, part 1 (1991) and the approach in ACI 318. Similar diagrams (Fig. A-23) may be derived for members subjected to shear and axial compressive forces or prestress, the influence of which is covered consistently by using the “truss-model with crack friction”.

The shear force component V_f for members with shear reinforcement is different to the ultimate shear force V_{ct} for members without transverse reinforcement. Due to the fact that the web is reinforced by the stirrups, the value for V_f is higher than that of V_{ct} , and the size effect, as well as the influence of the longitudinal reinforcement ratio, are far less pronounced.

The state of stress is defined at the crack, and from this definition the principal stresses between cracks can be evaluated. The resulting biaxial stress field is represented by the superposition of the two trusses in Fig. A-25. These trusses are statically admissible stress-fields for the web in the B-region of a beam, so that the “truss model with crack friction” fulfils the requirements of a lower-bound method, provided safe strength limits are defined in the constitutive laws for the shear transfer mechanisms at the crack.

These models demonstrate that both approaches, discrete and smeared ones, result in similar design models, and only the failure criteria are different. In discrete shear transfer approaches, friction values are explicitly checked, whereas in smeared approaches limits for the strut angle or the strength of the struts are empirically derived. It is important to note that any controversy over the “standard method” versus the “variable strut angle method” is futile and unproductive. More important is whether the behavior and the test results are realistically and economically covered as is the case for the “truss-model with crack friction”.

The “truss-model with crack friction” also fulfils an indispensable requirement for a modern design code, namely that the resulting shear design procedure is consistent with the design rules for strut-and-tie models, which is important for practicing engineers. The resultant truss models are clearly defined so that transition from the B-region, where the “truss-model with crack friction” applies, to the D-region, where the strut and tie model applies is seamless. This result is also relevant for future ACI 318 and AASHTO-LRFD Codes, because the design format for the “truss-model with crack friction” is very similar to that for the present shear design rules of ACI 318, since both use “concrete terms”.

A. 3.1 Concluding Remarks

The smeared models of both the Modified Compression Field Theory (MCFT) and the Fixed-Angle Softened –Softened Truss Model (FA-STM) have been adjusted so that they provide excellent agreement with test data for a wide range of test variables. However, both models are sufficiently complicated that computer programming of the models is almost a necessity for their practical use. Further, the models cannot be readily used to check the appropriateness of an existing design.

The Truss-Model with Crack Friction provides a failure mechanism approach that is easy to understand and readily useable to check an existing design. Further, the approach provides a rational explanation for why the V_c term of the AASHTO Standard Specification and ACI Code 318 is appropriate.

However, the basic difference is that while the V_c term in the AASHTO Standard Specification and ACI 318 is assumed to be the shear force at diagonal cracking, the V_c term for the “truss-model with crack friction” is a function of the shear that can be transferred by friction across the inclined crack in a B-region. While the two V_c terms may have similar values the basic concepts associated with each are fundamentally different with the V_c term of the “truss-model with crack friction usually being less than the shear force at diagonal cracking. The appropriate angle of the truss associated with the crack for the “truss-model with crack friction” will vary with the type of cracking, “flexure-shear” or “web-shear”, anticipated for the B-region being checked. Thus it is rational to relate the effectiveness of the transverse reinforcement to the type of diagonal cracking predicted. A simplified failure mechanism with V_c related to the “truss-model with crack friction” concept and the contribution of the transverse reinforcement determined using a variable angle truss whose angle is dependent on the type of diagonal cracking is a simplified and rational approach justified by theory, experience, and the economy of the result.

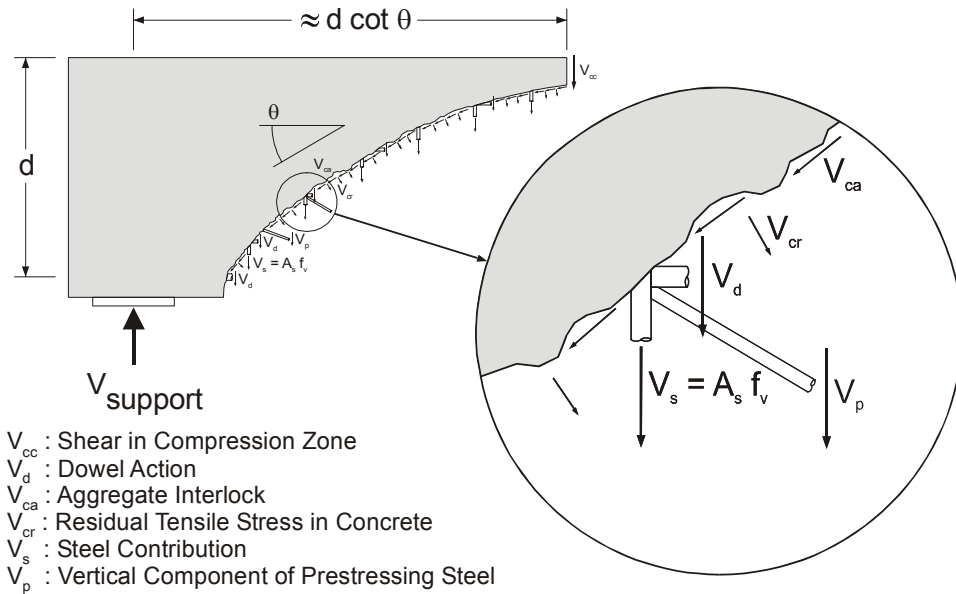


Figure A-1 Shear Transfer/Actions Contributing to Shear Resistance

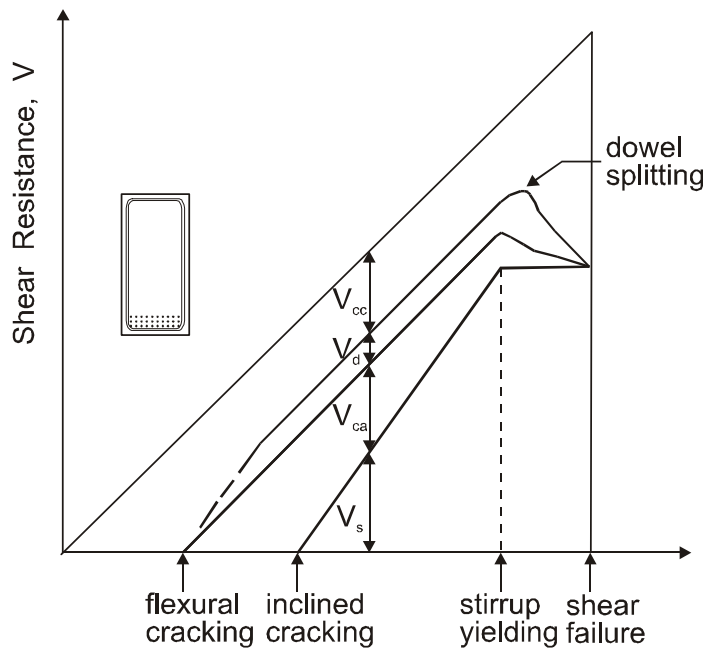


Figure A-2 Distribution of Internal Shear Resistance (ASCE-ACI Committee 426, 1973)

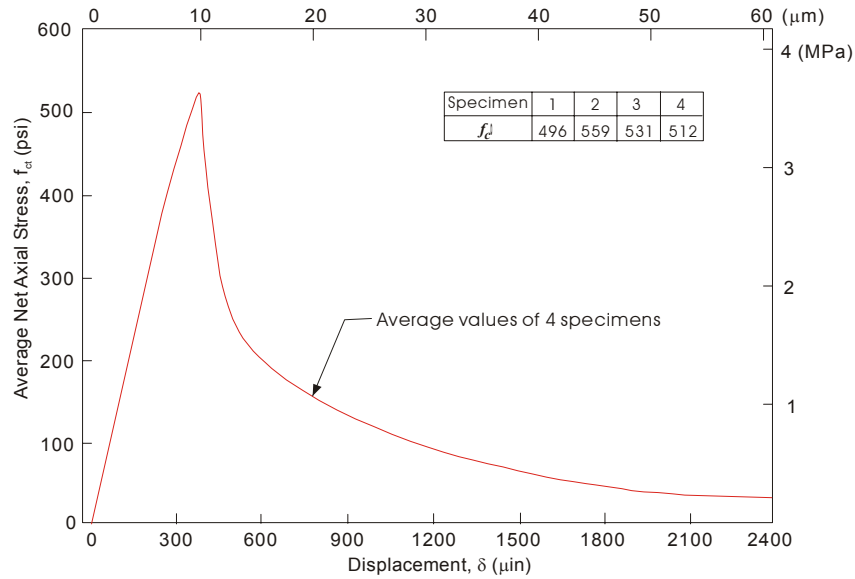


Figure A-3 Response of Concrete in Uniaxial Tension (Gopalaratnam and Shah, 1985)

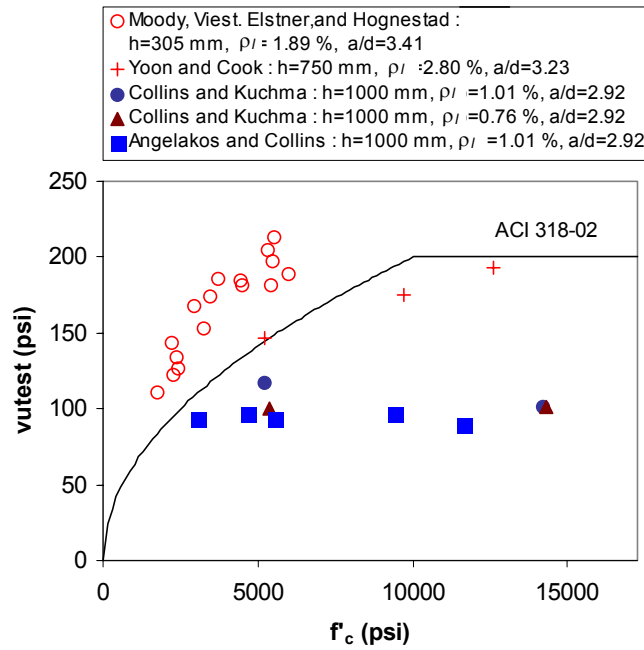


Figure A-4 Influence of Concrete Compressive Strength on Shear Strength (Kuchma and Kim, 2002)

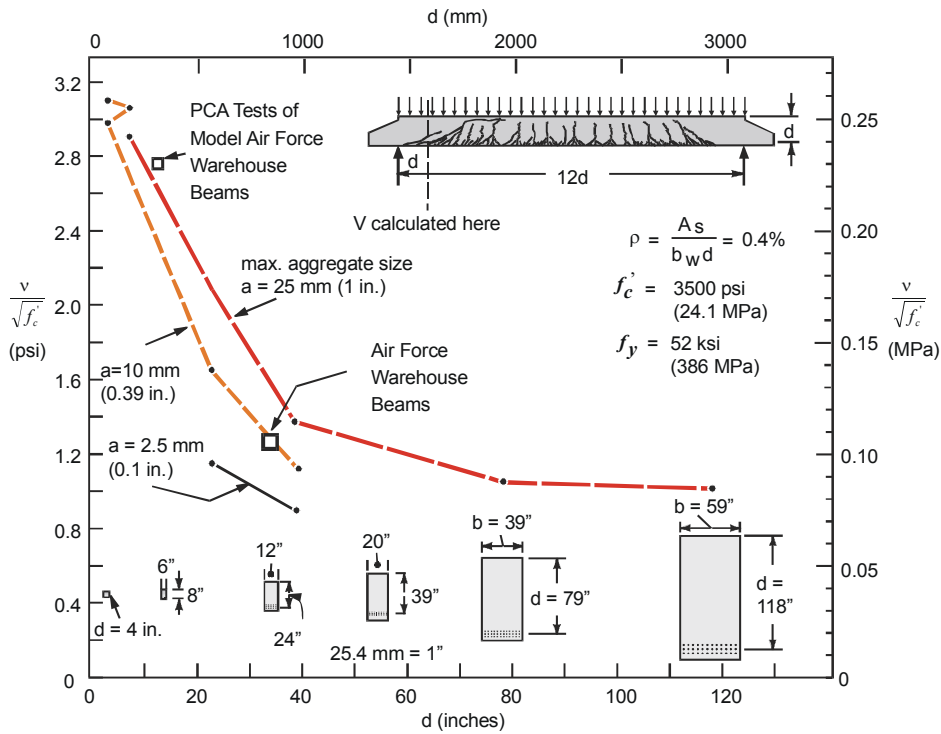


Figure A-5 Size Effect in Shear (Kuchma and Collins, 1998)

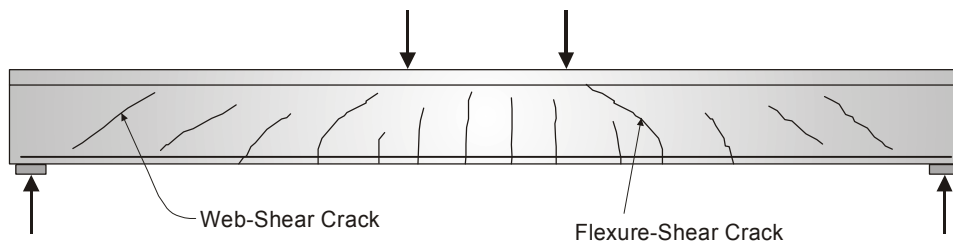


Figure A-6 Types of Inclined Cracks

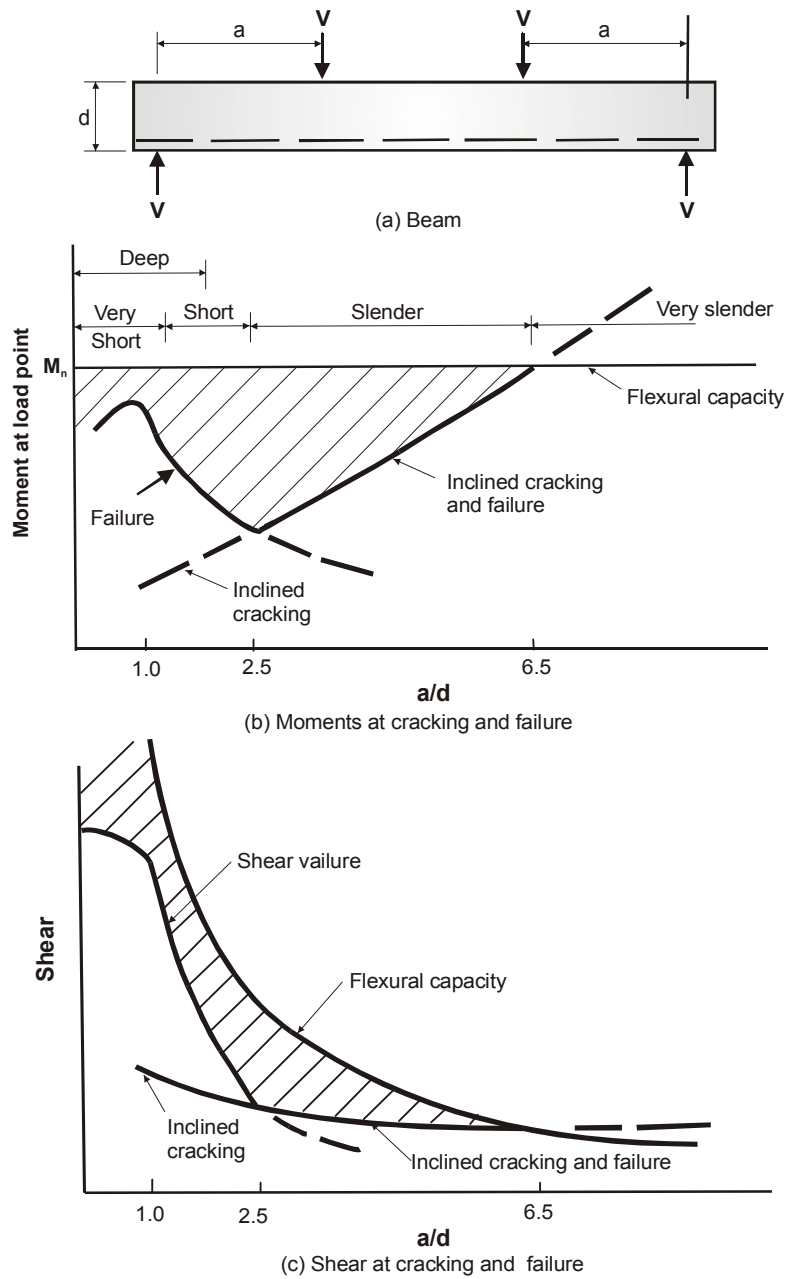


Figure A-7 Effect of a/d on Shear Strength of Beams without Stirrups (McGregor, 1988)

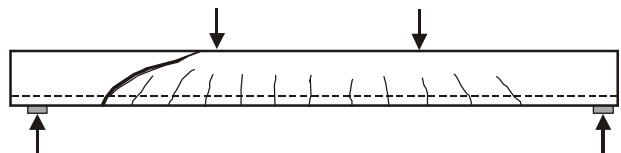


Figure A-8 Diagonal Tension Failure (ASCE-ACI 426, 1973)

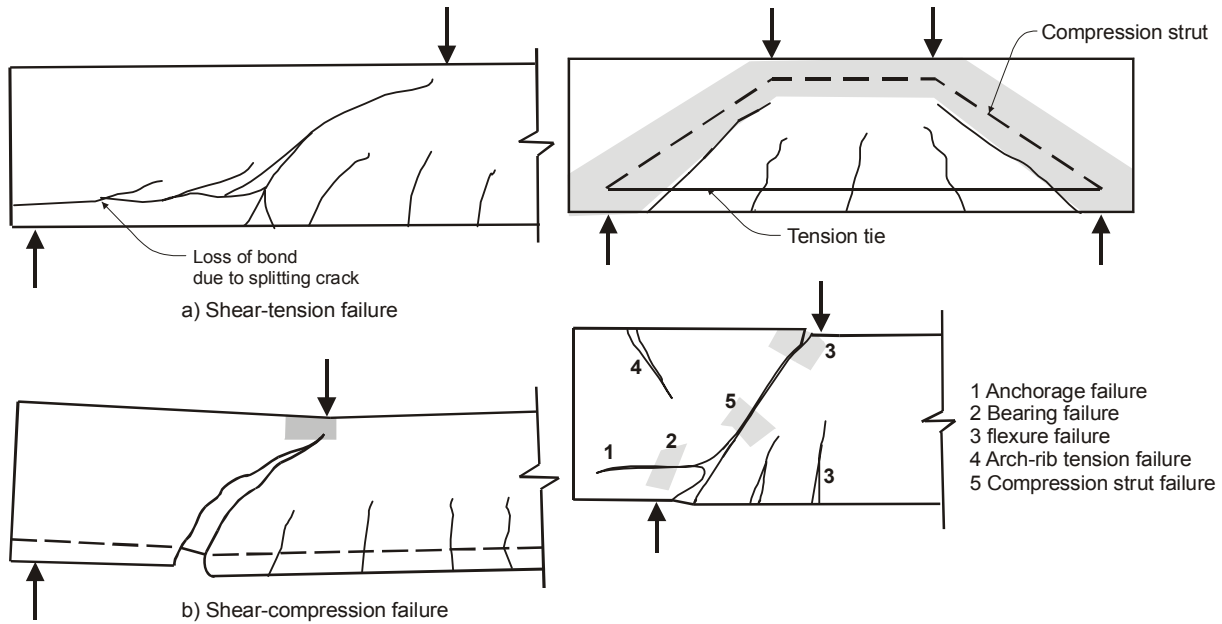


Figure A-9 Modes of Shear Failures in Short Beams (ASCE-ACI 426, 1973)

Figure A-10 Modes of Failures in Deep Beams (ASCE-ACI 426, 1973)

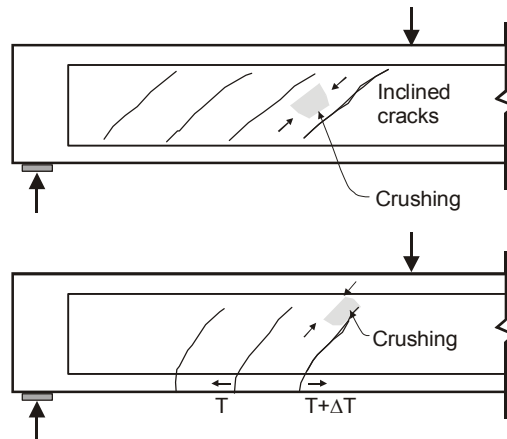


Figure A-11 Modes of Shear Failures of I-Beams (ASCE-ACI 426, 1973)

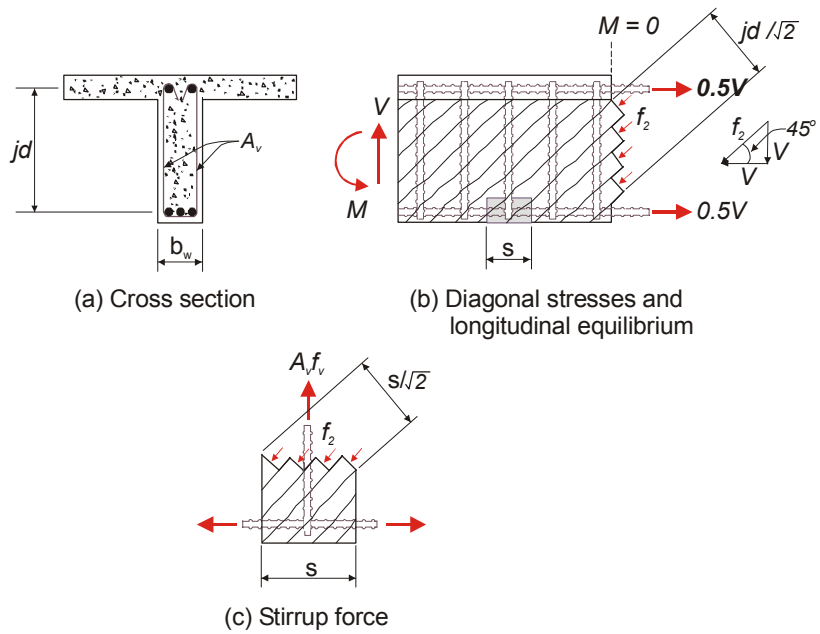


Figure A-12 Equilibrium Conditions for 45° Truss Model (Collins and Mitchell, 1991)

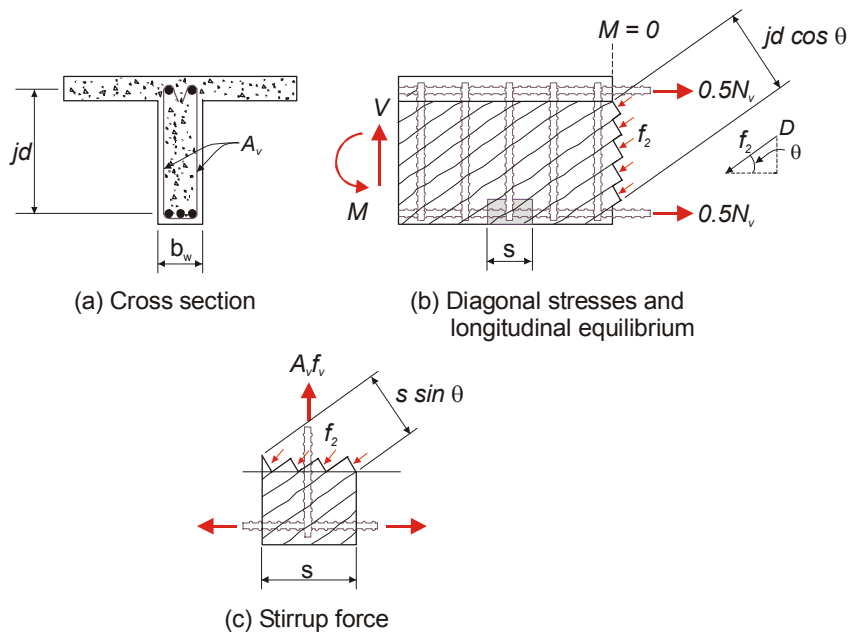


Figure A-13 Equilibrium Conditions for Variable-Angle Truss Model (Collins and Mitchell, 1991)

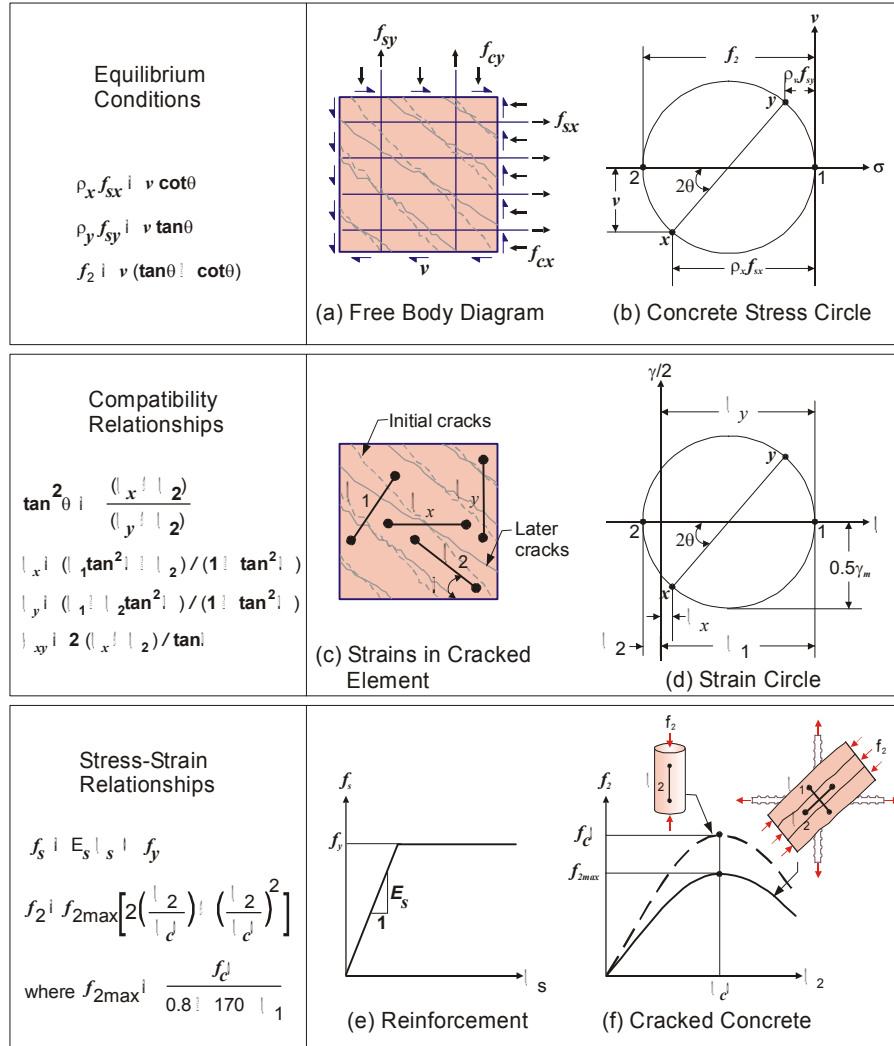


Figure A-14 Basic Relationships for Compression Field Theory (Mitchell and Collins, 1974)



Figure A-15 Shear Panel Test (Vecchio and Collins, 1982)

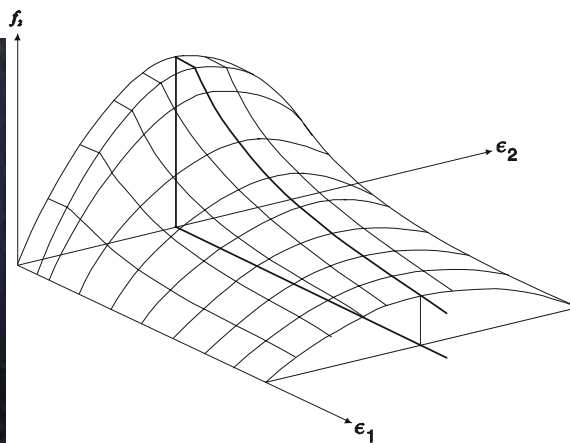


Figure A-16 Compressive Stress-Strain Relationship for Cracked Concrete (Vecchio and Collins, 1986)

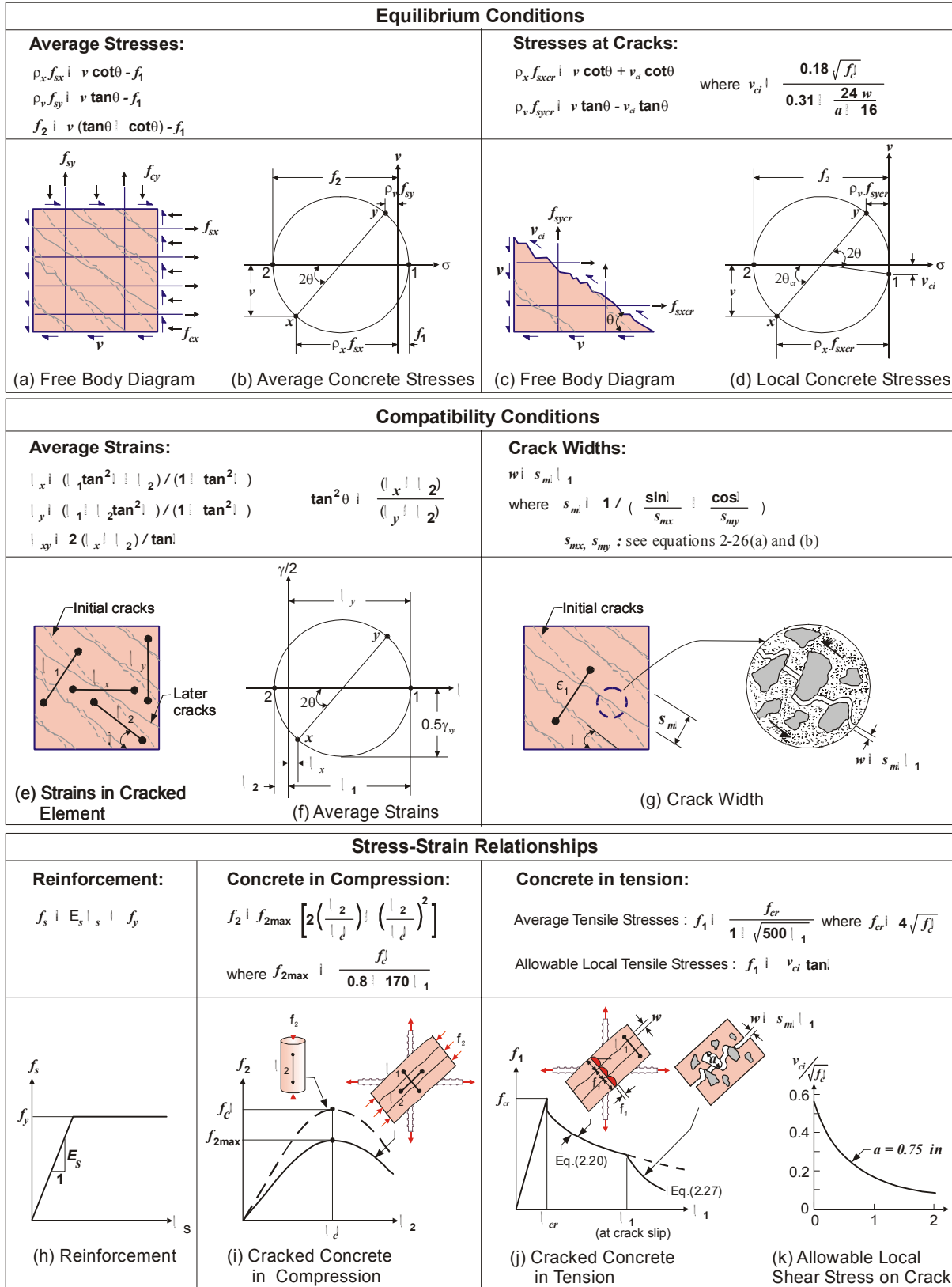


Figure A-17 Description of Modified Compression Field Theory (Vecchio and Collins, 1986)

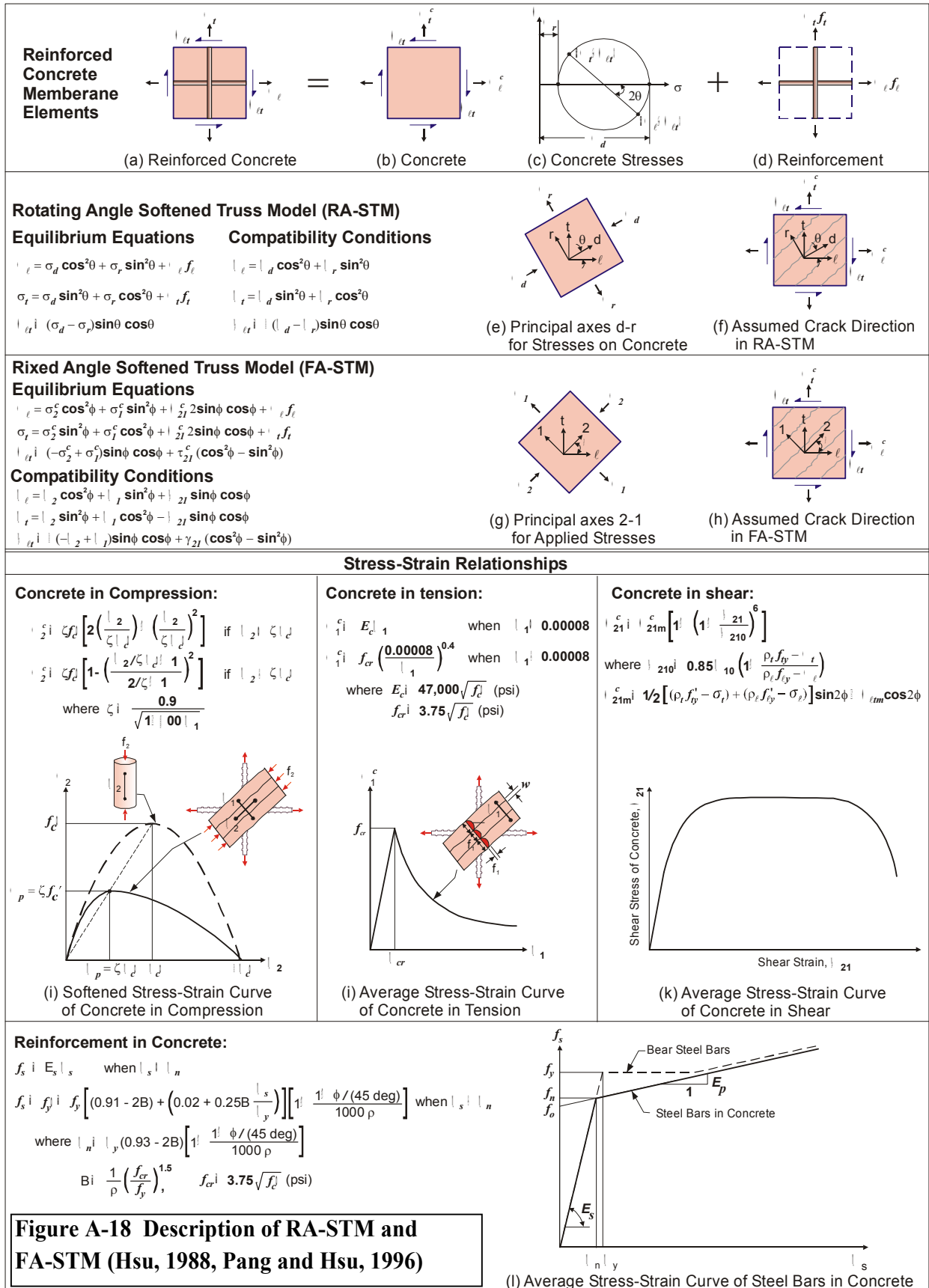


Figure A-18 Description of RA-STM and FA-STM (Hsu, 1988, Pang and Hsu, 1996)

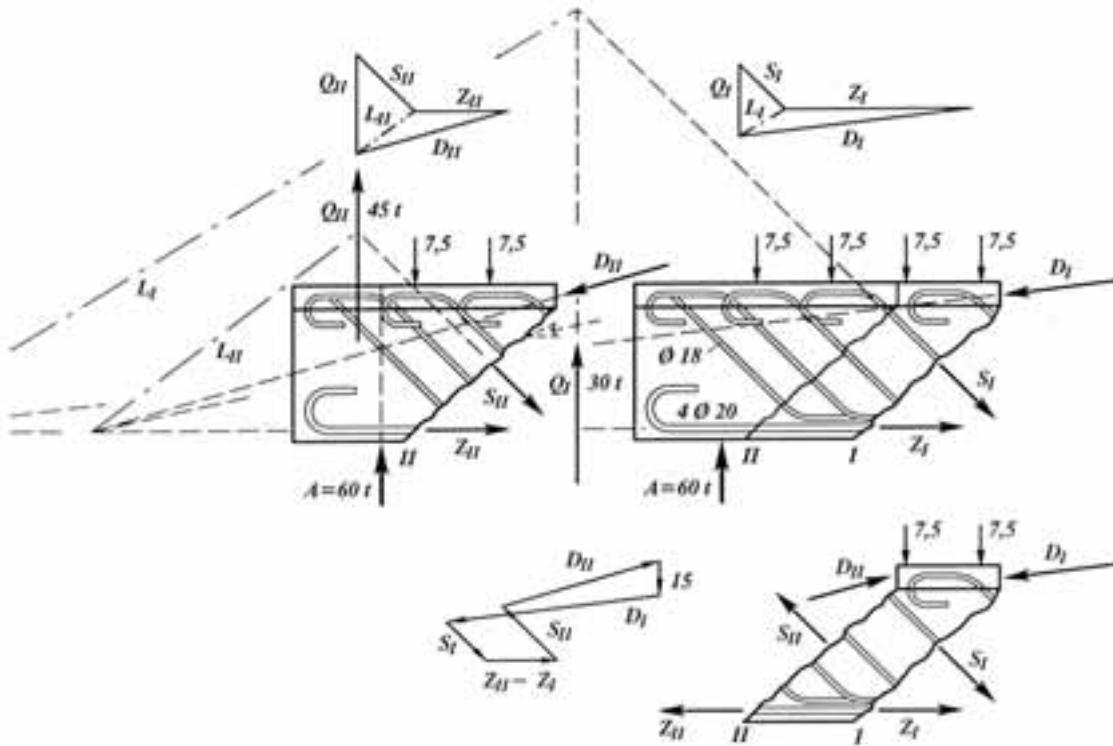
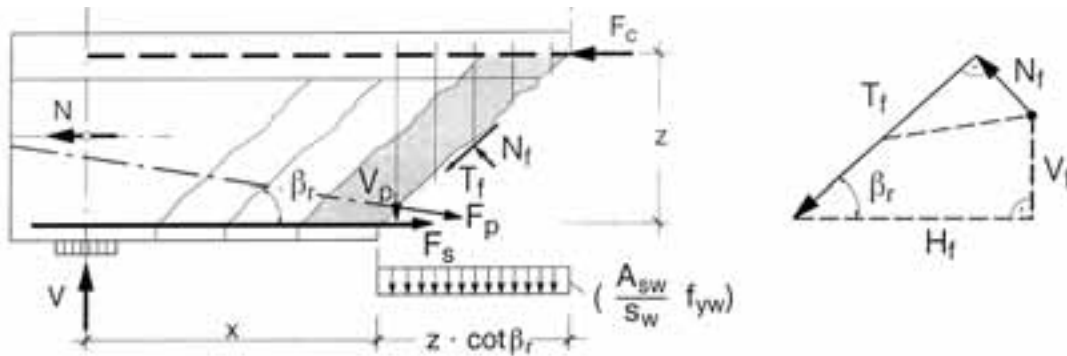


Figure A-19 The Approach by Morsch (1909,1922) for Shear Design



a) free-body with forces acting on it

b) forces due to friction

Figure A-20 Free-Body of an End Support of a Beam with Applied Forces

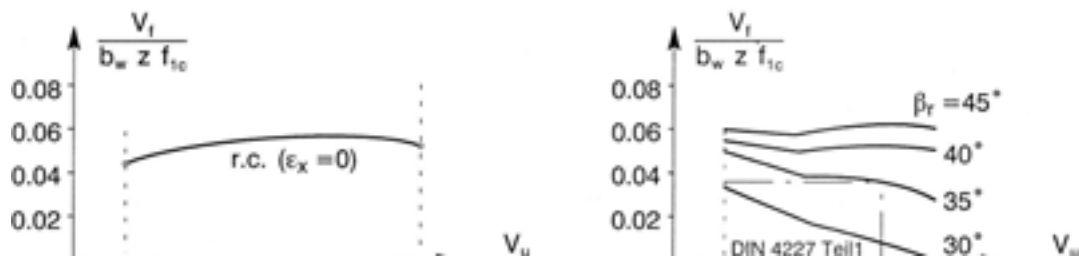


Figure A-21 Results of Parameter Studies for the Shear Force Component V_f (Kirmair, 1985 and 1987)

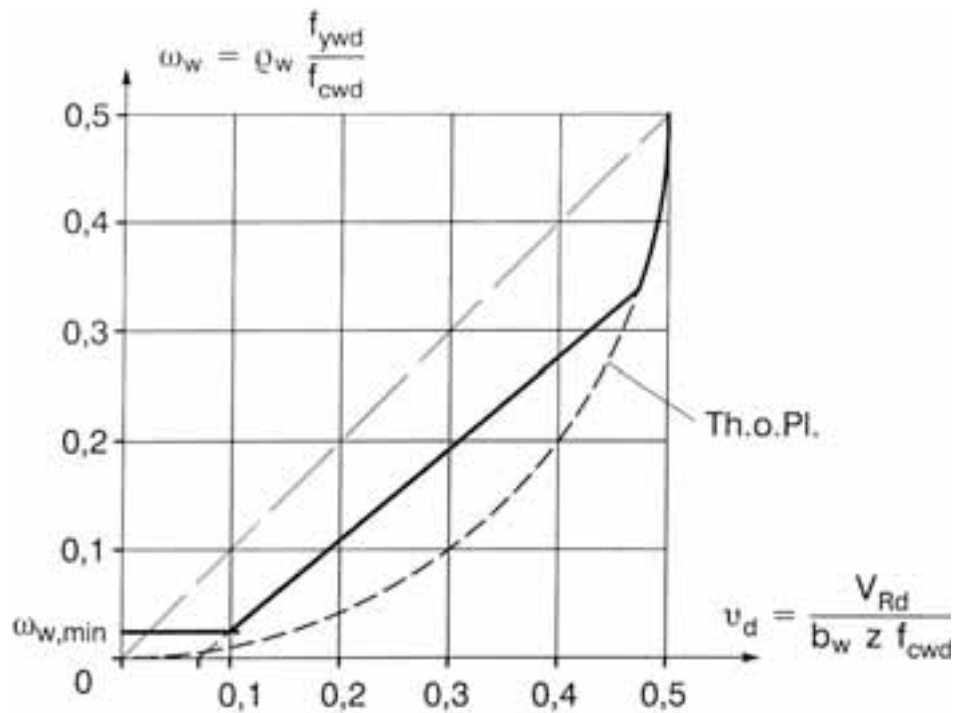


Figure A-22 Dimensioning Diagram for the Design of Vertical Stirrups for RC Members without Axial Forces

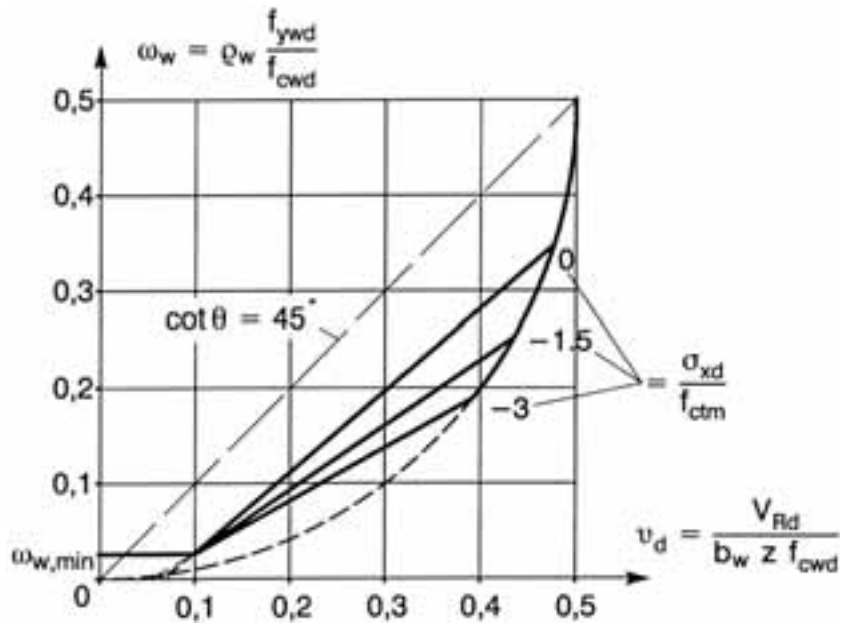


Figure A-23 Dimensioning Diagram for Vertical Stirrups for Prestressed Concrete Members and Members with Axial Compression

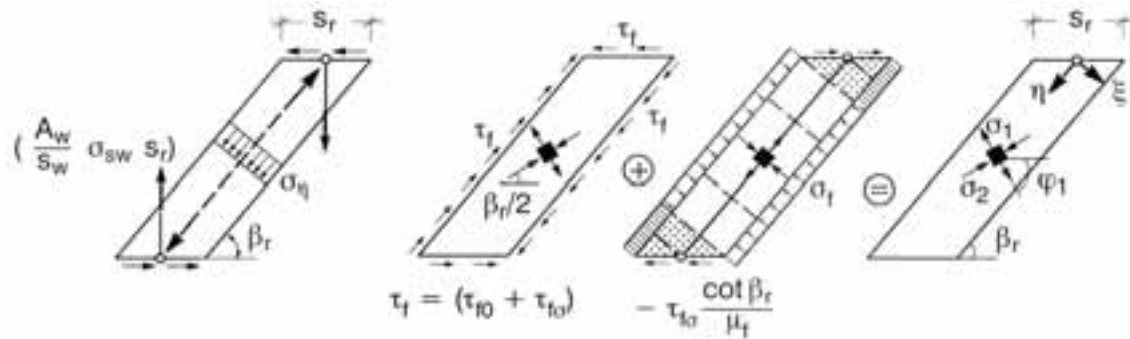
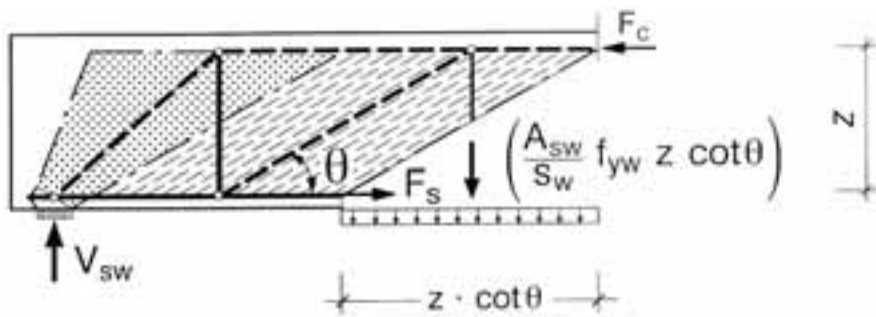
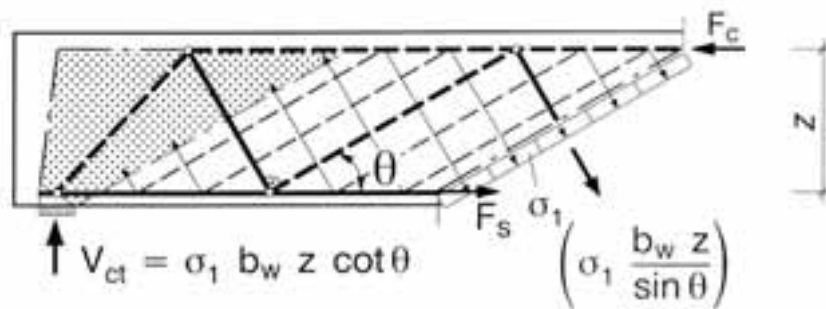


Figure A-24 Forces and Stresses in the Discrete Concrete Struts between the Inclined Cracks



a) truss model with uniaxial compression field in B-region



b) biaxial tension-compression field in concrete for low shear

Figure A-25 Models for B-regions with Shear Force

Appendix B: Shear Design Provisions

This appendix presents the shear design provisions in the most widely used national codes of practice, together with other significant emerging design approaches. The shear design provisions in existing codes of practice are presented in Section B.1. These codes include: *ACI 318-02*; *AASHTO Standard Specification (1989)*; *CSA A23.A-94 (Canadian Standards: Design of Concrete Structures, 1994)*; *AASHTO-LRFD Bridge Design Specifications (2001)*; *CSA A23.3 2004 edition (Collins, 2002)*; *Eurocode EC2, Part 1 (1991) and (2003)*; *German Code (DIN, 2001)*; the *Japanese Code (JSCE Standards, 1986)*; and the *AASHTO Guide Specifications for Design and Construction of Segmental Bridges*. In Section B.2 the shear design approach developed by A. Koray Tureyen and Robert J. Frosch (2002) and the *AASHTO LRFD Bridge Design Specifications (1979)* are also summarized. These design approaches are used in the comparison of different approaches in Appendix D.

B.1 Shear Design Provisions in Codes of Practice

B.1.1 ACI 318-02

B.1.1.1 Non-prestressed members

As discussed in Section A.2.2, when the 45° truss model was introduced into the American literature, it was observed to be conservative. For example, the 45° truss model predicts zero shear strength for beams without shear reinforcement, clearly underestimating the shear capacity for such beams. To account for the concrete contribution to shear resistance, as documented by ACI-ASCE Committee 326 (1962), the concept of a concrete contribution, V_c , was added to the steel contribution, V_s , from the 45° truss as shown in Fig. B-1.

In 1963, ACI 318 set the concrete contribution equal to the shear at inclined cracking because beams without shear reinforcement often failed simultaneously with inclined cracking. The concrete contribution term, V_c , for slender non-prestressed members has remained unchanged through ACI 318-02. Except for those members designed with the strut-and-tie method, the nominal shear strength, V_n , of non-prestressed members is the sum of the concrete contribution, V_c , and shear reinforcement contribution, V_s . Thus,

$$V_n = V_c + V_s \quad (\text{B-1})$$

where the concrete contribution term, V_c , can be calculated by either of the following two equations:

$$V_c = 2\sqrt{f'_c} b_w d \quad (\text{in., psi}) \quad (\text{B-2})$$

$$V_c = \left(1.9\sqrt{f'_c} + 2500\rho_w \frac{V_u d}{M_u} \right) b_w d \leq 3.5\sqrt{f'_c} b_w d \quad (\text{in., psi}) \quad \text{where } \frac{V_u d}{M_u} \leq 1.0 \quad (\text{B-3})$$

Eq. (B-3) is seldom used by practicing engineers because of its added complexity and the fact that for most current beams it provides little increase in shear strength over that provided by Eq. (B-2).

The steel contribution V_s is calculated based on the 45° truss model as:

$$V_s = \frac{A_v f_v d}{s} \quad (\text{B-4})$$

where $V_s \leq 8\sqrt{f'_c} b_w d$ (*in.*, *psi*). This limit is imposed to avoid crushing of the concrete struts of the truss and to guard against excessive crack widths. Eqs.(B-2) and (B-3) expressed in SI units are:

$$V_c = \left(\frac{\sqrt{f'_c}}{6} \right) b_w d \quad (\text{mm}, \text{MPa}) \quad (\text{B-5})$$

$$V_c = \left(\sqrt{f'_c} + 120\rho_w \frac{V_u d}{M_u} \right) \frac{b_w d}{7} \leq 0.3\sqrt{f'_c} b_w d \quad (\text{mm}, \text{MPa}) \quad (\text{B-6})$$

To account for the effects of axial compression and tension, a modification factor or adjustment is applied to the Eq. (B-2) or (B-3). Further, unless a higher level of minimum shear reinforcement is provided, ACI 318 does not permit the use of a concrete compressive strength, f'_c , greater than 10 *ksi* (69 *MPa*) for shear strength calculations. The ACI prediction gives unconservative results for large members and lightly reinforced members without shear reinforcement.

B.1.1.2 Prestressed members

The nominal shear strength, V_n , of prestressed members also consists of a concrete contribution, V_c , and a shear reinforcement contribution, V_s . ACI 318 provides two methods for calculating the concrete contribution to the shear strength of prestressed members; a simplified method and a detailed method. The detailed method is presented in Section B.1.2 since it is same as AASHTO STD 1989. The simplified method, intended for building members, provides the following expression:

$$V_c = \left(0.6\sqrt{f'_c} + 700 \frac{V_u d}{M_u} \right) b_w d \quad (\text{in.}, \text{psi}) \quad (\text{B-7})$$

where $2\sqrt{f'_c} b_w d \leq V_c \leq 5\sqrt{f'_c} b_w d$ (*in.*, *psi*). The V_c in Eq. (B-7) also should not exceed the web-shear cracking strength, V_{cw} , that is discussed in Section B.1.2. Fig. B-2 shows the variation of V_c according to Eq. (B-7) for uniformly loaded prestressed members with f'_c equal to 5000 *psi*. As a member becomes more slender, the shear strength decreases. The shear strength predicted by this method usually gives conservative results.

B.1.2 AASHTO STD 1989

The AASHTO STD method for calculating the shear strength of prestressed concrete members is the same as the detailed method of ACI 318. The components of resistance are the contribution of the concrete, the shear reinforcement and the vertically component of the

prestressing force, V_c , V_s , and V_p , respectively. The V_c term is the shear force causing first diagonal cracking while V_s is calculated by the 45° truss analogy of Eq. (B-4) with a limitation of $V_s \leq 8\sqrt{f'_c}b_wd$ (in., psi).

Shear cracks in prestressed concrete members appear as shown in Fig. B-3. The two possible shear crack types, web-shear cracking and flexure-shear cracking, are treated differently and the V_c term is expressed in terms of those two types. Web-shear cracking occurs in high shear regions when the principal tensile stress reaches the tensile strength of the concrete. Fig. B-4 shows the stresses on a small element located at the centroid of a beam segment. For the Mohr's circle in Fig. B-4(c), the principal tensile stress, f_1 , can be written as:

$$f_1 = \sqrt{v^2 + \left(\frac{f_{pc} - f_v}{2}\right)^2} - \left(\frac{f_{pc} + f_v}{2}\right) \quad (\text{B-8})$$

Assuming that the vertical stresses, f_v , is negligibly small, Eq. (B-8) can be simplified to:

$$f_1 = \sqrt{v^2 + \left(\frac{f_{pc}}{2}\right)^2} - \left(\frac{f_{pc}}{2}\right) \quad (\text{B-9})$$

Because web-shear cracking occurs when the principal tensile stress, f_1 , reaches the tensile strength of the concrete, f_t , the f_1 in Eq. (B-9) can be replaced by f_t . Then, the shear stress for web-shear cracking, v_{cw} , is:

$$v_{cw} = f_t \sqrt{1 + \frac{f_{pc}}{f_t}} \quad (\text{B-10})$$

For thin-webbed members, the web-shear cracking force, V_{cw} , is:

$$V_{cw} = v_{cw}b_wd \quad (\text{B-11})$$

where b_w = web thickness.

If draped strands are used, the vertical component of the prestressing force, V_p , will also resist shear. Thus,

$$V_{cw} = v_{cw}b_wd + V_p \quad (\text{B-12})$$

Therefore, the web-shear cracking force, V_{cw} , can be rewritten as:

$$V_{cw} = f_t \sqrt{1 + \frac{f_{pc}}{f_t}} b_wd + V_p \quad (\text{B-13})$$

The Specifications permit two methods for calculating V_{cw} . The first method is by limiting f_t to $4\sqrt{f'_c}$ (psi), which is a conservative value of the tensile strength, at the centroidal axis or at the junction of the flange and web if the centroidal axis lies in the flange. Test data are consistent with a tensile strength of between 4 and $5\sqrt{f'_c}$ (psi). For the second method the tensile strength of the concrete, f_t , is taken conservatively as $3.5\sqrt{f'_c}$ (psi). Then, Eq. (B-13) becomes:

$$V_{cw} = 3.5\sqrt{f'_c} \sqrt{1 + \frac{f_{pc}}{3.5\sqrt{f'_c}}} b_w d + V_p \quad (\text{in., psi}) \quad (\text{B-14})$$

and for customary values of f'_c and f_{pc} and AASHTO Standard I-Beam dimensions, the web-shear cracking force, V_{cw} , can be approximated as:

$$V_{cw} = (3.5\sqrt{f'_c} + 0.3f_{pc})b_w d + V_p \quad (\text{in., psi}) \quad (\text{B-15})$$

As can be seen in Fig. B-5, both Eqs.(B-14) and (B-15) give very similar web-shear cracking strengths

Flexure-shear cracking occurs in regions of high moment combined with significant shear and at slightly higher shear forces than those for flexural cracking. As shown in Fig. B-6, as the loading on a beam increases flexural cracks form in and near the maximum moment region. When it is assumed that the first shear crack may be initiated by a flexural crack which occurs at a section at least $d/2$ away from the load point, the relationship between the moment, M , and the shear, V , is:

$$M_{cr} = M - V\left(\frac{d}{2}\right) = V\left(\frac{M}{V} - \frac{d}{2}\right) \quad (\text{B-16})$$

where M_{cr} is the cracking moment due to the load, excluding the self-weight of the member. It should be noted that the term V is also due to the live loads only. Eq. (B-16) can be rearranged by solving for V as:

$$V = \frac{M_{cr}}{\frac{M}{V} - \frac{d}{2}} \quad (\text{B-17})$$

Eq. (B-17) gives the shear force corresponding to the flexural crack that may grow into a shear crack at a later loading stage. However, it is not the flexure-shear cracking force. Shear cracking does not develop until slightly higher shear forces than those for flexural cracking. The increment in shear force between flexural cracking and flexure-shear cracking was evaluated empirically. The effect of the shear force due to dead load also needs to be included, especially for composite members and, thus, the shear force at flexure-shear cracking, V_{ci} , becomes:

$$V_{ci} = 0.6\sqrt{f'_c}b_wd + V_d + \frac{M_{cr}}{\frac{M}{V} - \frac{d}{2}} \quad (in., psi) \quad (B-18)$$

The increment in shear, $0.6\sqrt{f'_c}b_wd$, necessary to cause inclined cracking is a conservative approximation to the average value of that increment of $\sqrt{f'_c}b_wd$ (*in., psi*) reported in University of Illinois Bulletin 493. For incorporation into the AASHTO Standard Specification, Eq. (B-18) was simplified by dropping the $d/2$ term so that:

$$V_{ci} = 0.6\sqrt{f'_c}b_wd + V_d + \frac{V_i M_{cr}}{M_{max}} \quad (in., psi) \quad (B-19)$$

where $V_{ci} \geq 1.7\sqrt{f'_c}b_wd$ (*in., psi*) and $d \geq 0.8h$. The definition of all the variables used in Eq. (B-19) is as follows:

f'_c = compressive strength of concrete at 28 days

b_w = width of web of a flanged member

d = distance from extreme compressive fiber to centroid of the prestressing force, or to centroid of negative moment reinforcement for precast girder bridges made continuous

V_d = shear force at section due to unfactored dead load

V_i = factored shear force at section due to externally applied loads occurring simultaneously with M_{max}

$M_{cr} = \frac{I}{y_t}(6\sqrt{f'_c} + f_{pe} - f_d)$ (*in., psi*): moment causing flexural cracking at section due to

externally applied loads. Again, $6\sqrt{f'_c}$ (*psi*) was taken as the modulus of rupture of concrete. That value was intended as a conservative approximation to the actual modulus of rupture of $7.5\sqrt{f'_c}$ (*psi*) measured in control tests on the concrete for the prestressed beams reported in University of Illinois Bulletin 493.

M_{max} = maximum factored moment at section due to externally applied loads

f_{pc} = compressive stress in concrete (after allowance for all prestress losses) at the centroid of the cross-section resisting externally applied loads or at the junction of web and flange when the centroid lies within the flange. (In a composite member, f_{pc} is the resultant compressive stress at the centroid of the composite section, or at the junction of web and flange when the centroid lies within the flange, due to both prestress and moments resisted by the precast member acting alone.)

f_{pe} = compressive stress in concrete due to effective prestress forces only (after allowance for all prestress losses) at extreme fiber of section where tensile stress is caused by externally applied loads

f_d = stress due to unfactored dead load, at extreme fiber of section where tensile stress is caused by externally applied loads

- y_t = distance from centroidal axis of gross section, neglecting reinforcement, to extreme fiber in tension
 I = moment of inertia about the centroid of the cross section

Note that while the vertical component of the prestressing, V_p , adds to the shear strength V_{cw} for web-shear cracking, there is no effect of the same vertical component on the shear strength for flexure-shear cracking, V_{ci} . Thus, draping strands increases the web-shear cracking load but can actually decrease the flexure shear cracking load by decreasing the effective depth, d .

B.1.3 CSA A23.3-94 (Canadian Standards: Design of Concrete Structures, 1994)

The Canadian Standard CSA A23.3-94 provides two methods for predicting the shear strength of reinforced concrete members - the Simplified Method and the General Method. The simplified method is similar to the ACI 318 method except that the effect of member size is considered. The general method is based on the modified compression field theory (MCFT) and thus has the same background as the AASHTO LRFD method. The Canadian code also recommends the use of the strut-and-tie method for the design of deep beams and other portions of members in which the variation in strain is complex (D regions). Strut-and-tie provisions are not presented here.

B.1.3.1 Simplified Method

The simplified method is based on the 45° truss model. The shear resistance is also divided into two components, V_c and V_s . The concrete contribution, V_c , can be taken by:

$$V_c = 0.2\sqrt{f'_c}b_wd \text{ (mm, MPa) when } A_v \geq \frac{0.06\sqrt{f'_c}b_w s}{f_y} \text{ or } d \leq 300 \text{ mm} \quad (\text{B-20})$$

$$\text{or } V_c = \frac{260}{1000 + d}\sqrt{f'_c}b_wd \geq 0.1\sqrt{f'_c}b_wd \text{ (mm, MPa)}$$

$$\text{when } A_v < \frac{0.06\sqrt{f'_c}b_w s}{f_y} \text{ or } d > 300 \text{ mm} \quad (\text{B-21})$$

The steel contribution, V_s , is calculated as:

$$V_s = \frac{A_v f_y d}{s} \text{ where } V_s \leq 0.8\sqrt{f'_c}b_wd \text{ (mm, MPa)} \quad (\text{B-22})$$

B.1.3.2 General Method

The general method is based on the MCFT. The general method provides an integrated procedure for the shear design of structural concrete members by accounting for the influence of

all actions on a section, including prestressing, axial loading, and flexure, in the determination of the required amount of shear reinforcement. This approach represents a significant departure from the ACI and AASHTO Standard Specifications in which additional shear design relationships are required for the design of sections subjected to combined actions. The AASHTO LRFD specifications described in Section B.1.4 and the CSA specifications described in Section B.1.5 also provide this same type of comprehensive design approach.

In the general method, the nominal shear strength of a beam is given as:

$$V_{rg} = V_{cg} + V_{sg} + V_p \leq 0.25f'_c b_w d_v + V_p \quad (\text{B-23})$$

$$\text{where } V_{cg} = \beta \sqrt{f'_c} b_w d_v \text{ (mm, MPa) : concrete contribution} \quad (\text{B-24})$$

$$\text{and } V_{sg} = \frac{A_v f_y d_v (\cot \theta + \cot \alpha) \sin \alpha}{s} \text{ : steel contribution} \quad (\text{B-25})$$

V_p = component in the direction of the applied shear of the effective prestressing force

β = factor accounting for shear resistance of cracked concrete, see Table B-1 and Table B-2

f'_c = specified compressive strength of concrete

b_w = effective web width

d_v = lever arm of resisting flexural moment $\geq 0.9d$

d = effective depth, i.e., distance from extreme compressive fiber to centroid of the longitudinal tension reinforcement

A_v = area of shear reinforcement within spacing, s

f_y = specified yield strength of reinforcement

θ = angle of inclination of diagonal compressive stresses to the longitudinal axis of the member

α = angle of inclined stirrups to longitudinal axis

s = spacing of shear reinforcement

The limit on V_{rg} is imposed to prevent concrete crushing in the web prior to yielding of the shear reinforcement.

To utilize this approach, the designer calculates the state of longitudinal strain (ϵ_x - as influenced by the ultimate axial load, shear force, bending moment, prestressing force, and stiffness of the longitudinal reinforcement), and either a crack spacing or a shear intensity factor. Using these two values, the coefficient, β , is obtained from a table and utilized to find the concrete contribution to shear resistance, V_{cg} , as well as the angle of the diagonal compression field, θ . The contribution of the shear reinforcement, V_{sg} , is directly related to the cotangent of the angle θ .

The factor β and the angle θ are given in Tables B-1 and B-2, respectively Table B-1 is for members with at least the minimum shear reinforcement while Table B-2 is for members with

less than the minimum shear reinforcement. The reason for dividing members into two categories is that members having at least the minimum required amount of transverse reinforcement will have well-distributed diagonal cracks. For such members, the crack spacings are taken as 12 inches (300 mm) and the maximum aggregate size is assumed to be 0.75 inches (19 mm). There is assumed to be no significant size effect for members having at least the minimum required amount of transverse reinforcement. The minimum required area of shear reinforcement is proportional to $\sqrt{f'_c}$ and is as follows:

$$A_{v\min} = 0.72\sqrt{f'_c} \frac{b_w s}{f_y} \quad (\text{in., psi}) \quad (\text{B-26a})$$

$$\text{or } A_{v\min} = 0.06\sqrt{f'_c} \frac{b_w s}{f_y} \quad (\text{mm, MPa}) \quad (\text{B-26b})$$

The longitudinal strain, ε_x , can be calculated as

$$\varepsilon_x = \frac{M_f/d_v + 0.5N_f + 0.5(V_f - V_p)\cot\theta - A_p f_{po}}{(E_s A_s + E_p A_p)} \quad (\text{B-27})$$

where,

M_f = factored moment at section

N_f = factored axial load normal to cross-section, occurring simultaneously with V_f , with tension positive and compression negative

V_f = factored shear force at section

A_p = area of prestressing strands

f_{po} = a parameter taken as modulus of elasticity of prestressing tendons multiplied by the locked in difference in strain between the prestressing tendons and the surrounding concrete

E_s = modulus of elasticity of reinforcement

A_s = area of reinforcement in tension zone

E_p = modulus of elasticity of prestressing strand

The critical section may be taken at a distance of $0.5d_v \cot\theta$ from a concentrated load or support. By contrast, in the simplified method, the critical section is taken at a distance d_v from the support.

In designing by the General Method, the engineer needs to calculate ε_x and either v_f/f'_c or s_z . From Tables B-1 and B-2, the values for β and θ can be found after the use of Eq. (B-27). The concrete contribution can then be found using Eq. (B-24) and the required amount of shear reinforcement can be determined using Eq. (B-25). Note that the θ values in the code were chosen so that the cost of both the transverse and longitudinal reinforcement required for shear is minimized. Values also ensure that the strain in the transverse reinforcement is at least equal to an assumed yield strain of 0.002.

The crack spacing parameter, s_z , needs to be determined to calculate the shear strength for members without shear reinforcement. The crack spacing parameter, s_z , is the lesser of d_v and the maximum distance between layers of crack control reinforcement but does not need to exceed 2000 mm. The size effect relationship for members without shear reinforcement is based on this crack spacing parameter, s_z . The reason is that crack spacing may be related to the distance between cracks and that crack widths – which influence the aggregate interlock mechanism – are roughly proportional to crack spacing for any given level of longitudinal strain.

B.1.4 AASHTO LRFD Bridge Design Specifications (2001)

The shear provisions in the AASHTO (American Association of State Highway and Transportation Officials) LRFD Bridge Design Specification (1994) are also based on the MCFT and thus are very similar to the General Method in CSA A23.3-94. The concrete contribution, V_c , to shear resistance is:

$$V_c = 0.0316\beta\sqrt{f'_c}b_vd_v \text{ (in., ksi)} \quad (\text{B-28})$$

where b_v is the effective web width. The steel contribution, V_s , is calculated as:

$$V_s = \frac{A_v f_y d_v (\cot \theta + \cot \alpha) \sin \alpha}{s} \quad (\text{B-29})$$

The values of β and θ are given in Tables B-3 and B-4, respectively

For non-prestressed concrete sections not subjected to axial tension and containing at least the minimum amount of transverse reinforcement or having an overall depth of less than 16.0 inches, a simplified procedure is also allowed which is identical to the ACI 318 traditional method for reinforced concrete members. That is, $\beta=2.0$, and $\theta = 45^\circ$.

The required minimum amount of transverse reinforcement is proportional to $\sqrt{f'_c}$ as follows:

$$A_v \geq 0.0316\sqrt{f'_c} \frac{b_v s}{f_y} \text{ (in., ksi)} \quad (\text{B-30a})$$

$$A_v \geq 0.0830\sqrt{f'_c} \frac{b_v s}{f_y} \text{ (mm, MPa)} \quad (\text{B-30b})$$

The minimum amount of transverse reinforcement required by Eq. (B-30) is about 38 % more than the amount required by the CSA A23.3-94 and ACI 318-02.

B.1.5 CSA A23.3 2004 edition (M.P. Collins, 2002)

The MCFT is the basis for the general shear provisions of the CSA and the AASHTO LRFD. In order to overcome concerns by practicing engineers over difficulties in using the

LRFD specifications, the CSA specifications presented below were developed to provide a simpler way to obtain θ and β . In this proposed method, the iteration procedure was removed for design purposes by taking $\theta = 30$ degrees for evaluating the demand of shear on the longitudinal reinforcement. In this approach, the nominal strength is defined by Eq. (B-31).

$$V_r = V_c + V_s + \phi_p V_p \leq 0.25 f'_c b_w d_v + \phi_p V_p \quad (\text{B-31})$$

where $V_c = \beta \sqrt{f'_c} b_w d_v$ (*in., psi*) : concrete contribution (B-32)

and $V_s = \frac{A_v f_y d_v (\cot \theta + \cot \alpha) \sin \alpha}{s}$: steel contribution (B-33)

As shown in the Fig. B-7, the longitudinal strain, ε_x , is computed at mid-depth of the cross-section by:

$$\varepsilon_x = \frac{M_f / d_v + 0.5 N_f + V_f - \phi_p V_p - A_p f_{po}}{2(E_s A_s + E_p A_p)} \quad (\text{B-34a})$$

When ε_x is negative, it is taken as either zero or recalculated by changing the denominator of Eq. (B-34a) such that the equation becomes:

$$\varepsilon_x = \frac{M_f / d_v + 0.5 N_f + V_f - \phi_p V_p - A_p f_{po}}{2(E_s A_s + E_p A_p + E_c A_{ct})} \quad (\text{B-34b})$$

However ε_x shall not be taken as less than 0.2×10^{-3} . For members having less than minimum shear reinforcement, as required by Eq. (B-37), the equivalent crack spacing parameter, s_{ze} , is calculated as:

$$s_{ze} = \frac{1.38 s_z}{0.63 + a_g} \quad (\text{in. units}) \quad (\text{B-35})$$

where a_g = maximum aggregate size (*in.*). Then, the factor accounting for the shear resistance of cracked concrete, β , can be computed from:

$$\beta = \frac{4.8}{(1 + 1500 \varepsilon_x)} \frac{51}{(39 + s_{ze})} \quad (\text{in. unit}) \quad (\text{B-36})$$

The minimum area of shear reinforcement is:

$$A_{v_{\min}} = 0.72 \sqrt{f'_c} \frac{b_w s}{f_y} \quad (\text{in., psi}) \quad (\text{B-37})$$

It should be noted that the minimum shear reinforcement is required only if the factored shear force exceeds V_c , rather than $V_c / 2$ as required by ACI 318. Further, that minimum amount of shear reinforcement is greater than the minimum amount required by ACI 318. For members having at least minimum transverse reinforcement, with the longitudinal strain, ε_x , computed from Eq. (B-34), the angle of the diagonal compression field, θ , is calculated as:

$$\theta = 29 + 7000\varepsilon_x \quad (\text{B-38})$$

and the coefficient, β , is obtained from Eq. (B-36) with the equivalent crack spacing parameter, s_{ze} , set to 12 inches.

The iteration procedure is completely removed in this method and there are trade-offs made between simplicity, generality, and accuracy. Collins (2002), in his proposal, reported that this approach had been checked against a database of 413 large reinforced and prestressed concrete beams. The average shear capacity ratio $V_{test}/V_{prediction}$ was 1.16 with a coefficient of variation of 16.9 % and a 1%-fractile value of $V_{test}/V_{prediction}$ of 0.77.

B.1.6 Eurocode EC2 Part 1 (1991)

The first version of the Eurocode EC2, Part 1 (1991) is based partly on Plasticity Theory as developed by Thürlimann (1975, 1983) and by Nielsen (1984). It provides two methods, the standard method and the variable strut inclination method. The standard method is basically a combination of a concrete contribution term and a steel contribution term based on the 45° truss model. The method is applicable for concrete strengths ranging from $12 \leq f'_c \leq 50 \text{ MPa}$.

B.1.6.1 Standard Method

The total shear resistance consists of the concrete contribution, V_{cd} , and the steel contribution, V_{wd} . Thus, the total shear resistance V_{Rd3} is:

$$V_{Rd3} = V_{cd} + V_{wd} \leq V_{Rd2,max} \quad (\text{B-39})$$

where

V_{cd} = concrete contribution taken as equal to V_{Rd1}

$V_{wd} = \frac{A_{sw}f_{ywd}(0.9d)}{s}$ = the steel contribution

A_{sw} = area of shear reinforcement within spacing, s

f_{ywd} = yield strength of shear reinforcement

$V_{Rd2,max}$ = upper limit on shear resistance to prevent web crushing

V_{Rd1} is the shear capacity of members without shear reinforcement based on an empirical formula:

$$V_{Rd1} = \beta\tau_{rd}k(1.2 + 40\rho_\ell)b_w d \quad (\text{mm, MPa}) \quad (\text{B-40})$$

where,

$\beta = \frac{2.5d}{x}$, ($1.0 \leq \beta \leq 5.0$) is an enhancement factor that can be applied if the member is loaded by a concentrated load situated at a distance, $x \leq 2.5d$, from the face of the support. Otherwise, $\beta = 1.0$.

τ_{rd} = basic design shear strength ($= 0.25f_{ctk0.05}$)

$f_{ctk0.05}$ = lower 5% fractile characteristic tensile strength ($= 0.7f_{ctm}$)

f_{ctm} = mean value of the concrete tensile strength ($= 0.30(f_{ck})^{2/3}$)

f_{ck} = characteristic cylinder compressive strength of concrete ($\cong 0.9 f_c'$)

$k = (1.6 - d / 1000) \geq 1.0$ (mm unit)

$$\rho_\ell = \frac{A_{s\ell}}{b_w d} \leq 0.02$$

$A_{s\ell}$ = area of longitudinal reinforcement in tension

b_w = effective web width

d = effective depth

Thus, Eq. (B-40) can be simplified as follows:

$$V_{Rd1} = 0.0525k\beta(f_{ck})^{2/3}(1.2 + 40\rho_\ell)b_w d \quad (\text{mm, MPa}) \quad (\text{B-41})$$

The shear strength provided by V_{Rd1} increases as the amount of longitudinal reinforcement increases, and decreases as the depth of the member increases. It should be noted that the values for τ_{Rrd} and thus of V_{Rd1} were regarded as unsafe for the application of the EC2, Part 1 in Germany. In Germany, in the application document for EC 2 the value for τ_{Rd} was reduced to:

$$\tau_{Rd} = 0.090f_{ck}^{1/3} \quad (\text{B-42})$$

The upper limit on the total shear resistance is determined by the resistance V_{Rd2} which is the web crushing shear force based on Plasticity Theory. The maximum value of V_{Rd2} is expressed in terms of the effective stress in the compression strut:

$$V_{Rd2,\max} = 0.5\nu f_{cd} b_w (0.9d) \quad (\text{B-43})$$

where, f_{cd} = the factored design strength, taken as $f_{cd} = f_{ck} / 1.5$ and

$$\nu = 0.7 - \frac{f_{ck}}{200} \geq 0.5 \quad \text{is the effectiveness factor} \quad (\text{B-44})$$

The minimum amount of shear reinforcement depends on the concrete compressive strength and the steel yield strength. Table B-5 shows the requirement for minimum shear reinforcement.

B.1.6.2 Variable strut inclination method

The variable strut inclination method is based on a variable-angle truss. This method assumes that transverse reinforcement carries all the shear. The concrete contribution to shear

resistance is considered using flatter truss angles. The shear resistance of members with shear reinforcement is:

$$V_{Rd3} = \frac{A_{sw}f_{ywd}(0.9d)}{s} \cot \theta \quad (\text{B-45})$$

where

$0.4 < \cot \theta < 2.5$: for beams with constant longitudinal reinforcement, or

$0.5 < \cot \theta < 2.0$: for beams with curtailed longitudinal reinforcement

Eq. (B-45) is based on a truss model with yielding of the shear reinforcement. The maximum shear resistance provided by a section, based on the crushing of struts, can be obtained from equilibrium at a section as:

$$V_{Rd2} = \frac{vf_{cd}b_w(0.9d)}{\cot \theta + \tan \theta} \quad (\text{B-46})$$

From Eq. (B-45), the smaller the angle, the higher is the shear capacity provided by the shear reinforcement. However, the shear capacity given by Eq. (B-46) decreases as θ decreases below 45° . From the lower-bound theory of plasticity, therefore, a limitation on the effectiveness of the shear reinforcement is given as:

$$\frac{A_{sw}f_{ywd}}{b_ws} \leq 0.5vf_{cd} \quad (\text{B-47})$$

In design, the actual failure condition can be obtained by equating the applied shear force to the resistance V_{Rd2} and finding the largest value of $\cot \theta$ which requires the least amount of shear reinforcement. Once $\cot \theta$ is found, the shear resistance, V_{Rd3} , can be calculated from the Eq. (B-45). For analysis purpose, the angle θ can be found by equating V_{Rd3} to V_{Rd2} as follows:

$$\tan \theta \geq \frac{1}{\sqrt{\left(\frac{vf_{cd}}{\rho_{sw}f_{ywd}} - 1\right)}} \quad (\text{B-48a})$$

$$\text{or } \cot \theta \leq \sqrt{\left(\frac{vf_{cd}}{\rho_{sw}f_{ywd}} - 1\right)} \quad (\text{B-48b})$$

where θ should be calculated using Eq. (B-48) and those conditions applied to Eq. (B-45).

B.1.7 Eurocode EN 1992-1-1 (2003)

B.1.7.1 General Remarks

The Eurocode EC2, part 1 (1991) has been revised and the final revised draft was published in April 2003 for comments by the different European nations. The Eurocode EC2 is applicable up to concrete strengths of $f_{ck} = 90 \text{ MPa}$, which corresponds to about $f'_c = 91.6 \text{ MPa}$. The characteristic value f_{ck} for the cylinder strength is defined as a 5%-fractile. By contrast f'_c is a 9%-fractile, and the relation between the two quantities is $f_{ck} = f'_c - 1.6 \text{ (MPa)}$.

The format of the new EC 2 is such that, for many applications, only recommended rules or values are given and the values used in different countries are subject to a national Annex. In the following the recommended values are given.

The design value for the uniaxial concrete compressive strength, based on f_{ck} , is:

$$f_{cd} = \alpha_{cc} f_{ck} / \gamma_c \quad (\text{B-49})$$

where γ_c is the partial safety factor for concrete (normally $\gamma_c = 1.50$)

α_{cc} is the coefficient taking account of long term effects on the compressive strength and of unfavorable effects resulting from the way the load is applied.

The value of α_{cc} for use in each country should lie between 0.8 and 1.0 and may be found in its National Annex. The recommended value is 1.

The value of the design tensile strength, f_{ctd} , is defined as:

$$f_{ctd} = \alpha_{ct} f_{ctk,0.05} / \gamma_c \quad (\text{B-50})$$

where γ_c is the partial safety factor for concrete (normally $\gamma_c = 1.50$)

α_{ct} is a coefficient taking account of long term effects on the tensile strength and of unfavorable effects, resulting from applied loading patterns.

The value of α_{ct} for use in each country may be found in its National Annex. The recommended value is 1.0.

B.1.7.2 Members Not Requiring Shear Reinforcement

The design value for the shear resistance $V_{Rd,c}$ is given by:

$$V_{Rd,c} = \left[0.12k(100\rho_l f_{ck})^{1/3} - 0.15\sigma_{cp} \right] b_w d \quad (\text{mm, MPa}) \quad (\text{B-51})$$

Where, f_{ck} is in MPa

$$k = 1 + \sqrt{\frac{200}{d}} \leq 2.0 \quad (\text{mm unit})$$

$$\rho_l = \frac{A_{sl}}{b_w d} \leq 0.02$$

- A_{sl} = the area of the tensile reinforcement, which extends $l_{bd} + d$ beyond the section considered, where l_{bd} is a bond development length (see Fig. B-8).
- b_w = the smallest width of the cross-section in the tensile area (mm)
- σ_{cp} = $N_{Ed} / A_c > -0.2f_{cd}$ (MPa)
- N_{Ed} = the axial force in the cross-section due to loading or prestressing ($Newtons$) ($N_{Ed} < 0$ for compression). The influence of imposed deformations on N_{Ed} may be ignored.
- A_c = the area of concrete cross section (mm^2)
- $V_{Rd,c}$ is in Newtons

The following minimum value is given:

$$V_{Rd,c} = (v_{\min} - 0.15\sigma_{cp})b_w d \text{ where } v_{\min} = 0.035k^{3/2}f_{ck}^{1/2} \quad (B-52a)$$

$$\text{which leads to: } V_{Rd,c} = (0.035k^{3/2}f_{ck}^{1/2} - 0.15\sigma_{cp})b_w d \quad (B-52b)$$

$$= \left[0.035(1 + \sqrt{200/d})^{3/2}f_{ck}^{1/2} - 0.15\sigma_{cp} \right] b_w d \quad (B-52c)$$

B.1.7.3 Members Requiring Shear Reinforcement

In the section on shear design only one design method is presented and this is the truss model with variable angles for the inclined struts.

The design of members with shear reinforcement is based on a truss model, whereby the values for the angle θ of the inclined struts in the web are limited as follows:

$$1 \leq \cot \theta \leq 2.5 \quad (B-53)$$

For members with vertical shear reinforcement, the shear resistance, V_{Rd} , is the smaller of:

$$V_{Rd,s} = \frac{A_{sw}}{s} z f_{ywd} \cot \theta \quad (B-54)$$

Note: If Eq. (B-56) is used the value of f_{ywd} should be reduced to $0.8f_{ywk}$ in Eq. (B-54).

$$\text{and } V_{Rd,max} = [(\alpha_{cw} \nu_1 f_{cd} / (\cot \theta + \tan \theta))] b_w z \quad (B-55)$$

where: A_{sw} = the cross-sectional area of the shear reinforcement

s = the spacing of the stirrups

f_{ywd} = the design yield strength of the shear reinforcement

f_{ywk} = the characteristic yield strength of the shear reinforcement

ν_1 = follows from Eq. (B-56)

α_{cw} = a coefficient taking account of the interaction of the stress in the compression chord and any applied axial compressive stress

- θ = the angle between inclined concrete struts and the main tension chord
 b_w = the minimum width between tension and compression chords
 z = the inner lever arm, for a member with constant depth, corresponding to the maximum bending moment in the element under consideration. In the shear analysis of reinforced concrete without axial force, the approximate value $z \approx 0.9d$ may be used.

The value of ν_1 and α_{cw} for use in each country may be found in its National Annex. The recommended value of ν_1 is as follows:

$$\nu_1 = 0.6(1 - f_{ck} / 250) \quad \text{where } f_{ck} \text{ is in MPa} \quad (\text{B-56a})$$

For reinforced and prestressed members, if the design stress of the shear reinforcement is below 80% of the characteristic yield stress, f_{yw} , ν_1 may be taken as:

$$\nu_1 = 0.6 \quad \text{for } f_{ck} \leq 60 \text{ MPa} \quad (\text{B-56b})$$

$$\nu_1 = 0.9 - f_{ck} / 200 > 0.5 \quad \text{for } f_{ck} > 60 \text{ MPa} \quad (\text{B-56c})$$

The recommended value of α_{cw} is as follows:

$$1 \quad \text{for non-prestressed structures} \quad (\text{B-57a})$$

$$(1 + \alpha_{cp} / f_{cd}) \quad \text{for } 0 < \alpha_{cp} \leq 0.25 f_{cd} \quad (\text{B-57b})$$

$$1.25 \quad \text{for } 0.25 < \alpha_{cp} \leq 0.5 f_{cd} \quad (\text{B-57c})$$

$$2.5(1 + \alpha_{cp} / f_{cd}) \quad \text{for } 0.5 < \alpha_{cp} \leq 1.0 f_{cd} \quad (\text{B-57d})$$

where α_{cp} is the mean compressive stress, measured positive (only in Eq. B-57), in the concrete due to the design axial force. This stress should be obtained by averaging it over the concrete section and taking account of the reinforcement. The value of α_{cp} need not be calculated at a distance less than $0.5d \cot \theta$ from the edge of the support.

Where the web contains grouted ducts with a diameter $\phi > b_w / 8$ the shear resistance $V_{Rd,max}$ should be calculated on the basis of a nominal web thickness given by:

$$b_{w,nom} = b_w - 0.5 \sum \phi \quad (\text{B-58a})$$

where ϕ is the outer diameter of the duct and $\sum \phi$ is determined for the most unfavorable level.

For non-grouted ducts, grouted plastic ducts and unbonded tendons the nominal web thickness is:

$$b_{w,nom} = b_w - 1.2 \sum \phi \quad (\text{B-58b})$$

The value 1.2 in Eq. (B-58b) is introduced to take account of splitting of the concrete struts due to transverse tension. If adequate transverse reinforcement is provided this value may be reduced to 1.0.

B.1.8 German Code DIN 1045-1 (2001)

B.1.8.1 General Remarks

In 2001 the new German code DIN 1045-1 was published and thereby replaced the previous codes DIN 1045 (1988) for reinforced concrete structures and DIN 4227 (1988) for prestressed concrete structures. The work on this code was parallel to that on the new EC 2 Code and many rules are similar. In the case of differences the new EC 2 allows different national application rules under the same principles so that the new German code may also be applied when the Eurocode becomes effective in about 5 years.

The DIN is applicable up to concrete strengths of $f_{ck} = 100 \text{ MPa}$, which corresponds to about $f'_c = 101.6 \text{ MPa}$. As in the Eurocode, the characteristic value f_{ck} for the cylinder strength is defined as the 5%-fractile, whereas f'_c is the 9%-fractile, so that $f_{ck} = f'_c - 1.6$ (MPa).

The design value for the uniaxial concrete compressive strength based on f_{ck} is:

$$f_{cd} = \alpha_{cc} f_{ck} / \gamma_c \quad (\text{B-59})$$

where: γ_c is the partial safety factor for concrete (normally $\gamma_c = 1.50$), and

$\alpha_{cc} = 0.85$. This coefficient takes account of long term effects on the compressive strength and the difference between cylinder strength and uniaxial compressive strength (prism strength). Higher values $\alpha < 1$ may be used, if justified, for short time loading.

No value is defined for the design tensile strength, f_{ctd} .

B.1.8.2 Members Not Requiring Shear Reinforcement

The design value for the shear resistance $V_{Rd,ct}$ is given by:

$$V_{Rd,ct} = \left[0.10 \eta_1 k (100 \rho_l f_{ck})^{1/3} - 0.12 \sigma_{cd} \right] b_w d \quad (\text{mm, MPa}) \quad (\text{B-60})$$

where: f_{ck} = characteristic concrete strength (MPa)

η_1 = 1 for normal concrete

= $0.4 + 0.6 \rho / 2200$ with ρ in (kg/m^3) for lightweight concrete

k = $1 + \sqrt{\frac{200}{d}} \leq 2.0$ (mm unit)

ρ_l = $\frac{A_{sl}}{b_w d} \leq 0.02$, longitudinal reinforcement ratio

A_{sl} = area of the tensile reinforcement, which extends d beyond the section considered and is anchored there effectively (see Fig. B-9)

b_w = smallest width of the cross-section in the tensile area (mm)

σ_{cd} = N_{Ed} / A_c (MPa)

N_{Ed} = design value of the axial force in the cross-section due to loading or prestressing
($N_{Ed} < 0$ for compression)
 A_c = area of concrete cross section (mm^2)

B.1.8.3 Members with Shear Reinforcement

The design of members with shear reinforcement is based on a truss model, with a limit given for the angle θ of the inclined struts in the web as follows:

$$0.58 \leq \cot \theta = \frac{(1.20 - 1.40 \sigma_{cd} / f_{cd})}{(1 - V_{Rd,c} / V_{Sd})} \leq 3.0 \text{ for normal concrete} \quad (\text{B-61})$$

$$\leq 2.0 \text{ for lightweight concrete}$$

where $V_{Rd,c}$ = shear force component of concrete section with shear reinforcement

$$V_{Rd,c} = \left[\eta_1 \cdot \beta_{ct} \cdot 0.10 \cdot f_{ck}^{1/3} \left(1 - 1.2 \cdot \frac{\sigma_{cd}}{f_{cd}} \right) \right] \cdot b_w \cdot z \text{ (mm, MPa)} \quad (\text{B-62})$$

$$\beta_{ct} = 2.4$$

$$\eta_1 = 1.0 \text{ for normal concrete; lightweight concrete see Eq. (B-60)}$$

$$\sigma_{cd} = N_{Ed} / A_c = \text{design value of axial concrete stress at centroid of section}$$

$$N_{Ed} = \text{design value of normal force due to loading and prestressing}$$

($N_{Ed} < 0$ for compression)

The internal lever arm, z , may normally be taken as $z \approx 0.9d$. For members with inclined prestressing tendons a sufficient amount of longitudinal reinforcement must be placed in the tension chord to take the axial tensile forces due to shear. For z , no higher value than $z = d - c_{nom}$ is allowed, where c_{nom} = concrete cover for the longitudinal reinforcement in the compression zone.

The design value of the shear force $V_{Rd,sy}$ for vertical shear reinforcement is:

$$V_{Rd,sy} = \frac{A_{sw}}{s_w} f_{yd} z \cot \theta \quad (\text{B-63})$$

where: s_w = spacing of shear reinforcement in longitudinal direction

$$A_{sw} = \text{cross-sectional area of shear reinforcement}$$

$$f_{ywd} = \text{design yield strength of shear reinforcement}$$

$$\theta = \text{angle between inclined concrete struts and the main tension chord}$$

The maximum design value of the shear force $V_{Rd,max}$ is determined by the compressive strength of the inclined struts in the web, and for members with vertical shear reinforcement its value is:

$$V_{Rd,max} = [(\alpha_c f_{cd} / (\cot \theta + \tan \theta))] b_w z \quad (mm, MPa) \quad (B-64)$$

where: $\alpha_c = 0.75\eta_1$ = reduction factor for the strength of the struts
 $\eta_1 = 1$ for normal concrete; lightweight concrete (see above)
 b_w = minimum width between tension and compression chords

Where the web contains grouted ducts with a sum of diameters $\phi > b_w / 8$, the shear resistance $V_{Rd,max}$ must be calculated on the basis of a nominal web thickness given by:

$$b_{w,nom} = b_w - 0.5 \sum \phi \quad \text{when } f_{ck} \leq 50 \text{ MPa} \quad (B-65a)$$

$$b_{w,nom} = b_w - 1.0 \sum \phi \quad \text{when } f_{ck} > 50 \text{ MPa} \quad (B-65b)$$

where ϕ is the outer diameter of the duct and $\sum \phi$ is determined for the most unfavorable level.

For non-grouted ducts and unbonded tendons the nominal web thickness is:

$$b_{w,nom} = b_w - 1.3 \sum \phi \quad (B-65c)$$

The additional tensile force due to shear in the longitudinal reinforcement has to be considered:

$$\Delta F_{sd} = 0.5 |V_{Ed}| (\cot \theta - \cot \alpha) \quad (B-66)$$

where: α = angle between shear reinforcement and axis of member
 V_{Ed} = design value of applied shear force

B.1.9 Japanese Code (JSCE Standards, 1986)

B.1.9.1 Background

The JSCE Code requires the designer to examine three limit states: ultimate, serviceability and fatigue. This review covers the provisions for shear for the ultimate and serviceability limit states only. As shown in Table B-6, the JSCE Code uses five different load and resistance factors. Two factors, γ_m and γ_b , are associated with the design capacity of the member and are equivalent in many respects to the ϕ values of US Codes. Two factors, γ_f and γ_a , relate to member forces for design and are equivalent in many respects to the load factors of US Codes. The fifth factor, γ_i , governs safety through comparison of the design capacity and the design force and it has a value that depends on the importance of the structure. Typical values for the five γ factors are listed in Table B-7. For design those factors are combined as shown in Table B-8.

B.1.9.2 Shear Considerations- Ultimate Limit State

Design for shear requires examination of the capacities V_{yd} and V_{wcd} where

V_{yd} = design shear capacity, and

V_{wcd} = design ultimate diagonal compressive capacity of web concrete.

It is assumed that, after inclined cracking, the shear force is carried by shear reinforcing steel and that the load carrying system is a truss type mechanism. Members can then lose their resistance to shear by yielding of the shear reinforcing steel that are the tension web chords of the truss or by compressive failure of the web concrete. V_{sd} defines the strength of the shear steel yield mechanism and V_{wcd} defines the strength for web concrete crushing.

V_{yd} is the sum of the shear components carried by the concrete, V_{cd} , the shear reinforcement, V_{sd} and the vertical component of the prestress force, V_{ped} :

$$V_{yd} = V_{cd} + V_{sd} + V_{ped} \quad (\text{B-67})$$

V_{cd} equals the design shear capacity of linear members without shear reinforcement and its value is as follows:

$$V_{cd} = f_{ycd} b_w d / \gamma_b \quad (\text{B-68})$$

Where $\gamma_b = 1.3$. The value of the stress f_{ycd} depends on the depth of the member, its reinforcement ratio, and axial stress, and the concrete strength and is given by:

$$f_{ycd} = 0.9 \beta_d \beta_p \beta_n (f_c')^{1/3} \quad (\text{kgf/cm}^2) \quad (\text{B-69})$$

where $\beta_d = (100/d)^{1/4} \leq 1.5$ and where d is in cm

$$\beta_p = (100\rho_w)^{1/3} \leq 1.5$$

$$\beta_n = 1 + M_o / M_d \leq 2.0 \quad (N_d' \geq 0)$$

$$= 1 + 2M_o / M_d \geq 0 \quad (N_d' < 0)$$

$$\rho_w = A_s / (b_w d)$$

M_d is the design flexural moment

M_o is the decompression moment that causes an extreme bottom fiber stress of zero when combined with the axial stresses, as shown in Fig. B-12.

The effects on shear strength of the effective depth, the longitudinal reinforcement ratio and axial forces are shown in Fig. B-11.

For a member without vertical prestressing and with vertical stirrups V_{sd} is:

$$V_{sd} = (A_w f_{wyd} / s_s) z / \gamma_b \quad (\text{B-70})$$

where f_{wyd} is to be taken not greater than $4,000 \text{ kgf/cm}^2$, z is to be taken as $d/1.15$ and γ_b as 1.15. The stress f_{wyd} is limited to $4,000 \text{ kgf/cm}^2$ because excessive inclined crack widths at shear failure reduce the shear carried by aggregate interlock on crack planes, and reduce the dowel action of the tension reinforcement. Stirrups resist shear forces as tension web chord members of the assumed truss system and also prevent inclined cracks from propagating along the tension reinforcement.

V_{ped} is given by:

$$V_{ped} = P_{ed} \sin \alpha_p / \gamma_b \quad (\text{B-71})$$

where P_{ed} = effective prestress force in the longitudinal tendon

α_p = angle between prestressing force and the longitudinal axis of member

and $\gamma_b = 1.15$

For lightweight concrete Eq. (B-69) values should be taken as 70 % of those for normal weight concrete.

Where members are directly supported, the strength V_{yd} need be examined no closer than $h/2$ to the support where h is the overall depth of the member. Between that section and the support, shear reinforcement equal to that at $h/2$ need be provided only.

The diagonal compressive capacity of the web concrete is given by:

$$V_{wcd} = f_{wcd} b_w d / \gamma_b \quad (\text{B-72})$$

where $f_{wcd} = 4\sqrt{f'_c}$ kgf/cm² and $\gamma_b = 1.3$.

Where the diameter of the duct of a prestressed member is equal to or greater than 1/8 times the web width, the width used in Eq. (B-68) must be less than b_w . The web width is reduced by one half the total amount of duct diameters in the cross-section. Except for circular members, the web width b_w is the minimum width within the effective depth. For circular members the web width equals the side length of a square with the same area and for a hollow circular member, the total width of the webs equals that for a square box having the same area.

Because inclined cracking often reduces the resistance of members without shear reinforcement, stirrups not less than 0.15 % of the concrete area must be provided along the length of the member. This minimum amount of shear reinforcement is required even when not necessary according to computations because sudden failure due to inclined cracking can be caused by concrete shrinkage and temperature differences. This reinforcement is necessary to provide adequate member ductility and re-establish the load carrying mechanism after inclined cracking. With that amount of stirrup reinforcement, the shear strength provided by the stirrups becomes approximately equal to V_{cd} . The spacing of such stirrups is not to exceed 40 cm (15.75 in) or three quarters of the effective depth.

Where stirrups are required by computation the spacing is not to exceed 30 cm or 1/2 the effective depth. That spacing is to be maintained to a length equal to d beyond where shear reinforcement is calculated as necessary. Ends of stirrups must be embedded in the compressive side of the concrete.

Both reinforced and prestressed concrete belong to the same group when the ultimate flexural strength is controlled by yielding of the tension reinforcement. Therefore the safety of prestressed members against failure in shear may be examined in the same manner as reinforced concrete members.

B.1.9.3 Shear Considerations - Serviceability Limit State

Clause 3.10.3.1 Because inclined cracking can significantly influence the durability of a structure, examination is required for shear cracking at the serviceability limit state. No examination is required if: (1) for reinforced concrete members the unfactored design shear force V_d is less than the design shear capacity of the concrete V_{cd} , and (2) for prestressed concrete members if V_d is less than $V_{cd} + V_{ped}$. For beams whose stirrup strain is less than $1,000 \times 10^{-4}$ and the service load does not exceed 0.7 times the ultimate load, the shear crack width does not have a significant effect. In general, when the stress in the shear reinforcement due to permanent loads is less than that shown in Table B-9, precise examination is not required. The stress in the vertical stirrup reinforcement is given by:

$$\sigma_{wd} = (V_{pd} - V_{cd})s / (A_w z) \quad (\text{B-73})$$

where V_{pd} is the design shear force produced by permanent loads. When the crack width due to variable loads is significantly greater than that due to permanent loads, computation of the stress in the shear reinforcement must consider the effect of the variable loads.

Clause 3.10.3.2 For prestressed concrete members the diagonal tensile stress in the concrete is limited to the following values of the design tensile strength of the concrete: (1) Where there is no tensile stress in the precompressed tensile zone: 35 % for shear alone or 50 % for shear and torsion; (2) Where the tensile stress in the precompressed tensile zone does not exceed the design tensile strength of the concrete: 75 % for shear alone or 95 % for shear and torsion. The design tensile strength of the concrete is $0.38(f'_c)^{2/3} \text{ kgf/cm}^2$. Where flexural cracking is predicted, the shear strength of the member must satisfy Clause 3.10.3.1.

B.1.10. AASHTO Guide Specifications for Design and Construction of Segmental Concrete Bridges – 2nd Edition 1999

B. 1.10.1. Background

The Segmental Concrete Bridge Guide Specifications were first published in 1989. The Specifications contained a simplified version of the ACI 318 Building Code provisions for shear. Since then, most segmental concrete bridges in the U.S.A. have been designed using those Specifications. The Specifications require minimum shear reinforcement throughout the length of segmental members regardless of the shear stress level.

The advantages of these alternate shear procedures (Freyermuth, 2003), as compared to the AASHTO-LRFD Specifications for shear, are reported to be:

- (1) The use of a limiting nominal shear stress of $12\sqrt{f'_c}$.

During 2002-2003 two Florida DOT segmental bridges, ostensibly designed in accordance with the AASHTO-LRFD Bridge Design Specifications, experienced web shear cracking that required repair or retrofit procedures. In response, Florida DOT limited the total nominal shear stress to $12\sqrt{f'_c}$ rather than the $0.25 f'_c$ of the AASHTO-LRFD Specifications. That same limiting nominal shear stress value is a requirement of the second edition of the AASHTO Segmental Concrete Bridge Guide Specifications.

(2) The use of a constant value of 45 degrees for the angle of inclination for truss diagonals in beams with shear reinforcement.

With that assumption there is no need to make separate calculations for the longitudinal tension reinforcement required to resist shear forces. The horizontal component to the truss diagonal force is provided by satisfaction of traditional detailing rules concerning termination of longitudinal reinforcement in tension zones.

(3) A limit on the concrete contribution to the shear capacity of $4\sqrt{f'_c}$ in areas of web shear cracking and $2\sqrt{f'_c}$ in areas of flexure-shear cracking.

While those limits typically require more stirrups to resist shear than the AASHTO-LRFD Specifications, the relatively small cost of additional stirrups, or small increase in web thickness, is considered an appropriate design investment.

(4) A reduction in the design time and training costs compared to the use of the AASHTO-LRFD Specifications

B.1.10.2 Guide

The relevant provisions are Articles 12.1 Scope, 12.2 General Requirements, and 12.3 Traditional Shear and Torsion Design for Plane Section Type Regions. This review is limited to the content of those provisions dealing with design for shear.

Scope – Article 12.1 states that the provisions are limited to: (1) the shear design of prestressed concrete segmental bridges; and (2) to B regions (bending regions) as defined in the AASHTO-LRFD Specifications. Article 12.1.5 defines the applied shear, V_u , as the shear due to factored dead load (V_{UDL}) including continuity effects, factored live load (V_{ULL}), and any other factored ultimate load cases specified. The applied shear due to the component of the effective longitudinal prestress force acting in the direction of the section being examined, (V_p), is considered as a load effect. The vertical component of that prestress force is considered to reduce the applied shear only on the webs for tendons which cross the webs and are anchored or fully developed by anchorages, deviators or internal ducts located in the outer one third of the webs. That vertical component can add to, or subtract from, shear on a cross-section.

General Requirements – Article 12.2 requires: (1) consideration of the effects of axial tension due to creep, shrinkage and thermal effects in restrained members; (2) components of inclined flexural compression or tension in variable depth members; and (3) the effects of openings or ducts in members. In the latter case, for shear stress calculations the diameters of ungrouted ducts, or one half the diameters of grouted ducts, is to be subtracted from the web width at the level of the ducts.

Values of $\sqrt{f'_c}$ used in design are not to exceed 100psi, the design yield stress for non-prestressed transverse shear reinforcement is not to exceed 60,000 psi, and that of prestressed reinforcement is not to exceed the effective prestress plus 60,000 psi, nor f_{py} , the specified yield strength of the prestressing steel. For pretensioned members the reduced prestress in the transfer length is to be used in computing f_{pc} (the axial prestress in the member) and V_p . The prestress force is assumed

to vary linearly from zero, at the point where bonding begins, to a maximum at the end of the transfer length. The transfer length is taken as 50 strand diameters.

Shear effects can be neglected in areas of members where $V_u \leq \Phi V_c/2$. However, minimum stirrup capacity not less than the equivalent of two No.4 Grade 60 bars at one foot on centers is required per web in such areas.

In lieu of more detailed calculations the shear that can be carried by the concrete, V_c , for nominal shear strength calculations may be taken as:

$$V_c = 2K\sqrt{f'_c}b_wd \quad (\text{B-74})$$

where

$$K = \sqrt{1 + \frac{f_{pc}}{2\sqrt{f'_c}}} \leq 2.0 \quad (\text{B-75})$$

Where V_u exceeds $\Phi V_c/2$ the capacity of the shear reinforcement is to exceed $50 b_w s$. Shear reinforcement is to consist of stirrups inclined at 45 degrees or more to the longitudinal tension reinforcement, welded wire fabric, longitudinal bars bent at an angle of 30 degrees or more with the tension reinforcement, well anchored prestressing steel, combinations of the above, and spirals. Shear reinforcement is to extend as a continuous tie from the extreme compression fiber, less cover, to the outermost tension reinforcement, and to be fully anchored at both ends. Maximum spacing of transverse reinforcement is not to exceed $0.5d$ in non-prestressed elements and $0.75h \leq 36$ inches in prestressed elements. Where V_u exceeds $6\Phi\sqrt{f'_c}b_wd$, these maximum spacing values are reduced by one half.

Flexural reinforcement, including tendons, is to extend beyond the theoretical termination point for at least $h/2$, where h is the member depth. Transverse reinforcement for shear is to be provided for a distance of $h/2$ beyond the point theoretically required.

Traditional Shear Design – Article 12.3 permits design by the methods detailed in it when $V_n = 12\sqrt{f'_c}b_wd$ and no concentrated load located within $2d$ of the support causes more than one-third of the shear at the support. Then

$$V_u \leq \phi V_n \quad (\text{B-76})$$

V_u must consider unfavorable effects of V_p and may also consider favorable effects, and

$$V_n = 12\sqrt{f'_c}b_wd \quad (\text{B-77})$$

$$V_n = V_c + V_s \quad (\text{B-78})$$

where V_c is given by Eq. (B-74)

$$\text{and} \quad V_s = \frac{A_v f_v d}{s} \quad (\text{B-79})$$

where d = distance from extreme compression fiber to centroid of prestressed reinforcement in tension chord, or $0.8h$, whichever, is greater.

The applied shear V_u in regions near supports may be reduced to the value at $h/2$ from the supports when both the following are satisfied: the support reaction in the direction of the applied shear introduces compression into the support region of the member; and no concentrated load occurs within a distance h from the face of the support.

B.2 Other Shear Design Approaches

B.2.1 Concrete Shear Strength: Another Perspective - A. Koray Tureyen and Robert J. Frosch (2003)

Frosch et al.(2003) calculate the shear strength using a free-body model of a cracked concrete member subject to shear stress and axial compression (Fig. B-13). Failure is assumed to occur when the principal tensile stress in the uncracked concrete above the neutral axis reaches the tensile strength of the concrete, f_t . From Fig. B-14 the relationship between the stresses and the tensile strength in the uncracked region can be obtained as:

$$\frac{\sigma}{2} - \sqrt{\tau^2 + \left(\frac{\sigma}{2}\right)^2} = -f_t \quad \text{or} \quad \tau = \sqrt{f_t^2 + f_t\sigma} \quad (\text{B-80})$$

Provided that a maximum shear stress, τ_{\max} , of $\frac{3}{2} \frac{V}{b_w c}$ and corresponding flexural stress

($\sigma = \frac{\sigma_m}{2}$) occur at the mid-depth of the compression zone ($c/2$) (Fig. B-13), the shear strength of the concrete can be derived as

$$V_c = \frac{2}{3} b_w c \sqrt{f_t^2 + f_t \frac{\sigma_m}{2}} \quad \text{or} \quad V_c = \left(16 + \frac{4\sigma_m}{3\sqrt{f_c'}}\right) \sqrt{f_c'} b_w c \quad (\text{B-81})$$

where b_w = beam width, in.

f_c' = specified compressive strength of concrete, psi

$f_t = 6\sqrt{f_c'}$ = concrete tensile strength

$c = kd$ = cracked transformed section neutral axis depth, in.

$k = \sqrt{2\rho n + (\rho n)^2} - \rho n$

d = effective depth, in.

$\rho = \frac{A_r}{b_w d}$ = reinforcement ratio

$n = \frac{E_r}{E_c}$ = modulus ratio

A_r = area of longitudinal tension reinforcement, in.²

$E_c = 57,000\sqrt{f_c'}$ = modulus of elasticity of concrete, psi

E_r = modulus of elasticity of reinforcement, psi

σ_m = stress of the extreme compression fiber at the cracking moment

For design purposes, Frosch et al. have proposed the following simplified equation for the shear strength of the concrete members:

$$V_c = 5\sqrt{f'_c} b_w c \quad (\text{psi and in.}) \quad (\text{B-82})$$

The invariant, 5, is substituted for the first term in parenthesis of Eq. (B-81). According to Frosch et al., this value is selected to provide conservative estimates of shear strength, and results in slightly more conservative values for $\rho < 0.8\%$.

Frosch et al. have found that the modulus of elasticity of the flexural reinforcement, (steel versus a fiber composite), influences the shear strength of a beam. This finding is essentially included in their equation because the location of the neutral axis (or the depth of uncracked concrete) depends on the modulus of elasticity of the reinforcement.

The concrete compressive strength is taken into account through the correlation with the concrete tensile strength as well as through its effect on the neutral axis depth. Increasing the compressive concrete strength decreases the modular ratio of reinforcement to concrete and the value of k , and therefore, the neutral axis depth decreases. Consequently, the effect of the compressive concrete strength is less than that in the expression $V_c = 2\sqrt{f'_c} b_w d$ of ACI 318.

Frosch et al. have pointed that there appears to be a decrease in shear strength as the effective depth increases. This trend was also observed for the shear strength data calculated by the equation of ACI 318 and is believed to be due to not taking into account the size effect effectively. Since the term related to the effective depth has not been changed herein, the same trend as the equation of ACI 318 is expected to appear.

Also, because this shear strength model assumes that the uncracked concrete contributes to the shear strength of reinforced concrete beams and neglects any interface shear transfer, it may result in more conservatism than ACI 318 when used for calculating the strength of beams with shear reinforcement. The extension of this model to prestressed concrete beams is currently being pursued by Frosch.

B.2.2 AASHTO 1979

The shear design approach included in AASHTO Standard Specifications for Highway Bridges (1979) is summarized following.

Prestressed concrete members shall be reinforced for diagonal tension stresses. Shear reinforcement shall be placed perpendicular to axis of the member. The area of web reinforcement shall be

$$A_v = \frac{(V_u - V_c)s}{2 f_{sy} jd} \quad (\text{B-83})$$

but not less than

$$A_v = 100b's / f_{sy} \quad \text{or} \quad \left(0.689 \frac{b's}{f_{sy}} \right) \quad (\text{B-84})$$

where f_{sy} shall not exceed 60,000 psi (415 MPa).

The concrete contribution to shear is:

$$V_c = 0.6 f'_c b' jd \quad (\text{B-85})$$

but not more than $180 b' jd$ or $(1.241 b' jd)$ where 1.241 is in units of MN/m^2 .

Web reinforcement may consist of :

- 1) Stirrups perpendicular to the axis of the member.
- 2) Welded wire fabric with wire located perpendicular to the axis of the member

The spacing of web reinforcement shall not exceed three-fourths the depth of the member.

The critical sections for shear in simply supported beams will usually not be near the ends of the spans where the shear is maximum, but at some point away from the ends in a region of high moment.

For the design of web reinforcement in simply supported members carrying moving loads, it is recommended that shear be investigated only in the middle half of the span length. The web reinforcement required at the quarter points should be used throughout the outer quarters of the span.

For continuous bridges whose individual spans consist of precast prestressed girders, web reinforcement shall be designated for the full length of interior spans and for the interior three-fourths of the exterior span.

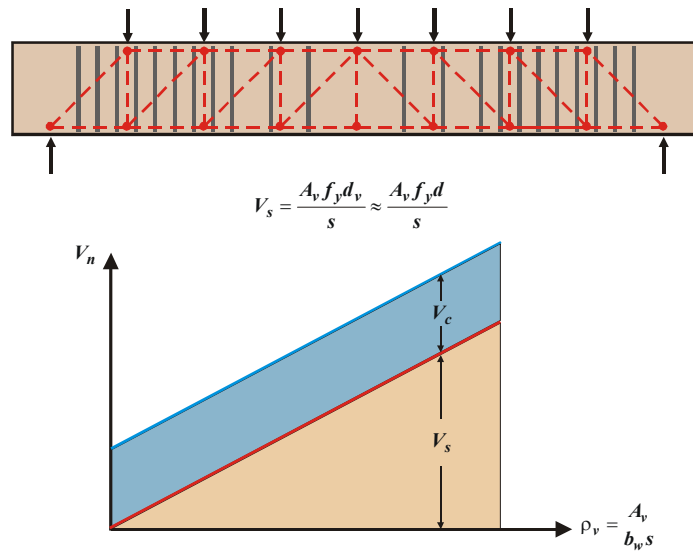


Fig. B-1 Concrete and Steel Contributions to Shear Strength

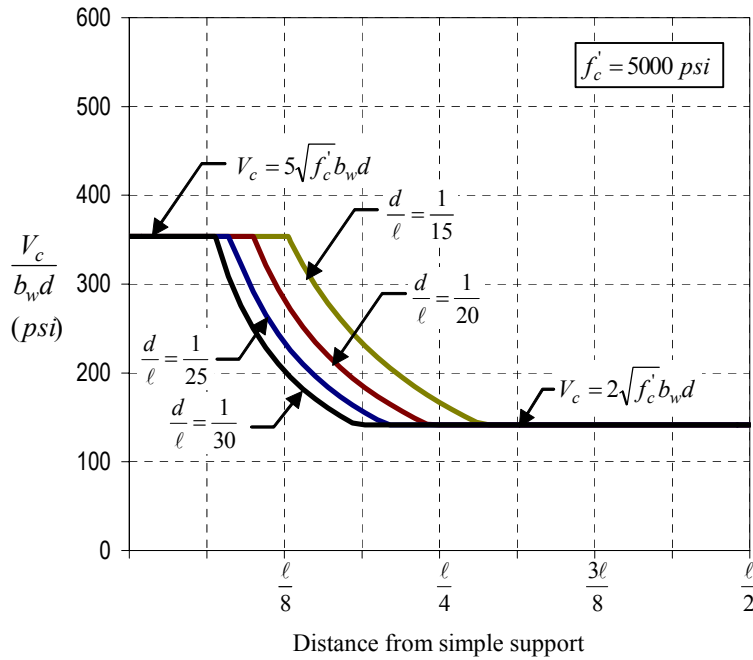


Fig. B-2 Eq. (B-7) for Uniformly Loaded Prestressed Members (ACI 318-02)

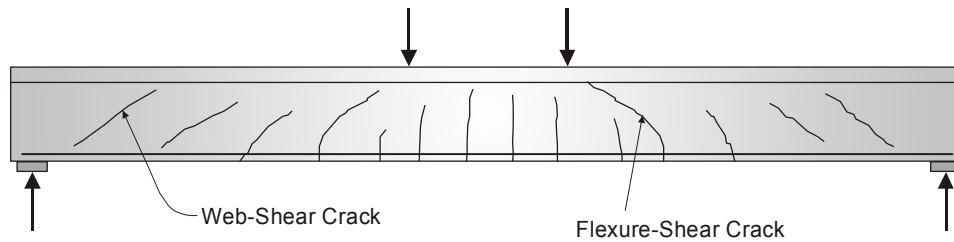


Fig. B-3 Typical Shear Cracks in Prestressed Concrete Members

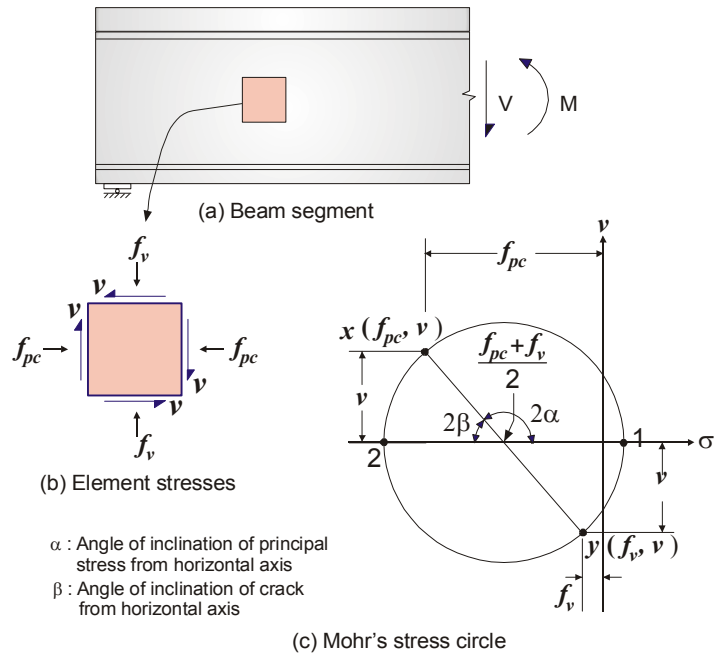


Fig. B-4 Derivation of Web-Shear Cracking Force, V_{cw}

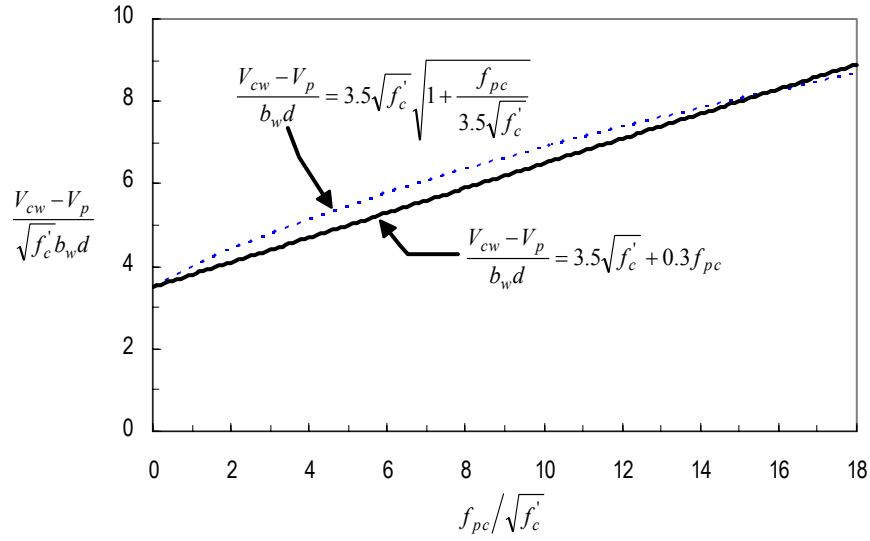


Fig. B-5 Approximation of Web-Shear Cracking Force, V_{cw}

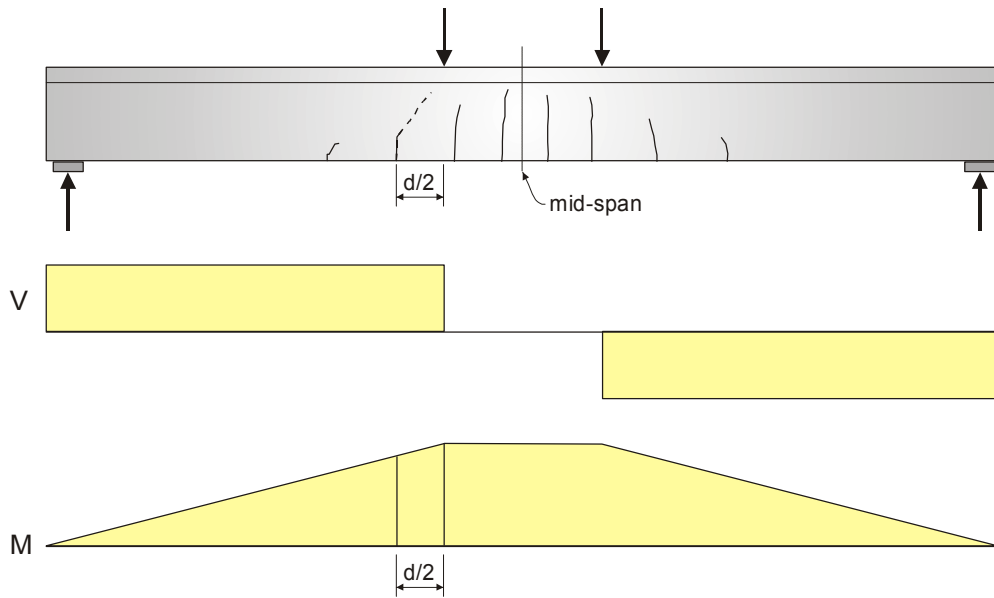


Fig. B-6 Derivation of Flexure-Shear Cracking Force, V_{ci}

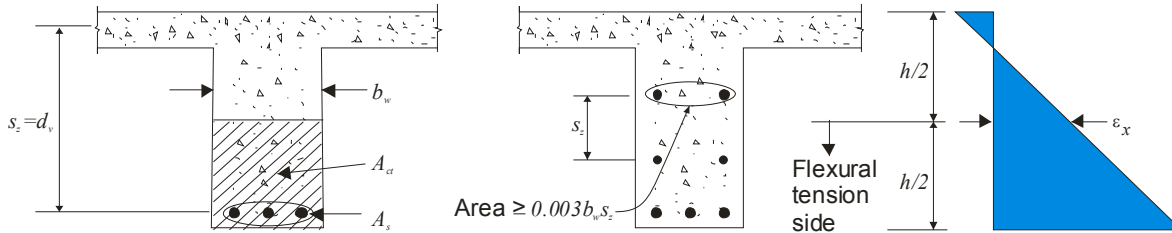
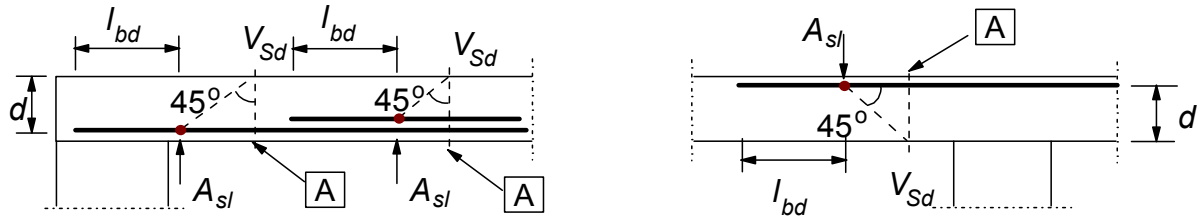
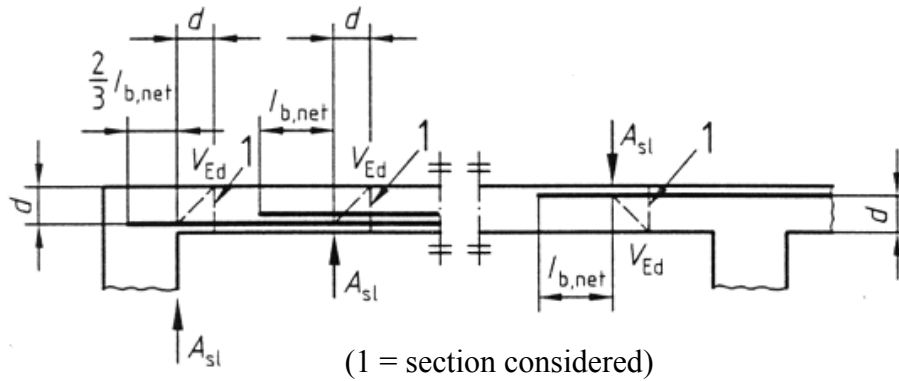


Fig. B-7 Terms in Shear Design Equations (Collins, 2002)



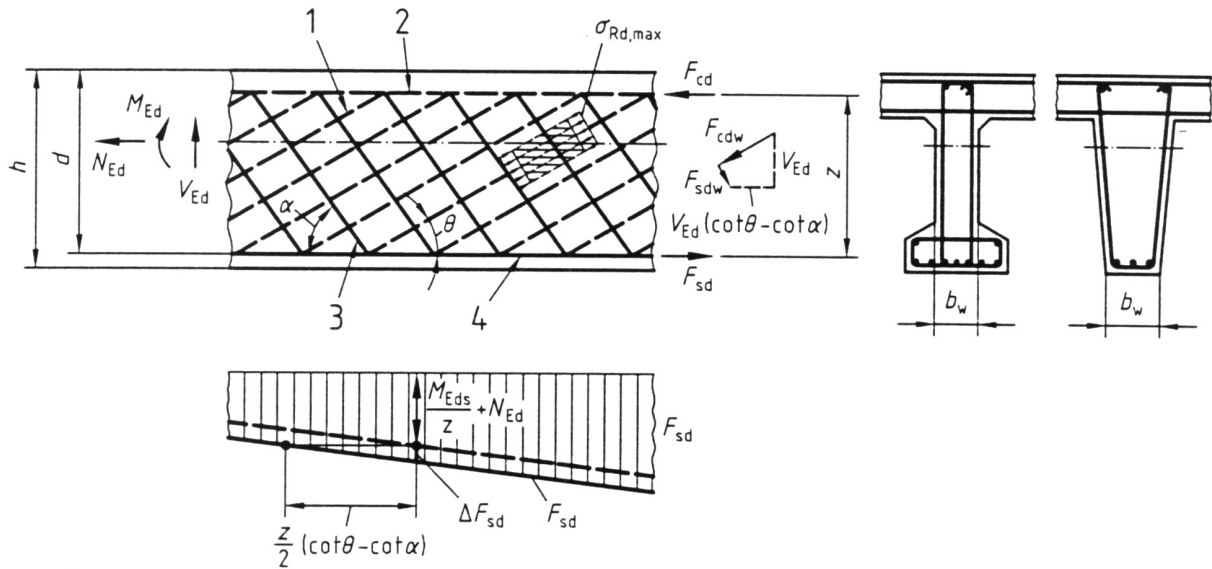
[A] - section considered

Fig. B-8 Definition of A_{sl} in Eq. (B-51)



(1 = section considered)

Fig. B-9 Definition of A_{sl} for Determining ρ_l in Eq. B-57 (Reineck, 2001)



1= strut, 2=compression chord, 3=tie; shear reinforcement, 4=tension chord; longitudinal reinforcement

Fig. B-10 Truss Model and Notation (Reineck, 2001)

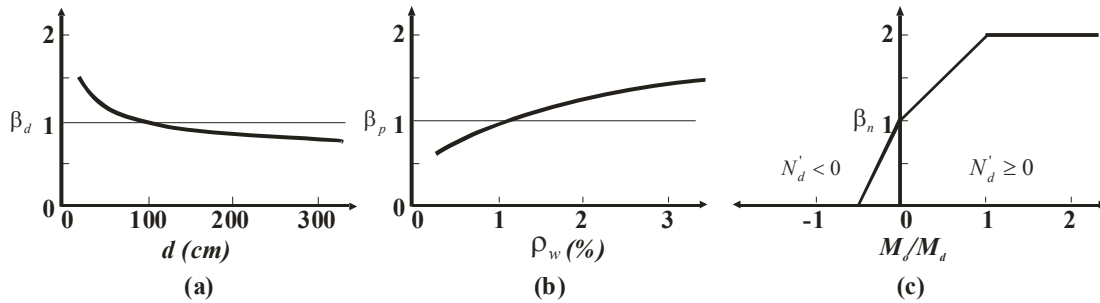


Fig. B-11 Influencing Factors on the Shear Strength (JSCE, 1986)

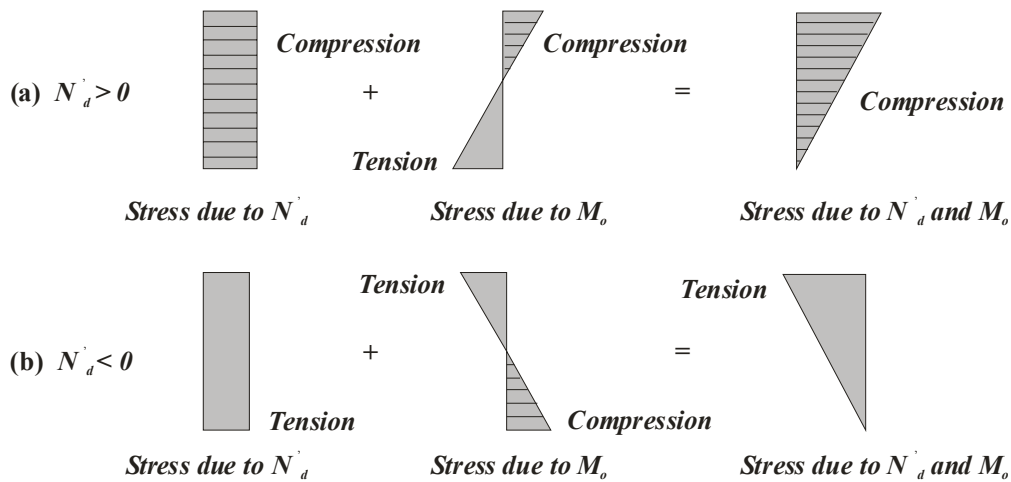


Fig. B-12 Meaning of Decompression Moment, M_o (JSCE, 1986)

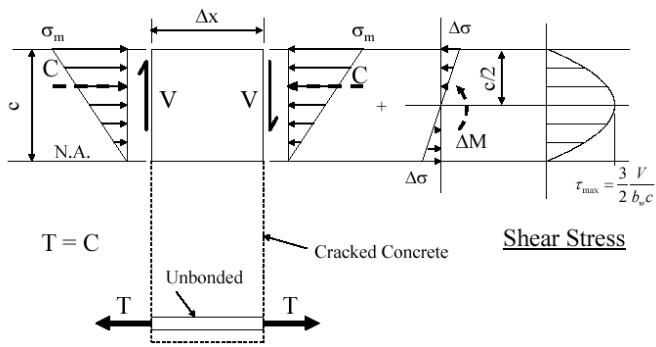


Figure B-13 Free-Body of Cracked Concrete Member

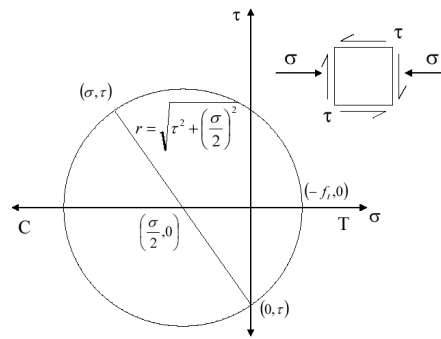


Figure B-14 Mohr's Stress Circle

Table B-1 Design Values of β and θ for Members with Transverse Reinforcement

$\frac{v_f^*}{f_c'}$		Longitudinal Strain, $\varepsilon_x \times 1000$						
		≤ 0	≤ 0.25	≤ 0.50	≤ 0.75	≤ 1.00	≤ 1.50	≤ 2.00
≤ 0.050	β	0.405	0.290	0.208	0.197	0.185	0.162	0.143
	θ	27.0°	28.5°	29.0°	33.0°	36.0°	41.0°	43.0°
≤ 0.075	β	0.405	0.250	0.205	0.194	0.179	0.158	0.137
	θ	27.0°	27.5°	30.0°	33.5°	36.0°	40.0°	42.0°
≤ 0.100	β	0.271	0.211	0.200	0.189	0.174	0.143	0.120
	θ	23.5°	26.5°	30.5°	34.0°	36.0°	38.0°	39.0°
≤ 0.125	β	0.216	0.208	0.197	0.181	0.167	0.133	0.112
	θ	23.5°	28.0°	31.5°	34.0°	36.0°	37.0°	38.0°
≤ 0.150	β	0.212	0.203	0.189	0.171	0.160	0.125	0.103
	θ	25.0°	29.0°	32.0°	34.0°	36.0°	36.5°	37.0°
≤ 0.200	β	0.203	0.194	0.174	0.151	0.131	0.100	0.083
	θ	27.5°	31.0°	33.0°	34.0°	34.5°	35.0°	36.0°
≤ 0.250	β	0.191	0.167	0.136	0.126	0.116	0.108	0.104
	θ	30.0°	32.0°	33.0°	34.0°	35.5°	38.5°	41.5°

$$* v_f = V_f / b_w d_v$$

Table B-2 Design Values of β and θ for Members without Transverse Reinforcement

s_z (mm)		Longitudinal Strain, $\varepsilon_x \times 1000$					
		≤ 0	≤ 0.25	≤ 0.50	≤ 1.00	≤ 1.50	≤ 2.00
≤ 125	β	0.406	0.309	0.263	0.214	0.183	0.161
	θ	27°	29°	32°	34°	36°	38°
≤ 250	β	0.384	0.283	0.235	0.183	0.156	0.138
	θ	30°	34°	37°	41°	43°	45°
≤ 500	β	0.359	0.248	0.201	0.153	0.127	0.108
	θ	34°	39°	43°	48°	51°	54°
≤ 1000	β	0.335	0.212	0.163	0.118	0.095	0.080
	θ	37°	45°	51°	56°	60°	63°
≤ 2000	β	0.306	0.171	0.126	0.084	0.064	0.052
	θ	41°	53°	59°	66°	69°	72°

Table B-3 Design Values of β and θ for Members with Transverse Reinforcement

$\frac{v^*}{f'_c}$		Longitudinal Strain, $\epsilon_x \times 1000$										
		≤ -0.20	≤ -0.10	≤ -0.05	≤ 0	≤ 0.125	≤ 0.25	≤ 0.50	≤ 0.75	≤ 1.00	≤ 1.50	≤ 2.00
≤ 0.075	θ	22.3°	20.4°	21.0°	21.8°	24.3°	26.6°	30.5°	33.7°	36.4°	40.8°	43.9°
	β	6.32	4.75	4.10	3.75	3.24	2.94	2.59	2.38	2.23	1.95	1.67
≤ 0.100	θ	18.1°	20.4°	21.4°	22.5°	24.9°	27.1°	30.8°	34.0°	36.7°	40.8°	43.1°
	β	3.79	3.38	3.24	3.14	2.91	2.75	2.50	2.32	2.18	1.93	1.69
≤ 0.125	θ	19.9°	21.9°	22.8°	23.7°	25.9°	27.9°	31.4°	34.4°	37.0°	41.0°	43.2°
	β	3.18	2.99	2.94	2.87	2.74	2.62	2.42	2.26	2.13	1.90	1.67
≤ 0.150	θ	21.6°	23.3°	24.2°	25.0°	26.9°	28.8°	32.1°	34.9°	37.3°	40.5°	42.8°
	β	2.88	2.79	2.78	2.72	2.60	2.52	2.36	2.21	2.08	1.82	1.61
≤ 0.175	θ	23.2°	24.7°	25.5°	26.2°	28.0°	29.7°	32.7°	35.2°	36.8°	39.7°	42.2°
	β	2.73	2.66	2.65	2.60	2.52	2.44	2.28	2.14	1.96	1.71	1.54
≤ 0.200	θ	24.7°	26.1°	26.7°	27.4°	29.0°	30.6°	32.8°	34.5°	36.1°	39.2°	41.7°
	β	2.63	2.59	2.52	2.51	2.43	2.37	2.14	1.94	1.79	1.61	1.47
≤ 0.225	θ	26.1°	27.3°	27.9°	28.5°	30.0°	30.8°	32.3°	34.0°	35.7°	38.8°	41.4°
	β	2.53	2.45	2.42	2.40	2.34	2.14	1.86	1.73	1.64	1.51	1.39
≤ 0.250	θ	27.5°	28.6°	29.1°	29.7°	30.6°	31.3°	32.8°	34.3°	35.8°	38.6°	41.2°
	β	2.39	2.39	2.33	2.33	2.12	1.93	1.70	1.58	1.50	1.38	1.29

$$*v = V / b_v d_v$$

Table B-4 Design Values of β and θ for Members without Transverse Reinforcement

s_{xe}^* (in)		Longitudinal Strain, $\epsilon_x \times 1000$										
		≤ -0.20	≤ -0.10	≤ -0.05	≤ 0	≤ 0.125	≤ 0.25	≤ 0.50	≤ 0.75	≤ 1.00	≤ 1.50	≤ 2.00
≤ 5	θ	25.4°	25.5°	25.9°	26.4°	27.7°	28.9°	30.9°	32.4°	33.7°	35.6°	37.2°
	β	6.36	6.06	5.56	5.15	4.41	3.90	3.26	2.86	2.58	2.21	1.96
≤ 10	θ	27.6°	27.6°	28.3°	29.3°	31.6°	33.5°	36.3°	38.4°	40.1°	42.7°	44.7°
	β	5.78	5.78	5.38	4.89	4.05	3.52	2.88	2.50	2.23	1.88	1.65
≤ 15	θ	29.5°	29.5°	29.7°	31.1°	34.1°	36.5°	39.9°	42.4°	44.4°	47.4°	49.7°
	β	5.34	5.34	5.27	4.73	3.82	3.27	2.64	2.27	2.01	1.68	1.46
≤ 20	θ	31.2°	31.2°	31.2°	32.3°	36.0°	38.8°	42.7°	45.5°	47.6°	50.9°	53.4°
	β	4.99	4.99	4.99	4.61	3.65	3.09	2.46	2.09	1.85	1.52	1.31
≤ 30	θ	34.1°	34.1°	34.1°	34.2°	38.9°	42.3°	46.9°	50.1°	52.6°	56.2°	59.0°
	β	4.46	4.46	4.46	4.43	3.39	2.82	2.19	1.84	1.61	1.30	1.10
≤ 40	θ	36.6°	36.6°	36.6°	36.6°	41.1°	45.0°	50.2°	53.7°	56.3°	60.2°	63.0°
	β	4.06	4.06	4.06	4.06	3.20	2.62	2.00	1.66	1.43	1.14	0.95
≤ 60	θ	40.8°	40.8°	40.8°	40.8°	44.5°	49.2°	55.1°	58.9°	61.8°	65.8°	68.6°
	β	3.50	3.50	3.50	3.50	2.92	2.32	1.72	1.40	1.18	0.92	0.75
≤ 80	θ	44.3°	44.3°	44.3°	44.3°	47.1°	52.3°	58.7°	62.8°	65.7°	69.7°	72.4°
	β	3.10	3.10	3.10	3.10	2.71	2.11	1.52	1.21	1.01	0.76	0.62

* $s_{xe} = \frac{1.38s_x}{0.63 + a_g}$ (in. units), where s_x = the lesser of d_v and the maximum distance between layers of crack control reinforcement (in.), a_g = maximum aggregate size (in.).

Table B-5 Minimum Shear Reinforcement Ratios ($A_{sw}/b_w s$)

Concrete Grade	Steel Grade		
	S220	S400	S500
12/15, 20/25	0.0016	0.0009	0.0007
25/30 to 35/45	0.0024	0.0013	0.0011
40/50 to 50/60	0.0030	0.0016	0.0013

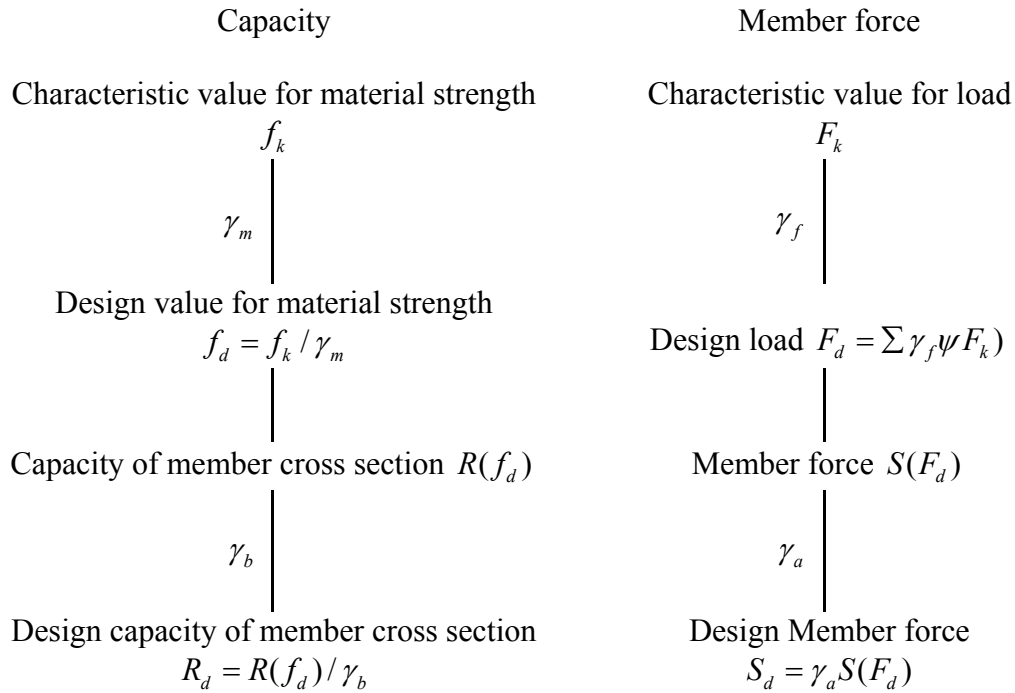
Table B-6 γ Factor Consideration

Contents Being Considered	Safety factors
Capacity of member cross section	
1. Variation of material strength	
(1) Where can be evaluated by records of tests for materials	Characteristic value, f_k
(2) Where cannot be evaluated by records of tests (Consider such conditions as lack or inadequacy of the records, degree of quality control, differences of material strength between test specimen and actual structure, and time dependent variation)	
2. Degree of influence on limit state	
3. Uncertainty in calculation, dimension error, importance of member and failure mode	
Member force	
1. Variation of loads	
(1) Where can be evaluated by statistical records of tests for materials	Characteristic value, F_k
(2) Where cannot be evaluated by statistical records of tests (Consider such conditions as lack or inadequacy of the statistical records, Variation of load during lifetime and uncertainty in evaluation of load)	
2. Degree of influence on limit state	
3. Probability of combination of loads	
4. Uncertainty in structural analysis	
Importance of structure, influence on society when the structure reaches a limit state	

Table B-7 Standard Values for γ Factors

Safety factor Limit States	Material Factor γ_m^*		Member Factor, γ_b	Structural Analysis Factor, γ_a	Load Factor, γ_f	Structure Factor, γ_i
	for Concrete γ_c	for Steel γ_s				
Ultimate Limit State	1.3	1.0	1.15 ~ 1.3*	1.0~1.2	1.0~1.2	1.0~1.2
Serviceability Limit State	1.0	1.0	1.0	1.0	1.0	1.0
Fatigue Limit State	1.3	1.0	1.0~1.1	1.0	1.0	1.0~1.1

* The value is recommended to increase shear capacity in seismic design.

Table B-8 Application of γ Factors

$$\text{Check } R_d / S_d \geq \gamma_i$$

Table B-9 Limiting Values for Reinforcement Stress Increments Due to Permanent Loads
(unit : kgf/cm^2)

Type of Reinforcement	Environmental Conditions for Corrosion of Reinforcement		
	Natural Environment	Corrosive Environment	Severely Corrosive Environment
Deformed Bars	1200	1000	800
Plain Bars	1000	800	600
Prestressing steel	1000	-	-

Appendix C: Shear Database

This appendix presents the shear database (SDB). The appendix begins with an introduction to the evolution and development of the database, describing the distribution of data in the SDB and suggesting where additional experimental research is required. In Section C.2, the effects of different parameters on the shear stresses at failure are presented.

C.1 Presentation of Shear Database

The development of a comprehensive database of shear test results was undertaken in order to provide the research and design communities with a resource for identifying research needs and for developing improved design code provisions. The resulting database is the largest database so far created and it provides new insights into the factors that affect shear strength. It can be used for the evaluation and comparison of different models for shear behavior and different relationships for shear strength.

Existing empirical design code provisions do not provide uniform levels of safety against failure. One reason is because only a small portion of the existing test results are typically used to evaluate or develop code provisions. Another is that the types of members in the test database do not well represent the types of structures that will be designed using the provisions.

One of the complications in developing this shear database was that only a brief summary of experimental test results are typically published in technical journals. There is often insufficient information on geometric details and material characteristics. For this reason, it takes a considerable amount of time for researchers to do literature surveys, and consequently researchers often examine only a limited number of test results before engaging in an experimental research program. Researchers often repeat previous experiments and focus on studying a relatively limited number and range of governing factors. The development of this database was a joint effort by the University of Illinois and the University of Stuttgart, Germany, undertaken with the objective of making research results more accessible and more comparable and, thus, providing a basis for improving the design code. In the creation of this database, about 600 papers or reports summarizing the results of experiment research on the shear resistance of concrete beams were identified. From 108 of the papers processed to date, 2187 individual beam test results have been extracted and subsequently utilized to evaluate the strength relationships used in various shear models, code provisions and other empirical equations. The shear database (SDB) includes tabularized data on both reinforced and prestressed concrete members. Information on the material, geometry, and test data from each experiment are shown in Table C-1.

C.1.1 Shear Test Data for Reinforced Concrete Members

Fig. C-1 provides an overview of the 1444-member reinforced concrete (RC) database. Of these members, 1379 beams were rectangular, 10 were I-shaped, and 55 were T-shaped; 385

beams had stirrups while 1059 of them did not. The vast majority of the tests (1268 of 1444, or about 90 %) consisted of simply supported beams subjected to one or two concentrated loads. 88 loading cases consisted of simply supported beams subjected to uniform loads; 96 cases consisted of continuous beams subjected to point loads. There are only two test results recorded for continuous beams that were subjected to uniform loads. The distribution of parameter values for the entire 1444-member RC database is shown in Fig. C-2. Only 409 of the test results were for beams with concrete strengths greater than 8000 psi and only 83 were for beams with depths greater than 30 inches. Almost half of the beams had shear span to depth ratios (a/d) less than 2.5. Such beams are generally considered as deep beams, and only 191 beams contained less than 1% longitudinal reinforcement.

A total of 409 RC High Strength Concrete (HSC), greater than 8000 psi, shear tests were extracted from 39 publications. The distribution of parameter values for the 409 beam RC HSC database is shown in Fig. C-3. In this bar chart, a second parameter is also reported in order to provide a more detailed description of the database. For example, 48 beams are shown to have cylinder compressive strengths, f'_c , between 8000 and 9000 psi, and among these, 29 beams were less than 10 inches in depth, 17 beams were between 10 and 20 inches in depth, and 2 beams were between 20 and 30 inches in depth. Only 14 % of the HSC RC beams were greater than 20 inches in depth and only 5 % of the HSC RC beams were greater than 30 inches in depth.

C.1.2 Shear Test Data for Prestressed Concrete Members

Fig. C-4 provides an overview of the 743-member prestressed concrete (PC) database. Of these members, 167 beams were rectangular, 535 were I-shaped, and 41 were T-shaped; 282 of the members contained shear reinforcement while 461 did not. For the loading conditions, 729 beams were simply supported and subjected to point loads; 6 beams were simply supported and subjected to uniformly distributed loads; 4 tests were on continuous beams subjected to point loads; and 4 tests were on continuous beams subjected to uniformly distributed loads. The distribution of parameter values for this database is shown in Fig. C-5. Only 115 beams had concrete compressive strengths greater than 8000 psi and only 67 beams were more than 30 inches deep. A total of 611 beams had a shear span to depth ratio (a/d) greater than 2.5 and 312 beams contained less than 1% longitudinal reinforcement.

Among the 115 HSC PC (greater than 8000 psi) members, 17 were noted to fail in flexure and 5 were reported with inadequate information for inclusion in the database. Thus, only 93 HSC PC shear tests could be included in the subsequent analysis.

The distribution of parameter values for the 115-member HSC PC database is shown Fig. C-6. The maximum cylinder compressive strength for all tests was about 14,000 psi. Only 31 out of 115 HSC PC beams were greater than 20 inches in depth and only 23 of them were greater than 30 inches in depth. About half of the HSC PC beams were heavily reinforced and most of the HSC PC beams had shear span to depth ratios greater than 2.5. Unfortunately, however, in the evaluation database, only 25 out of 115 HSC PC beams were greater than 20 inches in depth and only 20 of the HSC PC beam were greater than 30 inches in depth.

C.2 Effect of Parameters

The database was used to investigate the influence of several major parameters on shear strength. In this section, the shear strength, $v_u = V_u / (b_w d)$ or normalized shear strength, $v_u / f'_c = V_u / (b_w d f'_c)$, is plotted for each primary parameter and observations are drawn from the analyses. This section presents in turn those observations for RC members without shear reinforcement, RC members with shear reinforcement, PC members without shear reinforcement, and PC members with shear reinforcement, respectively

Fig. C-7 shows the ultimate shear stresses of the 1444 RC members in the SDB. The large and lightly reinforced members without shear reinforcement (i.e., $h \geq 35 \text{ in}$, $\rho_l \leq 1.0\%$, $\rho_v = 0$) are shown with rectangular markers. The shear strengths of those members are the lowest among members with the same concrete strength and those shear strengths do not increase as the concrete strengths increase. For members with shear reinforcement, the same plot is less meaningful because shear strength is then strongly dependent on the amount of shear reinforcement. In Fig. C-8, the observed shear stresses at failure are plotted versus the concrete cylinder strength for the 743-member PC database. This plot illustrates that very few tests have been conducted in which specimens were cast with high strength concrete or were very heavily reinforced in shear.

In the remaining sections of this chapter, the influences of the major parameters on shear are examined for members with shear span to depth ratios greater than 2.4. Before their results were included in the database, members reported as flexural failure were removed and the flexural capacity of all members was checked against the possibility of flexural failure, i.e., $M_{failure} / M_n < 1.0$. The total number of beams examined in this section is 1359 of which 878 are RC members and 481 are PC members.

C.2.1 Reinforced Concrete Members without Shear Reinforcement

In this section, 718 RC members without shear reinforcement are studied.

C.2.1.1 Concrete Strength

In Fig. C-9, the shear strengths of RC members are plotted versus their concrete cylinder strength. Most of the beams had ultimate shear stresses ranging from 50 to 600 psi. In most cases the shear strength increases as the concrete strength increases. However, members greater than 30 inches in depth, with light amounts of longitudinal reinforcement ($\rho_l < 2.0\%$), do not follow such this trend as discussed previously in Section A.1.3.

In Fig. C-10 the shear strength ratio ($v_{u,test} / f'_c$) is plotted versus the concrete cylinder strength. The shear strength ratio clearly decreases with increasing concrete cylinder strength which means that the shear strength ($v_{u,test}$) itself increases less than in direct proportion to

concrete strength. In most codes of practice, shear strength is proportional to the concrete strength to an exponent between 0.25 and 0.5.

In both Figs. C-9 and C-10 the data points are subdivided into groups with three different depth levels. A size effect can be inferred from the three data point layers although there are some exceptions.

C.2.1.2 Effective Depth

Fig. C-11 shows shear strengths plotted versus effective depths. Although only a limited number of the test beams were large, the shear strength clearly decreases as the effective depth of the member increases. The shear strengths of the members having effective depths less than about 15 inches are very high. However, most of the small size members having shear strengths greater than about 350 psi contained large amounts of longitudinal reinforcement, i.e., $\rho_l \geq 3.0\%$. On the other hand, the lower boundaries of data points are for members with low amounts of longitudinal reinforcement. This means that the longitudinal reinforcement has a significant effect on shear strength. Further, the shear strengths of large and lightly reinforced concrete members are especially low.

Many of the major codes and empirical equations account for a size effect in shear. In these expressions, the shear strength decreases as a function of the member depth. However, the expressions vary, ranging from $1/d$, $1/\sqrt{d}$, $1/d^{1/3}$, and $1/d^{1/4}$. The CSA and the AASHTO LRFD consider the size effect relationship for members without shear reinforcement in a somewhat different manner, as was described in Appendix B. These codes consider size effect to be a crack spacing parameter that is related to the distance between cracks and that crack widths are roughly proportional to crack spacing for a given level of longitudinal strain. ACI 318-02 still does not include any consideration of the size effect.

C.2.1.3 Shear Span to Depth Ratio (Moment-shear ratio)

In both Figs. C-7 and C-13, shear strengths are plotted versus shear span to depth ratios (or moment-shear ratios). However, different subgroups are used in each of these plots. Many of the test beams had an a/d ratio around 2.5. The shear strengths of members with an a/d ratio of 2.5 are clearly higher than those of the members with an a/d ratio around 3.0. This result is due to the beneficial effect of direct load transfer to the support by arch action. From the Fig. C-12 it can be seen that most members having high shear strengths are heavily reinforced, and from Fig. C-13 that those members are mostly of small size except for some members with an a/d ratio around 2.5. Fig. C-13 also shows that the members having low shear strengths, with an a/d ratio of about 3.0, are of relatively large size.

Many code provisions and empirical equations include a variable related to the shear span to depth ratio, or moment to shear ratio, in their predictions of shear capacity. However, the a/d

ratio can not be clearly defined for members subjected to uniformly distributed load, and thus it is more appropriate to use the moment to shear ratio in design code expressions than an a/d ratio.

C.2.1.4 Longitudinal Reinforcement Ratio

Fig. C-14 shows a plot of shear strengths versus the longitudinal reinforcement ratios. More than half of the test beams were heavily reinforced (i.e., $\rho_\ell \geq 2.0\%$). This fact is unfortunate as it is not representative of design practice. Only a small number of test beams contain modest amounts of longitudinal reinforcement, i.e., $\rho_\ell \leq 1.0\%$.

As can be seen in Fig. C-14, the shear strength clearly increases as the longitudinal reinforcement increases and members with $\rho_\ell \leq 1.0\%$ have lower shear strengths. Further, as the member size becomes larger, the decreases in shear strengths of lightly reinforced members increase.

Most building codes or empirical formulae account for the influence of longitudinal reinforcement ratio directly or indirectly. For example, AASHTO LRFD considers the influence of longitudinal reinforcement by using the longitudinal strain, ε_x , which is a function of the longitudinal reinforcement amount as well as other sectional forces and sectional properties.

C.2.2 Reinforced Concrete Members with Shear Reinforcement

In this section, 160 RC members with shear reinforcement are studied. Because the shear strength of RC members with shear reinforcement strongly depends on the shear reinforcement strength, the shear reinforcement strength levels are divided into 6 groups in all plots; $\rho_v f_{vy} < 100$ psi, $100 \leq \rho_v f_{vy} < 150$ psi, $150 \leq \rho_v f_{vy} < 250$ psi, $250 \leq \rho_v f_{vy} < 500$ psi, $500 \leq \rho_v f_{vy} < 1000$ psi, $\rho_v f_{vy} \geq 1000$ psi.

C.2.2.1 Concrete Strength

Fig. C-15 shows the shear strengths of RC members with shear reinforcement plotted versus their concrete cylinder strengths. The shear strengths have a large scatter but depend on the shear reinforcement strength, i.e., $\rho_v f_{vy}$. Most of the beams have ultimate shear stresses ranging from 100 to 800 psi but several beams have shear strengths of up to 1700 psi. The shear strengths increase slowly with concrete compressive strength increase, although that trend is not very clear. The influence on the shear strength of concrete compressive strength for RC members with shear reinforcement appears to be relatively smaller than the same influence for RC members without shear reinforcement.

C.2.2.2 Effective Depth

Fig. C-16 shows shear strengths plotted versus the effective depths. The shear strengths of RC members having shear reinforcement amounts less than $\rho_v f_{vy} \leq 150$ psi and depths greater than 15 inches are almost constant. The shear strengths of smaller members with similar amounts of shear reinforcement strength are a little higher. RC members with high shear reinforcement amounts do not show any significant size effect.

C.2.2.3 Shear Span to Depth Ratio (Moment- Shear Ratio)

In Fig. C-17, shear strengths are plotted versus shear span to depth ratios, a/d (or moment-shear ratios). Although strengths for members with a/d ratios of about 2.5 show a large scatter, that result is because of different shear reinforcement strengths. In each subgroup having similar shear reinforcement strengths, shear strengths do not vary much with a/d ratio increases but remain almost constant. The a/d ratio does not seem to have a significant influence on the shear strength of RC members with shear reinforcement.

C.2.2.4 Longitudinal Reinforcement Ratio

Fig. C-18 plots shear strengths versus longitudinal reinforcement ratios. Most of the test beams were heavily reinforced (i.e., $\rho_\ell \geq 2.0\%$) and only a small number contained low amounts of longitudinal reinforcement (i.e., $\rho_\ell < 1.0$ or 2.0%).

As can be seen in Fig. C-18, for members in each subgroup having similar levels of shear reinforcement, the shear strength clearly increases as the longitudinal reinforcement ratio increases. Further, the increments in shear strength for members with large amounts of shear reinforcement are greater than those for members with lower amounts of shear reinforcement. One of the reasons for this could be that dowel action is enhanced by shear reinforcement. On the other hand, if for test purposes members are heavily reinforced against flexure in order to produce shear failures, then longitudinal strain are smaller than in lightly reinforced members and thus the shear strength increases.

C.2.2.5 Shear Reinforcement

Fig. C-19 plots shear strength versus the strength of the shear reinforcement. In members with shear reinforcement, a large portion of the shear is carried by the shear reinforcement after diagonal cracking has occurred. Thus, the shear resistance of members with shear reinforcement heavily depends on the amount of shear reinforcement. In most of the major design codes, the shear resistance is limited to avoid concrete web crushing. In Fig. C-20, normalized shear strengths are plotted ($v_{u,test} / f'_c$) versus normalized strengths of the shear reinforcement ($\rho_v f_{vy} / f'_c$). Several members have shear strengths greater than $0.25 f'_c$ while most of members

have shear strengths smaller than that value. The shear strength limit (without V_p) in the current AASHTO LRFD is $0.25f'_c$.

C.2.3 Prestressed Concrete Members without Shear Reinforcement

In this section, 321 PC members without shear reinforcement are studied.

C.2.3.1 Concrete Strength

In Fig. C-21 the shear strengths of PC members without shear reinforcement are plotted versus their concrete cylinder strengths, and in Fig. C-22 the normalized ultimate shear strength ratios ($v_{u,test} / f'_c$) of those members are plotted versus the ratios of the compressive stresses at the centroids to their concrete cylinder strengths. The ultimate shear stresses of the test beams range from 100 to 1200 psi and the ratios of the compressive stresses at the centroids to their concrete cylinder strengths range from about 0.02 to 0.25. From Fig. C-21 it can be clearly seen that shear strengths increase as concrete strengths increases. On the other hand Fig. C-22 shows that normalized ultimate shear strength ratios ($v_{u,test} / f'_c$) also increase as the ratios of the compressive stresses at the centroids to their concrete cylinder strengths (f_{pc} / f'_c) increase. This result is due to the beneficial effect of the axial compressive stress caused by prestressing. That stress delays the formation of cracking and also reduces crack width.

In most codes of practice, the compressive stresses due to prestressing are taken into account. However, the methods used vary widely. In both AASHTO LRFD and CSA 2004, the longitudinal strain becomes smaller as the axial compressive stress increases and this results in greater shear strength. ACI 318-02, Eurocode EC2 (2003), and the German Code (DIN, 2001) account for the prestress directly by using the axial stress at the centroid of the section. The Japanese Code (JSCE Standards, 1986) considers the decompression moment at the extreme fiber to account for axial load as well as prestress effects.

C.2.3.2 Effective Depth

Fig. C-23 shows shear strengths plotted versus effective depths. Unfortunately, there were only two beams having effective depths greater than 20 inches and thus the influence of effective depth on shear strength is not observable from the database.

C.2.3.3 Shear Span to Depth Ratio (Moment-Shear Ratio)

Fig. C-24 shows shear strengths versus shear span to depth ratios (or moment-shear ratios) for all PC members (592 beams). Fig. C-25 shows the same plots for members with shear span to depth ratios greater than 2.4.

From Fig. C-24 it can be seen that the shear span to depth ratio (moment-shear ratio) has a strong influence on the shear strengths of members with a/d ratios less than about 2.5 while it has less influence on strengths for members with a/d ratios greater than about 2.5. This result is because, for short shear span to depth ratios, a large portion of shear force can be directly transmitted to the support without crossing a shear crack. Typical sectional analysis based models or codes give very conservative predictions in these cases. Thus, all analysis in this report use only results for members with a/d ratios greater than 2.4.

C.2.3.4 Longitudinal Reinforcement Ratio

Fig. C-26 shows shear strengths versus the longitudinal reinforcement ratios. Shear strengths clearly increase as the longitudinal reinforcement ratio increases. As observed for RC members without shear reinforcement, PC members with $\rho_\ell \leq 1.0\%$ also have very low shear strengths.

PC members with high longitudinal prestressing steel ratios have large compressive stresses and thus higher shear strengths. On the other hand, if members are heavily reinforced against flexure to ensure shear failure for test purposes, the longitudinal strains are smaller than for lightly reinforced members; thus, the shear strength increases.

C.2.4 Prestressed Concrete Members with Shear Reinforcement

In this section, results for 160 PC members with shear reinforcement are examined. Because the shear strength of PC members with shear reinforcement depends strongly on the strength of the shear reinforcement strength as is the case for RC members with shear reinforcement, shear reinforcement strength levels are again divided into 6 groups in all plots; $\rho_v f_{vy} < 100$ psi, $100 \leq \rho_v f_{vy} < 150$ psi, $150 \leq \rho_v f_{vy} < 250$ psi, $250 \leq \rho_v f_{vy} < 500$ psi, $500 \leq \rho_v f_{vy} < 1000$ psi, $\rho_v f_{vy} \geq 1000$ psi.

C.2.4.1 Concrete Strength

Fig. C-27 shows the shear strengths of PC members with shear reinforcement plotted versus their concrete cylinder strengths. The shear strengths show a large scatter but they depend on the shear reinforcement strength, i.e., $\rho_v f_{vy}$. Shear strengths increase slowly as concrete compressive strengths increase unlike the situation for PC members without shear reinforcement. Thus, the influence of concrete compressive strength on the shear strength of PC members with shear reinforcement appears to be somewhat smaller than for PC members without shear reinforcement.

C.2.4.2 Effective Depth

Fig. C-28 shows the shear strengths of PC members with shear reinforcement plotted versus their effective depths. Although only a limited number of the members were large, there appears to be no size effect for PC members with shear reinforcement. In the AASHTO LRFD, it is assumed that there is no size effect for members having at least minimum shear reinforcement. This assumption seems reasonable, at least for PC members with shear reinforcement, from the data plotted in Fig. C-28.

C.2.4.3 Shear Span to Depth Ratio (Moment-shear ratio)

Fig. C-29 shows shear strengths versus the shear span to depth ratios (or moment-shear ratios) for PC members with shear reinforcement and with shear span to depth ratios greater than 2.4. From Fig. C-29 there is no clearly observable influence of the shear span to depth ratio on shear strength for PC members with shear reinforcement.

C.2.4.4 Longitudinal Reinforcement Ratio

Fig. C-30 shows shear strengths versus longitudinal reinforcement ratios. For members with similar shear reinforcement strengths, the shear strength clearly increases as the longitudinal reinforcement ratio increases. Members with large amounts of longitudinal prestressing steel will also have large compressive stresses which in turn increases the shear strength. Shear reinforcement also enhances dowelling resistance to shear displacements along the inclined crack.

C.2.4.5 Shear Reinforcement

Fig. C-31 plots shear strengths versus shear reinforcement strengths. Clearly the shear resistance of members with shear reinforcement depends strongly on the strength of the shear reinforcement. In Fig. C-32, normalized shear strengths are plotted ($v_{u,test} / f'_c$) versus the normalized strengths of the shear reinforcement ($\rho_v f_{vy} / f'_c$). While most members have shear strengths smaller than $0.25 f'_c$, some members with large amounts of shear reinforcement have shear strengths greater than $0.25 f'_c$, which is the shear strength limit (without V_p) in the current AASHTO LRFD.

Table C-1 List of Parameters Collected and Evaluated in Shear Database

Classification	Symbols	Content	Classification	Symbols	Content
Units	units	metric/US unit			
Concrete Properties	f _c	cylinder compressive strength of concrete	Prestressing Details	E _{ps}	modulus of elasticity of prestressed reinforcement
	ε _c	net compressive strain of concrete at compressive strength		ε _{psy}	yield strain of prestressed reinforcement
	f _{cu}	cubic compressive strength of concrete		ε _{pu}	rupture strain of prestressed reinforcement
	f _{cr}	cracking strength of concrete		ρ _{op}	ratio of prestressed reinforcement = A _{ps} /b _d
	f _{cr-mr}	modulus of rupture of concrete		ρ _{owp}	ratio of prestressed reinforcement = A _{ps} /b _{wd}
	f _{cr-un}	uniaxial tensile strength of concrete		d _p	distance from extreme compression fiber to centroid of prestressed tension reinforcement
	f _{cr-sp}	split-cylinder tensile strength		A _{ps}	area of prestressed reinforcement in tension zone
	f _{cr-dp}	double-punch tensile strength		d _{bp}	diameter of prestressed reinforcement
	agg	maximum aggregate size		F _{st}	applied force in prestressed reinforcement
	gamc	density of concrete		f _{st}	applied stress in prestressed reinforcement
age	age of specimen	F _{se}	effective force in prestressed reinforcement (after allowance for all prestress losses)		
Cross-Section	shape	rectangular/T-shape/I-shape	(con'd)	f _{se}	effective stress in prestressed reinforcement (after allowance for all prestress losses)
	b _{slab}	width of slab	V _p	vertical component of effective prestress force at section	
	t _{slab}	thickness of slab	f _{ps}	stress in prestressed reinforcement at nominal strength	
	h	overall depth of member	ρ _{owp'}	ratio of prestressed reinforcement = A' _{ps} /b _{wd}	
	b	width of member	d' _p	distance from extreme compression fiber to centroid of prestressed reinforcement on compression side	
	b _w	web width of member	A' _{ps}	area of prestressed reinforcement in compression zone	
	b _{top}	width of top flange	d' _{bp}	diameter of prestressed reinforcement on compression side	
	b _{bot}	width of bottom flange	F' _{se}	effective force in prestressed reinforcement on compression side (after allowance for all prestress losses)	
	t _{top}	thickness of top flange	f' _{se}	effective stress in prestressed reinforcement on compression side (after allowance for all prestress losses)	
	t _{bot}	thickness of bottom flange	Prestress method	pre-tension/post-tension	
A _g	gross area of section	Bond	bond status of prestressed reinforcement (bonded/unbonded)		
I _g	moment of inertia of gross-section	Vertical Shear Reinforcement	f _{vy}	yield strength of vertical reinforcement	
bar type	deformed/plain bar		f _{uv}	ultimate strength of vertical reinforcement	
f _y	yield strength of nonprestressed reinforcement		A _v	area of shear reinforcement perpendicular to flexural tension reinforcement	
f _u	ultimate tensile strength of nonprestressed reinforcement		sv	spacing of vertical web reinforcement	
E _s	modulus of elasticity of reinforcement		θ	angle between inclined stirrups and longitudinal axis of member	
ε _{py}	yield strain of reinforcement		ρ _{ov}	vertical shear reinforcement ratio(=A _v /(b _w *sv))	
ρ _o	ratio of nonprestressed tension reinforcement =A _s /b _d		f _{yh}	yield strength of horizontal web reinforcement	
ρ _{ow}	ratio of nonprestressed tension reinforcement =A _s /b _{wd}		A _h	area of shear reinforcement parallel to flexural tension	
d	distance from extreme compression fiber to centroid of nonprestressed reinforcement on the layer of tension side		sh	spacing of horizontal web reinforcement	
A _s	area of nonprestressed longitudinal reinforcement on flexural tension side having distance d from extreme compression fiber		ρ _{oh}	horizontal shear reinforcement ratio(=A _v h/(b _w *sh))	
db	bar diameter on the layer of tension side	Test Set-up	Diagram	diagram of setting specimen	
ns	number of longitudinal reinforcement on flexural tension side		Set-Up	support condition & loading form	
sc	side cover		a/d	shear span to depth ratio	
dc	distance from extreme compression fiber to centroid of nonprestressed reinforcement on the layer of compression side		Lent	entire length of specimen	
A _{sc}	area of nonprestressed longitudinal reinforcement on flexural compression side having distance dc from extreme		L	distance between center of supports	
dbc	bar diameter on the layer of compression side		a	shear span measured from center of support to center of loading point	
f _{pci}	compressive strength of concrete at time of initial prestress		a'	distance between concentrated load and face of support	
age@ps	days after casting when the prestressing forces were transmitted to the concrete beams		L _n	distance between face of supports	
y _{ps}	distance from centroidal axis of gross section, neglecting reinforcement, to prestressed reinforcement in tension		M _n	nominal moment strength at section	
y _b	distance from centroidal axis of gross section, neglecting reinforcement, to extreme fiber in tension		M _{cr}	moment causing flexural cracking at section due to externally applied loads (ACI eq. 11-11)	
y _t	distance from centroidal axis of gross section, neglecting reinforcement, to extreme fiber in compression	M _{uf}	bending moment occurring simultaneously with shear force V _{ult} at the cross section considered		
f _{pc}	compressive stress in concrete (after allowance for all prestress losses) at centroid of cross section resisting externally applied loads or at junction of web and flange when	V _{nf}	shear force when a member reaches its flexural capacity		
f _{pe}	compressive stress in concrete due to effective prestress forces only (after allowance for all prestress losses) at extreme fiber of section where tensile stress is caused by externally applied loads	V _{ult} /V _{nf}	ratio of ultimate shear force to shear force at flexural failure		
strand type	type of prestressing steel (1,2,3,4,5,6,7) 1. seven-wire strand (f _{pu} =270 ksi) 2. seven-wire strand (f _{pu} =250 ksi) 3. three- and four-wire strand (f _{pu} =250 ksi) 4. prestressing wire 5. smooth prestressing bars (f _{pu} =145 ksi) 6. smooth prestressing bars (f _{pu} =160 ksi) 7. deformed prestressing bars	V _{cr}	cracking shear force		
f _{py}	yield strength of prestressed reinforcement	V _{ult}	ultimate shear force		
f _{pu}	ultimate tensile strength of prestressed reinforcement	ν _u	ultimate shear stress		
		V _{n,pred}	nominal shear capacity predicted by codes or other researchers such as ACI, LRFD, and etc.		
		V _{ult} /V _{n,pred}	shear strength ratio of test values to prediction		
		L-D	load-deflection diagram		
		Crack diagram	crack diagram		
		Failure mode1	failure mode defined by authors		
		Failure mode2	failure mode defined by ratio of V _{ult} /V _{nf} (V _{ult} /V _{nf} <1.0 : shear failure, V _{ult} /V _{nf} >1.0 : flexural failure)		

Note) This table is to illustrate the details of information compiled into SDB. The notations used in this table do not necessarily represent those used in other part of this report.

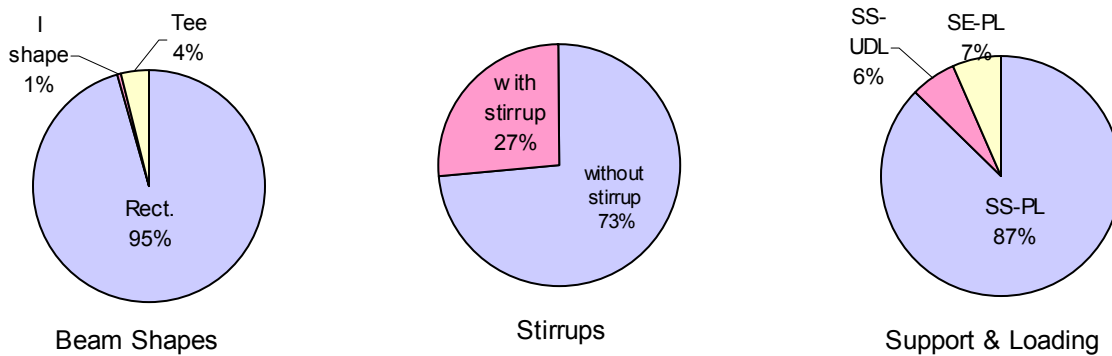


Fig. C-1 General Characteristics of RC Beams in Database (1444 tests)

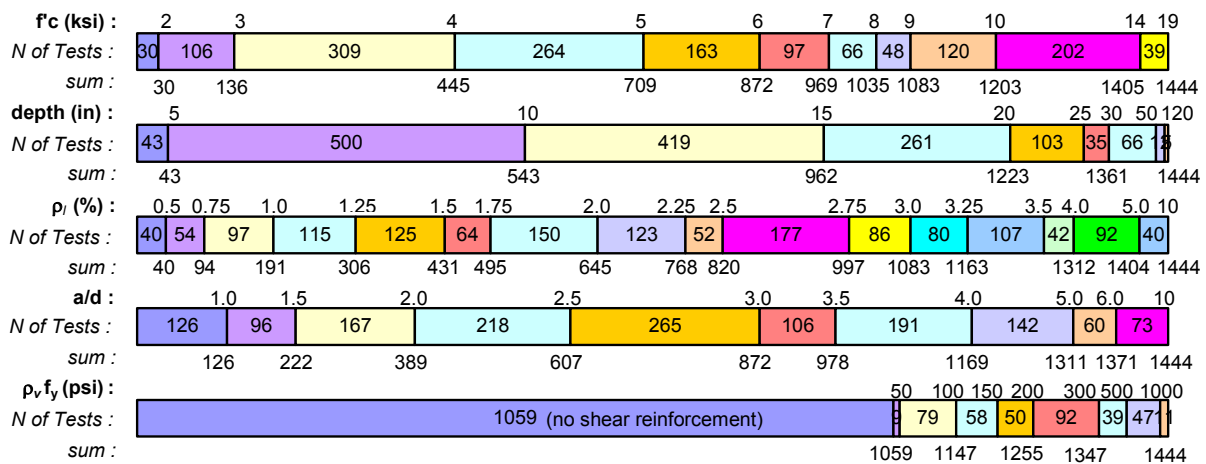


Fig. C-2 Distribution of Parameters of RC Beams in Database (1444 tests)

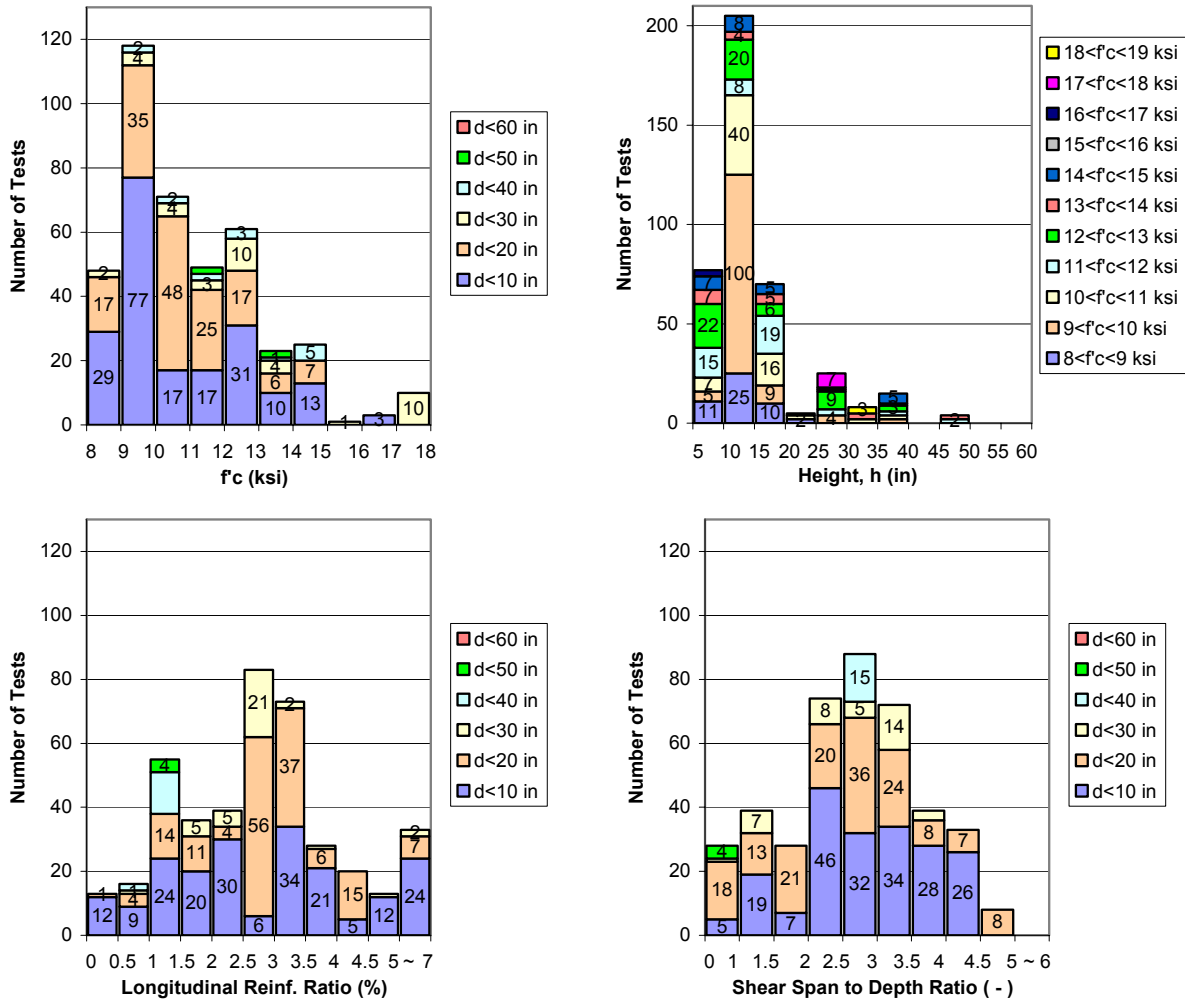


Fig. C-3 Distribution of Parameters of RC High Strength Concrete Beams in Database (409 tests)

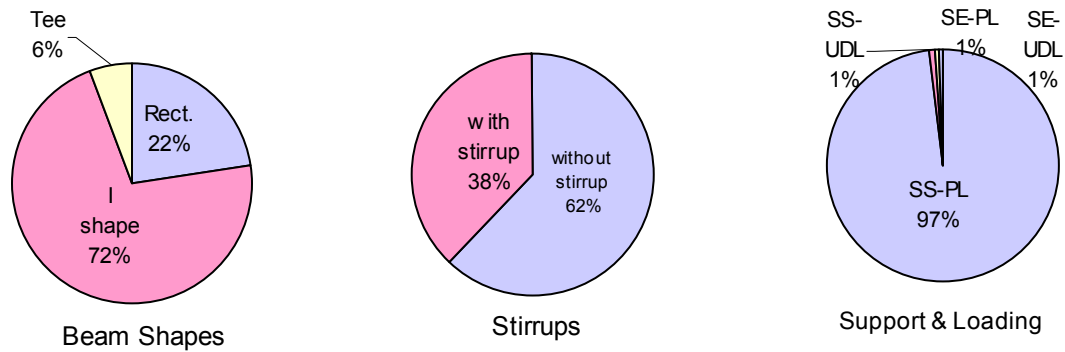


Fig. C-4 General Characteristics of PC Beams in Database (743 tests)

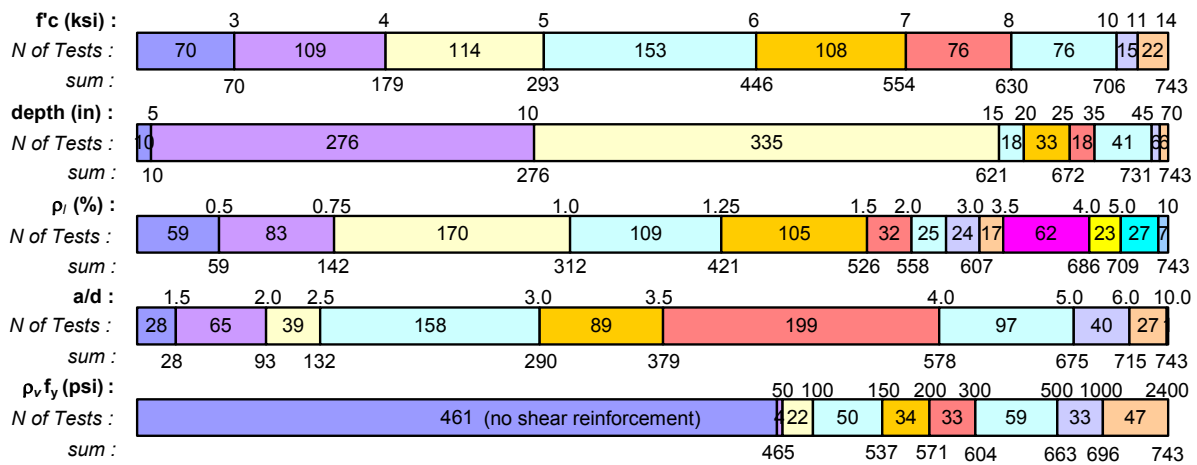


Fig. C-5 Distribution of Parameters of PC Beams in Database (743 tests)

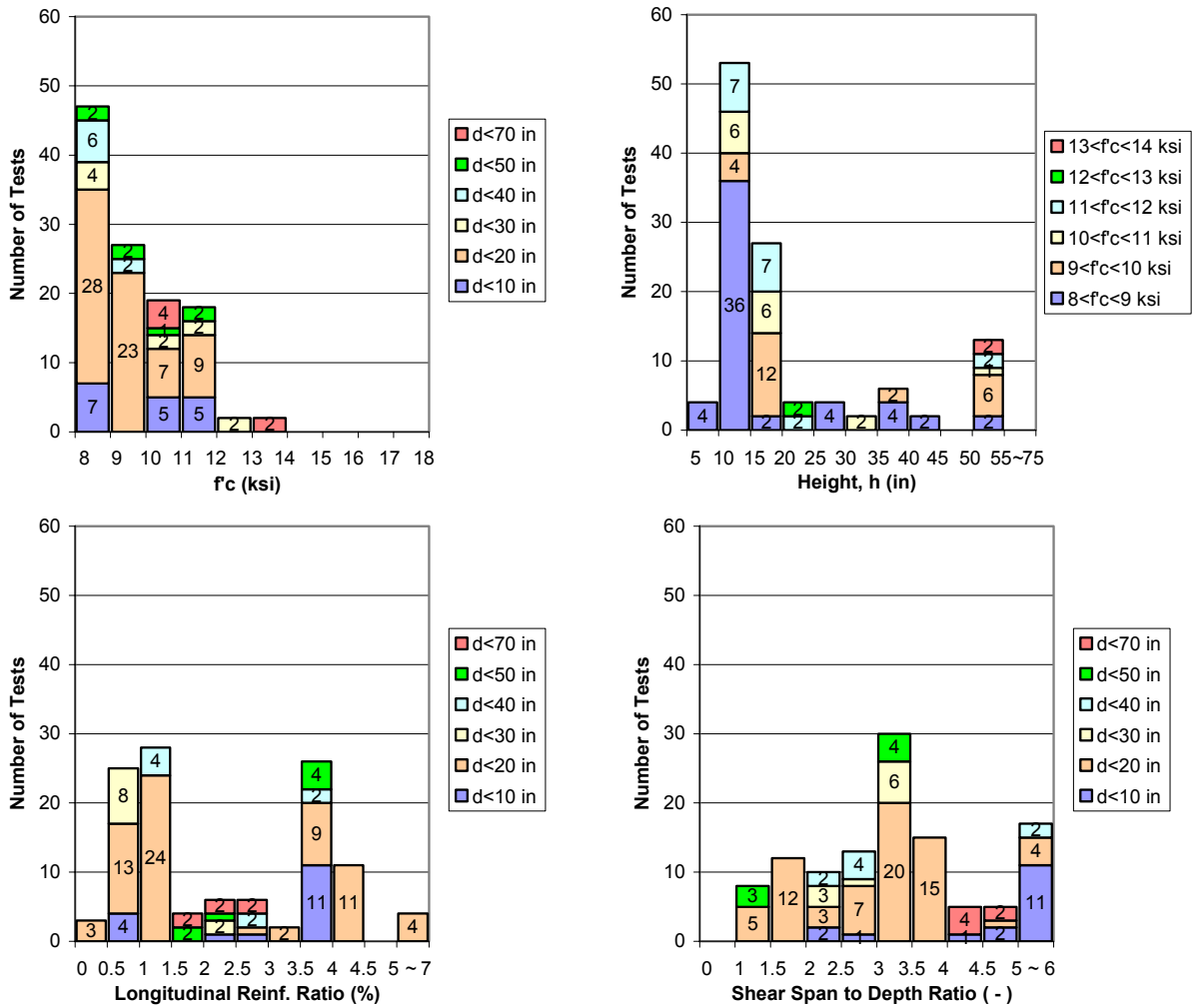


Fig. C-6 Distribution of Parameters of PC High Strength Concrete Beams in Database (115 tests)

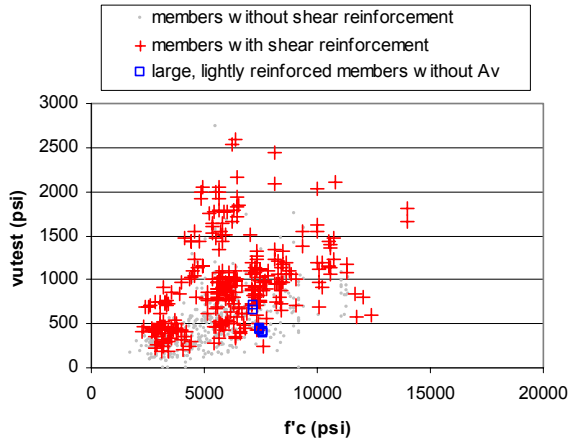


Fig. C-7 Ultimate Shear Stress ($v_{u,test}$) at Failure versus Concrete Compressive Strength (f'_c) of RC Members

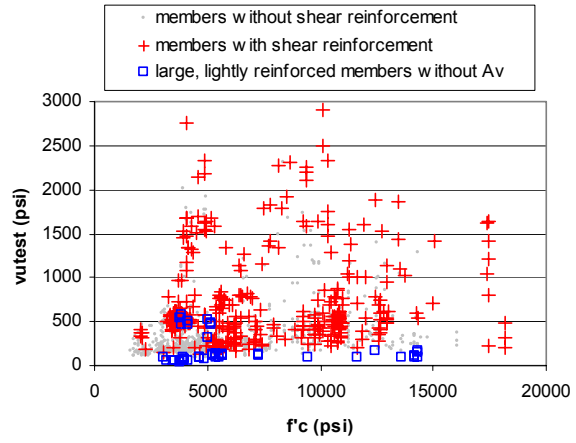


Fig. C-8 Ultimate Shear Stress ($v_{u,test}$) at Failure versus Concrete Compressive Strength (f'_c) of PC Members

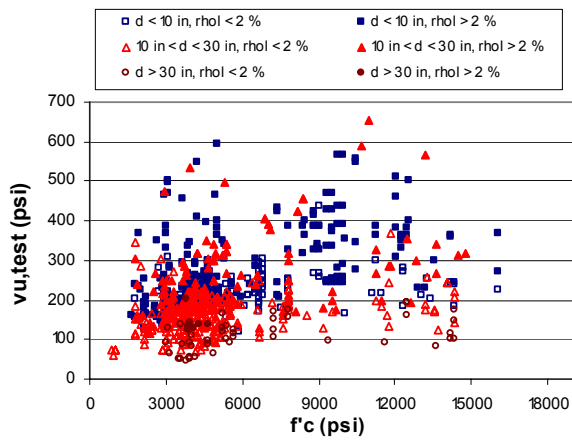


Fig. C-9 Ultimate Shear Stress ($v_{u,test}$) at Failure versus Concrete Compressive Strength (f'_c) of RC Members without Shear Reinforcement

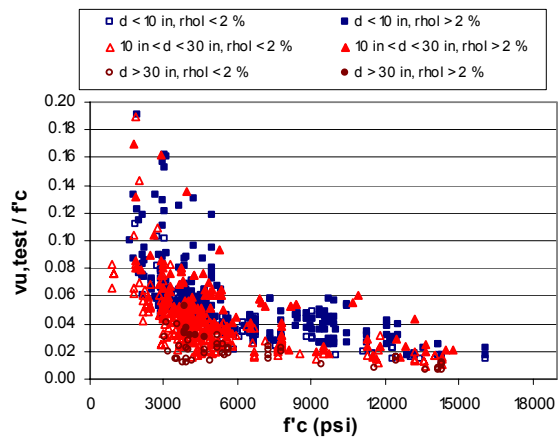


Fig. C-10 Ultimate Shear Strength Ratio ($v_{u,test}/f'_c$) versus Concrete Compressive Strength (f'_c) of RC Members without Shear Reinforcement

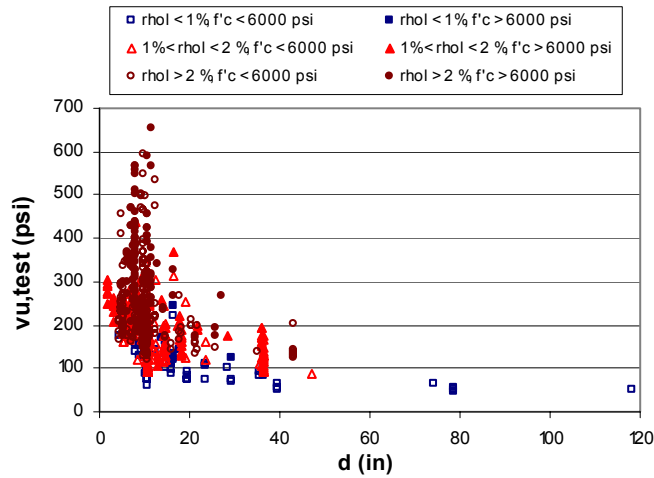


Fig. C-11 Ultimate Shear Stress ($v_{u,test}$) at Failure versus Effective Depth of RC Members without Shear Reinforcement

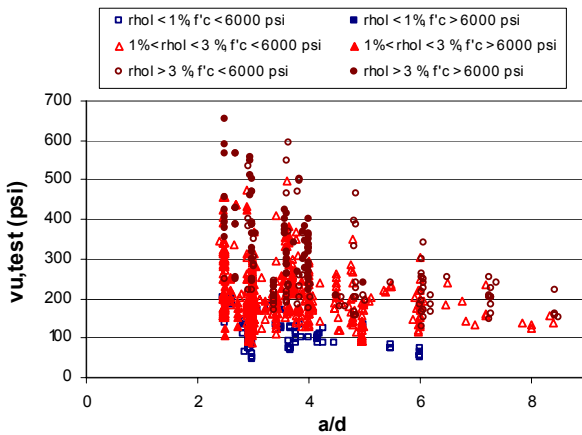


Fig. C-12 Ultimate Shear Stress ($v_{u,test}$) at Failure versus Shear Span to Depth Ratio for RC Members without Shear Reinforcement

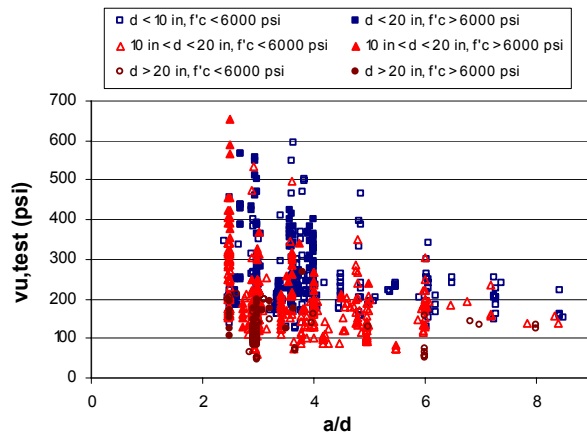


Fig. C-13 Ultimate Shear Stress ($v_{u,test}$) at Failure versus Shear Span to Depth Ratio for RC Members without Shear Reinforcement

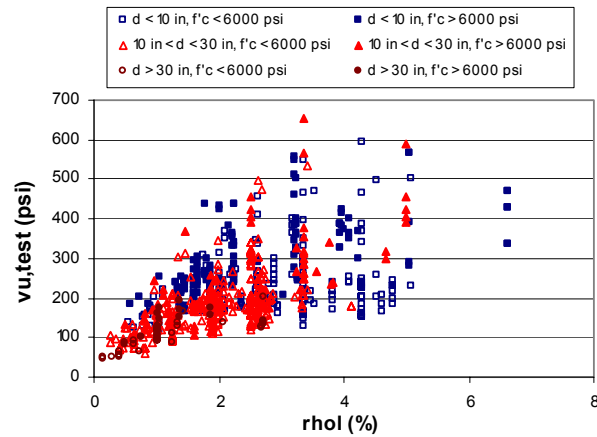


Fig. C-14 Ultimate Shear Stress ($v_{u,test}$) at Failure versus Longitudinal Reinforcement Ratio for RC Members without Shear Reinforcement

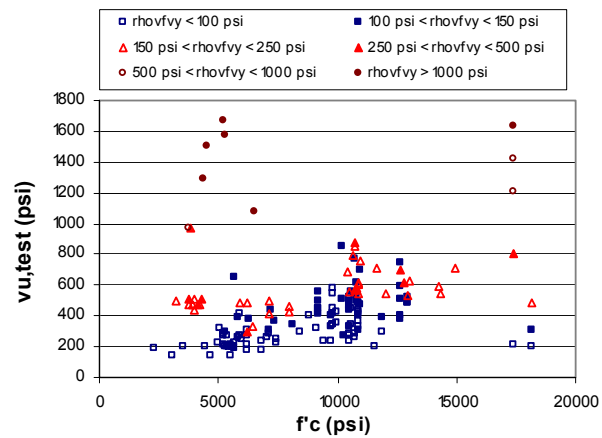


Fig. C-15 Ultimate Shear Stress ($v_{u,test}$) at Failure versus Concrete Compressive Strength (f'_c) of RC Members with Shear Reinforcement

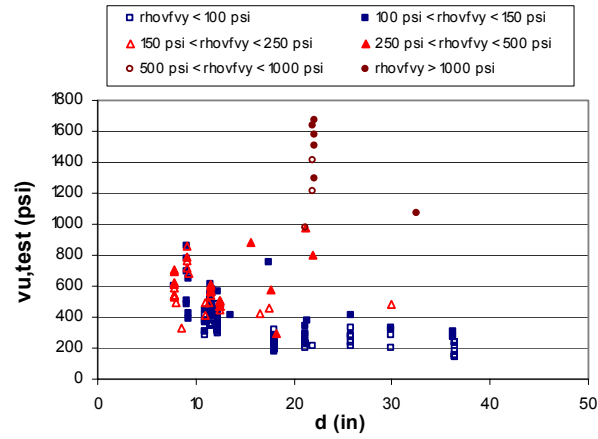


Fig. C-16 Ultimate Shear Stress ($v_{u,test}$) at Failure versus Effective Depth of RC Members with Shear Reinforcement

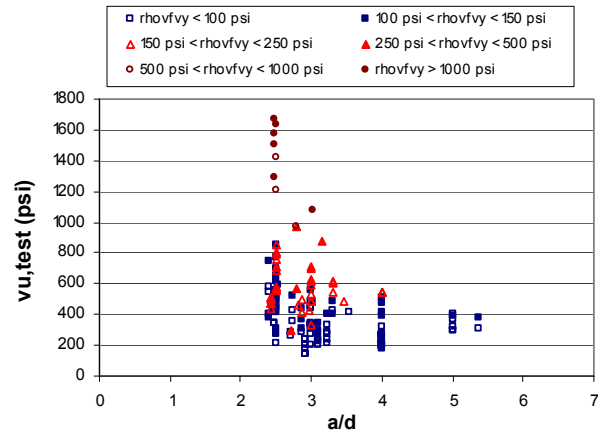


Fig. C-17 Ultimate Shear Stress ($v_{u,test}$) at Failure versus Shear Span to Depth Ratio for RC Members with Shear Reinforcement

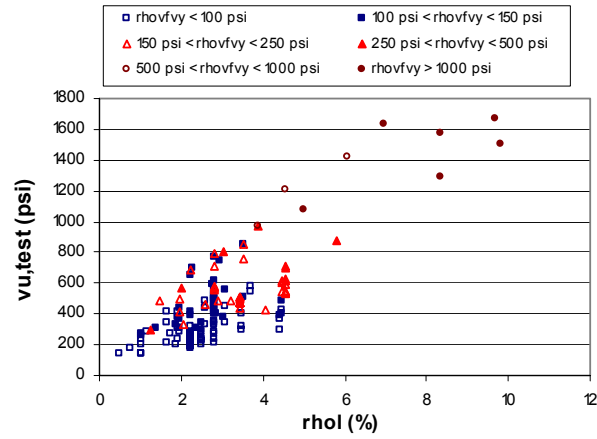


Fig. C-18 Ultimate Shear Stress ($v_{u,test}$) at Failure versus Longitudinal Reinforcement Ratio for RC Members with Shear Reinforcement

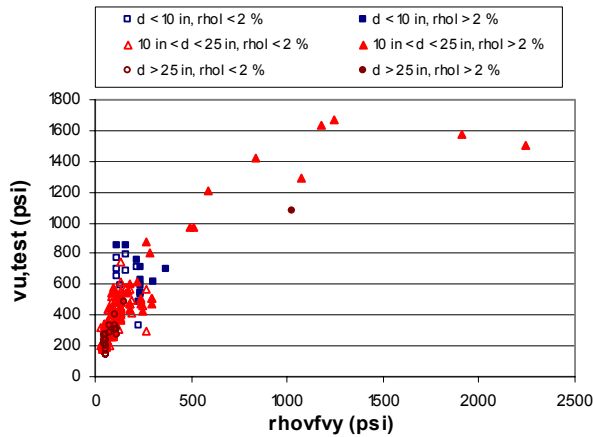


Fig. C-19 Ultimate Shear Stress ($v_{u,test}$) at Failure versus Strength of Shear Reinforcement for RC Members with Shear Reinforcement

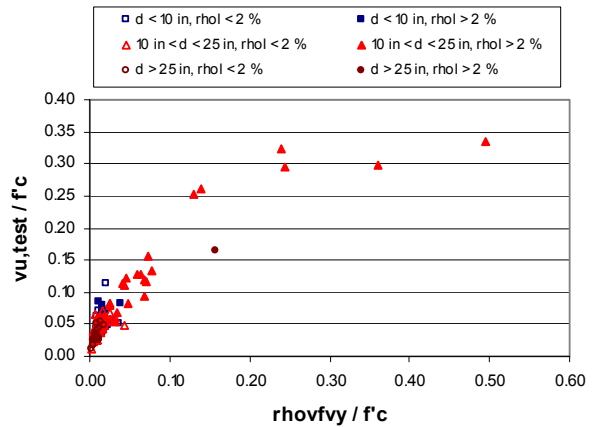


Fig. C-20 Normalized Ultimate Shear Stress ($v_{u,test}$) at Failure versus Normalized Strength of Shear Reinforcement for RC Members with Shear Reinforcement

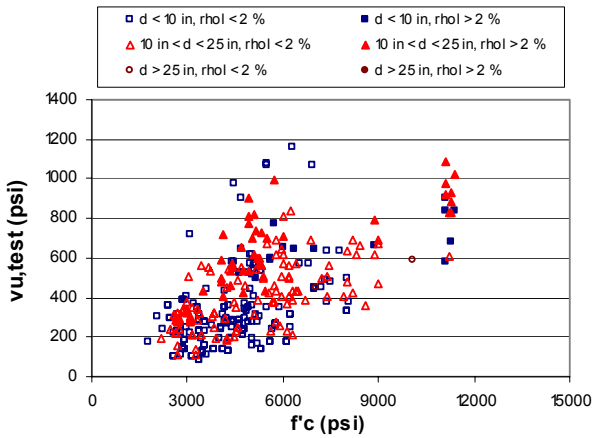


Fig. C-21 Ultimate Shear Stress ($v_{u,test}$) at Failure versus Concrete Compressive Strength (f'_c) of PC Members without Shear Reinforcement

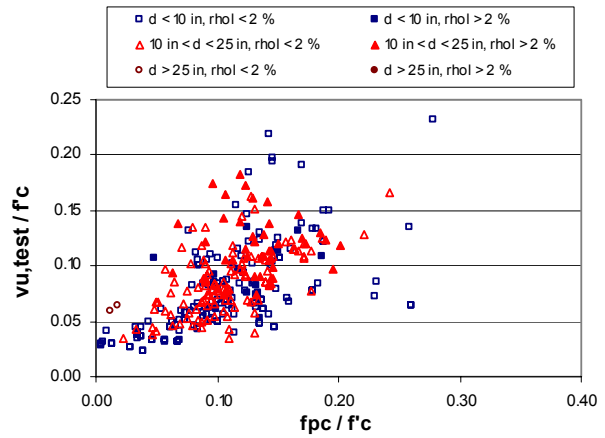


Fig. C-22 Normalized Ultimate Shear Strength Ratio ($v_{u,test}/f'_c$) versus Ratio of Compressive Stress at Centroid to Concrete Compressive Strength (f_{pc}/f'_c) of PC Members without Shear Reinforcement

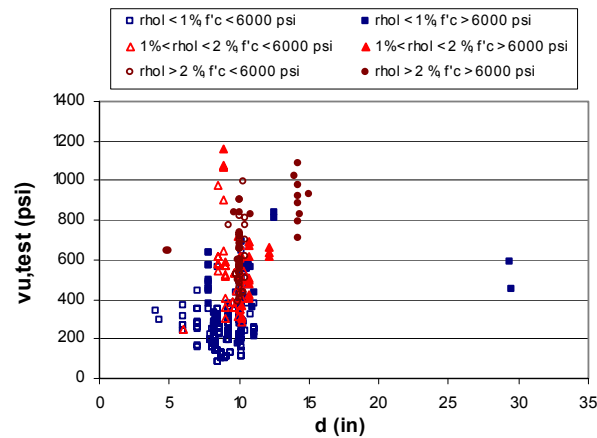


Fig. C-23 Ultimate Shear Stress ($v_{u,test}$) at Failure versus Effective Depth of PC Members without Shear Reinforcement

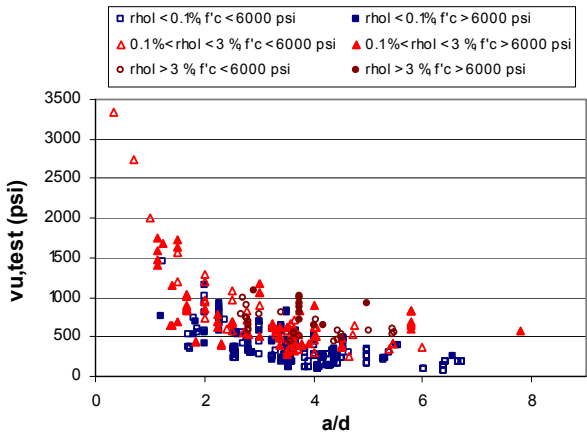


Fig. C-24 Ultimate Shear Stress ($v_{u,test}$) at Failure versus Shear Span to Depth Ratio for All PC Members without Shear Reinforcement

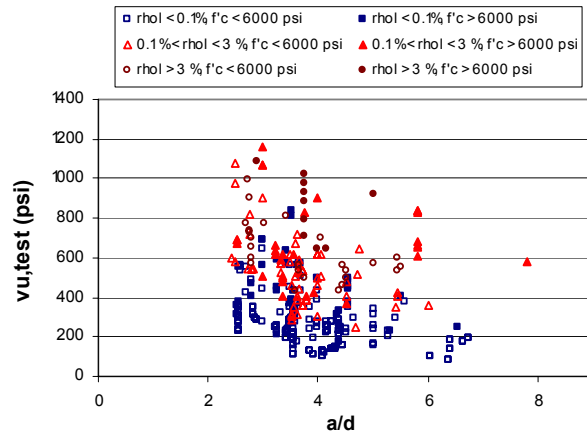


Fig. C-25 Ultimate Shear Stress ($v_{u,test}$) at Failure versus Shear Span to Depth Ratio for PC Members without Shear Reinforcement ($a/d > 2.4$)

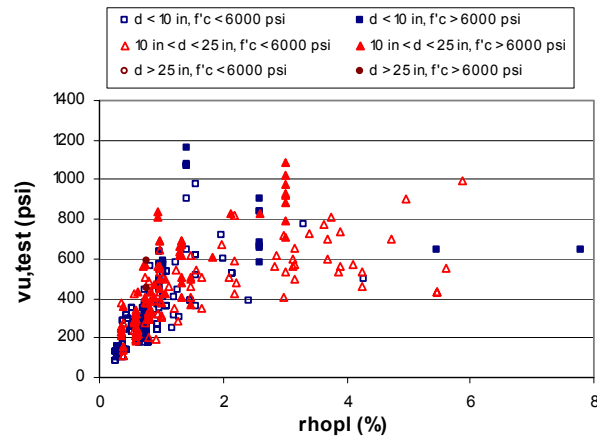


Fig. C-26 Ultimate Shear Stress ($v_{u,test}$) at Failure versus Longitudinal Reinforcement Ratio for PC Members without Shear Reinforcement

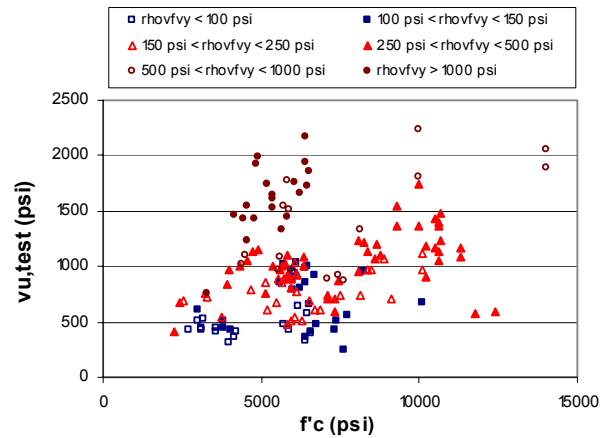


Fig. C-27 Ultimate Shear Stress ($v_{u,test}$) at Failure versus Concrete Compressive Strength (f'_c) of PC Members with Shear Reinforcement

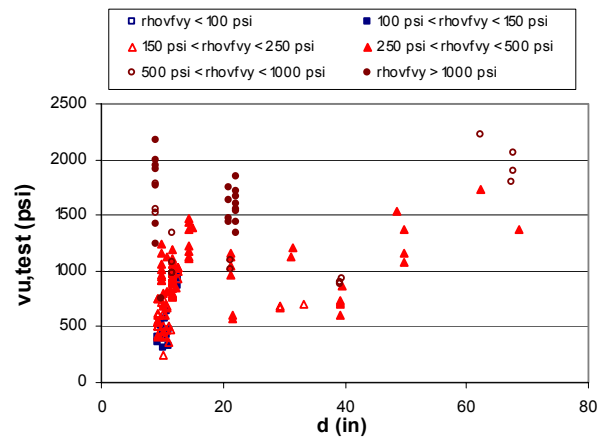


Fig. C-28 Ultimate Shear Stress ($v_{u,test}$) at Failure versus Effective Depth of PC Members with Shear Reinforcement

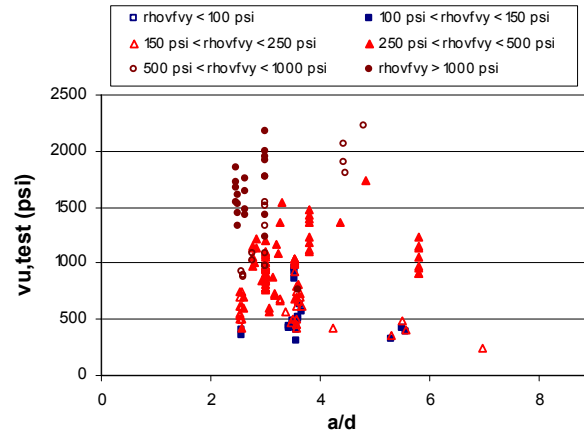


Fig. C-29 Ultimate Shear Stress ($v_{u,test}$) at Failure versus Shear Span to Depth Ratio for PC Members with Shear Reinforcement

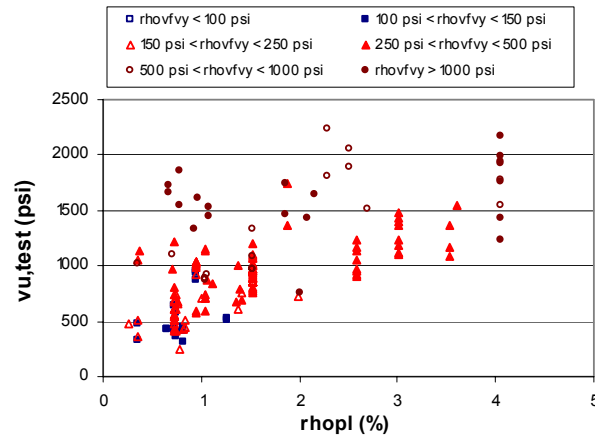


Fig. C-30 Ultimate Shear Stress ($v_{u,test}$) at Failure versus Longitudinal Reinforcement Ratio for PC Members with Shear Reinforcement

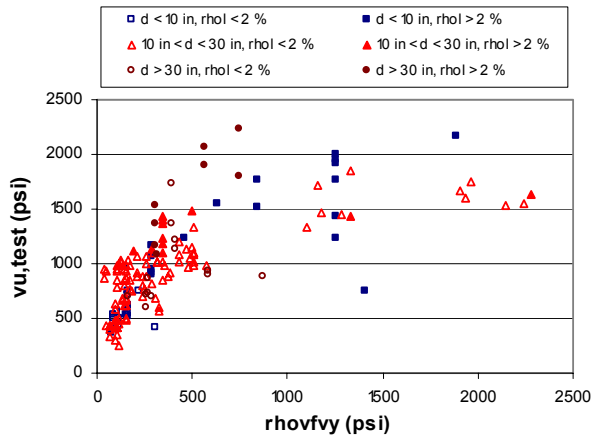


Fig. C-31 Ultimate Shear Stress ($v_{u,test}$) at Failure versus Strength of Shear Reinforcement for PC Members with Shear Reinforcement

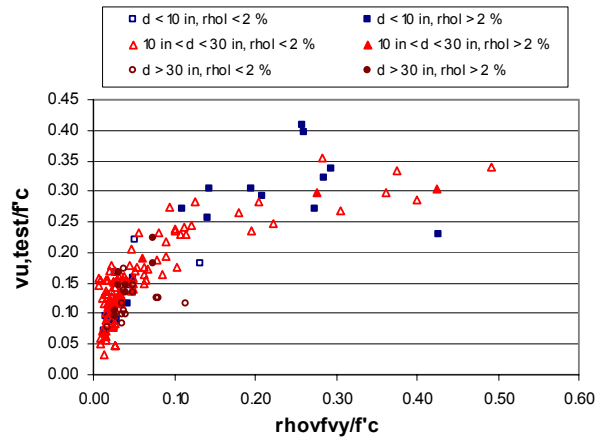


Fig. C-32 Ultimate Shear Stress ($v_{u,test}$) at Failure versus Strength of Shear Reinforcement for PC Members with Shear Reinforcement

APPENDIX D: Evaluation of Shear Design Provisions

In this appendix an evaluation of several shear design approaches is presented. In Section D.1, the relative strengths and weaknesses of six different codes of practice are assessed based on statistical values of strength ratios for the experimental test data of the shear database presented in Appendix C. In Section D.2, the selected shear design approaches are evaluated using selected members from the shear database.

D.1 Initial Assessment of Codes of Practice

A total of 1359 test results are compared to predictions by six national design codes. These codes are: *AASHTO Standard Specification (1989) (same as ACI 318-02)*; *AASHTO LRFD Bridge Design Specifications (2001)*; *CSA A23.3 2004 edition (Collins, 2002)*; *Japanese Code (JSCE Standards, 1986)*; *Eurocode EC2, Part 1(2003)*; and the *German Code (DIN, 2001)*.

Comparisons are made only for members with shear span to depth ratios (a/d ratios) greater than 2.4 and that satisfy the check that the measured ultimate moment was less than the calculated yield moment, $M_u < M_y$. These two restrictions reduced the total number of test results in the database from just over 2000 to 1359 of which 878 are RC members and 481 are PC members. For this comparison, all strength reduction factors and material strength reduction factors are set equal to unity.

D.1.1 Comparison of Predicted Strengths and Limitations of Codes

Table D-1 provides the Means and COVs for the ratio of V_{test}/V_{code} for the six codes of practice examined. The categories of test data are divided by member type reinforced or prestressed, (RC or PC), and whether or not shear reinforcement (A_v) was provided. The number of data points used to calculate the Mean and COV are shown in the third row labeled “count”.

The following observations can be made from an examination of the data in Table D-1:

(i) The COV for these methods ranged from 0.147 to 0.687 with most COVs being between 0.3 and 0.4. For making relative evaluations, a COV of less than 0.15 may be considered excellent, from 0.15 - 0.20 very good, from 0.20 - 0.25 good, from 0.25 - 0.30 reasonable, from 0.30 – 0.35 poor, and greater than 0.35 is bad.

(ii) The overall COV for the ACI 318 method (AASHTO Standard Specification) is bad; with the provisions performing most poorly for reinforced concrete (i.e. non-prestressed) members that do not contain shear reinforcement. The performance of the ACI provisions for the other three subcategories of members ranged from 0.221 to 0.277, a result considered good to reasonable. Clearly from Table D-1, the deficiency in the ACI provisions is with its expression for the shear strength of reinforced concrete beams without shear reinforcement. ACI Committee 445 on Shear and Torsion has been re-examining that expression at the request of ACI Committee 318-E which is charged with initiating changes to the ACI 318 Code provisions that deal with shear and torsion. In particular, ACI 318-E has identified that the expression needs a factor that reduces the shear strength as the depth of the member increases. ACI-ASCE 445 has identified that, not only does such a factor need to be introduced, but that the expression also probably needs to vary with the reinforcement ratio and to perhaps be less dependent on the concrete strength than the current formula.

(iii) The overall performances of the LRFD and CSA provisions are very similar, which is not surprising considering that they both are derived from the modified compression field theory. The overall performances for all subcategories were good to reasonable. Further for PC members with shear reinforcement the performance of both methods was essentially excellent.

(iv) The overall performance of the JSCE method was reasonable; with the best performance being for RC members with shear reinforcement.

(v) The performance for the EC2 and DIN methods were uniformly poor to bad.

(vi) Another very important measure of performance is the variation in the Mean for all categories of test data. As can be seen, the Mean for ACI ranged from 1.21 for PC members with shear reinforcement to 1.54 for RC members without shear reinforcement. The lowest variation in the Mean was for the LRFD and CSA methods. That result suggests that these methods provide the most uniform factor of safety against failure. The largest variation was for the DIN method in which the Mean ranged from 1.25 to 2.59.

(vii) If one of the six design methods were to be selected purely on the basis of performance, then either the LRFD or CSA method would be selected. This conclusion is particularly applicable if the prime emphasis is on the performance of PC members containing shear reinforcement.

Table D-2 presents the Means and COVs for non-prestressed (RC) members that do not contain shear reinforcement. Subcategories divide the members into normal and high-strength concrete members, small and large size members, stocky and slender members, and members with light and heavy amounts of longitudinal tension reinforcement.

The following observations can be made from an examination of the data in Table D-2.

(i) The COV for the ACI method is essentially bad for all categories. There is also a large variation in the Means which is of particular concern for members with depths greater than 24 inches for which the Mean is 0.76 and for members lightly reinforced in flexure ($\rho_{ol} < 1\%$) for which the Mean is 0.88.

(ii) The CSA, LRFD, and JSCE provisions all have relatively good COVs and a limited variation in Means.

(iii) The COVs for the EC2 and DIN methods are slightly higher than for the CSA, LRFD and JSCE provisions as is the variation in Means over the subcategories.

Table D-3 presents the Means and COVs for non-prestressed (RC) members that contain shear reinforcement ($A_v > 0$) for all six codes examined. The subcategories are normal and high strength concrete members, small and large sized members, members with light and heavy amounts of shear reinforcement, and members with light and heavy amounts of longitudinal tension reinforcement.

The following observations can be made from reviewing Table D-3.

(i) The COVs for all codes of practice are considerably lower for most categories of members with shear reinforcement than for members without shear reinforcement. The COVs for the LRFD, CSA, and JSCE provisions are particularly good. The COV for the EC2 method is the largest, particularly for normal strength concrete members, for small sized members, and for heavily reinforced members.

(ii) The variations in the Means for the LRFD, CSA, and JSCE methods are reasonably low. The variations in the Mean for the ACI method is reasonable, with the lowest Means being recorded for large members and those containing small amounts of flexural reinforcement.

(iii) The variation in Means for the EC2 and DIN methods are very large.

Table D-4 presents Means and COVs for prestressed concrete members without shear reinforcement. The subcategories are normal and high strength concrete members, small and large size members, short and slender members, and members with light and heavy amounts of longitudinal tension reinforcement.

The following observations can be made from Table D-4.

(i) The first four methods (ACI, LRFD, CSA, and JSCE) all result in similar COVs for all subcategories.

(ii) The COVs for members cast with high strength concretes are significantly less than those for other subcategories for most of the codes.

(iii) The COVs for the two subcategories containing the smallest number of test results were generally much smaller than for other subcategories.

(iv) The variations in the Means for the ACI, LRFD, and CSA methods are significantly less than for the other three codes.

(v) The EC2, and particularly the DIN, methods are conservative for all categories of test data.

Table D-5 presents the Means and COVs for prestressed members that contain shear reinforcement for all six codes examined. The subcategories of member types are normal and high-strength concrete members, small and large size members, short and slender members, members with light and heavy amounts of shear reinforcement, and members with light and heavy amounts of longitudinal tension reinforcement.

From Table D-5, the following observations can be made.

(i) The COVs for the LRFD and CSA methods are very good to excellent and reasonably consistent across all subcategories. The variations in the Means for LRFD and CSA methods are also very small.

(ii) The COV for the ACI method is also good and the variation in the Mean is similarly low.

(iii) The COV for the JSCE method is reasonable and consistent. The variation in Mean for the JSCE method is small.

(iv) The performance of the EC2 method was poor both in terms of the COV and the variation in the Mean.

(v) The performance of the DIN method was reasonable but not as good as the LRFD, CSA, ACI or JSCE provisions.

Table D-6 presents the Means and COVs for specifically selected types of members that highlight the strengths and weaknesses of the six codes of practice examined. The characteristics of each member subcategory are described by footnotes to the table where the number key is given in parentheses in row 2 of the table.

The following observations can be made from Table D-6:

(i) The Mean for the ACI provisions is particularly low for large members that do not contain shear reinforcement and have small amounts of longitudinal reinforcement.

(ii) The COVs for the LRFD and CSA methods are particularly good for PC members containing shear reinforcement. The variations in the Mean by these two methods varied considerably between large high-strength concrete RC members without shear reinforcement and that for large high-strength concrete PC members without shear reinforcement.

(iii) The variations in the Means for the JSCE, EC2 and DIN methods are large for these distinctively different subcategories.

D.1.2 Summary of Observations

For the four broad categories of RC members with and without shear reinforcement and PC members with and without shear reinforcement, a different version of Table D-1 is given in Table D-7 in accordance with which the performance of the codes can be further compared.

The important observations made from an examination of Tables D-1 through D-7 are as follows:

(i) The variation in the Means of the LRFD and CSA methods between major categories is small relative to other codes.

(ii) The COVs of the LRFD and CSA methods are the lowest of the six codes examined and reasonably uniform over all the subcategories of member types.

(iii) There is little difference in the COVs and Means between the LRFD and CSA methods for all categories and subcategories. This result is to be anticipated because both of methods were derived from the modified compression field theory.

(iv) The overall performance of the ACI provisions, considering the variations in the COVs and Means between the categories is reasonable to good, except for non-prestressed (RC) members without shear reinforcement.

(v) The overall performance of the JSCE provisions is reasonable, with the best COV being for RC members with shear reinforcement.

(vi) The overall performance of the EC2 and DIN methods is poor.

(vii) Using the variations in the Means for the four major member categories and the values of the COVs in each of these categories, the shear design provisions of the LRFD and CSA methods provide the most accurate and consistent predictions of capacity.

In utilizing the shear database of test results for assessing the accuracy of codes of practice, the shortcomings of past experimental research efforts in shear are very evident. Researchers have unfortunately focused the majority of their efforts on testing members without shear reinforcement, that have rectangular cross-sections, that are simply supported, that are loaded by point loads, and that are heavily reinforced in flexure. Because the distribution of members in the experimental test database does not well represent what is built using design code provisions, the results presented in Table D-1 to D-7 do not provide a full assessment of the reliability of those codes. For this reason, further comparisons of the different shear design approaches are desirable using selected members that are representative of actual members built in field.

D.1.3 Remarks on Relationships between Statistical Values and Safety of Design Approach

In the evaluation of the results, it is useful to consider the relationship between the Mean, the COV, and the Fractile value. For the development of codes of practice, the Fractile level refers to the percentage of members that, if designed by the provisions, would be expected to fail if the full factored load were applied to the test structure. This concept is now illustrated in an example using data from Table D-7 for all members for the ACI provisions. As shown in Fig.D-1 the mean ratio of $V_{\text{test}}/V_{\text{aci}}$ is 1.44, the standard deviation, σ , is 0.53, and the corresponding Coefficient of Variation (COV) is 0.37. Note that the standard deviation is the square root of the square of the differences between the mean and individual data points divided by the number of samples while the COV is the standard deviation divided by the mean. Using a commonly assumed Gaussian distribution of experimental data, it is then possible to calculate the likelihood that a test result may be less than any selected $V_{\text{test}}/V_{\text{code}}$ ratio. In this example, the percentage of the test data beneath $V_{\text{test}}/V_{\text{code}} = 1.0$ is equal to 20.45%.

The appropriate Fractile level (predicted percentage of cases for which the design strength is less than the ultimate design force (i.e. $\phi V_n \leq V_u$)), is frequently a source of debate at code committee meetings. Opinions range from the proper value being as low as 5% to it being acceptable that the value can be as high as 30%. The drawback to a procedure having a large COV is that the design code relationship needs to be adjusted (calibrated) so that it is very conservative for most design situations in order to keep the risk of a failure to low. If the design code relationship is not adjusted (calibrated) to an appropriate Mean, then the values used in the load factors and strength reduction factors cease to have their intended meaning. The properties of the data used for derivation of the current ACI Code expression for the shear strength of beams without shear reinforcement are not very representative of the properties of the beams now most frequently designed in practice. Further the scatter in the original data effectively required the use of a strength reduction factor for shear considerably less than that for flexure. The use of a database with specimen properties more representative of those used in practice and the use of a low fractile value such as 5% should allow the use of a strength reduction factor for shear only marginally lower than that for flexure.

The influence of the selected Fractile level, F , and the required Mean, u , for the $V_{\text{test}}/V_{\text{code}}$ ratio is illustrated by using the following relationship and the preceding ACI example

$$F = \Phi\left(\frac{x_0 - \mu}{\sigma}\right) \text{ and thus } u = \frac{1}{\Phi^{-1}(F) \cdot COV + 1}$$

For ACI, the current Mean, $u = 1.44$, and the Fractile level is 20.45%. If the Fractile level is reduced to 10%, which corresponds to a more conservative margin of safety against failure, then the design code relationship needs to be adjusted so that the ratio of $V_{\text{test}}/V_{\text{code}}$ is 1.90. In Table D-8, the relationship between the Fractile level and the required Mean for the shear provisions of the ACI Code is shown based on the results in the shear experimental database.

The calibration of design code relationships using the COVs found from test data assumes that the member types in the experimental database are representative of the members designed

using the code relations. While this is not completely valid, it is probably the best possible way to proceed given the available information.

The calibration of a design code relationship must also consider that it is important to create a relationship with simple constants so that the designer and the checker can more easily remember the relationship and so as not to imply a level of precision in the relationship inconsistent with the accuracy of the relationship.

D.2 Evaluation of Shear Design Provisions Using Selected Members from Shear Database

In Section D.1, a statistical evaluation of six design provisions was made using an extensive database of test results. One drawback to this approach is that the database is heavily weighted towards a narrow range of test results. Another concern is that the database is so large that it is very difficult to identify the conditions under which design provisions provided a reasonable estimate of capacity, are overly conservative, or are unsafe. Thus, in this section members, which are considered to have properties close to those of actual members in the field, are selected from the database and used for evaluations of the different shear design approaches.

D.2.1 Overview of Selected Database

A total of 64 reinforced concrete (RC) members and 85 prestressed concrete (PC) members were selected for the comparison of approaches presented in this section. All selected members contained the traditional ACI minimum amount of shear reinforcement ($\rho_v f_y > 50$ psi), had an overall depth of at least 20 inches, and were cast with concrete having measured compressive strengths of at least 4000 psi. The number of members selected was further reduced by removing those members for which the test reports indicated that anchorage or flexural failures may have occurred. Furthermore, members were removed so that the final database would consist of a relatively evenly weighted set considering section shape, depth, concrete strength, and strength of shear reinforcement ($\rho_v f_y$). While all the RC beams selected had shear span to depth ratios (a/d) greater than 2.4, 16 PC members had shear span to depth ratios (a/d) of less than 2.4 in order to include data for large high strength concrete girders tested very recently. The smallest a/d ratio of these members was 1.56.

Table D-9 provides information on the sectional shapes of the 64 selected RC members. Of these members, 46 beams were rectangular, and 18 were I-shaped. The vast majority of the tests (61 of 64, or about 95 %) consisted of simply supported beams subjected to one or two concentrated loads. Only three tests were on continuous beams of which two were subjected to a point load and only one was tested using uniformly distributed loads.

The distribution of parameters values for the 64 RC members is shown in Fig. D-2. Of these test results, 40 beams had concrete strengths greater than 6 ksi. While all members had overall depths greater than 20 inches, about a half of them had an effective depth greater than 25 inches. About half of the members had longitudinal reinforcement ratios less than 3 %, and for only two of them was this ratio less than 1 %. Longitudinal ratios are based on the web widths of members. More than one half of the beams had shear span to depth ratios (a/d) greater than 3.0, and about one half of the members had shear reinforcement strengths ($\rho_v f_y$) less than 100 psi but not less than 50 psi.

Information on the sectional shapes and loading geometries of the 85 selected PC members are shown in Table D-10. Most of them (79 of 85, or about 93 %) were I-shaped, and only five were rectangular. Of these members, 27 members had composite deck slabs. Most of these members (77 of 85, or about 91 %) were simply supported and subjected to concentrated loads. Six of them were simply supported beams subject to uniform loading and two of them were continuous beams subject to point loads.

Fig. D-3 shows the distribution of parameters values for the 85 PC members. More than one half of the PC members had cylinder compressive strengths, f'_c , greater than 6 ksi, and 11 of them had concrete strengths greater than 10 ksi. More than one half of the members were greater than 25 inches in depth and 12 of them were deeper than 50 inches. 52 of the members had longitudinal reinforcement ratios less than 3 % and only 3 had longitudinal reinforcement ratios less than 1 %. 11 members had a/d ratios between 1.5 and 2.0, and 13 members had a/d ratios of between 2.0 and 2.5. These members were included in order to include recently tested large prestressed concrete members, cast with high strength concrete, in this evaluation. However, the majority of the PC members had a/d ratios greater than 2.5. More than one half of the members had shear reinforcement strengths ($\rho_v f_y$) less than 500 psi but not less than 100 psi. However, as can be seen from Fig. D-3, a large number of the members (38 of 85 or 45 %) had relatively heavy amounts of shear reinforcement.

D.2.2 Assessment of Accuracy of Shear Design Provisions

Six national design codes, Response 2000 and the Frosch method are compared to the test results of this selected design database. These codes/methods compared are: *ACI 318-02 (which is the same as the AASHTO Standard Specification 1989)*; *AASHTO LRFD Bridge Design Specifications (2001)*; *A draft of CSA A23.3 2004 edition (Collins, 2002)*; *Response 2000 (Bentz & Collins, 2000)*; *Truss Model with Crack Friction (Reineck, 2001)*; *AASHTO Segmental Guide Specification (1999)*, *Simplified Shear Design (Tureyen & Frosch, 2003)*; and the *AASHTO Standard Bridge Design Specifications (1979)*.

Table D-11 shows a summary comparing the predictions by the eight approaches for the RC members. The ratios of the shear strengths measured in the experiments and the calculated shear strengths with resistance factors removed, $V_{\text{Test}}/V_{\text{Pred}}$, for all eight approaches are compared. In Table D-11 information is summarized in three horizontal blocks. The first block provides statistical values of $V_{\text{Test}}/V_{\text{Pred}}$ ratios such as the mean, standard deviation (STDEV), and coefficient of variation (COV). The second block gives the percentage of the calculated values of $V_{\text{Test}}/V_{\text{Pred}}$ that lie within the ranges shown in the first column. For example, the ACI approach has 7.8 % of the RC beams within a $V_{\text{Test}}/V_{\text{ACI}}$ ratio of 0.65 to 0.85. The third block shows significant statistical values for the $V_{\text{Test}}/V_{\text{Pred}}$ values for the 64 RC members assuming that the data follow a “normal distribution”. For example, the value of 5% for the ACI method means that 5 % of members can be expected to have $V_{\text{Test}}/V_{\text{Pred}}$ ratios below 0.587.

The mean values of $V_{\text{Test}}/V_{\text{Pred}}$ ratios range from 1.019 (R2k) to 1.296 (ACI) and COVs range from 0.108 (R2k) to 0.333 (ACI). From the statistical values, it is apparent that the Response 2000 method (R2k) gives the best shear strength prediction for the 64 RC members. The next best prediction is by the CSA method, followed by the AASHTO LRFD, and the TMwCF methods with the mean values for the AASHTO LRFD, and the TMwCF methods being slightly higher than those of the CSA method. The COVs for the STD79, Frosch, and

ASBI methods follow in that order while their mean values are comparable (approximately 1.25). The ACI method gives the highest mean value and the largest COV. In fact the combination of the mean and the COV values for the ACI method mean that the ACI method is not conservative in many cases even though it has the highest mean value.

The second block of information on the distribution of $V_{\text{Test}}/V_{\text{Pred}}$ ratios shows that in the AASHTO LRFD, CSA, R2k, and TMwCF methods, the strength ratios follow a relatively narrow distribution. For the Frosch and STD79 methods the ratios exhibit a wider distribution although the Frosch approach is very conservative for some members and the STD79 method is unconservative for some cases. The approach for RC members by the ACI and ASBI methods is basically identical except for the maximum limitation on the shear strength. Thus, the distribution trends of these approaches are very similar. Unfortunately, both approaches give the worst distributions of $V_{\text{Test}}/V_{\text{Pred}}$, which is to be expected because they account for concrete compressive strength only while there are many other parameters influencing the shear that can be carried by the concrete.

The 5% fractile values in the third block also provide a good indication of whether an approach is conservative or not. The 5% fractile values of the AASHTO LRFD, CSA, R2k, and TMwCF methods are very similar and range from 0.822 to 0.857, which is close enough to 1.0 when used with current strength reduction factors. These four methods can be said to provide good levels of safety. The Frosch and STD79 approaches have 5% fractile values of 0.724 and 0.756, respectively. These methods can be said to provide moderate levels of safety. The 5% fractile values of the ACI and ASBI approaches are 0.587 and 0.692, respectively which in combination with currently used strength reduction factors provide a less than desirable level of safety.

Table D-12 compares predictions by the eight approaches for 85 PC members. The mean values of $V_{\text{Test}}/V_{\text{Pred}}$ ratios range from 1.090 (STD79) to 1.515 (ASBI) and COVs range from 0.131 (CSA) to 0.383 (STD79). R2k gives a mean value of 1.107 and a COV of 0.170, and more than 80% of the members had strength ratios ($V_{\text{Test}}/V_{\text{R2k}}$) of between 0.85 and 1.3. For all members, including both RC and PC, R2k gives very accurate and consistent predictions supporting a conclusion that the MCFT is one of the most advanced and accurate theories for understanding and predicting shear behavior. For the PC members the CSA, AASHTO LRFD and ACI predictions give reasonable mean values and COVs that provided a reasonable margin of safety. The predictions by these approaches are very close to each other but the mean and the COV for the ACI method are a little higher than those of the CSA and AASHTO LRFD methods. COVs obtained using the ASBI, Frosch, and TMwCF approaches followed in that order and their mean values were similar (between 1.3 and 1.5). The STD79 method gives the largest COV with a very large scatter in the strength ratios ($V_{\text{Test}}/V_{\text{Pred}}$). For the STD79 approach about 15% of the PC members had $V_{\text{Test}}/V_{\text{STD79}}$ ratios below 0.65. Use of this approach would be unsafe.

The 5% fractile values for all approaches, except the STD79 approach, were between 0.78 and 0.99, providing a reasonable level of safety for PC members. The STD79 approach had 5% fractile values of 0.404 indicating again that shear strengths predicted by this approach would be unsafe unless an unrealistically small strength reduction factor is used.

D.2.2.1 Compressive Strength (f'_c)

Consideration of the influences of either concrete compressive strength or tensile strength is included for all the approaches presented here. In the ACI 318-02 (ACI), the AASHTO LRFD Bridge Design Specifications (AASHTO LRFD), the CSA 2004 (CSA), the Response 2000 (R2k), the AASHTO Segmental Guide Specification (ASBI), and the Simplified Shear Design (Frosch) methods, the shear strength is proportional to $(f'_c)^{0.5}$, while in the Truss Model with Crack Friction (TMwCF) and the AASHTO Standard Bridge Design Specifications (1979, STD79) methods, the shear strength is proportional to (f'_c) . Figs. D-4 and D-5 show the strength ratio ($V_{\text{Test}}/V_{\text{Pred}}$) versus concrete compressive strength (f'_c) for the database of 64 RC members and 85 PC members, respectively.

The ACI 318-02 (Eq. 11-3) predictions for RC members have a large scatter with coefficient of variation of 0.333 and tend to result in a decreasing strength ratio ($V_{\text{Test}}/V_{\text{ACI}}$) as f'_c increases. However, this trend can be caused not only by f'_c but also by other parameters such as member depth, longitudinal reinforcement ratio, and shear span to depth ratio. However, the ACI 318-02 Eq. 11-3 does not consider those effects to be significant parameters. Most of the unconservative results obtained by the ACI method are for members that are lightly reinforced against flexure and have relatively small amount of stirrups as discussed in Sections D.2.2.3 and D.2.2.5. For PC members (Fig. D-5), the ACI 318-02 method provides a good estimate of capacities with a reasonable margin of safety up to very high concrete strengths.

As shown in Figs. D-4 and D-5, both the AASHTO LRFD and the CSA approaches provide very similar predictions as both approaches are based on the MCFT. Both approaches give good predictions for both RC and PC members, with no discernible descending or ascending trends as the concrete strength increases. Note that the AASHTO LRFD and CSA methods provide a unified design approach for both RC and PC members, unlike many other traditional methods where RC and PC members are treated separately. While the AASHTO LRFD and CSA methods have many assumptions and simplifications adopted from the MCFT, the R2k method is a computer based analysis program that incorporates all the features of the MCFT. Thus, it is not surprising that R2k gave the best result of all the approaches.

The TMwCF approach gives a reasonable level of predictions for RC members but with a slightly descending trend as the concrete strength increases. In the TMwCF method, the concrete contribution to shear is mainly provided by the vertical component of the friction forces at the diagonal crack, V_{fd} , and that component is proportional to the concrete compressive strength as mentioned above. While the angle of the diagonal compression strut is fixed as 40 degrees for RC members, the angle of the compression strut depends on the tensile strength of the concrete and the axial stress at the centroid of the member for PC members. Thus, the angle of the inclined strut for PC members can be more realistic than that for RC members. This results in a descending trend in the strength plot for RC members while no such trend is observable for PC members. However, the scatter of the $V_{\text{Test}}/V_{\text{TMwCF}}$ ratios is greater in PC members than in RC members.

The ASBI method gives predictions that are very similar to those of the ACI method for RC members. However, there is less scatter than with the ACI method. The only difference between these two approaches is the maximum limitation on shear capacity. That value is $10\sqrt{f'_c}b_wd$ in the ACI method, and $12\sqrt{f'_c}b_wd$ in the ASBI method. Thus, the strength ratios, which are very conservative for the ACI method, are less conservative for the ASBI method. The ASBI

approach basically gives the same trends as the ACI approach and is also unconservative for members lightly reinforced against flexure as discussed in Section D.2.2.3. For PC members, the concrete contribution term in the ASBI method is somewhat similar to the web-shear cracking strength, V_{cw} , in the ACI method, but a little more conservative in most cases. For all values of concrete compressive strength, the ASBI approach provides a reasonable margin of safety for PC members.

The Frosch approach does not show any specific trend over the concrete compressive strength range considered here and thus that approach seems to realistically consider the influence of concrete compressive strength for RC members as well as PC members. However, there are some overly conservative results for both RC and PC members due to the influence of other parameters such as the longitudinal reinforcement ratio, shape of section, and amount of shear reinforcement. These effects are explained in subsequent sections.

The STD79 approach shows a slightly ascending trend for RC members as the concrete strength increases. This result is because the concrete compressive strength in this approach is limited to 3 ksi. Above that strength the concrete contribution to shear is basically fixed at $180b_wjd$ psi. For all other approaches a limitation on the compressive strength was not applied because the assessment of the applicability of these approaches to high strength concrete members was one of objectives of this study. However, this method yields very unconservative results for all members with concrete strength greater than 3 ksi if the limitation is not applied. Hence, applying the limitation is thought to be more appropriate. A similar trend can be seen for PC members, but unlike the case for RC members the trend is mainly due to the effect of shear reinforcement as explained in Section D.2.2.5.

Other parameters may affect these observations on how well an approach accounts for the influence of concrete strength on shear. However, in for all eight approaches no severe descending or ascending trend was found for this parameter.

D.2.2.2 Depth of member (d)

For members without shear reinforcement, the size effect has recently become recognized as an important parameter for understanding shear behavior. Thus, the influence of member depth is taken into account in the AASHTO LRFD, the CSA, and the R2k approaches. In the ACI 318-02, the ASBI, the Frosch, and the STD79 approaches, however, the size effect is not considered. In the AASHTO LRFD, the CSA, and the R2k approaches, member depth is indirectly accounted for in shear strength by using a crack spacing parameter that affects the crack width and thus the shear strength. In the TMwCF, the shear strength of members without shear reinforcement cannot be calculated. Therefore, for such cases, this approach adopts Loov's equation (Eq. 2-45) in which the shear strength is proportional to $1/d^{1/3}$.

In members with shear reinforcement, it is usually considered that no severe size effect exists. Thus, none of the above approaches considers the member depth as a significant parameter for the shear of members with shear reinforcement. As can be seen from Fig. D-6 for RC members, and Fig. D-7 for PC members, there is no apparent descending or ascending trend with member depth for all approaches except the STD79 approach. However, the trend in the STD79 approach is not due to member depth but due to the effective amount of shear reinforcement as explained in Section D.2.2.5. Therefore, it can be stated that no significant size

effect exists for any of the eight approaches when members contain at least minimum shear reinforcement

D.2.2.3 Longitudinal Reinforcement Ratio (ρ_ℓ)

The longitudinal reinforcement ratio affects the amount of longitudinal strain and thereby affects crack width, interface shear transfer, dowel action, and thus the shear strength. The influence of longitudinal reinforcement is accounted for in most major codes but in different ways. While the AASHTO LRFD, the CSA, the R2k, and the Frosch approaches account for the influence of longitudinal reinforcement, the ACI, TMwCF, ASBI, and STD79 approaches do not.

In ACI 318-02, Eq. 11-3 does not consider the influence of longitudinal reinforcement but in the alternate Eq. 11-5 the shear strength is proportional to longitudinal reinforcement ratio, ρ_ℓ , for RC members. Note that ACI 318-02 Eq. 11-3 is controls for this analysis. As can be seen in Fig. D-8, the ACI 318-02 Eq. 11-3 underestimates the shear strength of lightly reinforced RC members but is also very conservative for heavily reinforced RC members. For PC members the prestressing steel ratio is usually directly related to the axial stress level in the PC member. Thus, as the prestressing steel ratio increases, the axial stress also usually increases. ACI 318-02 uses Eq. 11-10 (flexure-shear cracking strength) and Eq. 11-12 (web-shear cracking strength) added to shear reinforcement contribution, if any, for shear strength calculations of PC members. In ACI 318-02, the influence of longitudinal reinforcement ratio is not considered to affect the shear strength of PC members. However, Eq. 11-12 (web-shear cracking strength) accounts for the influence of axial stress at the centroid of section. Thus, as can be seen in Fig. D-9, for PC members this ACI approach may capture part of the influence of the longitudinal reinforcement ratio.

In the AASHTO LRFD, CSA, and R2k approaches, the effect of the amount of longitudinal reinforcement is incorporated because it is reflected in the longitudinal strain. Thus the longitudinal reinforcement ratio affects crack width and shear strength. For the same magnitude of loading, as the longitudinal reinforcement ratio decreases, flexural stress and strain increase. Subsequently, crack width increases, interface shear transfer decreases, and the shear strength is reduced. As can be seen in Figs. D-8 and D-9, these three approaches account realistically for the influence of the longitudinal reinforcement ratio.

As explained in Appendix A, the TMwCF approach almost corresponds to the MCFT when the longitudinal strain ε_x is 0.001 for RC members. The shear strength of RC members with longitudinal reinforcement ratios less than about 2 to 3 % is usually governed by Eq. 2-45 because most of those members have light amounts of shear reinforcement and the TMwCF approach is not applicable for such members. In Eq. 2-45, the shear strength is proportional to $(\rho_\ell)^{1/3}$ and the approach gives conservative results for members within this range. For RC members with longitudinal reinforcement ratios greater than about 2 to 3 %, the TMwCF approach seems to give an ascending trend as longitudinal reinforcement ratio increases. For PC members, the TMwCF approach considers axial stress in the determination of the angle of the inclined strut. This approach seems to capture a part of the influence of the longitudinal reinforcement ratio as can be seen in Fig. D-9.

For RC members, the ASBI approach gives a trend, which is very similar to the ACI approach for the reason explained in Section D.2.2.1. For PC members, the ASBI approach

accounts for the influence of axial stress at the centroid of section in a similar manner to the ACI 318-02 Eq. 11-12 (web shear cracking strength). However, the ASBI approach always gives more conservative shear strengths than ACI 318-02 Eq. 11-12.

The Frosch approach considers the influence of longitudinal reinforcement ratio in a different way from the other approaches. In the Frosch approach, the shear strength of a member is proportional to the area of the flexural compression zone of the cracked concrete section. Thus, as the longitudinal reinforcement ratio increases, the compression depth increases which leads to increase in the area of the compression zone. Therefore, the larger the amount of longitudinal reinforcement, the higher is the shear strength. However, as can be seen in Fig. D-8, this approach clearly gives an ascending trend as the longitudinal reinforcement ratio increases. For PC members, a similar trend, but less marked trend is shown in Fig. D-9. The Frosch approach does not capture the influence of the longitudinal reinforcement ratio effectively.

In the STD79 approach, there is no consideration of the influence of the longitudinal reinforcement ratio. The approach gives unconservative results for members with low amounts of longitudinal reinforcement for both RC and PC members. There is a slight ascending trend for RC members with a large scatter as the longitudinal reinforcement increases. The reason that this approach does not show any strong ascending trend for RC members, as is the case for the ACI approach, is because most RC members with large amounts of longitudinal reinforcement also have a large amount of stirrups, and this approach does not have any limitation on shear strength. Thus, unconservatism in the strength of the stirrup contribution for those members balances the conservatism in the strength of the concrete contribution. For PC members, the STD79 approach gives a very large scatter for members with light amounts of longitudinal reinforcement. However, this trend is strongly influenced by the amount of shear reinforcement as discussed in Section D.2.2.5.

D.2.2.4 Shear span to depth ratio (a/d)

The span to depth ratio (a/d) takes account of the relative values of shear and moment applied to the member. In ACI 318-02, Eq. 11-3 does not presume any influence of the a/d ratio but Eq. 11-5 considers it by using an M/Vd ratio for RC members. For PC members, Eq. 11-10 (flexure-shear cracking strength) also considers the a/d ratio by using an M/Vd ratio. In the AASHTO LRFD and CSA approaches, the influence of the combined sectional forces on the state of strain is directly considered. However, the ASI, Frosch, and STD79 approaches do not include any a/d ratio effect in their shear strength calculations. The TMwCF approach also does not include any effect of span to depth ratio (a/d), but in Eq. 2-45, which is adopted for cases where the TMwCF approach should not be applied, the shear strength is proportional to the inverse of the a/d ratio.

As can be seen in Fig. D-10, the distribution of a/d ratios for RC members is heavily concentrated between 2.4 and 4.5. This is because shear failures can be easily ensured in this range of a/d ratios. When a member is very slender, (an a/d ratio greater than about 6), its response is more likely to be governed by flexure than by shear. For the limited property ranges of the selected members it is hard to observe any differences in the trends for the eight approaches. The AASHTO LRFD, CSA, R2k, and TMwCF approaches result in narrow scatters, while the TMwCF approach gives an ascending trend. The ACI, ASBI, Frosch, and STD79 approaches do not show any descending or ascending trend but have a large scatter. For PC

members, the ACI, AASHTO LRFD, CSA, and R2k approaches all give good predictions over the full range of a/d ratios, while the TMwCF, ASBI, Frosch, and STD79 approaches give relatively large scatters.

D.2.2.5 Shear Reinforcement Strength ($\rho_v f_{vy}$)

The shear resistance of members with shear reinforcement depends heavily on the strength of the shear reinforcement. The contribution of the shear reinforcement to the shear strength of members depends on the angle of diagonal compression, often analogous with the angle of diagonal cracking. As the crack angle becomes flatter, the contribution of the shear reinforcement to the shear strength becomes larger. Thus, the accurate prediction of the crack angle in a beam is very important for accurate predictions of shear strength. While the ACI 318-02, ASBI, and Frosch approaches use a 45° truss model, the AASHTO LRFD, CSA, R2k, and TMwCF approaches use a variable angle truss model. On the other hand, the STD79 approach effectively uses about a 27-degree crack angle for the stirrup contribution to shear for PC members and 45 degrees for RC members. For all approaches except the STD79 approach the shear resistance is limited to avoid the possibility of concrete web crushing.

As shown in Fig. D-12, the ACI 318-02 approach gives an ascending trend as the strength of the shear reinforcement increases. The ACI 318-02 prediction for RC members also gives unconservative predictions for members with light amount of shear reinforcement. Note that many such members also have light amounts of longitudinal reinforcement and, as explained in section D.2.2.3, this unconservative result mainly comes from not considering the effect of the longitudinal reinforcement ratio on shear strength. For members with heavy amounts of shear reinforcement, the ACI approach gives very conservative predictions, resulting primarily from the limitation on the maximum of shear resistance that can be provided by the shear reinforcement. This result means that the maximum shear resistance limitation for shear reinforcement is a conservative rather than a necessary limitation. For PC members, the ACI approach gives good predictions with a reasonable margin of safety.

The AASHTO LRFD, CSA, and R2k approaches give reasonable predictions for all shear reinforcement levels for both RC and PC members. This result comes from a reasonably close prediction of the crack angle as well as a good representation of the concrete contribution to shear strength.

The TMwCF approach does not result in any trend for RC members as stirrup strength increases, but it does give a slightly wider scatter than the approaches based on the MCFT. The few members that are somewhat unconservative are high strength concrete members. For PC members with stirrup strengths less than about 300 psi, the TMwCF approach gives very conservative results. In the TMwCF approach the compressive stress in the inclined strut is limited by the ratio of the stirrup spacing to the flexural lever arm, and for members with light amounts of stirrups that stress can be as low as $0.45f'_c$. That limit causes the conservative results. For PC members with stirrup strengths greater than about 300 psi the approach gives good results with an almost constant strength ratio (V_{Test}/V_{TMwCF}).

The ASBI approach gives almost the same trend for RC members as the ACI approach but shows slightly less scatter as mentioned previously. For PC members the ASBI approach has a

larger scatter than the ACI approach and tends to be more conservative as the stirrup strength increases.

The Frosch approach also gives predictions that are similar to the ACI and ASBI approaches for RC members. This result shows that although the Frosch method is very different to the ACI Eq. 11-3, it does not give significantly better results for members of customary proportions than those obtained using ACI Eq. 11-3. For PC members, the Frosch approach gives a trend similar to the ASBI approach but a little less conservative than ASBI. Some of the members for which the predictions are very conservative are members with relatively wide top flanges or deck slabs. In the Frosch approach, the shear strength of the member depends on the depth of flexural compression, and the compression area of the I or T shaped beams is the flexural compression depth times a width that is the top flange or deck slab thickness added to web width. The flexural compression depth of an I or T shaped beam having a wide top flange or slab becomes small and thus leads to a small compression area. For to this reason, the Frosch approach gives very conservative results for very wide flanged members.

The STD79 approach gives a trend that is different to the other approaches that are based on 45-degree truss models. In the STD79 approach the concrete strength is limited to 3 ksi, as mentioned previously, and thus the concrete contribution to shear strength is sharply curtailed. For this reason for RC members the trend for the STD79 approach depends very strongly on the V_c prediction. Thus the conservatism comes from the high strength concrete used in some members. For RC members with heavy amounts of shear reinforcement, the STD79 approach tends to be unconservative because there is no limit on the shear strength of such members. For PC members, the STD79 approach also gives the worst distribution of strength ratio (V_{Test}/V_{Pred}). For members with heavy amounts of shear reinforcement, the STD79 approach gives very unsafe predictions due to the low crack angle assumed in this method regardless of any other member characteristics. The stirrup contribution calculated by the STD79 approach is double that for the 45-degree truss model usually used for PC members with shear reinforcement.

D.2.3 Summary of Assessment

The following findings can be made from this examination of selected RC and PC members with shear reinforcement.

1. The ACI provisions give good predictions of the shear strengths of PC members with shear reinforcement. They also provide a reasonable margin of safety. However, for RC members, ACI Eq. 11-3 gives unconservative predictions of the shear strength for members lightly reinforced in flexure; these members are also likely to have light amounts of shear reinforcement. The ACI approach becomes increasingly conservative as the longitudinal reinforcement ratio increases; the members that have large amounts of longitudinal reinforcement are also likely to have relatively larger amounts of shear reinforcement. For RC members with heavy amounts of shear reinforcement, ACI Eq. 11-3 gives conservative results due to its low limitation on maximum shear strength in order to avoid web concrete crushing.
2. No significant size effect exists for either RC or PC members with shear reinforcement.

3. The AASHTO LRFD and CSA approaches, which are both based on the modified compression field theory, give very similar results with good levels of accuracy for both RC and PC members. These methods also provide a unified method of shear design for both RC and PC members and they consider all sectional forces in a consistent manner.

4. Response 2000 (R2k) is a computer-based program that utilizes MCFT. R2k gives a good agreement with test results for both RC and PC members. This software can provide an easy and practical tool for accurate calculations of the shear strength of RC and PC members with all sectional forces applied.

5. The TMwCF approach is a simplified method that utilizes a crack friction model. This approach provides a reasonably accurate level of shear strength predictions for both RC and PC members with shear reinforcement. However, for RC members it tends to be slightly unconservative as the concrete strength increases. It also gives conservative results for PC members with relatively light amounts of shear reinforcement.

6. For RC members the ASBI approach is basically the same as the ACI approach except for the maximum shear strength limitation. For PC members, the concrete contribution, V_c in ASBI, is very similar to the web-shear cracking force, V_{cw} in ACI. However, for PC members the ASBI approach gives more conservative results than the ACI approach. The flexure-shear cracking strength, V_{ci} in ACI, is removed and thus the approach is simpler than the ACI approach. The strength ratios, V_{Test}/V_{ASBI} , show an ascending trend as the longitudinal reinforcement ratio increases for both RC and PC members.

7. The Frosch approach accounts only for the shear strength of the uncracked flexural compression zone. The strength ratios, V_{Test}/V_{Frosch} , show an ascending trend as the longitudinal reinforcement ratio increases for both RC and PC members. This approach gives very conservative results for members with wide flanges or wide slabs. It should be also noted that in this approach the web width of member does not result in any difference in the shear strength for the tee-beams where the neutral axis lies in the top flange. That is, a T-beam with a very thick web and or one with very thin web have similar shear strengths for this approach.

8. The STD79 approach seems relatively unsatisfactory because in this approach the concrete contribution to shear for concrete strengths above 3 ksi is fixed at that for members with concrete strengths of 3 ksi. Once this limitation removed, then it gives very unconservative results since the concrete contribution term, V_c , becomes too large in most cases, i.e., in normal and high strength concrete members. This approach also gives very unconservative results for PC members with heavy amounts of shear reinforcement due to the basic assumption that the crack angle is always 27 degrees for all PC members. That assumption leads to a stirrup contribution that is double that calculated using a 45-degree truss model.

Table D-1 Code Assessment for Broad Categories (RC and PC with and without Av)

Member Type		All	RC	RC	RC	PC	PC	PC
With or without Av			Both	No Av	With Av	Both	No Av	With Av
count	(#)	1359	878	718	160	481	321	160
ACI	Mean	1.44	1.51	1.54	1.35	1.32	1.38	1.21
	COV	0.371	0.404	0.418	0.277	0.248	0.247	0.221
LRFD	Mean	1.38	1.37	1.39	1.27	1.40	1.44	1.32
	COV	0.262	0.262	0.266	0.224	0.261	0.290	0.154
CSA	Mean	1.31	1.25	1.27	1.19	1.41	1.46	1.31
	COV	0.275	0.274	0.282	0.218	0.261	0.287	0.147
JSCE	Mean	1.51	1.36	1.35	1.38	1.80	1.85	1.70
	COV	0.321	0.280	0.293	0.216	0.292	0.297	0.272
EC2	Mean	1.85	1.74	1.75	1.70	2.06	2.13	1.91
	COV	0.409	0.336	0.328	0.373	0.470	0.343	0.687
DIN	Mean	2.05	1.95	2.10	1.25	2.25	2.59	1.58
	COV	0.395	0.368	0.327	0.267	0.413	0.345	0.357

Table D-2 Reinforced Concrete Members without Shear Reinforcement

f'c	(KSI)	all	<8	>8	all	all	all	all	all	all
d	(in)	all	all	all	<24	>24	all	all	all	all
a/d ratio	(-)	all	all	all	all	all	<3	>3	all	all
rho	(%)	all	all	all	all	all	all	all	<1	>1
count	(#)	718	577	141	659	59	172	546	76	642
ACI	Mean	1.54	1.57	1.43	1.61	0.76	1.68	1.50	0.88	1.62
	COV	0.418	0.415	0.421	0.386	0.344	0.441	0.404	0.380	0.387
LRFD	Mean	1.39	1.38	1.44	1.42	1.06	1.47	1.37	1.14	1.42
	COV	0.266	0.264	0.273	0.259	0.178	0.316	0.242	0.193	0.262
CSA	Mean	1.27	1.26	1.31	1.28	1.09	1.33	1.25	1.27	1.29
	COV	0.282	0.290	0.251	0.285	0.175	0.298	0.275	0.282	0.287
JSCE	Mean	1.35	1.35	1.35	1.37	1.16	1.54	1.30	1.20	1.37
	COV	0.293	0.295	0.287	0.296	0.176	0.295	0.277	0.190	0.298
EC2	Mean	1.75	1.74	1.78	1.79	1.32	1.97	1.68	1.42	1.79
	COV	0.328	0.326	0.333	0.324	0.192	0.340	0.310	0.209	0.327
DIN	Mean	2.10	2.09	2.14	2.15	1.59	2.36	2.02	1.71	2.15
	COV	0.327	0.326	0.333	0.323	0.190	0.340	0.310	0.207	0.327

Table D-3 Reinforced Concrete Members with Shear Reinforcement

f'c	(KSI)	all	<8	>8	all	all	all	all	all	all
d	(in)	all	all	all	<24	>24	all	all	all	all
ρ _h v x f _y	(psi)	all	all	all	all	all	1-200	>200	all	all
ρ _h	(%)	all	all	all	all	all	all	all	<2	>2
count	(#)	160	66	94	139	21	125	35	28	132
ACI	Mean	1.35	1.27	1.40	1.40	1.00	1.34	1.39	1.06	1.41
	COV	0.277	0.290	0.263	0.259	0.229	0.280	0.266	0.278	0.256
LRFD	Mean	1.27	1.19	1.33	1.28	1.25	1.33	1.08	1.27	1.27
	COV	0.224	0.206	0.223	0.222	0.244	0.213	0.192	0.232	0.223
CSA	Mean	1.19	1.12	1.25	1.21	1.05	1.21	1.12	1.19	1.19
	COV	0.218	0.225	0.204	0.217	0.171	0.223	0.185	0.218	0.218
JSCE	Mean	1.38	1.27	1.45	1.40	1.25	1.39	1.33	1.28	1.40
	COV	0.216	0.200	0.210	0.220	0.141	0.222	0.190	0.170	0.220
EC2	Mean	1.70	1.54	1.81	1.72	1.57	1.89	1.04	1.46	1.75
	COV	0.373	0.433	0.324	0.382	0.274	0.309	0.257	0.295	0.378
DIN	Mean	1.25	1.10	1.36	1.30	0.96	1.28	1.15	1.01	1.30
	COV	0.267	0.233	0.251	0.253	0.213	0.276	0.200	0.246	0.252

Table D-4 Prestressed Concrete Members without Shear Reinforcement

f'c	(KSI)	all	<8	>8	all	all	all	all	all	all
d	(in)	all	all	all	<12	>12	all	all	all	all
a/d ratio	(%)	all	all	all	all	all	<3	>3	all	all
ρ _h	(-)	all	all	all	all	all	all	all	<1	>1
count	(#)	321	292	29	305	16	55	266	203	118
ACI	Mean	1.38	1.40	1.14	1.38	1.22	1.47	1.36	1.32	1.46
	COV	0.247	0.247	0.101	0.249	0.132	0.240	0.247	0.170	0.318
LRFD	Mean	1.44	1.43	1.59	1.42	1.85	1.60	1.41	1.26	1.75
	COV	0.290	0.293	0.247	0.289	0.194	0.312	0.278	0.200	0.265
CSA	Mean	1.46	1.44	1.61	1.44	1.85	1.63	1.42	1.27	1.78
	COV	0.287	0.293	0.217	0.288	0.161	0.328	0.269	0.211	0.249
JSCE	Mean	1.85	1.83	2.02	1.82	2.42	2.21	1.78	1.66	2.18
	COV	0.297	0.307	0.178	0.294	0.205	0.285	0.282	0.282	0.242
EC2	Mean	2.13	2.12	2.29	2.09	2.86	2.56	2.04	1.87	2.58
	COV	0.343	0.356	0.192	0.339	0.272	0.312	0.335	0.336	0.262
DIN	Mean	2.59	2.57	2.81	2.54	3.49	3.12	2.48	2.27	3.14
	COV	0.345	0.358	0.190	0.342	0.269	0.313	0.338	0.341	0.262

Table D-5 Prestressed Concrete Members with Shear Reinforcement

	f _c (KSI)	all	<8	>8	all	all	all	all	all	all
d	(in)	all	all	all	<24	>24	all	all	all	all
ρ _h × f _y	(psi)	all	all	all	all	all	1-200	>200	all	all
ρ _h	(%)	all	all	all	all	all	all	all	<1	>1
count	(#)	160	120	40	137	23	66	94	63	97
ACI	Mean	1.21	1.23	1.14	1.20	1.26	1.24	1.18	1.33	1.12
	COV	0.221	0.225	0.199	0.228	0.173	0.204	0.231	0.191	0.214
LRFD	Mean	1.32	1.34	1.27	1.35	1.17	1.43	1.25	1.36	1.30
	COV	0.154	0.155	0.144	0.142	0.184	0.121	0.152	0.149	0.155
CSA	Mean	1.31	1.32	1.27	1.33	1.18	1.40	1.24	1.37	1.26
	COV	0.147	0.150	0.133	0.136	0.178	0.114	0.150	0.143	0.141
JSCE	Mean	1.70	1.64	1.86	1.66	1.95	1.80	1.62	1.74	1.67
	COV	0.272	0.285	0.216	0.267	0.259	0.306	0.229	0.343	0.207
EC2	Mean	1.91	1.96	1.75	1.99	1.40	2.69	1.35	2.31	1.64
	COV	0.687	0.748	0.369	0.697	0.323	0.644	0.223	0.814	0.379
DIN	Mean	1.58	1.52	1.76	1.57	1.60	1.87	1.38	1.67	1.52
	COV	0.357	0.402	0.194	0.374	0.240	0.365	0.250	0.456	0.249

Table D-6 Mean and COV for Selected Types of Members

type	RC or PC	RC	RC	RC	RC	PC	PC	PC	PC	PC
f _c	(KSI)	>8	all	all	all	>8	all	all	all	>8
d	(in)	>24	>24	all	all	>12	>12	all	all	>12
ρ _h × f _y	(psi)	0	0	<200	<200	0	0	<200	<200	<200
ρ _h	(%)	all	<1	<2	all	all	<2	<2	all	all
count	(#)	(1)	(2)	(3)	(4)	(5)	(6)	(7)	(8)	(9)
count	(#)	16	18	27	125	11	7	64	66	3
ACI	Mean	0.66	0.53	1.08	1.34	1.17	1.31	1.25	1.24	1.09
	COV	0.341	0.260	0.272	0.280	0.107	0.156	0.205	0.204	0.188
LRFD	Mean	1.03	0.95	1.29	1.33	1.95	1.52	1.44	1.43	1.25
	COV	0.192	0.139	0.218	0.213	0.190	0.107	0.121	0.121	0.146
CSA	Mean	1.11	1.03	1.17	1.21	1.94	1.69	1.40	1.40	1.23
	COV	0.229	0.129	0.212	0.223	0.161	0.218	0.114	0.114	0.143
JSCE	Mean	1.04	1.08	1.30	1.39	2.30	2.54	1.80	1.80	1.85
	COV	0.218	0.125	0.159	0.222	0.078	0.289	0.310	0.306	0.064
EC2	Mean	1.21	1.18	1.51	1.89	2.58	3.39	2.69	2.69	2.26
	COV	0.236	0.129	0.257	0.309	0.168	0.279	0.654	0.644	0.162
DIN	Mean	1.45	1.43	1.02	1.28	3.16	4.13	1.86	1.87	1.91
	COV	0.236	0.134	0.241	0.276	0.161	0.277	0.372	0.365	0.160

(1) Large High-Strength RC Members without Shear Reinforcement

(2) Large RC Members without Shear Reinforcement and with Light Longitudinal Reinforcement

(3) RC Members with Light Shear Reinforcement and Light Longitudinal Reinforcement

(4) Large RC Members with Light Shear Reinforcement

(5) Large High-Strength PC Members without Shear Reinforcement

(6) Large PC Members without Shear Reinforcement and with Light Longitudinal Reinforcement

(7) PC Members with Light Shear Reinforcement and Light Longitudinal Reinforcement

(8) Large PC Members with Light Shear Reinforcement

(9) Large High-Strength PC members with Light Shear Reinforcement

Table D-7 Comparison of Code Performance across Four Broad Categories

Member Type		All	RC	RC	RC	PC	PC	PC	Largest Variation in Mean	Largest Variation in COV	Lowest COV & Category	Highest COV & Category
With or without Av			Both	No Av	With Av	Both	No Av	With Av				
count	(#)	1359	878	718	160	481	321	160				
ACI	Mean	1.44	1.51	1.54	1.35	1.32	1.38	1.21	0.34	0.20	0.221	0.418
	COV	0.371	0.404	0.418	0.277	0.248	0.247	0.221				
LRFD	Mean	1.38	1.37	1.39	1.27	1.40	1.44	1.32	0.17	0.14	0.154	0.290
	COV	0.262	0.262	0.266	0.224	0.261	0.290	0.154				
CSA	Mean	1.31	1.25	1.27	1.19	1.41	1.46	1.31	0.27	0.14	0.147	0.287
	COV	0.275	0.274	0.282	0.218	0.261	0.287	0.147				
JSCE	Mean	1.51	1.36	1.35	1.38	1.80	1.85	1.70	0.50	0.08	0.216	0.297
	COV	0.321	0.280	0.293	0.216	0.292	0.297	0.272				
EC2	Mean	1.85	1.74	1.75	1.70	2.06	2.13	1.91	0.43	0.36	0.328	0.687
	COV	0.409	0.336	0.328	0.373	0.470	0.343	0.687				
DIN	Mean	2.05	1.95	2.10	1.25	2.25	2.59	1.58	1.34	0.09	0.267	0.357
	COV	0.395	0.368	0.327	0.267	0.413	0.345	0.357				

Table D-8 Relationship Between Selected Fractile Level and Required Mean

ACI (COV = 0.37)

F	$\Phi^{-1}(F)$	u
0.05	-1.645	2.56
0.10	-1.282	1.90
0.15	-1.036	1.62
0.20	-0.842	1.45
0.2045	-0.8258	1.44
0.25	-0.674	1.33
0.30	-0.524	1.24

Table D-9 Beam shapes and loading geometries for reinforced concrete members

Shape	# of tests	(%)	Loading Geometry	# of tests	(%)
Rectangular	46	72	simply supported beams with point load	61	95
I-shape	18	28	continuous beams with point load	2	3
T-shape	0	0	continuous beam with uniform load	1	2

Table D-10 Beam shapes and loading geometries for prestressed concrete members

Shape	# of tests	(%)	Loading Geometry	# of tests	(%)
Rectangular	5	6	simply supported beams with point load	77	91
I-shape	79	93	simply supported beams with uniform load	6	7
T-shape	1	1	continuous beams with point load	2	2

Table D-11 Comparison of predictions by various approaches (64 RC members)

Ratio of V_{Test}/V_{Pred}	V_{Test}/V_{ACI}	V_{Test}/V_{LRFD}	V_{Test}/V_{CSA}	V_{Test}/V_{R2k}	V_{Test}/V_{TMwCF}	V_{Test}/V_{ASBI}	V_{Test}/V_{Frosch}	V_{Test}/V_{STD79}
# of Beams	64	64	64	64	64	64	64	64
Mean	1.296	1.214	1.105	1.019	1.237	1.233	1.257	1.263
STDEV	0.431	0.217	0.172	0.110	0.236	0.329	0.324	0.308
COV	0.333	0.179	0.156	0.108	0.191	0.267	0.258	0.244
Distribution	(%)	(%)	(%)	(%)	(%)	(%)	(%)	(%)
>2	7.8	0.0	0.0	0.0	0.0	1.6	3.1	0.0
1.3~2.0	31.3	32.8	17.2	1.6	39.1	35.9	28.1	35.9
0.85~1.3	51.6	64.1	78.1	93.8	50.0	53.1	67.2	57.8
0.65~0.85	7.8	3.1	4.7	4.7	10.9	7.8	1.6	4.7
0.5~0.65	1.6	0.0	0.0	0.0	0.0	1.6	0.0	1.6
<0.5	0.0	0.0	0.0	0.0	0.0	0.0	0.0	0.0
max	2.444	1.730	1.483	1.347	1.890	2.036	2.147	1.911
99.90%	2.633	1.887	1.639	1.359	1.970	2.253	2.261	2.218
99%	2.301	1.720	1.506	1.275	1.788	2.000	2.012	1.981
95%	2.006	1.571	1.388	1.200	1.626	1.775	1.790	1.770
75%	1.587	1.361	1.221	1.093	1.396	1.455	1.476	1.471
50%	1.296	1.214	1.105	1.019	1.237	1.233	1.257	1.263
25%	1.005	1.068	0.989	0.945	1.077	1.011	1.039	1.055
5%	0.587	0.857	0.822	0.838	0.848	0.692	0.724	0.756
1%	0.291	0.709	0.704	0.763	0.686	0.466	0.503	0.545
0.10%	-0.041	0.542	0.572	0.678	0.504	0.213	0.253	0.308
min	0.624	0.786	0.824	0.755	0.681	0.624	0.764	0.641

Table D-12 Comparison of predictions by various approaches (85 PC members)

Ratio of V_{Test}/V_{Pred}	$V_{Test} /$ V_{ACI}	$V_{Test} /$ V_{LRFD}	$V_{Test} /$ V_{CSA}	$V_{Test} /$ V_{R2k}	$V_{Test} /$ V_{TMwCF}	$V_{Test} /$ V_{ASBI}	$V_{Test} /$ V_{Frosch}	$V_{Test} /$ V_{STD79}
# of Beams	85	85	85	85	85	85	85	85
Mean	1.318	1.243	1.261	1.107	1.328	1.515	1.455	1.090
STDEV	0.206	0.174	0.165	0.188	0.333	0.300	0.292	0.417
COV	0.156	0.140	0.131	0.170	0.251	0.198	0.200	0.383
Distribution	(%)	(%)	(%)	(%)	(%)	(%)	(%)	(%)
>2	0.0	0.0	0.0	0.0	4.7	4.7	3.5	2.4
1.3~2.0	47.1	42.4	45.9	11.8	47.1	69.4	67.1	21.2
0.85~1.3	52.9	57.6	52.9	81.2	45.9	25.9	28.2	52.9
0.65~0.85	0.0	0.0	1.2	7.1	2.4	0.0	1.2	9.4
0.5~0.65	0.0	0.0	0.0	0.0	0.0	0.0	0.0	5.9
<0.5	0.0	0.0	0.0	0.0	0.0	0.0	0.0	8.2
max	1.820	1.654	1.595	1.803	2.691	2.334	2.619	2.543
99.90%	1.956	1.783	1.773	1.689	2.361	2.444	2.359	2.383
99%	1.798	1.649	1.646	1.544	2.104	2.213	2.134	2.062
95%	1.657	1.530	1.532	1.416	1.876	2.008	1.935	1.776
75%	1.457	1.361	1.372	1.234	1.553	1.717	1.652	1.372
50%	1.318	1.243	1.261	1.107	1.328	1.515	1.455	1.090
25%	1.179	1.126	1.149	0.980	1.103	1.312	1.258	0.809
5%	0.980	0.957	0.989	0.798	0.780	1.021	0.975	0.404
1%	0.839	0.838	0.876	0.669	0.551	0.816	0.775	0.118
0.10%	0.680	0.704	0.749	0.524	0.295	0.585	0.551	-0.203
min	0.887	0.860	0.821	0.787	0.815	0.912	0.845	0.260

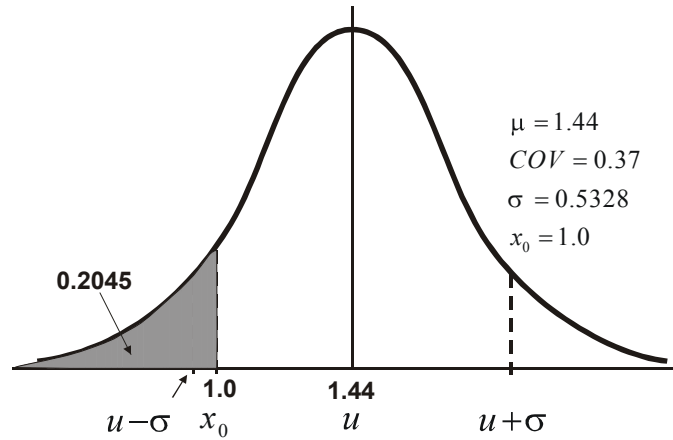


Figure D-1 Distribution of Ratio V_{test}/V_{aci} for All Test Data (Gaussian Distribution of Data Assumed)

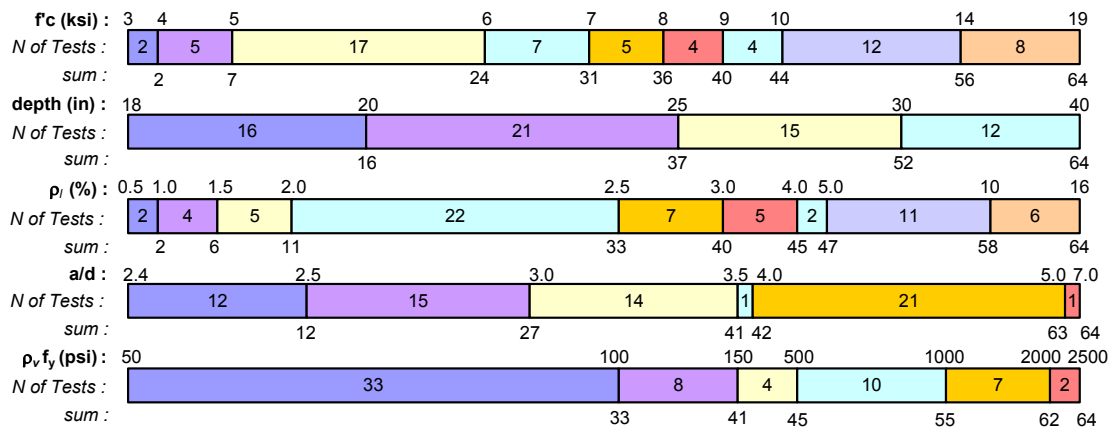


Figure D-2 Range in parameters for reinforced concrete members

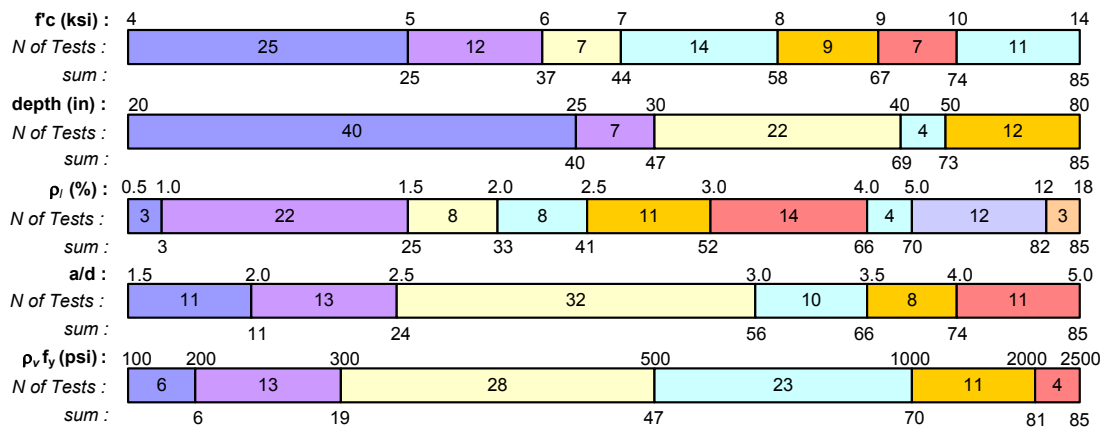


Figure D-3 Range in parameters for prestressed concrete members

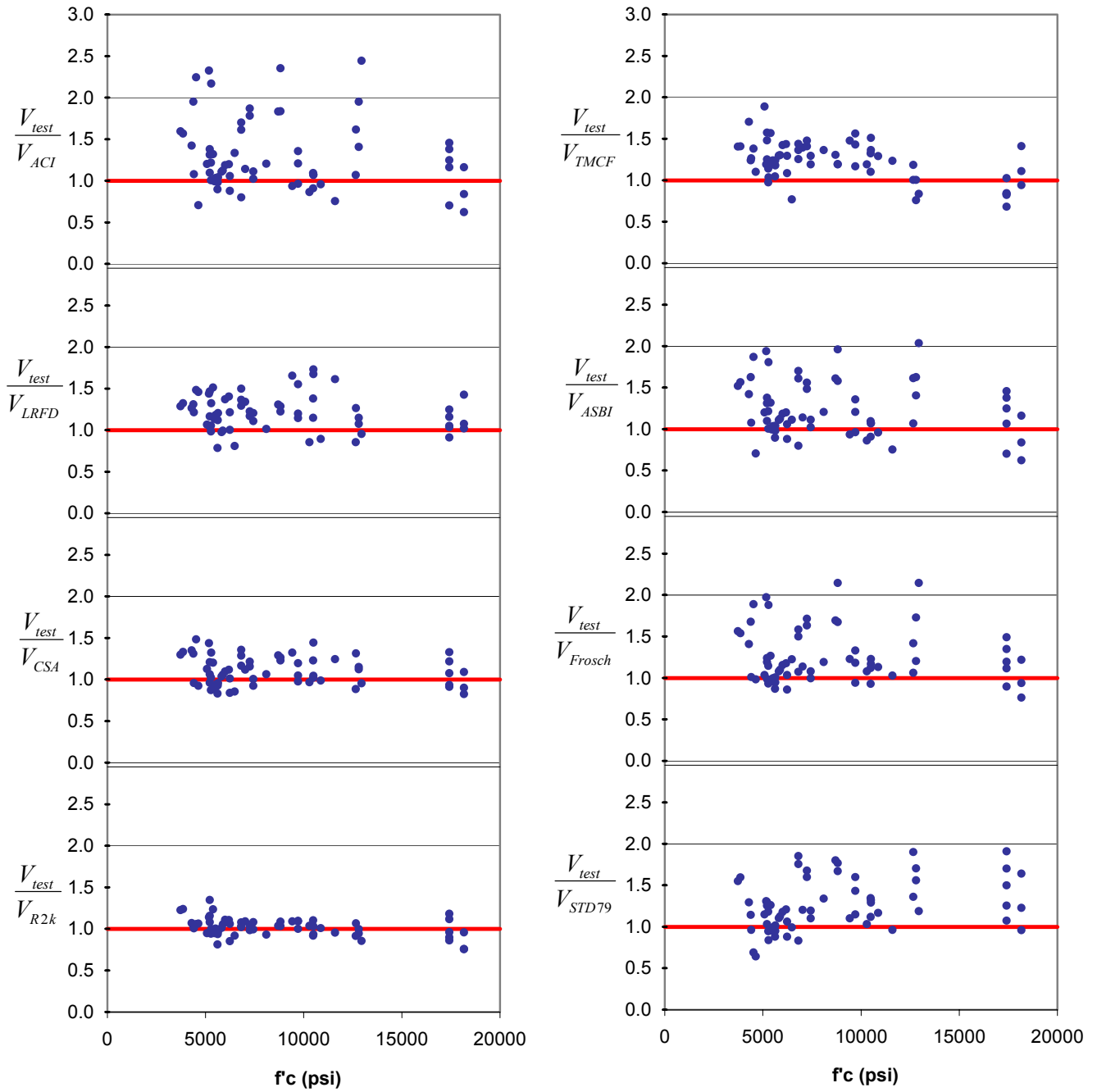


Figure D-4 Strength ratio (V_{Test}/V_{Pred}) versus concrete compressive strength ($f'c$) for 64 RC members

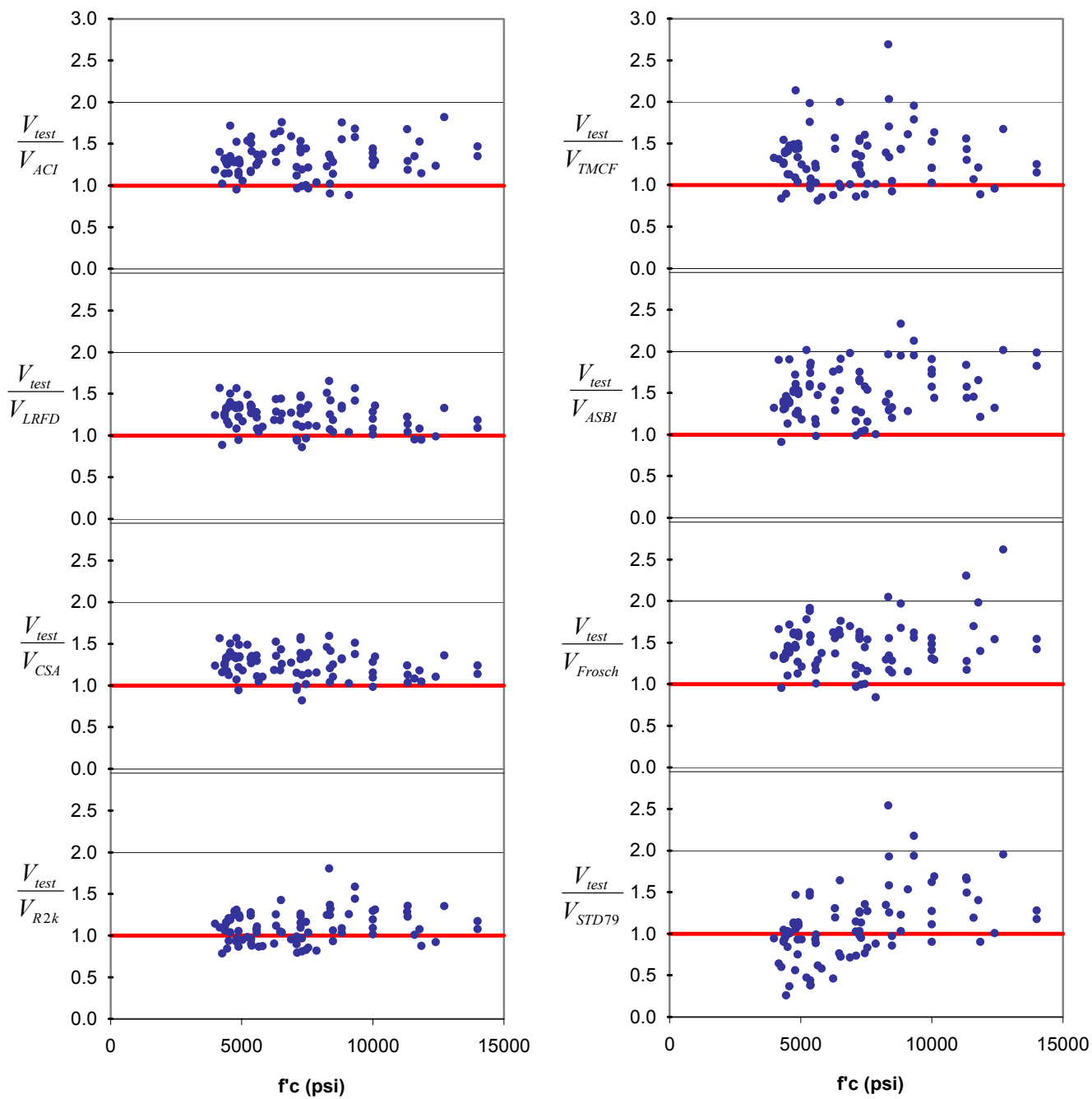


Figure D-5 Strength ratio (V_{Test}/V_{Pred}) versus concrete compressive strength ($f'c$) for 85 PC members

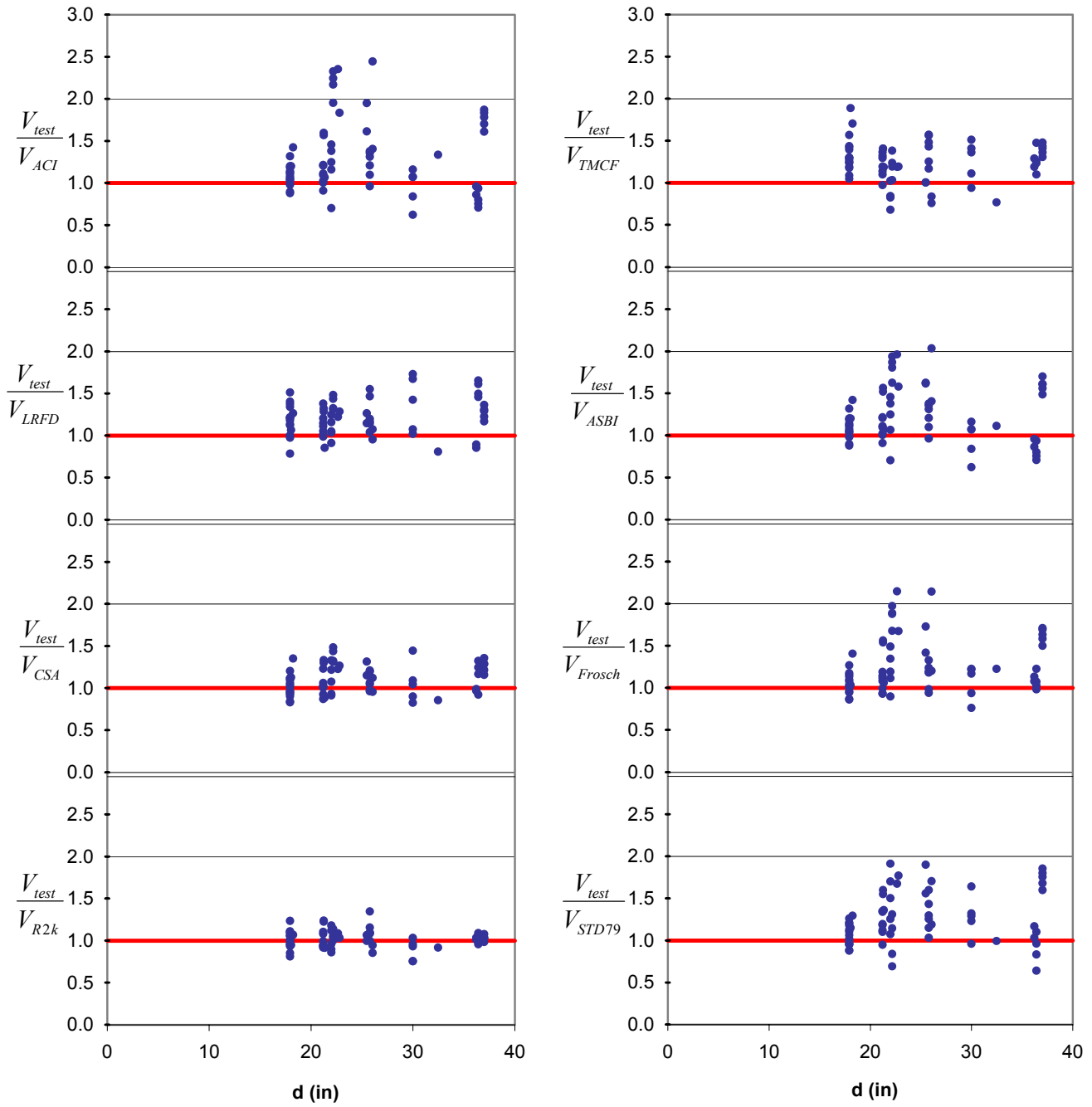


Figure D-6 Strength ratio (V_{Test}/V_{Pred}) versus member depth (d) for 64 RC members

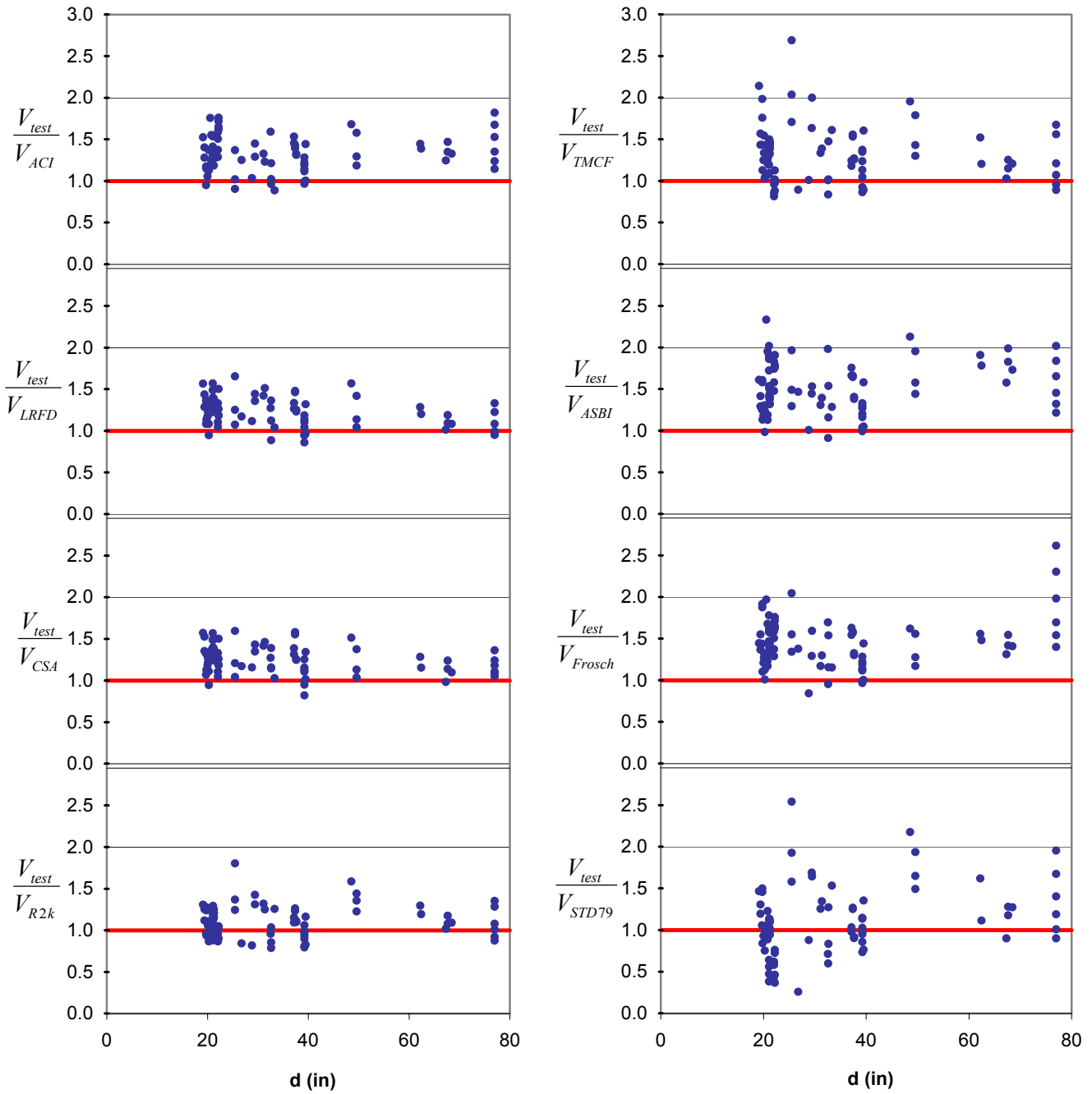


Figure D-7 Strength ratio (V_{Test}/V_{Pred}) versus member depth (d) for 85 PC members

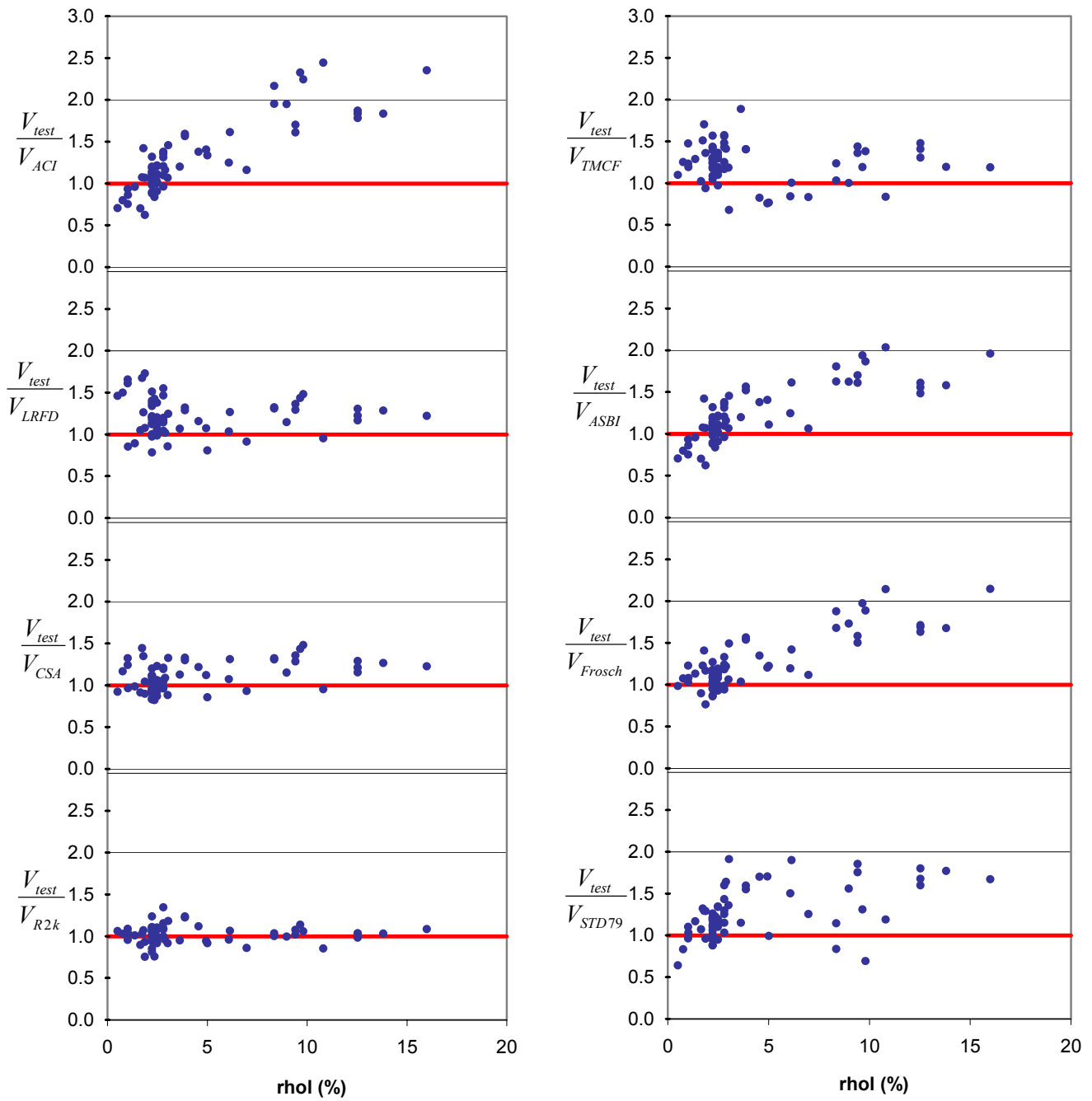


Figure D-8 Strength ratio (V_{Test}/V_{Pred}) versus longitudinal reinforcement ratio (ρ_l) for 64 RC members

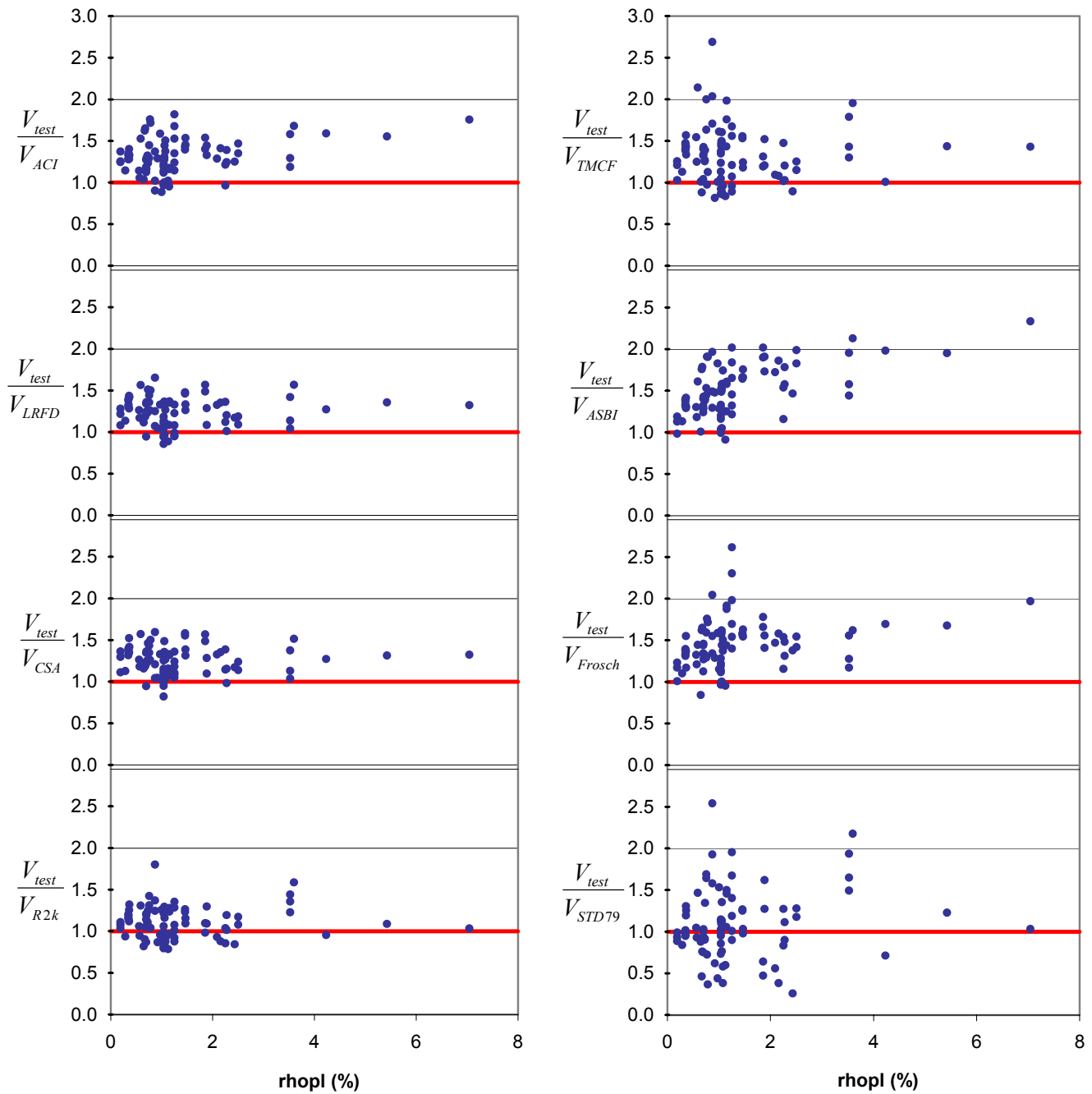


Figure D-9 Strength ratio (V_{Test}/V_{Pred}) versus versus longitudinal reinforcement ratio (ρ_l) for 85 PC members

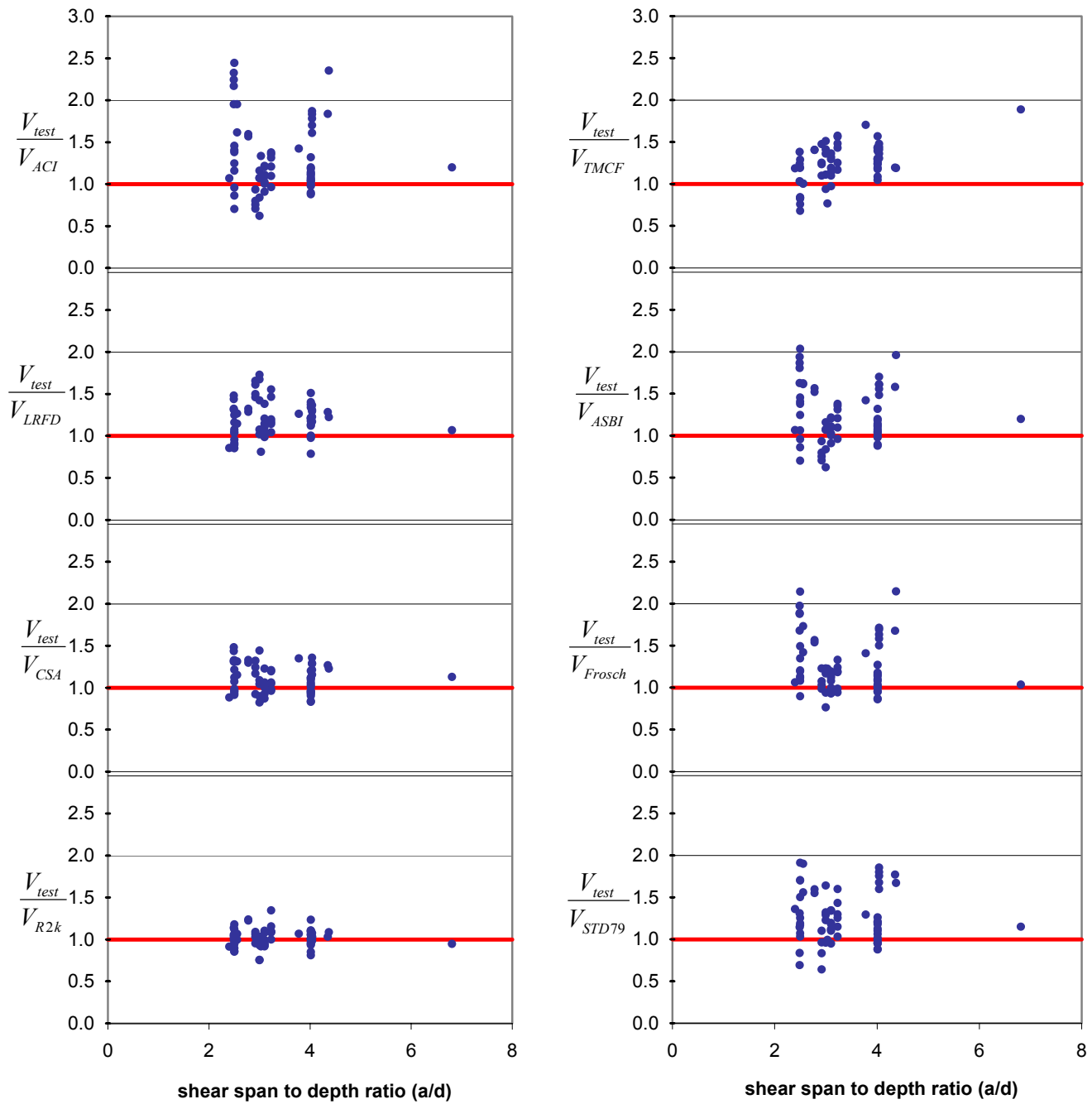


Figure D-10 Strength ratio (V_{Test}/V_{Pred}) versus shear span to depth ratio (a/d) for 64 RC members

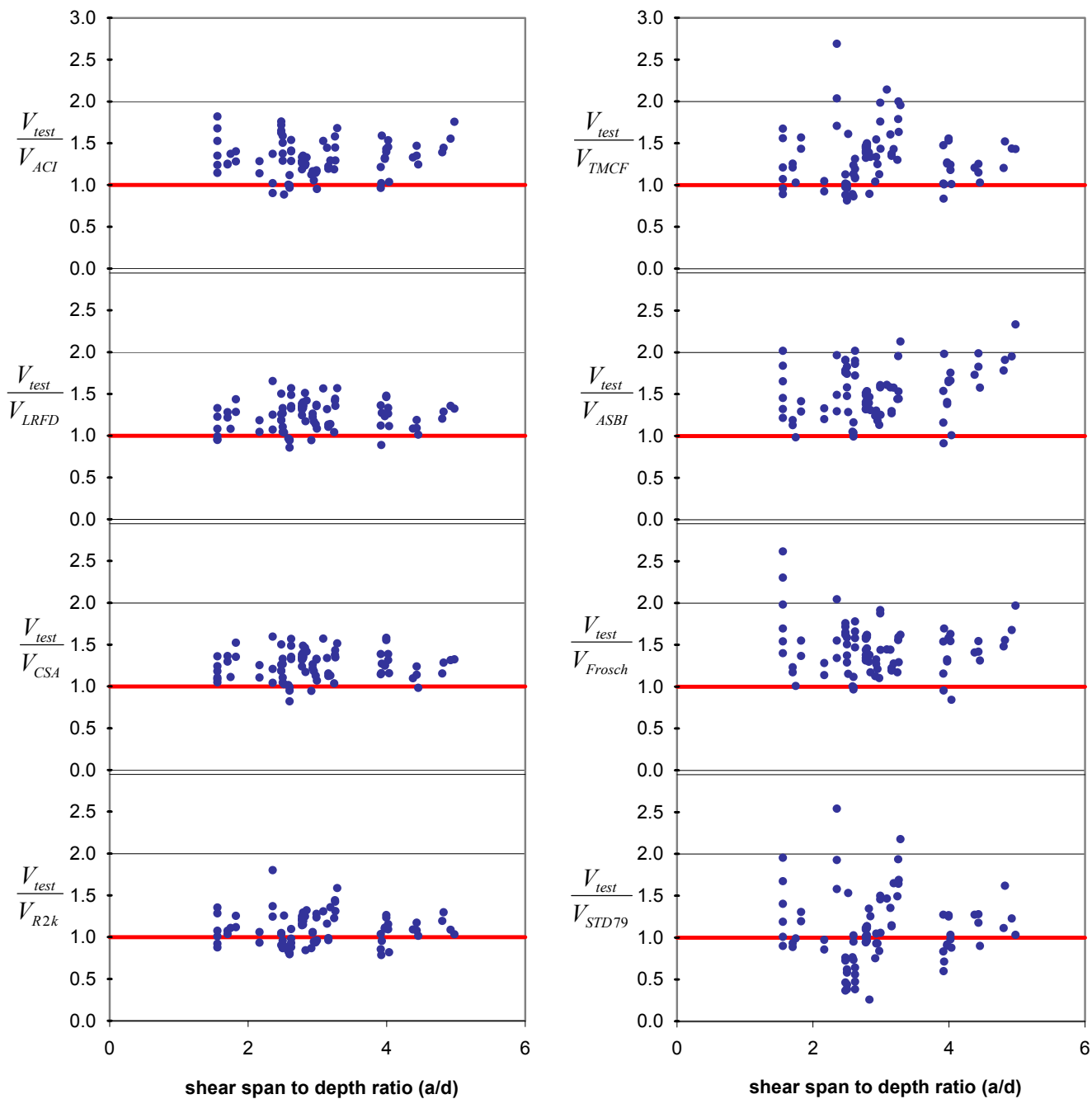


Figure D-11 Strength ratio (V_{Test}/V_{Pred}) versus shear span to depth ratio (a/d) for 85 PC members

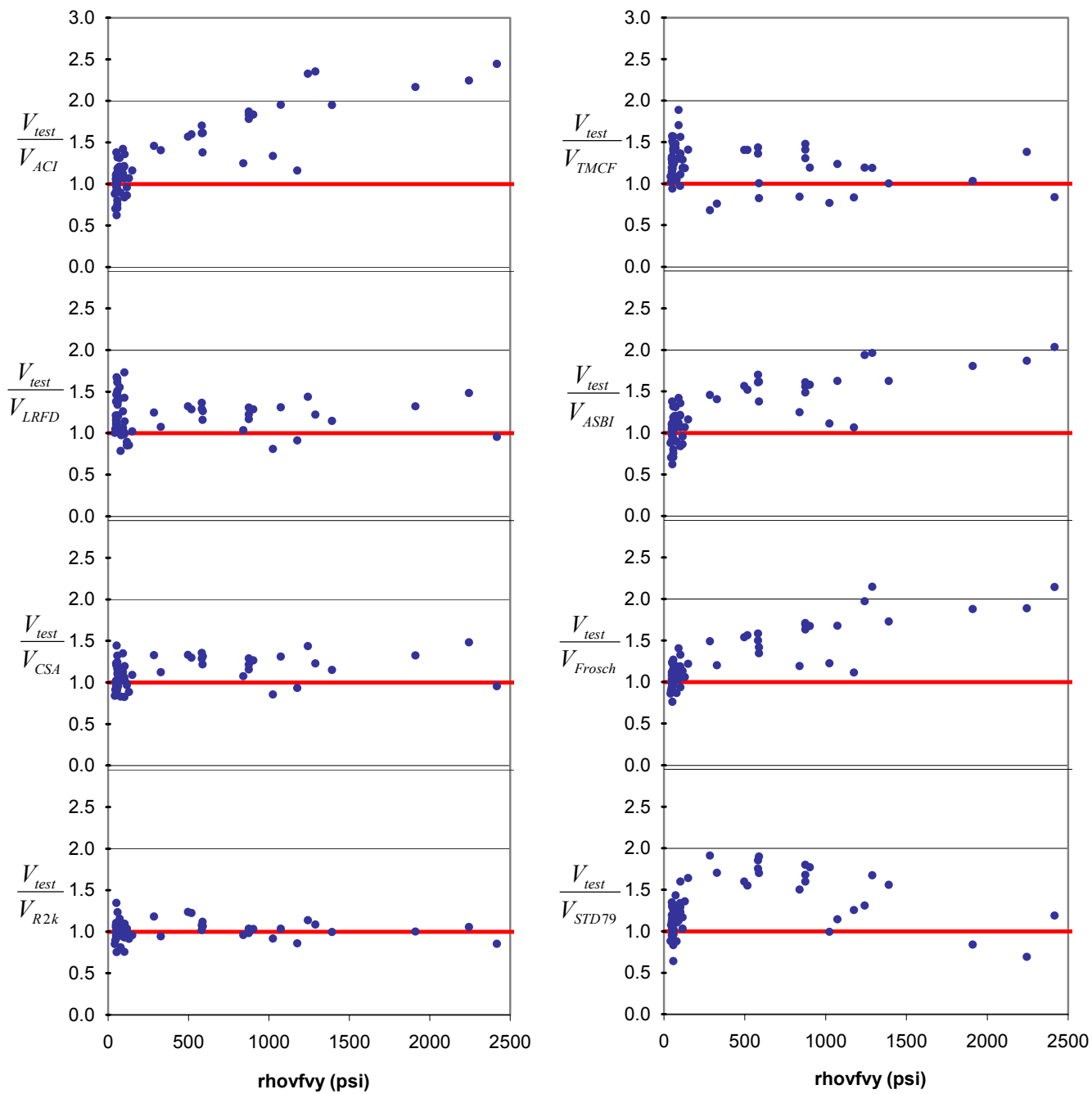


Figure D-12 Strength ratio (V_{Test}/V_{Pred}) versus shear reinforcement strength ($\rho_v f_{vy}$) for 64 RC members

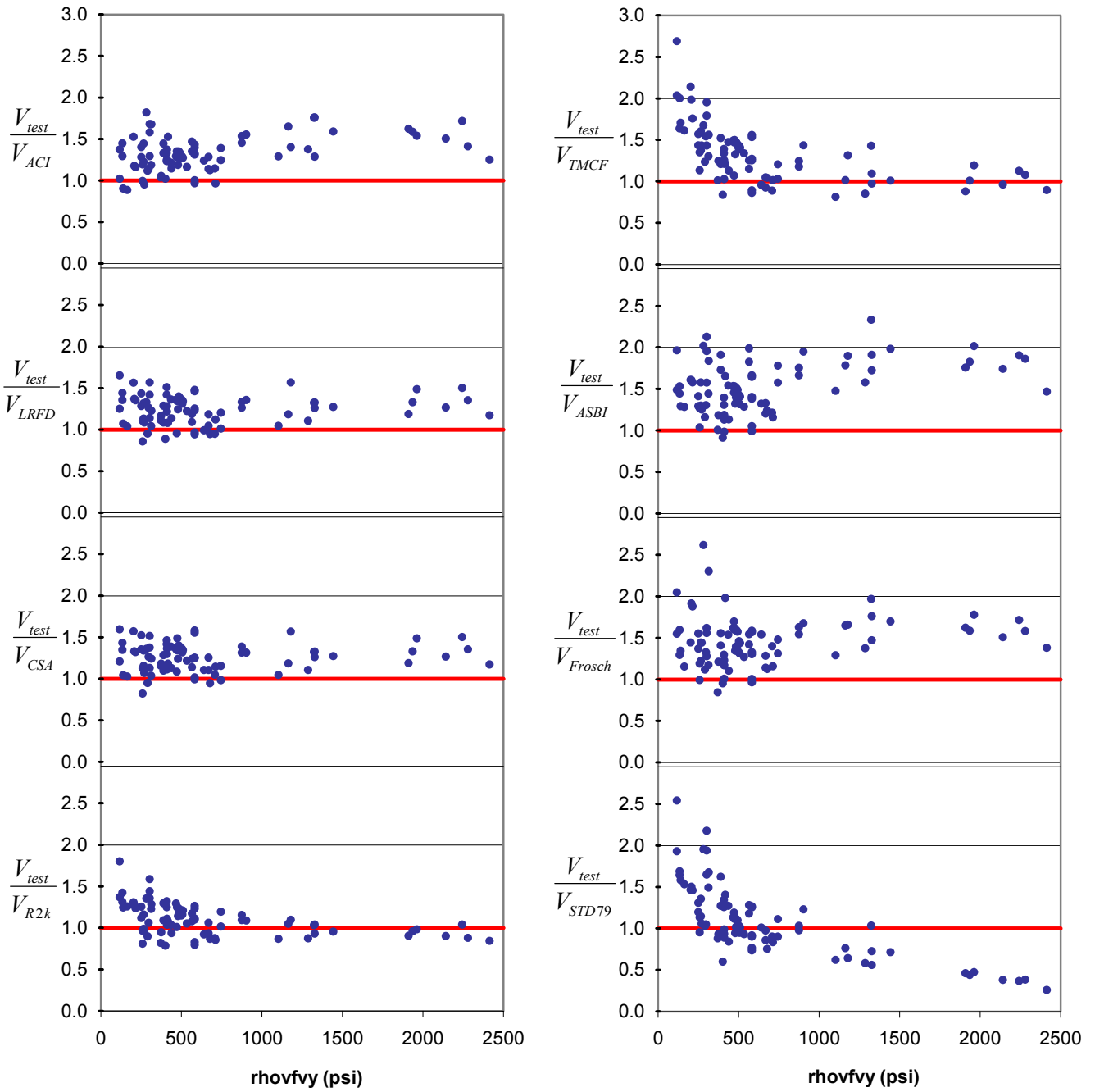


Figure D-13 Strength ratio (V_{Test}/V_{Pred}) versus shear reinforcement strength ($\rho_v f_{vy}$) for 85 PC members

APPENDIX E: Field Performance Data and Practitioner Experience

A survey of the design practice of 26 different state departments of transportation and federal lands bridge design agencies was conducted. This survey included both a written questionnaire and either a telephone briefing on the response to the questionnaire or a written response. The objective of the questionnaire was to determine the status of conversion to LRFD, identify specific problems and practices with respect to concrete element shear design, to ascertain preferences for shear design methodologies, and to provide a vehicle for organizations to express their opinion of the current LRFD shear design methodology.

Of the 26 agencies polled, 21 responded, and these states are Alaska, Arkansas, California, Delaware, FHWA CFLHD, Florida, Georgia, Illinois, Kansas, Kentucky, Mississippi, Missouri, Montana, Nevada, New Hampshire, New Jersey, Oregon, Pennsylvania, Tennessee, Texas, and Washington.

The questionnaire and the responses are included in Sections E.1 and E.2, respectively. A summary of the results of the questionnaire was presented in Section 2.4.

E.1 Questionnaire for NCHRP 12-61 Simplified Shear Provisions

Design:

- I. Does your agency currently use the AASHTO LRFD Specification, including the Modified Compression Field Theory (MCFT) shear provisions (Section 5.8.3.3)?
- II. Does your agency use any modifications to the provisions? (e.g. pre-set θ and β values, simplified approach to critical section determination, other)
- III. Have you had difficulty applying the LRFD MCFT shear provisions?
- IV. Does the lack of a unique solution for shear design cause problems for your agency?
- V. Do the LRFD MCFT shear provisions produce designs significantly different than the AASHTO Standard Specifications provisions for your bridges?
- VI. Does your agency use the 1979 Interim AASHTO provisions (or previous editions) for prestressed member shear design? (Allowed by footnote to Section 9.20 of the Standard Specifications)
- VII. Do you have a preference for approach to shear design? $V_c+V_s+V_p$; mechanically-understandable; relatively simple to apply; examples?
- VIII. What types of bridges are most often designed by your agency?
 - IX. Have you encountered cases where a particular method of shear design eliminated a bridge type from consideration?
 - X. What would you say is the most important design issue, with respect to concrete shear design, that your agency faces?
 - XI. Do the LRFD shear design provisions increase the design time significantly?
 - XII. Are the LRFD shear provisions acceptable and clear for continuous beam design?

- XIII. Do you use the Segmental Guide Specification shear design procedures for any of your box girder designs?

Field/Existing Structures:

- I. Has your agency had problems in the field that could be directly attributable to a given shear design approach? This can include any previously-used design procedure?
- II. Has your agency had problems in fabrication of precast elements or construction of any bridge elements that are attributable to a specific shear design procedure?
- III. Has your agency had cases where existing and/or recently-designed structures will not work or rate if load rated using the LRFD approach?

E.2 Responses to the Questionnaire for NCHRP 12-61 Simplified Shear Provisions

Design:

- I. Does your agency currently use the AASHTO LRFD Specification, including the Modified Compression Field Theory (MCFT) shear provisions (Section 5.8.3.3)?
 - 1) Yes, all new bridges.
 - 2) Yes, all new bridges; converting Bridge Design Manual to LRFD.
 - 3) Yes, have changed to LRFD, for all but steel boxes.
 - 4) Yes.
 - 5) Yes, on approx 99 percent of new bridges; all but one designer has changed over. MCFT is nice because it can be used for many elements.
 - 6) Yes.
 - 7) Mostly converted to LRFD.
 - 8) About 50 percent are done with LRFD; trying to figure out how to implement standard shear designs for I girders.
 - 9) In transition, but have not done any new concrete designs with LRFD.
 - 10) Some LRFD designs on newer structures; several LRFD designs with LFD check. Some strut and tie designs have been done, but that method has been found to be quite difficult.
 - 11) In process of switching over to LRFD; have completed several designs to date.
 - 12) Currently in transition to LRFD and in evaluation stage of whether to use MCFT or allow simplified method.
 - 13) In process of converting, still fairly green with LRFD.
 - 14) LRFD implementation is only in development stage; not adopted as yet for production.
 - 15) Not at this time; have one bridge in design by LRFD right now.
 - 16) No, doing first LRFD right now.
 - 17) No; other programs have impeded implementation.
 - 18) Have not converted yet; not enough support software.
 - 19) No.
 - 20) No.
 - 21) Yes, since 1997.

II. Does your agency use any modifications to the provisions? (e.g. pre-set θ and β values, simplified approach to critical section determination, other)

- 1) No.
- 2) Yes, use simplification to avoid iterations for angle.
- 3) No, but some smoothing on β and values.
- 4) Yes.
- 5) No, use tables in document.
- 6) No.
- 7) No modifications to the shear provisions. However, do use software, and if it includes simplifications, then those are used. The simplifications that are in LRFD for non-prestressed members often are not of use, because the demand is higher; thus to keep members at a similar size to the Standard Specifications, complete advantage must be taken of all mechanisms on the resistance side.
- 8) Yes, Standard Specifications method for shear capacity may be used with LRFD loadings.
- 9) No, not there yet.
- 10) No in-house changes; not to the point where we would be comfortable making changes yet.
- 11) No, and in limited calculations done to date the crack angle was set at 45-degrees and the concrete contribution, β , set to 2.
- 12) No changes formulated, but would welcome any modifications or simplifications, including the 'traditional' method.
- 13) No, but we would certainly preset some of the values as soon as our experience shows how it can be done. One designer investigated the current simplified method, but it proved too conservative for a precast slab unit.
- 14) No.
- 15) No.
- 16) No.
- 17) Not yet.
- 18) No, but have used $\beta = 2$ and $\theta = 26.5$ for non-prestressed cases.
- 19) No.
- 20) No.
- 21) No.

III. Have you had difficulty applying the LRFD MCFT shear provisions?

- 1) Yes, the learning curve is steep, even with training.
- 2) Yes with non-prestressed elements, such as footings and pile caps.
- 3) Yes, not simple enough and not clear where the numbers came from. Nice that strut and tie is now included, but difficult to follow in practice.
- 4) Yes.
- 5) Many of the younger engineers, who learned MCFT in school have had no problems. They have had more problems with V_{ci} and V_{cw} method. There have not been any problems with checking.
- 6) General problem with LRFD is that it is a 'black box'.

- 7) Absolutely. Several days of training by M. Collins helped, but still hard to pick up. Can't apply it by hand, thus hard to check. Code not clear on how to apply. Use of simplified method too conservative when coupled with increase in demand that is part of LRFD. Additionally, we have not been able to arrive at standard shear steel designs for P/S girders, which was easily accomplished with the Standard Specifications methods.
- 8) Yes, complex. Difficult to apply by hand. Not a lot of confidence with the method, because it is not tested in field. Why throw out all previous experience? Method takes more time. Still trying to arrive at standard shear designs for girders. Not sure that you get a better design with LRFD methods. Software not there yet.
- 9) Don't know yet.
- 10) Strut and tie difficult to apply, examples are always simply supported. Have had problems in continuous members.
- 11) Not applicable.
- 12) The short answer is a qualified yes. It takes some serious academic study to understand the new shear provisions. We are quite certain the provisions are a more accurate description of true behavior. However, as written, they are not appropriate for a design code. We opine that codes which work for the everyday designer are short, to the point, and also incorporate new knowledge all at the same time.
- 13) Several designers have indicated that it is too busy of a process for most 'bread/butter' type of structures. It requires software to do the iterations and can't readily be hand checked.
- 14) Yes, as you are aware, Dr. Collins has produced several generations of the equations in LRFD. All are a pain.
- 15) We have had trouble applying all the LRFD Specifications. Have had trouble developing in-house software due to complexity.
- 16) No. For new designers it takes about the same effort to learn as V_{ci} and V_{cw} method. However, some quick and intuitive checks would be nice.
- 17) Not applicable.
- 18) Iterative process difficult, especially without software.
- 19) No, we have not implemented LRFD design yet.
- 20) Not applicable.
- 21) No, however it is not the easiest thing to understand the first time using it for design.

IV. Does the lack of a unique solution for shear design cause problems for your agency?

- 1) Yes.
- 2) No.
- 3) No.
- 4) Not enough experience to answer.
- 5) No. There have not been any checking problems and iteration is not an issue.
- 6) No.
- 7) No unique solution is a problem.
- 8) Have not experienced any problems yet.

- 9) Not there yet.
- 10) Yes for the strut and tie models when checking, otherwise not sure yet.
- 11) Not applicable.
- 12) Yes, code should be short and to the point.
- 13) Too busy of a process, but otherwise not a problem.
- 14) Very much so. We need to be able to quickly spot check designs. When all possible paths have to be evaluated, this takes too much time and makes errors hard to spot.
- 15) No, not necessarily.
- 16) Not yet.
- 17) No.
- 18) Iteration adds effort and makes it more difficult.
- 19) It does have the potential to complicate the design.
- 20) Yes.
- 21) We are unaware of any problems.

V. Do the LRFD MCFT shear provisions produce designs significantly different than the AASHTO Standard Specifications provisions for your bridges?

- 1) Not tracked.
- 2) Not getting very different results. Second edition changes made results similar to Standard Specifications.
- 3) Much better with new tables, closer to old AASHTO. Before steel at quarter point was a concern, now distributed more toward ends. Some congestion at ends, but not so much of a shear steel problem.
- 4) Not anymore.
- 5) In first edition there was a noticeable increase in shear steel, but now not a big deal. There is more steel near the quarter points.
- 6) No.
- 7) More shear steel, as much as 40-50% more with skewed bridges. Sometimes have had to add strand.
- 8) No.
- 9) No.
- 10) It requires significantly more steel than the Standard Specifications. This may occur for stirrups, for longitudinal steel, or a combination of both. Often see more stirrups within 'd' of the beam end.
- 11) Not applicable.
- 12) At this time, we are not certain about this question in regard to the resistance side of the equation. At this juncture, we have more concern about the significant increase in design shear forces on the loading side.
- 13) Not enough experience to answer yet.
- 14) 'Significant' is relative. It does cause additional stirrups in some areas of a beam.
- 15) Don't know.
- 16) Not that we have noticed.
- 17) Probably not. We are conservative because of seismic.
- 18) 10-15% increase in stirrups at supports.
- 19) We have not investigated the design differences.

- 20) Not sure.
- 21) There have been minor differences in the amount of stirrups used, but nothing significant.

VI. Does your agency use the 1979 Interim AASHTO provisions (or previous editions) for prestressed member shear design? (Allowed by footnote to Section 9.20 of the Standard Spec.)

- 1) No.
- 2) Yes, 1979 method is embedded in girder design program.
- 3) No.
- 4) No.
- 5) No.
- 6) No.
- 7) No.
- 8) Yes in past, but it has not been used in recent past.
- 9) No.
- 10) No.
- 11) Yes.
- 12) No.
- 13) Yes, exclusively, until conversion to LRFD.
- 14) Yes, exclusively and without any ill effect.
- 15) No.
- 16) No.
- 17) No.
- 18) Yes, occasionally, but P/S usage is small.
- 19) Yes, on simple spans only.
- 20) Yes.
- 21) No. Not familiar enough with these provisions to know if we used them prior to LRFD implementation.

VII. Do you have a preference for approach to shear design? $V_c+V_s+V_p$; mechanically-understandable; relatively simple to apply; examples?

- 1) Simple is better, even though recognize that nearly all methods require software today.
- 2) Like the MCFT, because concrete contribution and tension are linked. Once familiar with MCFT it is easier. New engineers have trouble with V_{ci} and V_{cw} method.
- 3) Need a simple method. The MCFT concept is OK, but how it has been put into the code needs better documentation and peer review. Changes in table values have raised concerns with engineers. The method for design should be easy to understand and give a feel for behavior, something similar to rectangular stress block for bending.
- 4) No.

- 5) The method should be easy to apply without mistakes. The $V_c+V_s+V_p$ approach is a good way to present the method. Designers do not always care about the method being completely mechanically-understandable.
- 6) Method should be simple, not a black box.
- 7) Yes, simpler is better.
- 8) Iterative part is a problem in current method.
- 9) Simpler is better.
- 10) Prefer simpler methods, and iteration is distasteful. We are comfortable with the $V_c+V_s+V_p$ concept.
- 11) Relatively simple $V_c+V_s+V_p$ would be preferred.
- 12) We would welcome any simplifications. We are certain that the provisions are a more accurate description of true behavior. However, as written, they are not appropriate for a design code.
- 13) Should still allow simpler methods. If amounts of steel required between several shear design methods, why use the complicated method? You don't need extreme accuracy.
- 14) Yes, but we give up a lot since concurrent web shear and moment cannot be obtained for continuous bridges.
- 15) The old AASHTO Specifications were easy to use.
- 16) Yes, for checking. With simpler methods can see contributions of different mechanisms.
- 17) All of the above.
- 18) Keep something simple in the specifications.
- 19) The 1979 and current standard specifications have worked well for us.
- 20) Yes.
- 21) The $V_c+V_s+V_p$ approach seems straightforward enough, even with the complexity of calculating the individual terms.

VIII. What types of bridges are most often designed by your agency?

- 1) P/S girders, boxes and slabs. Generally simple span designs; we are not thrilled with continuity due to detailing concerns.
- 2) P/S girders.
- 3) AASHTO Type III and VI girders, bulb tees, and precast segmental. Many are simple span made continuous, but not counted on.
- 4) P/S concrete.
- 5) Bulb tees, decked-bulb tees and WSDOT series P/S girders. Many simple spans, some continuous for live load.
- 6) Not a lot of concrete bridges, but some P/S girders and some boxes.
- 7) P/S girders 80-90%. Simple-span for both dead load and live load. Deck made continuous with crack control steel, but not counted in design.
- 8) P/S girders. Both simple spans and simple span made continuous for live load are used. Most simple spans have a continuous deck that is not counted.
- 9) About 50 percent of new bridges are concrete. Mostly precast 'New England' bulb tees.
- 10) P/S haunched slabs, P/S I-girders and K-sections. Just beginning to use PT slabs.
- 11) Prestressed concrete I-girders or steel plate girders are the majority.

- 12) Concrete deck on stringers, and concrete deck on prestressed I-beams and bulb T-beams.
- 13) Concrete CIP slabs, box girders, I shapes, bulb tees.
- 14) Simple span for dead load, continuous for live load prestressed beams.
- 15) Prestressed beam bridges.
- 16) CIP PT box girders and some P/S girders.
- 17) CIP PT box girders, slabs, and some P/S girders, which are made continuous for live load.
- 18) Steel composite with concrete deck, with some P/S girder bridges.
- 19) CIP deck with P/S concrete I girders continuous for live load.
- 20) P/S girders.
- 21) Concrete box beams (either adjacent or spread) for any span 25-feet or greater. Rigid frames, box culvert and the occasional timber bridge for shorter spans.

IX. Have you encountered cases where a particular method of shear design eliminated a bridge type from consideration?

- 1) No.
- 2) Not yet.
- 3) No. LRFD shear design seems OK, particularly after modifications.
- 4) No.
- 5) No types eliminated.
- 6) Possible elimination could have happened, but not sure.
- 7) No, but for high skews shallower P/S beams may no longer work due to increased shear demand from new distribution factors.
- 8) Don't know.
- 9) Not yet.
- 10) No.
- 11) No.
- 12) No.
- 13) No.
- 14) No.
- 15) No.
- 16) No.
- 17) No.
- 18) No.
- 19) No.
- 20) No.
- 21) No, but the small structures we typically do (<100 feet) the bridge type is usually set during scoping (and similar to previous projects), so shear design would not be a determining factor in the type of structure used.

X. What would you say is the most important design issue, with respect to concrete shear design, that your agency faces?

- 1) The correct calculation of V_c , particularly after the section cracks.

- 2) Shear design for the negative moment region, and the longitudinal reinforcement design at mid-span.
- 3) Getting the calculations correct and being confident about the result.
- 4) How to apply the new specifications to existing bridges logically.
- 5) Load rating, particularly as related to the distribution of shear demand.
- 6) Understanding what appears to be a ‘black box’ method.
- 7) Trying to arrive at a standard shear design for all girders of a given size, which was possible with the Standard Specifications, but has not been so far with LRFD.
- 8) Need to have a simplified design method for checking.
- 9) A simpler method.
- 10) Developing a comfort level with the new methods, the learning curve. The lack of a hand method is an important issue for shear design, too.
- 11) Not applicable yet.
- 12) Larger specified design shear forces and complex shear resistance provisions.
- 13) Need a method to verify your design by hand. Too dependent on software, which may all come from one source.
- 14) The most important issues are speed, simplicity, and repeatability from one designer to another.
- 15) Simplicity, ease of use, and the ‘black box’ effect of the current method.
- 16) Keeping the designs easy to produce.
- 17) Congestion of shear reinforcement at bent caps, i.e. constructability. Also, not being able to check by hand is a concern, and software should show physically what is going on.
- 18) Simplicity and hand check methods with no iterations and one answer.
- 19) Not aware of any specific shear design issues.
- 20) LRFD needs to be simplified.
- 21) No critical issues that I am aware of.

XI. Do the LRFD shear design provisions increase the design time significantly?

- 1) Not really, design has to be automated; so design time is then not an issue.
- 2) Not with a computer, and not any more than V_{ci} and V_{cw} method. Hand checks do take more time though.
- 3) Yes, if you want to understand the result; no, if you just use the software.
- 4) No.
- 5) No increase in design time, difference is ‘peanuts’ with respect to previous method. In fact, many of the same parameters are required in both methods.
- 6) Don’t know yet.
- 7) Some increase, but not major.
- 8) Yes, anything in LRFD has increased design time.
- 9) Don’t know yet.
- 10) Design time is increased, even after the learning curve is accounted for.
- 11) They would increase design time, but once a process is laid out, I do not foresee the increased time to be significant.
- 12) Yes; however, time is not as important as clarity and understandability of the provisions themselves.
- 13) By hand, yes; by software, no.

- 14) Yes.
- 15) I think so. The LRFD Specifications increase the design time in almost all areas.
- 16) Maybe a little, but that is difficult to discern from the learning curve. In terms of total design, not that big a deal.
- 17) Not applicable.
- 18) Yes, especially without software.
- 19) It appears so, yes.
- 20) Probably.
- 21) No, we have beam design programmed into MathCAD. There was some initial programming time, but now the user need only fill in variables that change from project to project (θ and β , etc.)

XII. Are the LRFD shear provisions acceptable and clear for continuous beam design?

- 1) Not sure, probably they are, but they have not been used a lot.
- 2) No, particularly in the negative moment region.
- 3) Strut and tie method is a good addition, but frustrating to follow, particularly for continuous beams.
- 4) Yes.
- 5) Provisions need to be clarified for continuity cases, in general. Change of calculated longitudinal strain from tension flange to mid-depth helped.
- 6) Don't know yet.
- 7) Provisions are not clear. PCI examples are also not clear.
- 8) Don't know yet.
- 9) Don't know yet.
- 10) No, they are not clear to us.
- 11) Not applicable.
- 12) No.
- 13) Don't know yet, have not done any continuous beams with LRFD.
- 14) No, the same issues of concurrent shear and moment still exist.
- 15) Don't know. We have not done any continuous beams using LRFD.
- 16) Yes.
- 17) No, but better if proposed revisions go through in 2004.
- 18) Don't know yet.
- 19) Future clarification would be helpful.
- 20) No.
- 21) The vast majority of bridges are single spans. To my knowledge, we have not done a continuous beam design within the last several years, since we have been using LRFD.

XIII. Do you use the Segmental Guide Specifications shear design procedures for any of your box girder designs?

- 1) No.
- 2) Only on segmental bridges, and spliced-girder bridges done to LRFD.
- 3) No.
- 4) No.

- 5) No.
- 6) Yes, for one bridge.
- 7) No.
- 8) No.
- 9) No.
- 10) No, we very rarely, almost never design box girder bridges.
- 11) Not applicable.
- 12) No.
- 13) No, not in this office.
- 14) No, we do no segmental bridges.
- 15) We haven't done any segmental box girders. If we do, we would use the Guide Specifications.
- 16) No.
- 17) No.
- 18) No, we have never designed a box girder.
- 19) No.
- 20) No.
- 21) Unfamiliar with this specification.

Field/Existing Structures:

- I. Has your agency had problems in the field that could be directly attributable to a given shear design approach. This can include any previously-used design procedure.
 - 1) Yes, but not any designed with LRFD. Some 1950's and 1960's vintage bridges have inadequate shear reinforcement that has led to a retrofit program. This was also partly due to heavier trucks and increased tire pressures.
 - 2) No.
 - 3) There have been problems with using the LRFD provisions for two segmental bridges, potentially stemming from the lack of principal tension stress checks in the webs. Additional PT (about 50 percent more) was added during construction of one of the bridges.
 - 4) No.
 - 5) One older bridge in inventory has had a problem with growing shear cracks. This apparently was due to significantly heavier truck weights than used in the design. The bridge has now been replaced.
 - 6) No.
 - 7) No.
 - 8) No.
 - 9) No.
 - 10) Have had problems with cracking across hooks at bearing seats, which apparently is a development problem. This has occurred on 1930's vintage simple-span T-beam bridges. Additionally, have had some diagonal cracking near the dead load inflection points of 1950's vintage bridges, and this has required retrofit with epoxy shear bars.
 - 11) Low shear ratings (using Virtis) have occurred in negative moment regions of structures designed with Load Factor Design.
 - 12) No.

- 13) No.
- 14) None, including those designed prior to the drastic reduction in allowable concrete shear.
- 15) We have had some shear cracking in T-beams and bridge edge beams that were designed before 1976. That was about the time that the allowable shear was lowered to its current value. Since that time we have not had a problem.
- 16) No.
- 17) No.
- 18) Have had some shear cracking in negative moment region of continuous P/S girder bridges.
- 19) No.
- 20) No.
- 21) Not to my knowledge.

II. Has your agency had problems in fabrication of precast elements or construction of any bridge elements that are attributable to a specific shear design procedure.

- 1) Not aware of any specific problems, but stirrup spacing is often tight.
- 2) Have had problems at the ends of P/S girders, where the splitting reinforcement (4 percent of P/S) is supposed to be located within $h/5$ of the end. Proposing $h/4$ to ease the congestion.
- 3) No.
- 4) No.
- 5) Congestion of shear steel usually not a problem. Congestion of confinement steel is a problem, however.
- 6) No.
- 7) Not yet, but LRFD method may produce unacceptable shear steel quantities for high skews and shallow beams, which worked by Standard Specifications.
- 8) Hard to say, because it is difficult to trace problem back to cause.
- 9) Have had diagonal cracks in webs near ends after strand release. Could be fabricator problem.
- 10) No, but have used self-leveling concrete to avoid compaction problems in congested areas.
- 11) Not applicable.
- 12) No.
- 13) No.
- 14) Not directly. Any prestressed beam with deflected strands requires dense patterns at the beam ends.
- 15) No not generally. There is a slight problem in getting all the shear steel into the ends of prestressed beams. It is getting quite congested.
- 16) No.
- 17) Joint shear designs of column footings or pile caps using some of the earlier seismic criteria were too congested.
- 18) No.
- 19) No.
- 20) No.

- 21) Not necessarily specific to a shear design procedure, but we have had some difficulty with the number of stirrups and the amount of end block steel conflicting at the ends of box beams. It has led to fabrication problems, either with changes at the shop drawing phase or adjustments made during fabrication (i.e. stirrups at spacings different from the plans or stirrups that shift in the form and create groups of bars). We have made an effort with recent box beam project to reduce the amount of overlapping or repetitive end block steel so that there is more flexibility in its placement and so that the stirrups are placed correctly.

III. Has your agency had cases where existing and/or recently-designed structures will not work or rate if load rated using the LRFD approach?

- 1) Not using LRFD for load rating (LRFR), yet.
- 2) LRFR will be a problem if newer bridges don't 'rate'. AASHTO guide is forthcoming.
- 3) There is a real debate over LRFR right now, may use older specification for rating older bridges.
- 4) Yes, almost every multi-column bent.
- 5) Some load ratings must use grid models to develop actual shear force distributions.
- 6) If load rating is a problem with new specification, then go back to older specification that worked.
- 7) This could be a problem, although load rating is done solely on flexure, here.
- 8) Don't know yet.
- 9) Not using LRFR yet, but this likely will be an issue.
- 10) We are just starting to explore LRFR now; thus, no problems yet.
- 11) We have not rated structures LRFD, as of yet.
- 12) Not sure.
- 13) Don't know yet.
- 14) We have not made specific checks. Others have reported such problems exist.
- 15) There is lots of controversy with LRFR. LRFR is not ready yet.
- 16) Have not looked into this yet. Whether it's a problem depends on how the system is set up.
- 17) Not applicable.
- 18) This would be a problem if LRFR caused something not to rate that previously did rate.
- 19) We have not investigated existing structures using LRFD.
- 20) Don't know.
- 21) Our ratings continue to be done in LFD. There was one LRFD designed bridge that had a perfectly acceptable beam design using the HL93 truck and the design tandem. However, when rated using LFD and one of the Delaware design trucks (S335 – a tandem load), it rated at just under 1.0. An additional pair of strands was added so that the design met both criteria.

APPENDIX F: Recommended Revisions to Shear Provisions of AASHTO LRFD Concrete Provisions

F.1 Scope

This Appendix details the revisions to the shear provisions of Section 5.8.3 of the LRFD Provisions recommended as a result of this study. There are three major differences between the existing shear provisions and those recommended here: (1) An explicit requirement is introduced into Section 5.8.3.2 that unless the member is built integrally into the support, then the shear stress in the member must not exceed $0.18f'_c$ unless a strut and tie model is used to design the D-Region near the end of the beam; (2) The replacement of the MCFT based provisions of the existing Section 5.8.3.4.2 with a new Section 5.8.3.4.3 that contains more simplified MCFT provisions, based on the 2004 CSA provisions; and (3) The introduction into a new Section 5.8.3.4.2 of a simplified procedure for shear design of both prestressed and nonprestressed sections. The two major changes, additional to the proposed simplified provisions, are discussed in Sections F.2 and F.3, respectively. The proposed simplified provisions and the basis for those recommendations are discussed in Section F.4. The complete recommended revised provisions are presented in the same format as the existing Section 5.8.3 of the AASHTO-LRFD in Section F.5. Deletions are shown by strikeouts and insertions by underlining. Accompanying the provisions is a revised commentary that explains the basis for the provisions.

F.2. Maximum Shear Stress Limit

Parallel with this project NCHRP 12-61 on “Simplified Shear Design of Structural Concrete Members”, there was project NCHRP 12-56 on “Application of the LRFD Bridge Design Specifications to High-Strength Structural Concrete: Shear Provisions.” In project 12-56 tests were conducted on 63-inch deep bulb-tee girders with a 10-inch thick cast in place concrete deck slab. Concrete strengths for the girders ranged between 8 and 18 ksi and several of them were highly prestressed with up to forty-two 0.6-inch diameter, 270 Grade, strands placed in the lower flange of the girder. Design shear stresses for the girders varied between 0.05 and 0.25 f'_c . The girders were subjected to uniformly distributed loads that were increased slowly until failure occurred. The shear reinforcement for the girders was designed using the AASHTO LRFD provisions of the existing Section 5.8.3. For several of the girders, as the applied shear stresses exceeded 0.14 f'_c , the girders failed violently due to a horizontal shearing failure along the intersection between the web of the girder and the lower flange. Details of the failures are provided in Kim (F.1) and Kuchma et al. (F.2) and are included in the final report for Project 12-56.

The explosive horizontal shearing failures typically removed the bottom third of the web for a distance of about two beam depths from the end of the girder. The exact cause of the failure was not obvious. However, it was clear that, with the beam loaded on top and supported on the bottom, there was a problem created by the funneling of compression forces into the reaction. The inclined cracks for the depth of the beam from the support all focused on the reaction as apparent from Figure C5.8.3.4.2-1 of the proposed revised commentary. The narrowing of the ends of the compression struts as they approached the support caused flaking of the concrete at the end of the struts before the explosive failure occurred. Further, as can be seen from Figure C5.8.3.4.2-1, the angles to the horizontal of the struts in the ends of the beams was greater than for inclined cracks at a distance “ d_v ” or more from the support. Thus, the transverse reinforcement in the end of the beam is not as

effective as that at a distance greater than “ d_v ” from the support. The MCFT, the basis for the existing AASHTO LRFD shear provisions, was derived from tests on plate elements uniformly loaded along their edges. Such plate elements realistically represent the conditions in the shear span of the girders at a distance greater than “ d_v ” from the face of the support, but not conditions within that distance unless the girder is built integrally with a transverse member of a similar depth or is continuous over the support.

There is reason to believe that this horizontal shear stress failure is also a function of the I-shape of the girder and that the same type of failure is less likely in girders with rectangular sections. The NCHRP 12-56 girders were reinforced differently at each end so that two shear tests could be made on sections with different properties at each end. After failure occurred at the first end, that end of the girder was repaired and reinforced and testing then continued until the other end failed. Often repair involved filling in the width of the girder between the faces of the web and the edges of the bottom flange with concrete for a depth of the girder from the support. Such repairs were sufficient to allow failure to be reached at the other end of the girder. In the 1950s and 1960s the University of Illinois, (Bulletin 493), made a large number of tests on small scale prestressed concrete I-girders and the provisions of the AASHTO Standard Specifications are based largely on the results of those tests. While concrete strengths in those tests were typically only 3 to 4 ksi, shear stresses as high as $0.25f'_c$ were achieved without horizontal shear failures along the intersection of the girder web and the bottom flange. However, those tests were made before the decision was taken to eliminate girder end blocks. Thus all the small-scale beams achieving shear stresses above $0.18f'_c$ had end blocks making them similar in some respects to the repaired girders of project 12-56.

The failure of the project 12-56 girders often occurred within the length where the transfer of stress occurs between the strands and the concrete due to anchorage of the prestress of the strands. Initially there were concerns that the horizontal shear failures may have been precipitated by bond failures of the strands. However, following careful instrumentation of the strands protruding from the end of the beam in subsequent tests in which the same horizontal shear failures occurred, no evidence of strand slip prior to failure was found. However, other instrumentation was used that recorded displacements for a grid covering the length and depth of the beam for the distance from one beam depth to two beam depths from the support. The measured displacements showed that shortly before failure the bottom flange of the beam started displacing towards the center of the beam consistent with the final mode of failure.

The ability of the web of a girder to carry large shear stresses above reactions, without concrete crushing of the web, or horizontal shear failure along the interface between the web and the bottom flange for a beam without an end block, is very dependent on end design details and the limiting shear stress needs to be less than that in the current AASHTO LRFD provisions. On the other hand, the maximum shear stress limits of the AASHTO STD, ACI and ASBI provisions are too conservative. From this study it is concluded that the maximum shear stress limit is related to the concrete crushing rather than diagonal tension cracking. Accordingly the shear stress limit should be a fraction of f'_c rather than $\sqrt{f'_c}$ and less than in the current AASHTO LRFD specifications. Based on the available test results a maximum shear stress limit of $0.18f'_c$ is recommended unless members are cast integrally with supports.

The limitation on shear strength is principally imposed to guard against diagonal compression failure. The diagonal compressive stress, f_d is determined as,

$$f_d = \frac{V_u}{\phi (b_v d_v \sin \theta \cos \theta)} \quad (\text{F-1})$$

$$\text{or } \frac{V_n}{b_v d_v} = f_d \sin \theta \cos \theta \quad (\text{F-2})$$

The AASHTO STD and ACI 318-02 methods limit V_s to $8\sqrt{f'_c} b_v d_v$ which therefore limits V_n to $10 - 14\sqrt{f'_c} b_v d_v$, depending on the level of axial prestress. If θ is taken as 45 degrees and $d_v = 0.9d$, then that limit corresponds to a diagonal compressive stress limit f_d of $22 - 30\sqrt{f'_c}$. If $f'_c = 5000$, psi then the f_d limit is $30\sqrt{f'_c} = 0.42 f'_c$ and if $f'_c = 10,000$ psi, then the f_d limit is $30\sqrt{f'_c} = 0.3 f'_c$.

The AASHTO LRFD Specifications limits the maximum shear stress to $0.25 f'_c$. When $v/f'_c = 0.25$, the lowest permissible angle of diagonal compression in the LRFD method is 28 degrees. That angle corresponds to a diagonal compressive stress limit of $f_d = 0.60 f'_c$.

In the German Standard (DIN), the limit on shear strength is also determined from a limit on the uniform field of diagonal compression based on a variable-angle truss model representation.

$$V_{Rd,max} = [f_{cd} / (\cot \theta + \tan \theta)] b_w z \quad (\text{F-3})$$

$$= [\alpha_c f_{cd} \sin \theta \cos \theta] b_w z \quad (\text{F-4})$$

$$\text{or } \frac{V_{Rd,max}}{0.9 b_w d} = \alpha_c f_{cd} \cos \theta \sin \theta \quad (\text{F-5})$$

where α_c is the reduction factor for the strength of the struts and f_{cd} is the design value for the uniaxial concrete compressive strengths (i.e., $f_{cd} = 0.85 f_{ck} / 1.5$ where $f_{ck} = f'_c - 1.6$ MPa). The DIN method specifies α_c as $0.75 \eta_1$, where $\eta_1 = 1$ for normal weight concrete. Therefore, the DIN method limits that diagonal compressive stress f_d to approximately $0.4 f'_c$. For these three codes of practice, there is a wide range in the allowable diagonal compressive stress limits. Values range from 0.3 to $0.6 f'_c$. Another factor to be considered is that there is a concentration of the diagonal compressive stresses as forces funnel into a support. Based on the measured strains in the girders tested in NCHRP Project 12-56, as well as based on the results of elastic analyses, the diagonal compressive stress in the web above the support can be more than 50% greater than the stress in a uniform compression field. For this reason, and with the lower limit on theta of 30 degrees proposed in the simplified procedure, it is appropriate that the maximum shear stress be limited as follows:

$$v_{max} = f_d / \alpha \sin \theta \cos \theta = 0.6 f'_c / 1.5 \cos(30) \sin(30) \approx 0.18 f'_c \quad (\text{F-6})$$

F.3 Revision of General Procedure

The studies of practitioner experience reported in Appendix E show that one of the major concerns of practitioners with the existing provisions is that they lose their physical 'feel' for shear design and consequently they would use simplifications to the LRFD MCFT if those simplifications were reasonable. The studies reported in Appendixes B, C and D have shown that the CSA 2004 method provides predictions of measured shear strengths as good as those of the existing AASHTO

LRFD method while largely eliminating the need for the iterative procedures of the current LRFD method. Therefore, modification of the current general procedures of Section 5.8.3.4.2 of the current LRFD method by adoption of the CSA 2004 method is proposed.

It is proposed that the values of β and θ no longer need to be determined from tables but can be determined from relatively simple equations. Further, it is proposed that the expression for the longitudinal strain ϵ_x at the middepth of the member can be simplified by removing its dependence on the value of θ . ϵ_x is then determined directly from an equation involving the factored forces calculated as acting on the section and section properties only. Appropriate changes are proposed in Section 5.8.3 for the General Procedure both for “Sections Containing at Least Minimum Transverse Reinforcement” and for “Sections Containing Less than Minimum Transverse Reinforcement.”

F.4 Simplified Shear Provisions

This section summarizes the process and criteria that the contractor used in the selection of the proposed Simplified Shear Design Specifications. Section F.4.1 describes the process and criteria used to develop those simplified provisions. Section F.4.2 presents the positive attributes of the shear design methods reviewed. Section F.4.3 presents the basis and derivation of the proposed Simplified Provisions.

F.4.1 Process and Criteria for Development of Simplified Provisions

In the previous sections, the contractor presented evidence that the draft CSA specifications were a simple, accurate, and comprehensive design approach that overcame the difficulties associated with the use of the tables in Section 5.8.3 of the existing LRFD specifications by enabling Beta and Theta to be calculated using simple algebraic expressions. However, as a result of a meeting with the project panel in September 2003 the contractor came to appreciate that the draft CSA Specifications were not what the panel envisaged for simplified provisions and that simplified provisions should be developed that were not based on the MCFT. A majority of the panel believed that the model that is the basis of the LRFD provisions was too complicated, with the result that the provisions were often being used blindly. The panel expressed concern with having to evaluate the angle theta to determine the contribution of the shear reinforcement because that action complicated the design process.

In response it was suggested that if it was assumed that the Sectional Design Model would be replaced by provisions similar to the draft CSA Specifications, then simplified provisions should be developed that took a different approach. As a consequence the contractor developed the following selection criteria for an approach that would address the perceived shortcomings of the draft CSA specifications:

- 1) The simplified Specifications should be directly usable without iteration to evaluate the capacity of a member. This is not possible in the 2004 CSA Specifications as the value for V_u is included in the equation for calculating ϵ_x , which in turn is used for calculating V_c and V_s as follows:

$$V_c = \beta \sqrt{f'_c} b_v d_v \quad (\text{F-7})$$

and

$$V_s = \frac{A_v f_y d_v \cot \theta}{s} \quad (\text{F-8})$$

where

$$\beta = \frac{4.8}{(1+1500\varepsilon_x)}, \theta = 29 + 7000\varepsilon_x, \text{ and } \varepsilon_x = \frac{M_u/d_v + 0.5N_u + V_u - \phi_p V_p - A_p f_{po}}{2(E_s A_s + E_p A_p)} \quad (\text{F-9})$$

2) The simplified Specifications should be useful in conducting field evaluations by providing the engineer with lower bound estimates to the loads at which shear cracking is expected to occur in the member. This is a restrictive criterion because if V_c in the provisions is an estimate of the diagonal cracking load, then it may be unrealistic to assume that V_c can simultaneously be a measure of the concrete contribution to capacity in the ultimate limit state. However, if V_c is a lower bound estimate of the shear force that causes diagonal cracking, then it is necessary to justify that this value of V_c is not an overstatement of the concrete contribution in the ultimate limit state. Because this criterion is partly a service load criterion its importance for strength-based specifications can be questioned. However, if this criterion is not used in the Specifications then this relationship should, as a minimum, be discussed in the Commentary to the Specifications.

3) The basis of the Specifications should be readily understandable and easily explainable by one engineer to another while still being based on a sound mechanistic model for strength.

4) The Specifications should allow rapid and reliable designs and rapid and reliable checks of designs by others.

5) The Specifications should not try to be a simplification of the existing LRFD specifications, as are the 2004 CSA specifications.

6) The Specifications should avoid the necessity of calculating the angle theta. If a simple relationship is to be suggested for calculating theta, then there needs be a default value that can be used if the engineer does not wish to make this calculation.

7) The Specifications do not need to enable the effects of all actions (axial load, moment, shear, and prestressing) to be considered simultaneously as this is done already in the LRFD Shear Design Specifications and it will likely be accounted for in future versions of Sectional Design Model (Section 5.8.3).

8) The simplified Specifications should provide a safe and reasonably accurate estimate of the required strength of the shear reinforcement for the types of members likely to be designed by these Specifications, (the design database prepared by the contractor), and where the best estimate of the required amount of shear reinforcement is determined both by using the results from the experimental database and from the application of program Response 2000.

9) Where the required strength of the shear reinforcement by the simplified Specifications ($\rho_v f_y$) differs substantially from what is required by use of the existing AASHTO Standard specifications, the LRFD specifications, and more importantly program Response 2000, then the reasons for the required amount of shear reinforcement should be well justified and results should be conservative.

F.4.2 Positive Attributes of Different Shear Design Approaches

The contractor evaluated all of the shear design approaches reviewed previously in conjunction with the criteria described in Section F.4.1. These approaches included:

- 1) AASHTO Standard Specification 1989 (AASHTO STD) and ACI 318-02;
- 2) AASHTO LRFD;
- 3) CSA 2004;
- 4) AASHTO 1979;
- 5) ASBI-AASHTO Segmental Bridge Guide Specifications;
- 6) Method by Frosch;

- 7) Truss Model with Crack Friction;
- 8) EuroCode 2;
- 9) JSCE; and
- 10) DIN.

The contractor identified the following positive attributes of the different shear design approaches:

1) In the AASHTO STD, ACI 318-02 and in the ASBI methods, the calculated value for V_c is an estimate of the diagonal cracking load. This result was considered not only to be useful for assessing the condition of a member in the field, but to also be important in the design process for determining if cracking is expected in a member under service load levels.

2) The consideration of two types of diagonal cracking, web-shear and flexure-shear, as used in the AASHTO STD and ACI 318-02 methods, was useful for characterizing shear behavior. As confirmed by the review of experimental test data, and by the results being obtained in NCHRP project 12-56, in web-shear regions – typically near the end of a simply supported member or in the region of contraflexure and over a central support in continuous beams– diagonal cracking in prestressed members does not occur until much higher shear stresses, and the angle of diagonal cracking is much flatter, than in reinforced concrete beams. By contrast, diagonal cracking in flexure-shear zones and in reinforced concrete beams occurs under much lower shear stresses, the cracks are rather steep, and sometimes in excess of 45 degrees.

3) The AASHTO LRFD method requires a minimum amount of shear reinforcement that is larger than in most other codes. This result was considered desirable as it was observed from the experimental test database that members with very low amounts of shear reinforcement were the ones most likely to fail under loads less than the calculated code capacities. For reinforced concrete (non-prestressed) beams with transverse reinforcement limited to the 50 psi minimum shear reinforcement required by the AASHTO STD and ACI 318-02 methods, a significant fraction of the members showed capacities less than the code calculated capacities.

4) The draft CSA, AASHTO1979, AASHTO LRFD, Truss Model with Crack Friction, Eurocode2, JSCE, and DIN methods all allow the designer to use an angle θ flatter than 45 degrees when evaluating the contribution of shear reinforcement to shear capacity. This allowance is supported by experimental test data that shows that for web-shear type cracking the angle of diagonal cracking is much flatter than 45 degrees, usually around 30 degrees, and can be reliably calculated using Mohr's circle of stress. That same observation is not, however, supported by the test data for situations where flexure-shear cracking governs. It is important to recognize the influence of accounting for the angle θ on the amount of shear reinforcement that is required in a member. When θ is assumed to be 45 degrees, 1.73 times as much shear reinforcement is required for the same shear design force than if θ is taken as 30 degrees; $\cot(30) = 1.73$. This difference is most important in the end regions of members, (and the interior supports of continuous members), when the shear force is high so that the fraction of the total shear force supported by stirrups (V_s/V_n) is large. This result is illustrated in Fig. F-1 for a member with 6000 psi concrete and where the concrete contribution is taken as $V_c = 4\sqrt{f'_c} b_v d_v$ (in, psi units).

5) The AASHTO LRFD, DIN, and Eurocode 2 methods allow the engineer to design a member to support a much larger shear stress than is permitted in other codes of practice. In the AASHTO LRFD, this shear design force limit is $V_n = 0.25 f'_c b_v d_v + V_p$ while in AASHTO STD and ACI 318-02 the limit is $V_n \approx 10 \sim 14 \sqrt{f'_c} b_w d$. To illustrate this difference, when $f'_c = 10,000$, the LRFD limit

is 2500 psi plus the stress that is taken by the vertical component of the prestressing. By contrast, the AASHTO STD and ACI 318-02 limit is just 1000-1400 psi.

F.4.3 Derivation of Simplified Provisions

F.4.3.1 Overview

After consideration of the provisions in numerous codes of practice and of other suggested shear design approaches, a simplified method is proposed that shares the approach taken in the current AASHTO Standard Specifications and in ACI 318-02 where the structure is divided into regions of web-shear and flexure-shear cracking. The ability to estimate the diagonal cracking load for the purpose of service evaluations is considered important to include in the AASHTO LRFD Specifications particularly because the use of the AASHTO Standard Specifications is likely to be discontinued in the near future. However, the proposed simplified specifications differ from the current AASHTO Standard Specifications in the expressions for V_{cw} , the assumed angle for θ , the maximum shear stress permitted for design, the minimum required amount of shear reinforcement, and requirements for the amount of longitudinal tension reinforcement that must be developed at the face of the support. Further, the expressions for V_{cw} and V_{ci} are taken so that they are lower bounds to the likely values for web-shear cracking and flexure-shear cracking, respectively, and so that they are therefore also valid lower bounds to the shear that can be carried by the concrete at failure.

F.4.3.2 Web-Shear Cracking Strength, V_{cw}

The V_{cw} expression for the proposed simplified Specifications, as is the case for the current AASHTO STD and ACI 318-02 methods, was derived from a consideration of the elastic distribution of stresses as described in the following.

The stresses on the small element of a flexural member are shown in Fig. F-2(b). From the Mohr's circle in Fig. F-2(c), the principal tensile stress, f_1 , can be derived as:

$$f_1 = \sqrt{v^2 + \left(\frac{f_{pc} - f_v}{2}\right)^2} - \left(\frac{f_{pc} + f_v}{2}\right) \quad (\text{F-10})$$

Assuming that the vertical stresses, f_v , is negligibly small in most cases, Eq.(F-10) can be simplified as follows:

$$f_1 = \sqrt{v^2 + \left(\frac{f_{pc}}{2}\right)^2} - \left(\frac{f_{pc}}{2}\right) \quad (\text{F-11})$$

Because web-shear cracking occurs when the principal tensile stress, f_1 , reaches the tensile strength of the concrete, f_t , the f_1 in Eq.(F-11) can be replaced by f_t . Then, the shear stress when web-shear cracking occurs, v_{cw} , is:

$$v_{cw} = f_t \sqrt{1 + \frac{f_{pc}}{f_t}} \quad (\text{F-12})$$

Thus, the web-shear cracking force, V_{cw} , can be expressed as:

$$V_{cw} = v_{cw} b_v d_v \quad (\text{F-13})$$

Consistent with the current specifications it is suggested that d_v need not be taken less than the greater of $0.9d_e$ or $0.72h$, where d_e is effective depth and h is overall depth.

If draped strands are used, the vertical component of the prestressing force, V_p , will also resist shear. Thus,

$$V_{cw} = v_{cw} b_v d_v + V_p \quad (\text{F-14})$$

Therefore, the web-shear cracking force, V_{cw} , can be rewritten as:

$$V_{cw} = f_t \sqrt{1 + \frac{f_{pc}}{f_t}} b_v d_v + V_p \quad (\text{F-15})$$

The tensile strength of the concrete, f_t , needs to be determined if Eq. (F-15) is to be used. Fig. F-3 presents the cracking stress measured by split cylinder test results as a function of concrete compressive strength. In the figure, the uniaxial tensile strength is shown to be approximately 0.65 times the tensile strength measured by split cylinder tests. Further, there is considerable variation in the tensile strength as a function of the compressive cylinder strength. The uniaxial tensile strength can be expected to vary from about 2.6 to $5.2\sqrt{f'_c}$ with a median value of around $4\sqrt{f'_c}$.

Thus, the tensile strength of the concrete, f_t , can be taken as somewhere between $2\sqrt{f'_c} \sim 4\sqrt{f'_c}$ (psi) where f'_c is in psi. While a tensile cracking strength close to $4\sqrt{f'_c}$ is believed to provide an accurate estimate of the diagonal cracking strength, due to the wide range of variation of the tensile cracking strength, it is considered to be safer to use $2\sqrt{f'_c}$ as the lower bound of the tensile strength of the concrete, f_t . On the other hand, while the tensile strength value of $2\sqrt{f'_c}$ provides a lower bound of diagonal cracking strength in Eq. (F-15), it is also believed to be a good estimate of the diagonal cracking load in a reinforced concrete member or a prestressed member with a low level of prestressing. Further, because in accordance with the concept of the TCMF this value of V_c is used as the shear that can be carried by the concrete at failure, it is better to use a lower, than a higher, estimate of the tensile strength. Thus Eq. (F-15) becomes:

$$V_{cw} = 2\sqrt{f'_c} \sqrt{1 + \frac{f_{pc}}{2\sqrt{f'_c}}} b_v d_v + V_p \quad (\text{in., psi}) \quad (\text{F-16})$$

Eq. (F-16) can be linearized for simplicity with a slight adjustment to provide a better fit with experimental test data. Then, V_{cw} , can be approximated as:

$$V_{cw} = (2.0\sqrt{f'_c} + 0.3f_{pc}) b_v d_v + V_p \quad (\text{in., psi}) \quad (\text{F-17})$$

or

$$V_{cw} = (0.06\sqrt{f'_c} + 0.3f_{pc}) b_v d_v + V_p \quad (\text{in., ksi}) \quad (\text{F-18})$$

Fig. F-4 illustrates the web-shear cracking strengths calculated by AASHTO STD (& ACI 318), Eqs. (F-16) and (F-17) or (F-18). As seen from Fig. F-4, while Eq. (F-18) gives $1.5\sqrt{f'_c b_v d_v}$ (in psi unit) less web-shear cracking strength than the AASHTO STD (& ACI 318) method, both Eqs. (F-16) and (F-17) or (F-18) give very similar web-shear cracking strengths for $f_{pc} / \sqrt{f'_c}$ (in psi unit) ratios between 0 and 14. For a 10,000 psi concrete Eqs. (F-16) and (F-17) are therefore realistic up to prestress values of 1,400 psi. Justifications for using the lower bound value for V_{cw} , as related not only to web-shear cracking but also to the concrete contribution at ultimate capacity, are provided in Appendix G.

F.4.3.3 Flexure-Shear Cracking Strength, V_{ci}

For flexure-shear cracking of beams, the same type of expression as that used in the AASHTO STD and ACI318-02 methods for prestressed beams is adopted.

As shown in Fig. F-5, as loading increases flexural cracks form in and near the maximum moment region. Assuming that the first shear crack may be initiated by a flexural crack which occurs at a section at least $d/2$ away from the load point, the relationship between moment, M , and shear, V , is:

$$M_{cr} = M - V\left(\frac{d}{2}\right) = V\left(\frac{M}{V} - \frac{d}{2}\right) \quad (\text{F-19})$$

where M_{cr} is the cracking moment due to the applied load, excluding the self-weight of the member. It should be noted that the terms M and V are also due to the live loads only. Eq. F-19 can be rearranged by solving for V as:

$$V = \frac{M_{cr}}{\frac{M}{V} - \frac{d}{2}} \quad (\text{F-20})$$

Because flexure-shear cracking occurs at slightly higher shear forces than flexural cracking, the margin between shear cracking and flexural cracking was evaluated empirically. Thus, the increment in shear, $0.02\sqrt{f'_c b_v d_v}$ (in. and ksi units, which is equivalent to $0.63\sqrt{f'_c b_v d_v}$ in psi units), was inserted into the Eq. (F-20), which is a conservative approximation to the average value of that increment of $\sqrt{f'_c b_w d}$ (in. and ksi units) reported in University of Illinois Bulletin 493. Note that this increment is slightly different from the value of $0.6\sqrt{f'_c b_w d}$ (in. and psi units) in the AASHTO STD and ACI 318 methods. The shear force due to dead load also needs to be included, especially for composite members and, thus, the shear force at flexure-shear cracking, V_{ci} , becomes:

$$V_{ci} = 0.63\sqrt{f'_c b_v d_v} + V_d + \frac{M_{cr}}{\frac{M}{V} - \frac{d}{2}} \quad (\text{in. and psi units}) \quad (\text{F-21})$$

For simplification, the $d/2$ term was dropped, and thus Eq. (F-21) becomes:

$$V_{ci} = 0.63\sqrt{f'_c}b_v d_v + V_d + \frac{V M_{cr}}{M} \quad (\text{in. and psi units}) \quad (\text{F-22})$$

A minimum strength of $0.06\sqrt{f'_c}b_v d_v$ (in. and ksi unit) is imposed on Eq. F-22, which is equivalent to $V_{ci} \geq 1.9\sqrt{f'_c}b_v d_v$ (in. and psi unit). The coefficient of 0.06 was selected so as to provide a uniform minimum V_c contribution over the length of the member independent of whether a web- or flexure-shear cracking region was being designed. The coefficient of 0.06 (ksi units) is also very close to the traditional coefficient of 1.7 (psi units) when it is considered that $d_v = 0.9d$.

$$V_{ci,\min} = 1.7\sqrt{f'_c}b_w d \text{ (psi units)} = 1.7b_v d_v / \sqrt{1000} / 0.9 = 0.0597\sqrt{f'_c}b_v d_v \text{ (ksi units)} \quad (\text{F-23})$$

Thus, the shear force at flexure-shear cracking, V_{ci} , becomes:

$$V_{ci} = 0.02\sqrt{f'_c}b_v d_v + V_d + \frac{V M_{cr}}{M} \geq 0.06\sqrt{f'_c}b_v d_v \quad (\text{in., ksi}) \quad (\text{F-24})$$

$$V_{ci} = 0.63\sqrt{f'_c}b_v d_v + V_d + \frac{V M_{cr}}{M} \geq 1.9\sqrt{f'_c}b_v d_v \quad (\text{in., psi}) \quad (\text{F-25})$$

where M and V are due to the live loads only.

F.4.3.4 Stirrup Contribution, V_s

For the stirrup contribution, the variable-angle truss model has been adopted in which the angle of compression strut can be flatter than 45° , i.e., $\theta \leq 45^\circ$.

From Fig. F-6, it can be seen that the vertical component of the diagonal compression force must be balanced by the tension in the stirrups over the length $jd \cot \theta$:

$$\frac{A_v f_v}{s} = \frac{V}{jd} \tan \theta \quad (\text{F-26})$$

Because the term jd in Eq. F-26 can be replaced by d_v (effective shear depth, which is the same as jd but need not be taken less than the greater of $0.9d_e$ or $0.72h$), the stirrup contribution becomes:

$$V_s = \frac{A_v f_y d_v}{s} \cot \theta \quad (\text{F-27})$$

The angle of inclination of strut at web-shear cracking can be derived from the Mohr's Circle in Fig. F-2 as:

$$\cot \theta = \frac{f_{pc} + f_t}{v} = \frac{f_{pc} + f_t}{f_t \sqrt{1 + \frac{f_{pc}}{f_t}}} = \sqrt{1 + \frac{f_{pc}}{f_t}} \quad (\text{F-28})$$

Thus, $\cot \theta = \sqrt{1 + \frac{f_{pc}}{f_t}}$, and this equation can also be linearized using the first two terms of a Taylor Series expansion as:

$$\cot \theta = 1 + 0.36 \frac{f_{pc}}{f_t} \quad (\text{F-29})$$

Figure F-7 compares the angles of inclination of the strut from Eqs. (F-28) and (F-29). It can be seen that the linearized equation (Eq. F-29) and the nonlinear one (Eq. F-28) have the same angle values when $\theta = 45^\circ$ and $\theta = 29^\circ$, and in between those two points the linearized equation gives a slightly steeper angle than the nonlinear one, which means a more conservative and desirable result in terms of the stirrup contribution.

The compression strut angle, θ , is a function of the ratio of f_{pc} / f_t . The sensitivity of the strut angle along with the ratio of f_{pc} / f_t is an important issue because small changes in the strut angle, θ , can make a significant difference in the contribution of the stirrup reinforcement to shear capacity. Figure F-8 shows the crack angle obtained from Eq. (F-29) for different tensile strength definitions of the concrete tensile strength, f_t , versus the ratio of $f_{pc} / \sqrt{f_c'}$. As the value selected for the concrete tensile strength, f_t , decreases, the change in crack angle, θ , becomes more rapid and the angle becomes flatter as the ratio of $f_{pc} / \sqrt{f_c'}$ increases.

Thus, in terms of the compression strut angle, θ , using $4\sqrt{f_c'}$ (in psi unit) as the concrete tensile strength, f_t , results in more conservative estimation of stirrup contribution than using $2\sqrt{f_c'}$ (in psi unit). That result is desirable because it leads to safer shear design. Then Eq. (F-29) becomes:

$$\cot \theta = 1.0 + 3.0 \frac{f_{pc}}{\sqrt{f_c'}} \leq 1.8 \quad (\text{in ksi unit}) \quad (\text{F-30})$$

$$\text{or} \quad \cot \theta = 1.0 + 0.09 \frac{f_{pc}}{\sqrt{f_c'}} \leq 1.8 \quad (\text{in psi unit}) \quad (\text{F-31})$$

Note that a lower bound to the compression strut angle, θ , is imposed in Eqs. (F-30) and (F-31) so that the strut angle cannot become flatter than 29 degrees for design purposes.

In addition for high moment and high shear regions such as regions near interior supports in a continuous beam, and in reinforced concrete beams, diagonal cracking in flexure-shear zones occurs at low shear stresses and the cracks are steep. Sometimes crack angles can be greater than 45 degrees. To account for this situation, $\cot \theta = 1.0$ or $\theta = 45^\circ$ needs to be used when V_{ci} governs or $M_u > M_{cr}$.

F.4.3.5 Minimum Reinforcement Ratio, $A_{v,\min}$

To prevent brittle shear failures, and minimize member size effects, a minimum amount of shear reinforcement needs to be provided. Based on the studies reported in this document the

recommended minimum amount of shear reinforcement is the same as the current LRFD requirement:

$$A_v \geq 0.0316 \sqrt{f'_c} \frac{b_v s}{f_y} \quad (\text{in. and ksi units}) \quad (\text{F-32})$$

F.4.3.6 Tensile Capacity of Longitudinal Reinforcement

The ability of cracked concrete to transmit tensile stress at a crack reduces the required amount of transverse reinforcement but increases the stresses in the longitudinal reinforcement. Thus, the consequences of the tension caused by shear, as well as that caused by moment and axial tension, need to be considered. Assuming that the stirrups are yielding and that only the reinforcement on the flexural tension side of the member resists tension, the amount of longitudinal reinforcement required to avoid yielding of the longitudinal reinforcement can be expressed as:

$$A_s f_y + A_{ps} f_{ps} \geq \left[\frac{M_u}{d_v \phi} + 0.5 \frac{N_u}{\phi} + \left(\frac{V_u}{\phi} - 0.5 V_s - V_p \right) \cot \theta \right] \quad (\text{F-33})$$

which is the same as the current LRFD requirement.

F.4.3.7 Summary of Proposed Simplified Provisions

For greater ease of understanding than the presentation in Section F.5 the proposed simplified shear design relationships are summarized here

Shear Design Procedure

In the proposed approach, the shear strength is taken as the sum of a lower bound to the diagonal cracking strength (V_c), a shear reinforcement contribution (V_s), and the vertical component of the prestressing steel (V_p) for regions where V_{cw} determines the value of V_c . Thus,

$$V_n = V_c + V_s \leq 0.25 f'_c b_v d_v \quad (\text{F-34})$$

For non-prestressed concrete members, the concrete contribution term, V_c , can be calculated as:

$$V_c = 0.06 \sqrt{f'_c} b_v d_v \quad (\text{in, ksi}) \quad (\text{F-35})$$

$$V_c = 2 \sqrt{f'_c} b_v d_v \quad (\text{in, psi}) \quad (\text{F-36})$$

The steel contribution, V_s , is calculated by the 45° truss analogy as:

$$V_s = \frac{A_v f_y d_v}{s} \quad (\text{F-37})$$

For prestressed concrete members, the concrete contribution term, V_c , can be calculated as the lesser of V_{cw} or V_{ci} :

$$\text{Web-shear cracking: } V_{cw} = (0.06 \sqrt{f'_c} + 0.3 f_{pc}) b_v d_v + V_p \quad (\text{in., ksi}) \quad (\text{F-38})$$

$$V_{cw} = (2.0\sqrt{f'_c} + 0.3f_{pc})b_v d_v + V_p \quad (\text{in., psi}) \quad (\text{F-39})$$

$$\text{Flexure-shear cracking: } V_{ci} = 0.02\sqrt{f'_c}b_v d_v + V_d + \frac{V M_{cr}}{M} \geq 0.06\sqrt{f'_c}b_v d_v \quad (\text{in., ksi}) \quad (\text{F-40})$$

$$V_{ci} = 0.63\sqrt{f'_c}b_v d_v + V_d + \frac{V M_{cr}}{M} \geq 1.9\sqrt{f'_c}b_v d_v \quad (\text{in., psi}) \quad (\text{F-41})$$

where M and V are due to the live loads only.

For the stirrup contribution,

$$V_s = \frac{A_v f_y d_v}{s} \cot \theta \quad (\text{F-42})$$

$$\text{where } \cot \theta = 1.0 + 3.0 \frac{f_{pc}}{\sqrt{f'_c}} \leq 1.8 \quad (\text{in ksi unit}) \quad (\text{F-43})$$

$$\text{or } \cot \theta = 1.0 + 0.09 \frac{f_{pc}}{\sqrt{f'_c}} \leq 1.8 \quad (\text{in psi unit}) \quad (\text{F-44})$$

but $\cot \theta = 1.0$ when V_{ci} governs or $M_u > M_{cr}$.

Minimum Shear Reinforcement

$$A_v \geq 0.0316\sqrt{f'_c} \frac{b_v s}{f_y} \quad (\text{in., ksi}) \quad (\text{F-45})$$

Tensile Capacity of Longitudinal Reinforcement

$$A_s f_y + A_{ps} f_{ps} \geq \left[\frac{M_u}{d_v \phi} + 0.5 \frac{N_u}{\phi} + \left(\frac{V_u}{\phi} - 0.5V_s - V_p \right) \cot \theta \right] \quad (\text{F-46})$$

Design Procedure using the Proposed Simplified Provisions

The steps in the design process are illustrated in the flowchart in Fig. F-9. For prestressed concrete members, it is shown that the designer uses the lower of V_{cw} and V_{ci} for V_c . If $V_{ci} < V_{cw}$, the designer compares M_u and M_{cr} . If $M_u > M_{cr}$, then $\cot \theta = 1.0$, otherwise, $\cot \theta = 1.0 + 3 \frac{f_{pc}}{\sqrt{f'_c}} \leq 1.8$ (in ksi unit).

F.5 Proposed Revised Section 5.8.3 of AASHTO LRFD

As a result of the recommendations summarized in this Appendix, it is proposed that the existing Section 5.8.3 of the AASHTO LRFD provisions be revised as detailed here. Insertions and deletions are shown directly for the existing text by underlying and strikeouts, respectively, for both the Specifications and the Commentary of the existing AASHTO LRFD provisions.

5.8.3 Sectional Design Model

5.8.3.1 General

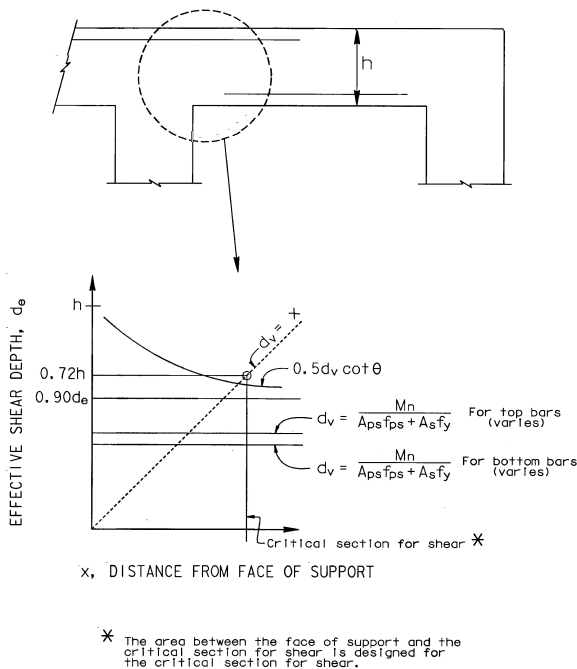
The sectional design model may be used for shear design where permitted in accordance with the provisions of Article 5.8.1

In lieu of the methods specified herein, the resistance of members in shear or in shear combined with torsion may be determined by satisfying the conditions of equilibrium and compatibility of strains and by using experimentally verified stress-strain relationships for reinforcement and for diagonally cracked concrete. Where consideration of simultaneous shear in a second direction is warranted, investigation shall be based either on the principles outlined above or on a three-dimensional strut-and-tie model.

5.8.3.2 Sections Near Supports

The provisions of Article 5.8.1.2 shall be considered.

Where the reaction force in the direction of the applied shear introduces compression into the end region of a member, the location of the critical section for shear shall be taken as d_v from the internal face of the support as illustrated in Figure 1.



C5.8.3.1

In the sectional design approach, the component is investigated by comparing the factored shear force and the factored shear resistance at a number of sections along its length. Usually this check is made at the tenth points of the span and at locations near the supports.

See Article 5.10.11.4.1c for additional requirements for Seismic Zones 3 and 4.

An appropriate nonlinear finite element analysis or a detailed sectional analysis would satisfy the requirements of this article. More information on appropriate procedures and a computer program that satisfies these requirements are given by Collins and Mitchell (1991). One possible approach to the analysis of biaxial shear and other complex loadings on concrete members is outlined in Rabbat and Collins (1978), and a corresponding computer-aided solution is presented in Rabbat and Collins (1976). A discussion of the effect of biaxial shear on the design of reinforced concrete beam-to-column joints can be found in Pauley and Priestley (1992).

C5.8.3.2

Loads close to the support are transferred directly to the support by compressive arching action without causing additional stresses in the stirrups.

The traditional approach to proportioning transverse reinforcement involves the determination of the required stirrup spacing at discrete sections along the member. The stirrups are then detailed such that this spacing is not exceeded over a length of the beam extending from the design section to the next design section out into the span. In such an approach, the shear demand and resistance provided is assumed to be as shown in Figure C1. There are, however, more theoretically exact stirrup designs. Knowledge of these may help to reconcile published research to traditional design practice.

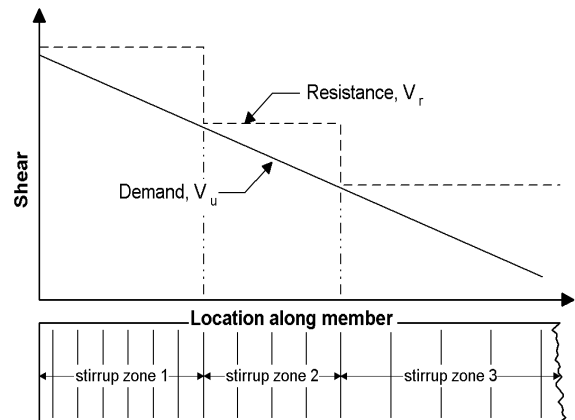


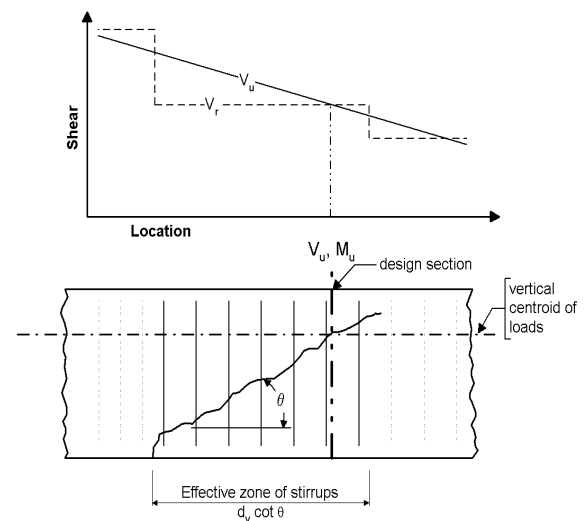
Figure C5.8.3.2-1 Traditional Shear Design.

Figure 5.8.3.2-1 Critical Section for Shear.

Otherwise, the design section shall be taken at the internal face of the support. Where the beam-type element extends on both sides of the reaction area, the design section on each side of the reaction shall be determined separately based upon the loads on each side of the reaction and whether their respective contribution to the total reaction introduces tension or compression into the end region.

For post-tensioned beams, anchorage zone reinforcement shall be provided as specified in Article 5.10.9. For pretensioned beams, a reinforcement cage confining the ends of strands shall be provided as specified in Article 5.10.10. For nonprestressed beams supported on bearings that introduce compression into the member, only minimal transverse reinforcement may be provided between the inside edge of the bearing plate or pad and the end of the beam.

Unlike flexural failures, shear failures occur over an inclined plane and a shear crack typically intersects a number of stirrups. The length of the failure along the longitudinal axis of the member is approximately $d_v \cot \theta$. Each of the stirrups intersected by this crack participates in resisting the applied shear. The relationship between the location of the design section and the longitudinal zone of stirrups that resist the shear at that design section is a function of the vertical position of the load applied to the member, including its selfweight, and the projection along the longitudinal axis of the beam of the inclined cracks at that location. Ideally, the design section could be located by determining where the vertical centroid of the applied loads intersects a shear crack inclined at an angle θ as shown in Figure C2.

**Figure C5.8.3.2-2 Theoretical Shear Design Section Location.**

For typical cases where the applied load acts at or above the middepth of the member, it is more practical to take the traditional approach as shown in Figure C1 or a more liberal yet conservative approach as shown in Figure C3. The approach taken in Figure C3 has the effect of extending the required stirrup spacing for a distance of $0.5d_v \cot \theta$ toward the bearing.

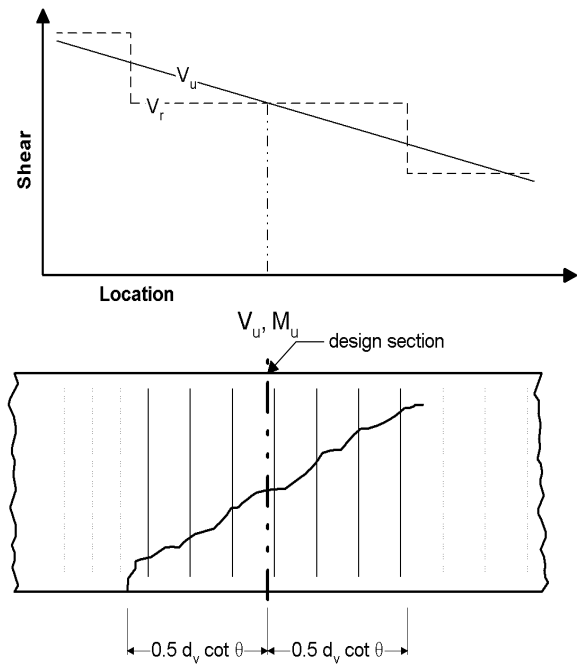


Figure C5.8.3.2-3 Simplified Design Section For Loads Applied at or Above the Middepth of the Member.

If the significant portion of the loads being resisted by the member are applied at a bearing resting on top of the member, the shear failure zone extends for a distance of approximately $d_v \cot \theta$ beyond the point of load application as shown in Figure C4. As with the previous case, all of the stirrups falling within the failure zone may be assumed effective in resisting the applied shear force. The traditional approach shown in Figure C1 is even more conservative in this case.

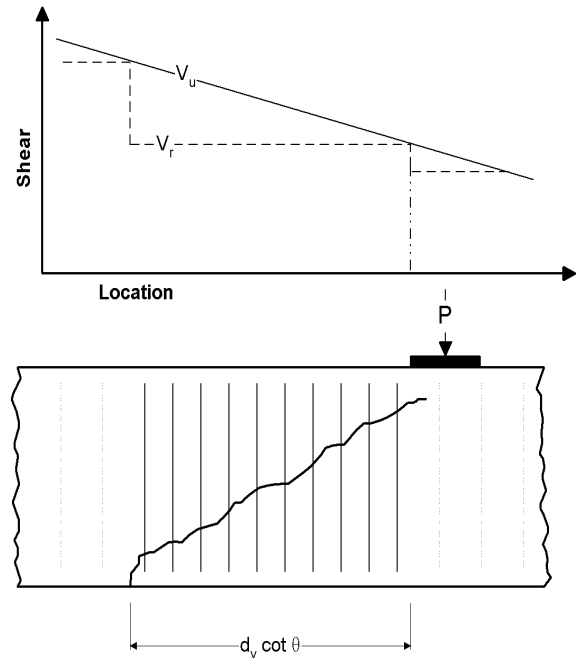


Figure C5.8.3.2-4 Effective Transverse Reinforcement to Members Subjected Primarily to Concentrated Loads.

Figure C5 shows a case where an inverted T-beam acts as a pier cap and the longitudinal members are supported by the flange of the T. In this case, a significant amount of the load is applied below the middepth of the member, and it is more appropriate to use the traditional approach to shear design shown in Figure C1.

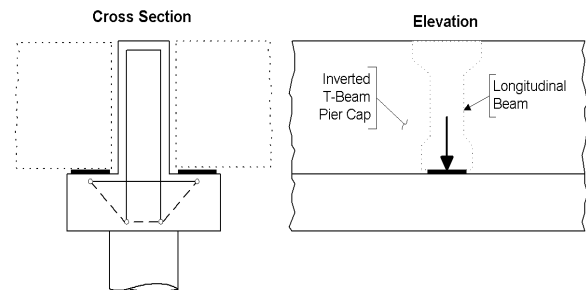


Figure C5.8.3.2-5 Inverted T-Beam Pier Cap.

The T-beam pier cap shown in Figure C5 acts as a beam ledge and should be designed for the localized effects caused by the concentrated load applied to the T-beam flange. Provisions for beam ledge design are given in Article 5.13.2.5.

If the shear stress at the design section calculated in accordance with 5.8.2.9 exceeds $0.18f'_c$ and the beam-type element is not built integrally with the support, its end region shall be designed using the strut-and-tie model specified in Article 5.6.3.

Where a beam is loaded on top and its end is not built integrally into the support, all the shear funnels

down into the end bearing. Where the beam has a thin web so that the shear stress in the beam exceeds $0.18f'_c$, there is the possibility of a horizontal shear failure along the interface between the web and the lower flange of the beam. Usually the inclusion of additional transverse reinforcement cannot prevent this type of failure and either the section size must be increased or the end of the beam designed using a strut-and-tie model.

5.8.3.3 Nominal Shear Resistance

The nominal shear resistance, V_n , shall be determined as the lesser of:

$$V_n = V_c + V_s + V_p, \text{ except as specified in Article 5.8.3.4.2} \quad (5.8.3.3-1)$$

$$V_n = 0.25f'_c b_v d_v + V_p \quad (5.8.3.3-2)$$

in which, except as specified in Article 5.8.3.4.2

$$V_c = 0.0316\beta\sqrt{f'_c} b_v d_v \quad (5.8.3.3-3)$$

$$V_s = \frac{A_v f_y d_v (\cot \theta + \cot \alpha) \sin \alpha}{s} \quad (5.8.3.3-4)$$

where:

b_v = effective web width taken as the minimum web width within the depth d_v as determined in Article 5.8.2.9 (in.)

d_v = effective shear depth as determined in Article 5.8.2.9 (in.)

s = spacing of stirrups (in.)

β = factor indicating ability of diagonally cracked concrete to transmit tension and shear as specified in Article 5.8.3.4

θ = angle of inclination of diagonal compressive stresses as determined in Article 5.8.3.4 (°)

α = angle of inclination of transverse reinforcement to longitudinal axis (°)

C5.8.3.3

The shear resistance of a concrete member may be separated into a component, V_c , that relies on tensile and shear stresses in the concrete, a component, V_s , that relies on tensile stresses in the transverse reinforcement, and a component, V_p , that is the vertical component of the prestressing force.

The expressions for V_c and V_s apply to both prestressed and nonprestressed sections, with the terms β and θ depending on the applied loading and the properties of the section.

The upper limit of V_n , given by Eq. 2, is intended to ensure that the concrete in the web of the beam will not crush prior to yield of the transverse reinforcement.

where $\alpha = 90^\circ$, Eq. 4 reduces to:

$$V_s = \frac{A_v f_y d_v \cot \theta}{s} \quad (C5.8.3.3-1)$$

The angle θ is, therefore, also taken as the angle between a strut and the longitudinal axis of a member.

A_v = area of shear reinforcement within a distance s (in.²)

V_p = component in the direction of the applied shear of the effective prestressing force; positive if resisting the applied shear (kip)

5.8.3.4 Procedures for Determining Shear Resistance ~~Determination of β and θ~~

5.8.3.4.1 Simplified Procedure for Nonprestressed Sections Not Greater than 16.0 IN Deep

For concrete footings in which the distance from point of zero shear to the face of the column, pier or wall is less than $3d_v$ with or without transverse reinforcement, and for other nonprestressed concrete sections not subjected to axial tension and containing at least the minimum amount of transverse reinforcement specified in Article 5.8.2.5, or having an overall depth of less than 16.0 in., the following values may be used:

$$\beta = 2.0$$

$$\theta = 45^\circ$$

5.8.3.4.2 Simplified Procedure for Prestressed and Nonprestressed Sections

For concrete beams not subject to significant axial tension, prestressed and nonprestressed, and containing at least the minimum amount of transverse reinforcement specified in Article 5.8.2.5, V_n in Article 5.8.3.3 may be determined with V_p taken as zero and V_c taken as the lesser of V_{ci} and V_{cw} , where:

V_{ci} = nominal shear resistance provided by concrete when inclined cracking results from combined shear and moment (kip)

V_{cw} = nominal shear resistance provided by concrete when inclined cracking results from excessive principal tensions in web (kip)

- V_{ci} shall be determined by

$$V_{ci} = 0.02\sqrt{f'_c} b_v d_v + V_d + \frac{V_i M_{cr}}{M_{\max}} \geq 0.06\sqrt{f'_c} b_v d_v$$

(5.8.3.4.2-1)

where:

V_d = shear force at section due to unfactored dead load and includes both DC and DW (kip)

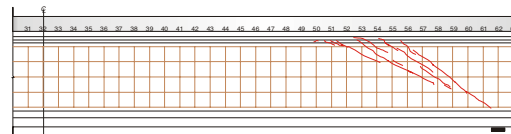
C5.8.3.4.1

With β taken as 2.0 and θ as 45° , the expressions for shear strength become essentially identical to those traditionally used for evaluating shear resistance. Recent large-scale experiments (*Shioya et al. 1989*), however, have demonstrated that these traditional expressions can be seriously unconservative for large members not containing transverse reinforcement and therefore an overall depth limit of 16.0 in. is imposed for use of this article.

C5.8.3.4.2

Article 5.8.3.4.2 is based on the recommendations of NCHRP Report XX1 (*Hawkins et al. 2005*). The concepts of Article 5.8.3.4.2 are compatible with the concepts of ACI Code 318-05 and AASHTO Standard Specifications for Highway Bridges 1996 for evaluations of the shear resistance of prestressed concrete members. However, those concepts are modified so that this article applies to both prestressed and nonprestressed sections.

The nominal shear resistance V_n is the sum of the shear resistances V_c and V_s provided by the concrete and shear reinforcement, respectively. Both V_c and V_s depend on the type of inclined cracking that occurs at the given section. There are two types of inclined cracking: flexure-shear cracking and web-shear cracking for which the associated resistances are V_{ci} and V_{cw} , respectively. Figure C1 shows the development of both types of cracking when increasing uniform load was applied to a 63-inch bulb-tee girder. NCHRP Report XX2 (*Hawkins et al. 2005*).



(a) Load 1

V_i = factored shear force at section due to externally applied loads occurring simultaneously with M_{max} (kip)

M_{cr} = moment causing flexural cracking at section due to externally applied loads (kip-in)

M_{max} = maximum factored moment at section due to externally applied loads (kip-in)

M_{cr} shall be determined by:

$$M_{cr} = (I_c / \gamma_t) (0.2 \sqrt{f'_c} + f_{pe} - f_d) \quad (5.8.3.4.2-2)$$

where:

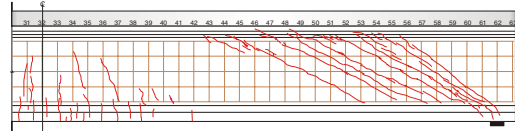
I_c = moment of inertia of section resisting externally applied factored loads (in⁴)

γ_t = distance from centroidal axis of gross section resisting externally applied factored loads, neglecting reinforcement, to extreme fiber in tension (in)

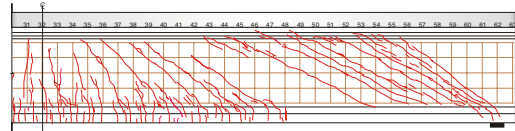
f_{pe} = compressive stress in concrete due to effective prestress forces only (after allowance for all prestress losses), at extreme fiber of section where tensile stress is caused by externally applied loads (ksi)

f_d = stress due to unfactored dead load, at extreme fiber of section where tensile stress is caused by externally applied loads (ksi)

In Eq. 5.8.3.4.2-1, M_{max} and V_i shall be determined from the load combination causing maximum moment at the section.



(b) Load 2



(c) Load 3

Figure C5.8.3.4.2-1 – Development of Shear Cracking with Increasing Loads for Uniformly Loaded Bulb Tee Beam. Load 1 < Load 2 < Load 3.

Web-shear cracking begins from an interior point in the web of the member before either flange in that region cracks in flexure. In Figure C1, at load 1, web-shear cracking developed in the web of the member adjacent to the end support. Flexure-shear cracking is initiated by flexural cracking. Flexural cracking increases the shear stresses in the concrete above the flexural crack. In Figure C1, flexural cracking had developed in the central region of the beam by load 2 and by load 3, the flexural cracks had become inclined cracks as flexural cracking extended towards the end support with increasing load.

For sections with shear reinforcement equal to or greater than that required by Article 5.8.2.5, the shear carried by the concrete may drop below V_c shortly after inclined cracking, and the shear reinforcement may yield locally. However, sections continue to resist increasing shears until resistances provided by the concrete again reach V_c . Thus, V_{ci} and V_{cw} are measures of the resistance that can be provided by the concrete at the nominal shear resistance of the section and are not directly equal to the shears at inclined cracking.

The angle θ of the inclined crack, and therefore of the diagonal compressive stress, is greater for a web-shear crack than a flexure-shear crack. Consequently, for a given section the value of V_s associated with web-shear cracking is greater than that associated with flexure-shear cracking.

V_{ci} is the sum of the shear ($V_i M_{cr} / M_{max}$) required to cause flexural cracking at the given section plus the increment of shear necessary to develop the flexural crack into a shear crack. For a non-composite beam, the total cross section resists all applied shears, dead and live, I_c equals the moment of inertia of the gross section and V_d equals the unfactored dead load shear acting on the section. In this case Eq. 1 can be used directly.

- V_{cw} shall be determined by

$$V_{cw} = (0.06\sqrt{f'_c} + 0.30f_{pc})b_v d_v + V_p \quad (5.8.3.4.2-3)$$

where:

f_{pc} = compressive stress in concrete (after allowance for all prestress losses) at centroid of cross section resisting externally applied loads or at junction of web and flange when the centroid lies within the flange (ksi). In a composite member, f_{pc} is the resultant compressive stress at the centroid of the composite section, or at junction of web and flange, due to both prestress and moments resisted by precast member acting alone.

- V_s shall be determined using Eq. 5.8.3.3-4 with $\cot \theta$ taken as follows:

Where V_{ci} is less than V_{cw} , $\cot \theta = 1.0$

Where V_{ci} is greater than V_{cw} ,

$$\cot \theta = 1.0 + 3(f_{pc} / \sqrt{f'_c}) \leq 1.8 \quad (5.8.3.4.2-4)$$

5.8.3.4.3.2 General Procedure

5.8.3.4.3a Sections Containing At least Minimum Transverse Reinforcement

For sections containing at least the minimum amount of transverse reinforcement specified in Article 5.8.2.5, the values of β and θ shall be determined as follows: as specified in Table 1. In using this table, ϵ_x shall be taken as the calculated longitudinal strain at the middepth of the member when the section is subjected to M_u , N_u , and V_u as shown in Figure 1.

For a composite beam, part of the dead load is resisted by only part of the final section. Where the final gross concrete section is achieved with only one addition to the initial concrete section, (two-stage construction), Eq. 1 can be used directly. In Eq. 2 appropriate section properties are used to compute f_d and in Eq. 1 the shear due to dead load V_d and that due to other loads V_i are separated. V_d is the total shear force due to unfactored dead loads acting on the part of the section carrying the dead loads acting prior to composite action plus the unfactored superimposed dead load acting on the composite member. The term V_i may be taken as $(V_u - V_d)$ and M_{max} as $M_u - M_d$ where V_u and M_u are the factored shear and moment at the given section due to the total factored loads M_d is the moment due to unfactored dead load at the same section.

Where the final gross section is developed with more than one concrete composite addition to the initial section (multiple-stage construction), it is necessary to trace the build up of the extreme fiber flexural stresses to compute M_{cr} . For each stage in the life history of the member, the increments in the extreme fiber flexural stress at the given section due to the unfactored loads acting on that section are calculated using the section properties existing at that stage. V_d , V_i and M_{max} are calculated in the same manner as for two-stage construction.

C5.8.3.4.3

In the 2005 Edition of this Specification a simplified procedure for prestressed and nonprestressed sections was inserted as Article 5.8.3.4.2 and the general procedure was renumbered as Article 5.8.3.4.3. In addition the provisions of the general procedure were revised to be consistent with the CSA provisions for the same procedure.

The shear resistance of a member may be determined by performing a detailed sectional analysis that satisfies the requirements of Article 5.8.3.1. Such an analysis, see Figure C1, would show that the shear stresses are not

$$\beta = \frac{4.8}{(1 + 1500 \varepsilon_x)} \quad (5.8.3.4.3-1)$$

$$\theta = 29 + 7000 \varepsilon_x \quad (5.8.3.4.3-2)$$

~~For sections containing less transverse reinforcement than specified in Article 5.8.2.5, the values of β and θ shall be as specified in Table 2. In using this table, ε_x shall be taken as the largest calculated longitudinal strain which occurs within the web of the member when the section is subjected to M_u , N_u , and V_u as shown in Figure 2.~~

The strain, ε_x shall be taken as the calculated longitudinal strain at the middepth of the member when the section is subjected to M_u , N_u , and V_u as shown in Figure 1.

Unless more accurate calculations are made, ε_x shall be determined as follows:

~~If the section contains at least the minimum transverse reinforcement as specified in Article 5.8.2.5:~~

$$\varepsilon_x = \frac{\left(\frac{M_u}{d_v} + 0.5N_u + 0.5(V_u - V_p) \cot \theta - A_{ps} f_{po} \right)}{2(E_s A_s + E_p A_{ps})} \quad (5.8.3.4.2-1)$$

$$\varepsilon_x = \frac{M_u / d_v + 0.5N_u + V_u - V_p - A_{ps} f_{po}}{2(E_s A_s + E_p A_{ps})} \quad (5.8.3.4.3-3)$$

where

- V_u and M_u shall be taken as positive quantities and M_u shall not be taken less than $(V_u - V_p)d_v$.
- The areas A_s and A_{ps} for reinforcement terminated at less than their development length from the given section shall be reduced in proportion to their lack of full development.
- Where the calculated ε_x is negative, ε_x shall be taken as zero or the value recalculated

uniform over the depth of the web and that the direction of the principal compressive stresses changes over the depth of the beam. The more direct procedure given herein assumes that the concrete shear stresses are essentially uniformly distributed over an area b_v wide and d_v deep, that the direction of principal compressive stresses (defined by angle θ) remains constant over d_v , and that the shear strength of the section can be determined by considering the biaxial stress conditions at just one location in the web. See Figure C2.

~~Members containing at least the minimum amount of transverse reinforcement have a considerable capacity to redistribute shear stresses from the most highly strained portion of the cross-section to the less highly strained portions. Because of this capacity to redistribute, it is appropriate to use the middepth of the member as the location at which the biaxial stress conditions are determined. Members that contain no transverse reinforcement, or contain less than the minimum amount of transverse reinforcement, have less capacity for shear redistribution. Hence, for such members, it is appropriate to perform the biaxial stress calculations at the location in the web subject to the highest longitudinal tensile strain, see Figure 2.~~

The longitudinal strain, ε_x , can be determined by the procedure illustrated in Figure C3. The actual section is represented by an idealized section consisting of a flexural tension flange, a flexural compression flange, and a web. The area of the compression flange is taken as the area on the flexural compression side of the member, i.e., the total area minus the area of the tension flange as defined by A_{ct} . After diagonal cracks have formed in the web, the shear force applied to the web concrete, $V_u - V_p$, will primarily be carried by diagonal compressive stresses in the web concrete. These diagonal compressive stresses will result in a longitudinal compressive force in the web concrete of $(V_u - V_p) \cot \theta$. Equilibrium requires that this longitudinal compressive force in the web needs to be balanced by tensile forces in the two flanges, with half the force, that is $0.5 (V_u - V_p) \cot \theta$, being taken by each flange. ~~To avoid a trial and error iteration process, it is a~~ A convenient simplification is to take this flange force due to shear as $V_u - V_p$. ~~This amounts to taking $0.5 \cot \theta = 1.0$ in the numerator of Eqs. 1, 2 and 3.~~ This simplification does not cause a significant loss of accuracy. After the required axial forces in the two flanges are calculated, the resulting axial strains, ε_t and ε_c , can be calculated based on the axial force-axial strain relationship shown in Figure C4.

For members containing at least the minimum amount of transverse reinforcement, ε_x can be taken as:

$$\varepsilon_x = \frac{\varepsilon_t + \varepsilon_c}{2} \quad (C5.8.3.4.32-1)$$

with the denominator of the equation replaced by $2(E_s A_s + E_{ps} A_{ps} + E_c A_{ct})$, except that ε_x shall not be taken less than -0.20×10^{-3} .

- Where the axial tension is large enough to crack the flexural compression face of the section, the resulting increase in ε_x shall be considered. In lieu of more accurate calculations ε_x value from Eq. 5.8.3.4.3-1 shall be doubled.
- Within the transfer length, f_{po} shall be increased linearly from zero at the location where the bond between the strands and concrete commences to its full value at the end of the transfer length.

and

The initial value of ε_x should not be taken greater than 0.001.

If the section contains less than the minimum transverse reinforcement as specified in Article 5.8.2.5

$$\varepsilon_x = \frac{\left(\frac{M_u}{d_v} + 0.5N_u + 0.5(V_u - V_p) \cot \theta - A_{ps} f_{po} \right)}{E_s A_s + E_p A_{ps}} \quad (5.8.3.4.2.2)$$

The initial value of ε_x should not be taken greater than 0.002.

If the value of ε_x from Eqs. 1 or 2 is negative, the strain shall be taken as:

$$\varepsilon_x = \frac{\left(\frac{M_u}{d_v} + 0.5N_u + 0.5(V_u - V_p) \cot \theta - A_{ps} f_{po} \right)}{2(E_c A_c + E_s A_s + E_p A_{ps})} \quad (5.8.3.4.2.3)$$

where:

A_{ct} = area of concrete on the flexural tension side of the member as shown in Figure 1 (in.²)

A_{ps} = area of prestressing steel on the flexural tension side of the member, as shown in Figure 1 (in.²)

A_s = area of nonprestressed steel on the flexural tension side of the member at the section under consideration, as shown in Figure 1 (in.²). In calculating A_s for use in this equation, bars

where ε_t and ε_c are positive for tensile strains and negative for compressive strains. If, for a member subject to flexure, the strain ε_c is assumed to be negligibly small, then ε_x becomes one half of ε_t . This is the basis for the expression for ε_x given in Eq. 3. For members containing less than the minimum amount of transverse reinforcement, Eq. 2 makes the conservative simplification that ε_x is equal to ε_t .

In some situations, it will be more appropriate to determine ε_x using the more accurate procedure of Eq. C1 rather than the simpler Eqs. 1 through 3. For example, the shear capacity of sections near the ends of precast, pretensioned simple beams made continuous for live load will be estimated in a very conservative manner by Eqs. 1 through 3 because, at these locations, the prestressing strands are located on the flexural compression side and, therefore, will not be included in A_{ps} . This will result in the benefits of prestressing not being accounted for by Eqs. 1 through 3.

For pretensioned members, f_{po} can be taken as the stress in the strands when the concrete is cast around them, i.e., approximately equal to the jacking stress. For post-tensioned members, f_{po} can be conservatively taken as the average stress in the tendons when the post-tensioning is completed.

Note that in both Table 1 and Table 2, the values of β and θ given in a particular cell of the table can be applied over a range of values. Thus from Table 1, $\theta=34.4^\circ$ and $\beta=2.26$ can be used provided that ε_x is not greater than 0.75×10^{-3} and v_u/f'_c is not greater than 0.125. Linear interpolation between the values given in the tables may be used, but is not recommended for hand calculations. Assuming a value of ε_x larger than the value calculated using Eqs. 1, 2 or 3, as appropriate, is permissible and will result in a higher value of θ and a lower value of β . Higher values of θ will typically require more transverse shear reinforcement, but will decrease the tension force required to be resisted by the longitudinal reinforcement.

Figure C5 illustrates the shear design process by means of a flow chart. This figure is based on the simplified assumption that $0.5 \cot \theta = 1.0$.

~~which are terminated at a distance less than their development length from the section under consideration shall be ignored~~

f_{po} = a parameter taken as modulus of elasticity of prestressing tendons multiplied by the locked-in difference in strain between the prestressing tendons and the surrounding concrete (ksi). For the usual levels of prestressing, a value of 0.7 f_{pu} will be appropriate for both pretensioned and post-tensioned members

N_u = factored axial force, taken as positive if tensile and negative if compressive (kip)

M_u = factored moment, taken as positive quantity, but not to be taken less than $V_u d_v$ (kip-in.)

V_u = factored shear force, taken as positive quantity (kip)

The flexural tension side of the member shall be taken as the half-depth containing the flexural tension zone, as illustrated in Figure 1.

5.8.3.4.3b Sections Containing Less Than Minimum Transverse Reinforcement

For sections containing less transverse reinforcement than specified in Article 5.8.2.5, the value for θ shall still be calculated by Eq. 5.8.3.4.3-2 whereas the value for β shall be determined by:

$$\beta = \frac{4.8}{(1 + 1500 \epsilon_x)} \frac{51}{(39 + s_{xe})} \quad (5.8.3.4.3-4)$$

~~Within the transfer length, f_{po} shall be increased linearly from zero at the location where the bond between the strands and concrete commences to its full value at the end of the transfer length.~~

~~The flexural tension side of the member shall be taken as the half depth containing the flexural tension zone, as illustrated in Figure 1.~~

The crack spacing parameter s_{xc} Table 2, shall be determined as:

$$s_{xe} = s_x \frac{1.38}{a_g + 0.63} \leq 80 \text{ in.} \quad (5.8.3.4.3-5)$$

where:

a_g = maximum aggregate size (IN)

s_x = the lesser of either d_v or the maximum distance between layers of longitudinal crack control reinforcement, where the area of the reinforcement in each layer is not less than $0.003b_v s_x$ as shown in Figure 2-3.

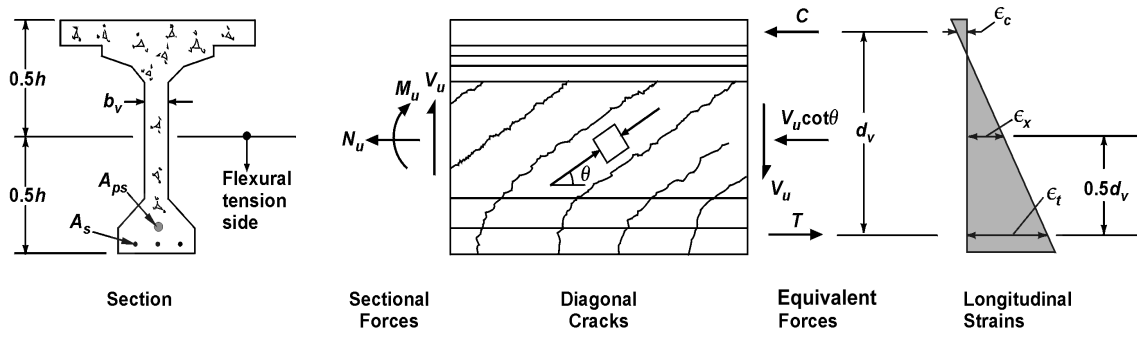


Figure 5.8.3.4.3.2-1 Illustration of Shear Parameters for Section Containing at Least the Minimum Amount of Transverse Reinforcement, $V_p=0$.

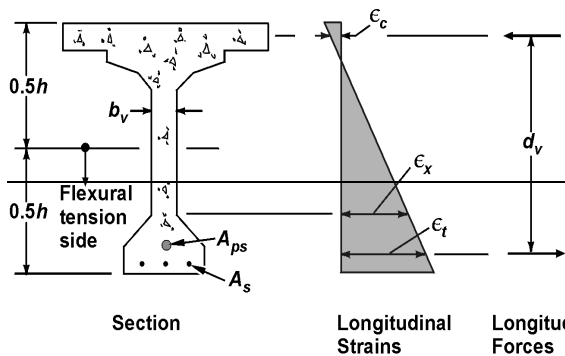


Figure 5.8.3.4.2-2 Longitudinal Strain, ϵ_x , for Sections Containing Less than the Minimum Amount of Transverse Reinforcement.

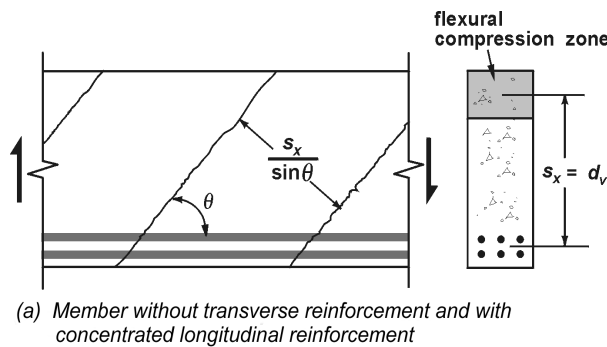


Figure 5.8.3.4.32-23 Definition of Crack Spacing Parameter, s_x .

For sections containing a specified amount of transverse reinforcement, a shear moment interaction diagram, see Figure C6, can be calculated directly from the procedures in this article. For a known concrete strength and a certain value of ϵ_x , each cell of Table 1 corresponds to a certain value of v_u/f'_c , i.e., a certain value of V_u . This value of V_u requires an amount of transverse reinforcement expressed in terms of the parameter $A_v f_y / (b_v s)$. The shear capacity corresponding to the provided shear reinforcement can be found by linearly interpolating between the values of V_u corresponding to two consecutive cells where one cell requires more transverse reinforcement than actually provided and the other cell requires less reinforcement than actually provided. After V_u and θ have been found in this manner, the corresponding moment capacity M_u can be found by calculating, from Eqs. 1 through 3, the moment required to cause this chosen value of ϵ_x , and calculating, from Eq. 5.8.3.5.1, the moment required to yield the reinforcement. The predicted moment capacity will be the lower of these two values. In using Eqs. 5.8.2.9.1, 5.8.3.5.1 and Eqs. 1 through 3 of the procedure to calculate a V_u - M_u interaction diagram, it is appropriate to replace V_u by V_u , M_u by M_u and N_u by N_u and to take the value of ϕ as 1.0. With an appropriate spreadsheet, the use of shear moment interaction diagrams is a convenient way of performing shear design and evaluation.

The values of β and θ in Eqs. 5.8.3.4.3-1, 5.8.3.4.3-2 and 5.8.3.4.3-4 listed in Table 1 and Table 2 are based on calculating the stresses that can be transmitted across diagonally cracked concrete. As the cracks become wider, the stress that can be transmitted decreases. For members containing at least the minimum amount of transverse reinforcement, it is assumed that the diagonal cracks will be spaced about 12.0 in. apart. For members without transverse reinforcement, the spacing of diagonal cracks inclined at θ° to the longitudinal reinforcement is assumed to be $s_x/\sin\theta$, as shown in Figure 32. Hence, deeper members having larger values of s_x are calculated to have more widely spaced cracks and hence, cannot transmit such high shear stresses. The ability of the crack surfaces to transmit shear stresses is influenced by the aggregate size of the concrete. Members made from concretes that have a smaller maximum aggregate size will have a larger value of s_{xe} and hence, if there is no transverse reinforcement, will have a smaller shear strength.

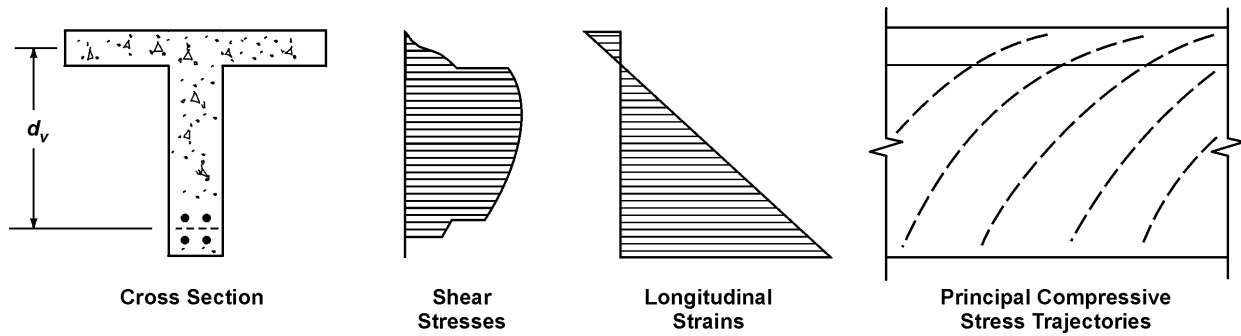


Figure C5.8.3.4.3.2-1 Detailed Sectional Analysis to Determine Shear Resistance in Accordance with Article 5.8.3.1.

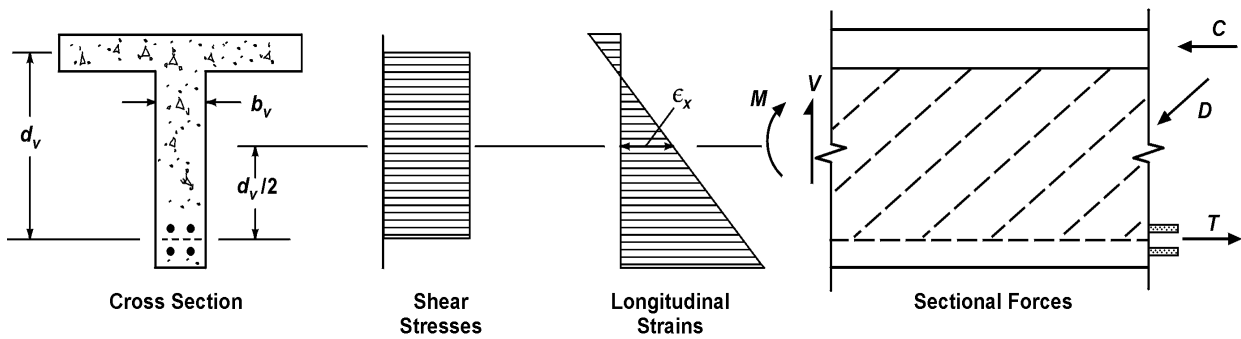


Figure C5.8.3.4.3.2-2 More Direct Procedure to Determine Shear Resistance in Accordance with Article 5.8.3.4.3.2.

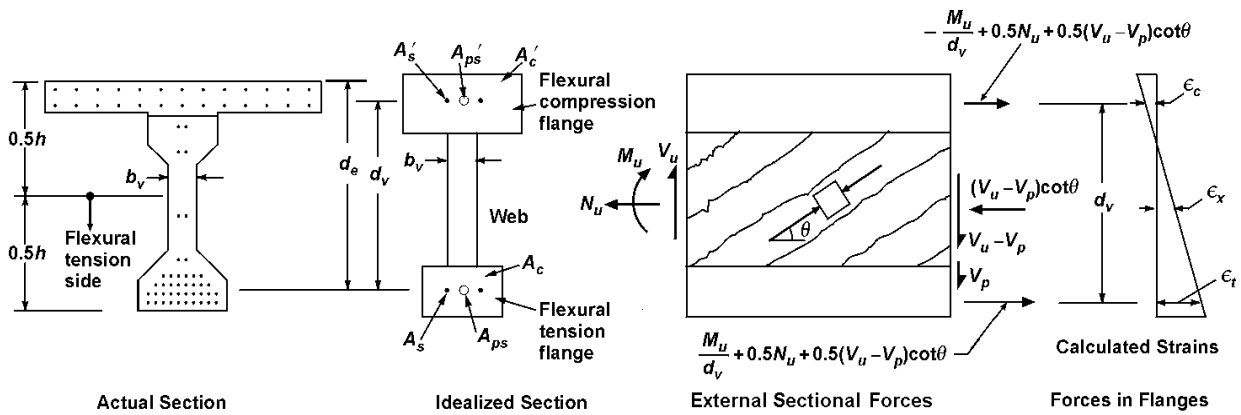


Figure C5.8.3.4.3.2-3 More Accurate Calculation Procedure for Determining ϵ_x

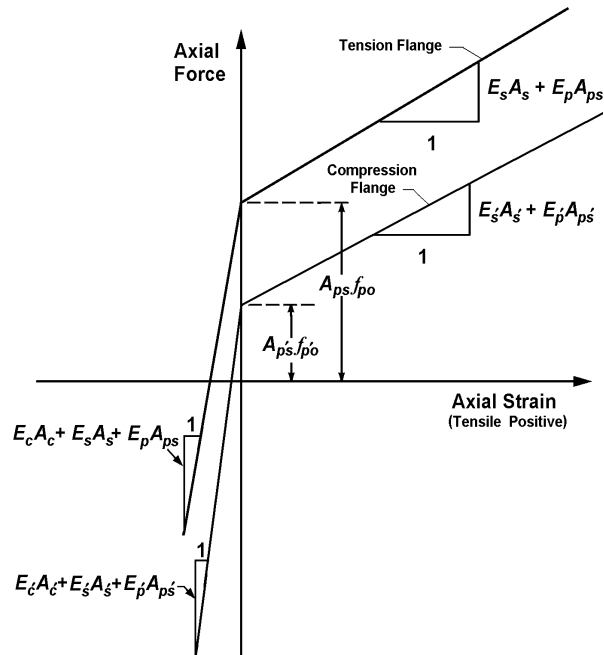
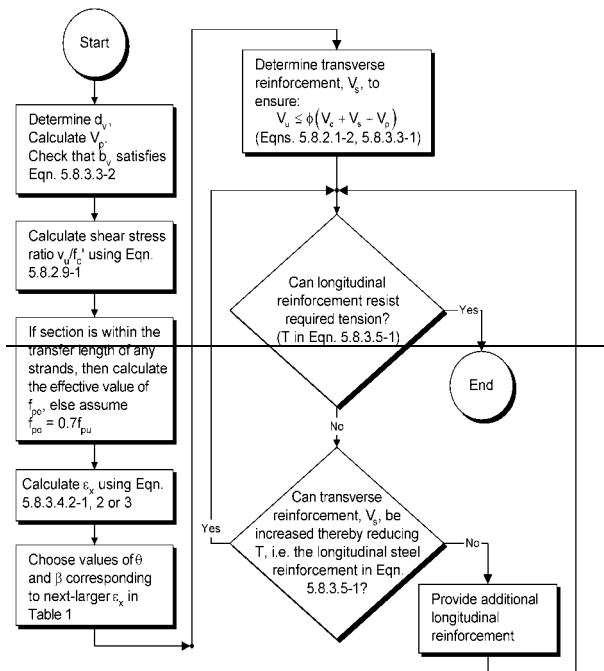


Figure C5.8.3.4.3.2-4 Assumed Relations Between Axial Force in Flange and Axial Strain of Flange.



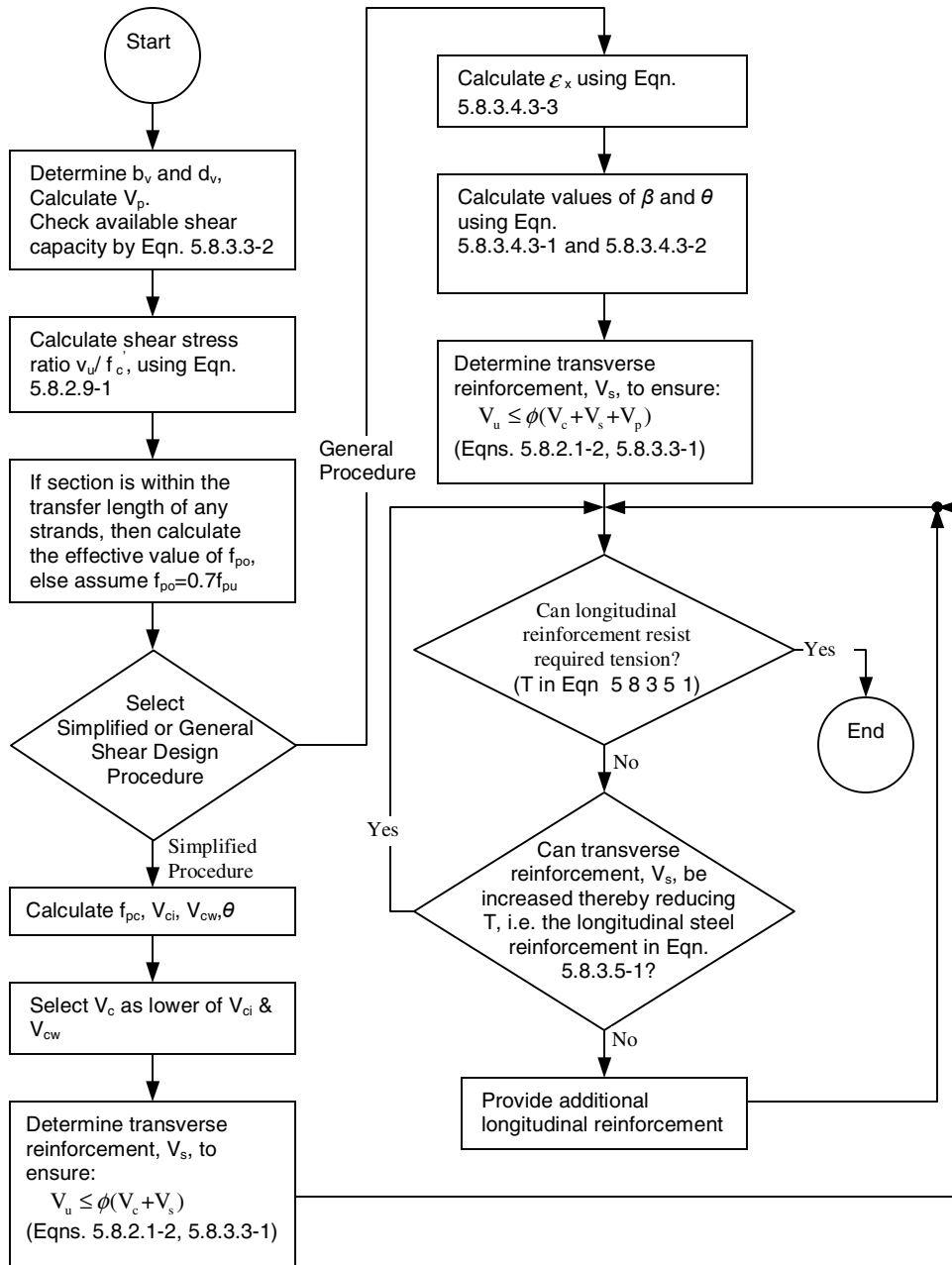


Figure C5.8.3.4.3.2-5 Flow Chart for Shear Design of Section Containing at Least Minimum Transverse Reinforcement.

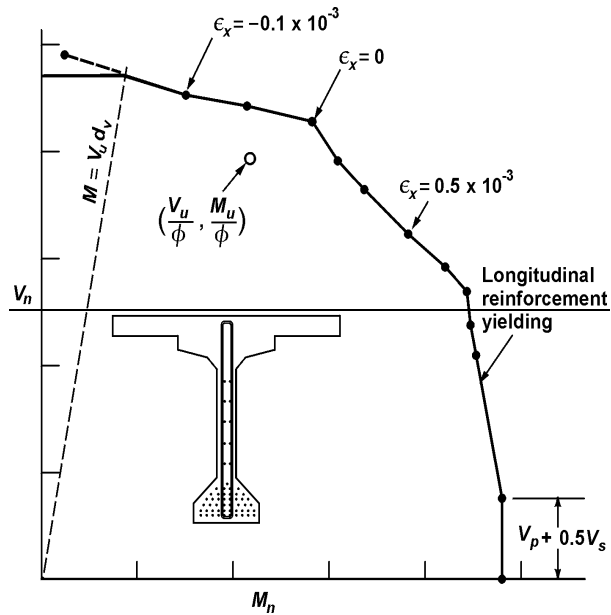


Figure C5.8.3.4.2-6 Typical Shear-Moment Interaction Diagram.

More details on the procedures used in deriving the tabulated values of θ and β are given in Collins and Mitchell (1991).

Table 5.8.3.4.2-1 Values of θ and β for Sections with Transverse Reinforcement.

$\frac{V_u}{f'_c}$	$\epsilon_x \times 1,000$								
	≤ -0.20	≤ -0.10	≤ -0.05	≤ 0	≤ 0.125	≤ 0.25	≤ 0.50	≤ 0.75	≤ 1.00
≤ 0.075	22.3 6.32	20.4 4.75	21.0 4.10	21.8 3.75	24.3 3.24	26.6 2.94	30.5 2.59	33.7 2.38	36.4 2.23
≤ 0.100	18.1 3.79	20.4 3.38	21.4 3.24	22.5 3.14	24.9 2.91	27.1 2.75	30.8 2.50	34.0 2.32	36.7 2.18
≤ 0.125	19.9 3.18	21.9 2.99	22.8 2.94	23.7 2.87	25.9 2.74	27.9 2.62	31.4 2.42	34.4 2.26	37.0 2.13
≤ 0.150	21.6 2.88	23.3 2.79	24.2 2.78	25.0 2.72	26.9 2.60	28.8 2.52	32.1 2.36	34.9 2.21	37.3 2.08
≤ 0.175	23.2 2.73	24.7 2.66	25.5 2.65	26.2 2.60	28.0 2.52	29.7 2.44	32.7 2.28	35.2 2.14	36.8 1.96
≤ 0.200	24.7 2.63	26.1 2.59	26.7 2.52	27.4 2.51	29.0 2.43	30.6 2.37	32.8 2.14	34.5 1.94	36.1 1.79
≤ 0.225	26.1 2.53	27.3 2.45	27.9 2.42	28.5 2.40	30.0 2.34	30.8 2.14	32.3 1.86	34.0 1.73	35.7 1.64
≤ 0.250	27.5 2.39	28.6 2.39	29.1 2.33	29.7 2.33	30.6 2.12	31.3 1.93	32.8 1.70	34.3 1.58	35.8 1.50

Table 5.8.3.4.2-2 Values of θ and β for Sections with Less than Minimum Transverse Reinforcement.

f_{xe} (in.)	$\epsilon_x \times 1000$										
	≤ 0.20	≤ 0.10	≤ 0.05	≤ 0	≤ 0.125	≤ 0.25	≤ 0.50	≤ 0.75	≤ 1.00	≤ 1.50	≤ 2.00
≤ 5	25.4 6.36	25.5 6.06	25.9 5.56	26.4 5.15	27.7 4.41	28.9 3.91	30.9 3.26	32.4 2.86	33.7 2.58	35.6 2.21	37.2 1.96
≤ 10	27.6 5.78	27.6 5.78	28.3 5.38	29.3 4.89	31.6 4.05	33.5 3.52	36.3 2.88	38.4 2.50	40.1 2.23	42.7 1.88	44.7 1.65
≤ 15	29.5 5.34	29.5 5.34	29.7 5.27	31.1 4.73	34.1 3.82	36.5 3.28	39.9 2.64	42.4 2.26	44.4 2.01	47.4 1.68	49.7 1.46
≤ 20	31.2 4.99	31.2 4.99	31.2 4.99	32.3 4.61	36.0 3.65	38.8 3.09	42.7 2.46	45.5 2.09	47.6 1.85	50.9 1.52	53.4 1.31
≤ 30	34.1 4.46	34.1 4.46	34.1 4.46	34.2 4.43	38.9 3.39	42.3 2.82	46.9 2.19	50.1 1.84	52.6 1.60	56.3 1.30	59.0 1.10
≤ 40	36.6 4.06	36.6 4.06	36.6 4.06	36.6 4.06	41.2 3.20	45.0 2.62	50.2 2.00	53.7 1.66	56.3 1.43	60.2 1.14	63.0 0.95
≤ 60	40.8 3.50	40.8 3.50	40.8 3.50	40.8 3.50	44.5 2.92	49.2 2.32	55.1 1.72	58.9 1.40	61.8 1.18	65.8 0.92	68.6 0.75
≤ 80	44.3 3.10	44.3 3.10	44.3 3.10	44.3 3.10	47.1 2.71	52.3 2.11	58.7 1.52	62.8 1.21	65.7 1.01	69.7 0.76	72.4 0.62

5.8.3.5 Longitudinal Reinforcement

At each section the tensile capacity of the longitudinal reinforcement on the flexural tension side of the member shall be proportioned to satisfy:

$$A_s f_y + A_{ps} f_{ps} \geq \frac{M_u}{d_v \phi_f} + 0.5 \frac{N_u}{\phi_c} + \left(\frac{V_u}{\phi_v} - 0.5 V_s - V_p \right) \cot \theta \quad (5.8.3.5-1)$$

where:

V_s = shear resistance provided by the transverse reinforcement at the section under investigation as given by Eq. 5.8.3.3-4, except V_s shall not be taken as greater than V_u/ϕ (kip)

θ = angle of inclination of diagonal compressive stresses used in determining the nominal shear resistance of the section under investigation as determined by Article 5.8.3.4 (°)

ϕ, ϕ_v, ϕ_c = resistance factors taken from Article 5.5.4.2 as appropriate for moment, shear and axial resistance

The area of longitudinal reinforcement on the flexural tension side of the member need not exceed the

C5.8.3.5

Shear causes tension in the longitudinal reinforcement. For a given shear, this tension becomes larger as θ becomes smaller and as V_c becomes larger. The tension in the longitudinal reinforcement caused by the shear force can be visualized from a free-body diagram such as that shown in Figure C1.

Taking moments about Point 0 in Figure C1, assuming that the aggregate interlock force on the crack, which contributes to V_c , has a negligible moment about Point 0, and neglecting the small difference in location of V_u and V_p leads to the requirement for the tension force in the longitudinal reinforcement caused by shear.

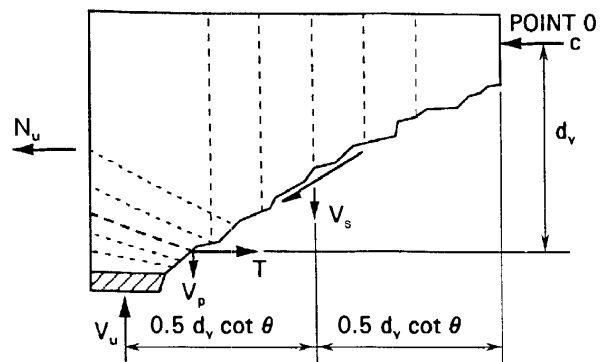


Figure C5.8.3.5-1 Forces Assumed in Resistance Model Caused by Moment and Shear.

At maximum moment locations, the shear force changes sign, and hence the inclination of the diagonal

area required to resist the maximum moment acting alone. This provision applies where the reaction force or the load introduces direct compression into the flexural compression face of the member.

Eq. 1 shall be evaluated where simply-supported girders are made continuous for live loads. Where longitudinal reinforcement is discontinuous, Eq. 1 shall be reevaluated.

compressive stresses changes. At direct supports including simply-supported girder ends and bent/pier caps pinned to columns, and at loads applied directly to the top or bottom face of the member, this change of inclination is associated with a fan-shaped pattern of compressive stresses radiating from the point load or the direct support as shown in Figure C2. This fanning of the diagonal stresses reduces the tension in the longitudinal reinforcement caused by the shear; i.e., angle θ becomes steeper. The tension in the reinforcement does not exceed that due to the maximum moment alone. Hence, the longitudinal reinforcement requirements can be met by extending the flexural reinforcement for a distance of $d_v \cot \theta$ or as specified in Article 5.11, whichever is greater.

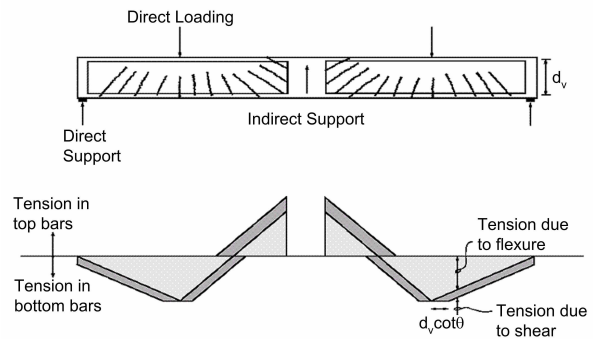


Figure C5.8.3.5-2 Force Variation in Longitudinal Reinforcement Near Maximum Moment Locations.

At the inside edge of the bearing area of simple end supports to the section of critical shear, the longitudinal reinforcement on the flexural tension side of the member shall satisfy:

$$A_s f_y + A_{ps} f_{ps} \geq \left(\frac{V_u}{\phi_v} - 0.5V_s - V_p \right) \cot \theta \quad (5.8.3.5-2)$$

Eqs. 1 and 2 shall be taken to apply to sections not subjected to torsion. Any lack of full development shall be accounted for.

5.8.3.6 Sections Subjected to Combined Shear and Torsion

5.8.3.6.1 Transverse Reinforcement

The transverse reinforcement shall not be less than the sum of that required for shear, as specified in Article 5.8.3.3, and for the concurrent torsion, as specified in Articles 5.8.2.1 and 5.8.3.6.2.

In determining the tensile force that the reinforcement is expected to resist at the inside edge of the bearing area, the values of V_u , V_s , V_p , and θ , calculated for the section d_v from the face of the support may be used. In calculating the tensile resistance of the longitudinal reinforcement, a linear variation of resistance over the development length or the transfer length may be assumed.

C5.8.3.6.1

The shear stresses due to torsion and shear will add on one side of the section and offset on the other side. The transverse reinforcement is designed for the side where the effects are additive.

Usually the loading that causes the highest torsion differs from the loading that causes the highest shear.

5.8.3.6.2 Torsional Resistance

The nominal torsional resistance shall be taken as:

$$T_n = \frac{2A_o A_t f_y \cot \theta}{s} \quad (5.8.3.6.2-1)$$

where:

A_o = area enclosed by the shear flow path, including any area of holes therein (in.²)

A_t = area of one leg of closed transverse torsion reinforcement (in.²)

θ = angle of crack as determined in accordance with the provisions of Article 5.8.3.4 with the modifications to the expressions for v and V_u herein (°)

For combined shear and torsion, ε_x shall be determined using Eq. 5.8.3.4.3.2-1 or Eq. 5.8.3.4.2-2, as appropriate, with V_u replaced by:

$$V_u = \sqrt{V_u^2 + \left(\frac{0.9 p_h T_u}{2A_o} \right)^2} \quad (5.8.3.6.2-2)$$

The angle θ shall be as specified in either Table 5.8.3.4.3.2-1 or 35° Table 5.8.3.4.2-2, as appropriate, with the shear stress, v , taken as:

(b) For box sections

$$v_u = \frac{V_u - \phi V_p}{\phi b_v d_v} + \frac{T_u p_h}{\phi A_{oh}^2} \quad (5.8.3.6.2-3)$$

(c) For other sections

$$v_u = \sqrt{\left(\frac{V_u - \phi V_p}{\phi b_v d_v} \right)^2 + \left(\frac{T_u p_h}{\phi A_{oh}^2} \right)^2} \quad (5.8.3.6.2-4)$$

where:

p_h = perimeter of the centerline of the closed transverse torsion reinforcement (in.)

Although it is sometimes convenient to design for the highest torsion combined with the highest shear, it is only necessary to design for the highest shear and its concurrent torsion, and the highest torsion and its concurrent shear.

C5.8.3.6.2

The term A_o can usually be taken as $0.85 A_{oh}$. The justification for this generally conservative substitution is given in Collins and Mitchell (1991).

Where torsion must be investigated for a box girder, the shear stress due to shear and the shear stress due to torsion will add together on one side of the box girder. Even if the webs of box girders were designed individually using refined analysis, the box girder must be checked for torsion as a single whole-width unit.

For other cross-sectional shapes, such as a rectangle or an "I," there is the possibility of considerable redistribution of shear stresses. To make some allowance for this favorable redistribution, it is safe to use a root-mean-square approach in calculating the nominal shear stress for these cross-sections, as indicated in Eqs. 2 and 4.

A_{oh} = area enclosed by centerline of exterior closed transverse torsion reinforcement, including area of any holes (in.²)

T_u = factored torsional moment (kip-in.)

ϕ = resistance factor specified in Article 5.5.4.2

5.8.3.6.3 Longitudinal Reinforcement

The provisions of Article 5.8.3.5 shall apply as amended, herein, to include torsion.

The longitudinal reinforcement shall be proportioned to satisfy Eq. 1:

$$A_s f_y + A_{ps} f_{ps} \geq \frac{M_u}{\phi d_v} + \frac{0.5N_u}{\phi} + \cot \theta \sqrt{\left(\frac{V_u}{\phi} - 0.5V_s - V_p \right)^2 + \left(\frac{0.45 p_h T_u}{2A_o \phi} \right)^2} \quad (5.8.3.6.3-1)$$

C5.8.3.6.3

To account for the fact that on one side of the section the torsional and shear stresses oppose each other, the equivalent tension used in the design equation is taken as the square root of the sum of the squares of the individually calculated tensions in the web.

References

Hawkins, N.M., D.A. Kuchma, R.F. Mast, M.L. Marsh, and K-H. Reineck. Simplified Shear Design of Structural Concrete Members. NCHRP Report XX1. TRB, National Research Council, Washington, D.C. 2005

Hawkins, N.M., D.A. Kuchma, H.G. Russell, G.J. Klein, and N.S. Anderson. Application of the LRFD Bridge Design Specifications to High-Strength Structural Concrete: Shear Provisions. NCHRP Report XX2. TRB, National Research Council, Washington, D.C. 2006.

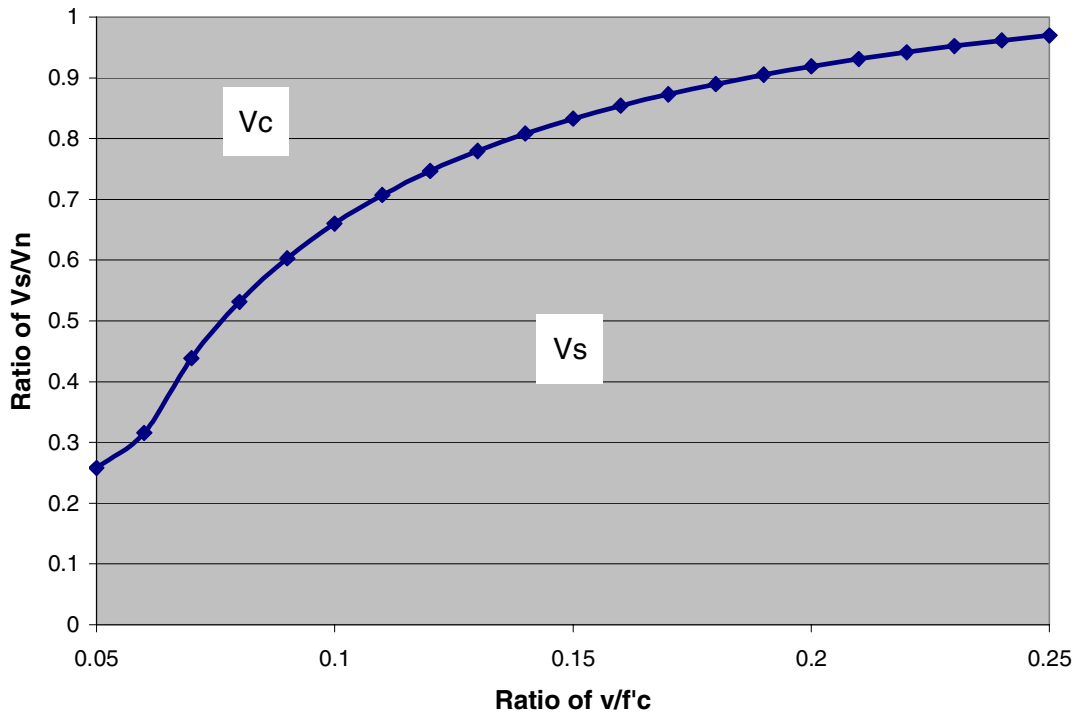


Figure F-1 Influence of Shear Stress Design Ratio on Fraction of Shear Supported by Stirrups

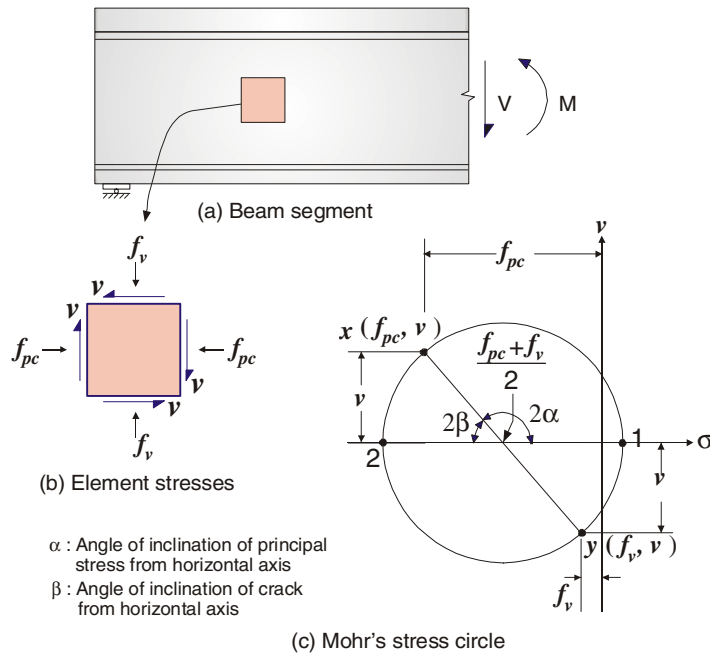


Figure F-2 Derivation of Web-Shear Cracking Force, V_{cw}

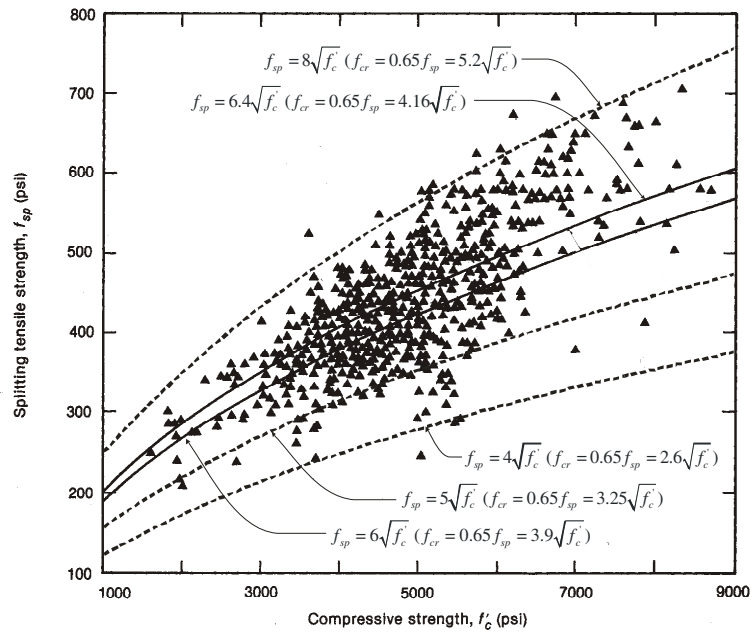


Figure F-3 Variation in Tensile Strength of Concrete (Sher et al, 1979)

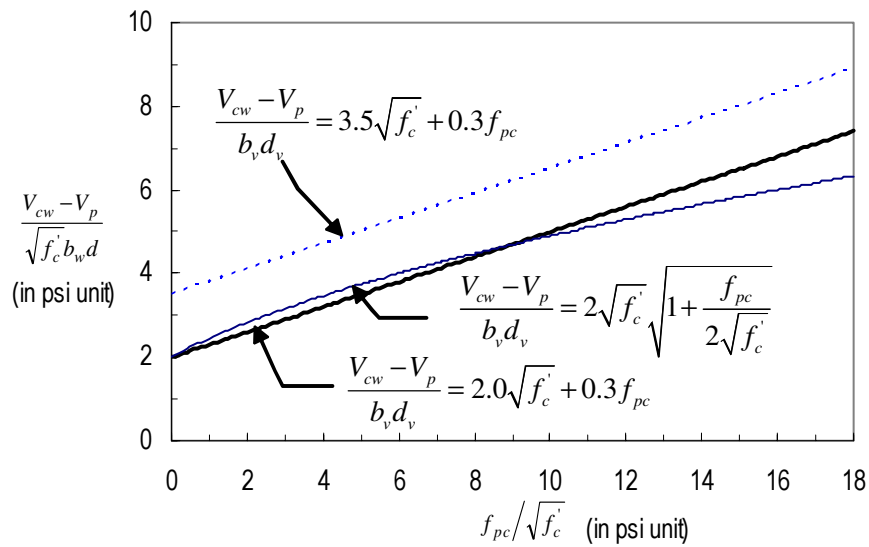


Figure F-4 Approximation of Web-Shear Cracking Force, V_{cw}

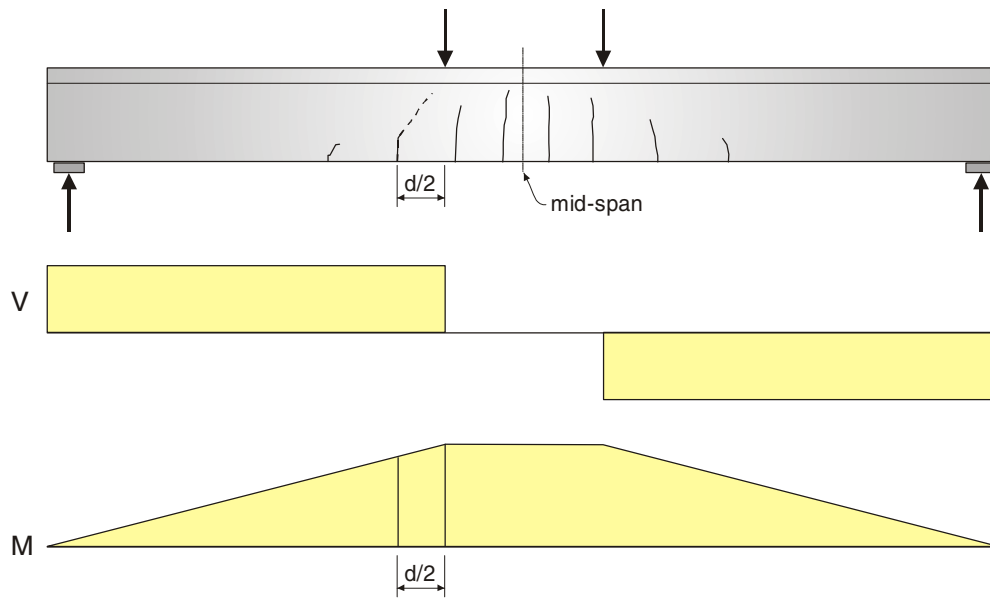


Figure F-5 Derivation of Flexure-Shear Cracking Force, V_{ci}

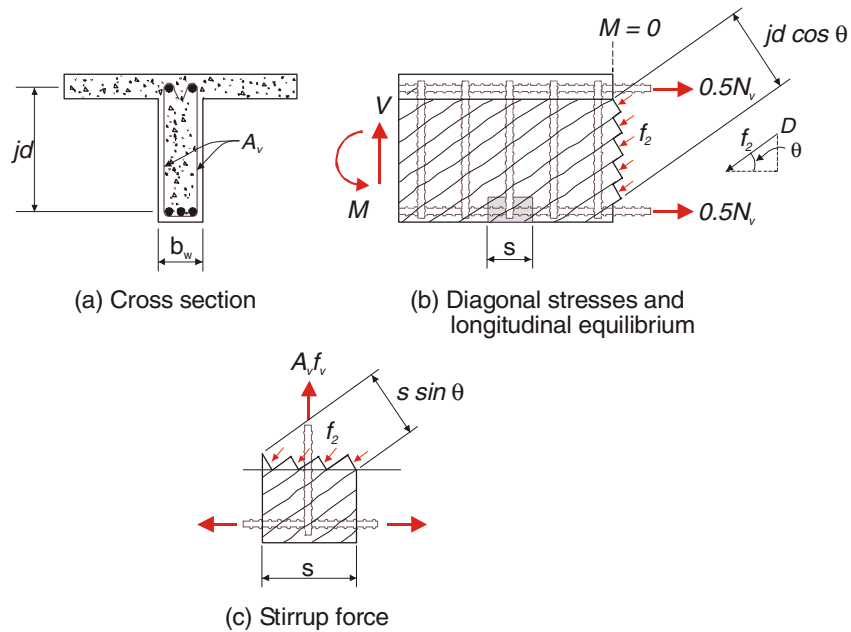


Figure F-6 Equilibrium Conditions for Variable-Angle Truss Model

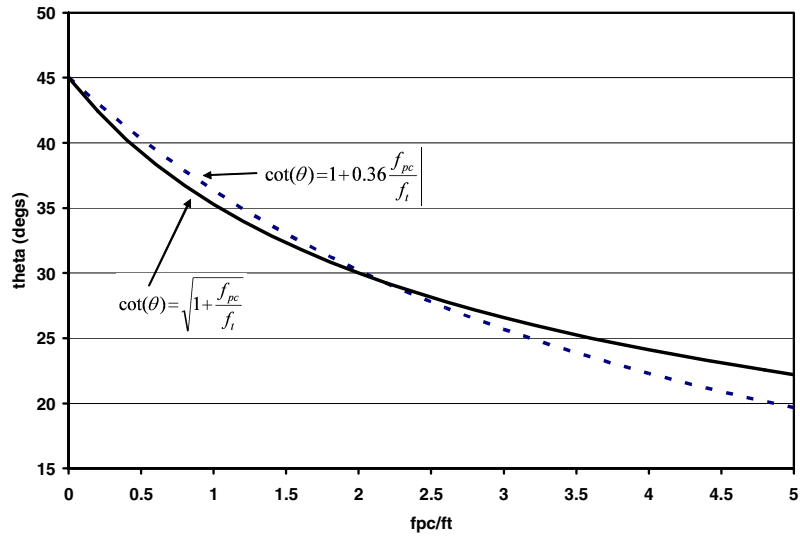


Figure F-7 Comparison of the Angle of Inclination of Strut

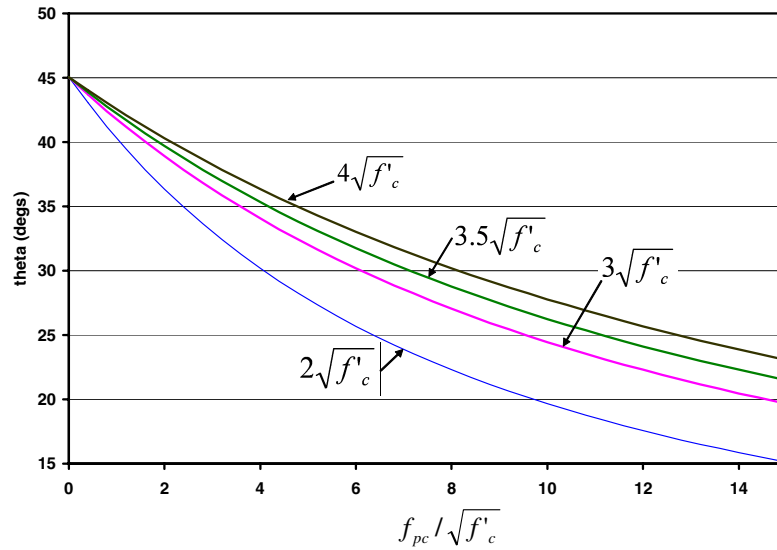


Figure F-8 Comparison of the Angle of Inclination of Strut versus $f_{pc} / \sqrt{f'_c}$

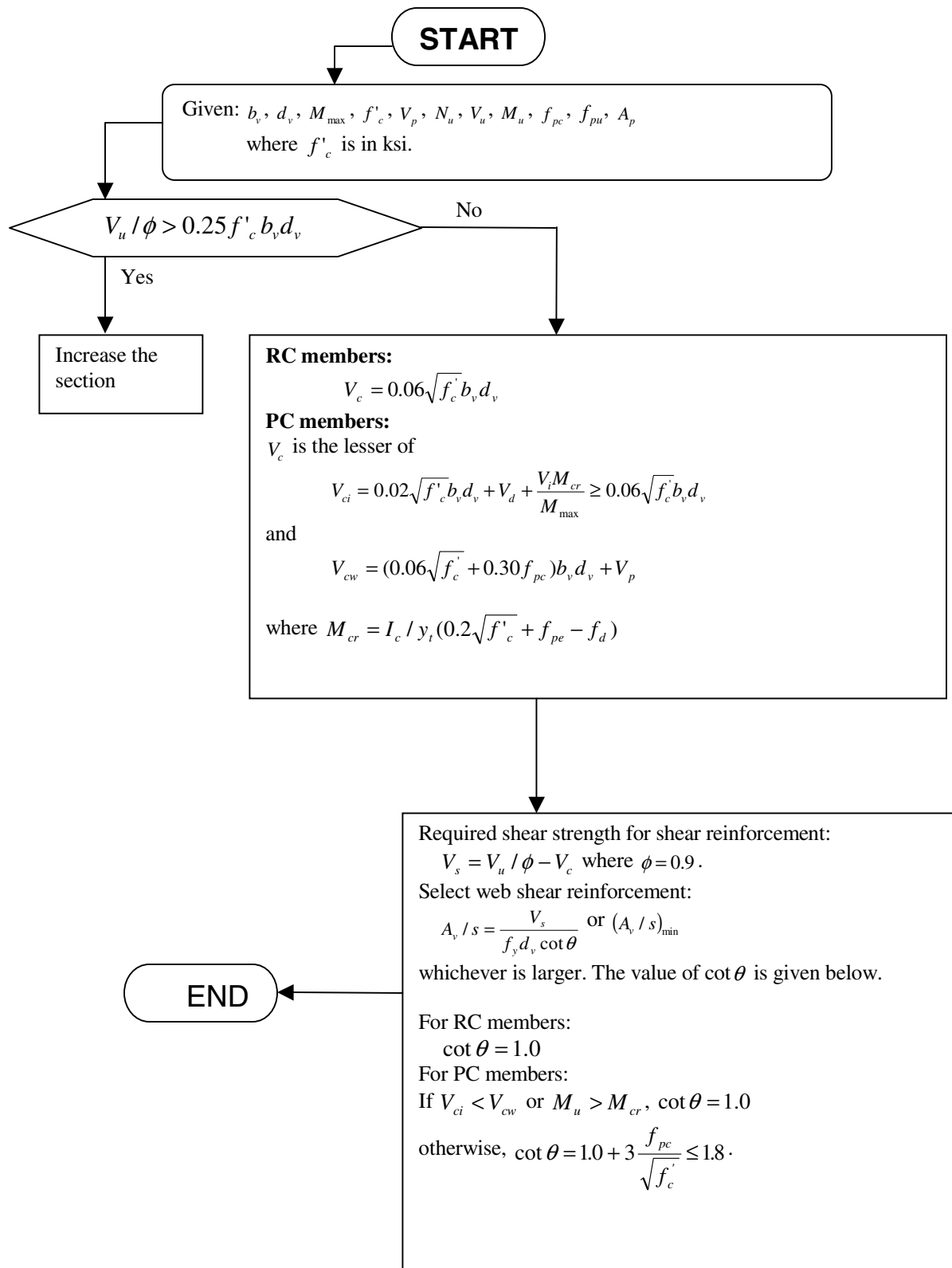


Figure F-9 Flowchart of Simplified Shear Design Procedure

APPENDIX G: Evaluation of Proposed Simplified Provisions with Selected Shear Database

In this appendix, the proposed simplified shear design provisions are evaluated and validated using with test data. In Section G.1, the overall performance and safety of the proposed simplified provisions (V_{test}/V_{prop}) are examined using the selected shear database and results compared with the predictions of the *AASHTO LRFD Bridge Design Specifications (2001)*; *CSA A23.3 2004 edition (Collins, 2003)*; and *AASHTO Standard Specification (1989) (same as ACI 318-02)* methods. Section G.2 examines the accuracy and safety of the proposed simplified provisions for also predicting the web-shear cracking load of PC members. In Section G.3, the significance of the compression strut angle is studied. Section G.4 provides an evaluation of the flexure-shear cracking strength predictions using test results from NCHRP Project 12-56.

G.1 Evaluation of Overall Performance of Simplified Proposed Provisions

The databases used in this section are presented in Tables G-1 and G-2, which are basically same as the databases used in Section D.2 of Appendix D. The only difference is that the number of PC members is reduced from 85 to 83 due to redundancy. Thus, these selected databases consist of 64 reinforced concrete (RC) members and 83 prestressed concrete (PC) members. All selected members contained the ACI 318 required minimum amount of shear reinforcement ($\rho_v f_y > 50$ psi), had an overall height of at least 20 inches, and were cast with concrete having measured compressive strengths of at least 4000 psi. In this comparison, all strength reduction factors and material strength reduction factors are set equal to unity.

In Figs. G-1 through G-4, the measured to calculated strength ratios ($V_{test}/V_{n,Prop}$, $V_{test}/V_{n,CSA}$, $V_{test}/V_{n,LRFD}$, and $V_{test}/V_{n,STD}$) are plotted versus the test parameters of f'_c , d (depth), ρ_l (longitudinal reinforcement ratio), and $\rho_v f_y$ (strength of shear reinforcement) for both the selected RC and PC members. The overall performance of the four different methods is also compared in Table G-3.

The results of the evaluation using the AASHTO Standard Specification are shown in Fig. G-1, where the mean strength ratio for RC members is 1.296 and for PC members is 1.322. There is more scatter in the RC member strength ratios (coefficient of variation (COV) = 0.333) than in the PC member strength ratios (COV = 0.160). For RC members, the provisions become less conservative as ρ_l decreases, with some unconservative strengths occurring for members with less than 2% longitudinal reinforcement. It can also be seen that some unconservative results also occur for RC members containing light amounts of shear reinforcement ($\rho_v f_y < 150$ psi). For PC members, the prestressing steel ratio is usually directly related to the axial stress level in the PC member. Thus, as the prestressing steel ratio increases, the axial stress level is also usually increasing. Although the influence of longitudinal reinforcement ratio is not considered to affect the shear strength of PC members, the web-shear cracking strength, V_{cw} , accounts for the influence of axial stress at the centroid of section. Thus, the influence of the longitudinal reinforcement ratio on shear strength is partly captured by AASHTO STD approach in an indirect manner. It is also observed that AASHTO STD method provides very conservative results for the members with relatively heavy amount of shear reinforcement. That result is due to its conservative limit on maximum shear strength.

By contrast with the AASHTO STD results, use of the LRFD shear design specifications results in strength predictions, Fig. G-2, that provide safe and accurate estimates of measured capacities for both RC and PC members, with no observable trends for the four selected test parameters. For RC members, the mean strength ratio is 1.214 with a COV of 0.179 while for PC members the mean strength ratio is 1.227 with a COV of 0.145. In the AASHTO LRFD method, the effect of the amount of longitudinal reinforcement is reflected in the longitudinal strain resulting from the combination of sectional forces. The longitudinal reinforcement ratio affects both crack width and shear strength. For the same magnitude of loading, as the longitudinal reinforcement ratio decreases, flexural stress and strain increase. Consequently, crack width increases, interface shear transfer decreases, and the shear strength are reduced. As shown in Fig. G-2, the AASHTO LRFD method accounts realistically for the influence of the longitudinal reinforcement ratio. It is also apparent that AASHTO LRFD method gives a reasonably constant margin of safety for all shear reinforcement levels for both RC and PC members.

Figure G-3 shows that the CSA 2004 method gives very good estimation of the shear capacity of both RC and PC members. The mean value of the strength ratios ($V_{\text{test}}/V_{n,\text{CSA}}$) is 1.105 with a COV of 0.156 for RC members, and the mean strength ratio is 1.245 with a COV of 0.134 for PC members. The overall trends of the results with the selected parameters and the accuracy of the method is very similar to that of the AASTHO LRFD method as both provisions have a common basis in the MCFT. It is proposed in this document that the CSA 2004 method be used to replace the AASHTO LRFD general procedure method.

Comparison of Figs G-3 and G-4 shows that the proposed simplified method gives results for both RC and PC members similar to those of the AASTHO STD method. The proposed simplified method provides conservative strength ratios ($V_{\text{test}}/V_{n,\text{Prop}}$) for all members except some RC members with relatively small amount of longitudinal reinforcement ($\rho_l < 2\%$) and containing light amounts of shear reinforcement ($\rho_v f_y < 150$ psi). The mean value of the strength ratios ($V_{\text{test}}/V_{n,\text{Prop}}$) is 1.309 with a COV of 0.291 for RC members, and the mean strength ratio is 1.542 with a COV of 0.189 for PC members.

To examine the overall accuracy and safety of the proposed provisions as the level of prestressing changes, the strength ratio ($V_{\text{test}}/V_{\text{Prop}}$) is plotted as a function of the level of prestressing, $f_{pc} / \sqrt{f'_c}$, in Fig. G-5. Different symbols are used to denote the level of shear reinforcement provided. This figure illustrates that the proposed simplified method provides conservative estimates of shear capacities, with reasonably constant factor of safety, over a wide range of prestress levels without any ascending or descending trend.

If the discussion of the proposed simplified provisions was terminated here, it might reasonably be concluded that the proposed simplified approach does not provide any improvement over that of the ACI 318 (AASHTO Standard) approach. It would also be reasonable to conclude that the current LRFD approach is considerably more accurate, although sometimes less conservative, than the proposed simplified approach. However, comparisons with experimental test data should only ever be part of the necessary evaluation because the types of experiments conducted in the laboratory do not well represent what is built in the field. For this reason the contractor also created a design database with which the predictions of the different methods are compared. The comparisons in Appendix H provide that perspective.

G.2 Evaluation of Web-Shear Cracking Strength, V_{cw}

In order to appreciate the basis for the selection of the proposed V_{cw} expression, it is useful to examine the scatter in the shear strength of PC members without shear reinforcement, A_v . In such tests, the ultimate capacity is directly dependent on V_c and, based on observations, that capacity typically occurs shortly after diagonal cracking has developed. Figure G-6 presents the normalized shear stress at failure as a function of the level of prestressing ($f_{pc} / \sqrt{f_c'}$) for PC members without shear reinforcement. For the left and bottom axes, f_c' is in psi units while on the right and top axes, f_c' is in ksi units. In this plot, the lower solid line is the proposal while the higher broken line is the expression for V_{cw} in the AASHTO Standard Specifications and ACI 318-02. That latter expression is:

$$V_{cw} = (3.5\sqrt{f_c'(\text{psi})} + 0.3f_{pc})b_w d \approx (0.11\sqrt{f_c'(\text{ksi})} + 0.3f_{pc})b_w d \quad (\text{G-1})$$

Based on this plot, it is observed that the proposed approach for V_{cw} represents a lower bound to the test data whereas the expression in the AASHTO Standard Specifications and ACI318-02 is closer to the mean of the ultimate strength for these data.

As mentioned previously in Appendix F, it needs to be demonstrated that the web-shear cracking strength V_{cw} provides a safe estimation of the concrete contribution at ultimate in order to be able to use the relationship $V_n = V_c + V_s$. Thus, it is worthwhile to also compare the concrete contribution at ultimate for members with shear reinforcement to the proposed expression for V_{cw} . In Fig. G-7, the normalized shear stresses, based on the measured concrete contribution at ultimate, $V_{c,\text{test}} / \sqrt{f_c'} b_w d_v$, of the selected members in Table G-2 are plotted versus the prestress level ($f_{pc} / \sqrt{f_c'}$) where $V_{c,\text{test}} = V_{\text{test}} - V_{s,\text{Prop}}$. Members whose shear strengths were governed by the maximum shear limit or whose concrete contributions were governed by flexure-shear strength values are not included in Fig. G-7. This figure is for web-shear cracking strengths only. The results in Fig. G-7 indicate that the expression for web-shear cracking strength and the proposed approach for calculation of the steel contribution provide a safe low bound for members with shear reinforcement.

All girders tested in NCHRP Project 12-56 also had shear reinforcement and were cast with high strength concrete. Table G-4 lists the inclined cracking loads (w_{cr}) in kips/ft, and the cracking shear forces (V_{cr}) for those beams along with selected specimen details. Because the shear force varied along the span under the uniform load applied in these experiments, the cracking shear force is very sensitive to the cracking location. Thus, the values for cracking shear force provided in Table G-4 are those when the diagonal crack first crossed mid-height of the member as shown in Fig. G-8. As can be seen from the last column of Table G-4, the normalized cracking shear strengths, $V_{cr} / \sqrt{f_c'} b_w d$, ranged from 4.6 to 11.7, so that the largest value was more than twice of the smallest.

In Table G-5, the web-shear cracking strengths calculated by the AASHTO STD (or ACI) method and the proposed simplified provision are compared with the test results. The assumed crack location was $h/2$ away from the face of the support in both approaches. In most cases, the AASHTO STD and ACI approach provide good estimates of the web-shear cracking strengths

with an average ratio, $V_{cr,test} / V_{cr,STD}$, of 1.15. The calculated cracking strengths using the proposed simplified approach are very conservative with an average ratio, $V_{cr,test} / V_{cr,Prop}$, of 1.70. Thus, as observed already for members with and without shear reinforcement, the proposed approach for calculating V_{cw} also provides a conservative and safe estimate for members with shear reinforcement and high strength concrete.

G.3 Evaluation of Compression Strut Angle

The contribution of the shear reinforcement in members with shear reinforcement is directly proportional to the value of $\cot \theta$ since $V_s = \frac{A_v f_y d_v \cot \theta}{s}$. In order to evaluate the accuracy of this expression for calculating the effectiveness of the shear reinforcement, the experimentally measured effectiveness of the shear reinforcement is compared with that given by the proposed expression.

In Fig. G-9, the value of $\cot(\theta)$ is plotted versus the level of prestressing ($f_{pc} / \sqrt{f'_c}$) for selected members. The experimentally measured contribution of the shear reinforcement ($V_{s, test}$) is equal to the measured shear capacity (V_{test}) less the calculated concrete contribution (V_{cw}) by the proposed expression. Thus, in Fig. G-9,

$$\cot \theta = \frac{V_{test} - V_{cw}}{\rho_v f_y b_v d} \quad (\text{G-2})$$

For Fig. G-9, members whose strengths were governed by the maximum shear strength limit of $0.18\sqrt{f'_c} b_v d_v$ are not shown because the magnitude of the steel contribution for those members would be meaningless for the foregoing approach. Such members have very heavy amounts of shear reinforcement and are therefore likely to have had anchorage failures or diagonal crushing failures before the stirrups yielded.

The results of Fig. G-9 illustrate that the proposed expression for $\cot(\theta)$ provides conservative results in most cases. This result is probably due to two reasons. First, the concrete shear cracking strength in the proposed approach is a conservative estimate of the actual cracking strength in order that the value is a lower bound appropriate for use as the concrete contribution at the ultimate capacity. Second, the value of the compression strut angle is conservative when $M_u > M_{cr}$. However, in combination these two concepts provide an appropriate approach for ensuring against any unconservative shear designs of RC and PC members. This issue is examined further in the comparisons with the design database in Appendix H. The expressions for $\cot(\theta)$ are particularly conservative for members with small amounts of shear reinforcement. This result is probably because in lightly reinforced members there is strain hardening of the stirrups and the conservative estimates for V_c increase the conservatism of this approach.

G.4 Evaluation of Flexure-Shear Cracking Strength, V_{ci}

As discussed in Appendix F, the proposed simplified approach adopts the flexure-shear cracking strength expression of the AASHTO STD method with very small changes in constants. In order to investigate the accuracy of simplified proposed approach, the flexure-shear cracking strengths of girders tested in NCHRP Project 12-56 are examined here. Figure. G-10 shows the flexure-shear cracks that developed and the corresponding distributed loads for those girders for

that cracking. Twelve test results from six girders were available at the time this report was written. In these tests the West ends of Girders 5 and 6 did not develop flexure-shear cracks until failure and for the East end of Girder 6 an investigation of the flexure-shear cracking strength was not possible due to the failure mode for the West end. Thus, those specimens are not included in this examination of the flexure-shear cracking strength. As can be seen from Fig. G-10, flexure-shear cracking occurs in regions of high moment combined with significant shear. The dotted vertical line in each figure is the location of the section where flexure-shear cracking shear forces were obtained, and corresponded to the load at which the diagonal crack crossed mid-height of the girder.

Table G-6 lists the flexure-shear cracking forces as measured in the tests and the same strengths calculated by the proposed simplified approach. The ratios of $V_{ci, test} / V_{ci, Prop}$ indicate that the proposed simplified approach somewhat over-predicted the measured flexure-shear cracking strengths but provides strengths reasonably close to the test results with an average value of 0.86. The AASHTO STD and ACI Code expression was derived from tests on 12-inch deep beams subject to concentrated loads and for which the critical section for flexure-shear cracking is a unique location. By contrast, the beams tested in the 12-56 project were much deeper and the location for flexure-shear cracking less unique. Thus, in the 12-56 tests cracking was to be expected at the weakest location within a reasonable distance from the centerline of the beam. Thus, it is reasonable that the simplified proposed approach gives a slight over-estimation of the flexure-shear cracking strength. The worst result for the simplified proposed approach is that for G5E for which the strength ratio, $V_{ci, test} / V_{ci, Prop}$, is 0.73 and where flexure-shear cracking occurred at 9.2 ft away from midspan ($M/V=28.9$). However, the accuracy of flexure-shear cracking strengths calculated by the simplified proposed approach seems reasonable.

The angles of the flexure-shear cracks in all girders were about 45 degrees or even steeper in some cases. Thus, in the simplified proposed approach, when the flexure-shear cracking strength, V_{ci} , governs, the compression strut angle used in determining the stirrup contribution is taken as 45 degrees.

Table G-1 Database of Selected Reinforced Concrete Members (64 Members)

Reference (Author)	Beam Name	shape	f'_c	d	b_w	a/d	Loading	ρ_l	$\rho_v f_y$	Vtest*
		R/T/I	(psi)	(in)	(in)	(-)	Geometry	(%)	(psi)	(kips)
Angelakos, Bentz Collins (2003)	DBO530M	R	4640	36.42	11.81	2.92	SS-1PL	0.50	58	59.1
	DB165M	R	9425	36.42	11.81	2.92	SS-1PL	1.01	58	101.6
	DB180M	R	11600	36.42	11.81	2.92	SS-1PL	1.01	58	88.8
Bresler; Scordelis (1963)	C-1	R	4290	18.25	6.10	3.78	SS-PL	1.80	92	35.3
	C-3	R	5080	18.06	6.10	6.81	SS-PL	3.63	92	31.0
Ceruti, Marti. (1987)	CM2_B	TI	6482	32.48	5.91	3.03	SE-UDL	5.01	1024	284.4
Collins Kuchma (1999)	SE100A-M-69	R	10295	36.22	11.61	2.50	SE-2PL	1.03	117	116.1
	SE100B-M-69	R	10875	36.22	11.61	2.50	SE-2PL	1.36	117	131.1
	BM100	R	6815	36.42	11.81	2.92	SS-1PL	0.76	58	76.9
	1	R	5280	21.21	12.00	3.10	SS-2PL	2.49	100	76.0
	2	R	5280	21.21	12.00	3.10	SS-2PL	2.49	50	50.0
	3	R	10490	21.21	12.00	3.10	SS-2PL	2.49	50	59.0
	4	R	10490	21.21	12.00	3.10	SS-2PL	2.49	50	71.0
	5	R	8100	21.21	12.00	3.10	SS-2PL	2.49	100	86.0
Johnson Ramirez (1989)	7	R	7440	21.21	12.00	3.10	SS-2PL	2.49	50	63.0
	8	R	7440	21.21	12.00	3.10	SS-2PL	2.49	50	58.0
	S4-1	R	12659	21.34	9.84	2.40	SS-2PL	3.02	130	79.6
Kong, Rangan. (1998)	Ss2-26-1	R	5820	17.94	10.00	4.01	SS-1PL	2.23	81	46.5
	Ss2-29a-1	R	5630	17.94	10.00	4.01	SS-1PL	2.23	54	35.9
	Ss2-29b-1	R	5460	17.94	10.00	4.01	SS-1PL	2.23	54	36.0
	Ss2-29a-2	R	5390	17.94	10.00	4.01	SS-1PL	2.23	59	48.7
	Ss2-29b-2	R	6000	17.94	10.00	4.01	SS-1PL	2.23	59	45.5
	Ss2-29d-2	R	4410	17.94	10.00	4.01	SS-1PL	2.23	59	37.1
	Ss2-29e-2	R	7030	17.94	10.00	4.01	SS-1PL	2.23	59	46.4
	Ss2-318-1	R	5880	17.94	10.00	4.01	SS-1PL	2.23	92	49.5
	Ss2-321-1	R	5620	17.94	10.00	4.01	SS-1PL	2.23	79	36.8
	Ss2-318-2	R	5640	17.94	10.00	4.01	SS-1PL	2.23	63	39.8
	Ss2-321-2	R	5510	17.94	10.00	4.01	SS-1PL	2.23	54	37.5
	Ss2-313.5-3	R	6190	17.94	10.00	4.01	SS-1PL	2.23	65	48.0
	Ss2-318-3	R	6240	17.94	10.00	4.01	SS-1PL	2.23	49	39.3
Ss2-321-3	R	6240	17.94	10.00	4.01	SS-1PL	2.23	42	31.6	
Levi Marro (1989/1993)	RC 60 A1	TI	6815	37.01	4.72	4.04	SS-PL	9.41	583	222.6
	RC 60 A2	TI	6815	37.01	4.72	4.04	SS-PL	9.41	583	210.9
	RC 60 B1	TI	7250	37.01	4.72	4.04	SS-PL	12.53	875	265.5
	RC 60 B2	TI	7250	37.01	4.72	4.04	SS-PL	12.53	875	278.6
	RC 70 B1	TI	8700	37.01	4.72	4.04	SS-PL	12.53	875	299.0
Lyngberg (1976)	5A-0	TI	3727	21.26	4.72	2.78	SS-2PL	3.88	518	97.8
	5B-0	TI	3857	21.26	4.72	2.78	SS-2PL	3.88	497	97.8
Rangan (1991)	I-1	I	5293	22.17	2.91	2.49	SS-2PL	8.35	1910	101.9
	I-2	I	4379	22.17	2.91	2.49	SS-2PL	8.35	1074	83.4
	I-3	I	4524	22.17	2.48	2.49	SS-2PL	9.81	2244	83.0
	I-4	I	5177	22.17	2.52	2.49	SS-2PL	9.66	1242	93.5
Reineck (1991)	Stb III	TI	8822	22.80	3.03	4.35	SS-PL	13.81	903	119.2
	Stb I	TI	8822	22.64	3.03	4.37	SS-PL	15.99	1289	151.8
Roller Russell (1990)	No.1	R	17420	22.00	14.00	2.50	SS-1PL	1.65	45	66.8
	No.2	R	17420	22.00	14.00	2.50	SS-1PL	3.04	286	246.7
	No.3	R	17420	22.00	14.00	2.50	SS-1PL	4.56	588	372.1
	No.4	R	17420	22.00	14.00	2.50	SS-1PL	6.08	840	436.1
	No.5	R	17420	22.00	14.00	2.50	SS-1PL	6.97	1176	502.3
	No.6	R	10500	30.00	18.00	3.00	SS-1PL	1.73	53	149.6
	No.7	R	10500	30.00	18.00	3.00	SS-1PL	1.88	102	177.1
	No.8	R	18170	30.00	18.00	3.00	SS-1PL	1.88	53	108.5
	No.9	R	18170	30.00	18.00	3.00	SS-1PL	2.35	102	168.5
	No.10	R	18170	30.00	18.00	3.00	SS-1PL	2.89	150	263.5
Stroband (1997)	1	I	12806	26.04	3.54	2.50	SS-PL	4.95	328	71.9
	2	I	12668	25.48	3.54	2.56	SS-PL	6.14	589	118.7
	3	I	12806	25.48	3.54	2.56	SS-PL	8.98	1391	199.3
	4	I	12943	26.04	3.54	2.50	SS-PL	10.81	2417	256.6
Yoon Cook Mitchell (1996)	N1-N	R	5220	25.79	14.76	3.23	SS-1PL	2.80	51	102.7
	N2-S	R	5220	25.79	14.76	3.23	SS-1PL	2.80	51	81.6
	N2-N	R	5220	25.79	14.76	3.23	SS-1PL	2.80	73	108.6
	M I-N	R	9715	25.79	14.76	3.23	SS-1PL	2.80	51	91.0
	M2-S	R	9715	25.79	14.76	3.23	SS-1PL	2.80	73	124.1
	M2-N	R	9715	25.79	14.76	3.23	SS-1PL	2.80	103	154.9

* For members subjected to uniformly distributed load (UDL), 'Vtest' values are end shear force.

Table G-2 Database of Selected Prestressed Concrete Members (83 Members)

Reference (Author)	Beam Name	shape R/T/I	f' _c (psi)	d (in)	b _w (in)	a/d (-)	Loading Geometry	ρ _p (%)	f _{pe} (ksi)	ρ _v f _y (psi)	V _{test} * (kips)
Cumming Shield French (1998)	IA	I	11330	49.61	6.00	3.24	SS-1PL	3.52	123.0	313	322.2
	IB	I	11330	49.61	6.00	3.19	SS-1PL	3.52	123.0	303	347.6
	IIC	I	9315	49.61	6.00	3.25	SS-1PL	3.52	123.0	303	408.0
	IID	I	9315	48.56	6.00	3.29	SS-1PL	3.60	123.0	303	448.9
Gregor, Collins (1995)	CM5_A	I	8381	31.14	5.91	2.84	SE-1PL	0.37	215.3	410	208.2
	CM6_A	I	8251	31.37	5.91	2.82	SE-1PL	0.73	215.3	410	224.4
Kaufman Ramirez (1988)	I-2	I	8340	25.50	6.00	2.35	SS-2PL	0.87	175.1	117	145.0
	I-3	I	8370	25.50	6.00	2.35	SS-2PL	0.87	180.5	139	100.0
	I-4	I	8370	25.50	6.00	2.35	SS-2PL	0.87	183.7	117	110.0
	II-1	I	9090	33.33	6.00	2.52	SS-2PL	1.00	179.4	164	140.0
Kordina, Weber (1984)	D2	I	4447	26.77	3.94	2.83	SS-PL	2.43	67.9	2414	123.7
	1E	I	10280	68.50	6.00	4.38	SS-UDL	1.70	160.7	388.9	572.0
Kuchma Kim (2004)	1W	I	10280	68.50	6.00	4.38	SS-UDL	1.70	160.7	388.9	662.0
	2E	I	9940	67.32	6.00	4.46	SS-UDL	2.05	156.6	744.9	742.9
	2W	I	9940	67.32	6.00	4.46	SS-UDL	2.05	156.6	744.9	851.8
	3E	I	14230	67.67	6.00	4.43	SS-UDL	2.26	153.0	565.0	785.0
	3W	I	14230	67.67	6.00	4.43	SS-UDL	2.26	153.0	565.0	854.0
	5E	I	17800	70.00	6.00	4.29	SS-UDL	1.25	172.4	169.0	521.2
	5W	I	17800	70.00	6.00	4.29	SS-UDL	1.25	172.4	140.3	437.8
	6E	I	17800	67.67	6.00	4.43	SS-UDL	2.26	163.1	557.1	760.7
6W	I	17800	67.67	6.00	4.43	SS-UDL	2.26	172.2	557.1	612.3	
Leonhardt Koch Rostásy (1974)	IP3-re	I	4258	32.63	11.81	3.92	SS-PL	1.13	9.5	402	204.8
	T.P3-ii	I	7540	32.66	5.91	3.92	SS-PL	2.25	102.5	713	232.7
	T.P3-re	I	7540	32.66	5.91	3.92	SS-PL	2.25	102.5	436	232.7
	T.P4	I	6884	32.56	3.15	3.93	SS-PL	4.23	98.7	1444	202.3
Levi Marro (1989)	PC 30A1	I	4350	37.65	4.72	3.97	SS-PL	0.73	139.0	583	197.8
	PC 30A2	I	4350	37.65	4.72	3.97	SS-PL	0.73	134.7	583	194.5
	PC 60A1	I	7250	37.42	4.72	4.00	SS-PL	1.46	120.0	583	268.4
	PC 60A2	I	7250	37.42	4.72	4.00	SS-PL	1.46	114.8	583	271.4
	PC 60B1	I	7250	37.18	4.72	4.02	SS-PL	1.47	115.3	875	298.3
	PC 60B2	I	7250	37.18	4.72	4.02	SS-PL	1.47	115.3	875	314.7
Lyngberg (1976)	2A-3	I	4727	21.26	4.72	2.78	SS-2PL	1.05	134.9	473	113.8
	2B-3	I	4916	21.26	4.72	2.78	SS-2PL	1.05	134.5	494	115.8
	3A-2	I	4510	21.26	4.72	2.78	SS-2PL	0.70	135.1	510	109.9
	3B-2	I	3988	21.26	4.72	2.78	SS-2PL	0.70	135.1	480	97.3
	4A-1	I	4568	21.26	4.72	2.78	SS-2PL	0.35	139.2	491	105.4
	4B-1	I	4408	21.26	4.72	2.78	SS-2PL	0.35	134.1	506	102.1
Malone, Ramierz (2000)	PC6S	I	6496	29.46	5.98	3.26	SS-1PL	0.76	164.1	134	116.9
	PC10S	I	10092	29.43	5.98	3.26	SS-1PL	0.76	163.3	134	120.0
Rangan (1991)	II-1	I	6525	22.21	2.52	2.48	SS-2PL	0.77	168.2	1327	103.6
	II-2	I	4568	22.21	2.48	2.48	SS-2PL	0.78	168.2	2244	85.2
	II-3	I	6467	22.21	2.87	2.48	SS-2PL	0.68	168.2	1164	110.0
	II-4	I	6235	22.21	2.91	2.48	SS-2PL	0.67	168.2	1910	107.8
	III-1	I	5800	22.07	2.60	2.50	SS-2PL	1.08	168.2	1287	82.7
	III-2	I	5365	22.07	2.60	2.50	SS-2PL	1.08	168.2	2142	87.8
	III-3	I	5655	22.07	3.03	2.50	SS-2PL	0.92	168.2	1103	89.1
	III-4	I	5365	22.07	2.87	2.50	SS-2PL	0.97	168.2	1936	101.8
	IV-1	I	5380	21.08	2.44	2.62	SS-2PL	2.16	168.2	2280	84.3
	IV-2	I	4785	21.08	2.52	2.62	SS-2PL	2.09	168.2	1327	75.9
	IV-3	I	5220	21.08	2.83	2.62	SS-2PL	1.86	168.2	1963	104.5
	IV-4	I	4162	21.08	2.83	2.62	SS-2PL	1.86	168.2	1180	87.8
Reineck, et al. (1991)	Spb III	I	8822	20.79	3.03	4.92	SS-PL	5.43	103.1	903	138.5
	Spb I	I	8822	20.55	2.95	4.98	SS-PL	7.04	103.1	1323	159.6
Russell Bruce Roller (2003)	BT6Live	I	11780	77.00	6.00	1.56	SS-3PL	1.25	158.9	417	592.0
	BT6Dead	I	11590	77.00	6.00	1.56	SS-3PL	1.25	158.9	472	557.0
	BT7Live	I	12400	77.00	6.00	1.56	SS-3PL	1.25	158.9	641	614.0
	BT7Dead	I	12730	77.00	6.00	1.56	SS-3PL	1.25	158.9	282	605.0
	BT8Live	I	11850	77.00	6.00	1.56	SS-3PL	1.25	158.9	708	599.0
	BT8Dead	I	11310	77.00	6.00	1.56	SS-3PL	1.25	158.9	315	564.0
Shahawy Batchelor (1996)	A0-00-R_N	I	8480	39.25	6.00	2.17	SS-1PL	1.04	154.0	669	313.0
	A0-00-R_S	I	8480	39.25	6.00	2.17	SS-1PL	1.04	154.0	669	276.0
	A1-00-M_N	I	7300	39.25	6.00	2.60	SS-1PL	1.04	154.0	259	141.0
	A1-00-M_S	I	7300	39.25	6.00	3.16	SS-1PL	1.04	154.0	259	168.0
	A1-00-R/2_N	I	7100	39.25	6.00	2.60	SS-1PL	1.04	154.0	291	166.0
	A1-00-R/2_S	I	7100	39.25	6.00	3.16	SS-1PL	1.04	154.0	266	173.0
	A1-00-R_N	I	7113	39.25	6.00	2.60	SS-1PL	1.04	154.0	583	210.0
	B0-00-R_N	I	7450	39.50	6.00	2.58	SS-1PL	1.06	153.8	583	220.0
	B0-00-R_S	I	7450	39.50	6.00	3.14	SS-1PL	1.06	153.8	266	206.0
	T5	I	7859	28.84	8.66	4.04	SS-PL	0.65	177.9	371	182.6
Teng Kong Poh (1998)	P-3a	R	5575	20.79	5.91	1.70	SS-1PL	0.19	137.2	411	98.4
	P-3b	R	5561	20.79	5.91	1.70	SS-1PL	0.19	188.6	411	103.4
	P-3e	R	5583	20.27	5.91	1.75	SS-1PL	0.19	179.5	411	106.8
	P1-1.5-WV	R	6303	19.42	6.30	1.82	SS-1PL	0.36	139.4	251	98.4
	P1-1.5-WVH	R	6313	19.42	6.30	1.82	SS-1PL	0.36	139.8	251	89.9
	A1-li	I	4503	19.83	3.94	2.98	SS-PL	0.29	154.6	440	62.6
Thürlimann Cafilisch Züricher Versuche (1970)	A2-re	I	5037	20.01	3.94	2.95	SS-PL	0.57	151.9	375	61.4
	A4-li	I	5342	19.76	3.94	2.99	SS-PL	1.15	144.8	207	62.4
	A4-re	I	5342	19.76	3.94	2.99	SS-PL	1.15	144.8	216	62.4
	B0-li	I	4808	19.73	3.94	2.99	SS-PL	1.15	138.0	271	53.4
	B1-li	I	4350	20.14	3.94	2.93	SS-PL	0.56	147.3	297	58.0
	B3-li	I	4884	20.25	3.15	2.92	SS-PL	0.70	146.8	677	66.4
	B3-re	I	4884	20.14	3.15	2.93	SS-PL	0.70	146.8	535	66.4
	B5-re	T	4808	19.14	3.94	3.09	SS-PL	0.59	148.8	203	58.2

* For members subjected to uniformly distributed load (UDL), 'V_{test}' values are end shear forces.

Table G-3 Comparison of Strength Ratios for Major Codes and Proposed Approach

Ratio of	64 RC members				83 PC members			
Ratio of V_{Test}/V_{Pred}	V_{Test}/V_{STD}	V_{Test}/V_{LRFD}	V_{Test}/V_{CSA}	V_{Test}/V_{Prop}	V_{Test}/V_{STD}	V_{Test}/V_{LRFD}	V_{Test}/V_{CSA}	V_{Test}/V_{Prop}
# of Beams	64	64	64	64	83	83	83	83
Mean	1.296	1.214	1.105	1.309	1.322	1.227	1.245	1.542
STDEV	0.431	0.217	0.172	0.291	0.211	0.177	0.167	0.292
COV	0.333	0.179	0.156	0.222	0.160	0.145	0.134	0.189
Distribution	(%)	(%)	(%)	(%)	(%)	(%)	(%)	(%)
>2	7.8	0.0	0.0	1.6	0.0	0.0	0.0	8.4
1.3~2.0	31.3	32.8	17.2	45.3	48.2	36.1	39.8	72.3
0.85~1.3	51.6	64.1	78.1	48.4	51.8	63.9	59.0	19.3
0.65~0.85	7.8	3.1	4.7	4.7	0.0	0.0	1.2	0.0
0.5~0.65	1.6	0.0	0.0	0.0	0.0	0.0	0.0	0.0
<0.5	0.0	0.0	0.0	0.0	0.0	0.0	0.0	0.0
max	2.444	1.730	1.483	2.059	1.820	1.654	1.595	2.396
99.9%	2.633	1.887	1.639	2.210	1.977	1.777	1.762	2.445
99%	2.301	1.720	1.506	1.987	1.814	1.640	1.634	2.221
95%	2.006	1.571	1.388	1.787	1.669	1.519	1.519	2.021
75%	1.587	1.361	1.221	1.506	1.464	1.346	1.357	1.738
50%	1.296	1.214	1.105	1.309	1.322	1.227	1.245	1.542
25%	1.005	1.068	0.989	1.113	1.179	1.107	1.132	1.345
5%	0.587	0.857	0.822	0.831	0.974	0.935	0.970	1.062
1%	0.291	0.709	0.704	0.632	0.829	0.813	0.856	0.863
0.1%	-0.041	0.542	0.572	0.408	0.667	0.677	0.727	0.638
min	0.624	0.786	0.824	0.711	0.887	0.860	0.821	1.008

Table G-4 Web-Shear Cracking Strengths of NCHRP Project 12-56 Girders

Test Specimen	f'_c (psi)	b_w (in)	d^* (in)	f_{se} (ksi)	f_{pc} (ksi)	V_p (kips)	w_{cr} (kips/ft)	x_{cr} (ft)	V_{cr} (kips)	$\frac{V_{cr}}{\sqrt{f'_c b_w d}}$
G1E	10280	6	68.5	160.7	0.858	-	15.2	2.5	334.4	8.0
G1W	10280	6	61.1	160.7	1.050	40.7	18.7	7.5	320.2	8.3
G2E	9940	6	67.32	156.6	1.029	-	18.7	2.7	410.0	10.2
G2W	9940	6	61.83	156.6	1.193	35.1	21.7	4.5	436.7	11.7
G3E	14230	6	67.67	153.0	1.198	-	16.2	3.0	350.4	7.2
G3W	14230	6	67.67	153.0	1.198	-	14.9	4.6	298.4	6.2
G4E	14230	6	67.67	162.4	1.272	-	14.0	3.4	297.7	6.1
G4W	14230	6	67.67	162.4	1.272	-	15.3	4.0	315.8	6.5
G5E	17800	6	70.00	172.4	0.777	-	16.8	2.1	369.6	6.6
G5W	17800	6	70.00	172.4	0.777	-	12.2	3.5	258.2	4.6
G6E	17800	6	67.67	163.1	1.350	-	16.5	4.6	330.6	6.1
G6W	17800	6	67.92	172.2	0.879	-	17.3	1.5	379.9	7.0

* d : The effective depth at the location of web-shear crack, x_{cr} .

Table G-5 Comparison of Cracking Strength Results and Predictions

Test Specimen	AASHTO STD & ACI				Proposed Approach				STD & ACI ratio		Proposed Approach ratio	
	w_{cr} (kips/ft)	x_{cr} (ft)	V_{cr} (kips)	$\frac{V_{cr}}{\sqrt{f'_c b_w d}}$	w_{cr} (kips/ft)	x_{cr} (ft)	V_{cr} (kips)	$\frac{V_{cr}}{\sqrt{f'_c b_w d}}$	$\frac{w_{cr,test}}{w_{cr,STD}}$	$\frac{V_{cr,test}}{V_{cr,STD}}$	$\frac{w_{cr,test}}{w_{cr,Prop}}$	$\frac{V_{cr,test}}{V_{cr,Prop}}$
G1E	11.7	3.04	251.7	6.0	7.7	3.04	166.4	3.99	1.30	1.33	1.97	2.01
G1W	13.3	3.04	286.3	7.7	9.6	3.04	208.1	5.60	1.41	1.08	1.94	1.54
G2E	12.3	3.04	265.6	6.6	8.4	3.04	180.9	4.49	1.52	1.54	2.23	2.27
G2W	13.8	3.04	297.3	8.0	10.1	3.04	217.7	5.89	1.58	1.46	2.15	2.01
G3E	14.6	3.04	314.1	6.5	9.9	3.04	214.1	4.42	1.11	1.12	1.63	1.64
G3W	14.6	3.04	314.1	6.5	9.9	3.04	214.1	4.42	1.03	0.95	1.50	1.39
G4E	14.5	3.04	312.1	6.4	10.3	3.04	222.1	4.59	0.97	0.95	1.36	1.34
G4W	14.5	3.04	312.1	6.4	10.3	3.04	222.1	4.59	1.06	1.01	1.48	1.42
G5E	13.6	3.04	295.1	5.2	8.5	3.04	183.8	3.28	1.23	1.26	1.97	2.01
G5W	13.6	3.04	295.1	5.2	8.5	3.04	183.8	3.28	0.90	0.88	1.43	1.40
G6E	16.4	3.04	355.1	6.5	11.1	3.04	240.5	4.44	1.01	0.93	1.48	1.37
G6W	13.8	3.04	298.8	5.5	8.8	3.04	189.5	3.49	1.25	1.28	1.97	2.00
Average:									1.20	1.15	1.76	1.70

Table G-6 Comparison of Flexure-Shear Cracking Strengths and Simplified Approach Predictions

Test Specimen	f'_c (ksi)	b (in)	d (in)	Test Results				Simplified Proposal		
				w_{ci} (kips/ft)	x_{ci} from mid-span, (ft)	V_{ci} (kips)	M_{cr} (kips.ft)	$M_{cr,Prop}$ (kips.ft)	$V_{ci,Prop}$ (kips)	$\frac{V_{ci,test}}{V_{ci,Prop}}$
G1E	10.28	12.0	68.50	23.5	5.8	137.1	6140.2	6321.2	157.3	0.87
G1W	10.28	12.0	62.22	23.5	4.2	97.9	6315.6	6320.1	114.4	0.86
G2E	9.94	12.0	67.32	25.9	3.7	95.0	7290.9	7008.9	112.6	0.84
G2W	9.94	12.0	62.45	25.9	4.2	107.9	7243.5	7009.1	123.8	0.87
G3E	14.23	12.0	67.67	28.2	6.7	173.7	7444.5	7536.5	211.3	0.82
G3W	14.23	12.0	67.67	28.2	5.8	152.0	7580.2	7535.9	185.5	0.82
G4E	14.23	12.0	67.67	30.7	5.6	171.4	8743.2	7943.3	185.8	0.92
G4W	14.23	12.0	67.67	32.0	5.3	170.7	8784.0	7943.2	178.1	0.96
G5E	17.80	12.0	70.00	18.2	9.2	167.4	4543.1	5432.7	229.8	0.73
Average:								0.85		

RC members

Statistical Values	V _{test} /V _{n,STD}
N of Beams	64
Average	1.296
Stdev	0.431
COV	0.333

PC members

Statistical Values	V _{test} /V _{n,STD}
N of Beams	83
Average	1.322
Stdev	0.211
COV	0.160

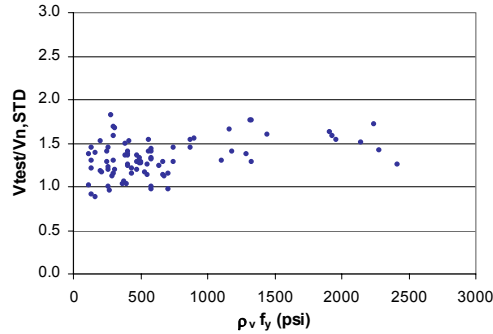
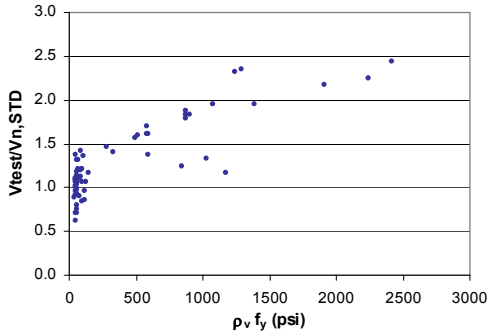
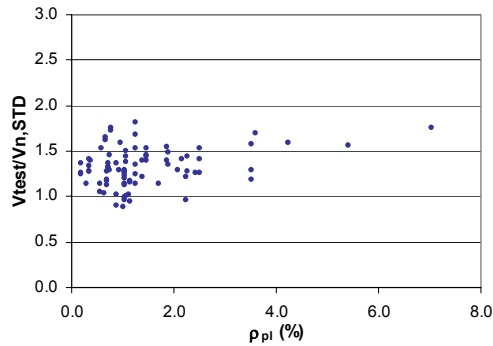
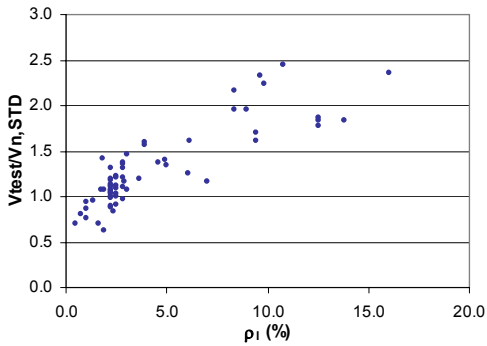
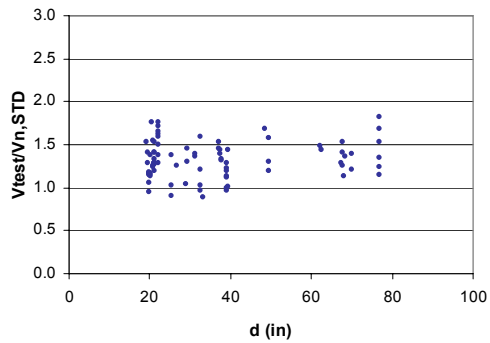
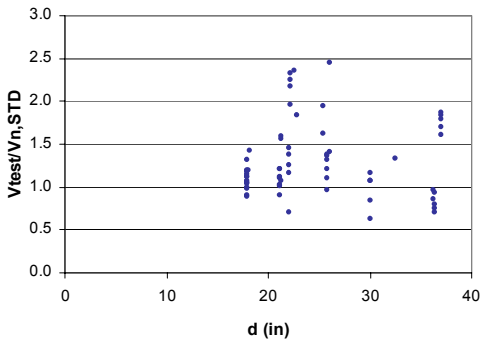
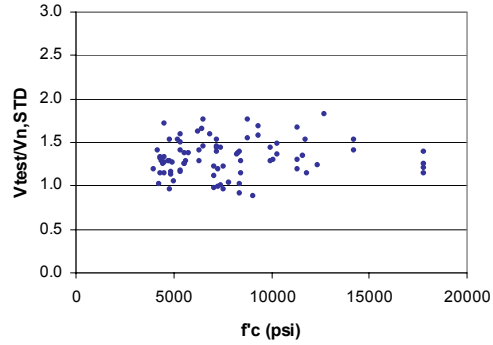
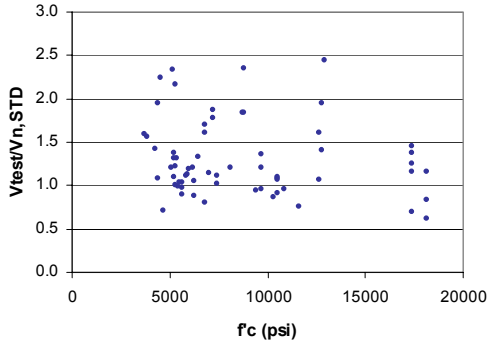
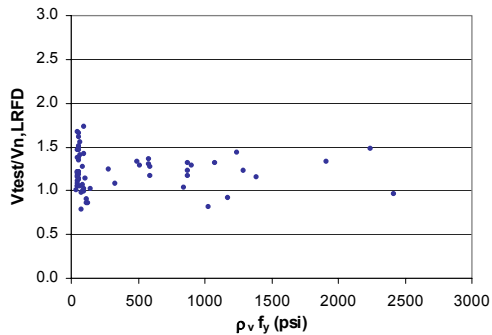
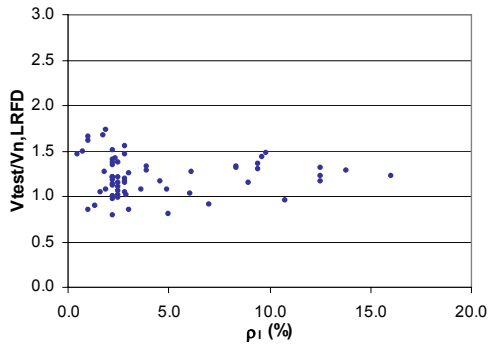
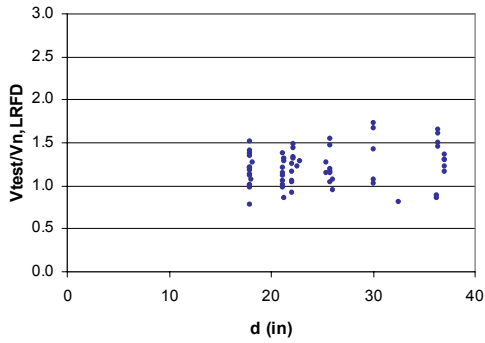
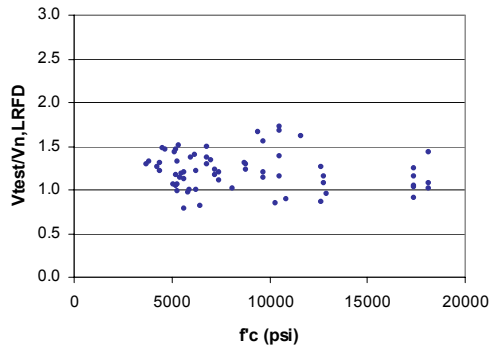


Figure G-1 Comparison of AASHTO STD Predictions and Test Results

RC members

Statistical Values	$V_{test}/V_{n,LRFD}$
N of Beams	64
Average	1.214
Stdev	0.217
COV	0.179



PC members

Statistical Values	$V_{test}/V_{n,LRFD}$
N of Beams	83
Average	1.227
Stdev	0.177
COV	0.145

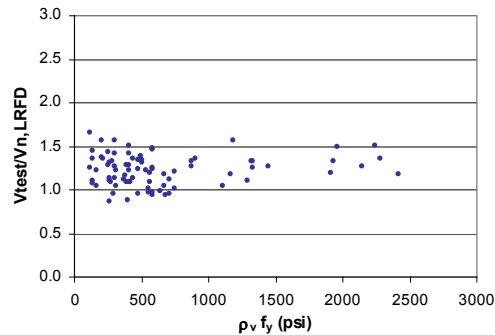
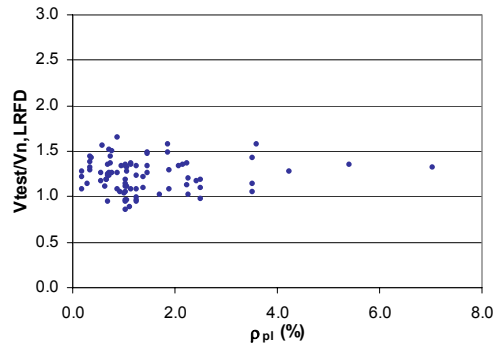
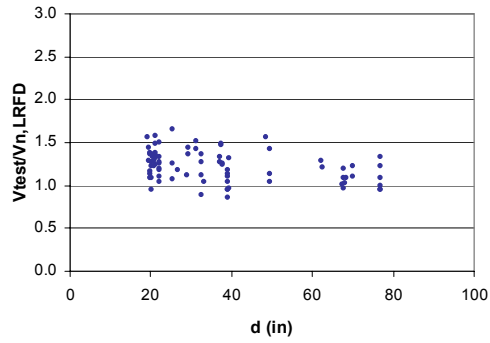
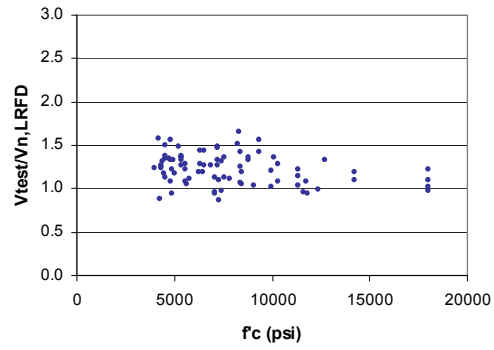
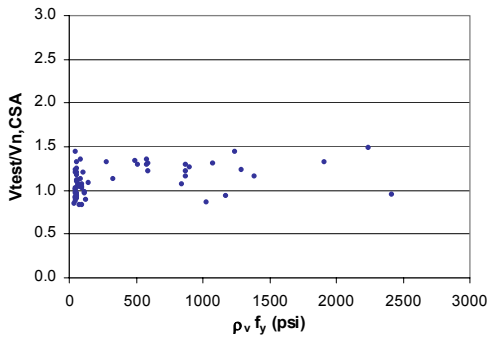
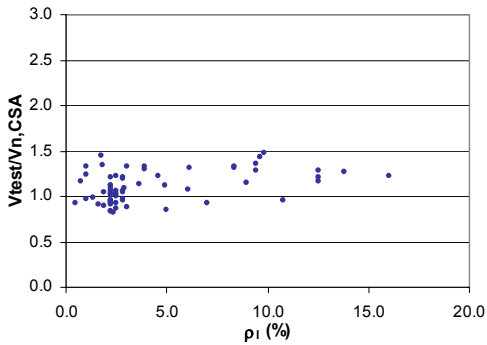
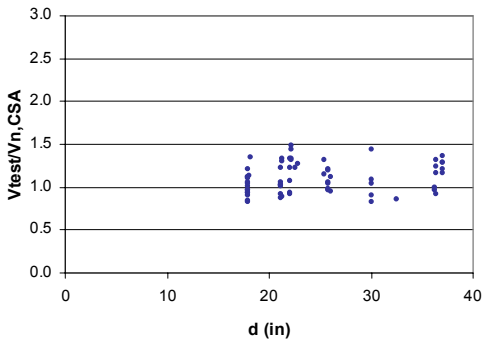
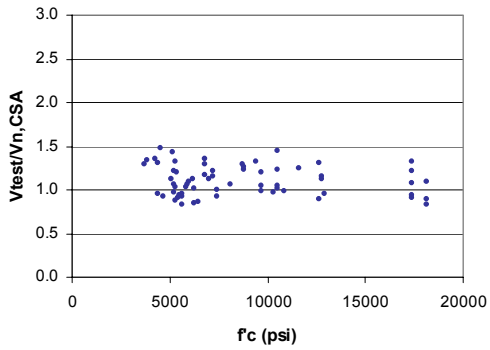


Figure G-2 Comparison of AASHTO LRFD Predictions and Test Results

RC members

Statistical Values	$V_{test}/V_{n,CSA}$
N of Beams	64
Average	1.105
Stdev	0.172
COV	0.156



PC members

Statistical Values	$V_{test}/V_{n,CSA}$
N of Beams	83
Average	1.245
Stdev	0.167
COV	0.134

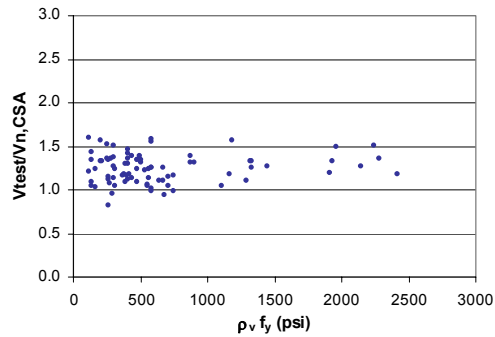
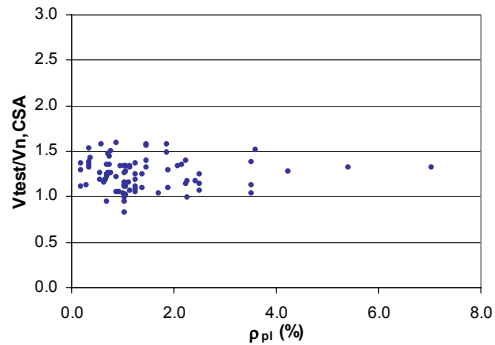
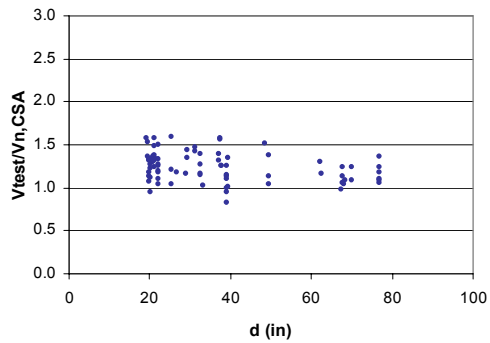
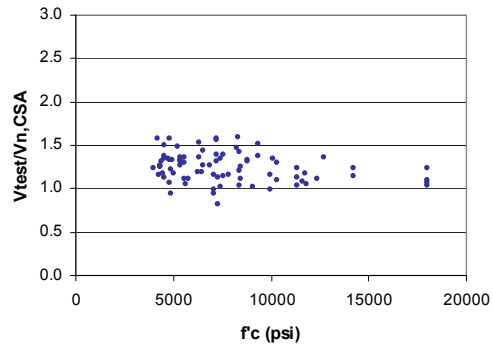


Figure G-3 Comparison of CSA 2004 Predictions and Test Results

RC members

Statistical Values	$V_{test}/V_{n,Prop}$
N of Beams	64
Average	1.309
Stdev	0.291
COV	0.222

PC members

Statistical Values	$V_{test}/V_{n,Prop}$
N of Beams	83
Average	1.542
Stdev	0.292
COV	0.189

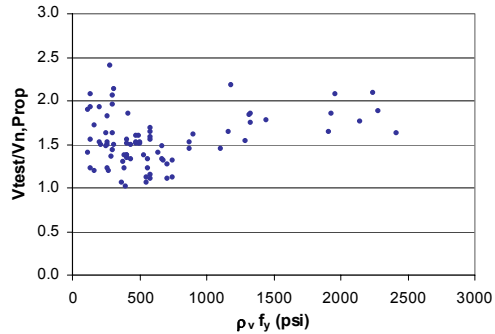
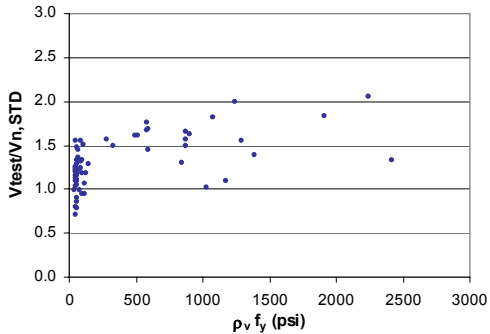
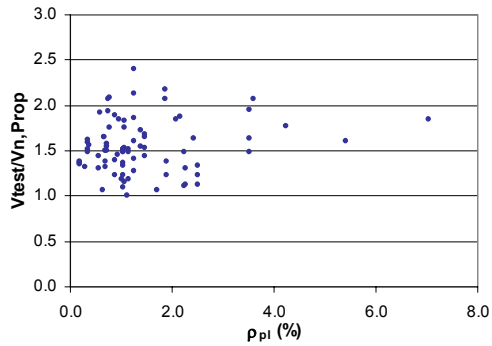
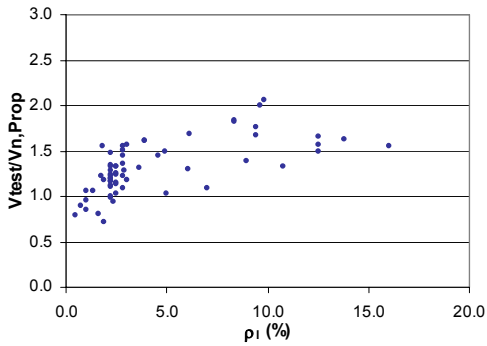
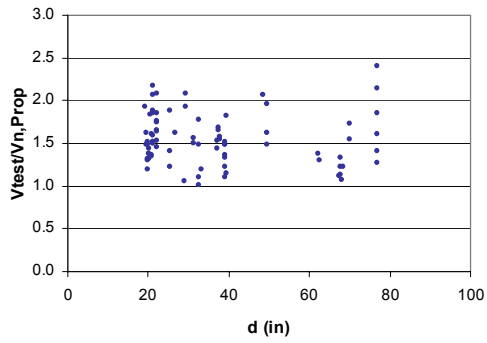
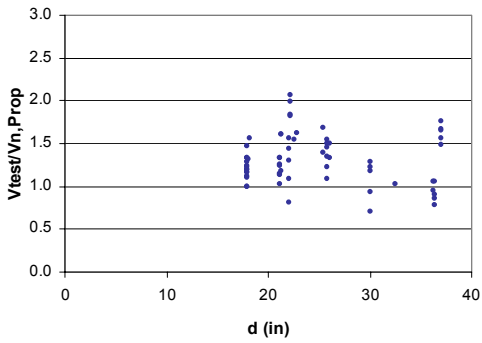
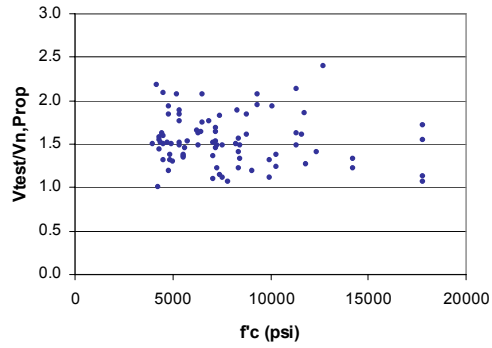
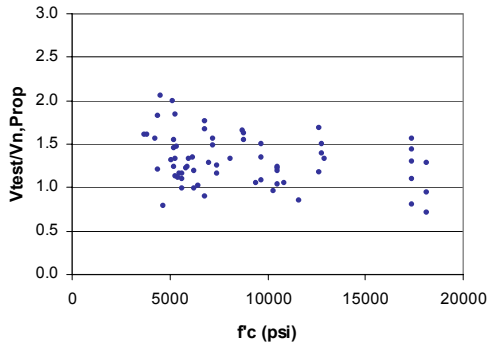


Figure G-4 Comparison of Simplified Approach Predictions and Test Results

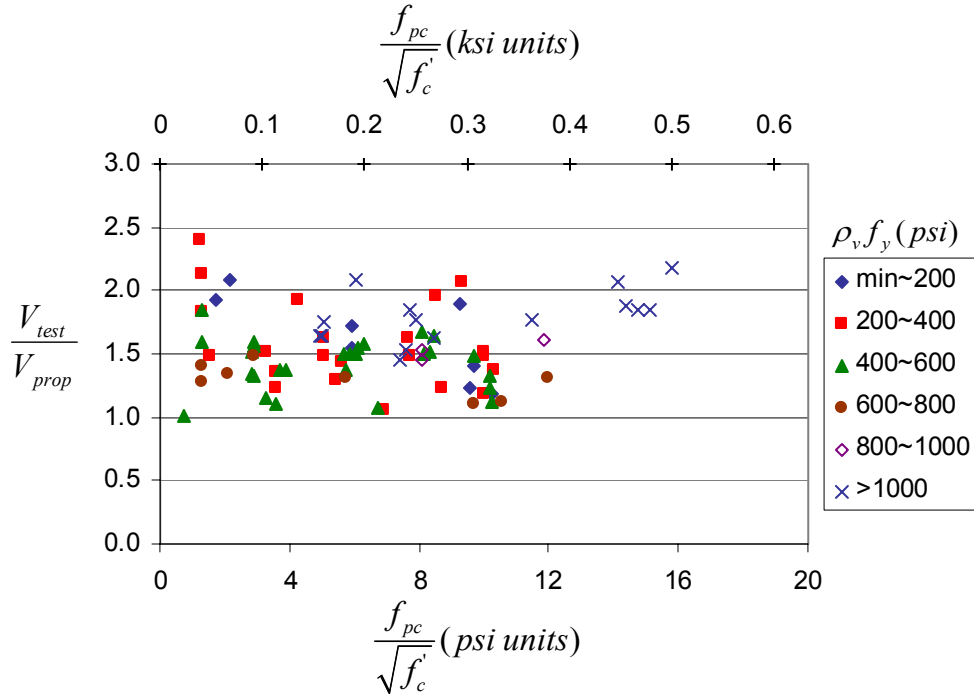


Figure G-5 Influence of Prestressing Level on Strength Ratio

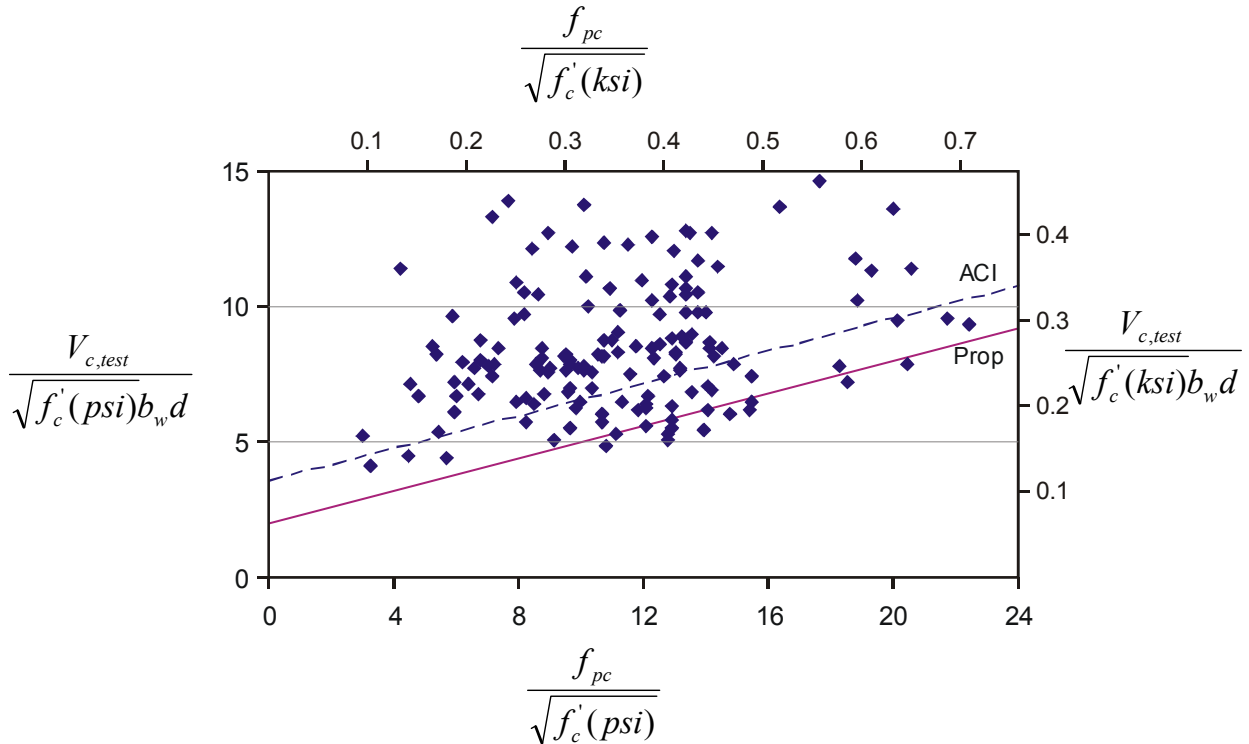


Figure G-6 Influence of Level of Prestressing on Concrete Contribution at Ultimate for Members without Shear Reinforcement

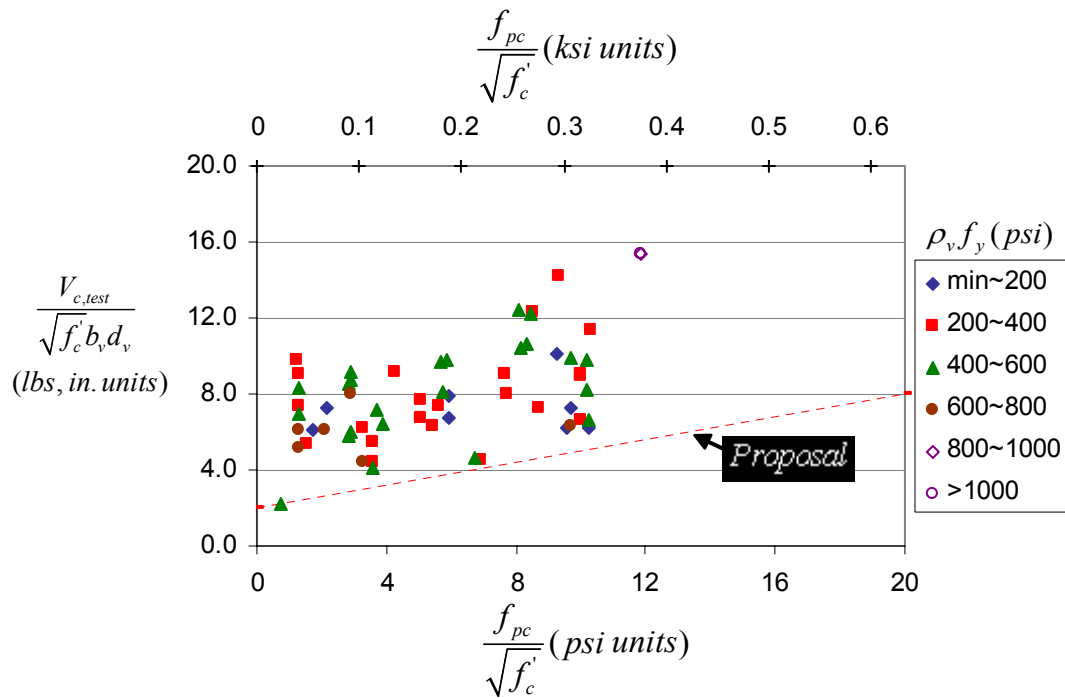


Figure G-7 Influence of Level of Prestressing on Concrete Contribution at Ultimate for Members with Shear Reinforcement

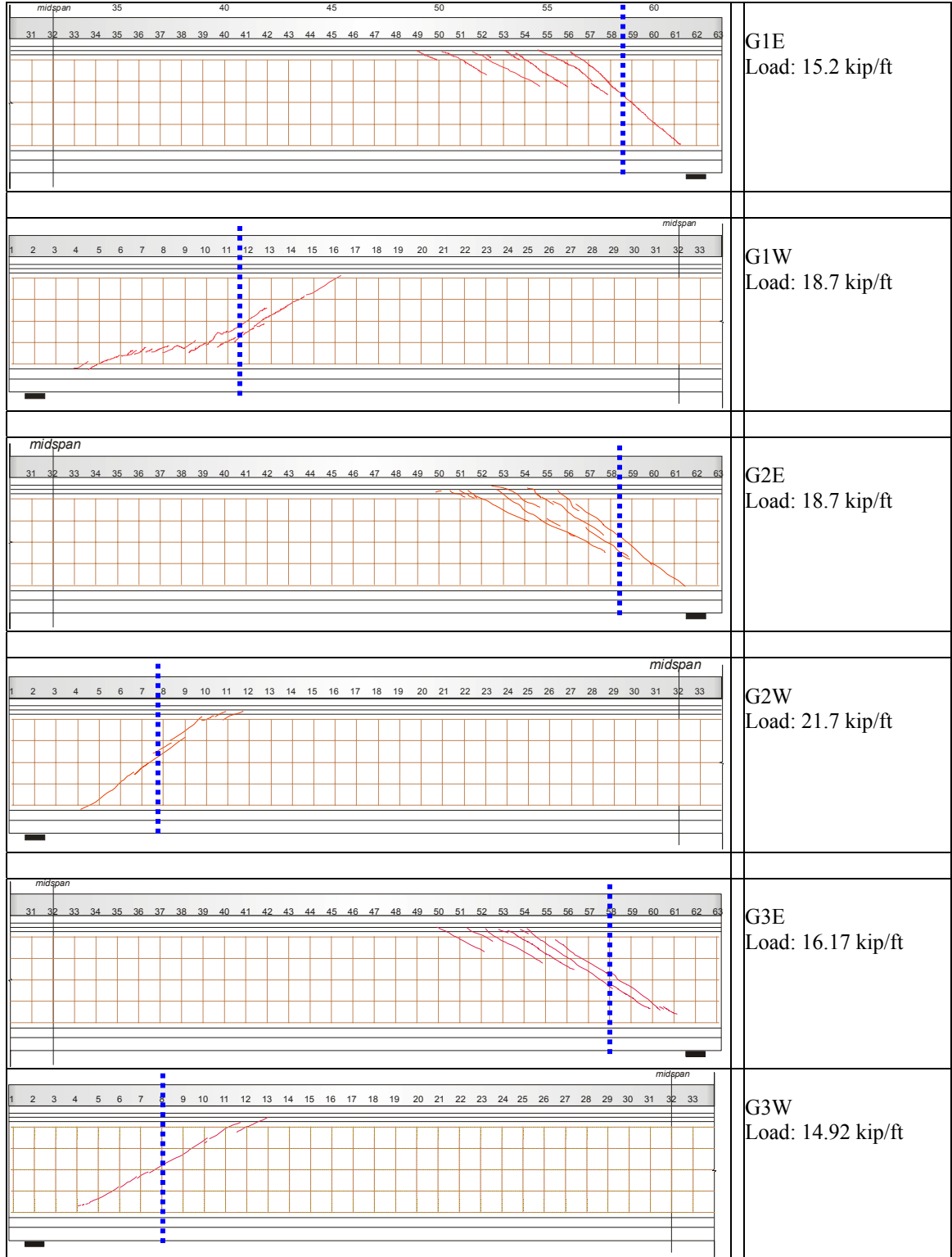


Figure G-8 Web-Shear Cracks for NCHRP 12-56 Girder Tests

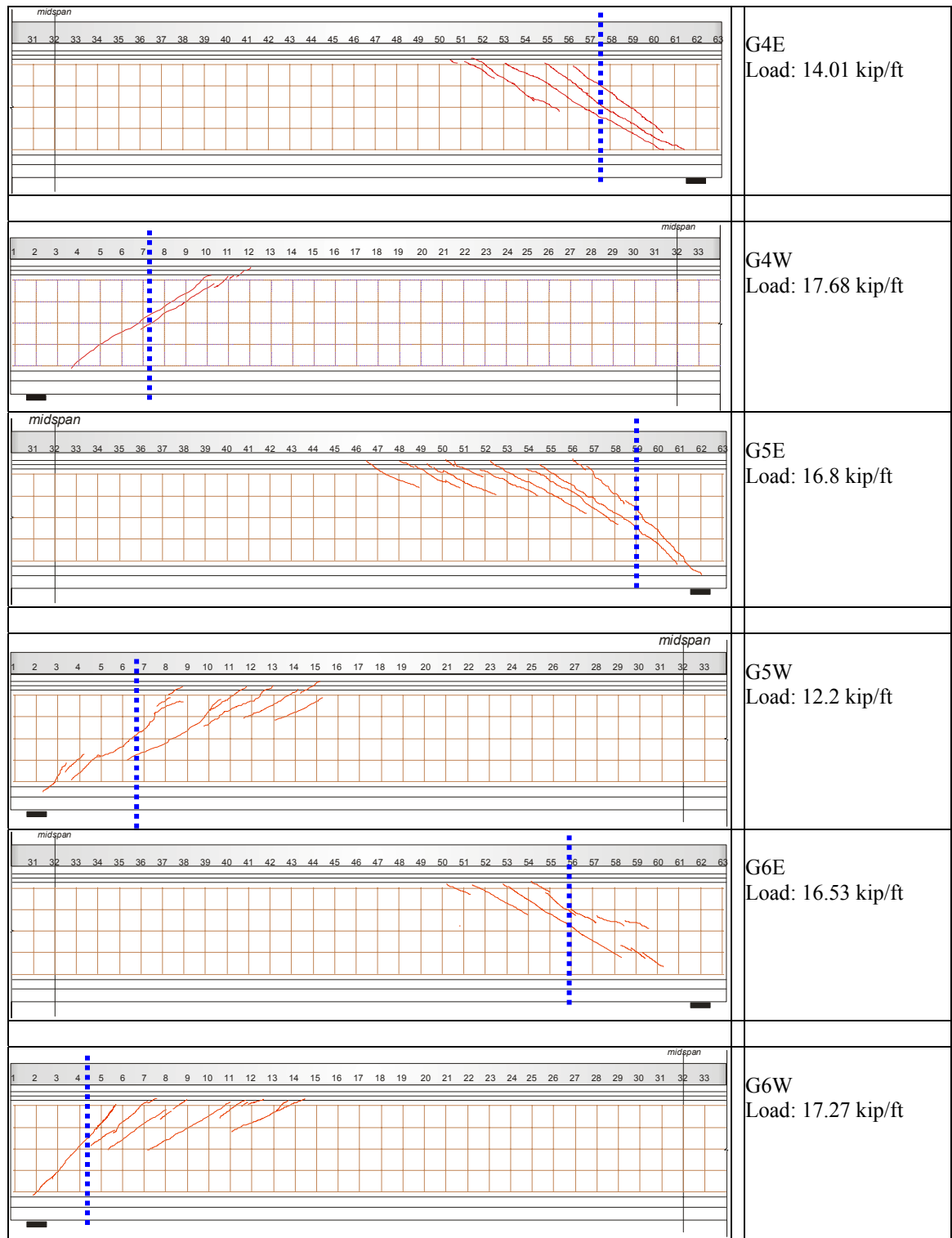


Figure G-8 Cont'd.

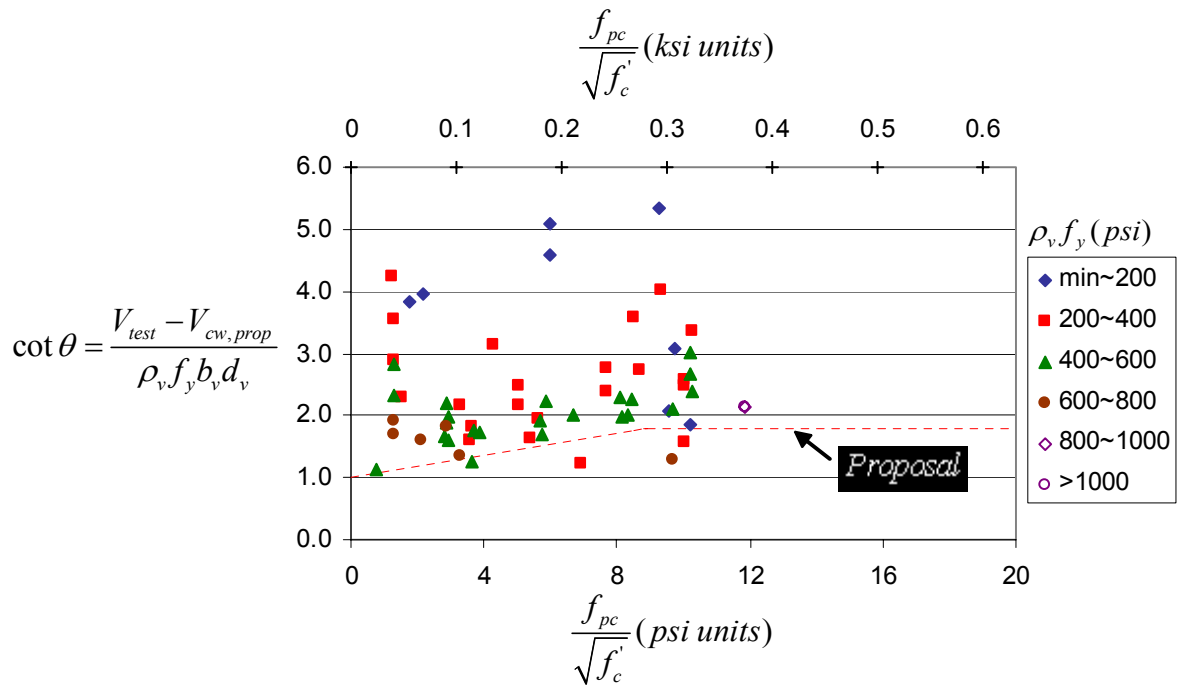


Figure G-9 Influence of Prestress Level on Compression Strut Angle, $\cot(\theta)$

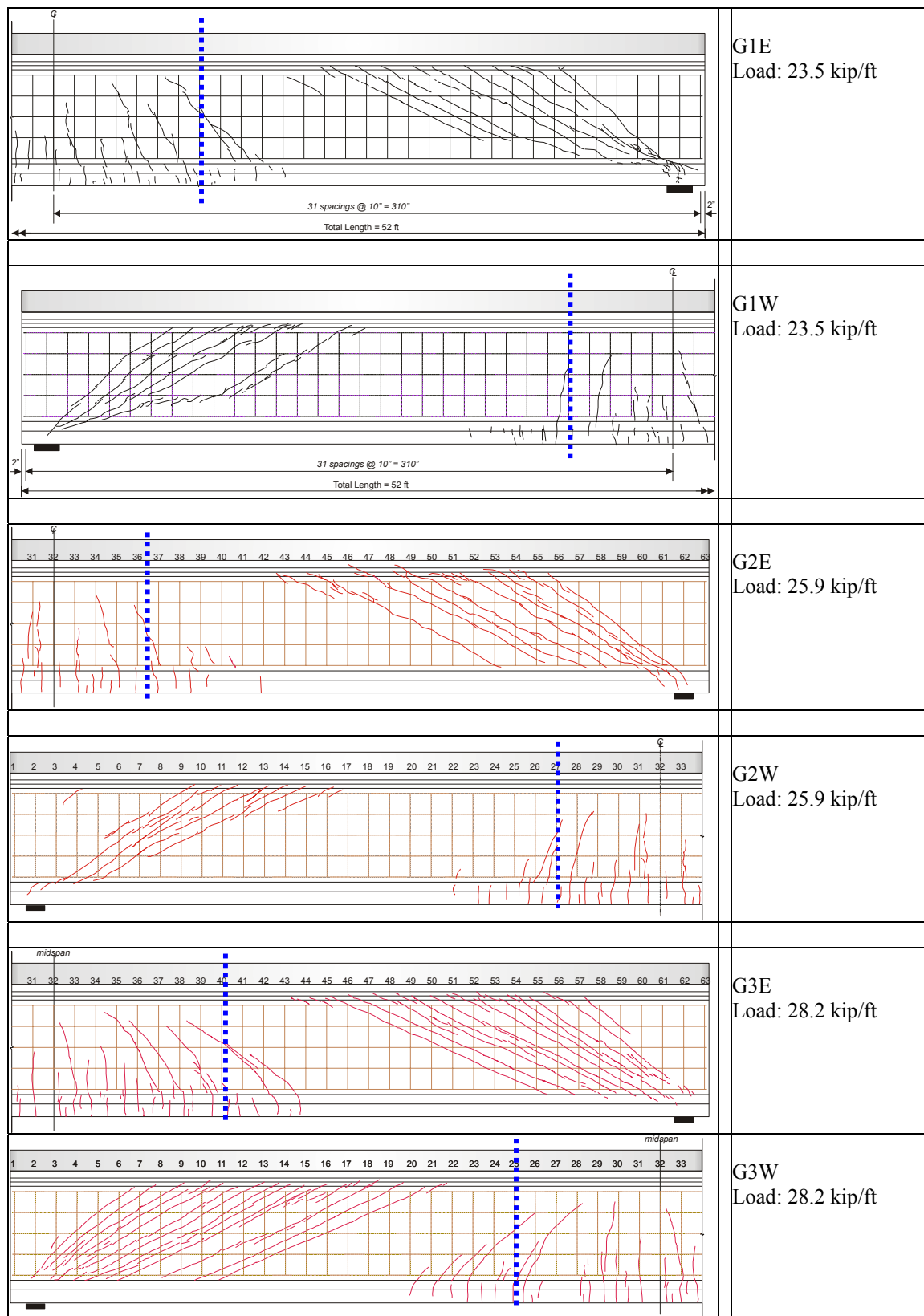


Figure G-10 Flexure-Shear Cracks for NCHRP 12-56 Girder Tests

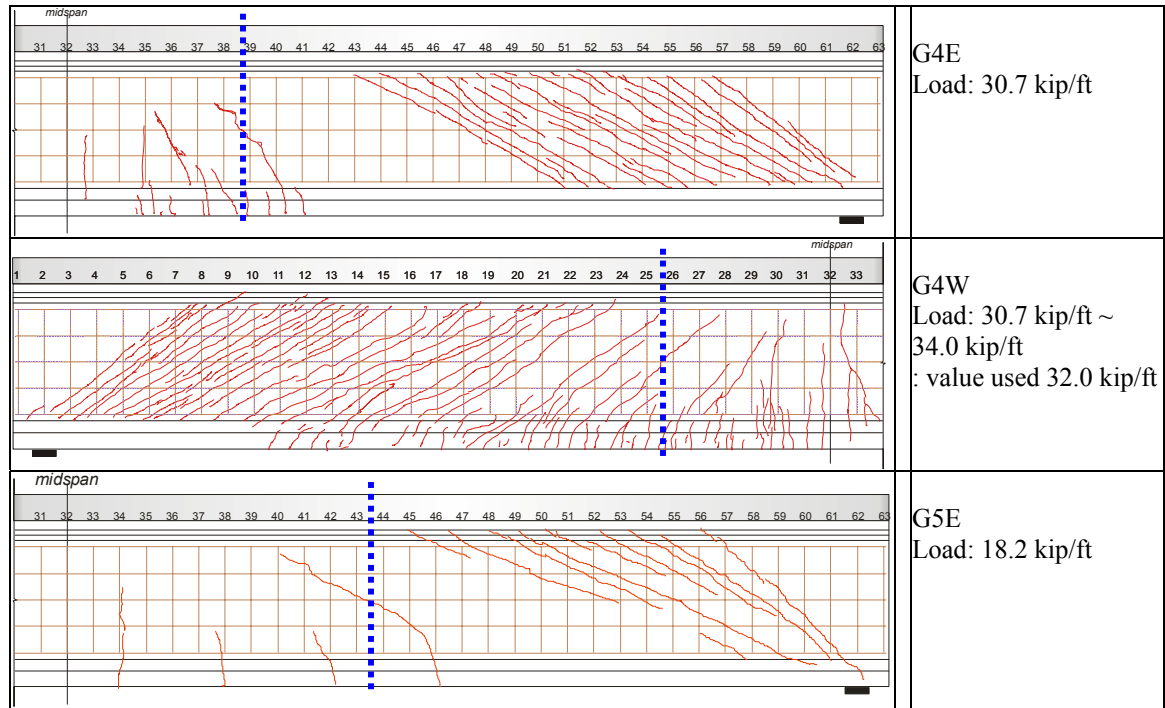


Figure G-10 Cont'd

Appendix H: Examination of Simplified Proposal Using Design Database

H.1 Presentation of Design Database

The proposal for simplified LRFD provisions is examined further in this Appendix using a Design Database intended to encompass the general loading and continuity conditions (e.g., distributed loads), section characteristics and design shear levels likely to be encountered in practice. The Design Database consists of concrete members having the typical bridge sections that the Experimental Shear Database could not cover; e.g., 36 inch-deep I shapes, 72 inch-deep T shapes, 78 inch-deep box shapes, and 36 inch-deep rectangular shapes. Included are composite and non-composite sections, precast and prestressed/post-tensioned and non-prestressed members, and simple and continuous designs. Fig. H-1 shows the sectional shapes and strand profiles of the sections in Design Database.

Flexural Design of Members in Design Database

The studies reported in this Appendix are aimed at determining how shear reinforcement amounts, determined using the proposed simplified provisions, differ from those determined using the AASHTO Standard, 2004 AASHTO LRFD, 2004 CSA, and R2K methods. Accordingly, significant effort was devoted to defining situations where the shear reinforcement amounts were not controlled by minimum shear requirements. Otherwise, in such cases, ratios of shear reinforcement requirements in accordance the different methods would be meaningless. First, the largest shear stress that could be applied to a given section was determined by reducing the span length and proportioning the strands or reinforcing bars, for prestressed members, so that the extreme fiber concrete stresses did not exceed the allowable stress limits specified in the 2004 AASHTO LRFD. Thereafter, the number of strands or reinforcing bars was reduced to 75%, 50%, or some other appropriate percentage of the maximum number of strands or bars determined in the first step. Then, the same approach was repeated for different span lengths.

For prestressed members the number of strands and the span lengths required to keep the extreme fiber concrete stresses less than the allowable stress limits were not the only the major issues studied. Differences resulting from draping strands or placing top strands were also studied. The latter considerations resulted in large conservatisms for some members in the Design Database for some of the different design methods. This issue is discussed in Section H.2.

Shear Design of the Members in Design Database

Five or six different sections in each member were designed using four different shear design approaches: the proposed simplified method (Proposal); the AASHTO Standard method (Standard); the 2004 AASHTO LRFD (LRFD) method; and the 2004 Canadian Code (CSA)

method. The following assumptions were made for consistency:

- (1) The compressive strut angle was taken as 45 degrees whenever the design flexural moment was greater than the cracking moment at the section under consideration.
- (2) The applied moment at 90 percent of the flexural capacity of the member was used to determine the design forces.
- (3) The resistance or material factors specified for shear in the applicable codes are shown in Table H-1. Different codes use different load factors and different resistance or material factors to achieve their intended levels of safety and reliability. If the differing factors specified in each code are used to obtain values of design shear forces and nominal shear resistances for comparison purposes, then the relative performance of the different methods will depend directly on those factors. Thus, for this study the demand and resistance relationships were deliberately decoupled, and all resistance or material factors set equal to 0.9.
- (4) No less than the minimum shear reinforcement requirement was provided for any case. Minimum shear reinforcement requirements used were those specified in the applicable code. Values are shown in Table H-2.

H.2 Comparison and Discussion of the Results

The amount of shear reinforcement required, the strut angle, and the concrete component of the shear capacity were compared for the proposed simplified method, the other three shear design codes, and *RESPONSE 2000, Reinforced Concrete Sectional Analysis Program using the Modified Compression Field Theory*. The minimum shear reinforcement requirements of the AASHTO LRFD were also enforced for analyses using *RESPONSE 2000 (R2k)*.

Table H-3 summarizes results for the members of the Design Database in terms of the relative ratios of the amounts of the required shear reinforcement for each approach to that of the R2K counterpart. Table H-3 contains six major columns. The first column lists the member type and the second lists the shear design procedure. The third column provides overall summary information on relative performance of the different design methods in terms of the number of cases studied for a particular beam type and the mean and coefficient of variation of those results for each of the four methods examined. The fourth through sixth columns provide a further breakdown of the information in column three. The governing relationship for assessing shear resistance is characterized as web-shear, transition, or flexure-shear for the information in columns four, five, and six, respectively. In a web-shear region V_{cw} is smaller than V_{ci} and M_u is also smaller than M_{cr} , which means that in the proposed simplified method V_{cw} governs the shear strength of the member at the section considered and the angle of compression strut is smaller than 45 degrees. In the flexure-shear region V_{ci} is smaller than V_{cw} , which means that in the

proposed simplified method V_{ci} governs the shear strength of the member at the section considered and the angle of compression strut is 45 degrees. A transition region is a location that does not belong to either a web-shear region or a flexure-shear region. In a transition region V_{cw} governs the shear strength of the member at the section considered and the angle of compression strut is 45 degrees. It should be noted that the values in Table H-3 included non-minimum shear reinforcement cases only (i.e., design cases where the required shear reinforcement is less than or equal to minimum shear reinforcement are not shown in Table H-3). Non-minimum means all approaches required shear reinforcement amounts at a given section greater than the minimum amount shown in Table H-2.

Tables H-4 through H-9 compare details for the concrete component of the shear capacity, the compressive strut (or crack) angle, and the amount of the required shear reinforcement for the five different design methods for each of the six design beams shown in Fig. H-1. All results, including minimum shear reinforcement cases, generated using the Design Database are shown.

Figures H-2 through H-7 provide graphical comparisons of the amount of required shear reinforcement for the five different approaches for different positions along the length of the beam. The horizontal axis is the distance from the support and that axis terminates at mid span of the beam

Figures H-8 through H-11 summarize comparison results for each of the six members of Fig. H-1 in terms of the $\rho_v f_y$ ratio required by each method to that required by the R2K results. The horizontal axis represents the amount of stirrup reinforcement required by the R2K method. The insert on each plot shows the mean, (m), and the standard deviation, (s), obtained from non-minimum cases. Also listed with each plot are the total number of cases included in the plot, including minimum cases, and the number of non-minimum cases. In the plots, the solid symbols represent non-minimum cases and the hollow symbols represent minimum cases.

Comparisons

The summary Table H-3, last row, shows that of the four methods the Proposal has the largest mean value (1.57) but the smallest coefficient of variation (0.23). The Proposal shows relatively large mean values for reinforced concrete members compared to the other approaches; e.g., R.C. rectangular single-span beams (1.78), R.C. T-shaped single-span beams (1.78), and R.C. rectangular continuous beams (1.35). Those mean values are slightly and consistently larger than those of the Standard (e.g., 1.50, 1.55, and 1.11), respectively, for the same members. This result is a reasonable since both provisions use similar equations - for R.C. members the V_c in the Proposal equals approximately $2\sqrt{f'_c}$ and the compressive strut angle equals 45 degrees. However, the term, d_v in the Proposal differs from that of d in the Standard and eventually produces a slightly larger required amount of shear reinforcement due to its reduced value in the

V_c term.

For the prestressed members, I-Beams and Bulb T-Beams, in the Design Database, the LRFD and the CSA methods are slightly more conservative than the Standard method. This issue is discussed in depth in the next section.

The Standard method shows the smallest mean value (1.26) and a modest coefficient of variations, 0.31. However, the Standard method is also non conservative for some members in the Design Database, especially in transition zone sections. The mean value for the Standard method in the transition zone is 0.90. This matter is also discussed in the next section.

Discussion of the Results

The LRFD and the CSA methods were conservative in the amount of required shear reinforcement, for specific cases, for members containing top strands. This conservatism is due to the code-based methods for taking account of top strands during evaluations of effective shear depth and longitudinal strain.

The CSA method provides the following simplified equation for longitudinal strain:

$$\varepsilon_x = \frac{M_f / d_v + V_f - V_p + 0.5N_f - A_p f_{po}}{2(E_s A_s + E_p A_p)} \quad (\text{CSA Eq. 11-13})$$

where M_f , V_f , and N_f are design forces and A_p is defined as *the area of tendons on the flexural tension side of the member*, i.e., the area of tendons in the bottom-half of the section. For this definition the strain increases or remains the same when top strands are provided since A_p is constant and M_f or V_f increases or remains the same. This result directly increases the strut angle θ , decreases the multiplier β , and hence requires more stirrups. However, intuitively, additional top strands should reduce the required amount of stirrups because they reduce the longitudinal strain in the member.

Second, a small conservatism may also result from the conservatively-drawn definition for the evaluation of “effective shear depth”. The LRFD method requires that the effective shear depth be taken as *the distance, measured perpendicular to the neutral axis, between the resultants of the tensile and compressive forces due to flexure; it need not be taken to be less than the greater of $0.9d_e$ or $0.72h$ (AASHTO LRFD Art. 5.8.2.7)*. The quantity d_e is in turn defined as the effective depth from extreme compression fiber to the centroid of the tensile force in the tensile reinforcement. A similar definition for effective shear depth is used in the CSA method and proposed in the Proposal. With this definition the effective shear depth is reduced if a large number of prestressing strands are provided at top of the section, the neutral axis lies above them and, hence, those strands are considered as tensile reinforcement. This situation commonly occurs in practice when top strands are provided to control flexural cracks at transfer and at

service loads in a short member where only a small number of bottom strands are required for flexural strength. The resultant shortened shear depth reduces V_c proportionally. This definition causes a slightly excessive reduction in V_c for members containing top strands that represent a significant fraction of the total number prestressing strands in the beam.

Consider for example a 43.5 in.-deep composite I-Beam containing 6 bottom strands and 2 top strands. This beam is the first member appearing in the Design Database of I-Beams, Table H-4. In this example, the neutral axis lies within the slab and therefore above the top strands. Hence the top strands should be considered as tensile steel according to the CSA or LRFD methods. Consequently, the calculated effective shear depth, d_v is 31.3 in., (see Table H-4), rather than the value of 37.4 in. for the same beam without top strands. The value of longitudinal strain, ϵ_x is equal to 0.0022 for d_v of 31.3 in., (all other data not included in the Table H-4 are provided in the Process 12-50 digital format, see Appendix I). By contrast the same strain equals 0.0018 if the top strands are not considered and hence the design moment and design shear force would have been smaller, (561 k ft and 163 kips, respectively). Finally, the amount of required shear reinforcement is equal to 882 psi, whereas that amount would have been only 523 psi if the top strands were omitted. The latter value is 125% of the *RESPONSE 2000* result where top strands are considered.

Another observation is that the Standard method appears to be unconservative for some members in the Design Database, especially in transition region sections; the mean values of the relative ratios of the transverse reinforcement amounts required by the Standard and R2k methods for Bulb T-beams and Box girders are 0.85 and 0.80, respectively. A closer examination revealed that in most of the non conservative cases M_u was greater than M_{cr} and V_{cw} governed, which implies that the Standard method does not incorporate moment effects explicitly in its equations while the LRFD and CSA methods do; e.g., the longitudinal strain increases as the moment increases in the LRFD and CSA methods. In the Proposal the additional criterion that θ equals 45 degrees if M_u exceeds M_{cr} implicitly precludes such unconservatism. By contrast, for the Proposal, mean values of the relative ratios for Bulb T-beams and Box girders were 1.68 and 1.35, respectively. This situation commonly occurs in a high-shear and high-moment region such as occurs over an interior support in a continuous beam. As an alternative, the ASBI provisions provide a higher level of assurance against web cracking by limiting the shear capacity to $2\sqrt{f'_c}$ over interior supports of continuous beams.

Closing Remarks

This Design Database study disclosed intrinsic code conservatisms or unconservatisms that the use of a limited experimental database could not have disclosed. However, any user of this

document should be careful before making any judgments based on this Design Database study. The Design Database does not reflect the actual probability distributions of bridges that are currently being built or that already exist even though considerable effort was spent in trying to achieve a database representative of a comprehensive range of practical design cases.

Additional information is provided in the Process 12-50 digital format so that a user can readily reproduce outputs and compare them with the results given by this Design Database study.

Figure H-1 Section Shapes and Strand Profile

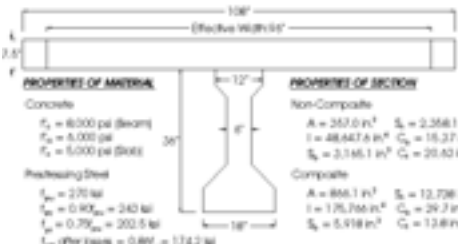
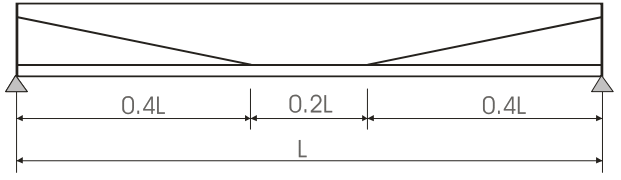
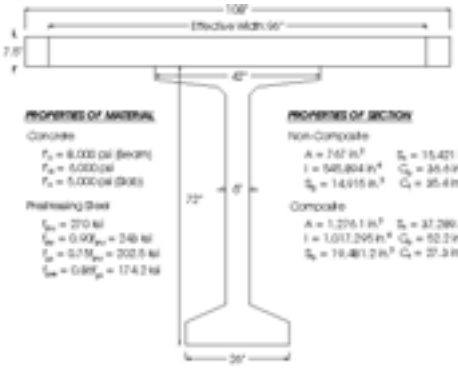
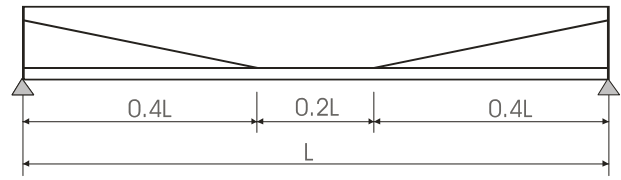
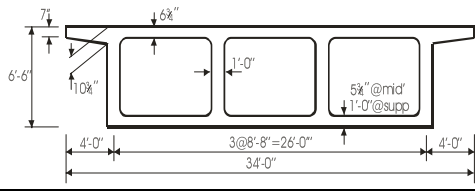
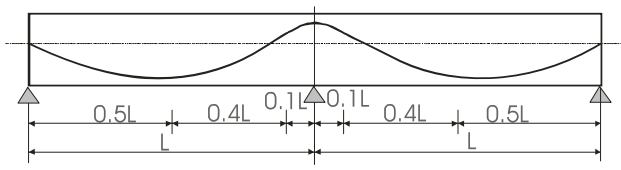
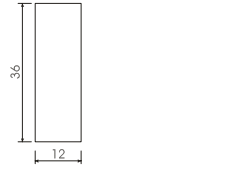
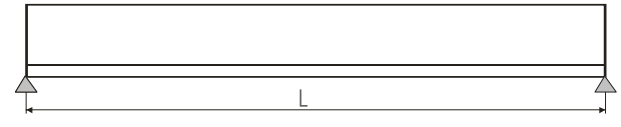
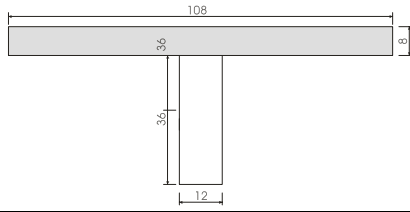
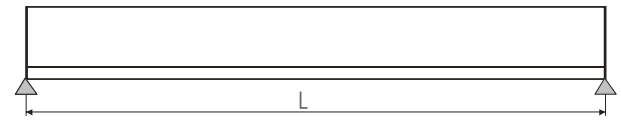
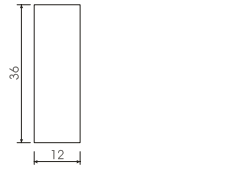
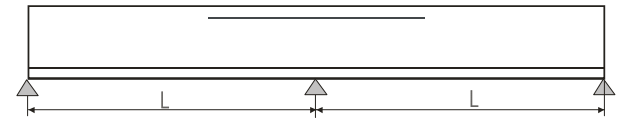
	Section (unit: in.)	Profile
PC	 <p>PROPERTIES OF MATERIAL</p> <p>Concrete $f_c = 8,000$ psi (beam) $f_c = 8,000$ psi $f_c = 5,000$ psi (bars)</p> <p>Reinforcing Steel $f_y = 270$ ksi $f_u = 0.93f_u = 243$ ksi $f_u = 0.79f_u = 202.5$ ksi f_u (for bars) = $0.89f_u = 174.2$ ksi</p> <p>PROPERTIES OF SECTION</p> <p>Non-Composite $A = 357.0$ in² $S_x = 2,358.1$ in³ $I = 48,647.8$ in⁴ $C_x = 16.27$ in $S_y = 3,146.1$ in³ $C_y = 20.43$ in</p> <p>Composite $A = 856.1$ in² $S_x = 12,738$ in³ $I = 175,756$ in⁴ $C_x = 29.7$ in $S_y = 5,918$ in³ $C_y = 13.88$ in</p>	
	 <p>PROPERTIES OF MATERIAL</p> <p>Concrete $f_c = 8,000$ psi (beam) $f_c = 8,000$ psi $f_c = 5,000$ psi (bars)</p> <p>Reinforcing Steel $f_y = 270$ ksi $f_u = 0.93f_u = 243$ ksi $f_u = 0.79f_u = 202.5$ ksi f_u (for bars) = $0.89f_u = 174.2$ ksi</p> <p>PROPERTIES OF SECTION</p> <p>Non-Composite $A = 747$ in² $S_x = 15,421$ in³ $I = 545,864$ in⁴ $C_x = 34.6$ in $S_y = 14,915$ in³ $C_y = 25.4$ in</p> <p>Composite $A = 1,276.1$ in² $S_x = 37,289.8$ in³ $I = 1,017,295$ in⁴ $C_x = 52.2$ in $S_y = 19,481.2$ in³ $C_y = 27.3$ in</p>	
	 <p>PROPERTIES OF MATERIAL</p> <p>Concrete $f_c = 8,000$ psi (beam) $f_c = 8,000$ psi $f_c = 5,000$ psi (bars)</p> <p>Reinforcing Steel $f_y = 270$ ksi $f_u = 0.93f_u = 243$ ksi $f_u = 0.79f_u = 202.5$ ksi f_u (for bars) = $0.89f_u = 174.2$ ksi</p> <p>PROPERTIES OF SECTION</p> <p>Non-Composite $A = 747$ in² $S_x = 15,421$ in³ $I = 545,864$ in⁴ $C_x = 34.6$ in $S_y = 14,915$ in³ $C_y = 25.4$ in</p> <p>Composite $A = 1,276.1$ in² $S_x = 37,289.8$ in³ $I = 1,017,295$ in⁴ $C_x = 52.2$ in $S_y = 19,481.2$ in³ $C_y = 27.3$ in</p>	
RC		
		
		

Table H-1 Resistance Factors or Material Factors

Proposal	AASHTO Standard	AASHTO LRFD	CSA
0.90	RC: 0.85 PC: 0.90	0.90	Concrete - 0.65 Steel - 0.85 Prestress - 0.90

Table H-2 Minimum Shear Reinforcement, $A_{v,min}$ (unit: in.²)

Proposal	AASHTO Standard	AASHTO LRFD	CSA
$\sqrt{f'_c} \frac{b_w s}{f_y}$	$50 \frac{b_w s}{f_y}$	$\sqrt{f'_c} \frac{b_w s}{f_y}$	$\sqrt{f'_c} \frac{b_w s}{f_y}$

* f'_c and f_y are in psi.

Table H-3 Relative Ratios of Amount of Required Shear Reinforcement to R2K Amount

Member	Approach*	Total			Web-Shear			Transition			Flexure-Shear		
		no.	mean	c.o.v.	no.	mean	c.o.v.	no.	mean	c.o.v.	no.	mean	c.o.v.
I Beam (Single Span)	std	38	1.36	0.28	29	1.43	0.22	9	1.12	0.45	0	0	0
	lrfd		1.98	0.33		1.76	0.32		2.69	0.11		0	0
	p		1.83	0.20		1.68	0.14		2.31	0.13		0	0
	csa		2.10	0.42		1.77	0.38		3.16	0.19		0	0
Bulb T (Single Span)	std	82	1.14	0.29	66	1.21	0.25	16	0.85	0.34	0	0	0
	lrfd		1.48	0.30		1.34	0.27		2.08	0.13		0	0
	p		1.38	0.18		1.30	0.15		1.68	0.10		0	0
	csa		1.43	0.45		1.24	0.46		2.22	0.10		0	0
RC Rect** (Single Span)	std	25	1.5	0.24									
	lrfd		1.23	0.24									
	p		1.78	0.22									
	csa		1.24	0.20									
RC T-Shape (Single Span)	std	35	1.55	0.15									
	lrfd		1.21	0.12									
	p		1.78	0.16									
	csa		1.18	0.12									
Box (Cont**)	std	18	0.77	0.26	6	0.66	0.38	11	0.8	0.20	1	0.08	0
	lrfd		1.06	0.14		1.13	0.09		1.04	0.15		0.85	0
	p		1.33	0.08		1.35	0.06		1.35	0.07		1.07	0
	csa		0.88	0.25		0.72	0.14		0.97	0.24		0.85	0
RC (Cont**)	std	15	1.11	0.22									
	lrfd		0.85	0.24									
	p		1.35	0.21									
	csa		0.9	0.19									
All	std	213	1.26	0.31	101	1.24	0.28	36	0.90	0.38	1	0.08	0
	lrfd		1.42	0.37		1.45	0.32		1.91	0.36		0.85	0
	p		1.57	0.23		1.41	0.19		1.74	0.24		1.07	0
	csa		1.40	0.48		1.36	0.48		2.07	0.44		0.85	0

* std – AASHTO Standard, lrfd – AASHTO LRFD, p – Proposal, csa – Canadian Code approach

** Rect - Rectangular, Cont - Continuous Span

*** All values are based on non-minimum cases, where non-minimum means all of the approaches required the shear reinforcement greater than the minimum requirements (see Table H-2) for a given section.

Table H-4 Summary of Results – Simply-Supported I Beam

beam no.	no. of bottom strands	location ft	d_v in	V_u kips	v_u ksi	M_{cr} k ft	M_u k ft	aashto standard			aashto lrfd			proposal			csa			r2k	
								V_{ci} kips	V_{cw} kips	$\rho_v f_y$ psi	V_c kips	$\rho_v f_y$ psi	θ deg	V_c kips	$\rho_v f_y$ psi	θ deg	V_c kips	$\rho_v f_y$ psi	θ deg	V_{cr} kips	$\rho_v f_y$ psi
1	6	2.9	31.3	171	0.911	920	612	274	87	492	27	804	43	52	537	36	17	882	44	83	320
	-	-	-	-	-	-	-	-	-	-	-	-	-	-	-	-	-	-	-	-	-
	6	3.6	31.3	151	0.804	915	725	209	88	382	28	699	43	52	446	36	15	840	46	63	260
	6	5.4	31.3	101	0.538	900	951	110	89	113	28	431	44	53	228	36	13	613	50	(80)	160
6	7.2	31.3	50	0.266	895	1087	55	89	50	28	141	44	53	89	35	13	258	50	(42)	89	
2	6	2.9	31.3	129	0.687	765	430	253	97	220	37	351	37	63	349	39	44	253	32	84	220
	-	-	-	-	-	-	-	-	-	-	-	-	-	-	-	-	-	-	-	-	-
	6	5	33	101	0.51	810	672	142	94	81	39	203	36	58	243	42	28	236	37	84	200
	6	7.5	35.2	67	0.317	875	881	85	89	50	37	89	41	52	113	46	26	104	39	(62)	89
6	10	37.4	34	0.152	945	1007	48	81	50	39	89	41	43	89	52	30	89	38	(27)	89	
3	6	2.9	31.3	74	0.394	661	229	252	98	50	63	89	22	62	89	36	78	89	29	91	89
	6	5	31.3	67	0.357	626	378	146	97	50	63	89	22	61	89	36	75	89	29	87	89
	6	10	33	50	0.253	581	672	73	99	50	42	89	34	61	89	37	42	89	33	(32)	89
	6	15	35.2	34	0.161	571	881	46	99	50	42	89	36	(46)	89	45	31	89	37	(32)	89
	6	20	37.4	17	0.076	596	1007	38	95	50	39	89	41	(38)	89	45	32	89	37	(15)	89
4	8	2.9	31.8	222	1.164	1184	797	348	82	777	26	1047	42	47	828	38	19	1092	43	85	460
	-	-	-	-	-	-	-	-	-	-	-	-	-	-	-	-	-	-	-	-	-
	8	3.6	31.8	197	1.032	1179	944	264	83	642	27	929	43	47	705	38	17	1043	45	95	380
	8	5.4	31.8	131	0.687	1164	1239	139	83	293	29	572	43	48	398	38	15	754	48	80	200
	8	7.2	31.8	66	0.346	1159	1416	67	84	50	28	226	44	48	101	38	14	335	48	(49)	89
5	8	2.9	31.8	181	0.949	1169	605	374	83	555	40	529	32	48	624	38	33	595	35	90	340
	-	-	-	-	-	-	-	-	-	-	-	-	-	-	-	-	-	-	-	-	-
	8	5	31.8	142	0.744	1139	944	191	85	345	28	636	43	49	436	37	21	613	41	91	220
	8	7.5	31.8	94	0.493	1119	1239	103	86	87	28	383	44	50	214	37	16	459	45	(80)	120
	8	10	31.8	47	0.246	1104	1416	51	87	50	28	120	44	(51)	89	45	15	197	47	(35)	89

* The values in parentheses represent the cases where the flexural shear cracking force governs for V_c .

Table H-4 Summary of Results – Simply-Supported I Beam (continued)

beam no.	no. of bottom strands	location ft	d_v in	V_u kips	v_u ksi	M_{cr} k ft	M_u k ft	aashto standard			aashto lrfd			proposal			csa			r2k	
								V_{ci} kips	V_{cw} kips	$\rho_v f_y$ psi	V_c kips	$\rho_v f_y$ psi	θ deg	V_c kips	$\rho_v f_y$ psi	θ deg	V_c kips	$\rho_v f_y$ psi	θ deg	V_{cr} kips	$\rho_v f_y$ psi
6	8	2.9	31.8	99	0.519	925	305	338	93	82	64	89	22	57	216	38	81	89	29	82	120
	8	5	32.5	89	0.456	890	503	194	94	50	65	89	22	57	167	38	79	89	29	89	100
	8	10	34.1	67	0.327	845	893	94	95	50	44	89	34	57	89	39	47	89	32	76	89
	8	15	35.7	45	0.21	835	1173	57	93	50	43	89	36	54	89	41	33	89	36	(38)	89
	8	20	37.4	22	0.098	860	1340	38	88	50	39	89	41	(38)	89	45	32	89	37	(19)	89
7	8	2.9	31.5	69	0.365	855	208	336	95	50	69	89	21	59	89	36	84	89	28	80	89
	8	7.5	32.5	60	0.308	676	503	128	104	50	65	89	22	66	89	34	80	89	29	78	89
	8	15	34.1	45	0.22	457	893	62	115	50	47	89	31	(62)	89	45	57	89	31	(51)	89
	8	22.5	35.7	30	0.14	327	1173	39	122	50	43	89	36	(39)	89	45	35	89	35	(25)	89
	8	30	37.4	15	0.067	282	1340	38	124	50	39	89	41	(38)	89	45	32	89	37	(13)	89
8	10	2.9	32.4	269	1.384	1428	967	416	81	1011	26	1253	42	45	1079	40	21	1246	41	85	640
	-	-	-	-	-	-	-	-	-	-	-	-	-	-	-	-	-	-	-	-	-
	10	3.6	32.4	239	1.229	1423	1145	315	81	853	27	1114	42	45	927	39	18	1188	43	95	520
	10	5.4	32.4	159	0.818	1408	1503	165	82	439	29	713	43	46	546	39	16	855	46	97	280
	10	7.2	32.4	80	0.412	1403	1718	79	82	50	29	296	44	46	180	39	16	384	46	(64)	120
9	10	2.9	32.4	220	1.132	1413	734	447	82	753	40	676	33	46	828	39	38	693	34	89	460
	-	-	-	-	-	-	-	-	-	-	-	-	-	-	-	-	-	-	-	-	-
	10	5	32.4	172	0.885	1383	1145	228	83	500	29	783	43	47	591	39	23	702	40	92	300
	10	7.5	32.4	115	0.592	1363	1503	121	84	201	29	474	43	48	321	38	18	532	44	(93)	160
	10	10	32.4	57	0.293	1348	1718	60	85	50	29	170	44	49	89	38	17	229	45	(46)	89
10	10	2.9	32.5	121	0.621	1169	374	417	91	199	57	138	21	55	330	39	85	89	28	83	160
	10	5	33.1	110	0.554	1134	617	237	92	136	67	94	22	55	275	39	82	89	29	90	140
	10	10	34.4	82	0.397	1084	1096	112	92	50	48	98	31	54	153	41	51	89	32	88	100
	10	15	35.7	55	0.257	1074	1439	66	89	50	43	89	36	51	89	43	34	89	36	(50)	89
	10	20	37	27	0.122	1104	1644	38	83	50	39	89	41	(38)	89	45	32	89	37	(21)	89

* The values in parentheses represent the cases where the flexural shear cracking force governs for V_c .

Table H-4 Summary of Results – Simply-Supported I Beam (continued)

beam no.	no. of bottom strands	location ft	d_v in	V_u kips	v_u ksi	M_{cr} k ft	M_u k ft	aashto standard			aashto lrfd			proposal			csa			r2k	
								V_{ci} kips	V_{cw} kips	$\rho_v f_y$ psi	V_c kips	$\rho_v f_y$ psi	θ deg	V_c kips	$\rho_v f_y$ psi	θ deg	V_c kips	$\rho_v f_y$ psi	θ deg	V_{cr} kips	$\rho_v f_y$ psi
11	10	2.9	32.3	84	0.433	1094	255	415	93	50	71	89	21	56	144	37	90	89	28	101	89
	10	7.5	33.1	73	0.368	920	617	157	102	50	67	89	22	64	89	35	84	89	29	95	89
	10	15	34.4	55	0.266	696	1096	74	112	50	54	89	27	72	89	33	63	89	30	(59)	89
	10	22.5	35.7	37	0.173	566	1439	45	118	50	43	89	36	(45)	89	45	36	89	35	(33)	89
	10	30	37	18	0.081	526	1644	37	119	50	39	89	41	(38)	89	45	32	89	37	(14)	89
12	12	2.9	32.9	319	1.616	1667	1143	483	78	1260	25	1473	41	42	1364	41	22	1430	41	107	820
	-	-	-	-	-	-	-	-	-	-	-	-	-	-	-	-	-	-	-	-	-
	12	3.6	32.9	282	1.429	1662	1354	365	78	1073	26	1297	42	42	1184	41	20	1350	42	96	700
	12	5.4	32.9	188	0.952	1647	1777	190	79	593	28	847	43	43	719	41	17	972	45	96	340
13	12	7.2	32.9	94	0.476	1642	2030	90	80	113	29	365	44	44	261	40	17	436	45	(71)	160
	12	2.9	32.9	260	1.317	1652	868	519	79	958	38	820	33	43	1065	41	41	801	33	92	618
	-	-	-	-	-	-	-	-	-	-	-	-	-	-	-	-	-	-	-	-	-
	12	5	32.9	203	1.028	1622	1354	264	81	660	37	729	37	45	762	40	25	804	39	90	412
	12	7.5	32.9	135	0.684	1602	1777	140	82	309	30	570	43	46	431	39	19	603	43	93	206
14	12	10	32.9	68	0.344	1587	2030	68	83	50	29	225	44	47	119	39	18	271	44	(51)	89
	12	2.9	32.9	150	0.76	1597	462	556	82	385	52	244	23	46	500	39	86	194	28	99	240
	12	5	32.9	135	0.684	1528	761	307	86	291	55	198	23	49	396	38	81	168	29	82	220
	12	10	32.9	102	0.517	1393	1354	134	94	87	39	276	36	57	203	35	37	246	34	92	140
	12	15	32.9	68	0.344	1298	1777	73	100	50	34	180	41	62	89	34	23	208	40	(58)	89
15	12	20	32.9	34	0.172	1239	2030	38	103	50	29	89	44	(38)	89	45	20	89	42	(26)	89
	12	2.9	32.8	100	0.508	1333	303	495	91	92	84	89	20	54	228	38	94	89	28	107	120
	12	7.5	33.5	87	0.433	1159	733	185	99	50	74	89	21	61	128	36	86	89	29	97	89
	12	15	34.6	65	0.313	935	1303	86	109	50	55	89	27	69	89	34	67	89	30	74	89
	12	22.5	35.7	43	0.201	810	1711	51	115	50	43	89	36	(51)	89	45	37	89	35	(37)	89
12	30	36.7	22	0.1	765	1955	37	114	50	38	89	41	(37)	89	45	32	89	37	(18)	89	

* The values in parentheses represent the cases where the flexural shear cracking force governs for V_c .

Table H-4 Summary of Results – Simply-Supported I Beam (continued)

beam no.	no. of bottom strands	location ft	d_v in	V_u kips	v_u ksi	M_{cr} k ft	M_u k ft	aashto standard			aashto lrfd			proposal			csa			r2k	
								V_{ci} kips	V_{cw} kips	$\rho_v f_y$ psi	V_c kips	$\rho_v f_y$ psi	θ deg	V_c kips	$\rho_v f_y$ psi	θ deg	V_c kips	$\rho_v f_y$ psi	θ deg	V_{cr} kips	$\rho_v f_y$ psi
16	12	2.9	32.8	82	0.417	1294	245	494	92	50	84	89	20	56	138	37	98	89	28	97	89
	12	9	33.5	70	0.348	985	707	153	108	50	74	89	21	69	89	33	88	89	28	96	89
	12	18	34.6	52	0.25	631	1257	72	127	50	60	89	24	(72)	89	45	81	89	29	(62)	89
	12	27	35.7	35	0.163	407	1650	43	139	50	46	89	34	(43)	89	45	42	89	33	(31)	89
	12	36	36.7	17	0.077	307	1885	37	143	50	44	89	36	(37)	89	45	36	89	35	(14)	89
17	14	2.9	31.3	171	0.911	1543	529	537	121	331	49	294	23	83	320	29	84	250	28	108	280
	14	5	31.3	155	0.825	1508	872	303	120	249	48	269	24	82	270	29	77	225	29	118	240
	14	10	31.6	116	0.612	1463	1551	139	118	52	37	325	37	80	150	30	36	285	34	113	140
	14	15	32.4	78	0.401	1453	2035	79	115	50	34	194	41	77	89	32	24	213	39	(68)	89
	14	20	33.2	39	0.196	1478	2326	43	110	50	30	89	44	(42)	89	45	22	89	41	(29)	89
18	14	2.9	33.2	116	0.582	1577	351	576	89	182	60	117	20	52	319	40	100	89	28	108	160
	14	7.5	33.8	101	0.498	1398	850	214	97	69	74	89	21	59	200	37	89	89	28	97	120
	14	15	34.7	76	0.365	1179	1511	98	106	50	55	89	27	66	89	35	69	89	30	83	89
	14	22.5	35.6	50	0.234	1049	1984	57	110	50	45	89	34	(57)	89	45	38	89	35	(46)	89
	14	30	36.6	25	0.114	1005	2267	37	109	50	38	89	41	(37)	89	45	32	89	37	(20)	89
19	14	2.9	33.2	98	0.492	1538	295	575	90	85	85	89	20	53	223	39	103	89	28	107	120
	14	9	33.8	84	0.414	1224	850	177	106	50	74	89	21	67	89	34	90	89	28	96	89
	14	18	34.7	63	0.303	875	1511	82	124	50	55	89	27	(82)	89	45	76	89	29	69	89
	14	27	35.6	42	0.197	646	1984	48	135	50	45	89	34	(48)	89	45	39	89	34	(38)	89
	14	36	36.6	21	0.096	546	2267	37	138	50	38	89	41	(37)	89	45	33	89	36	(16)	89
20	16	2.9	31.3	131	0.698	1548	397	565	119	129	57	153	20	81	201	30	97	89	28	114	180
	16	7.5	31.9	114	0.596	1418	961	216	121	50	55	123	21	83	133	30	85	89	28	103	140
	16	15	33.4	85	0.424	1269	1709	102	124	50	53	89	27	84	89	31	62	89	30	(89)	89
	16	22.5	34.9	57	0.272	1214	2243	61	121	50	42	89	36	(61)	89	45	36	89	35	(47)	89
	16	30	36.5	28	0.128	1249	2563	37	111	50	38	89	41	(37)	89	45	33	89	36	(22)	89

* The values in parentheses represent the cases where the flexural shear cracking force governs for V_c .

Table H-4 Summary of Results – Simply-Supported I Beam (continued)

beam no.	no. of bottom strands	location ft	d_v in	V_u kips	v_u ksi	M_{cr} k ft	M_u k ft	aashto standard			aashto lrfd			proposal			csa			r2k	
								V_{ci} kips	V_{cw} kips	$\rho_v f_y$ psi	V_c kips	$\rho_v f_y$ psi	θ deg	V_c kips	$\rho_v f_y$ psi	θ deg	V_c kips	$\rho_v f_y$ psi	θ deg	V_{cr} kips	$\rho_v f_y$ psi
21	16	2.9	31.3	111	0.591	1503	333	563	120	50	57	113	20	82	125	30	101	89	28	111	140
	16	9	31.9	95	0.496	1244	961	178	129	50	70	89	21	90	89	29	86	89	28	115	89
	16	18	33.4	71	0.354	965	1709	85	140	50	53	89	27	(85)	89	45	67	89	30	(73)	89
	16	27	34.9	47	0.224	810	2243	52	143	50	45	89	34	(51)	89	45	37	89	34	(41)	89
	16	36	36.5	24	0.11	790	2563	37	139	50	44	89	36	(37)	89	45	33	89	36	(19)	89
22	18	2.9	31.3	123	0.655	1722	370	636	119	83	57	139	20	81	168	30	104	89	28	112	160
	18	9	32.1	106	0.55	1463	1069	200	130	50	71	89	21	90	89	29	89	89	28	117	120
	18	18	33.5	79	0.393	1184	1900	94	140	50	53	89	27	(94)	89	45	72	89	29	(87)	89
	18	27	34.8	53	0.254	1029	2493	56	143	50	44	89	34	(56)	89	45	38	89	34	(46)	89
	18	36	36.2	26	0.12	1005	2849	37	137	50	43	89	36	(37)	89	45	34	89	36	(20)	89

* The values in parentheses represent the cases where the flexural shear cracking force governs for V_c .

Table H-5 Summary of Results – Simply-Supported Bulb-T

beam no.	no. of bottom strands	location ft	d _v in	V _u kips	v _u ksi	M _{cr} k ft	M _u k ft	aashto standard			aashto lrfd			proposal			csa			r2k	
								V _{ci} kips	V _{ew} kips	$\rho_v f_y$ psi	V _c kips	$\rho_v f_y$ psi	θ deg	V _c kips	$\rho_v f_y$ psi	θ deg	V _c kips	$\rho_v f_y$ psi	θ deg	V _{cr} kips	$\rho_v f_y$ psi
1	18	5.3	63.2	525	1.384	4670	3810	679	179	961	50	1253	42	106	903	36	33	1441	45	166	800
	-	-	-	-	-	-	-	-	-	-	-	-	-	-	-	-	-	-	-	-	-
	-	-	-	-	-	-	-	-	-	-	-	-	-	-	-	-	-	-	-	-	-
	18	7.5	63.2	365	0.963	4638	4789	384	179	539	55	857	43	106	789	45	32	1004	46	184	460
18	10.0	63.2	182	0.480	4621	5473	181	180	53	57	369	44	108	250	45	35	419	44	(138)	160	
2	18	5.3	65.0	442	1.133	4391	2834	730	203	664	77	690	35	130	703	37	65	707	35	176	500
	-	-	-	-	-	-	-	-	-	-	-	-	-	-	-	-	-	-	-	-	-
	18	7.2	65.9	376	0.951	4408	3612	501	204	486	75	598	37	130	557	37	55	634	37	176	390
	18	10.8	67.5	251	0.620	4473	4741	273	204	166	70	385	41	129	371	45	49	396	39	(205)	200
18	14.4	69.1	125	0.301	4572	5418	137	204	50	72	89	41	127	89	45	53	98	38	(104)	89	
3	18	5.3	64.4	356	0.921	4244	2139	761	197	462	95	352	26	124	520	37	150	300	29	179	360
	-	-	-	-	-	-	-	-	-	-	-	-	-	-	-	-	-	-	-	-	-
	18	10.0	65.9	271	0.685	4227	3612	366	200	230	82	339	34	126	332	37	71	347	34	199	230
	18	15.0	67.5	181	0.447	4244	4741	202	202	50	71	234	41	126	186	45	56	222	37	(166)	120
18	20.0	69.1	90	0.217	4293	5418	104	202	50	72	89	41	(104)	89	45	57	89	38	(75)	89	
4	18	5.3	63.8	258	0.674	4080	1483	787	193	221	108	179	23	120	315	36	160	136	29	180	190
	18	7.5	64.3	241	0.625	3998	2032	546	195	169	108	157	23	122	271	36	156	115	29	184	170
	18	15.0	65.9	181	0.458	3752	3612	248	203	50	84	174	34	127	133	35	97	125	32	181	120
	18	22.5	67.5	120	0.296	3620	4741	141	207	50	81	89	36	130	89	45	65	89	36	(110)	89
	18	30.0	69.1	60	0.145	3588	5418	77	210	50	72	89	41	(76)	89	45	60	89	37	(51)	89
5	18	5.3	69.1	202	0.487	4391	1133	880	180	96	152	89	21	103	230	38	181	89	28	129	144
	18	10.0	69.1	181	0.437	4014	2032	448	187	50	139	89	22	109	167	37	172	89	29	172	120
	18	20.0	69.1	135	0.326	3341	3612	199	202	50	109	89	27	123	89	45	139	89	30	(163)	89
	18	30.0	69.1	90	0.217	2882	4741	113	212	50	83	89	36	(112)	89	45	74	89	34	(83)	89
	18	40.0	69.1	45	0.109	2587	5418	70	218	50	72	89	41	(70)	89	45	60	89	37	(36)	89

* The values in parentheses represent the cases where the flexural shear cracking force governs for V_c.

Table H-5 Summary of Results – Simply-Supported Bulb-T (continued)

beam no.	no. of bottom strands	location ft	d_v in	V_u kips	v_u ksi	M_{cr} k ft	M_u k ft	aashto standard			aashto lrfd			proposal			csa			r2k	
								V_{ci} kips	V_{cw} kips	$\rho_v f_y$ psi	V_c kips	$\rho_v f_y$ psi	θ deg	V_c kips	$\rho_v f_y$ psi	θ deg	V_c kips	$\rho_v f_y$ psi	θ deg	V_{cr} kips	$\rho_v f_y$ psi
6	20	5.3	63.6	583	1.528	5097	4229	738	182	1097	47	1387	41	109	998	35	34	1592	45	167	940
	-	-	-	-	-	-	-	-	-	-	-	-	-	-	-	-	-	-	-	-	-
	-	-	-	-	-	-	-	-	-	-	-	-	-	-	-	-	-	-	-	-	-
	20	7.5	63.6	405	1.061	5064	5316	417	184	628	55	959	43	111	890	45	32	1109	46	184	560
	20	10.0	63.6	203	0.532	5048	6076	195	184	99	57	425	44	111	301	45	35	472	44	(163)	190
7	20	5.3	63.6	496	1.300	5048	3178	832	184	866	66	873	35	111	811	35	55	960	37	151	660
	-	-	-	-	-	-	-	-	-	-	-	-	-	-	-	-	-	-	-	-	-
	20	7.2	63.6	422	1.106	4998	4050	561	185	669	53	989	42	112	652	35	46	898	39	152	520
	20	10.8	63.6	281	0.736	4933	5316	296	186	297	57	628	43	113	522	45	39	638	42	204	280
	20	14.4	63.6	141	0.369	4900	6076	142	186	50	57	251	44	113	115	45	38	271	42	(122)	100
8	20	5.3	64.7	395	1.018	4687	2378	835	201	552	90	429	27	127	586	36	150	359	29	180	400
	-	-	-	-	-	-	-	-	-	-	-	-	-	-	-	-	-	-	-	-	-
	20	10.0	66.1	301	0.759	4654	4015	398	204	297	82	394	34	128	382	36	71	404	34	200	270
	20	15.0	67.6	201	0.496	4687	5269	219	205	50	71	281	41	128	234	45	56	265	37	166	140
	20	20.0	69.0	100	0.242	4736	6022	112	205	50	72	89	41	(111)	89	45	56	89	38	(88)	89
9	20	5.3	64.2	287	0.745	4523	1648	865	196	286	108	212	23	123	363	35	162	177	29	181	220
	20	7.5	64.6	268	0.691	4424	2258	597	199	229	109	187	23	125	316	35	158	154	29	185	200
	20	15.0	66.1	201	0.507	4178	4015	270	206	50	84	211	34	130	164	35	97	159	32	182	140
	20	22.5	67.6	134	0.330	4063	5269	152	211	50	81	99	36	134	89	45	65	112	36	123	89
	20	30.0	69.0	67	0.162	4030	6022	81	213	50	72	89	41	(81)	89	45	59	89	37	(56)	89
10	20	5.3	64.0	224	0.583	4359	1259	872	196	123	111	130	21	123	229	35	170	89	28	182	152
	20	10.0	64.6	201	0.519	4047	2258	449	203	50	130	89	22	128	166	34	161	89	29	182	126
	20	20.0	66.1	151	0.381	3505	4015	204	216	50	92	98	31	138	89	45	118	89	30	(173)	89
	20	30.0	67.6	100	0.247	3194	5269	118	226	50	81	89	36	(118)	89	45	70	89	35	(91)	89
	20	40.0	69.0	50	0.121	3030	6022	70	232	50	72	89	41	(70)	89	45	61	89	37	(41)	89

* The values in parentheses represent the cases where the flexural shear cracking force governs for V_c .

Table H-5 Summary of Results – Simply-Supported Bulb-T (continued)

beam no.	no. of bottom strands	location ft	d_v in	V_u kips	v_u ksi	M_{cr} k ft	M_u k ft	aashto standard			aashto lrfd			proposal			csa			r2k	
								V_{ci} kips	V_{cw} kips	$\rho_v f_y$ psi	V_c kips	$\rho_v f_y$ psi	θ deg	V_c kips	$\rho_v f_y$ psi	θ deg	V_c kips	$\rho_v f_y$ psi	θ deg	V_{cr} kips	$\rho_v f_y$ psi
11	22	5.3	64.0	639	1.664	5540	4632	799	187	1225	44	1518	41	114	1075	35	34	1726	45	168	1120
	-	-	-	-	-	-	-	-	-	-	-	-	-	-	-	-	-	-	-	-	-
	-	-	-	-	-	-	-	-	-	-	-	-	-	-	-	-	-	-	-	-	-
	22	7.5	64.0	444	1.156	5507	5823	450	187	717	53	1040	42	114	989	45	33	1203	45	183	640
22	10.0	64.0	222	0.578	5491	6655	210	187	139	58	460	43	114	347	45	36	513	44	(162)	220	
12	22	5.3	64.0	543	1.414	5491	3481	901	189	972	67	961	35	115	874	34	57	1044	37	152	760
	-	-	-	-	-	-	-	-	-	-	-	-	-	-	-	-	-	-	-	-	-
	22	7.2	64.0	462	1.203	5441	4436	608	189	761	53	1087	42	115	713	34	47	976	39	205	580
	22	10.8	64.0	308	0.802	5376	5823	319	190	357	57	697	43	116	589	45	40	695	42	152	320
22	14.4	64.0	154	0.401	5343	6655	153	191	50	57	285	44	117	141	45	39	297	42	(123)	116	
12	22	5.3	64.0	437	1.138	5409	2628	954	190	693	74	757	35	116	656	34	128	510	30	162	500
	-	-	-	-	-	-	-	-	-	-	-	-	-	-	-	-	-	-	-	-	-
	22	10.0	64.0	333	0.867	5261	4436	442	192	416	65	690	41	118	441	34	61	568	36	182	320
	22	15.0	64.0	222	0.578	5146	5823	235	195	121	66	405	41	120	329	45	45	423	40	(186)	190
22	20.0	64.0	111	0.289	5064	6655	115	196	50	57	165	44	(115)	89	45	42	172	41	(89)	89	
14	22	5.3	64.6	316	0.815	4949	1812	939	201	348	99	270	24	127	403	35	164	218	29	182	250
	22	7.5	64.9	294	0.755	4851	2484	647	203	287	100	240	24	128	356	35	159	192	29	185	230
	22	15.0	66.3	221	0.556	4621	4416	292	210	80	85	247	34	134	192	34	97	192	32	206	170
	22	22.5	67.6	147	0.362	4490	5795	163	214	50	81	125	36	136	89	45	64	139	36	(135)	89
	22	30.0	68.9	74	0.179	4457	6623	86	217	50	72	89	41	(85)	89	45	59	89	37	(62)	89
15	22	5.3	64.3	247	0.640	4802	1385	951	200	174	112	155	21	125	265	34	173	101	28	183	180
	22	10.0	64.9	221	0.568	4473	2484	487	207	89	109	134	23	131	196	34	163	89	29	183	150
	22	20.0	66.3	166	0.417	3948	4416	221	220	50	92	122	31	142	106	45	119	89	30	(173)	110
	22	30.0	67.6	110	0.271	3620	5795	126	228	50	81	89	36	(126)	89	45	70	89	35	(102)	89
	22	40.0	68.9	55	0.133	3456	6623	70	234	50	72	89	41	(70)	89	45	61	89	37	(44)	89

* The values in parentheses represent the cases where the flexural shear cracking force governs for V_c .

Table H-5 Summary of Results – Simply-Supported Bulb-T (continued)

beam no.	no. of bottom strands	location ft	d _v in	V _u kips	v _u ksi	M _{cr} k ft	M _u k ft	aashto standard			aashto lrfd			proposal			csa			r2k	
								V _{ci} kips	V _{ew} kips	$\rho_v f_y$ psi	V _c kips	$\rho_v f_y$ psi	θ deg	V _c kips	$\rho_v f_y$ psi	θ deg	V _c kips	$\rho_v f_y$ psi	θ deg	V _{cr} kips	$\rho_v f_y$ psi
16	22	5.3	64.2	202	0.524	4654	1121	956	201	54	141	89	21	127	171	34	179	89	28	182	134
	22	12.5	64.9	177	0.455	3998	2484	390	215	50	131	89	22	139	94	32	166	89	29	181	110
	22	25.0	66.3	132	0.332	3095	4416	179	235	50	105	89	27	156	89	45	137	89	30	(152)	89
	22	37.5	67.6	88	0.217	2488	5795	103	251	50	86	89	34	(103)	89	45	73	89	34	(82)	89
	22	50.0	68.9	44	0.106	2177	6623	70	260	50	72	89	41	(70)	89	45	62	89	36	(34)	89
17	24	5.3	64.3	693	1.796	5966	5025	858	191	1352	45	1646	41	116	1155	34	35	1845	44	169	1260
	-	-	-	-	-	-	-	-	-	-	-	-	-	-	-	-	-	-	-	-	-
	-	-	-	-	-	-	-	-	-	-	-	-	-	-	-	-	-	-	-	-	-
	24	7.5	64.3	481	1.247	5934	6317	483	191	802	53	1131	42	116	1084	45	34	1284	45	186	700
	24	10.0	64.3	241	0.625	5917	7220	224	192	177	58	508	43	118	389	45	37	553	43	-179	230
18	24	5.3	64.3	590	1.529	5917	3777	968	192	1082	60	1042	34	118	944	34	58	1126	36	153	840
	-	-	-	-	-	-	-	-	-	-	-	-	-	-	-	-	-	-	-	-	-
	24	7.2	64.3	501	1.299	5868	4813	652	193	848	51	1168	42	119	763	34	48	1047	39	153	660
	24	10.8	64.3	334	0.866	5802	6317	342	193	415	58	763	43	119	654	45	41	746	41	207	340
	24	14.4	64.3	167	0.433	5770	7220	163	195	54	58	319	44	120	170	45	41	322	41	(136)	130
19	24	5.3	64.3	474	1.229	5835	2851	1025	193	778	74	828	35	119	711	34	135	553	30	163	600
	-	-	-	-	-	-	-	-	-	-	-	-	-	-	-	-	-	-	-	-	-
	24	10.0	64.3	361	0.936	5688	4813	475	196	479	76	587	35	121	481	34	62	613	35	184	380
	24	15.0	64.3	241	0.625	5573	6317	251	198	162	67	450	41	123	374	45	47	458	39	186	210
	24	20.0	64.3	120	0.311	5491	7220	122	200	50	67	148	41	(122)	89	45	43	188	40	(97)	89
20	24	5.3	64.8	344	0.885	5376	1973	1013	205	411	100	303	24	130	446	34	166	257	29	183	290
	24	7.5	65.2	320	0.818	5294	2704	700	207	342	100	271	24	132	390	34	161	228	29	173	290
	24	15.0	66.4	240	0.602	5048	4807	313	213	120	83	288	34	136	220	34	99	221	32	207	180
	24	22.5	67.6	160	0.394	4916	6310	174	217	50	81	151	36	138	97	45	65	163	36	(136)	100
	24	30.0	68.9	80	0.194	4900	7211	91	219	50	72	89	41	(90)	89	45	59	89	37	(64)	89

* The values in parentheses represent the cases where the flexural shear cracking force governs for V_c.

Table H-5 Summary of Results – Simply-Supported Bulb-T (continued)

beam no.	no. of bottom strands	location ft	d_v in	V_u kips	v_u ksi	M_{cr} k ft	M_u k ft	aashto standard			aashto lrfd			proposal			csa			r2k	
								V_{ci} kips	V_{cw} kips	$\rho_v f_y$ psi	V_c kips	$\rho_v f_y$ psi	θ deg	V_c kips	$\rho_v f_y$ psi	θ deg	V_c kips	$\rho_v f_y$ psi	θ deg	V_{cr} kips	$\rho_v f_y$ psi
21	24	5.3	64.6	269	0.694	5228	1508	1027	205	219	112	178	21	130	294	34	176	129	28	184	200
	24	10.0	65.2	240	0.613	4916	2704	526	211	127	110	155	23	135	219	33	166	101	29	183	170
	24	20.0	66.4	180	0.452	4375	4807	237	223	50	105	107	27	145	139	45	121	89	30	(192)	120
	24	30.0	67.6	120	0.296	4047	6310	134	232	50	81	89	36	(134)	89	45	70	89	35	(111)	89
	24	40.0	68.9	60	0.145	3899	7211	73	237	50	72	89	41	(72)	89	45	61	89	37	(47)	89
22	24	5.3	64.5	220	0.568	5080	1220	1033	205	92	117	115	20	130	197	34	183	89	28	183	150
	24	12.5	65.2	192	0.491	4441	2704	421	218	50	143	89	21	141	114	32	168	89	29	216	89
	24	25.0	66.4	144	0.361	3522	4807	191	238	50	105	89	27	158	89	45	140	89	29	171	89
	24	37.5	67.6	96	0.237	2915	6310	110	253	50	86	89	34	(109)	89	45	74	89	34	(97)	89
	24	50.0	68.9	48	0.116	2620	7211	70	262	50	72	89	41	(70)	89	45	62	89	36	(46)	89
23	26	5.3	61.3	512	1.392	5852	3080	1027	222	847	64	906	35	149	697	31	125	632	30	182	600
	-	-	-	-	-	-	-	-	-	-	-	-	-	-	-	-	-	-	-	-	-
	26	10.0	62.3	390	1.043	5835	5200	485	224	503	74	633	35	150	466	32	60	665	36	203	400
	26	20.0	64.4	130	0.336	5901	7799	129	225	50	67	126	41	(129)	89	45	45	160	40	(101)	89
24	26	5.3	64.9	370	0.950	5802	2120	1088	209	466	95	363	25	133	479	34	168	293	29	184	330
	26	7.5	65.3	344	0.878	5704	2905	748	211	393	101	300	24	135	420	34	162	263	29	186	290
	26	15.0	66.4	258	0.648	5458	5164	334	217	157	89	275	31	140	243	33	101	246	31	208	220
	26	22.5	67.5	172	0.425	5343	6778	185	221	50	81	176	36	142	121	45	66	184	35	(149)	110
	26	30.0	68.6	86	0.209	5310	7746	96	223	50	72	89	41	(95)	89	45	59	89	37	(68)	89
25	26	5.3	64.7	289	0.744	5638	1620	1100	207	264	112	200	21	132	323	34	179	154	28	185	220
	26	10.0	65.3	258	0.658	5327	2905	563	214	166	110	176	23	138	245	33	167	126	29	184	190
	26	20.0	66.4	194	0.487	4785	5164	252	227	50	105	126	27	148	169	45	124	98	30	194	130
	26	30.0	67.5	129	0.319	4473	6778	142	235	50	81	95	36	(142)	89	45	71	92	35	(112)	89
	26	40.0	68.6	65	0.158	4309	7746	76	240	50	72	89	41	(76)	89	45	61	89	36	(51)	89

* The values in parentheses represent the cases where the flexural shear cracking force governs for V_c .

Table H-5 Summary of Results – Simply-Supported Bulb-T (continued)

beam no.	no. of bottom strands	location ft	d_v in	V_u kips	v_u ksi	M_{cr} k ft	M_u k ft	aashto standard			aashto lrfd			proposal			csa			r2k	
								V_{ci} kips	V_{cw} kips	$\rho_v f_y$ psi	V_c kips	$\rho_v f_y$ psi	θ deg	V_c kips	$\rho_v f_y$ psi	θ deg	V_c kips	$\rho_v f_y$ psi	θ deg	V_{cr} kips	$\rho_v f_y$ psi
26	26	5.3	64.6	236	0.609	5491	1310	1107	209	124	117	131	20	133	216	33	187	89	28	184	170
	26	12.5	65.3	207	0.528	4851	2905	450	223	50	144	89	21	145	132	31	170	89	28	182	140
	26	25.0	66.4	155	0.389	3932	5164	204	242	50	105	89	27	162	89	45	144	89	29	(169)	89
	26	37.5	67.5	103	0.254	3341	6778	116	257	50	86	89	34	(116)	89	45	75	89	34	(97)	89
	26	50.0	68.6	52	0.126	3030	7746	70	265	50	82	89	36	(70)	89	45	62	89	36	(49)	89
27	28	5.3	61.4	309	0.839	5622	1734	1096	226	287	97	259	23	152	311	31	172	192	28	193	240
	28	10.0	62.4	276	0.737	5359	3109	565	232	179	105	201	23	158	234	30	161	158	29	192	200
	28	20.0	64.4	207	0.536	4949	5527	258	243	50	90	184	31	165	167	45	115	124	30	201	140
	28	30.0	66.4	138	0.346	4752	7254	147	250	50	79	100	36	(147)	89	45	70	97	35	(117)	89
	28	40.0	68.5	69	0.168	4720	8290	80	253	50	82	89	36	(79)	89	45	63	89	36	(76)	89
28	28	5.3	61.2	253	0.689	5458	1402	1100	224	139	111	156	20	151	209	30	180	94	28	192	180
	28	12.5	62.4	221	0.590	4884	3109	452	237	50	108	127	21	161	127	29	164	89	28	224	140
	28	25.0	64.4	166	0.430	4096	5527	208	256	50	102	89	27	177	89	45	132	89	30	(177)	100
	28	37.5	66.4	111	0.279	3620	7254	120	269	50	85	89	34	(119)	89	45	73	89	34	(113)	89
	28	50.0	68.5	55	0.134	3440	8290	69	277	50	82	89	36	(70)	89	45	64	89	36	(61)	89
29	28	5.3	64.7	214	0.551	5786	1177	1189	214	55	165	89	20	138	161	32	198	89	28	183	150
	28	15.0	65.3	184	0.470	4687	3109	400	237	50	144	89	21	158	89	30	175	89	28	209	89
	28	30.0	66.4	138	0.346	3325	5527	181	266	50	115	89	24	(181)	89	45	155	89	29	(164)	89
	28	45.0	67.4	92	0.227	2390	7254	103	288	50	86	89	34	(103)	89	45	79	89	34	(79)	89
	28	60.0	68.5	46	0.112	1881	8290	69	300	50	82	89	36	(70)	89	45	64	89	36	(44)	89
30	30	5.3	58.5	330	0.940	5934	1855	1151	239	327	92	305	23	167	316	29	165	249	28	194	260
	30	10.0	59.3	296	0.832	5671	3327	591	246	211	91	269	24	172	245	29	152	215	29	194	220
	30	20.0	61.1	222	0.606	5261	5914	268	256	50	82	236	31	180	182	45	92	208	32	222	150
	30	30.0	62.9	148	0.392	5064	7763	152	263	50	75	135	36	(152)	89	45	58	156	36	(131)	89
	30	40.0	64.6	74	0.191	5031	8872	81	266	50	68	89	41	(80)	89	45	52	89	38	(76)	89

* The values in parentheses represent the cases where the flexural shear cracking force governs for V_c .

Table H-5 Summary of Results – Simply-Supported Bulb-T (continued)

beam no.	no. of bottom strands	location ft	d_v in	V_u kips	v_u ksi	M_{cr} k ft	M_u k ft	aashto standard			aashto lrfd			proposal			csa			r2k	
								V_{ci} kips	V_{cw} kips	$\rho_v f_y$ psi	V_c kips	$\rho_v f_y$ psi	θ deg	V_c kips	$\rho_v f_y$ psi	θ deg	V_c kips	$\rho_v f_y$ psi	θ deg	V_{cr} kips	$\rho_v f_y$ psi
31	30	5.3	61.6	271	0.733	5884	1502	1177	229	175	112	175	20	155	228	30	185	115	28	196	190
	30	12.5	62.6	237	0.631	5310	3328	482	242	52	109	145	21	165	145	29	166	91	28	228	150
	30	25.0	64.5	178	0.460	4523	5917	221	260	50	102	104	27	180	89	45	132	89	30	(182)	100
	30	37.5	66.4	118	0.296	4047	7766	126	273	50	85	89	34	(126)	89	45	73	89	34	(122)	89
	30	50.0	68.3	59	0.144	3866	8876	71	279	50	82	89	36	(70)	89	45	63	89	36	(64)	89
32	30	5.3	61.4	229	0.622	5737	1261	1179	228	63	111	131	20	154	155	30	191	89	28	191	150
	30	15.0	62.6	197	0.524	4720	3328	401	250	50	138	89	21	173	89	29	168	89	28	217	120
	30	30.0	64.5	148	0.382	3489	5917	184	278	50	112	89	24	(184)	89	45	146	89	29	(160)	89
	30	45.0	66.4	99	0.248	2685	7766	107	298	50	85	89	34	(106)	89	45	75	89	34	(99)	89
	30	60.0	68.3	49	0.120	2308	8876	69	310	50	82	89	36	(70)	89	45	64	89	36	(53)	89
33	32	5.3	59.0	287	0.811	5868	1594	1173	244	191	95	228	22	171	232	29	180	144	28	200	210
	32	12.5	60.5	251	0.691	5359	3533	485	257	54	105	163	21	182	149	29	161	115	28	231	160
	32	25.0	63.0	188	0.497	4703	6281	226	273	50	99	115	27	194	89	45	123	89	30	(198)	120
	32	37.5	65.6	126	0.320	4342	8244	131	285	50	84	89	34	(130)	89	45	71	89	34	(105)	89
	32	50.0	68.2	63	0.154	4277	9422	74	290	50	82	89	36	(73)	89	45	64	89	36	(69)	89
34	32	5.3	58.8	243	0.689	5720	1338	1175	243	69	107	152	20	170	157	29	187	89	28	189	160
	32	15.0	60.5	209	0.576	4769	3533	403	264	50	133	89	21	188	89	29	163	89	28	220	120
	32	30.0	63.0	157	0.415	3670	6281	188	289	50	99	89	27	(188)	89	45	135	89	29	(164)	89
	32	45.0	65.6	105	0.267	2980	8244	110	308	50	84	89	34	(110)	89	45	73	89	34	(104)	89
	32	60.0	68.2	52	0.127	2718	9422	69	318	50	82	89	36	(69)	89	45	65	89	36	(57)	89
35	34	5.3	57.2	257	0.749	6032	1415	1231	260	67	104	176	20	187	160	29	185	93	28	196	180
	34	15.0	57.9	221	0.636	5080	3736	421	277	50	101	142	21	201	89	29	156	89	28	252	89
	34	30.0	60.2	166	0.460	3965	6642	195	301	50	95	97	27	(195)	89	45	110	89	30	(190)	89
	34	45.0	62.5	111	0.296	3292	8718	113	320	50	75	89	36	(113)	89	45	62	89	35	(108)	89
	34	60.0	64.8	55	0.141	3030	9964	66	331	50	68	89	41	(66)	89	45	55	89	37	(61)	89

* The values in parentheses represent the cases where the flexural shear cracking force governs for V_c .

Table H-6 Summary of Results – Continuous Box Girder

beam no.	no. of strands	location ft	d_v in	V_u kips	v_u ksi	M_{cr} k ft	M_u k ft	aashto standard			aashto lrfd			proposal			csa			r2k
								V_{ci} kips	V_{cw} kips	$\rho_v f_y$ psi	V_c kips	$\rho_v f_y$ psi	θ deg	V_c kips	$\rho_v f_y$ psi	θ deg	V_c kips	$\rho_v f_y$ psi	θ deg	$\rho_v f_y$ psi
1	172	5.2	56.16	1733	0.643	17781	11086	2918	1859	50	677	118	21	1160	158	29	1047	77	28	203
	172	22	56.16	967	0.359	22655	34428	776	1715	100	541	77	31	(778)	110	45	566	77	32	99
	172	44	58.14	66	0.024	25520	46136	406	1563	50	482	77	36	(410)	77	45	377	77	36	77
	172	66	56.9	1098	0.402	23494	35124	875	1645	115	548	99	31	(879)	125	45	522	100	33	117
	172	88	56.16	2131	0.791	12787	1392	19714	2059	103	614	175	23	1361	207	29	1081	106	28	151
	172	104.61	58.17	2897	1.037	35733	38276	2844	1755	487	463	586	35	1190	726	45	410	583	35	495
2	172	5.2	56.16	1406	0.522	17322	8838	2896	1774	50	706	77	20	1076	100	29	1084	77	28	77
	172	28	56.16	760	0.282	22655	34428	639	1653	68	541	77	31	(640)	77	45	599	77	31	77
	172	56	58.14	52	0.018	25520	46136	406	1542	50	482	77	36	(410)	77	45	377	77	36	77
	172	84	56.9	863	0.316	23494	35124	717	1600	80	548	77	31	(719)	88	45	559	77	32	77
	172	112	56.16	1674	0.621	12787	1392	15519	1923	50	706	90	20	1225	131	29	1116	77	28	109
	172	134.54	58.98	2321	0.82	36288	41745	2160	1611	317	456	498	37	1033	546	45	403	466	35	417
3	172	5.2	56.16	1122	0.416	16939	6955	2873	1702	50	992	77	20	1004	77	29	1118	77	28	77
	172	36	56.16	591	0.219	22655	34428	528	1602	50	541	77	31	(527)	77	45	629	77	31	77
	172	72	58.14	40	0.014	25520	46136	406	1525	50	482	77	36	(410)	77	45	376	77	36	77
	172	108	56.9	671	0.246	23494	35124	589	1563	52	548	77	31	(589)	77	45	593	77	32	77
	172	144	56.16	1302	0.483	12787	1392	12101	1813	50	992	77	20	1114	77	29	1147	77	28	77
	172	174.49	59.5	1834	0.642	36655	44622	1650	1517	169	471	370	37	933	387	45	398	358	36	313
4	240	5.2	56.16	2189	0.812	21847	13302	3734	2207	75	624	189	22	1266	240	29	1146	122	28	198
	240	22	56.16	1215	0.451	27948	42900	931	2026	140	677	77	24	(933)	155	45	837	77	29	135
	240	44	56.16	81	0.03	31441	57296	394	1787	50	497	77	34	(396)	77	45	444	77	34	77
	240	66	56.16	1377	0.511	28903	43187	1060	1924	157	574	133	27	984	203	45	739	97	30	154
	240	88	56.16	2672	0.991	15801	575	73601	2439	177	583	258	23	1498	303	29	1188	172	28	219
	240	104.8	56.16	3646	1.353	44180	50239	3346	2022	678	361	796	34	1237	1044	45	421	779	34	781

* The values in parentheses represent the cases where the flexural shear cracking force governs for V_c .

Table H-6 Summary of Results – Continuous Box Girder (Continued)

beam no.	no. of strands	location ft	d_v in	V_u kips	v_u ksi	M_{cr} k ft	M_u k ft	aashto standard			aashto lrfd			proposal			csa			r2k
								V_{ci} kips	V_{cw} kips	$\rho_v f_y$ psi	V_c kips	$\rho_v f_y$ psi	θ deg	V_c kips	$\rho_v f_y$ psi	θ deg	V_c kips	$\rho_v f_y$ psi	θ deg	$\rho_v f_y$ psi
5	240	5.2	56.16	1774	0.658	21303	10600	3704	2101	50	706	115	20	1161	167	29	1200	77	28	125
	240	28	56.16	954	0.354	27948	42900	761	1949	100	677	77	24	(761)	111	45	902	77	29	99
	240	56	56.16	64	0.024	31441	57296	394	1761	50	497	77	34	(396)	77	45	443	77	34	77
	240	84	56.16	1082	0.401	28903	43187	863	1869	113	677	77	24	(864)	125	45	809	77	30	104
	240	112	56.16	2100	0.779	15801	575	57860	2273	50	624	164	22	1333	206	29	1240	77	28	150
	240	134.76	56.61	2919	1.074	44808	54442	2542	1827	473	408	637	35	1047	808	45	410	630	35	583
6	240	5.2	56.16	1414	0.525	20848	8338	3675	2011	50	706	77	20	1070	103	29	1250	77	28	83
	240	36	56.16	742	0.275	27948	42900	623	1887	67	783	77	22	(622)	77	45	908	77	29	77
	240	72	56.16	49	0.018	31441	57296	394	1740	50	497	77	34	(396)	77	45	443	77	34	77
	240	108	56.16	841	0.312	28903	43187	702	1824	78	677	77	24	(702)	86	45	876	77	29	77
	240	144	56.16	1633	0.606	15801	575	45033	2138	50	706	88	20	1198	127	29	1287	77	28	104
	240	174.72	57.03	2305	0.842	45225	57926	1939	1702	287	469	485	35	928	596	45	404	490	35	417
7	288	5.2	56.16	2451	0.909	24575	14391	4324	2427	99	583	248	23	1316	290	29	1233	149	28	219
	288	22	56.16	1355	0.503	31243	47496	1031	2229	159	783	77	22	(1033)	175	45	927	77	29	167
	288	44	56.16	90	0.033	34989	63200	394	1968	50	541	77	31	(396)	77	45	564	77	32	77
	288	66	56.16	1535	0.569	32198	47112	1188	2113	173	656	119	23	1001	261	45	919	84	29	171
	288	88	56.16	2980	1.106	32402	768	125914	2477	279	555	329	25	1552	363	29	1176	232	28	260
	288	104.8	56.16	4076	1.512	49147	58273	3577	2183	783	330	928	34	1258	1213	45	458	858	34	979
8	288	5.2	56.16	1985	0.736	23999	11464	4294	2311	50	624	165	22	1200	207	29	1289	77	28	135
	288	28	56.16	1065	0.395	31243	47496	840	2145	115	783	77	22	(840)	127	45	935	77	29	113
	288	56	56.16	71	0.026	34989	63200	394	1940	50	541	77	31	(396)	77	45	563	77	32	77
	288	84	56.16	1206	0.447	32198	47112	964	2054	126	783	77	22	943	148	45	929	77	29	125
	288	112	56.16	2342	0.869	32402	768	98962	2300	101	624	198	22	1375	253	29	1221	116	28	177
	288	134.8	56.16	3261	1.21	49792	62867	2722	1980	549	361	734	34	1055	953	45	438	701	34	760

* The values in parentheses represent the cases where the flexural shear cracking force governs for V_c .

Table H-6 Summary of Results – Continuous Box Girder (Continued)

beam no.	no. of strands	location ft	d_v in	V_u kips	v_u ksi	M_{cr} k ft	M_u k ft	aashto standard			aashto lrfd			proposal			csa			r2k
								V_{ci} kips	V_{cw} kips	$\rho_v f_y$ psi	V_c kips	$\rho_v f_y$ psi	θ deg	V_c kips	$\rho_v f_y$ psi	θ deg	V_c kips	$\rho_v f_y$ psi	θ deg	$\rho_v f_y$ psi
9	288	5.2	56.16	1581	0.586	23518	9015	4263	2213	50	791	77	18	1101	135	29	1289	77	28	89
	288	36	56.16	828	0.307	31243	47496	684	2077	79	783	77	22	(683)	88	45	942	77	29	77
	288	72	56.16	55	0.02	34989	63200	394	1917	50	541	77	31	(396)	77	45	562	77	32	77
	288	108	56.16	938	0.348	32198	47112	780	2006	87	783	77	22	(780)	97	45	938	77	29	77
	288	144	56.16	1821	0.676	32402	768	77001	2156	50	706	112	20	1231	163	29	1261	77	28	120
	288	174.8	56.16	2574	0.955	50221	66673	2078	1850	337	447	579	35	925	718	45	426	552	34	536

* The values in parentheses represent the cases where the flexural shear cracking force governs for V_c .

Table H-7 Summary of Results – Simply-Supported RC Rectangular Beam

beam no.	no. of bottom bars	location ft	d _v in	V _u kips	v _u ksi	M _u k ft	aashto standard		aashto lrfd			proposal		csa			r2k
							V _c kips	$\rho_v f_y$ psi	V _c kips	$\rho_v f_y$ psi	θ deg	V _c kips	$\rho_v f_y$ psi	V _c kips	$\rho_v f_y$ psi	θ deg	$\rho_v f_y$ psi
1	8	2.4	29.3	167	0.475	535	60.4	321	59	268	37	52	381	44	290	37	270
	-	-	-	-	-	-	-	-	-	-	-	-	-	-	-	-	-
	-	-	-	-	-	-	-	-	-	-	-	-	-	-	-	-	-
	8	3.6	29.3	111	0.316	702	60.4	161	61	131	36	52	204	43	161	37	200
8	4.8	29.3	56	0.159	803	60.4	50	53	77	41	52	77	44	77	37	97	
2	8	2.4	29.3	152	0.432	450	60.4	278	59	232	37	52	333	48	237	36	200
	-	-	-	-	-	-	-	-	-	-	-	-	-	-	-	-	-
	8	3	29.3	134	0.381	535	60.4	227	61	185	36	52	276	47	201	36	180
	8	4.5	29.3	89	0.253	702	60.4	99	61	80	36	52	134	45	104	37	130
8	6	29.3	45	0.128	803	60.4	50	61	77	36	52	77	45	77	37	77	
3	8	2.4	29.3	94	0.267	246	60.4	113	71	77	31	52	150	64	77	33	100
	8	3	29.3	89	0.253	301	60.4	99	65	77	34	52	134	61	77	33	85
	8	6	29.3	67	0.191	535	60.4	50	65	77	34	52	77	53	77	35	77
	8	9	29.3	45	0.128	702	60.4	50	61	77	36	52	77	48	77	36	77
	8	12	29.3	22	0.063	803	60.4	50	61	77	36	52	77	47	77	36	77
4	12	2.4	28.4	229	0.672	733	58.6	518	56	438	37	50	600	45	440	36	330
	-	-	-	-	-	-	-	-	-	-	-	-	-	-	-	-	-
	-	-	-	-	-	-	-	-	-	-	-	-	-	-	-	-	-
	12	3.6	28.4	153	0.449	962	58.6	295	58	246	37	50	352	44	264	37	230
12	4.8	28.4	76	0.223	1100	58.6	68	59	77	36	50	101	45	77	36	83	
5	12	2.4	28.4	208	0.61	616	58.6	456	56	387	37	50	531	49	368	35	280
	-	-	-	-	-	-	-	-	-	-	-	-	-	-	-	-	-
	12	3	28.4	183	0.537	733	58.6	383	58	319	37	50	450	47	317	36	235
	12	4.5	28.4	122	0.358	962	58.6	204	59	166	36	50	251	45	182	36	145
12	6	28.4	61	0.179	1100	58.6	50	59	77	36	50	77	45	77	36	77	

Table H-7 Summary of Results – Simply-Supported RC Rectangular Beam (Continued)

beam no.	no. of bottom bars	location ft	d _v in	V _u kips	v _u ksi	M _u k ft	aashto standard		aashto lrfd			proposal		csa			r2k
							V _c kips	$\rho_v f_y$ psi	V _c kips	$\rho_v f_y$ psi	θ deg	V _c kips	$\rho_v f_y$ psi	V _c kips	$\rho_v f_y$ psi	θ deg	$\rho_v f_y$ psi
6	12	2.4	28.4	128	0.376	337	58.6	221	68	128	31	50	270	64	133	33	155
	12	3	28.4	122	0.358	412	58.6	204	63	142	34	50	251	62	128	33	125
	12	6	28.4	92	0.27	733	58.6	116	63	77	34	50	153	53	87	34	90
	12	9	28.4	61	0.179	962	58.6	50	59	77	36	50	77	49	77	35	77
	12	12	28.4	31	0.091	1100	58.6	50	59	77	36	50	77	47	77	36	77
7	16	2.4	27.4	300	0.912	959	56.7	756	50	645	37	48	867	45	618	36	530
	-	-	-	-	-	-	-	-	-	-	-	-	-	-	-	-	-
	-	-	-	-	-	-	-	-	-	-	-	-	-	-	-	-	-
	16	3.6	27.4	200	0.608	1259	56.7	452	54	385	37	48	529	44	382	36	325
16	4.8	27.4	100	0.304	1439	56.7	149	57	122	36	48	191	45	134	36	140	
8	16	2.4	27.4	272	0.827	806	56.7	671	50	574	37	48	772	49	524	35	400
	-	-	-	-	-	-	-	-	-	-	-	-	-	-	-	-	-
	16	3	27.4	240	0.73	959	56.7	574	53	495	37	48	664	48	457	35	340
	16	4.5	27.4	160	0.487	1259	56.7	331	56	277	37	48	394	46	277	36	225
16	6	27.4	80	0.243	1439	56.7	88	57	77	36	48	123	46	83	36	90	
9	16	2.4	27.4	168	0.511	441	56.7	355	64	223	31	48	421	64	223	32	180
	16	3	27.4	160	0.487	540	56.7	331	59	243	34	48	394	62	214	33	190
	16	6	27.4	120	0.365	959	56.7	209	61	147	34	48	259	53	153	34	132
	16	9	27.4	80	0.243	1259	56.7	88	57	77	36	48	123	49	77	35	80
	16	12	27.4	40	0.122	1439	56.7	50	57	77	36	48	77	47	77	35	77

Table H-8 Summary of Results – Simply-Supported RC T-shape Beam

beam no.	no. of bottom bars	location ft	d _v in	V _u kips	v _u ksi	M _u k ft	aashto standard		aashto lrfd			proposal		csa			r2k
							V _c kips	$\rho_v f_y$ psi	V _c kips	$\rho_v f_y$ psi	θ deg	V _c kips	$\rho_v f_y$ psi	V _c kips	$\rho_v f_y$ psi	θ deg	$\rho_v f_y$ psi
1	20	2.9	33.3	378	0.946	1356	68.8	791	55	665	36	59	904	56	640	36	520
	-	-	-	-	-	-	-	-	-	-	-	-	-	-	-	-	-
	-	3.6	33.3	334	0.836	1605	68.8	681	61	581	37	59	782	54	563	36	450
	20	5.4	33.3	223	0.558	2107	68.8	403	66	343	37	-59	473	52	351	36	280
	20	7.2	33.3	111	0.278	2408	68.8	123	60	136	41	-59	162	52	121	36	150
2	20	2.9	33.3	312	0.781	1043	68.8	626	68	486	35	59	721	63	470	34	365
	-	-	-	-	-	-	-	-	-	-	-	-	-	-	-	-	-
	20	5	33.3	244	0.611	1627	68.8	456	66	387	37	-59	531	57	367	35	262
	20	7.5	33.3	163	0.408	2136	68.8	253	67	212	37	-59	306	53	222	36	155
	20	10	33.3	81	0.203	2441	68.8	50	60	77	41	-59	78	52	77	36	77
3	20	2.9	33.3	181	0.453	561	68.8	298	77	185	31	59	356	83	170	32	150
	20	5	33.3	164	0.41	924	68.8	255	72	186	34	59	309	74	161	33	135
	20	10	33.3	123	0.308	1642	68.8	153	74	105	34	-59	195	62	116	34	95
	20	15	33.3	82	0.205	2155	68.8	50	69	77	36	-59	81	56	77	35	77
	20	20	33.3	41	0.103	2463	68.8	50	69	77	36	-59	77	53	77	36	77
4	28	2.9	31.5	489	1.294	1754	65.1	1139	44	953	36	56	1290	54	908	35	850
	-	-	-	-	-	-	-	-	-	-	-	-	-	-	-	-	-
	-	3.6	31.5	433	1.146	2076	65.1	991	48	823	36	56	1126	52	805	36	720
	28	5.4	31.5	288	0.762	2725	65.1	607	61	522	37	-56	700	49	515	36	430
	28	7.2	31.5	144	0.381	3114	65.1	226	57	235	41	-56	276	49	204	36	165
5	28	2.9	31.5	407	1.077	1358	65.1	922	57	719	35	56	1049	61	689	34	600
	-	-	-	-	-	-	-	-	-	-	-	-	-	-	-	-	-
	28	5	31.5	318	0.841	2119	65.1	686	57	586	37	56	788	54	546	35	420
	28	7.5	31.5	212	0.561	2781	65.1	406	62	345	37	-56	476	51	344	36	265
	28	10	31.5	106	0.28	3179	65.1	126	65	102	36	-56	165	50	121	36	100

Table H-8 Summary of Results – Simply-Supported RC T-shape Beam (Continued)

beam no.	no. of bottom bars	location ft	d _v in	V _u kips	v _u ksi	M _u k ft	aashto standard		aashto lrfd			proposal		csa			r2k
							V _c kips	$\rho_v f_y$ psi	V _c kips	$\rho_v f_y$ psi	θ deg	V _c kips	$\rho_v f_y$ psi	V _c kips	$\rho_v f_y$ psi	θ deg	$\rho_v f_y$ psi
6	28	2.9	31.5	237	0.627	734	65.1	472	71	311	31	56	550	79	289	32	245
	28	5	31.5	215	0.569	1208	65.1	414	71	271	31	56	485	71	273	33	220
	28	10	31.5	161	0.426	2148	65.1	271	68	198	34	-56	326	59	205	34	150
	28	15	31.5	107	0.283	2820	65.1	128	65	105	36	-56	168	53	113	35	95
	28	20	31.5	54	0.143	3223	65.1	50	65	77	36	-56	77	50	77	36	77
7	36	2.9	31.3	576	1.534	2069	61.3	1461	44	1145	36	55	1557	55	1074	35	1190
	-	-	-	-	-	-	-	-	-	-	-	-	-	-	-	-	-
	-	3.6	31.3	510	1.358	2449	61.3	1276	44	1004	36	55	1362	54	954	35	990
	36	5.4	31.3	340	0.905	3215	61.3	799	57	639	37	-55	859	51	616	36	620
	36	7.2	31.3	170	0.453	3674	61.3	322	63	249	37	-55	356	51	254	36	200
8	36	2.9	31.3	484	1.289	1615	61.3	1203	46	893	34	55	1285	62	834	34	830
	-	-	-	-	-	-	-	-	-	-	-	-	-	-	-	-	-
	36	5	31.3	378	1.006	2520	61.3	906	52	714	36	55	971	56	662	35	580
	36	7.5	31.3	252	0.671	3308	61.3	552	62	437	37	-55	599	52	422	36	380
	36	10	31.3	126	0.335	3780	61.3	199	65	147	36	-55	226	51	160	36	140
9	36	2.9	31.3	284	0.756	877	61.3	642	69	412	32	55	693	80	372	32	340
	36	5	31.3	257	0.684	1445	61.3	566	69	362	32	55	613	72	349	32	295
	36	10	31.3	193	0.514	2569	61.3	387	67	264	34	-55	424	60	266	34	200
	36	15	31.3	128	0.341	3371	61.3	204	65	152	36	-55	232	54	153	35	130
	36	20	31.3	64	0.17	3853	61.3	50	65	77	36	-55	77	52	77	36	77

Table H-9 Summary of Results – Continuous RC Rectangular Beam

beam no.	A _s in. ²	location ft	d _v in	V _u kips	v _u ksi	M _u k ft	aashto standard		aashto lrfd			proposal		csa			r2k
							V _c kips	ρ _v f _y psi	V _c kips	ρ _v f _y psi	θ deg	V _c kips	ρ _v f _y psi	V _c kips	ρ _v f _y psi	θ deg	ρ _v f _y psi
1	2.9	2.7	28.8	70	0.203	249	60	50	60	77	36	51	79	45	77	36	104
	2.9	3.6	28.8	54	0.157	307	60	50	60	77	36	51	77	44	77	37	77
	2.9	7.2	28.8	8	0.022	391	60	50	60	77	36	51	77	46	77	36	77
	2.9	10.8	28.8	70	0.202	251	60	50	60	77	36	51	77	45	77	36	104
	2.9	14.4	28.8	132	0.381	112	60	226	60	185	36	51	277	50	184	35	233
	5.3	15.3	28.8	148	0.428	242	60	273	60	223	36	51	328	47	234	36	333
2	2.9	2.7	28.8	47	0.135	140	60	50	64	77	34	51	77	60	77	33	77
	2.9	7.2	28.8	27	0.078	307	60	50	60	77	36	51	77	49	77	35	77
	2.9	14.4	28.8	4	0.011	391	60	50	60	77	36	51	77	47	77	36	77
	2.9	21.6	28.8	35	0.101	251	60	50	60	77	36	51	77	52	77	35	77
	2.9	28.8	28.8	66	0.191	112	60	50	69	77	31	51	77	70	77	32	77
	5.3	33.3	28.8	85	0.247	454	60	92	60	77	36	51	128	49	83	35	96
3	2.9	2.7	28.8	34	0.097	97	60	50	69	77	31	51	77	70	77	32	77
	2.9	10.8	28.8	18	0.052	307	60	50	60	77	36	51	77	50	77	35	77
	2.9	21.6	28.8	3	0.007	391	60	50	60	77	36	51	77	47	77	36	77
	2.9	32.4	28.8	23	0.067	251	60	50	64	77	34	51	77	54	77	34	77
	2.9	43.2	28.8	44	0.127	112	60	50	69	77	31	51	77	80	77	31	77
	5.3	51.3	28.8	59	0.172	532	60	50	60	77	36	51	77	48	77	35	77
4	4.2	2.7	28.8	101	0.293	358	60	138	60	112	36	51	178	46	131	36	158
	4.2	3.6	28.8	78	0.226	441	60	71	60	77	36	51	104	44	80	37	138
	4.2	7.2	28.8	11	0.032	562	60	50	60	77	36	51	77	46	77	36	77
	4.2	10.8	28.8	100	0.29	361	60	135	60	110	36	51	176	45	129	36	158
	4.2	14.4	28.8	189	0.548	161	60	393	61	297	34	51	462	51	309	35	333
	7.9	15.3	28.8	213	0.615	348	60	460	57	391	37	51	537	48	377	36	396

Table H-9 Summary of Results – Continuous RC Rectangular Beam (Continued)

beam no.	A _s in. ²	location ft	d _v in	V _u kips	v _u ksi	M _u k ft	aashto standard		aashto lrfd			proposal		csa			r2k
							V _c kips	ρ _v f _y psi	V _c kips	ρ _v f _y psi	θ deg	V _c kips	ρ _v f _y psi	V _c kips	ρ _v f _y psi	θ deg	ρ _v f _y psi
5	4.2	2.7	28.8	67	0.194	201	60	50	64	77	34	51	77	60	77	33	77
	4.2	7.2	28.8	39	0.113	441	60	50	60	77	36	51	77	49	77	35	77
	4.2	14.4	28.8	6	0.016	562	60	50	60	77	36	51	77	47	77	36	77
	4.2	21.6	28.8	50	0.145	361	60	50	60	77	36	51	77	52	77	35	77
	4.2	28.8	28.8	95	0.274	161	60	119	69	77	31	51	158	71	77	32	108
	7.9	33.3	28.8	123	0.355	654	60	200	60	164	36	51	248	50	164	35	133
6	4.2	2.7	28.8	48	0.14	139	60	50	69	77	31	51	77	70	77	32	77
	4.2	10.8	28.8	26	0.075	441	60	50	60	77	36	51	77	50	77	35	77
	4.2	21.6	28.8	4	0.011	562	60	50	60	77	36	51	77	47	77	36	77
	4.2	32.4	28.8	33	0.097	361	60	50	64	77	34	51	77	54	77	34	77
	4.2	43.2	28.8	63	0.183	161	60	50	69	77	31	51	77	81	77	31	77
	7.9	51.3	28.8	86	0.248	765	60	93	60	77	36	51	128	50	82	35	88
7	5.5	2.7	28.8	129	0.374	457	60	219	60	179	36	51	269	46	195	36	213
	5.5	3.6	28.8	100	0.289	564	60	134	60	109	36	51	174	45	130	36	183
	5.5	7.2	28.8	14	0.041	718	60	50	60	77	36	51	77	47	77	36	77
	5.5	10.8	28.8	128	0.371	462	60	216	60	177	36	51	265	46	193	36	208
	5.5	14.4	28.8	242	0.701	205	60	546	59	424	35	51	632	53	420	35	479
	10.5	15.3	28.8	272	0.786	445	60	631	56	543	37	51	727	49	505	35	521
8	5.5	2.7	28.8	86	0.248	257	60	93	64	77	34	51	129	60	77	33	99
	5.5	7.2	28.8	50	0.144	564	60	50	60	77	36	51	77	49	77	35	77
	5.5	14.4	28.8	7	0.021	718	60	50	60	77	36	51	77	47	77	36	77
	5.5	21.6	28.8	64	0.185	462	60	50	60	77	36	51	77	52	77	35	77
	5.5	28.8	28.8	121	0.35	205	60	195	69	111	31	51	242	72	97	32	150
	10.5	33.3	28.8	157	0.454	835	60	299	58	250	37	51	358	51	236	35	196

Table H-9 Summary of Results – Continuous RC Rectangular Beam (Continued)

beam no.	A _s in. ²	location ft	d _v in	V _u kips	v _u ksi	M _u k ft	aashto standard		aashto lrfd			proposal		csa			r2k
							V _c kips	$\rho_v f_y$ psi	V _c kips	$\rho_v f_y$ psi	θ deg	V _c kips	$\rho_v f_y$ psi	V _c kips	$\rho_v f_y$ psi	θ deg	$\rho_v f_y$ psi
9	5.5	2.7	28.8	62	0.179	177	60	50	69	77	31	51	77	70	77	32	77
	5.5	10.8	28.8	33	0.096	564	60	50	60	77	36	51	77	51	77	35	77
	5.5	21.6	28.8	5	0.014	718	60	50	60	77	36	51	77	47	77	36	77
	5.5	32.4	28.8	43	0.124	462	60	50	64	77	34	51	77	55	77	34	77
	5.5	43.2	28.8	81	0.234	205	60	79	69	77	31	51	113	82	77	31	79
	10.5	51.3	28.8	109	0.316	978	60	161	60	132	36	51	205	51	131	35	125

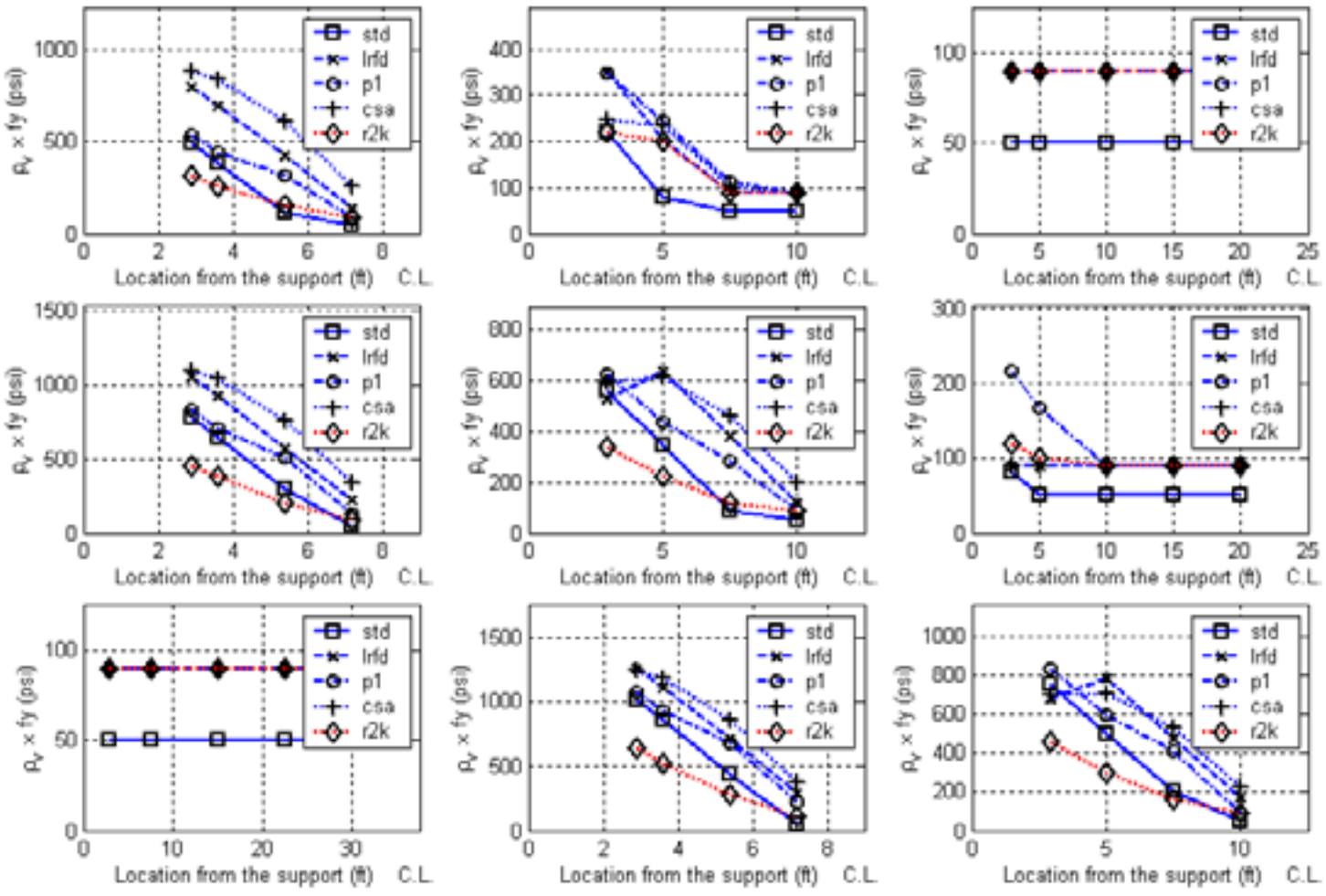


Figure H-2 Comparisons of Required Shear Reinforcement (Simply-Supported I Beam)

Beam Number		
1	2	3
4	5	6
7	8	9

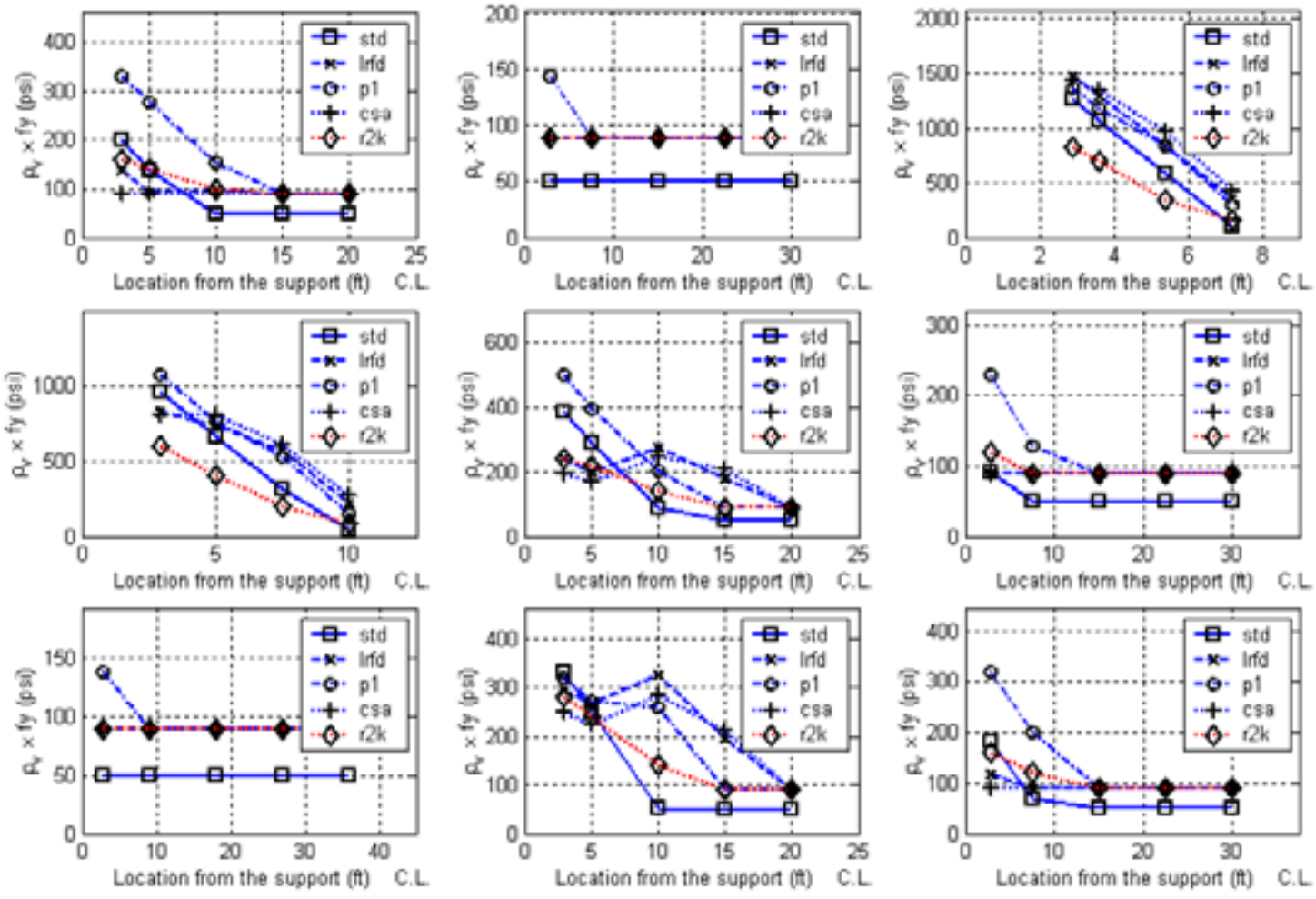
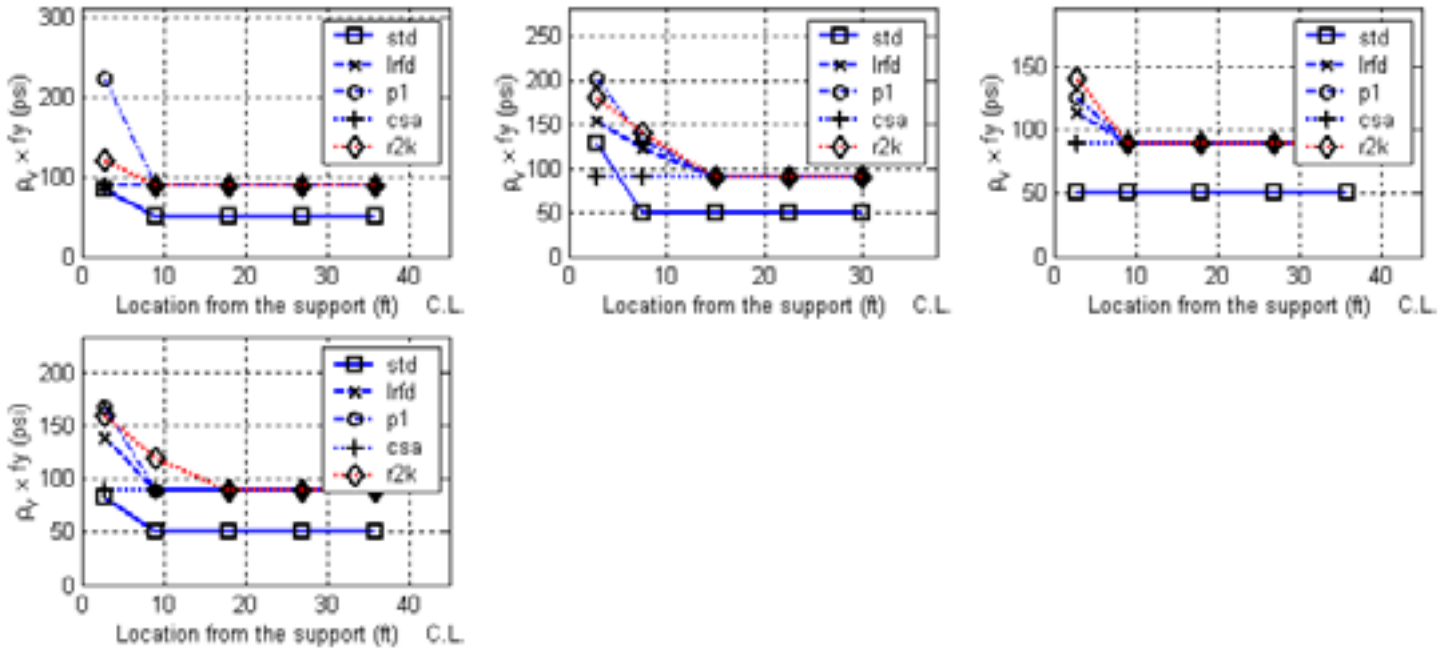


Figure H-2 Comparisons of Required Shear Reinforcement (Simply-Supported I Beam) -continued

Beam Number		
10	11	12
13	14	15
16	17	18



Beam Number		
19	20	21
22		

Figure H-2 Comparisons of Required Shear Reinforcement (Simply-Supported I Beam) -continued

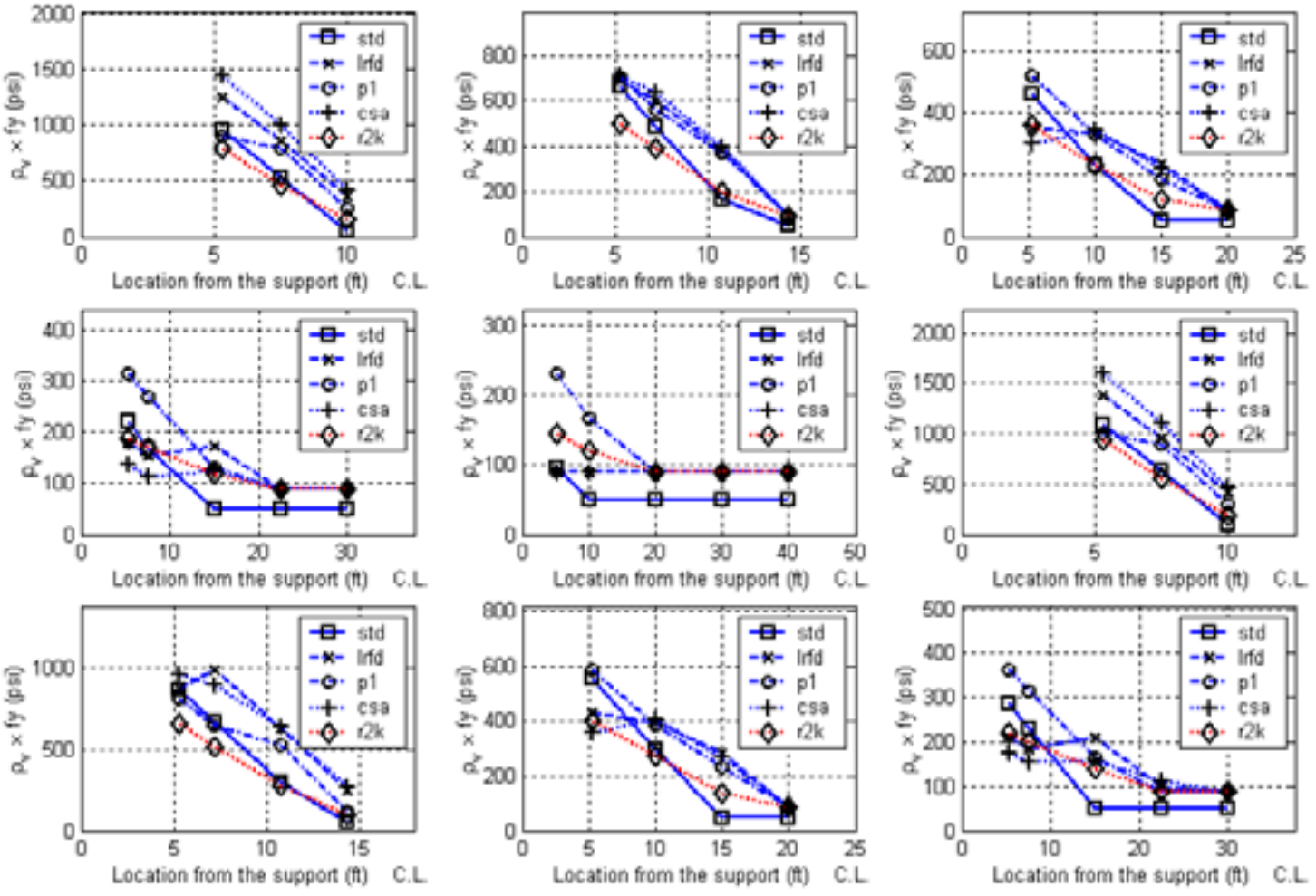
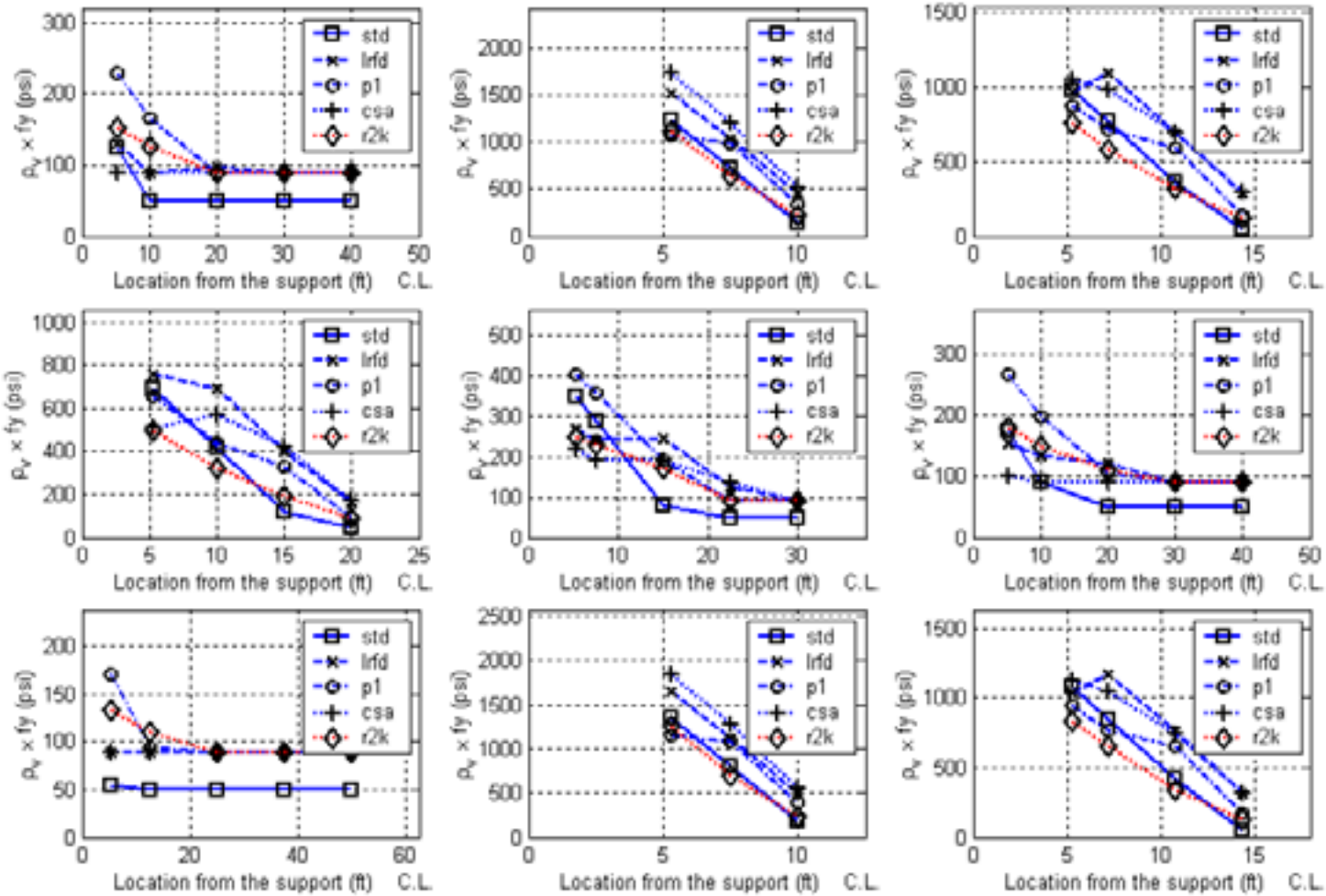


Figure H-3 Comparisons of Required Shear Reinforcement (Simply-Supported Bulb-T)

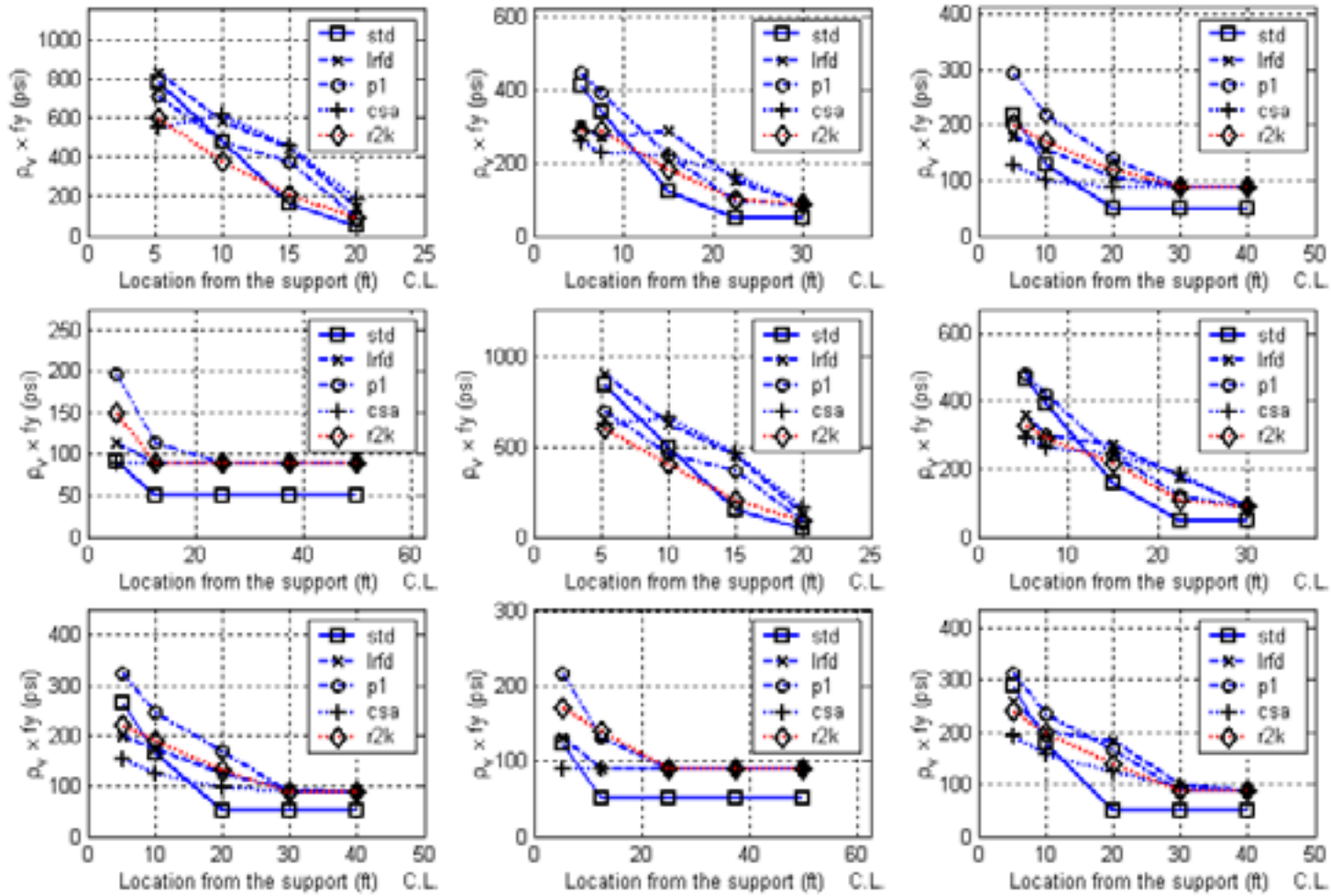
Beam Number

1	2	3
4	5	6
7	8	9



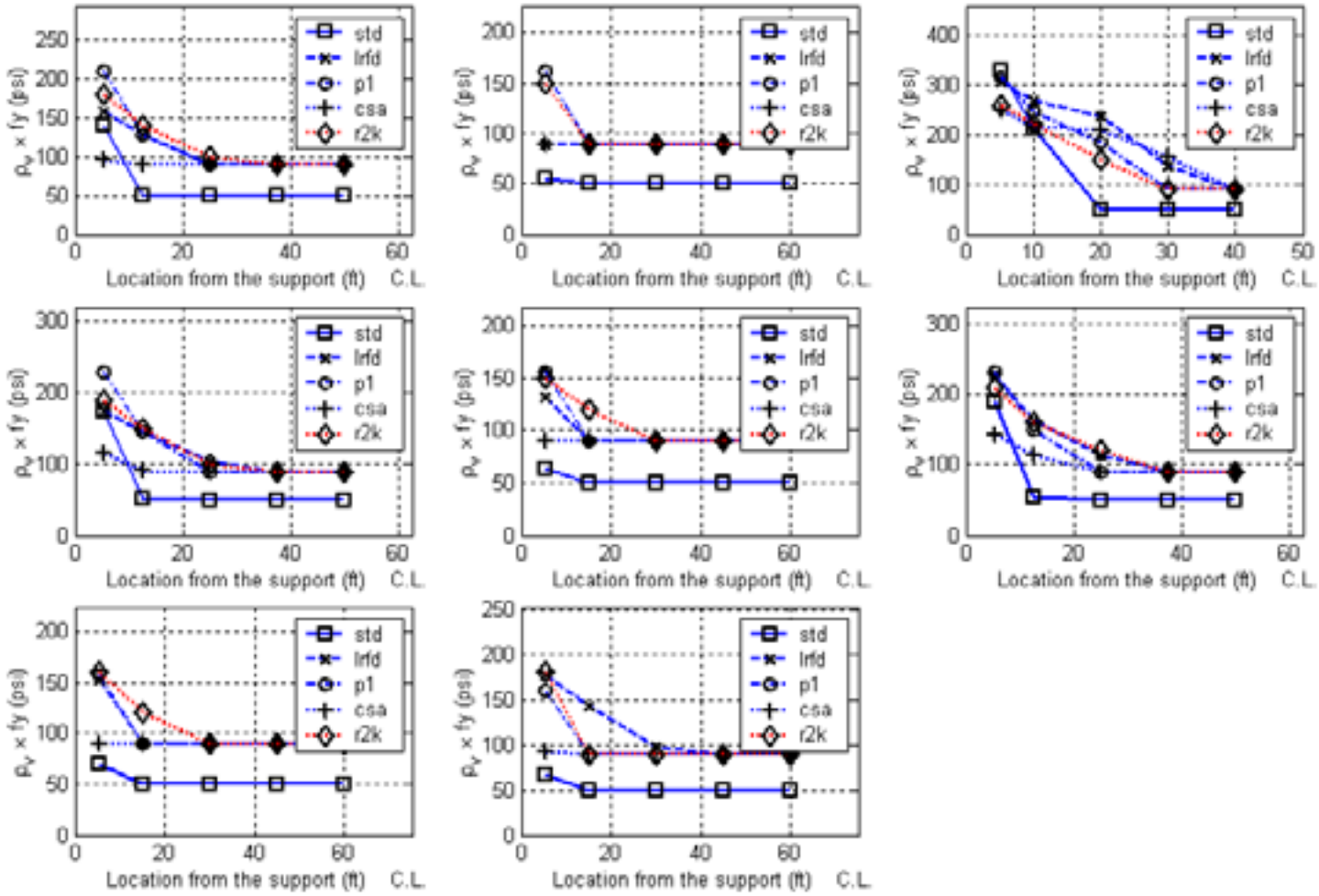
Beam Number		
10	11	12
13	14	15
16	17	18

Figure H-3 Comparisons of Required Shear Reinforcement (Simply-Supported Bulb-T) -continued



Beam Number		
19	20	21
22	23	24
25	26	27

Figure H-3 Comparisons of Required Shear Reinforcement (Simply-Supported Bulb-T) -continued



Beam Number		
28	29	30
31	32	33
34	35	

Figure H-3 Comparisons of Required Shear Reinforcement (Simply-Supported Bulb-T) –continued

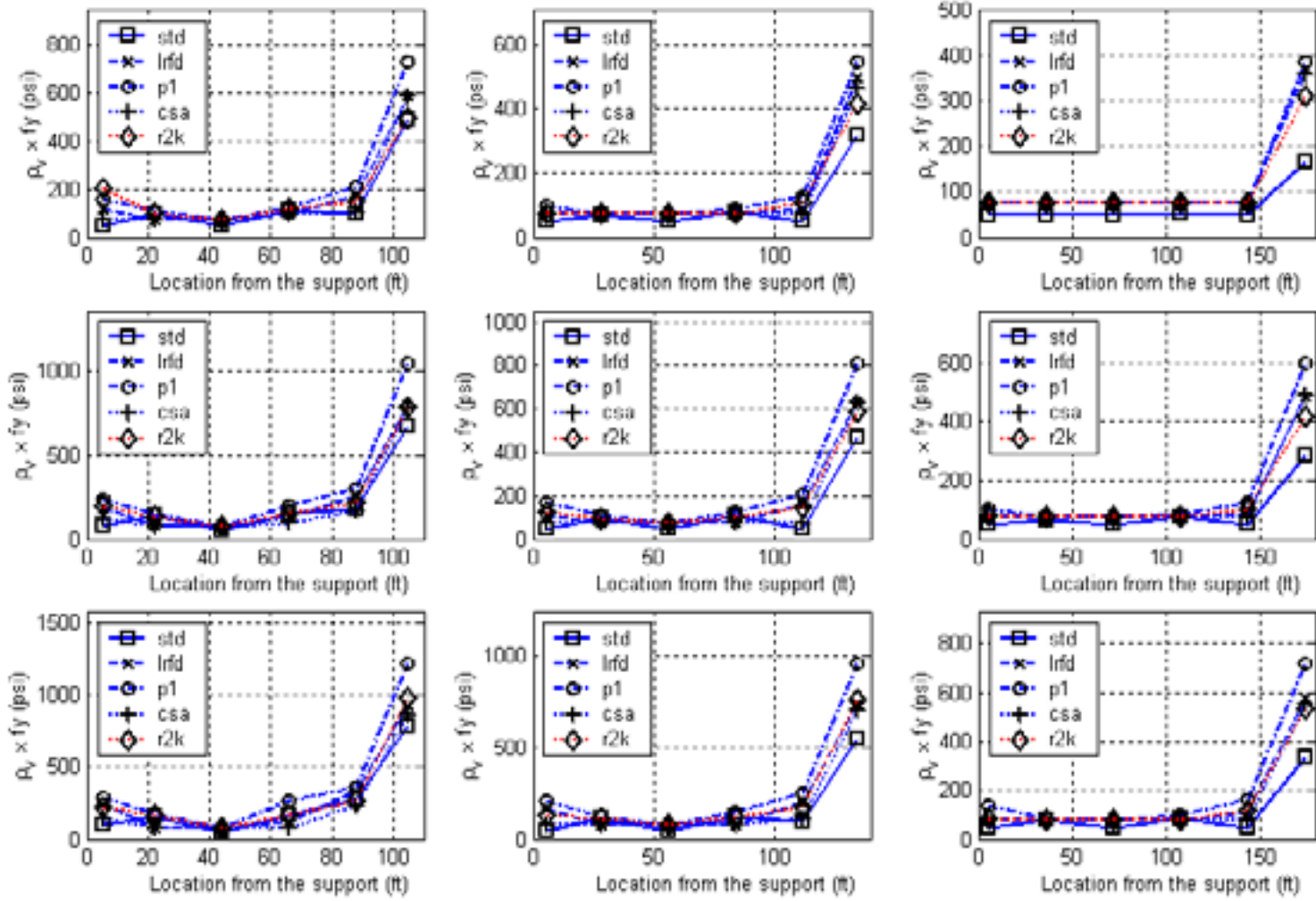
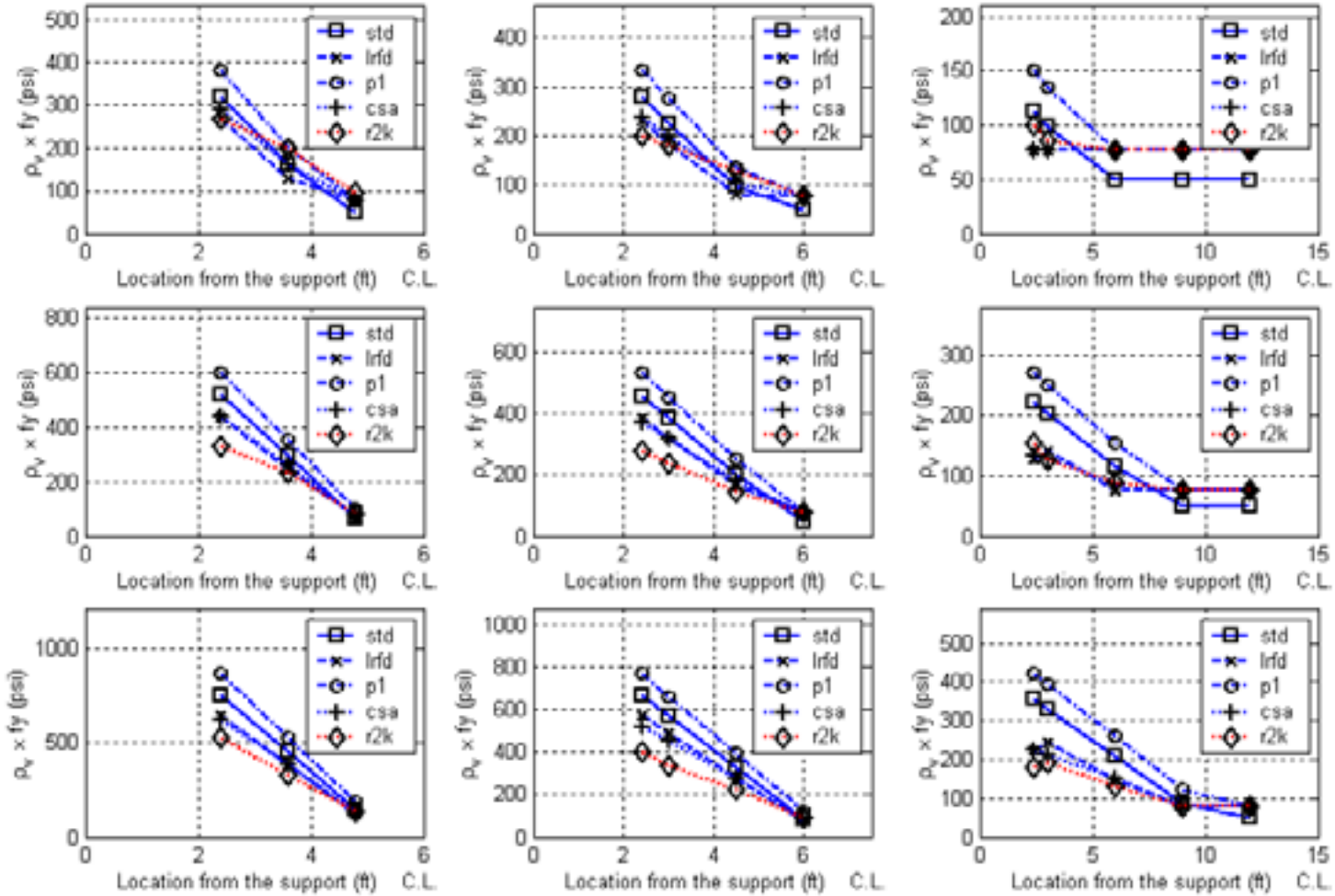


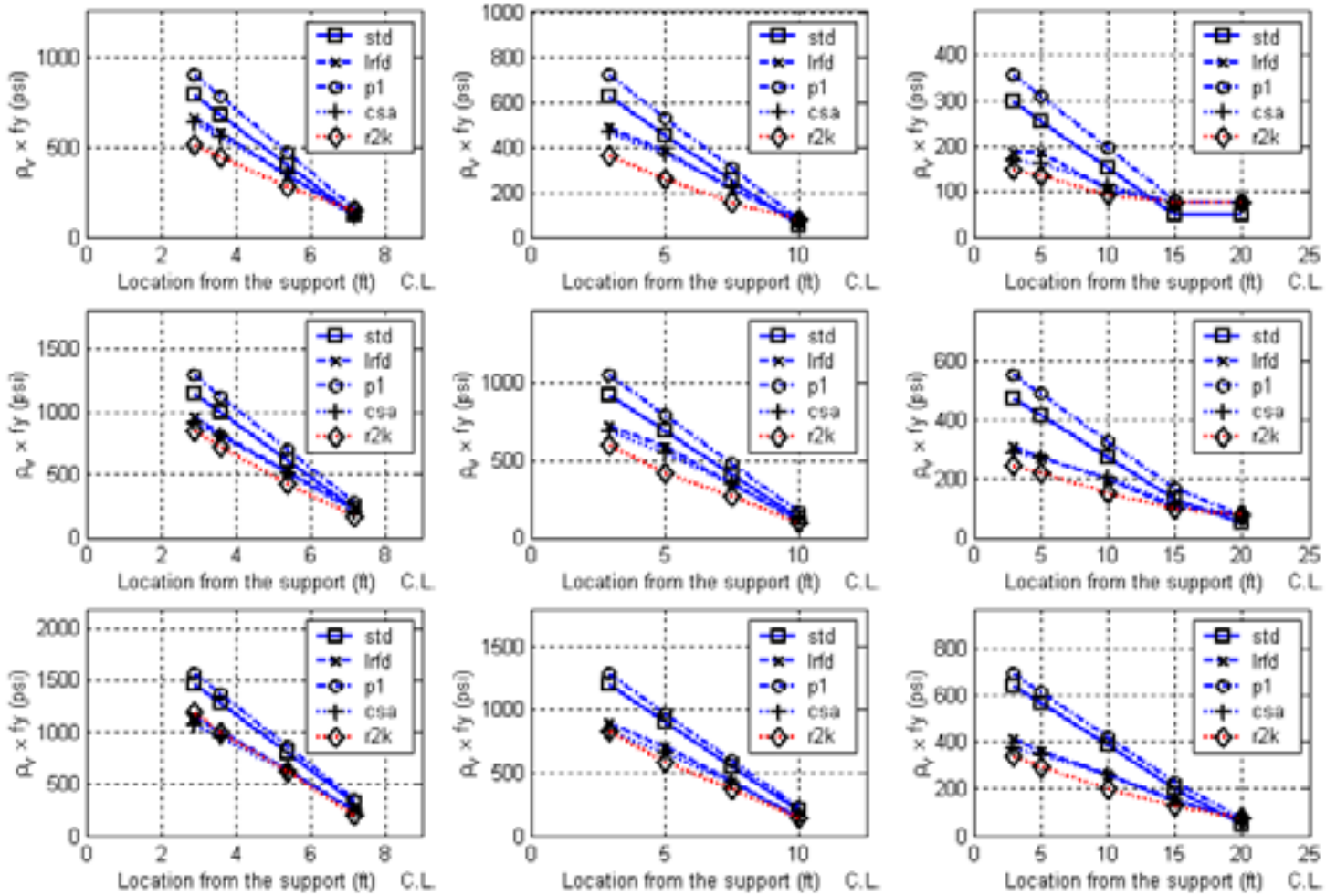
Figure H-4 Comparisons of Required Shear Reinforcement (Continuous Box Beam)

Beam Number		
1	2	3
4	5	6
7	8	9



Beam Number		
1	2	3
4	5	6
7	8	9

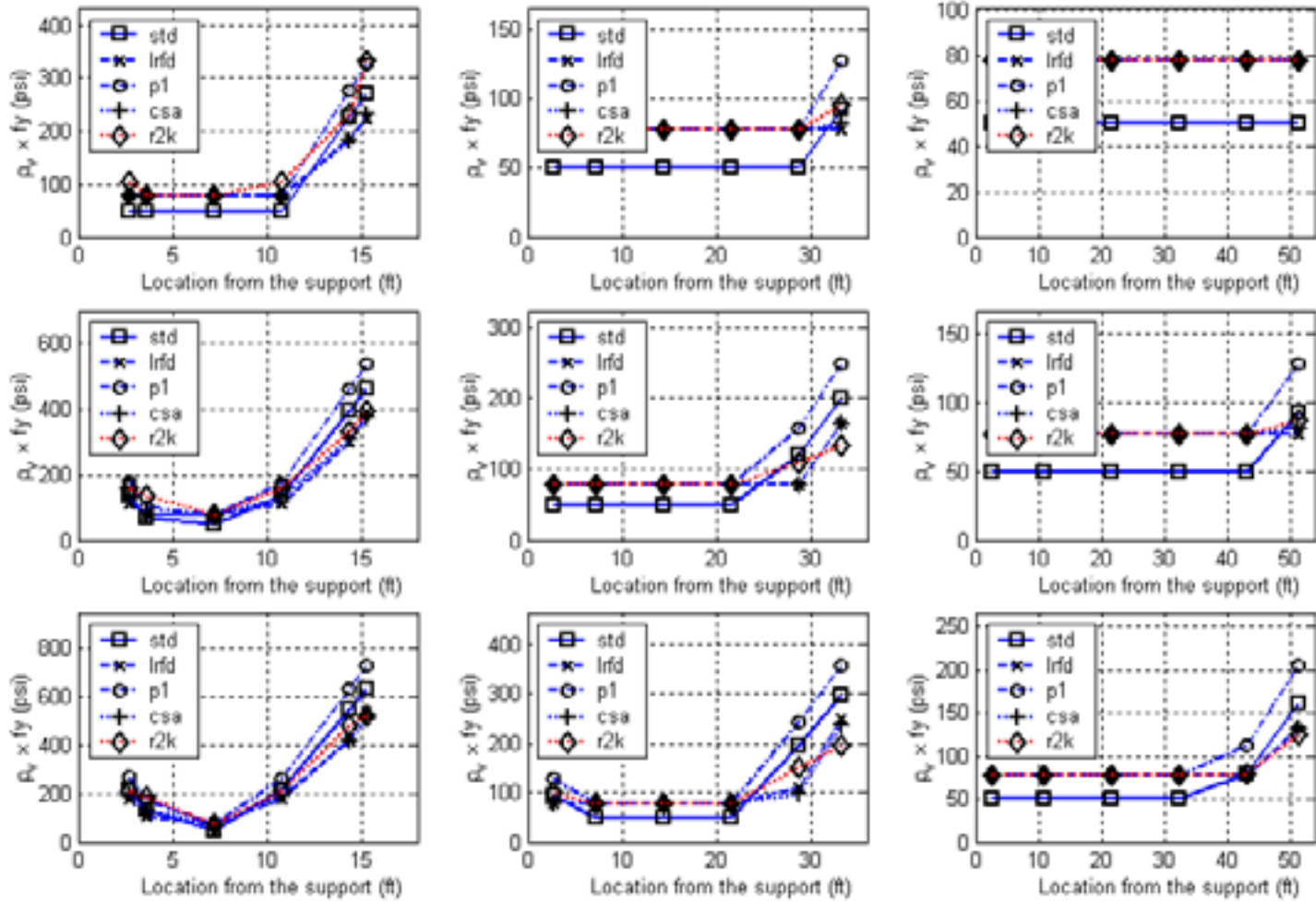
Figure H-5 Comparisons of Required Shear Reinforcement (Simply-Supported RC Rectangular Beam)



Beam Number

1	2	3
4	5	6
7	8	9

Figure H-6 Comparisons of Required Shear Reinforcement (Simply-Supported RC T-shape Beam)



Beam Number

1	2	3
4	5	6
7	8	9

Figure H-7 Comparisons of Required Shear Reinforcement Amounts (Continuous RC Rectangular Beam)

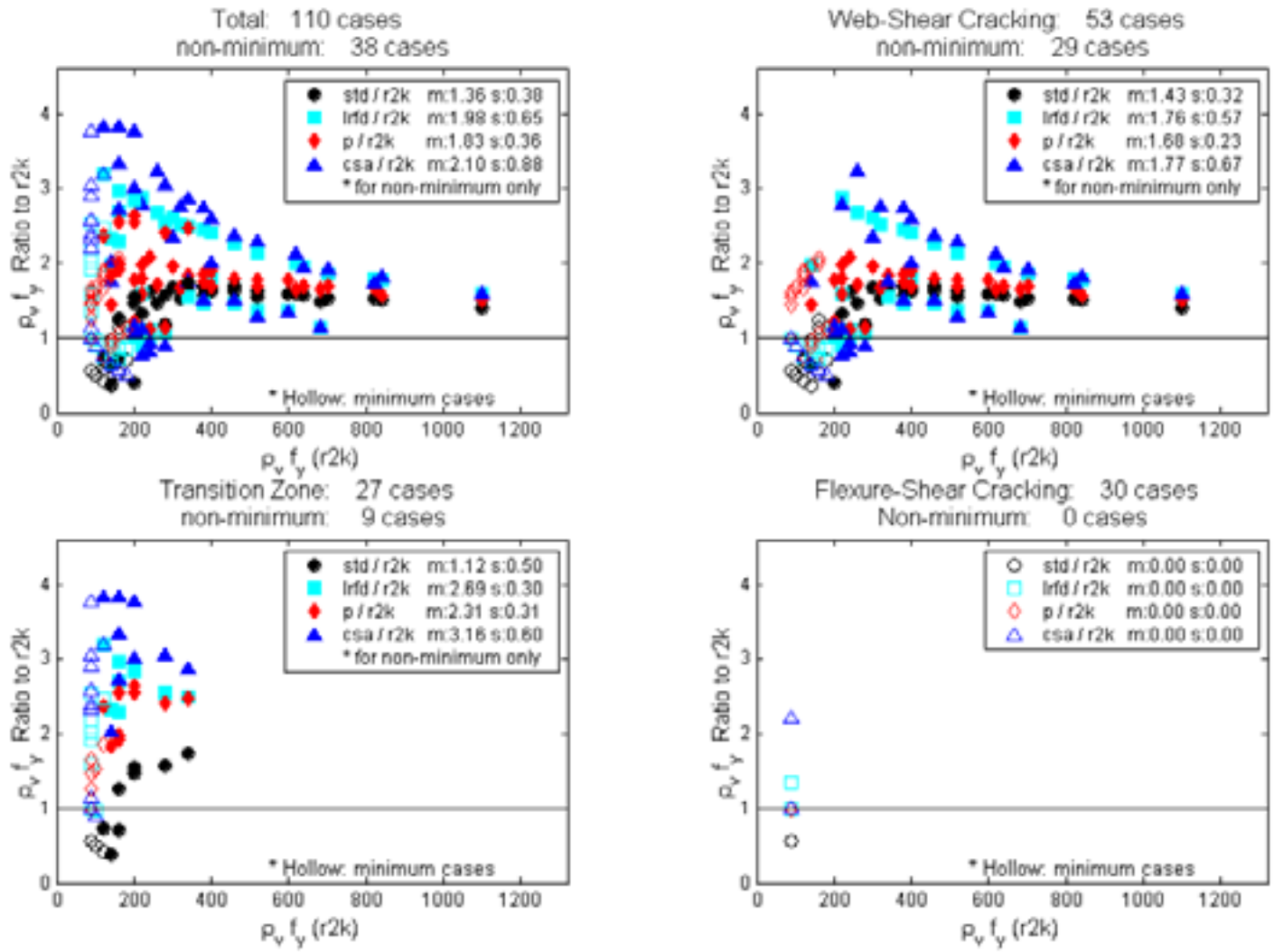


Figure H-8 I-Beams

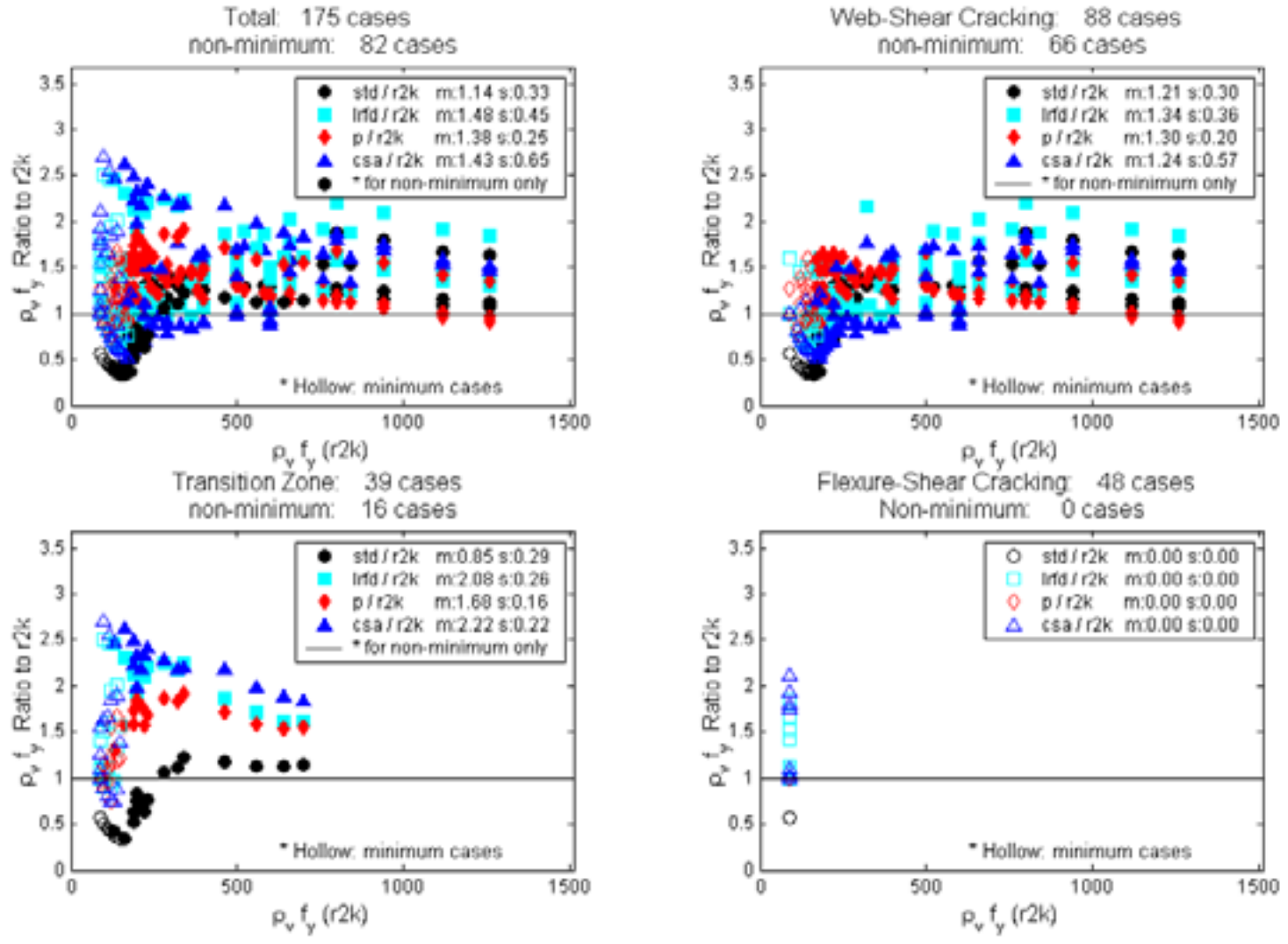


Figure H-9 Bulb-T Girders

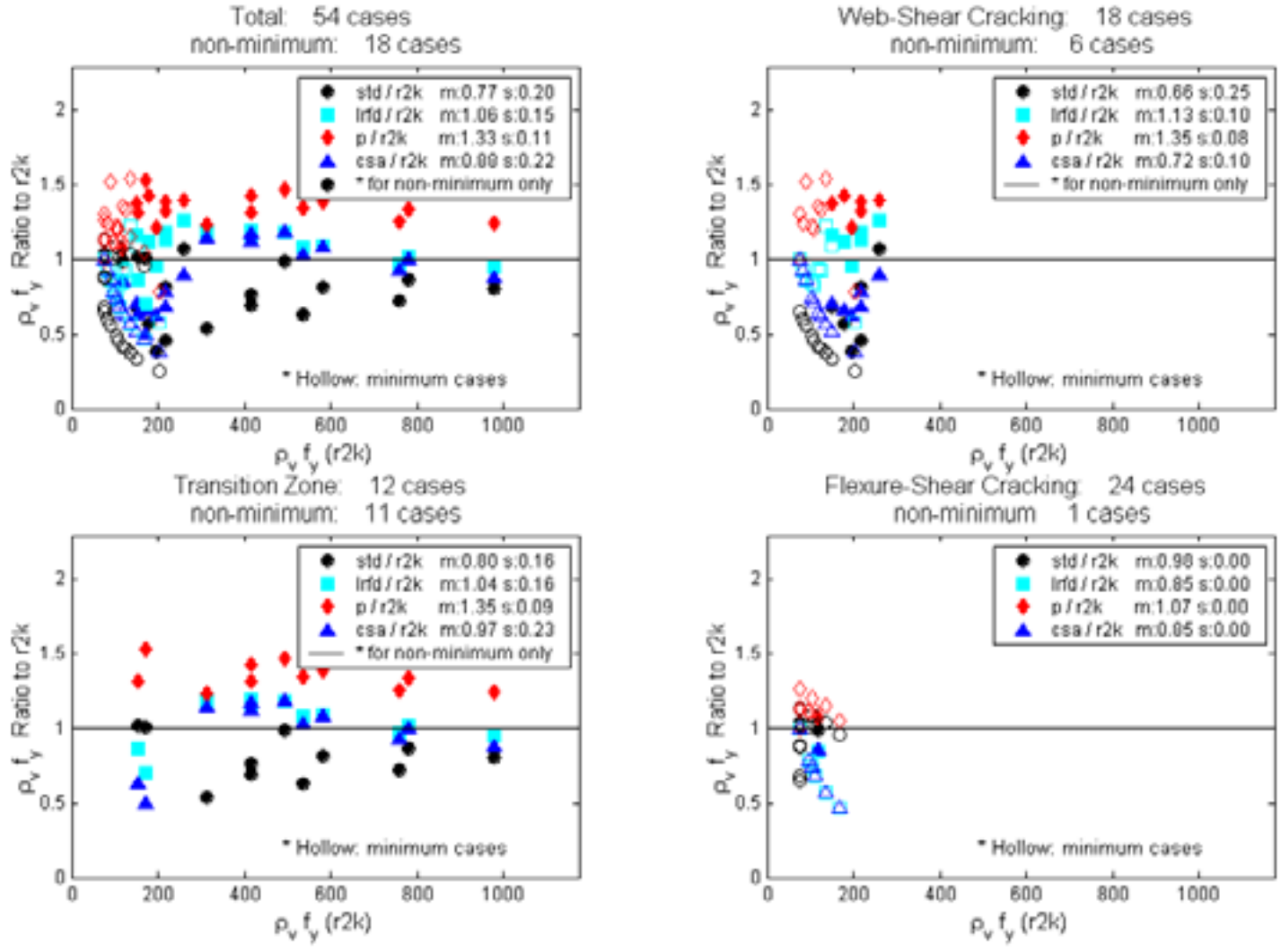


Figure H-10 Box Girders

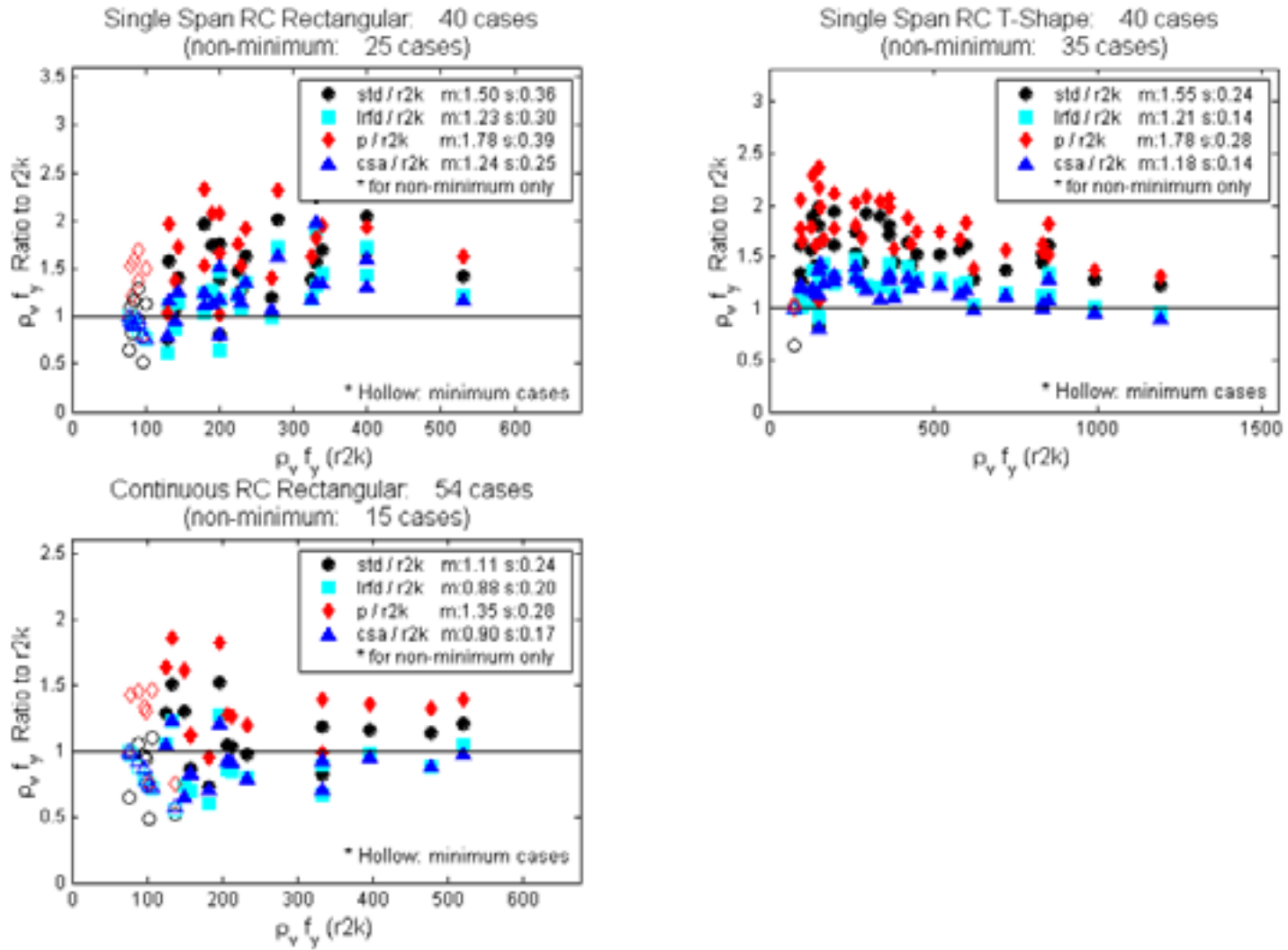


Figure H-11 RC Beams

Appendix I: Utilization of the Process 12-50

I.1 Application of the Process 12-50 to the Design Database

The Process 12-50 is a standardized pre-/post- process that can be used to generate inputs for various computational processes (CPs) (programs, spreadsheets, etc) and to compare the results of the CPs by importing them into a common viewer (e.g. NCHRP Viewer).

To apply the Process 12-50 to the completion of the NCHRP 12-61 project, the Design Databases were stored in the tables of Microsoft Access Database files so that the NCHRP Viewer could display them immediately on its window. The Non Automated Comparison procedure in the NCHRP 12-50 final report was adopted.

The data flow and processing procedures are summarized in Fig. I-1; **First**, input data was generated including member dimensions, number of strands or conventional reinforcing bars, span length, etc. For this step, a spreadsheet was used to aid in member selection and satisfaction of flexural design requirements that extreme fiber stresses should not exceed the allowable stress limits for transfer and service states. **Second**, computations were performed. The input data obtained in the first step were copied and pasted into a spreadsheet to calculate the amount of required shear reinforcement in accordance with the selected approaches. Conventional methods were used to generate the outputs for RESPONSE 2000 program. **Third**, an ASCII output was generated in a standardized format. The NCHRP Viewer requires an output of 8 tables designated as *POI (Point-Of-Interest)*, *ReportIDs*, *Results*, *SpecArticles*, *SpecVersion*, *SubReport*, *tblProcesses*, and *Units*. Among these tables, a user can generate or modify several tables, such as the *POI* and *Results* tables, depending on the user's objectives. The *POI* table, shown as box five in Fig. I-1 contains information about each point of interest. For box four of Fig. I-1 the first column indicates the Bridge ID. The second column, the Process ID, indicates a shear design approach that is associated with a computational process in the original NCHRP 12-50 test cases. Table I-1 includes the Process ID numbers and the corresponding design approaches. The third column in box four, ReportID, indicates the type of data reported. The Report IDs differ from those in the NCHRP 12-50 final report. The Report IDs are summarized in Table I-3. The sixth column, SubdomainID, indicates the test suite for which the results were created. Table I-2 contains the descriptions of the subdomains and the number of Design Database cases. The *Results* table contains information about computational outputs. **Fifth**, the Microsoft Access program is opened and the tables newly produced imported. For this step, the *tblProcesses* table was modified with the information of the shear design approaches as summarized in Table I-4. Results are saved as **.mdb and the Access program closed. Finally, the NCHRP Viewer is run by opening the **.mdb file and selecting the Process (Design Approach) ID of interest.

I.2 Installation of Program and Copy of Database

Detailed information about the members used in the Design Database can be viewed using the enclosed program *NCHRP Viewer*. Instructions for the installation of this program are provided below:

- (1) Copy all files under the directory of *D:\NCHRP12-61\Design_database\NCHRP Data Viewer* to your hard disk.
- (2) Double Click **setup.exe**.
- (3) Copy all files under the directory of *D:\NCHRP12-61\Design_database\Database* to your hard disk.
- (4) Run **NCHRP Viewer**.

I.3 How to View Design Database Using NCHRP Viewer

The Design Database results are stored in two mdb files; i.e., DesignDatabaseI.mdb and DesignDatabaseII.mdb. The former contains results for simply-supported members and the latter contains results for continuous members. The following is an explanation of how to view the Design Database results using the NCHRP Viewer.

- (1) Open the NCHRP Viewer.
- (2) Click File/Open on the menu bar on the left top corner.
- (3) Double-click DesignDatabaseI.mdb or DesignDatabaseII.mdb for simply-supported members or continuous members, respectively.
- (4) Click on the desired process and then on the click OK button. Processes (1) through (5) will show the amount of required shear reinforcement calculated in accordance with each stated design approach. Make a multiple choice among these. For comparisons of the five approaches, click (1) through (5). Process (6) will show all necessary information of the design sections for shear design such as beam dimensions, number of strands, effective prestressing force after all loss, etc. To view this item, click (6) only.
- (5) Make a choice in the scrolls such as ReportID, SubdomainID, BridgeID, etc.
- (6) Finally, click 'View Data' button on the upper and right side of the screen to display the data in tabular form

Fig. I-2 is a screen shot of the NCHRP Viewer window showing the required amounts of shear reinforcement calculated in accordance with the 2004 AASHTO LRFD Specifications, the AASHTO Standard Specifications, the proposed simplified method, the 2004 CSA method, and the RESPONSE 2000 program.

In Fig. I-2, the different components of the NCHRP Viewer are designated by letters A through D. The four components are as follows:

A. A dropdown list used to select the database that is displayed. The user can specify the Report ID, the Subdomain ID and the Bridge ID for the desired graph.

B. View Data Buttons. The 'Copy to Clipboard' button allows the user to copy the current graph appearing on the screen to the clipboard. The 'View Data' button opens another window and tabulates the graph data.

C. Graph window.

D. Specification information grid. This grid displays the specification numbers and descriptions as related to the Report ID currently showing on the screen. This option has not been implemented for the Design Database.

NCHRP 12-50 Glossary:

Subdomain – A subset of the entire test suite, so subdivided to create a more manageable set of data. The subdomain contains a set of data in the test suite representing a specific area of the specifications. (e.g., distribution factor subdomain, dead load, HL 93 load effects, stresses, etc.)

Bridge ID – A unique numerical value used to reference (tag) a specific bridge.

Computational Process (CP) – a unique method of computation. CPs can be software, hand calculations, or a set of examples from a published source.

Process ID – A unique numerical value used to reference a computational process that created a result. Unique Process ID's will be provided for different versions of the same computer program.

Report ID – A unique numerical value used to reference (tag) a single computational result, which may be from analysis, resistance computations, loads, or a specification value, and is a potential output item from one or more processes as defined above.

Location – Physical location along the structure.

Value – Value of the data.

Location ID – This field defines the type of point at *Location*

Table I-1. Process ID Table (Design Approaches)

Process ID	Design Approaches	Version
1	AASHTO Standard Specifications	2000 Interim
2	AASHTO LRFD Specifications	2004
3	Canadian Code	2004 CSA A23.3
4	Proposal	2004
5	RESPONSE 2000	1.0.5

Table I-2 NCHRP 12-61 Subdomain Content

Subdomain ID	Description	No. of members in Subdomain Test Suite
100	Composite Prestressed I-Sections	22 Simple span
101	Composite Prestressed Bulb T Sections	35 Simple span
102	Composite Reinforced Concrete Sections	9 Simple span
103	Non-Composite Reinforced Concrete Sections	9 Simple span
104	Non-Composite Reinforced Concrete Sections	9 Continuous span
105	Non-Composite Post-tensioned Box Sections	9 Continuous span

Table I-3 NCHRP 12-61 ReportIDs

ReportID	Stage	Description 1	Description 2	Description 3	Description 4	Description 5	Unit
60000		sectional height	h	in	Composite		
60001		web width	bw	in			
60002		moment of inertia	I _g	in ⁴	Beam only		
60003		distance from centroidal axis of gross section neglecting reinforcement to extreme fiber in tension	y _t	in	Beam only		
60004		gross area of section	A _g	in ²	Beam only		
60005		effective width	b _{eff}	in			
60006		flange thickness	t _f	in	slab thickness		
60007		area of nonprestressed tension reinforcement	A _s	in ²			
60008		distance from extreme compression fiber to centroid of prestressed reinforcement	d _s	in			
60009		area of prestressed reinforcement in tension zone	A _p	in ²			
60010		area of total prestressed reinforcement	A _{pa}	in ²			
60011		distance from extreme compression fiber to centroid of prestressed reinforcement in tension zone	d _p	in			
60012		distance from extreme compression fiber to centroid of total prestressed reinforcement	d _{ps}	in			
60013		effective steel prestress after losses	f _{se}	ksi			
60014		specified compressive strength of concrete	f _{cp}	ksi	Beam only		
60015		specified compressive strength of concrete	f _{cp_s}	ksi	Slab		

ReportID	Stage	Description 1	Description 2	Description 3	Description 4	Description 5	Unit
60016		factored axial load normal to cross section occurring simultaneously with V_u	N_u	kips			
60017		factored shear force at section	V_u	kips			
60018		shear force at section due to unfactored dead load	V_d	kips			
60019		vertical component of effective prestress force at section	V_p	kips			
60020		factored moment at section	M_u	k-ft			
60021		moment due to dead load	M_d	k-ft			
60022		distance from end support	x	ft			
60023		span length	L	ft			
60024		angle of inclination of diagonal compressive stresses to the longitudinal axis of the member	theta	deg			
60025		factor accounting for shear resistance of cracked concrete	beta	-			
65001		N/A	location	ft			
65002		N/A	Span	ft			
65003		effective depth or distance from the top fiber to the centroid of tension steel including prestressed steel	d_e	in			
65004		effective shear depth taken as the greater of $0.9d$ or $0.72h$	d_v	in			
65005		distance from extreme compression fiber to centroid of longitudinal tension reinforcement but need not be less than $0.8h$ for circular sections and pre-stressed members	d	in			
65006		distance from bottom fiber to center of gravity of the section	y_b	in			

ReportID	Stage	Description 1	Description 2	Description 3	Description 4	Description 5	Unit
65007		gross area of section	Agc	in ²	Composite		
65008		moment of inertia of gross composite section	Igc	in ⁴	Composite		
65009		distance from bottom fiber to center of gravity of the composite section	ybc	in	Composite		
65010		eccentricity of design load or prestressing force parallel to axis measured from the centroid of the section	e	in	Beam only		
65011		distance of composite section centroid from the centroid of precast unit	c	in	Composite		
65012		area of concrete on flexural tension side of member	Act	in ²			
65013		N/A	dcr	in			
65014		N/A	UncrA	in ²			
65015		modulus of elasticity of concrete	Ec	in ⁴			
65016		N/A	rho_s	-			
65017		specified yield strength of nonprestressed reinforcement	fy	psi			
65018		modulus of elasticity of nonprestressed reinforcement	Es	ksi			
65019		specified tensile strength of prestressing tendons	fpu	ksi			
65020		specified yield strength of prestressing tendons	fpy	ksi			
65021		modulus of elasticity of prestressing reinforcement	Ep	ksi			
65022		stress in the prestressing steel when the stress in the surrounding concrete is zero	fpo	ksi			
65023		effective stress in the prestressing steel after losses	fpe	ksi			
65024		compressive stress in concrete at centroid of cross section	fpc	ksi			

ReportID	Stage	Description 1	Description 2	Description 3	Description 4	Description 5	Unit
		resisting externally applied loads or at junction of web and flange when the centroid lies within the flange					
65025		stress due to unfactored dead load at extreme fiber of section where tensile stress is caused by externally applied loads	fd	ksi			
65026		effective prestressing force	Pe	kips			
65027		maximum aggregate size	ag	in			
65028		equivalent value of s_z which allows for influence of aggregate size	sz	in			
65029		crack spacing parameter	sz	in			
65030		factored shear force at section due to externally applied loads occurring simultaneously with M_{max}	V_i	kips			
65031		maximum factored moment at section due to externally applied loads	M_{max}	kip-ft			
65032		factored shear stress	v	psi			
65033		N/A	v/f_c	-			
65034		N/A	theta	deg			
65035		N/A	beta	-			
65036		N/A	ex	in/in			
65037		N/A	f_{pc}	ksi			
70000		N/A	x	ft			
70001		N/A	dv	in			
70002		N/A	V_u	k			
70003		N/A	v_u	ksi			

ReportID	Stage	Description 1	Description 2	Description 3	Description 4	Description 5	Unit
70004		cracking moment	Mcr	k_ft			
70005		N/A	Mu	k_ft			
70006		nominal shear strength provided by concrete when diagonal cracking results from combined shear and moment	Vci_std	k	AASHTO STANDARD		
70007		nominal shear strength provided by concrete when diagonal cracking results from excessive principal tensile stress in web	Vcw_std	k	AASHTO STANDARD		
70008		amount of required shear reinforcement	pvfy_std	psi	AASHTO STANDARD		
70009		nominal shear resistance provided by tensile stresses in the concrete	Vc_lrfd	k	AASHTO LRFD		
70010		amount of required shear reinforcement	pvfy_lrfd	psi	AASHTO LRFD		
70011		angle of inclination of diagonal compressive stresses to the longitudinal axis of the member	theta_lrfd	deg	AASHTO LRFD		
70012		nominal shear strength provided by concrete	Vc_p	k	Proposal		
70013		amount of required shear reinforcement	pvfy_p	psi	Proposal		
70014		angle of inclination of diagonal compressive stresses to the longitudinal axis of the member	theta_p	deg	Proposal		
70015		nominal shear strength provided by concrete	Vc_csa	k	CSA		
70016		amount of required shear reinforcement	pvfy_csa	psi	CSA		
70017		angle of inclination of diagonal compressive stresses to the longitudinal axis of the member	theta_csa	deg	CSA		
70018		shear strength when the first shear or flexure crack occurs	Vcr_r2k	k	R2K		

ReportID	Stage	Description 1	Description 2	Description 3	Description 4	Description 5	Unit
70019		amount of required shear reinforcement	pvfy_r2k	psi	R2K		
80000		amount of required shear reinforcement		psi			

Table I-4 tblTable Content

ProcessID	ProcessName	ExecutableName	ProcessAbbrev	Comments	Version	LegendText	SpecVersionID
1	AASHTO STANDARD	Standard	ST	Amount of required shear reinforcement			
2	AASHTO LRFD	LRFD	LR	Amount of required shear reinforcement			
3	Proposal	Proposal	PR	Amount of required shear reinforcement			
4	CSA	CSA	CS	Amount of required shear reinforcement			
5	RESPONSE2000	R2K	R2	Amnt of required shear reinforcement			
6	All Information	Spreadsheet	SS	For all information choose this only			

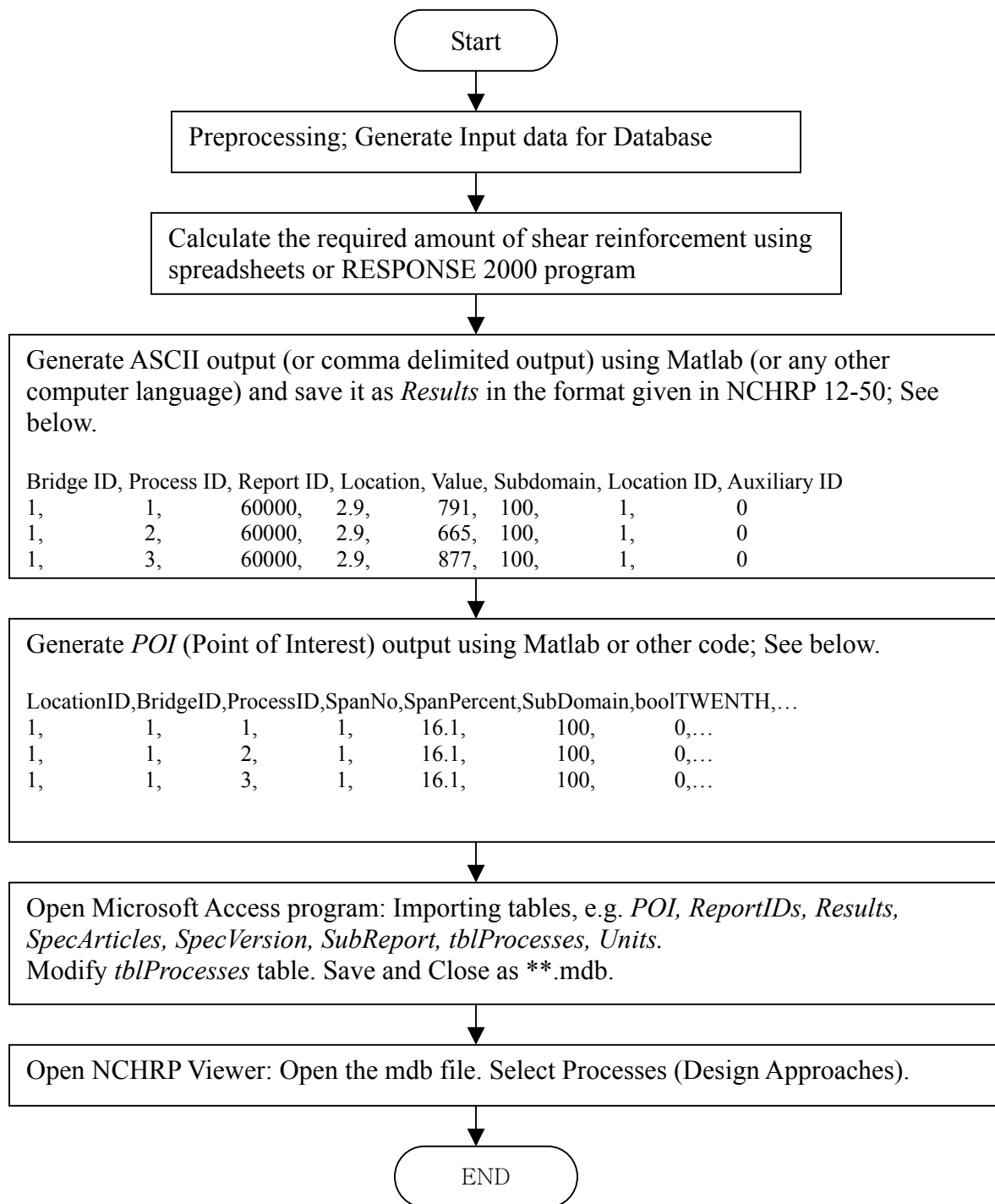


Figure I-1 Data Flow and Processing

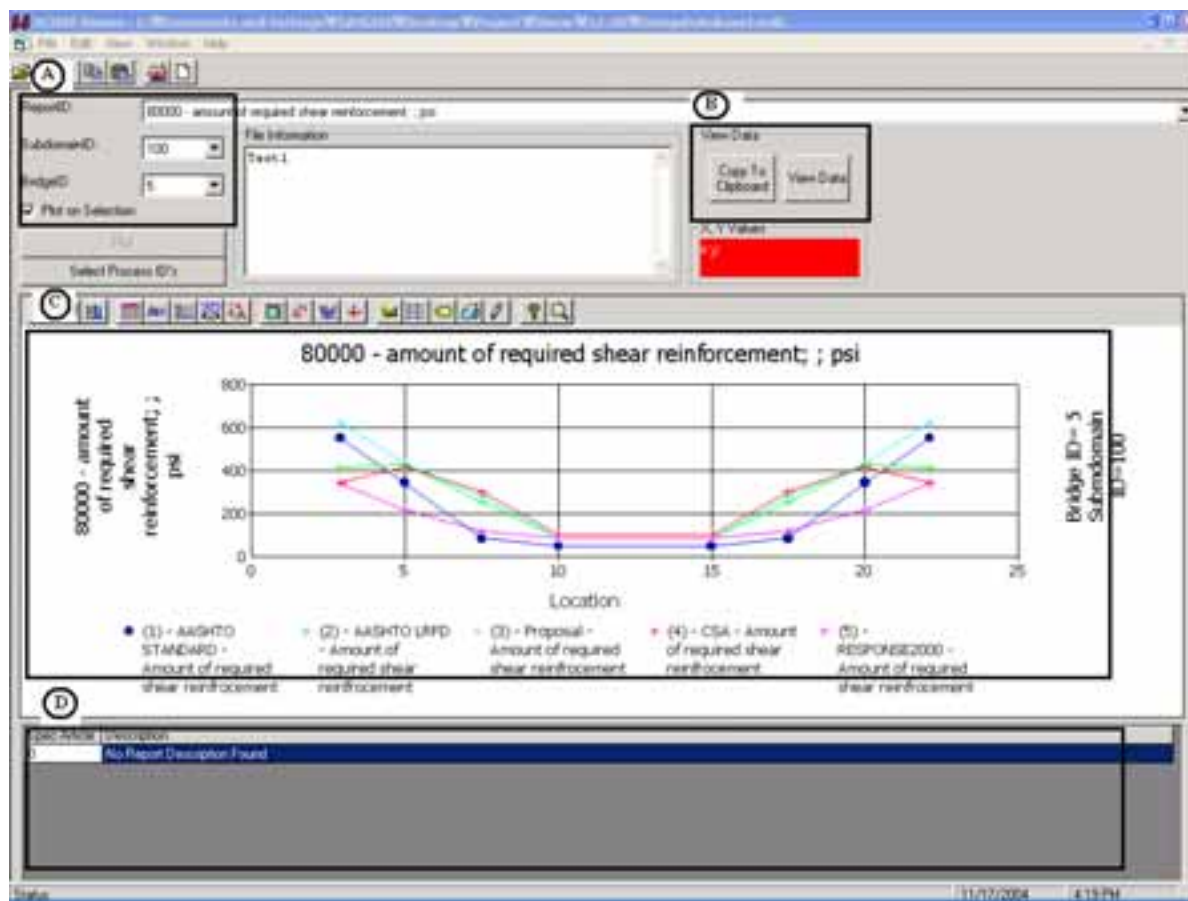


Figure I-2 NCHRP Viewer Window

Appendix J: Examples of Shear Design

The purpose of these design examples is to demonstrate the application of the shear design methods developed in Tasks 4 through 6, i.e., Proposal 1 (Modified STD Approach) and Proposal 2 (Modified CSA Approach). These design examples are based on real bridges that have been constructed, or on published design examples such as those in the PCI Bridge Design Manual.

These design examples show the shear design of three types of superstructure: simple-span non-composite precast pretensioned box beams with straight debonded strands, pretensioned I-beams with draped strands made continuous with unstressed reinforcement, and continuous cast-in-place post-tensioned box beams. The design examples also include the shear design of three types of non-prestressed substructure elements: cap beams, columns, and footings.

Section 5.8.3.2 of the AASHTO LRFD Specifications allows the location of the critical section for shear to be taken as the larger of $0.5d_v \cot(\theta)$ or d_v from the internal face of the support. However, the $0.5d_v \cot(\theta)$ value requires an initial assumption as to the value of theta and is therefore another drawback to use of the LRFD Sectional Design Model. In the following examples, the critical sections used are those used by the designers who provided the case studies on which these examples are based. The moments and shears acting at the specified critical sections are those calculated by the original designers.

J.1 Example 1: Precast, Pretensioned Non-Composite Box Beam

J.1.1 Example Description

This example demonstrates the shear design at a specific section of a 95-ft single-span AASHTO Type BIII-48 box beam bridge with no skew. The bridge is that of Example 9.2 of the PCI Bridge Design Manual. This non-composite pretensioned beam is 39-inch deep and simply supported. All strands are straight and some are debonded for a distance of 5ft from the end of the beam. The shear design is accomplished in accordance with the Proposal 1 (Modified STD Approach) and Proposal 2 (Modified CSA Approach).

J.1.2 Geometry and Loading

The beam is simply supported on a 95-ft single-span and is part of a bridge for which the superstructure consists of seven beams abutted as shown in Fig. J-1. The individual beams are transversely post-tensioned together to form the bridge through 8-in.-thick full-depth diaphragms located at quarter-points. The design live load is HL-93. As shown in Fig. J-2, the section at a distance of 42.74 in. from support is considered for shear design in this example.

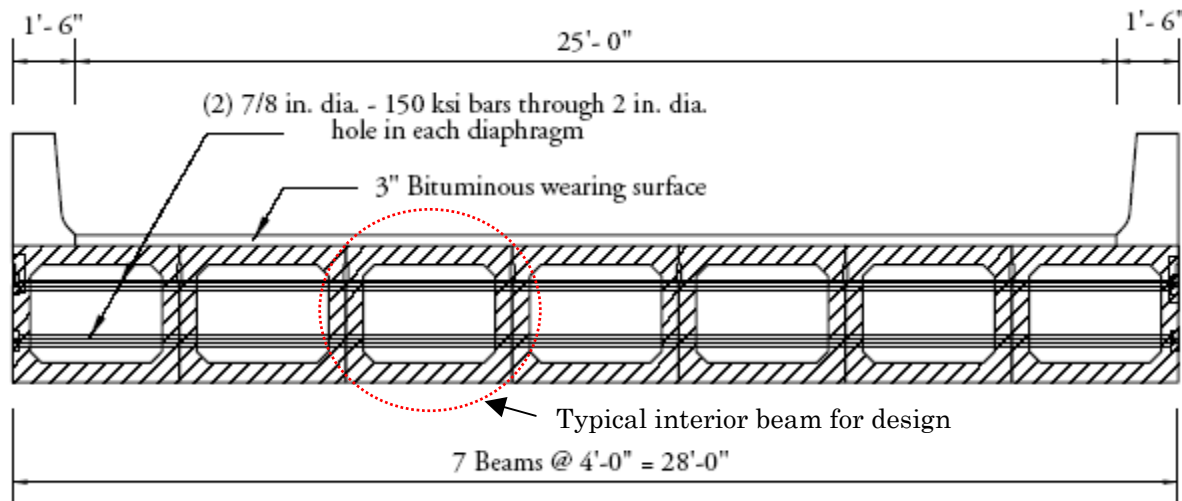


Figure J-1 Bridge Cross-Section

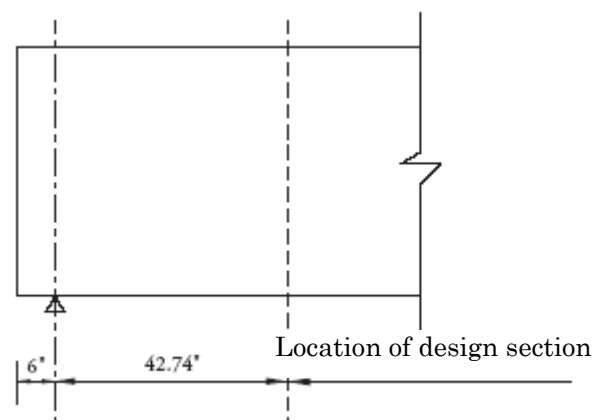


Figure J-2 Location of design section

J.1.3 Material Properties

The material properties are given in Table J-1.

Table J-1 Material Properties

CONCRETE PROPERTIES	
Concrete strength at 28 days, f'_c	5 ksi
Concrete unit weight, w_c	0.150 kcf
Modulus of elasticity of concrete, $E_c = 33,000(w_c)^{1.5} \sqrt{f'_c}$ [LRFD Eq. 5.4.2.4-1]	4,287ksi
PRESTRESSING STRANDS	
Type	0.5 in. dia., seven-wire, low-relaxation
Area of a strand	0.153 in ²
Ultimate strength, f_{pu}	270.0 ksi
Yield strength, f_{py} (=0.9 f_{pu}) [LRFD Table 5.4.4.1-1]	243.0 ksi
A parameter for prestressing, $f_{po} = 0.7 f_{pu}$	189 ksi
Effective prestress after all losses, f_{se}	171.6 ksi
Modulus of elasticity, E_p [LRFD Art. 5.4.4.2]	28,500 ksi
REINFORCING BARS	
Yield strength, f_y	#3 Grade 60 ksi
Modulus of elasticity, E_s [LRFD Art. 5.4.3.2]	29,000 ksi

J.1.4 Sectional Properties and Forces

The sectional properties and forces are given in Table J-2. Fig. J-3 provides detailed dimensions of the cross-section of AASHTO Box Beam Type BIII-48. The strand patterns at midspan and at the design section are shown in Figs. J-4 and J-5, respectively. Other basic calculations are also provided.

Table J-2 Sectional Properties and Forces

OVERALL GEOMETRY AND SECTIONAL PROPERTIES	
Span length, L	95 ft
Overall depth of girder, h	39 in.
Width of Web, b_v	10 in. (Width of each leg is 5 in.)
Area of cross-section of girder, A_g	813 in. ²
Moment of inertia, I_g	168,367 in. ⁴
Distance from centroid to extreme bottom fiber, y_b	19.29 in.
Distance from centroid to extreme top fiber, y_t	19.71 in.

Section modulus for the extreme bottom fiber, S_b	8,728 in ³
Section modulus for the extreme top fiber, S_t	8,542 in ³
Area of non-prestressed tension reinforcement, A_s	0 in ²
Distance from extreme compression fiber to centroid of longitudinal tension reinforcement, d_s	0 in
Area of prestressed tension reinforcement, A_p	=29(0.153)=4.437 in ²
Distance from the top fiber to the centroid of prestressed tendons, d_p	36.59 in
Weight of beam	0.847 kip/ft
SECTIONAL FORCES AT DESIGN SECTION	
Unfactored shear force caused by dead load, V_d	47.6 kips
Factored shear force, V_u	146.5 kips
Unfactored moment caused by dead load, M_d	176.0 ft-kips
Factored moment, M_u	424.6 ft-kips

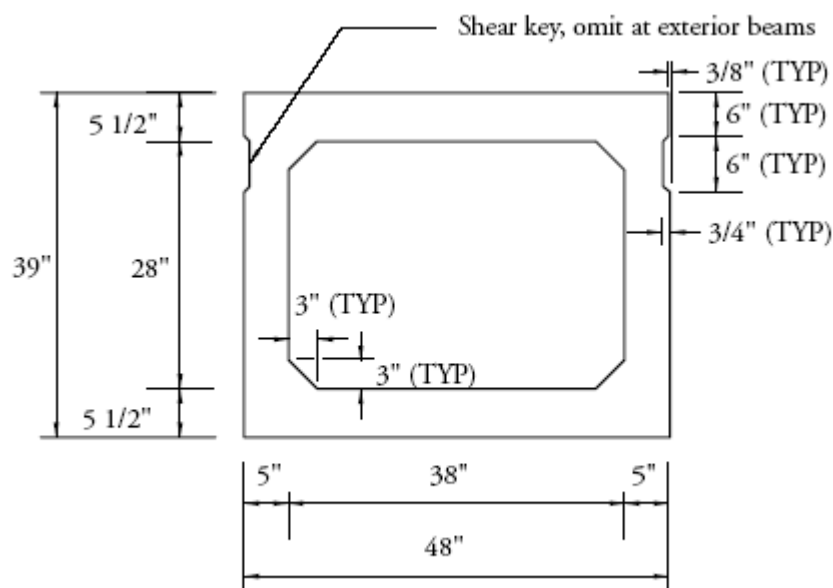


Figure J-3 Cross-Section of AASHTO Box Beam Type BIII-48

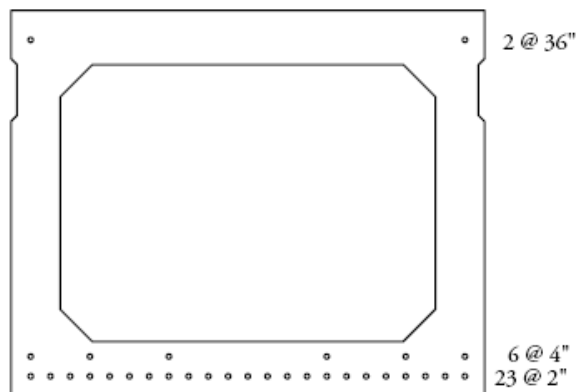


Figure J-4 Strand Pattern at Midspan

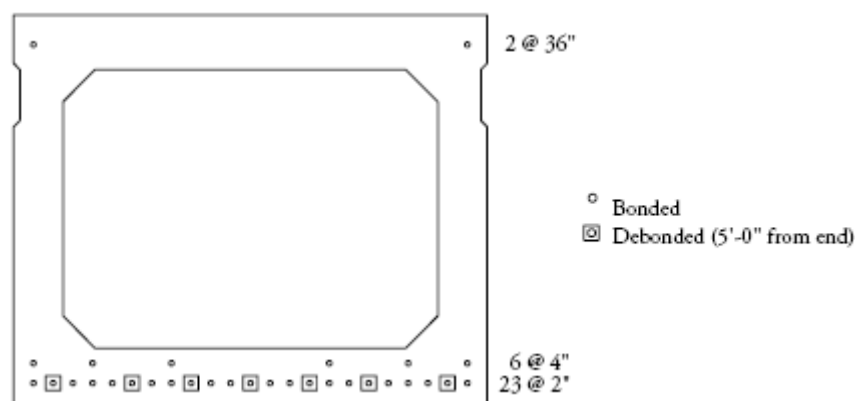


Figure J-5 Strand Pattern at the Design Section

Calculation of effective depth, d_v :

Note that only 22 strands (16@2 in. and 6@4 in.) are effective at the design section for shear, because 7 strands are debonded and the top level of strands is ignored. See Fig. J-5. The equivalent compressive block depth, a , is calculated by flexural analysis ($a=9.03$ in.).

The center of gravity of strand in tension at the design section is:

$$y_{bs} = \frac{16(2) + 6(4)}{22} = 2.55 \text{ in}$$

Therefore, $d_e = 39 - 2.55 = 36.45 \text{ in}$

d_v is the greater of:

$$d_e - a/2 = [36.45 - 0.5(9.03)] = 31.94 \text{ in}$$

$$0.9d_e = 0.9(36.45) = 32.81 \text{ in (Controls)}$$

$$0.72h = 0.72(39) = 28.08 \text{ in}$$

Therefore, $d_v = 32.81 \text{ in}$.

The design shear stress is:

$$v_u = \frac{V_u - \phi V_p}{\phi b_v d_v} = \frac{146.5 - 0}{(0.9)(10)(32.81)} = 0.496 \text{ ksi}$$

Thus, $v_u / f'_c = 0.496 / 5 = 0.099$

J.1.5 Shear Design by Proposal 1: Modified STD Approach

Shear design procedures in accordance with the Modified STD Approach are used to determine the amount and spacing of the shear reinforcement required at a section located 42.74 in. from the support.

a) Evaluation of Web-Shear Cracking Strength

Compute web-shear cracking strength, V_{cw} :

$$V_{cw} = (0.06\sqrt{f'_c} + 0.3f_{pc})b_v d_v + V_p$$

The effective prestress force is:

$$P_{se} = 24(0.153)(171.6) = 630.1 \text{ kips}$$

Compressive stress in concrete at the centroid of cross section due to prestress is:

$$f_{pc} = \frac{P_{se}}{A_g} = \frac{630.1}{813} = 0.775 \text{ ksi}$$

Therefore, $V_{cw} = [0.06\sqrt{5.0} + 0.3(0.775)](10)(32.81) + 0 = 120.3 \text{ kips}$

b) Evaluation of Flexure-Shear Cracking Strength

Compute flexure-shear cracking strength, V_{ci} :

$$V_{ci} = 0.02\sqrt{f'_c}b_v d_v + V_d + V_i \frac{M_{cr}}{M_{\max}} \geq 0.06\sqrt{f'_c}b_v d_v$$

$$V_i = V_u - V_d = 146.5 - 47.6 = 98.9 \text{ kips},$$

$$M_{\max} = M_u - M_d = 424.6 - 176.0 = 248.6 \text{ ft} \cdot \text{kips}.$$

Moment causing flexural cracking at the design section due to externally applied loads:

$$M_{cr} = \frac{I_g}{y_b} (0.2\sqrt{f'_c} + f_{pe} - f_d)$$

The center of gravity of strand pattern at the design section is:

$$y_{bs} = \frac{16(2) + 6(4) + 2(36)}{24} = 5.33 \text{ in}$$

The eccentricity of the strands at the design section is:

$$e = y_b - y_{bs} = 19.29 - 5.33 = 13.96 \text{ in}.$$

Compressive stress in concrete due to effective prestress forces only:

$$f_{pe} = \frac{P_{se}}{A_g} + \frac{P_{se}ey_b}{I_g} = \frac{630.1}{813} + \frac{630.1(13.96)(19.29)}{168,367} = 1.783 \text{ ksi}$$

Stress due to service dead load:

$$f_d = \frac{M_d y_b}{I_g} = \frac{176.0(12)(19.29)}{168,367} = 0.242 \text{ ksi}$$

$$\text{Therefore, } M_{cr} = \frac{168,367}{19.29} (0.2\sqrt{5.0} + 1.783 - 0.242) / 12 = 1,446.1 \text{ ft} \cdot \text{kips}$$

The flexure-shear cracking strength, V_{ci} , is:

$$V_{ci} = 0.02\sqrt{5.0}(10)(32.81) + 47.6 + \frac{98.9(1,446.1)}{248.6} = 637.6 \text{ kips}$$

$$> 0.06\sqrt{f'_c} b_v d_v = 0.06\sqrt{5.0}(10)(32.81) = 44.0 \text{ kips}$$

c) Evaluation of Concrete Contribution

The nominal shear strength provided by concrete is the lesser of V_{ci} and V_{cw} .

Web-shear cracking strength $V_{cw} = 120.3 \text{ kips}$ (Governs),

Flexure-shear cracking strength $V_{ci} = 637.6 \text{ kips}$

Thus, the nominal shear strength provided by concrete is:

$$V_c = 120.3 \text{ kips}$$

d) Evaluation of Required Transverse Reinforcement

Check if $V_u > 0.5\phi V_c$

$$V_u = 146.5 \text{ kips} > 0.5\phi V_c = 0.5(0.9)(120.3) = 54.1 \text{ kips}$$

Therefore, transverse reinforcement must be provided.

The shear force required is:

$$V_s = (V_u / \phi) - V_c = (146.5 / 0.9) - 120.3 = 42.5 \text{ kips}$$

The shear strength provided by transverse reinforcement is:

$$V_s = \frac{A_v f_y d_v (\cot \theta + \cot \alpha) \sin \alpha}{s} \quad [\text{LRFD Eq. 5.8.3.3-4}]$$

When vertical stirrups are used, $\alpha = 90^\circ$.

Since V_{cw} governs and $M_u = 424.6 \text{ ft} \cdot \text{kips} < M_{cr} = 1,446.1 \text{ ft} \cdot \text{kips}$, the angle of compressive strut is obtained as

$$\cot \theta = 1 + 3 f_{pc} / \sqrt{f'_c} \leq 1.80$$

$$\cot \theta = 1 + 3(0.775) / \sqrt{5.0} = 2.04 > 1.80 \text{ (Governs)}$$

Therefore, $\cot \theta = 1.80$.

The area of transverse reinforcement (in^2) within a spacing (s) is: (use $f_y = 60 \text{ ksi}$)

$$A_v / s = V_s / (f_y d_v \cot \theta) = 42.5 / [(60)(32.81)(1.80)] = 0.0120 \text{ in.}^2 / \text{in.}$$

Therefore, **use #3 single leg stirrups in each side of web at 18 in. spacing**

$$A_v / s \text{ provided} = 0.22 / 18 = 0.0122 \text{ in.}^2 / \text{in.} > A_v / s \text{ required} = 0.0120 \text{ in.}^2 / \text{in.}$$

$$\text{Then, provided } V_s = \frac{0.22 \times 60 \times 32.81 \times 1.80}{18} = 43.3 \text{ kips}$$

e) Checks

Maximum Spacing Limit of Transverse Reinforcement

Maximum spacing of transverse reinforcement shall not exceed the following:

$$\text{When } v_u / f'_c = 0.099 < 0.125, s_{\max} = 0.8d_v \leq 24.0 \text{ in.} \quad [\text{LRFD Eqs. 5.8.2.7-1}]$$

$$\begin{aligned} s_{\max} &\leq 24 \text{ in. (controls)} \\ &\leq 0.8d_v = (0.8)(32.81) = 26.25 \text{ in.} \end{aligned}$$

Since $s = 18 \text{ in.} < s_{\max} \leq 24 \text{ in.}$ O.K.

Minimum Reinforcement Requirement

The area of transverse reinforcement shall not be less than:

$$A_{v,\min} \geq 0.0316 \sqrt{f'_c} \frac{b_v s}{f_y} = 0.0316 \sqrt{5.0} \frac{(10)(18)}{60} = 0.212 \text{ in.}^2 < \text{provided } A_v = 0.22 \text{ in.}^2$$

O.K.

Maximum Nominal Shear Resistance

In order to ensure that the concrete in the web of the girder will not crush prior to yielding of the transverse reinforcement, the LRFD Specifications specify an upper limit of V_n as follows:

$$\begin{aligned} V_n &\leq 0.25 f'_c b_v d_v + V_p \quad (V_p = 0 \text{ in this example}) \\ V_n &= 120.3 + 43.3 = 163.6 \text{ kips} < 0.25 f'_c b_v d_v = 0.25(5.0)(10)(32.81) = 410.1 \text{ kips} \end{aligned}$$

O.K.

J.1.6 Shear Design by Proposal 2: Modified CSA Approach

Shear design procedures in accordance with the Modified CSA Approach are used to determine the amount and spacing of the shear reinforcement required at a section located at a distance of 42.74 in. from the support.

a) Evaluation of ε_x

Calculate the strain in the reinforcement on the flexural tension side, ε_x :

$$\begin{aligned} \varepsilon_x &= \frac{M_u / d_v + 0.5N_u + V_u - V_p - A_{ps}f_{po}}{2(E_s A_s + E_p A_{ps})} \leq 0.002 \\ \varepsilon_x &= \frac{424.6(12) / 32.81 + 0 + 146.5 - 0 - 3.366(189)}{2[(0 + 28,500)(3.366)]} = -1.743 \times 10^{-3} \end{aligned}$$

Since the value of ε_x is negative, a different equation must be used:

$$\varepsilon_x = \frac{M_u / d_v + 0.5N_u + V_u - V_p - A_{ps}f_{po}}{2(E_c A_c + E_s A_s + E_p A_{ps})} \leq 0.002$$

where A_c = area of concrete on the flexural tension side as shown in Fig. J-6.
 $= (0.5)(813) = 406.5 \text{ in}^2$

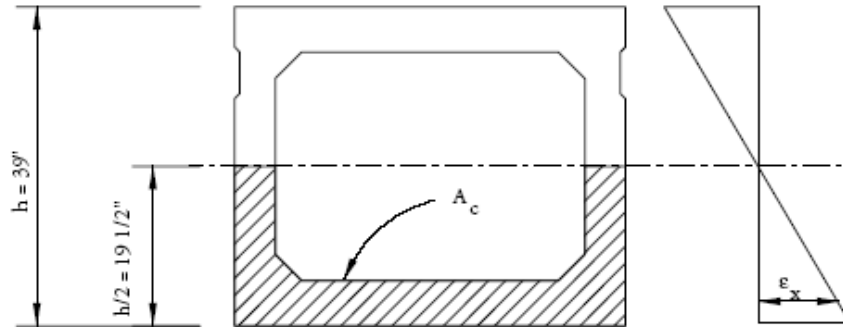


Figure J-6 Illustration of A_c

$$\varepsilon_x = \frac{424.6(12) / 32.81 + 0 + 146.5 - 0 - 3.366(189)}{2[(4,287)(406.5) + (28,500)(3.366)]} = -9.1 \times 10^{-5}$$

b) Evaluation of β and θ

Calculate θ from the longitudinal strain, ε_x .

$$\begin{aligned} \theta &= 29 + 7,000\varepsilon_x \\ &= 29 + 7,000(-9.1 \times 10^{-5}) = 28.4^\circ \end{aligned}$$

Assume that at least minimum shear reinforcement is provided. Then, the coefficient, β , is:

$$\begin{aligned} \beta &= \frac{4.8}{(1 + 1500\varepsilon_x)} \\ &= \frac{4.8}{[1 + 1,500(-9.1 \times 10^{-5})]} = 5.56 \end{aligned}$$

c) Evaluation of Concrete Contribution

The contribution of the concrete to the nominal shear resistance is:

$$\begin{aligned} V_c &= 0.0316\beta\sqrt{f'_c}b_vd_v \\ &= 0.0316(5.56)\sqrt{5.0}(10)(32.81) = 128.9 \text{ kips} \end{aligned}$$

d) Evaluation of Required Transverse Reinforcement

Check if $V_u > 0.5\phi(V_c + V_p)$

$$V_u = 146.5 \text{ kips} > 0.5\phi(V_c + V_p) = (0.5)(0.9)(128.9 + 0) = 58.0 \text{ kips}$$

Therefore, transverse shear reinforcement must be provided.

The shear resistance to be provided by transverse reinforcement is:

$$V_s = (V_u / \phi) - V_c - V_p = (146.5 / 0.9) - 128.9 - 0 = 33.9 \text{ kips}$$

The shear strength provided by transverse reinforcement is:

$$V_s = \frac{A_v f_y d_v (\cot \theta + \cot \alpha) \sin \alpha}{s} \quad [\text{LRFD Eq. 5.8.3.3-4}]$$

When vertical stirrups are used, $\alpha = 90^\circ$. Then, the required area of transverse reinforcement within a spacing (s) is: (use $f_y = 60$ ksi)

$$A_v / s = V_s / (f_y d_v \cot \theta) = 33.9 / [(60)(32.81) \cot 28.4^\circ] = 0.0093 \text{ in.}^2 / \text{in.}$$

Therefore, **use #3 single leg stirrups in each side of the web at 24 in. spacing**

$$A_v / s \text{ provided} = 0.22 / 24 = 0.0092 \text{ in.}^2 / \text{in.} \approx A_v / s \text{ required} = 0.0093 \text{ in.}^2 / \text{in.}$$

$$\text{Then, } V_s = \frac{0.22 \times 60 \times 32.81 \times \cot 28.4^\circ}{24} = 33.4 \text{ kips}$$

e) Checks

Maximum Spacing Limit of Transverse Reinforcement

Maximum spacing of transverse reinforcement may not exceed the following:

$$\text{When } v_u / f_c' = 0.099 < 0.125, s_{\max} = 0.8d_v \leq 24.0 \text{ in.} \quad [\text{LRFD Eqs. 5.8.2.7-1}]$$

$$\begin{aligned} s_{\max} &\leq 24 \text{ in. (controls)} \\ &\leq 0.8d_v = (0.8)(32.81) = 26.25 \text{ in.} \end{aligned}$$

Since $s = 24 \text{ in.}$ and $s_{\max} \leq 24 \text{ in.}$ O.K.

Minimum Transverse Reinforcement Requirement

The area of transverse reinforcement should not be less than:

$$A_{v,\min} \geq 0.0316 \sqrt{f_c'} \frac{b_v s}{f_y} = 0.0316 \sqrt{5.0} \frac{(10)(24)}{60} = 0.283 \text{ in.}^2 > \text{provided } A_v = 0.22 \text{ in.}^2$$

Therefore minimum transverse reinforcement governs. **Use #3 single leg stirrups in each web at 18 in. spacing.** Then,

$$A_v / s \text{ provided} = 0.22 / 18 = 0.0122 \text{ in.}^2 / \text{in.} > A_v / s \text{ required} = 0.283 / 24 = 0.0118 \text{ in.}^2 / \text{in.}$$

$$\text{And } V_s = \frac{0.22 \times 60 \times 32.81 \times \cot 28.4^\circ}{18} = 44.5 \text{ kips}$$

Maximum Nominal Shear Resistance

In order to ensure that the concrete in the web of the girder will not crush prior to yielding of the transverse reinforcement, the LRFD Specifications specify an upper limit on V_n as follows:

$$V_n \leq 0.25 f_c' b_v d_v + V_p \quad (V_p = 0 \text{ in this example})$$

$$V_n = 128.9 + 44.5 + 0 = 173.4 \text{ kips} < 0.25 f_c' b_v d_v = 0.25(5.0)(10)(32.81) = 410.1 \text{ kips}$$

O.K.

J.1.7 Summary and Conclusions

Shear design procedures in accordance with the Modified STD Approach and the Modified CSA Approach were used to determine the amount and spacing of the transverse reinforcement required at a section 42.74 in. from the support of a 95-ft single-span AASHTO Type BIII-48 box beam with straight strands and of which seven strands are debonded at the design section.. The shear design results are summarized in Table J-3. In this design example, the amounts of transverse reinforcement required by the two approaches are very similar.

Table J-3 Summary of Results

Required or calculated	Proposal 1: Modified STD Approach	Proposal 2: Modified CSA Approach
V_c , kips	120.3	128.9
V_s , kips	42.5	33.9
θ , deg.	29.0	28.4
Reinforcement Provided	single leg (each web) #3 bars @18 inches	single leg (each web) #3 bars @18 inches

J.2 Example 2: Three-Span Continuous Precast, Pretensioned Girders

J.2.1 Example Description

This example is based on Example 9.6 of the PCI Bridge Design Manual. The bridge uses 72-inch bulb-tee beams with harped (draped) pretensioned strands on 110-foot end spans and a 120-foot interior span. The beams are made continuous for live load by the addition of non-pretensioned reinforcement in the deck in the negative moment region. This example illustrates the shear design of the negative moment region of a beam made continuous with non-pretensioned reinforcement.

J.2.2 Geometry and Loading

As shown in Fig. J-7, the bridge is a three-span continuous structure and is designed to act compositely to resist all superimposed dead loads, live loads and impact. Design live load is AASHTO LRFD HL-93. The superstructure consists of four beams spaced at 12 ft centers as shown in Fig. J-8. The section at a distance of 7.10 ft from support, as indicated in Fig. J-7, is designed for shear in this example.

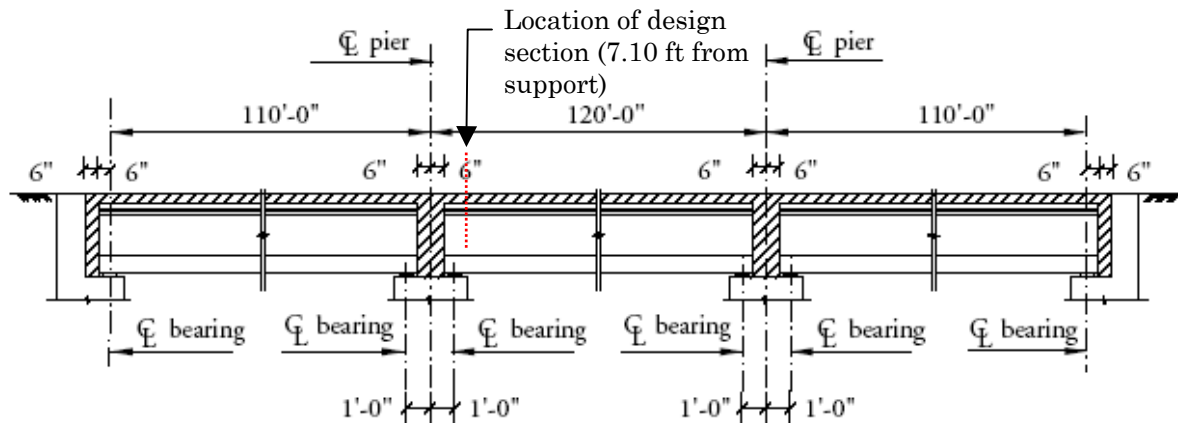


Figure J-7 Span Geometry

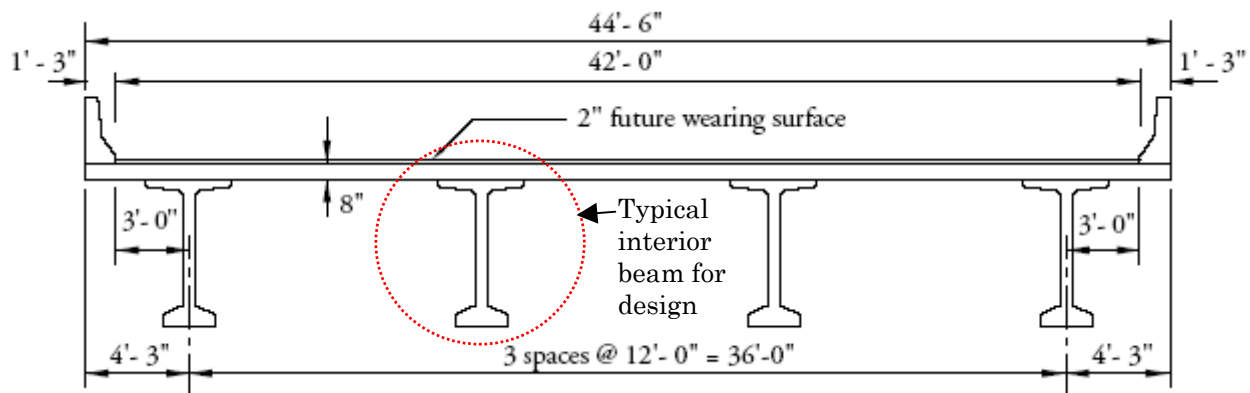


Figure J-8 Bridge Cross-Section

J.2.3 Material Properties

The material properties are given in Table J-4.

Table J-4 Material Properties and Basic Information

CONCRETE PROPERTIES	
Concrete strength of girder at 28 days, f'_c	7.0 ksi
Concrete strength of deck at 28 days, f'_c	4.0 ksi
Concrete unit weight, w_c	0.150 kcf
Modulus of elasticity of concrete for girder,	5,072 ksi
$E_{c,beam} = 33,000(w_c)^{1.5} \sqrt{f'_c}$ [LRFD Eq. 5.4.2.4-1]	
Modulus of elasticity of concrete for deck,	3,834 ksi
$E_{c,slab} = 33,000(w_c)^{1.5} \sqrt{f'_c}$ [LRFD Eq. 5.4.2.4-1]	
Modular ratio between slab and beam concrete, $n = E_{c,slab} / E_{c,beam}$	$= 0.7559$
PRESTRESSING STRANDS	
Type	0.5 in. dia., seven-wire, low-relaxation
Area of a strand	0.153 in ²
Ultimate strength, f_{pu}	270.0 ksi
Yield strength, f_{py} ($=0.9 f_{pu}$) [LRFD Table 5.4.4.1-1]	243 ksi
A parameter for prestressing, $f_{po} = 0.7 f_{pu}$	189 ksi
Effective prestress after all losses, f_{se}	152.9 ksi
Modulus of elasticity, E_p [LRFD Art. 5.4.4.2]	28,500 ksi
REINFORCING BARS	
Yield strength, f_y	#5 Grade 60 ksi
Modulus of elasticity, E_s [LRFD Art. 5.4.3.2]	29,000 ksi

J.2.4 Sectional Properties and Forces

The sectional properties and forces are given in Table J-5. Fig. J-9 provides details of the dimensions of the cross-section of a AASHTO Type IV beam and Fig. J-10 provides details for the composite section. The typical strand patterns at midspan and at the end are shown in Fig. J-11. Note that 12 strands are draped as shown in Fig. J-11. Some basic calculations are also provided in this sub-section.

Table J-5 Sectional Properties and Forces

OVERALL GEOMETRY AND SECTIONAL PROPERTIES	
Non-Composite Section	
Span length, L	120 ft
Overall depth of girder, h	72 in.
Width of web, b_w	6 in.
Area of cross-section of girder, A_g	767 in. ²
Moment of inertia, I_g	545,894 in. ⁴
Distance from centroid to extreme bottom fiber, y_b	36.60 in.

Distance from centroid to extreme top fiber, y_t	35.40 in.
Section modulus for the extreme bottom fiber, S_b	14,915 in ³
Section modulus for the extreme top fiber, S_t	15,421 in ³
Weight of beam	0.799 kip/ft
Composite Section	
Overall depth of the composite section, h_c	80 in.
Slab thickness, t_s	8.0 in.
Total transformed area of the composite section, A_c	1,412 in. ²
Moment of inertia of the composite section, I_c	1,097,252 in. ⁴
Distance from centroid of the composite section to extreme bottom fiber, y_{bc}	54.67 in.
Distance from centroid of the composite section to extreme top fiber of beam, y_{tg}	17.33 in.
Distance from centroid of the composite section to extreme top fiber of slab, y_{tc}	25.33 in.
Composite section modulus for the extreme bottom fiber of beam, S_{bc}	20,070 in ³
Composite section modulus for the extreme top fiber of beam, S_{tg}	63,315 in ³
Composite section modulus for the extreme top fiber of slab, S_{tc}	57,307 in ³
Area of non-prestressed tension reinforcement, A_s	0 in ²
Distance from extreme compression fiber to centroid of longitudinal tension reinforcement, d_s	0 in
Area of prestressed tension reinforcement, A_p	=44(0.153)=6.732 in ²
Distance from the top fiber to the centroid of prestressed tendons, d_p	74.18 in
SECTIONAL FORCES AT DESIGN SECTION	
Unfactored shear force due to beam weight, V_{dg}	42.3 kips
Unfactored shear force due to deck slab, V_{ds}	64.6 kips
Unfactored shear force due to superimposed dead load, V_{dw}	22.0 kips
Unfactored shear force due to total dead load, V_d	128.9 kips
Factored shear force, V_u	405.0 kips
Unfactored moment due to beam weight, M_{dg}	272.7 ft-kips
Unfactored moment due to deck slab, M_{ds}	417.1 ft-kips
Unfactored moment due to superimposed dead load, M_{dw}	-384.0 ft-kips
Unfactored moment due to total dead load, M_d	305.8 ft-kips
Factored moment, M_u	-2,877.6 ft-kips

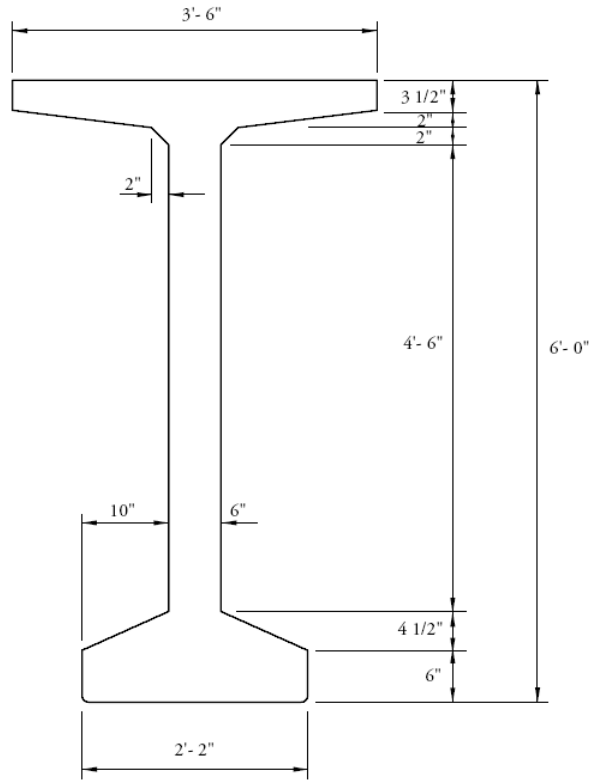


Figure J-9 Cross-Section of AASHTO-PCI, BT-72 Bulb-Tee Beam

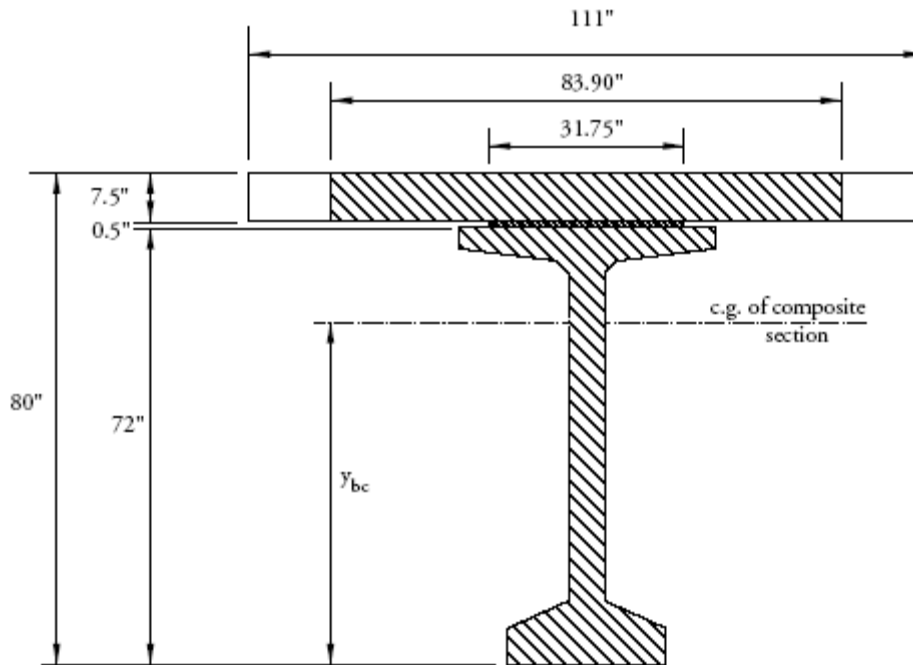


Figure J-10 Composite Section

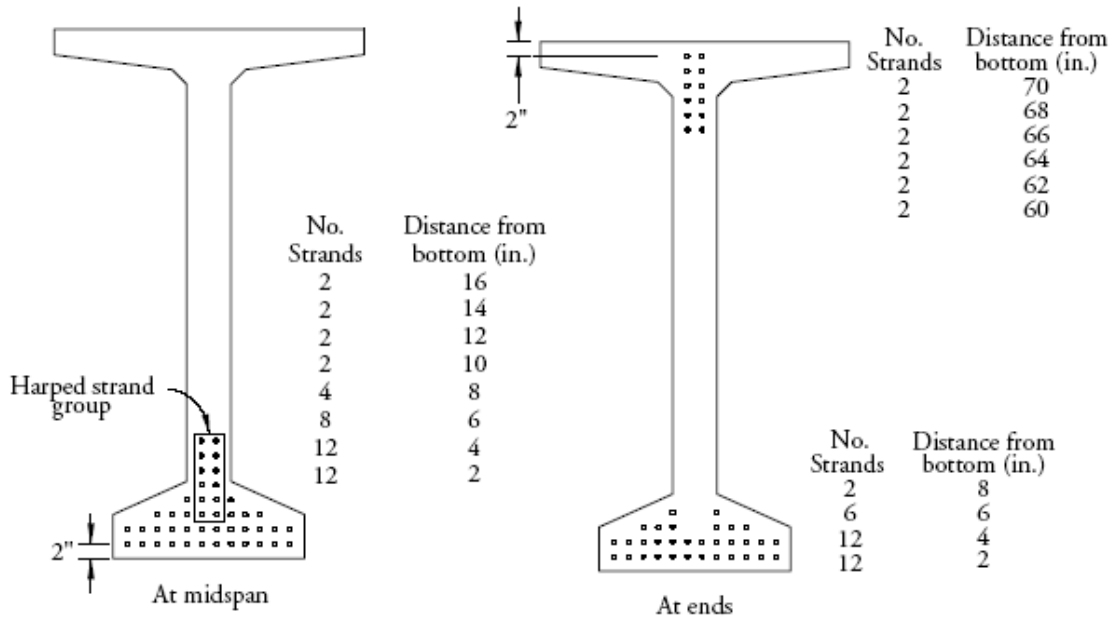


Figure J-11 Strand Pattern at Midspan and at Ends

Calculation of effective depth, d_v :

Note that the design section (7.10 ft from the interior support) is located in the negative moment zone. Thus, only the nonprestressed reinforcement in the slab is considered as the main reinforcement for flexure and the prestress reinforcement is neglected. The area of nonprestressed steel on the flexural tension side of the member is $A_s = 15.52 \text{ in}^2$ and the effective depth is $d_e = 76.25 \text{ in}$. The equivalent compressive block depth, a , is calculated by flexural analysis ($a = 6.02 \text{ in}$).

d_v is the greater of:

$$d_e - a/2 = [76.25 - 0.5(6.02)] = 73.24 \text{ in (Controls)}$$

$$0.9d_e = 0.9(76.25) = 68.63 \text{ in}$$

$$0.72h = 0.72(80.0) = 57.60 \text{ in}$$

Therefore, $d_v = 73.24 \text{ in}$.

The vertical component of the effective prestressing force, V_p , due to the 12 draped strands (with an angle of 7.2°) is:

$$V_p = 12(0.153)(152.9) \sin 7.2^\circ = 35.2 \text{ kips}$$

The design shear stress is:

$$v_u = \frac{V_u - \phi V_p}{\phi b_v d_v} = \frac{405.0 - 0.9(35.2)}{(0.9)(6)(73.24)} = 0.944 \text{ ksi}$$

Thus, $v_u / f'_c = 0.944 / 7.0 = 0.135$.

J.2.5 Shear Design by Proposal 1: Modified STD Approach

Shear design procedures in accordance with the Modified STD Approach are used to determine the amount and spacing of the shear reinforcement required at a distance of 7.10 ft from the interior support.

a) Evaluation of Web-Shear Cracking Strength

Compute web-shear cracking strength, V_{cw} :

$$V_{cw} = (0.06\sqrt{f'_c} + 0.3f_{pc})b_v d_v + V_p$$

The effective prestress force is:

$$P_{se} = 44(0.153)(152.9) = 1,029.3 \text{ kips}$$

The eccentricity of the strands at the design section is 18.79 in. The compressive stress in the concrete at the centroid of the cross section due to both pretensioning and moments and resisted by precast member alone is:

$$f_{pc} = \frac{P_{se}}{A_g} - \frac{P_{se}e(y_{bc} - y_b)}{I_g} + \frac{(M_{dg} + M_{ds})(y_{bc} - y_b)}{I_g}$$

$$f_{pc} = \frac{1,029.3}{767} - \frac{1,029.3(18.79)(54.67 - 36.60)}{545,894} + \frac{(272.7 + 417.1)(12)(54.67 - 36.60)}{545,894}$$

$$= 0.976 \text{ ksi}$$

Therefore, $V_{cw} = [0.06\sqrt{7.0} + 0.3(0.976)](6)(73.24) + 35.2 = 233.6 \text{ kips}$

b) Evaluation of Flexure-Shear Cracking Strength

Compute flexure-shear cracking strength, V_{ci} :

$$V_{ci} = 0.02\sqrt{f'_c}b_v d_v + V_d + V_i \frac{M_{cr}}{M_{\max}} \geq 0.06\sqrt{f'_c}b_v d_v$$

$$V_i = V_u - V_d = 405.0 - 128.9 = 276.1 \text{ kips},$$

$$M_{\max} = M_u - M_d = -2,877.6 - 305.8 = -3,183.4 \text{ ft} \cdot \text{kips}.$$

Moment causing flexural cracking at the design section due to externally applied loads:

$$M_{cr} = \frac{I_c}{y_{ic}}(0.2\sqrt{f'_c} + f_{pe} - f_d)$$

Because the beam at this section is under net negative moment, the compressive stress in the concrete due to effective prestress forces only, at the extreme fiber of the section where tensile stress is caused by externally applied loads, f_{pe} , should be evaluated at the top of the deck slab.

Pretension has no effect on the deck slab, therefore, $f_{pe} = 0$.

Stress due to service dead load:

$$f_d = \frac{M_{dw}y_{ic}}{I_c} = \frac{-384.0(12)(25.33)}{1,097,252} = 0.106 \text{ ksi}$$

Note that because this section is under net negative moment M_{dw} was evaluated conservatively by considering the dead load negative moment component as that resulting from the dead load acting on a continuous span.

Therefore,

$$M_{cr} = \frac{1,097,252}{25.33} (0.2\sqrt{4.0} + 0 - 0.106) / 12 = 1,061.3 \text{ ft} \cdot \text{kips}$$

The flexure-shear cracking strength, V_{ci} , is:

$$V_{ci} = 0.02\sqrt{7.0}(6)(73.24) + 128.9 + \frac{276.1(1,061.3)}{3,183.4} = 244.2 \text{ kips}$$

$$> 0.06\sqrt{f'_c}b_vd_v = 0.06\sqrt{7.0}(6)(73.24) = 69.76 \text{ kips}$$

c) Evaluation of Concrete Contribution

The nominal shear strength provided by the concrete is the lesser of V_{ci} and V_{cw} .

Web-shear cracking strength $V_{cw} = 233.6 \text{ kips}$ (Governs)

Flexure-shear cracking strength $V_{ci} = 244.2 \text{ kips}$

Thus, the nominal shear strength provided by concrete is:

$$V_c = 233.6 \text{ kips}$$

d) Evaluation of Required Transverse Reinforcement

Check if $V_u > 0.5\phi V_c$

$$V_u = 405.0 \text{ kips} > 0.5\phi V_c = 0.5(0.9)(233.6) = 105.1 \text{ kips}$$

Therefore, transverse reinforcement must be provided.

The shear force required is:

$$V_s = (V_u / \phi) - V_c = (405.0 / 0.9) - 233.6 = 216.4 \text{ kips}$$

The shear strength provided by transverse reinforcement is:

$$V_s = \frac{A_v f_y d_v (\cot \theta + \cot \alpha) \sin \alpha}{s} \quad [\text{LRFD Eq. 5.8.3.3-4}]$$

When vertical stirrups are used, $\alpha = 90^\circ$.

Since $M_u = 2,877.6 \text{ ft} \cdot \text{kips} > M_{cr} = 1,061.3 \text{ ft} \cdot \text{kips}$, the angle of compressive strut is 45° .

Therefore, the area of transverse reinforcement (in^2) within a spacing (s) is: (use $f_y = 60 \text{ ksi}$)

$$A_v / s = V_s / (f_y d_v \cot \theta) = 216.4 / [(60)(73.24)(\cot 45^\circ)] = 0.0492 \text{ in}^2 / \text{in}.$$

Therefore, **use #5 double leg stirrups at 12 in. spacing**

$$A_v / s \text{ provided} = 2(0.31) / 12 = 0.0517 \text{ in}^2 / \text{in}. > A_v / s \text{ required} = 0.0492 \text{ in}^2 / \text{in}.$$

Then, provided $V_s = \frac{0.62(60)(73.24) \cot 45.0^\circ}{12} = 227.0 \text{ kips}$

e) Checks

Maximum Spacing Limit of Transverse Reinforcement

Maximum spacing of transverse reinforcement shall not exceed the following:

When $v_u / f'_c = 0.135 > 0.125$, $s_{\max} = 0.4d_v \leq 12.0$ in. [LRFD Eqs. 5.8.2.7-1]

$$\begin{aligned} s_{\max} &\leq 12 \text{ in. (controls)} \\ &\leq 0.4d_v = (0.4)(73.24) = 29.30 \text{ in.} \end{aligned}$$

Therefore, $s_{\max} \leq 12$ in.

Actual spacing, $s = 12$ in. O.K.

Minimum Reinforcement Requirement

The area of transverse reinforcement shall not be less than:

$$A_{v,\min} \geq 0.0316 \sqrt{f'_c} \frac{b_v s}{f_y} = 0.0316 \sqrt{7.0} \frac{(6)(12)}{60} = 0.1003 \text{ in}^2 < \text{provided } A_v = 0.62 \text{ in}^2$$

O.K.

Maximum Nominal Shear Resistance

In order to ensure that the concrete in the web of the girder will not crush prior to yielding of the transverse reinforcement, the LRFD Specifications specify an upper limit of V_n as follows:

$$\begin{aligned} V_n &\leq 0.25 f'_c b_v d_v + V_p \\ V_n &= 233.6 + 227.0 = 460.6 \text{ kips} \\ &< 0.25 f'_c b_v d_v + V_p = 0.25(7.0)(6)(73.24) + 35.2 = 804.2 \text{ kips} \quad \text{O.K.} \end{aligned}$$

J.2.6 Shear Design by Proposal 2: Modified CSA Approach

Shear design procedures in accordance with the Modified CSA Approach are used to determine the amount and spacing of the shear reinforcement required at a distance of 7.10 ft from the interior support.

a) Evaluation of ε_x

Calculate the strain in the reinforcement on the flexural tension side, ε_x :

$$\begin{aligned} \varepsilon_x &= \frac{M_u / d_v + 0.5N_u + V_u - V_p - A_{ps}f_{po}}{2(E_s A_s + E_p A_{ps})} \leq 0.002 \\ &= \frac{2,877.6(12) / 73.24 + 0 + 405.0 - 35.2 - 12(0.153)(189)}{2[29,000(15.52) + 28,500(12)(0.153)]} = 0.492 \times 10^{-3} \end{aligned}$$

Note that there are 12 draped strands on the flexural tension side of the member which is taken as the half-depth of the member (LRFD Figure 5.8.3.4.2-3). Thus,

$$A_{ps} = 12(0.153) = 1.836 \text{ in}^2.$$

b) Evaluation of β and θ

Calculate θ from the longitudinal strain, ε_x .

$$\begin{aligned} \theta &= 29 + 7,000\varepsilon_x \\ &= 29 + 7,000(0.492 \times 10^{-3}) = 32.4^\circ \end{aligned}$$

Assume that at least minimum amount of shear reinforcement is provided. Then, the coefficient, β , is:

$$\beta = \frac{4.8}{(1+1500\varepsilon_x)}$$

$$= \frac{4.8}{[1+1,500(0.492 \times 10^{-3})]} = 2.76$$

c) Evaluation of Concrete Contribution

The contribution of the concrete to the nominal shear resistance is:

$$V_c = 0.0316\beta\sqrt{f'_c}b_vd_v$$

$$= 0.0316(2.76)\sqrt{7.0}(6.0)(73.24) = 101.4 \text{ kips}$$

d) Evaluation of Required Transverse Reinforcement

Check if $V_u > 0.5\phi(V_c + V_p)$

$$V_u = 405.0 \text{ kips} > 0.5\phi(V_c + V_p) = 0.5(0.9)(101.4 + 35.2) = 61.5 \text{ kips}$$

Therefore, transverse shear reinforcement must be provided.

The shear resistance to be provided by transverse reinforcement is:

$$V_s = (V_u / \phi) - V_c - V_p = (405.0 / 0.9) - 101.4 - 35.2 = 313.4 \text{ kips}$$

The shear strength provided by transverse reinforcement is:

$$V_s = \frac{A_v f_y d_v (\cot \theta + \cot \alpha) \sin \alpha}{s} \quad \text{[LRFD Eq. 5.8.3.3-4]}$$

When vertical stirrups are used, $\alpha = 90^\circ$. Then, the area of transverse reinforcement within a spacing (s) is: (use $f_y = 60$ ksi)

$$A_v / s = V_s / (f_y d_v \cot \theta) = 313.4 / [(60)(73.24) \cot 32.4^\circ] = 0.0453 \text{ in.}^2 / \text{in.}$$

Therefore, **use #5 double legs stirrups at 12 in. spacing**

$$A_v / s \text{ provided} = 2(0.31) / 12 = 0.0517 \text{ in.}^2 / \text{in.} > A_v / s \text{ required} = 0.0453 \text{ in.}^2 / \text{in.}$$

$$\text{Then, provided } V_s = \frac{0.62(60)(73.24) \cot 32.4^\circ}{12} = 357.8 \text{ kips}$$

e) Checks**Maximum Spacing Limit of Transverse Reinforcement**

Maximum spacing of transverse reinforcement shall not exceed the following:

When $v_u / f'_c = 0.135 > 0.125$, $s_{\max} = 0.4d_v \leq 12.0 \text{ in.}$ [LRFD Eqs. 5.8.2.7-1]

$$\begin{aligned} s_{\max} &\leq 12 \text{ in. (controls)} \\ &\leq 0.4d_v = (0.4)(73.24) = 29.30 \text{ in.} \end{aligned}$$

Therefore, $s_{\max} \leq 12 \text{ in.}$

Actual spacing, $s = 12 \text{ in.}$ O.K.

Minimum Reinforcement Requirement

The area of transverse reinforcement shall not be less than:

$$A_{v,\min} \geq 0.0316 \sqrt{f'_c} \frac{b_v s}{f_y} = 0.0316 \sqrt{7.0} \frac{(6)(12)}{60} = 0.100 \text{ in}^2 < \text{provided } A_v = 0.62 \text{ in}^2$$

O.K.

Maximum Nominal Shear Resistance

In order to ensure that the concrete in the web of the girder will not crush prior to yielding of the transverse reinforcement, the LRFD Specifications specify an upper limit on V_n as follows:

$$\begin{aligned} V_n &\leq 0.25 f'_c b_v d_v + V_p \\ V_n &= 101.4 + 357.8 + 35.2 = 494.4 \text{ kips} \\ &< 0.25 f'_c b_v d_v + V_p = 0.25(7.0)(6)(73.24) + 35.2 = 804.2 \text{ kips} \end{aligned}$$

O.K.

J.2.7 Summary and Conclusions

Shear design procedures in accordance with the Modified STD Approach and the Modified CSA Approach are used to determine the amount and spacing of the transverse reinforcement required at a given section of a 120-ft span 72-inch bulb-tee beam with harped (draped) pretensioned strands and that was made continuous for live load. Shear design results are summarized in Table J-6. While the concrete contribution, (including V_p), calculated by the Modified STD Approach was about 70% greater than that by the Modified CSA Approach, the difference in the amount of transverse reinforcement required by these two approaches is very small.

Table J-6 Summary of Results

Required or calculated	Proposal 1: Modified STD Approach	Proposal 2: Modified CSA Approach
$(V_c + V_p)$, kips	233.6	136.6
V_s , kips	216.4	313.4
θ , deg.	45.0	32.4
Reinforcement Provided	double leg #5 bars @12 inches	double leg #5 bars @12 inches

J.3 Example 3: Reinforced Concrete Cap Beam

J.3.1 Example Description

This design example demonstrates the shear design of a section of a 15-ft span cap beam sitting on three circular columns of 3-ft diameter. The cap beam supports a 3-lane superstructure consisting of six AASHTO Type IV beams.

J.3.2 Geometry and Loading

Each span of the two-span continuous beam is 15 feet long as shown in Fig. J-12. The section is 39-inches wide and 39-inches deep. The beam rests on three 3-ft diameter and 14-ft long columns. It is designed for HL20 Loading. As shown in the figure, the selected section AA, at a distance of 4.5 ft from the exterior support, is to be designed for shear.

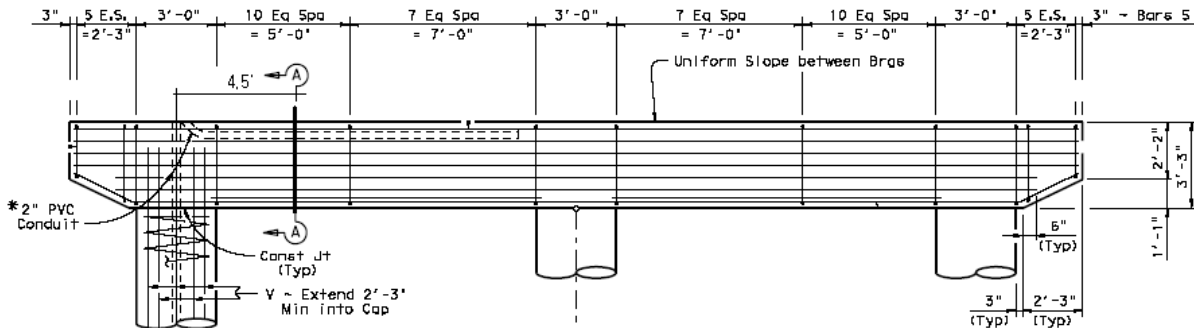


Figure J-12 Elevation View (PBS&J)

J.3.3 Material Properties

The material properties are given in Table J-7.

Table J-7 Material Properties

CONCRETE PROPERTIES	
Concrete strength at 28 days, f'_c	3.6 ksi
Concrete unit weight, w_c	0.150 kcf
Modulus of elasticity of concrete,	3,834 ksi
$E_c = 33,000(w_c)^{1.5} \sqrt{f'_c}$ [LRFD Eq. 5.4.2.4-1]	
REINFORCING BARS	
Yield strength, f_y	60 ksi
Modulus of elasticity, E_s [LRFD Art. 5.4.3.2]	29,000 ksi

J.3.4 Sectional Properties and Forces

The sectional properties and forces are summarized in Table J-8. Fig. J-13 provides cross-section details. Other basic calculations are also provided.

Table J-8 Sectional Properties and Forces

OVERALL GEOMETRY AND SECTIONAL PROPERTIES	
Span length, L	15 ft

Overall depth of beam, h	39 in.
Width of web, b_v	39 in.
Area of cross-section of beam, A_g	1,521 in. ²
Moment of inertia, I_g	192,787 in. ⁴
Distance from centroid to extreme bottom fiber, y_b	19.5 in.
Distance from centroid to extreme top fiber, y_t	19.5 in.
Section modulus for the extreme bottom fiber, S_b	9,987 in. ³
Section modulus for the extreme top fiber, S_t	9,987 in. ³
Area of non-prestressed tension reinforcement, A_s	9.36 in ² (6-#11 bars)
Distance from extreme compression fiber to centroid of longitudinal tension reinforcement, d_s	35.7 in
SECTIONAL FORCES AT DESIGN SECTION	
Unfactored shear force due to dead load, V_d	149.0 kips
Factored shear force, V_u	321.7 kips
Unfactored moment due to dead load, M_d	103.9 ft-kips
Factored moment, M_u	300.2 ft-kips

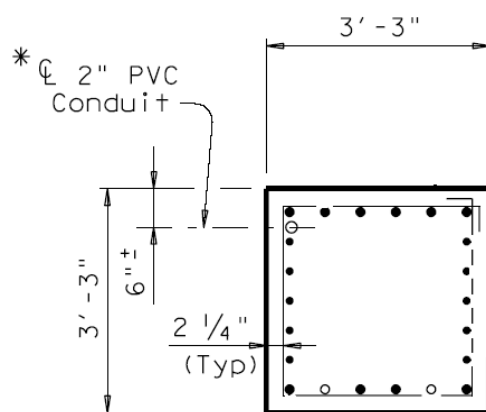


Figure J-13 Cross-Section (PBS&J)

Calculation of effective shear depth, d_v :

$$d_e = d_s = 35.7 \text{ in}$$

d_v is the greater of:

$$0.9d_e = 0.9(35.7) = 32.1 \text{ in (Controls)}$$

$$0.72h = 0.72(39) = 28.1 \text{ in}$$

Therefore, $d_v = 32.1 \text{ in}$.

The design shear stress is:

$$v_u = \frac{V_u}{\phi b_v d_v} = \frac{321.7}{(0.9)(39)(32.1)} = 0.286 \text{ ksi}$$

Thus, $v_u / f'_c = 0.286 / 3.6 = 0.079$.

J.3.5 Shear Design by Proposal 1: Modified STD Approach

Shear design procedures in accordance with the Modified STD Approach are used to determine the amount and spacing of the shear reinforcement required at a distance of 42.74 in. from the support.

a) Evaluation of Concrete Contribution

Compute nominal shear strength provided by concrete, V_c :

$$V_c = 0.06\sqrt{f'_c}b_v d_v = 0.06\sqrt{3.6}(39)(32.1) = 143 \text{ kips}$$

d) Evaluation of Required Transverse Reinforcement

Check if $V_u > 0.5\phi V_c$

$$V_u = 321.7 \text{ kips} > 0.5\phi V_c = 0.5(0.9)(143) = 64.4 \text{ kips}$$

Therefore, transverse reinforcement must be provided.

The shear force required is

$$V_s = (V_u / \phi) - V_c = (321.7 / 0.9) - 143 = 214 \text{ kips}$$

The shear strength provided by the transverse reinforcement is:

$$V_s = \frac{A_v f_y d_v (\cot \theta + \cot \alpha) \sin \alpha}{s} \quad [\text{LRFD Eq. 5.8.3.3-4}]$$

When vertical stirrups are used, $\alpha = 90$.

For RC members, the angle of the compressive strut is 45 degrees; i.e.,

$$\cot \theta = 1$$

Therefore, area of transverse reinforcement (in^2) required within a spacing (s) is:

(use $f_y = 60$ ksi)

$$A_v / s = V_s / (f_y d_v \cot \theta) = 214 / [(60)(32.1)(1.0)] = 0.11 \text{ in}^2 / \text{in.}$$

Use #5 four-leg stirrups at 11-in. spacing

$$A_v / s \text{ provided} = 0.31 \times 4 / 11 = 0.11 \text{ in}^2 / \text{in.} \geq A_v / s \text{ required} = 0.11 \text{ in}^2 / \text{in.}$$

Therefore, provided $V_s = \frac{0.31 \times 4 \times 60 \times 32.1 \times 1.0}{11} = 217 \text{ kips}$

e) Checks

Maximum Spacing Limitation for Transverse Reinforcement

Maximum spacing of transverse reinforcement shall not exceed the following:

When $v_u / f'_c = 0.099 < 0.125$, $s_{\max} = 0.8d_v \leq 24.0$ in. [LRFD Eqs. 5.8.2.7-1]

$$s_{\max} \leq 24 \text{ in. (controls)}$$

$$\leq 0.8d_v = (0.8)(32.1) = 25.7 \text{ in.}$$

Since $s = 11 \text{ in.} \leq 24 \text{ in.}$ O.K.

Minimum Reinforcement Requirement

The area of transverse reinforcement shall not be less than:

$$A_{v,\min} = 0.0316 \sqrt{f'_c} \frac{b_v s}{f_y} = 0.0316 \sqrt{3.6} \frac{(39)(12)}{60} = 0.468 \text{ in}^2 < \text{provided } A_v = 1.24 \text{ in}^2$$

O.K.

Maximum Nominal Shear Resistance

In order to ensure that the concrete in the web of the beam will not crush prior to yielding of the transverse reinforcement, the LRFD Specifications specify an upper limit on V_n as follows:

$$V_n \leq 0.25 f'_c b_v d_v$$

$$V_n = 143 + 217 = 360 \text{ kips} < 0.25 f'_c b_v d_v = 0.25(3.6)(39)(32.1) = 1126.7 \text{ kips O.K.}$$

J.3.6 Shear Design by Proposal 2: Modified CSA Approach

Shear design procedures in accordance with the Modified CSA Approach are used to determine the amount and spacing of the shear reinforcement required at a distance of 54 in. from the support.

a) Evaluation of ε_x

The design moment is :

$$M_u = 300.2 \text{ kips ft}$$

which shall not be less than the following value.

$$V_u \cdot d_v / 12 = 321.7(32.1) / 12 = 861 \text{ kips ft}$$

Therefore, substitute $V_u d_v$ for M_u in the ε_x calculation.

Calculate the strain in the reinforcement on the flexural tension side, ε_x :

$$\varepsilon_x = \frac{M_u / d_v + 0.5 N_u + V_u}{2(E_s A_s + E_p A_{ps})}$$

$$= \frac{861(12) / 32.1 + 0 + 321.7}{2[29,000(9.36) + 0]} = 1.2 \times 10^{-3} \leq 0.002 \quad \text{OK}$$

b) Evaluation of β and θ

Calculate θ from the longitudinal strain, ε_x .

$$\theta = 29 + 7000\varepsilon_x$$

$$= 29 + 7,000(1.2 \times 10^{-3}) = 37.4^\circ$$

Assume that at least minimum required amount of shear reinforcement is provided. Then, the coefficient, β , is:

$$\begin{aligned}\beta &= \frac{4.8}{(1 + 1500\varepsilon_x)} \\ &= \frac{4.8}{[1 + 1,500(1.2 \times 10^{-3})]} = 1.71\end{aligned}$$

c) Evaluation of Concrete Contribution

The contribution of the concrete to the nominal shear resistance is:

$$\begin{aligned}V_c &= 0.0316\beta\sqrt{f'_c}b_vd_v \\ &= 0.0316(1.71)\sqrt{3.6}(39)(32.1) = 128 \text{ kips}\end{aligned}$$

d) Evaluation of Required Transverse Reinforcement

Check if $V_u > 0.5\phi(V_c + V_p)$,

$$V_u = 321.7 \text{ kips} > 0.5\phi(V_c + V_p) = 0.5(0.9)(128 + 0) = 57.5 \text{ kips}$$

Therefore, transverse shear reinforcement must be provided.

The shear resistance required for the transverse reinforcement is:

$$V_s = (V_u / \phi) - V_c = (321.7 / 0.9) - 128 = 229 \text{ kips}$$

The shear strength provided by transverse reinforcement is:

$$V_s = \frac{A_v f_y d_v (\cot \theta + \cot \alpha) \sin \alpha}{s} \quad [\text{LRFD Eq. 5.8.3.3-4}]$$

When vertical stirrups are used, $\alpha = 90^\circ$. Then, the area of transverse reinforcement within a spacing (s) is: (use $f_y = 60$ ksi)

$$A_v / s = V_s / (f_y d_v \cot \theta) = 229 / [(60)(32.1) \cot 37.4^\circ] = 0.091 \text{ in.}^2 / \text{in.}$$

Use #5 four-leg stirrups at 12-in. spacing

$$A_v / s \text{ provided} = 0.31 \times 4 / 12 = 0.103 \text{ in.}^2 / \text{in.} > A_v / s \text{ required} = 0.091 \text{ in.}^2 / \text{in.}$$

e) Checks

Maximum Spacing Limitation for Transverse Reinforcement

Maximum spacing of transverse reinforcement shall not exceed the following

When $v_u / f'_c = 0.079 < 0.125$, $s_{\max} = 0.8d_v \leq 24.0$ in. [LRFD Eqs. 5.8.2.7-1]

$$s_{\max} \leq 24 \text{ in. (controls)}$$

$$\leq 0.8d_v = (0.8)(32.1) = 25.7 \text{ in.}$$

Since $s = 12$ in. ≤ 24 in. O.K.

Minimum Reinforcement Requirement

The area of transverse reinforcement shall not be less than:

$$A_{v,\min} = 0.0316 \sqrt{f'_c} \frac{b_v s}{f_y} = 0.0316 \sqrt{3.6} \frac{(39)(12)}{60} = 0.468 \text{ in}^2 < \text{provided } A_v = 1.24 \text{ in}^2$$

O.K.

Maximum Nominal Shear Resistance

In order to ensure that the concrete in the web of the beam will not crush prior to yielding of the transverse reinforcement, the LRFD Specifications specify an upper limit on V_n as follows:

$$V_n \leq 0.25 f'_c b_v d_v + V_p$$

$$V_s = \frac{A_v f_y d_v (\cot \theta + \cot \alpha) \sin \alpha}{s} = \frac{1.24 \cdot 60 \cdot 32.1 \cdot \cot(37.4)}{12} = 260 \text{ kips}$$

$$V_n = 128 + 260 + 0 = 388 \text{ kips} < 0.25 f'_c b_v d_v + 0 = 0.25(3.6)(39)(32.1) + 0 = 1126.7 \text{ kips}$$

O.K.

J.3.7 Summary and Conclusions

The required amounts of transverse reinforcement were four-leg #5 bar stirrups @12 inches and four-leg #5 bar stirrups @11 inches for Proposal 1 and 2, respectively. Table J-9 summarizes the results.

Table J-9 Summary of Results

Required or Calculated	Proposal 1: Modified STD Approach	Proposal 2: Modified CSA Approach
$(V_c + V_p)$, kips	143	128
V_s , kips	214	229
θ , deg.	45	37.4
Reinforcement Provided	four-leg #5 bars @11 inches	four-leg #5 bars @12 inches

J.4 Example 4: Reinforced Concrete Column and Footing

J.4.1 Example Description

This design example demonstrates shear design for two sections of a reinforced concrete column and footing, which are part of a pier designed by Modjeski and Masters, Inc.. The shear design is accomplished in accordance with the Proposal 1 (Modified STD Approach) and Proposal 2 (Modified CSA Approach). In the shear design of the footing, only one-way action is considered for a demonstration of proposals.

J.4.2 Geometry and Loading

The pier consists of 4 circular columns spaced 14'-1" apart on spread footings founded on sandy soil. Fig. J-14 shows an elevation of the pier. Each column is 39-inches in diameter and 18 ft tall. The footing size is 12'x12'x3'. The bridge supported by the pier was designed for the HS-25 live loading of the AASHTO Standard Specifications. Maximum shear occurs on column 1 at 0.0 ft from the bottom (top face of footing) and equals $V_t=44.8$ kips. The critical section for the footing is shown in Fig. J-15 and the design shear force is 21.9 k/ft.

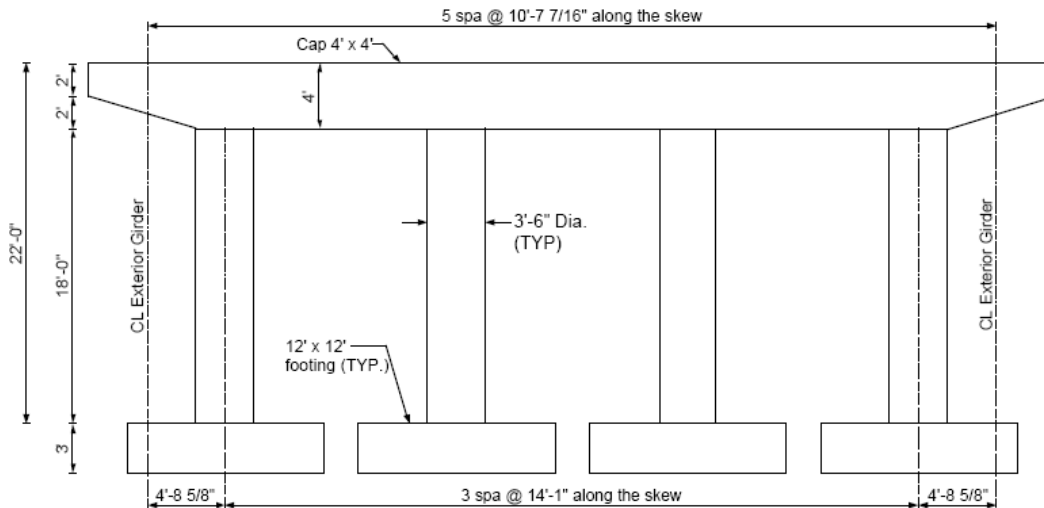


Figure J-14 Elevation (Modjeski and Masters, Inc.)

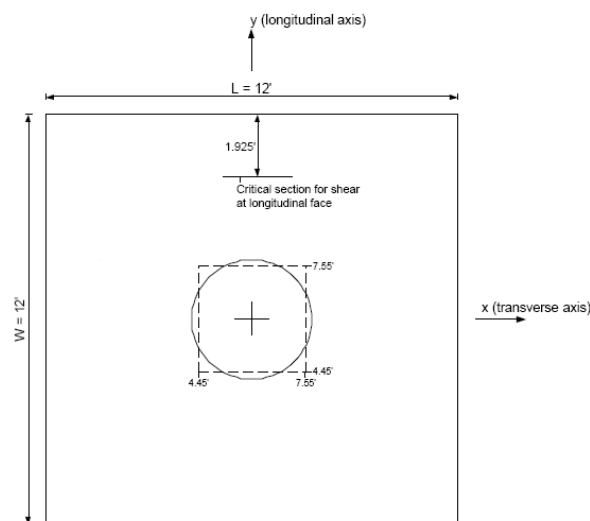


Figure J-15 Critical Section for Footing (Modjeski and Masters, Inc.)

J.4.3 Material Properties

The material properties are given in Table J-10.

Table J-10 Material Properties

CONCRETE PROPERTIES	
Concrete strength at 28 days, f'_c	3.0 ksi
Concrete unit weight, w_c	0.150 kcf
Modulus of elasticity of concrete, $E_c = 33,000(w_c)^{1.5}\sqrt{f'_c}$ [LRFD Eq. 5.4.2.4-1]	3,321ksi
REINFORCING BARS	
Yield strength, f_y	60 ksi
Modulus of elasticity, E_s [LRFD Art. 5.4.3.2]	29,000 ksi

J.4.4 Sectional Properties and Forces

The sectional properties and forces are summarized in Table J-11. Figures J-16 and J-17 provide cross-section details. Other basic calculations are also provided.

Table J-11 Sectional Properties and Forces

OVERALL GEOMETRY AND SECTIONAL PROPERTIES	COLUMN	FOOTING
Length (net), L	18 ft	-
Overall depth (or diameter) of member, h (or d_c)	39 in.	36 in.
Width of web, b_v	$\sqrt{1,370} = 37$ in.	12 in./ft
Area of cross-section of member, A_g	1,370 in. ²	432 in. ² /ft
Moment of inertia, I_g	149,292 in. ⁴	46,656 in. ⁴ /ft
Distance from centroid to extreme bottom fiber, y_b	21 in.	18 in.
Distance from centroid to extreme top fiber, y_t	21 in.	18 in.
Section modulus for the extreme bottom fiber, S_b	7,109 in. ³	2,592 in. ³ /ft
Section modulus for the extreme top fiber, S_t	7,109 in. ³	2,592 in. ³ /ft
Area of non-prestressed tension reinforcement, A_s	5.53 in. ² (7-#8 bars)	1.08 in. ² /ft (#9 bars @ 11.4 in. spacing)
Distance from extreme compression fiber to centroid of longitudinal tension reinforcement, d_s	34.1 in.	31.3 in.

SECTIONAL FORCES AT DESIGN SECTION

Unfactored shear force due to dead load, V_d	0.0 kips*	0.0 kips*
Factored shear force, V_u	44.8 kips	21.9 kips/ft
Unfactored moment due to dead load, M_d	0.0 ft-kips*	0.0 kips/ft*
Factored moment, M_u	491 ft-kips	20.7 ft-kips/ft
Factored axial force, N_u	1,062 kips (compression)	0.0 kips/ft

* These data are not available. For more accurate calculations, however, shear force and moment at a section due to unfactored dead load must be evaluated.

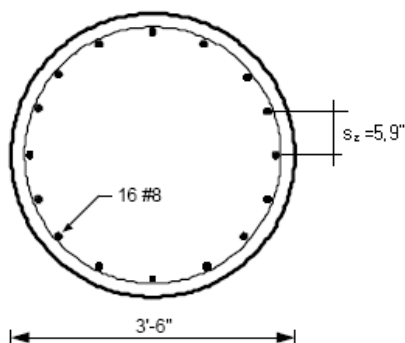


Figure J-16 Cross Section of Columns (Modjeski and Masters, Inc.)

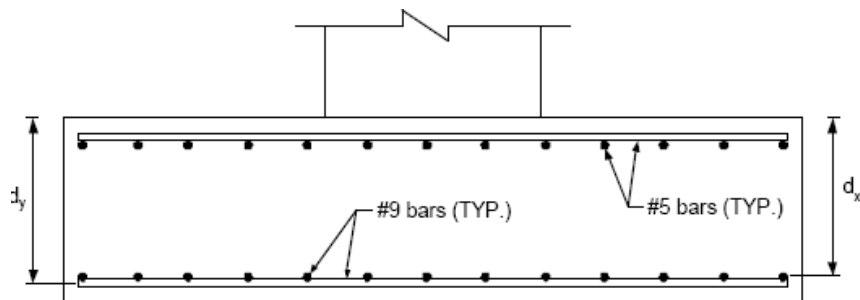


Figure J-17 Cross Section of Footings (Modjeski and Masters, Inc.)

Calculation of effective shear depth, d_v :

Column:

$$d_e = d_s = 34.1 \text{ in.}$$

d_v is the greater of:

$$0.9d_e = 0.9(34.1) = 30.7 \text{ in. (Controls)}$$

$$0.72h = 0.72(39) = 28.1 \text{ in.}$$

Therefore, $d_v = 30.7 \text{ in.}$

The design shear stress is:

$$v_u = \frac{V_u}{\phi b_v d_v} = \frac{44.8}{(0.9)(37)(30.7)} = 0.044 \text{ ksi}$$

Thus, $v_u / f'_c = 0.044 / 3.0 = 0.015$.

Footing:

$$d_e = d_s = 31.3 \text{ in.}$$

d_v is the greater of:

$$0.9d_e = 0.9(31.3) = 28.2 \text{ in. (Controls)}$$

$$0.72h = 0.72(36) = 25.9 \text{ in.}$$

Therefore, $d_v = 28.2 \text{ in.}$

The design shear stress is:

$$v_u = \frac{V_u}{\phi b_v d_v} = \frac{21.9}{(0.9)(12)(28.2)} = 0.072 \text{ ksi}$$

Thus, $v_u / f'_c = 0.044 / 3.0 = 0.015$.

J.4.5 Shear Design by Proposal 1: Modified STD Approach

Column:

Shear design procedures in accordance with the Modified STD Approach are used to determine the amount and spacing of the shear reinforcement required at a section 0.0 in. from the top face of column.

a) Evaluation of Concrete Contribution

Compute nominal shear strength provided by concrete, V_c :

$$V_c = 0.06\sqrt{f'_c}b_v d_v = 0.06\sqrt{3.0}(37)(30.7) = 118 \text{ kips}$$

d) Evaluation of Required Transverse Reinforcement

Check if $V_u > 0.5\phi V_c$

$$V_u = 44.8 \text{ kips} > 0.5\phi V_c = 0.5(0.9)(118) = 53.1 \text{ kips}$$

Therefore, transverse reinforcement is not required. However, ties (or spirals) should be spaced at least at 12-in. center-to-center for confinement of the column.

Footing:

Shear design procedures in accordance with the Modified STD Approach are used to determine the amount and spacing of the shear reinforcement required at a section located 23.1 in. from the edge of footing.

a) Evaluation of Concrete Contribution

Compute nominal shear strength provided by concrete, V_c :

$$V_c = 0.06\sqrt{f'_c}b_v d_v = 0.06\sqrt{3.0}(12)(36) = 44.9 \text{ kips}$$

d) Evaluation of Required Transverse Reinforcement

Check if $V_u > \phi V_c$

$$V_u = 21.9 \text{ kips} < \phi V_c = 0.9(44.9) = 40.4 \text{ kips}$$

Therefore, shear reinforcement is not required.

J.4.6 Shear Design by Proposal 2: Modified CSA Approach

Column:

Shear design procedures in accordance with the Modified CSA Approach are used to determine the amount and spacing of the shear reinforcement required at a distance of 0.0 in. from the top face of column.

a) Evaluation of ε_x

The design moment is

$$M_u = 491 \text{ kips ft}$$

which shall not be less than the following value.

$$V_u \cdot d_v / 12 = 44.8(30.7) / 12 = 115 \text{ kips ft} < M_u \quad \text{OK}$$

Calculate the strain in the reinforcement on the flexural tension side, ε_x :

$$\begin{aligned} \varepsilon_x &= \frac{M_u / d_v + 0.5N_u + V_u}{2(E_s A_s + E_p A_{ps})} \\ &= \frac{491(12) / 30.7 - 0.5(1062) + 44.8}{2[29,000(5.53) + 0]} = -9.2 \times 10^{-4} \end{aligned}$$

Since the value of ε_x is negative, the following equation must be used:

$$\begin{aligned} \varepsilon_x &= \frac{M_u / d_v + 0.5N_u + V_u}{2(E_c A_c + E_s A_s)} \\ &= \frac{491(12) / 30.7 - 0.5(1062) + 44.8}{2[3,321(1,370/2) + 29,000(5.53)]} = -6.0 \times 10^{-5} \end{aligned}$$

where A_c = area of concrete on the flexural tension side.

b) Evaluation of β and θ

Calculate θ from the longitudinal strain, ε_x .

$$\begin{aligned} \theta &= 29 + 7000\varepsilon_x \\ &= 29 + 7,000(-6.0 \times 10^{-5}) = 28.6^\circ \end{aligned}$$

Assume that at least the minimum amount of shear reinforcement required is provided. Then, the coefficient, β , is:

$$\begin{aligned} \beta &= \frac{4.8}{(1 + 1500\varepsilon_x)} \\ &= \frac{4.8}{[1 + 1,500(-6.0 \times 10^{-5})]} = 5.28 \end{aligned}$$

c) Evaluation of Concrete Contribution

The contribution of the concrete to the nominal shear resistance is:

$$\begin{aligned} V_c &= 0.0316\beta\sqrt{f'_c}b_vd_v \\ &= 0.0316(5.28)\sqrt{3.0}(37)(30.7) = 328.3 \text{ kips} \end{aligned}$$

d) Evaluation of Required Transverse Reinforcement

Check if $V_u > 0.5\phi(V_c + V_p)$

$$V_u = 44.8 \text{ kips} < 0.5\phi(V_c + V_p) = 0.5(0.9)(328.3 + 0) = 147.7 \text{ kips}$$

Therefore, transverse shear reinforcement is not required. If the section contains no transverse reinforcement, β should be calculated by the following equation.

$$\beta = \frac{4.8}{(1+1500\varepsilon_x)} \cdot \frac{51}{(39+s_{ze})} = \frac{4.8}{(1+1500(-6.0 \times 10^{-5}))} \cdot \frac{51}{(39+1.15)} = 6.7$$

Where the crack spacing parameter, s_z , shall be taken as d_v or as the maximum distance between layers of distributed longitudinal reinforcement, whichever is less.

From Fig. J-16, $s_z = 5.9$ in. and $s_{ze} = \frac{1.38s_z}{0.63+a_g} = \frac{1.38(5.9)}{0.63+0.75} = 1.15$.

Again, the contribution of the concrete to the nominal shear resistance is:

$$\begin{aligned} V_c &= 0.0316\beta\sqrt{f'_c}b_vd_v \\ &= 0.0316(6.7)\sqrt{3.0}(37)(30.7) = 416.5 \text{ kips} \end{aligned}$$

a half of which is larger than $V_u / \phi = 50.0 \text{ kips}$. Therefore, shear reinforcement is not required.

However, ties (or spirals) should be spaced at least at 12-in. center-to-center for confinement of the column.

Footings:

Shear design procedures in accordance with the Modified CSA Approach are used to determine the amount and spacing of the shear reinforcement at a section 23.1 in. from the edge of footing.

a) Evaluation of ε_x

The design moment is $M_u = 20.7 \text{ kips ft}$, which shall not be less than the following value.

$$V_u \cdot d_v / 12 = 21.9(28.2) / 12 = 51.5 \text{ kips ft}$$

Therefore, substitute $V_u d_v$ for M_u in the ε_x calculation.

Calculate the strain in the reinforcement on the flexural tension side, ε_x :

$$\begin{aligned} \varepsilon_x &= \frac{M_u / d_v + 0.5N_u + V_u}{2(E_s A_s + E_p A_{ps})} \\ &= \frac{51.5(12) / 28.2 + 0 + 21.9}{2[29,000(1.083) + 0]} = 7.0 \times 10^{-4} \end{aligned}$$

b) Evaluation of β and θ

Calculate θ from the longitudinal strain, ε_x .

$$\theta = 29 + 7000\varepsilon_x$$

$$= 29 + 7,000(7.0 \times 10^{-4}) = 33.9^\circ$$

Assume that at least the minimum amount of shear reinforcement required is provided. Then, the coefficient, β , is:

$$\begin{aligned}\beta &= \frac{4.8}{(1 + 1500\varepsilon_x)} \\ &= \frac{4.8}{[1 + 1,500(7.0 \times 10^{-4})]} = 2.34\end{aligned}$$

c) Evaluation of Concrete Contribution

The contribution of the concrete to the nominal shear resistance is:

$$\begin{aligned}V_c &= 0.0316\beta\sqrt{f'_c}b_vd_v \\ &= 0.0316(2.34)\sqrt{3.0}(12)(28.2) = 43.3 \text{ kips}\end{aligned}$$

d) Evaluation of Required Transverse Reinforcement

Check if $V_u > 0.5\phi(V_c + V_p)$

$$V_u = 21.9 \text{ kips} > 0.5\phi(V_c + V_p) = 0.5(0.9)(43.3 + 0) = 19.5 \text{ kips}$$

Therefore, shear reinforcement is not required.

J.4.7 Summary and Conclusions

Table J-12 summarizes the results. In the column, the shear reinforcement is not required for either approach. However, V_c values are very different. V_c increases as the axial compressive force increases in Proposal 2 while axial force effects are not reflected in Proposal 1. For the design of the footing, both approaches yield similar results.

Table J-12 (a) Summary of Results (Column)

Required or Calculated	Proposal 1: Modified STD Approach	Proposal 2: Modified CSA Approach
$(V_c + V_p)$, kips	118	328.3
V_s , kips	0	0
θ , deg.	45	28.6
Reinforcement Provided	#3 bars @ 12 in. (for confinement)	#3 bars @ 12 in. (for confinement)

Table J-12 (b) Summary of Results (Footing)

Required or Calculated	Proposal 1: Modified STD Approach	Proposal 2: Modified CSA Approach
$(V_c + V_p)$, kips	44.9	43.3

Reinforcement Provided	Not Required	Not Required
---------------------------	--------------	--------------

J.5 Example 5: Two-Span Continuous Post-Tensioned Box Bridge in Nevada

J.5.1 Example Description

This design example demonstrates shear design in the vicinity of the inflection point, (0.9L from the exterior support), of two-span, cast-in-place, post-tensioned box girder bridge. BERGER/ABAM provided the initial design data. This non-composite box girder is 60-inch deep and two-span continuous. The shear design is accomplished in accordance with the Proposal 1 (Modified STD Approach) and Proposal 2 (Modified CSA Approach).

J.5.2 Geometry and Loading

The beams are post-tensioned with the tendon profiles illustrated in Fig. J-18. The design girder is 120 ft long as shown on the left side of the figure. The design section is located 12 ft from the center of the mid-support, which corresponds to the inflection point.

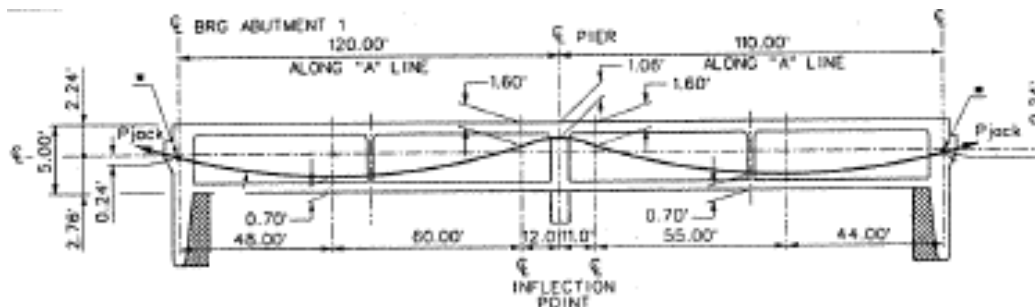


Figure J-18 Tendon Profiles (BERGER/ABAM)

J.5.3 Material Properties

The material properties are given in Table J-13.

Table J-13 Material Properties

CONCRETE PROPERTIES	
Concrete strength at 28 days, f'_c	4.0 ksi
Concrete unit weight, w_c	0.150 kcf
Modulus of elasticity of concrete, $E_c = 33,000(w_c)^{1.5}\sqrt{f'_c}$ [LRFD Eq. 5.4.2.4-1]	3,834 ksi
POST-TENSIONING STRANDS	
Type	0.5 in. dia., seven-wire, low-relaxation
Area of a strand	0.153 in ²
Ultimate strength, f_{pu}	270.0 ksi
Yield strength, f_{py} (=0.9 f_{pu}) [LRFD Table 5.4.4.1-1]	243 ksi
A parameter for prestressing, $f_{po} = 0.7 f_{pu}$	189 ksi
Modulus of elasticity, E_p [LRFD Art. 5.4.4.2]	28,500 ksi

REINFORCING BARS

Yield strength, f_y	60 ksi
Modulus of elasticity, E_s [LRFD Art. 5.4.3.2]	29,000 ksi

J.5.4 Sectional Properties and Forces

The sectional properties and forces are given in Table J-14. Fig. J-19 provides detailed dimensions of cross-section. Other basic calculations are also provided.

Table J-14 Sectional Properties and Forces

OVERALL GEOMETRY AND SECTIONAL PROPERTIES	
Span length, L	120 ft
Overall depth of girder, h	60 in.
Width of web, b_w	84 in.
Area of cross-section of girder, A_g	14,210 in. ²
Moment of inertia, I_g	7,699,484 in. ⁴
Distance from centroid to extreme bottom fiber, y_b	33.12 in.
Distance from centroid to extreme top fiber, y_t	26.88 in.
Section modulus for the extreme bottom fiber, S_b	232,472 in. ³
Section modulus for the extreme top fiber, S_t	286,439 in. ³
Area of non-prestressed tension reinforcement, A_s	18.6 in. ²
Distance from extreme compression fiber to centroid of longitudinal tension reinforcement, d_s	56.0 in
Area of prestressed tension reinforcement, A_p	53.09 in. ²
Distance from the bottom fiber to the centroid of prestressed tendons, d_p (negative moment region)	40.8 in
SECTIONAL FORCES AT DESIGN SECTION	
Unfactored shear force due to dead load, V_d	1,114 kips
Factored shear force, V_u	2,387 kips
Vertical component of the effective prestress force at the section considered, V_p	757 kips
Unfactored moment due to dead load, M_d	15,612 ft-kips
Factored moment, M_u	18,694 ft-kips

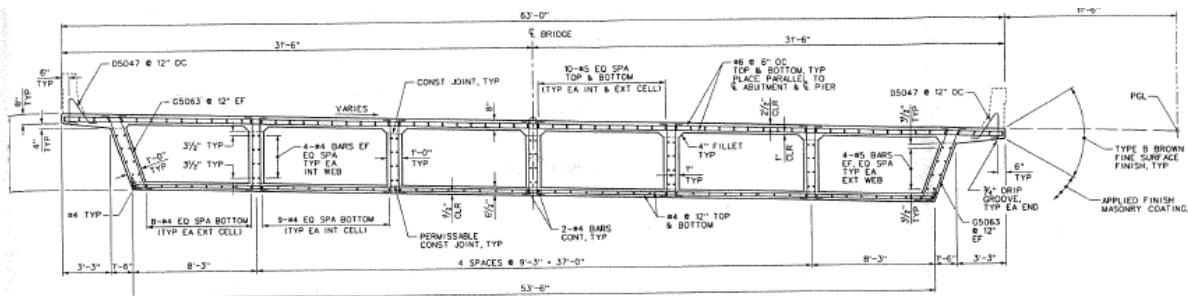


Figure J-19 Girder Cross-Section (BERGER/ABAM)

Effective depth or distance from the top fiber to the centroid of the tension steel including the prestressed steel is calculated as:

$$d_e = \frac{A_p f_{ps} d_p + A_s f_y d_s}{A_p f_{ps} + A_s f_y} = 42 \text{ in.} \quad [\text{LRFD Eqs. 5.7.3.3.1-2}]$$

where f_{ps} is the average stress in the prestressing steel, which can be calculated from [LRFD Eqs. 5.7.3.1.1-1].

The effective depth, d_v is the greater of:

$$0.9d_e = 0.9(42) = 37.8 \text{ in.}$$

$$0.72h = 0.72(60) = 43.2 \text{ in. (Controls)}$$

Therefore, $d_v = 43.2 \text{ in.}$

The design shear stress is:

$$v_u = \frac{V_u - \phi V_p}{\phi b_v d_v} = \frac{2,387 - 0.9(757)}{(0.9)(84)(43.2)} = 0.522 \text{ ksi}$$

Thus, $v_u / f_c' = 0.522 / 4 = 0.131$

J.5.5 Shear Design by Proposal 1: Modified STD Approach

Shear design procedures in accordance with the Modified STD Approach are used to determine the amount and spacing of the shear reinforcement at a section located 11.0 ft. from the center of the central support.

a) Evaluation of Web-Shear Cracking Strength

Compute web-shear cracking strength, V_{cw} :

$$V_{cw} = (0.06\sqrt{f_c'} + 0.3f_{pc})b_v d_v + V_p$$

The effective prestress forces are:

$$P_{se} = (53.09)(178) = 9,450 \text{ kips}$$

Compressive stress in concrete at the centroid of cross section due to prestress is:

$$f_{pc} = \frac{P_{se}}{A_g} = \frac{9,450}{14,210} = 0.67 \text{ ksi}$$

Therefore,

$$V_{cw} = [0.06\sqrt{4.0} + 0.3(0.67)](84)(43.2) + 757 = 1,922 \text{ kips}$$

b) Evaluation of Flexure-Shear Cracking Strength

Compute flexure-shear cracking strength, V_{ci} :

$$V_{ci} = 0.02\sqrt{f'_c}b_v d_v + V_d + V_i \frac{M_{cr}}{M_{\max}} \geq 0.06\sqrt{f'_c}b_v d_v$$

$$V_i = V_u - V_d = 2,387 - 1,114 = 1,273 \text{ kips} ,$$

$$M_{\max} = M_u - M_d = 18,694 - 15,612 = 3,082 \text{ ft} \cdot \text{kips} .$$

Moment causing flexural cracking at the design section due to externally applied loads:

$$M_{cr} = \frac{I_g}{y_t} (0.2\sqrt{f'_c} + f_{pe} - f_d)$$

The eccentricity of the strands at the design section is:

$$e = d_p - (h - y_t) = 40.8 - (60.0 - 26.88) = 7.7 \text{ in}.$$

Compressive stress in concrete due to effective prestress forces only:

$$f_{pe} = \frac{P_{se}}{A_g} + \frac{P_{se}ey_t}{I_g} = 0.67 + \frac{9,450(7.7)(26.88)}{7,699,484} = 0.92 \text{ ksi}$$

Stress due to service dead load:

$$f_d = \frac{M_d y_t}{I_g} = \frac{(15,612)(12)(26.88)}{7,699,484} = 0.65 \text{ ksi}$$

Therefore,

$$M_{cr} = \frac{7,699,484}{26.88} (0.2\sqrt{4.0} + 0.92 - 0.65) / 12 = 15,992 \text{ ft} \cdot \text{kips}$$

The flexure-shear cracking strength, V_{ci} , is:

$$V_{ci} = 0.02\sqrt{4.0}(84)(43.2) + 1,114 + \frac{1,273(15,992)}{3,082} = 7,733 \text{ kips}$$

$$> 0.06\sqrt{f'_c}b_v d_v = 0.06\sqrt{4.0}(84)(43.2) = 435 \text{ kips}$$

c) Evaluation of Concrete Contribution

The nominal shear strength provided by the concrete is the lesser of V_{ci} and V_{cw} .

Web-shear cracking strength $V_{cw} = 1,922 \text{ kips}$ (Governs)

Flexure-shear cracking strength $V_{ci} = 7,733 \text{ kips}$

Thus, the nominal shear strength provided by the concrete is:

$$V_c = 1,922 \text{ kips}$$

d) Evaluation of Required Transverse Reinforcement

Check if $V_u > 0.5\phi V_c$

$$V_u = 2,387 \text{ kips} > 0.5\phi V_c = 0.5(0.9)(1,922) = 865 \text{ kips}$$

Therefore, transverse reinforcement must be provided.

The shear force required is

$$V_s = (V_u / \phi) - V_c = (2,387 / 0.9) - 1,922 = 730 \text{ kips}$$

The shear strength provided by the transverse reinforcement is:

$$V_s = \frac{A_v f_y d_v (\cot \theta + \cot \alpha) \sin \alpha}{s} \quad [\text{LRFD Eq. 5.8.3.3-4}]$$

When vertical stirrups are used, $\alpha = 90^\circ$.

Since V_{cw} governs but $M_u = 18,694 \text{ ft} \cdot \text{kips} > M_{cr} = 15,992 \text{ ft} \cdot \text{kips}$, the angle of compressive strut is 45 degrees; i.e., $\cot \theta = 1$.

Therefore, area of transverse reinforcement (in^2) within a spacing (s) is: (use $f_y = 60 \text{ ksi}$)

$$A_v / s = V_s / (f_y d_v \cot \theta) = 730 / [(60)(43.2)(1.0)] = 0.28 \text{ in}^2 / \text{in}.$$

Therefore, **use double-leg #4 bars in each web at 10 in. spacing**

$$A_v / s \text{ provided} = 0.2 \times 2 \times 7 / 10 = 0.28 \text{ in}^2 / \text{in} > A_v / s \text{ required} = 0.28 \text{ in}^2 / \text{in}.$$

$$\text{Then, provided } V_s = \frac{0.2 \times 2 \times 7 \times 60 \times 43.2 \times 1.0}{10} = 726 \text{ kips}$$

Maximum Nominal Shear Resistance

In order to ensure that the concrete in the web of the girder will not crush prior to yielding of the transverse reinforcement, the LRFD Specifications specify an upper limit on V_n as follows:

$$V_n \leq 0.25 f'_c b_v d_v + V_p$$

$$V_n = 1,922 + 726 = 2,648 \text{ kips}$$

$$< 0.25 f'_c b_v d_v + V_p = 0.25(4.0)(84)(43.2) + 757 = 4,386 \text{ kips O.K.}$$

J.5.6 Shear Design by Proposal 2: Modified CSA Approach

Shear design procedures in accordance with the Modified CSA Approach are used to determine the amount and spacing of the shear reinforcement required at a section located 11.0 ft. from the centerline of the center support.

a) Evaluation of ε_x

Calculate the strain in the reinforcement on the flexural tension side, ε_x :

$$\begin{aligned} \varepsilon_x &= \frac{M_u / d_v + 0.5 N_u + V_u - V_p - A_{ps} f_{po}}{2(E_s A_s + E_p A_{ps})} \\ &= \frac{18,694(12) / 43.2 + 0 + 2,387 - 757 - 53.09(189)}{2[29,000(18.6) + 28,500(53.09)]} = -7.82 \times 10^{-4} \end{aligned}$$

Since the value of ε_x is negative, a different equation must be used:

$$\varepsilon_x = \frac{M_u / d_v + 0.5N_u + V_u - V_p - A_{ps}f_{po}}{2(E_c A_c + E_s A_s + E_p A_{ps})}$$

Where the area of concrete on the flexural tension side is the area above mid-height for the negative moment region; i.e., $A_c = 8,126 \text{ in.}^2$.

$$\varepsilon_x = \frac{18,694(12) / 43.2 + 0 + 2,387 - 757 - 53.09(189)}{2[(3,834)(8,126) + (29,000)(18.6) + (28,500)(53.09)]} = -4.8 \times 10^{-5}$$

b) Evaluation of β and θ

Calculate θ from the longitudinal strain, ε_x .

$$\begin{aligned}\theta &= 29 + 7000\varepsilon_x \\ &= 29 + 7,000(-4.8 \times 10^{-5}) = 28.7^\circ\end{aligned}$$

Assume that at least the minimum amount of shear reinforcement required is provided. Then, the coefficient, β , is:

$$\begin{aligned}\beta &= \frac{4.8}{(1 + 1500\varepsilon_x)} \\ &= \frac{4.8}{[1 + 1,500(-4.8 \times 10^{-5})]} = 5.18\end{aligned}$$

c) Evaluation of Concrete Contribution

The contribution of the concrete to the nominal shear resistance is:

$$\begin{aligned}V_c &= 0.0316\beta\sqrt{f'_c}b_v d_v \\ &= 0.0316(5.18)\sqrt{4.0}(84)(43.2) = 1,187 \text{ kips}\end{aligned}$$

d) Evaluation of Required Transverse Reinforcement

Check if $V_u > 0.5\phi(V_c + V_p)$

$$V_u = 2387 \text{ kips} > 0.5\phi(V_c + V_p) = 0.5(0.9)(1187 + 757) = 874.8 \text{ kips}$$

Therefore, transverse shear reinforcement must be provided.

The shear resistance required for the transverse reinforcement is:

$$V_s = (V_u / \phi) - V_c - V_p = (2,387 / 0.9) - 1,187 - 757 = 708.3 \text{ kips}$$

The shear strength provided by the transverse reinforcement is:

$$V_s = \frac{A_v f_y d_v (\cot \theta + \cot \alpha) \sin \alpha}{s} \quad \text{[LRFD Eq. 5.8.3.3-4]}$$

When vertical stirrups are used, $\alpha = 90^\circ$. Then, the area of transverse reinforcement within a spacing (s) is: (use $f_y = 60 \text{ ksi}$)

$$A_v / s = V_s / (f_y d_v \cot \theta) = 708.3 / [(60)(43.2) \cot 28.7^\circ] = 0.15 \text{ in.}^2 / \text{in.}$$

Therefore, **use #3 double-leg stirrups in each web at 10 in. spacing**

$$A_v / s \text{ provided} = 0.11 \times 2 \times 7 / 10 = 0.154 \text{ in.}^2 / \text{in.} > A_v / s \text{ required} = 0.15 \text{ in.}^2 / \text{in.}$$

$$\text{Then, provided } V_s = \frac{0.11 \times 2 \times 7 \times 60 \times 43.2 \times \cot 28.7^\circ}{10} = 729 \text{ kips}$$

e) Checks

Maximum Spacing Limitation of Transverse Reinforcement

Maximum spacing of transverse reinforcement may not exceed the following:

When $v_u / f'_c = 0.131 > 0.125$, $s_{\max} = 0.4d_v \leq 12.0 \text{ in.}$ [LRFD Eqs. 5.8.2.7-1]

$$\begin{aligned} s_{\max} &\leq 12 \text{ in. (controls)} \\ &\leq 0.4d_v = (0.4)(43.2) = 17.3 \text{ in.} \end{aligned}$$

Since $s = 12 \text{ in.} < 12 \text{ in.}$ O.K.

Maximum Nominal Shear Resistance

In order to ensure that the concrete in the web of the girder will not crush prior to yielding of the transverse reinforcement, the LRFD Specifications specify an upper limit on V_n as follows:

$$\begin{aligned} V_n &\leq 0.25f'_c b_v d_v + V_p \\ V_n &= 1,209 + 732 + 757 = 2,698 \text{ kips} \\ &< 0.25f'_c b_v d_v + V_p = 0.25(4.0)(84)(43.2) + 757 = 4,386 \text{ kips O.K.} \end{aligned}$$

J.5.7 Summary and Conclusions

The shear reinforcement required by Proposal 1 is almost twice as much as that required by Proposal 2. This result is mainly due to the discrepancy in the angle assumed for the compressive strut. In Proposal 1, that angle is conservatively taken as 45 degrees when the factored moment is greater than the cracking moment.

Table J-15 Summary of Results

Required or Calculated	Proposal 1: Modified STD Approach	Proposal 2: Modified CSA Approach
$(V_c + V_p)$, kips	1,922	1,944
V_s , kips	730	708
θ , deg.	45	28.7
Reinforcement Provided	double-leg #4 bars @ 10 in.	double-leg #3 bars @ 10 in.

J.6 Example 6: Shear Design Example of a Multi-Post Bent Cap

J.6.1 Example Description

This design example is from Tennessee DOT and is for a multi-post bent cap beam that is 86 feet wide. The beam is supported on four columns distributed at 22 ft centers below the beam. Fig. J-20 shows the elevation of the multi-post bent. The design section is taken at the internal face of the first pier in the first bay. Shear design is accomplished in accordance with the Proposal 1 (Modified CSA Approach) and Proposal 2 (Modified STD Approach). Since the design section is in the D-region, the Strut-and-Tie method is also used for shear design.

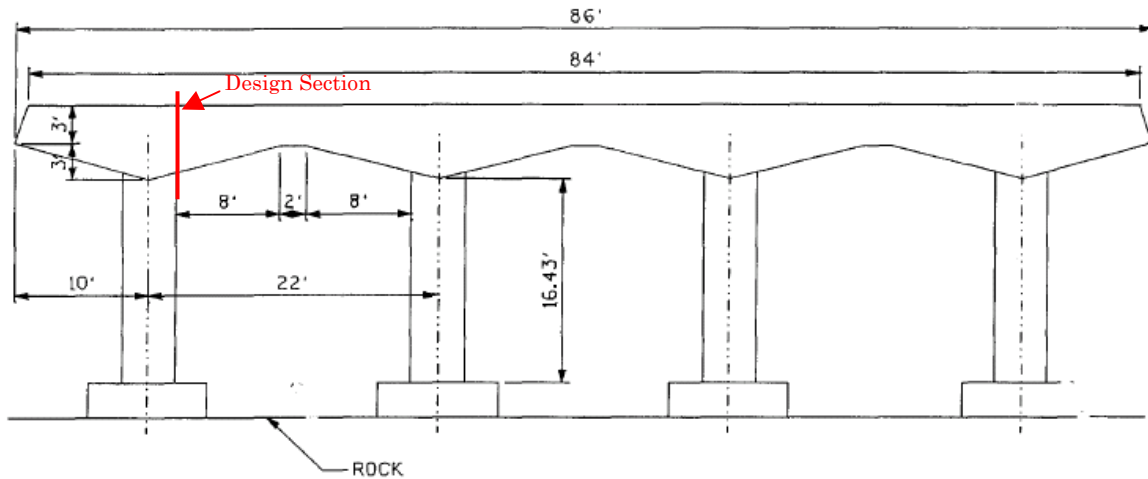


Figure J-20 Elevation of a Multi-Post Bent

J.6.2 Geometry and Loading

Fig. J-21 shows the load pattern and the design section dimensions. The design section was taken at the interior face of the first pier. Fig. J-22 gives the reinforcement layout for typical sections.

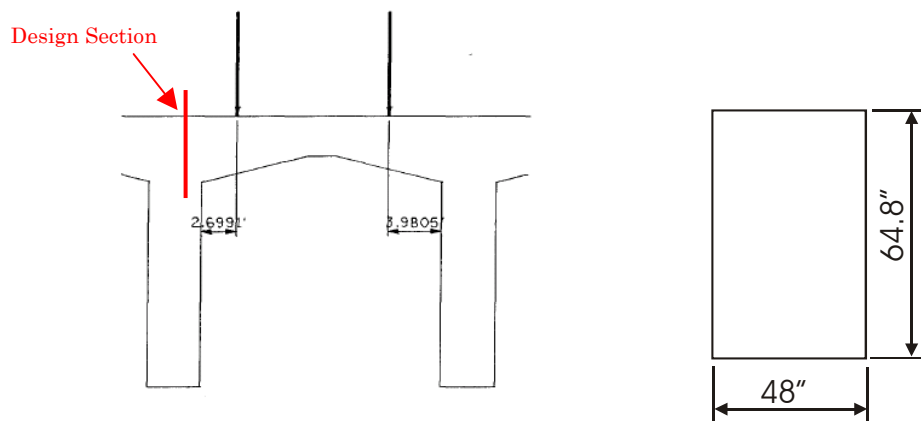


Figure J-21 Elevation of a Multi-Post Bent

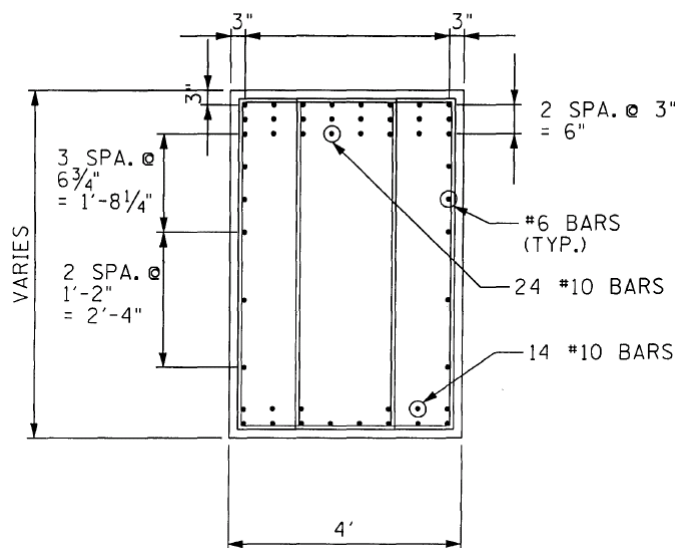


Figure J-22 Reinforcement Layout for sections through cap

J.6.3 Material Properties

The material properties are given in Table J-16.

Table J-16 Material Properties

CONCRETE PROPERTIES	
Concrete strength at 28 days, f'_c	3.0 ksi
Concrete unit weight, w_c	0.150 kcf
Modulus of elasticity of concrete, $E_c = 33,000(w_c)^{1.5}\sqrt{f'_c}$ [LRFD Eq. 5.4.2.4-1]	3,321ksi
REINFORCING BARS	
Yield strength, f_y	60 ksi(#10, #6)
Modulus of elasticity, E_s [LRFD Art. 5.4.3.2]	29,000 ksi

J.6.4. Sectional Properties and Forces

The sectional properties and forces are given in Table J-17.

Table J-17 Sectional Properties and Forces

OVERALL GEOMETRY AND SECTIONAL PROPERTIES	
Span length, L	22 ft
Overall depth of girder, h	64.8 in.
Width of web, b_v	48 in.
Area of cross-section of girder, A_g	3,110.4 in. ²
Moment of inertia, I_g	1,088,390.8 in. ⁴
Distance from centroid to extreme bottom fiber, y_b	32.4in.
Distance from centroid to extreme top fiber, y_t	32.4 in.
Section modulus for the extreme bottom fiber, S_b	33,592 in ³

Section modulus for the extreme top fiber, S_t	33,592 in ³
Area of non-prestressed tension reinforcement, A_s	30.48 in ²
Distance from extreme compression fiber to centroid of longitudinal tension reinforcement, d_s	58.8 in
Area of prestressed tension reinforcement, A_p	
Distance from the bottom fiber to the centroid of prestressed tendons, d_p	
Weight of beam	Varies with sections
SECTIONAL FORCES AT DESIGN SECTION*	
Unfactored shear force due to dead load, V_d	
Factored shear force, V_u	1222.4 kips
Unfactored moment due to dead load, M_d	
Factored moment, M_u	3477.1 ft-kips

*Negative moment, bottom is in compression

For variable depth members, LRFD requires components of inclined flexural compression shall be considered when calculating shear resistance. The flexural compression C_c at bottom side is:

$$C_c = \frac{M_u}{d_e - a/2} = \frac{3477.1 \times 12}{58.8 - 0.5(20)} = 855 \text{ kips}$$

Therefore the shear resistance for the flexural compression is:

$$V_{comp} = C_c \tan(\theta) = 855 \times \frac{3}{10} = 256.5 \text{ kips}$$

Calculation of effective depth, d_v :

The compressive block depth, $a = 20$ in

$$d_e = d_s = 58.8 \text{ in}$$

$$d_v = \max \left\{ \begin{array}{l} d_e - a/2 \\ 0.9d_e \\ 0.72h \end{array} \right\} = \max \left\{ \begin{array}{l} 58.8 - 0.5(20) = 48.8 \\ 0.9(58.8) = 52.92 \\ 0.72(64.8) = 46.66 \end{array} \right\} = 52.92 \text{ in}$$

The design shear stress is:

$$v_u = \frac{V_u - V_{comp} - \phi V_p}{\phi b_v d_v} = \frac{1222.4 - 256.5 - 0}{(0.9)(48)(52.92)} = 0.423 \text{ ksi}$$

Thus, $v_u / f'_c = 0.423 / 3.0 = 0.141 < 0.18$

J.6.5. Shear Design by Proposal 1: Modified STD Approach

Shear design procedures in accordance with the Modified STD Approach are used to determine the required amount and spacing of the shear reinforcement.

a) Evaluation of concrete contribution V_c

$$\begin{aligned} V_c &= 0.06\sqrt{f'_c}b_vd_v \\ &= 0.06\sqrt{3.0}(48)(52.92) = 264.0 \text{ kips} \end{aligned}$$

d) Evaluation of Required Transverse Reinforcement

Check if $V_u > 0.5\phi V_c$

$$V_u - V_{comp} = 965.9 \text{ kips} > 0.5\phi V_c = 0.5(0.9)(264.0) = 118.8 \text{ kips}$$

Therefore, transverse reinforcement must be provided.

The shear force required is

$$V_s = (V_u - V_{comp}) / \phi - V_c = (965.9 / 0.9) - 264 = 809.2 \text{ kips}$$

The shear strength provided by the transverse reinforcement is:

$$V_s = \frac{A_v f_y d_v}{s} \quad \text{[LRFD Eq. 5.8.3.3-4]}$$

$$A_v / s = V_s / (f_y d_v) = 809.2 / [(60)(52.92)] = 0.255 \text{ in.}^2 / \text{in.}$$

Therefore, **use 4-#6 bars at a spacing of 4.5 in.**

$$A_v = 4(0.44) = 1.76 \text{ in.}^2 \text{ and } s = 4.5 \text{ in.}$$

$$\frac{A_v}{s} (\text{provided}) = 1.76 / 4.5 = 0.39 \text{ in.}^2 / \text{in.} > \frac{A_v}{s} (\text{required}) = 0.255 \text{ in.}^2 / \text{in.}$$

$$\text{Then, provided } V_s = \frac{1.76 \times 60 \times 52.92}{4.5} = 1242 \text{ kips}$$

e) ChecksMaximum Spacing Limitation on Transverse Reinforcement

Maximum spacing of the transverse reinforcement shall not exceed the following:

$$\text{When } v_u / f'_c = 0.178 \geq 0.125, s_{\max} = 0.4d_v \leq 12.0 \text{ in.} \quad \text{[LRFD Eqs. 5.8.2.7-1]}$$

$$\begin{aligned} s_{\max} &\leq 12 \text{ in. (controls)} \\ &\leq 0.4d_v = (0.4)(52.92) = 21 \text{ in.} \end{aligned}$$

Since $s = 4.5 \text{ in.} \leq s_{\max} = 12 \text{ in.}$ O.K.

Minimum Reinforcement Requirement

The area of transverse reinforcement shall not be less than:

$$A_{v,\min} \geq 0.0316\sqrt{f'_c} \frac{b_v s}{f_y} = 0.0316\sqrt{3.0} \frac{(48)(4.5)}{60} = 0.197 \text{ in.}^2 < \text{provided } A_v = 1.76 \text{ in.}^2$$

O.K.

Maximum Nominal Shear Resistance

In order to ensure that the concrete in the web of the girder will not crush prior to yielding of the transverse reinforcement, the LRFD Specifications specify an upper limit on V_n as follows:

$$V_n \leq 0.25 f'_c b_v d_v + V_p$$

$$V_c + V_s = 264 + 1242 = 1506 \text{ kips} < 0.25 f'_c b_v d_v = 0.25(3.0)(48)(52.92) = 1905 \text{ kips}$$

Then $V_n = 1506 \text{ kips} > (V_u - V_{comp}) / \phi = 1073 \text{ kips}$ O.K.

J.6.6 Shear Design by Proposal 2: Modified CSA Approach

Shear design procedures in accordance with the Modified CSA Approach are used to determine the required amount and spacing of the shear reinforcement.

a) Evaluation of ε_x

Calculate the strain in the reinforcement on the flexural tension side, ε_x :

$$\begin{aligned} \varepsilon_x &= \frac{M_u / d_v + 0.5 N_u + V_u - V_p - A_{ps} f_{po}}{2(E_s A_s + E_p A_{ps})} \leq 0.002 \\ &= \frac{3477.1(12) / 52.92 + 0 + 1222.4 - 256.5 - 0 - 0}{2[(29,000)(30.48)]} = 0.992 \times 10^{-3} \end{aligned}$$

b) Evaluation of β and θ

Calculate θ from the longitudinal strain, ε_x .

$$\begin{aligned} \theta &= 29 + 7000 \varepsilon_x \\ &= 29 + 7,000(0.992 \times 10^{-3}) = 35.9^\circ \\ \cot \theta &= 1.381 \end{aligned}$$

Assume that at least the minimum amount of shear reinforcement required is provided. Then, the coefficient, β , is:

$$\beta = \frac{4.8}{(1 + 1500 \varepsilon_x)} = \frac{4.8}{(1 + (1500)(0.992 \times 10^{-3}))} = 1.929$$

c) Evaluation of Concrete Contribution

The contribution of the concrete to the nominal shear resistance is:

$$\begin{aligned} V_c &= 0.0316 \beta \sqrt{f'_c} b_v d_v \\ &= 0.0316(1.929) \sqrt{3.0} (48)(52.92) = 268.2 \text{ kips} \end{aligned}$$

d) Evaluation of Required Transverse Reinforcement

Check if $V_u > 0.5 \phi (V_c + V_p)$

$$V_u - V_{comp} = 965.9 \text{ kips} > 0.5 \phi (V_c + V_p) = 0.5(0.9)(268.2 + 0) = 120.7 \text{ kips}$$

Therefore, transverse shear reinforcement must be provided.

The required shear resistance for the transverse reinforcement is:

$$V_s = (V_u - V_{comp}) / \phi - V_c - V_p = (965.9 / 0.9) - 268.2 - 0 = 805 \text{ kips}$$

The shear strength provided by the transverse reinforcement is:

$$V_s = \frac{A_v f_y d_v (\cot \theta + \cot \alpha) \sin \alpha}{s} \quad [\text{LRFD Eq. 5.8.3.3-4}]$$

When vertical stirrups are used, $\alpha = 90^\circ$. Then, the area of transverse reinforcement within a spacing of (s) is: (use $f_y = 60$ ksi, $\cot \theta = 1.381$)

$$A_v / s = V_s / (f_y d_v \cot \theta) = 805 / [(60)(52.92)(1.381)] = 0.184 \text{ in.}^2 / \text{in.}$$

Therefore, **use 4-#6 bars at a spacing of 4.5 in.**

$$A_v = 4(0.44) = 1.76 \text{ in.}^2 \text{ and } s = 4.5 \text{ in.}$$

$$\frac{A_v}{s} (\text{provided}) = 1.76 / 4.5 = 0.39 \text{ in.}^2 / \text{in.} > \frac{A_v}{s} (\text{required}) = 0.184 \text{ in.}^2 / \text{in.}$$

$$\text{Then, provided } V_s = \frac{1.76 \times 60 \times 52.92 \times 1.381}{4.5} = 1715 \text{ kips}$$

e) Checks

Maximum Spacing Limitation on Transverse Reinforcement

Maximum spacing of transverse reinforcement shall not exceed the following:

$$\text{When } v_u / f'_c = 0.178 \geq 0.125, s_{\max} = 0.4d_v \leq 12.0 \text{ in.} \quad [\text{LRFD Eqs. 5.8.2.7-1}]$$

$$\begin{aligned} s_{\max} &\leq 12 \text{ in. (controls)} \\ &\leq 0.4d_v = (0.4)(52.92) = 21 \text{ in.} \end{aligned}$$

Since $s = 4.5 \text{ in.} \leq s_{\max} = 12 \text{ in.}$ O.K.

Minimum Reinforcement Requirement

The area of transverse reinforcement should not be less than:

$$A_{v,\min} \geq 0.0316 \sqrt{f'_c} \frac{b_v s}{f_y} = 0.0316 \sqrt{3.0} \frac{(48)(4.5)}{60} = 0.197 \text{ in.}^2 < \text{provided } A_v = 1.76 \text{ in.}^2$$

O.K.

Maximum Nominal Shear Resistance

In order to ensure that the concrete in the web of the girder will not crush prior to yielding of the transverse reinforcement, the LRFD Specifications specify an upper limit on V_n as follows:

$$V_n \leq 0.25 f'_c b_v d_v + V_p, \quad (V_p = 0 \text{ in this example})$$

$$V_c + V_s = 268.2 + 1715 = 1983 \text{ kips} > 0.25 f'_c b_v d_v = 0.25(3.0)(48)(52.92) = 1905 \text{ kips}$$

Then $V_n = 1905 \text{ kips} > (V_u - V_{\text{comp}}) / \phi = 1073 \text{ kips}$ O.K.

J.6.7 Shear Design (STRUT AND TIE)

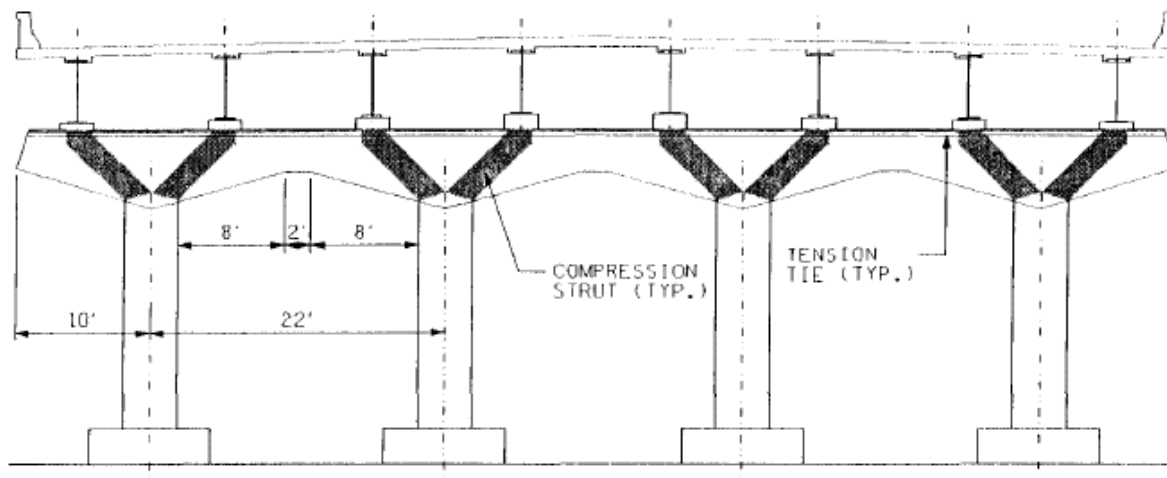


Figure J-23 Strut-and-Tie Model

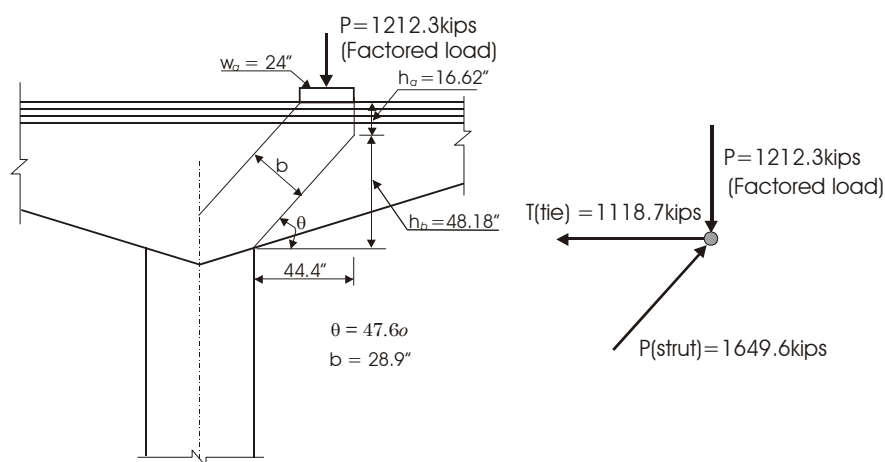


Figure J-24 Strut-and-Tie Model

a) Geometry Properties

The bearing width is : $w_a = 24in.$

$$h_a = 3 + 3 + 3 + 6d_b = 9 + 6 \times 1.27 = 16.62in.$$

$$h_b = 64.8 - h_a = 64.8 - 16.62 = 48.18in.$$

Therefore the strut angle is:

$$\theta = \arctan\left(\frac{48.18}{44.4}\right) = 47.3^\circ$$

The strut width can be given as :

$$b = w_b \sin(\theta) + h_a \cos(\theta) = 28.9in.$$

b) Interior forces

Compressive force in strut:

$$P_{strut} = P_{bearing} / \sin(\theta) = 1212.3 / \sin(47.3) = 1649.6kips$$

Tensile force in ties:

$$T_{tie} = P_{bearing} / \tan(\theta) = 1212.3 / \tan(47.3) = 1118.7 \text{ kips}$$

c) Strut

The tensile strain in the concrete in the direction of the tension tie is:

$$\varepsilon_s = \frac{f_y}{E_s} = \frac{60}{29000} = 0.00207$$

The principal tensile strain of concrete is :

$$\varepsilon_1 = \varepsilon_s + (\varepsilon_s + 0.002) \cot^2 \theta = 0.00207 + (0.00207 + 0.002)(0.923)^2 = 0.00554$$

The limiting compressive stress f_{cu} is:

$$f_{cu} = \frac{f'_c}{0.8 + 170\varepsilon_1} = \frac{3}{0.8 + (170)(0.00554)} = 1.72 \text{ ksi} \leq 0.85f'_c = 2.55 \text{ ksi}$$

$$f_{cu} = 1.72 \text{ ksi}$$

Then

$$P_n = f_{cu} A_{cs} = (1.72)(48)(28.9) = 2386 \text{ kips} > P_{strut} = 1649.6 \text{ kips} \quad \text{O.K.}$$

d) Tie

$$P_n = f_y A_s = (60)(30.48) = 1828.8 \text{ kips} > T_{tie} = 1118.7 \text{ kips} \quad \text{O.K.}$$

f) Node Region Check

The limiting compressive stress in the node region is:

$$f_{limit} = 0.85\phi f'_c = (0.85)(0.70)(3.0) = 1.785 \text{ ksi}$$

Compressive stress in the strut is:

$$f_{strut} = P_{strut} / A_{cs} = 1649.6 / ((48)(28.9)) = 1.19 \text{ ksi} \leq 1.785 \text{ ksi}$$

Compressive stress under bearing is:

$$f_{bearing} = P_{bearing} / A_c = 1212.3 / ((48)(24)) = 1.05 \text{ ksi} \leq 1.785 \text{ ksi} \quad \text{O.K.}$$

g) Crack control reinforcement

The required area of crack control reinforcement with a spacing of 12 inches is :

$$A_{required} = \frac{0.003 \times (36 \text{ in}) \times (12 \text{ in})}{1 \text{ ft}} = 1.296 \frac{\text{in}^2}{\text{ft}}$$

Try #6 bars spaced @ 6 inches vertically and at 12 inches horizontally:

$$A_s = \frac{0.44 \times 2 + 0.44}{1 \text{ ft}} = 1.32 \frac{\text{in}^2}{\text{ft}} \geq 1.296 \frac{\text{in}^2}{\text{ft}}, \text{ O.K.}$$

J.6.8. Summary and Conclusions

The design results by the Modified STD Approach and the Modified CSA Approach are summarized in Table J-18. The required amounts of transverse reinforcement by those two approaches are very similar. Those two methods require large amounts of shear reinforcement while only minimum reinforcement is required by the strut-and-tie method. The reason is that the design section is within the D-region and strut-and-tie method is more appropriate for shear design in this region even though the LRFD Specifications allow the use of the sectional design method.

Table J-18 Summary of Results

Required or calculated	Proposal 1: Modified STD	Proposal 2: Modified CSA
	Approach	Approach
$(V_c + V_p)$, kips	264	268.2
V_s , kips	809.2	805
θ , deg.	45.0	35.9
Reinforcement Provided	4- #6 bars @4.5 inches	4- #6 bars @4.5 inches

J.7 Example 7: Type IV Beam

J.7.1 Example Description

This example demonstrates the shear design of a section of a 100-ft span AASHTO Type IV beam bridge. Bridge details were provided by Tim Bradberry of the Texas Department of Transportation. The bridge consists of 3 spans with each span simply supported. The composite pretensioned beams are 54-inch deep and have an 8 in. thick deck. Shear design is accomplished in accordance with Proposal 1 (Modified STD Approach) and Proposal 2 (Modified CSA Approach).

J.7.2 Geometry and Loading

This bridge has 3 spans, each span is simply supported, and the span lengths are 100-ft, 120-ft, and 100-ft as shown in Fig. J-25. Design live load is HS-20, and the section at a distance of 4.93 ft from the support, as marked in Fig. J-25, is designed for shear. As shown in Fig. J-26, the typical interior beam among five beams is designed in this example.

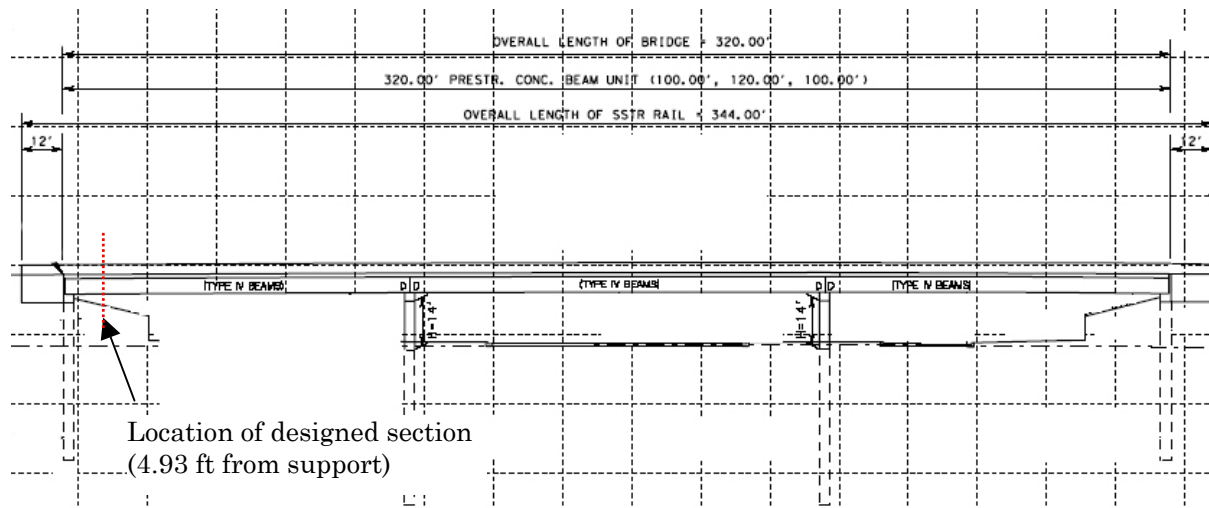


Figure J-25 Bridge Span Geometry

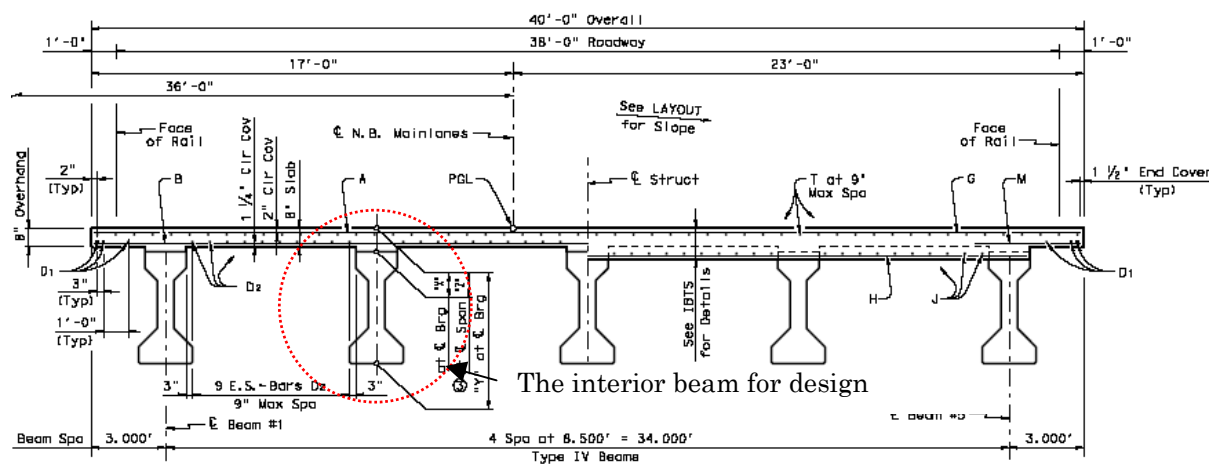


Figure J-26 Bridge Cross-Section

J.7.3 Material Properties

The material properties are given in Table J-19.

Table J-19 Material Properties

CONCRETE PROPERTIES	
Concrete strength of girder at 28 days, f'_c	6.5 ksi
Concrete strength of deck at 28 days, f'_c	4.0 ksi
Concrete unit weight, w_c	0.150 kcf
Modulus of elasticity of concrete for girder,	4,888 ksi
$E_{c,beam} = 33,000(w_c)^{1.5} \sqrt{f'_c}$ [LRFD Eq. 5.4.2.4-1]	
Modulus of elasticity of concrete for deck,	3,834 ksi
$E_{c,slab} = 33,000(w_c)^{1.5} \sqrt{f'_c}$ [LRFD Eq. 5.4.2.4-1]	
Modular ratio between slab and beam concrete, n	$= E_{c,slab} / E_{c,beam} = 0.784$
PRESTRESSING STRANDS	
Type	0.5 in. dia., seven-wire, low-relaxation
Area of a strand	0.153 in ²
Ultimate strength, f_{pu}	270.0 ksi
Yield strength, f_{py} ($=0.9 f_{pu}$)	243 ksi
[LRFD Table 5.4.4.1-1]	
A parameter for prestressing, $f_{po} = 0.7 f_{pu}$	189 ksi
Effective prestressing stress after all losses, f_{se}	148.2 ksi
Modulus of elasticity, E_p [LRFD Art. 5.4.4.2]	28,500 ksi
REINFORCING BARS	
Yield strength, f_y	#3, #4 :60 ksi
Modulus of elasticity, E_s [LRFD Art. 5.4.3.2]	29,000 ksi

J.7.4 Sectional Properties and Forces

The sectional properties and forces are given in Table J-20. Fig. J-27 provides detailed dimensions for the cross-section of an AASHTO Type IV beam. The typical strand pattern at midspan is shown in Fig. J-28, and the strand pattern at the design section is given in Table J-21. Note that 8 strands are draped as shown in Table J-21. Some basic calculations are also provided in this sub-section.

Table J-20 Sectional Properties and Forces

OVERALL GEOMETRY AND SECTIONAL PROPERTIES	
Non-Composite Section	
Span length, L	98.58 ft
Overall depth of girder, h	54.0 in.
Width of web, b_v	8.0 in.
Area of cross-section of girder, A_g	789 in. ²
Moment of inertia, I_g	260,403 in. ⁴
Distance from centroid to extreme bottom fiber,	24.75 in.
y_b	

Distance from centroid to extreme top fiber, y_t	29.25 in.
Section modulus for the extreme bottom fiber, S_b	10,521 in ³
Section modulus for the extreme top fiber, S_t	8,902 in ³
Weight of beam	0.821 kip/ft
Composite Section	
Overall depth of the composite section, h_c	62 in.
Slab thickness, t_s	8.0 in.
Total transformed area of the composite section, A_c	1,604 in. ²
Moment of inertia of the composite section, I_c	708,041 in. ⁴
Distance from centroid of the composite section to extreme bottom fiber, y_{bc}	41.66 in.
Distance from centroid of the composite section to extreme top fiber of beam, y_{tg}	12.34 in.
Distance from centroid of the composite section to extreme top fiber of slab, y_{tc}	20.34 in.
Composite section modulus for the extreme bottom fiber of beam, S_{bc}	16,996 in ³
Composite section modulus for the extreme top fiber of beam, S_{tg}	57,378 in ³
Composite section modulus for the extreme top fiber of slab, S_{tc}	34,810 in ³
Area of non-prestressed tension reinforcement, A_s	0 in ²
Distance from extreme compression fiber to centroid of longitudinal tension reinforcement, d_s	0 in
Area of prestressed tension reinforcement, A_p	=40(0.153)=6.120 in ²
Distance from the top fiber to the centroid of prestressed tendons, d_p	55.93 in
SECTIONAL FORCES AT DESIGN SECTION	
Unfactored shear force due to beam weight, V_{dg}	36.4 kips
Unfactored shear force due to deck slab, V_{ds}	37.7 kips
Unfactored shear force due to superimposed dead load, V_{dw}	8.3 kips
Unfactored shear force due to total dead load, V_d	82.4 kips
Factored shear force, V_u	265.0 kips
Unfactored moment due to beam weight, M_{dg}	189.6 ft-kips
Unfactored moment due to deck slab, M_{ds}	196.2 ft-kips
Unfactored moment due to superimposed dead load, M_{dw}	43.4 ft-kips
Unfactored moment due to total dead load, M_d	429.2 ft-kips
Factored moment, M_u	1,125.0 ft-kips

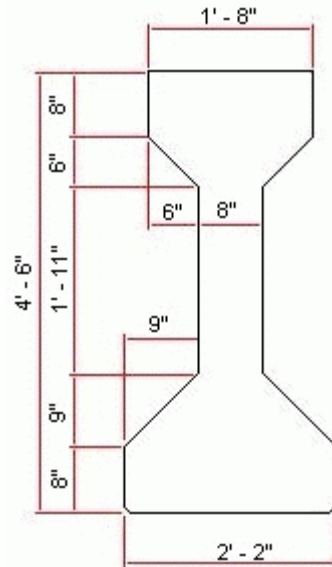


Figure J-27 Cross-Section of AASHTO Box Beam Type BIII-48

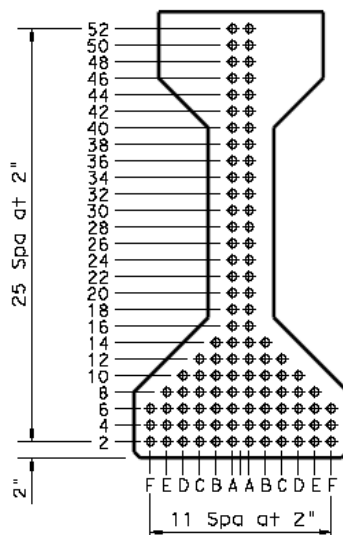


Figure J-28 Typical Strand Pattern at Midspan

Table J-21 Strand Pattern at the Design Section (a total of 40 strands, 8 draped strands)

Dist. from bottom (in.)	2.0	4.0	6.0	8.0	46.0	48.0	50.0	52.0
Strands/Row at End	10	10	10	2	2	2	2	2
Strands/Row at CL	12	12	12	4	0	0	0	0

Calculation of effective depth, d_v :

Note that 8 strands are draped, and $d_e = 49.40$ in at the design section for shear. The equivalent compressive block depth, a , is calculated by flexural analysis ($a = 8.40$ in.).

Then, d_v is the greater of:

$$d_e - a/2 = [49.4 - 0.5(8.4)] = 45.20 \text{ in (Controls)}$$

$$0.9d_e = 0.9(49.40) = 44.46 \text{ in}$$

$$0.72h = 0.72(62) = 43.40 \text{ in}$$

Therefore, $d_v = 45.20 \text{ in}$.

The vertical component of the effective prestressing force, V_p , due to the 8 draped strands is 17.17 kips. Then, the design shear stress is:

$$v_u = \frac{V_u - \phi V_p}{\phi b_v d_v} = \frac{265.0 - 0.9(17.17)}{(0.9)(8.0)(45.20)} = 0.767 \text{ ksi}$$

Thus, $v_u / f'_c = 0.767 / 6.5 = 0.118$

J.7.5 Shear Design by Proposal 1: Modified STD Approach

Shear design in accordance with the Modified STD Approach is used to determine the amount and spacing of the shear reinforcement required at a section located 4.93 ft from the support.

a) Evaluation of Web-Shear Cracking Strength

Compute web-shear cracking strength, V_{cw} :

$$V_{cw} = (0.06\sqrt{f'_c} + 0.3f_{pc})b_v d_v + V_p$$

The effective prestress force is:

$$P_{se} = 40(0.153)(148.2) = 907.0 \text{ kips}$$

The eccentricity of the strands at the design section is 12.15 in. Then, the compressive stress in the concrete at the centroid of cross section due to both pretensioning and moments and resisted by the precast member alone is:

$$f_{pc} = \frac{P_{se}}{A_g} - \frac{P_{se}e(y_{bc} - y_b)}{I_g} + \frac{(M_{dg} + M_{ds})(y_{bc} - y_b)}{I_g}$$

$$f_{pc} = \frac{907.0}{789} - \frac{907.0(12.15)(41.66 - 24.75)}{260,403} + \frac{(189.6 + 196.2)(12)(41.66 - 24.75)}{260,403} = 0.735 \text{ kips}$$

Therefore,

$$V_{cw} = [0.06\sqrt{6.5} + 0.3(0.735)](8)(45.20) + 17.17 = 152.2 \text{ kips}$$

b) Evaluation of Flexure-Shear Cracking Strength

Compute flexure-shear cracking strength, V_{ci} :

$$V_{ci} = 0.02\sqrt{f'_c}b_v d_v + V_d + V_i \frac{M_{cr}}{M_{\max}} \geq 0.06\sqrt{f'_c}b_v d_v$$

$$V_i = V_u - V_d = 265.0 - 82.4 = 182.6 \text{ kips},$$

$$M_{\max} = M_u - M_d = 1,125.0 - 429.2 = 695.8 \text{ ft} \cdot \text{kips}.$$

Moment causing flexural cracking at the design section due to externally applied loads:

$$M_{cr} = \frac{I_c}{y_{bc}} (0.2\sqrt{f'_c} + f_{pe} - f_d)$$

Compressive stress in concrete due to effective prestress forces only:

$$f_{pe} = \frac{P_{se}}{A_g} + \frac{P_{se} e y_b}{I_g} = \frac{907.0}{789} + \frac{907.0(12.15)(24.75)}{260,403} = 2.197 \text{ ksi}$$

Stress due to service dead load:

$$f_d = \frac{M_d y_b}{I_g} = \frac{429.2(12)(24.75)}{260,403} = 0.490 \text{ ksi}$$

Therefore,

$$M_{cr} = \frac{708,041}{41.66} (0.2\sqrt{6.5} + 2.197 - 0.490) / 12 = 3,139.8 \text{ ft} \cdot \text{kips}$$

The flexure-shear cracking strength, V_{ci} , is:

$$V_{ci} = 0.02\sqrt{6.5}(8.0)(45.20) + 82.4 + \frac{182.6(3,139.8)}{695.8} = 924.8 \text{ kips}$$

$$> 0.06\sqrt{f'_c} b_v d_v = 0.06\sqrt{6.5}(8.0)(45.20) = 55.3 \text{ kips}$$

c) Evaluation of Concrete Contribution

The nominal shear strength provided by concrete is the lesser of V_{ci} and V_{cw} .

Web-shear cracking strength $V_{cw} = 152.2 \text{ kips}$ (Governs)

Flexure-shear cracking strength $V_{ci} = 924.8 \text{ kips}$

Thus, the nominal shear strength provided by concrete is:

$$V_c = 152.2 \text{ kips}$$

d) Evaluation of Required Transverse Reinforcement

Check if $V_u > 0.5\phi V_c$

$$V_u = 265.0 \text{ kips} > 0.5\phi V_c = 0.5(0.9)(152.2) = 68.5 \text{ kips}$$

Therefore, transverse reinforcement must be provided.

The shear force required is

$$V_s = (V_u / \phi) - V_c = (265.0 / 0.9) - 152.2 = 142.2 \text{ kips}$$

The shear strength provided by the transverse reinforcement is:

$$V_s = \frac{A_v f_y d_v (\cot \theta + \cot \alpha) \sin \alpha}{s} \quad [\text{LRFD Eq. 5.8.3.3-4}]$$

When vertical stirrups are used, $\alpha = 90^\circ$.

Since V_{cw} governs and $M_u = 1,125.0 \text{ ft} \cdot \text{kips} < M_{cr} = 3,139.8 \text{ ft} \cdot \text{kips}$, the angle of the compressive strut is obtained as:

$$\cot \theta = 1 + 3f_{pc} / \sqrt{f'_c} \leq 1.80$$

$$\cot \theta = 1 + 3(0.735) / \sqrt{6.5} = 1.86 > 1.80 \text{ (Governs)}$$

Therefore, $\cot \theta = 1.80$.

Therefore, area of transverse reinforcement (in^2) within a spacing (s) is: (use $f_y = 60$ ksi)

$$A_v / s = V_s / (f_y d_v \cot \theta) = 142.2 / [(60)(45.20)(1.8)] = 0.0291 \text{ in}^2 / \text{in}.$$

Therefore, **use #4 double leg stirrups at 12 in. spacing**

$$A_v / s \text{ provided} = 2(0.20) / 12 = 0.0333 \text{ in}^2 / \text{in}. > A_v / s \text{ required} = 0.0291 \text{ in}^2 / \text{in}.$$

Then, provided $V_s = \frac{0.40(60)(45.20)(1.80)}{12} = 162.7 \text{ kips}$.

e) Checks

Maximum Spacing Limitation of Transverse Reinforcement

Maximum spacing of transverse reinforcement shall not exceed the following:

When $v_u / f'_c = 0.118 < 0.125$, $s_{\max} = 0.8d_v \leq 24.0 \text{ in}$. [LRFD Eqs. 5.8.2.7-1]

$$\begin{aligned} s_{\max} &\leq 24 \text{ in. (controls)} \\ &\leq 0.8d_v = (0.8)(45.20) = 36.16 \text{ in.} \end{aligned}$$

Since $s = 12 \text{ in.} < s_{\max} \leq 24 \text{ in.}$ O.K.

Minimum Reinforcement Requirement

The area of transverse reinforcement shall not be less than:

$$A_{v,\min} \geq 0.0316 \sqrt{f'_c} \frac{b_v s}{f_y} = 0.0316 \sqrt{6.5} \frac{(8)(12)}{60} = 0.129 \text{ in}^2 < \text{provided } A_v = 0.40 \text{ in}^2$$

O.K.

Maximum Nominal Shear Resistance

In order to ensure that the concrete in the web of the girder will not crush prior to yielding of the transverse reinforcement, the LRFD Specifications specify an upper limit on V_n as follows:

$$\begin{aligned} V_n &\leq 0.25 f'_c b_v d_v + V_p \\ V_n &= 152.2 + 162.7 = 314.9 \text{ kips} \\ &< 0.25 f'_c b_v d_v + V_p = 0.25(6.5)(8)(45.20) + 17.17 = 604.8 \text{ kips} \end{aligned}$$

O.K.

J.7.6 Shear Design by Proposal 2: Modified CSA Approach

Shear design in accordance with the Modified CSA Approach is used to determine the amount and spacing of the shear reinforcement required at a section located 4.93 ft from the support.

a) Evaluation of ϵ_x

Calculate the strain in the reinforcement on the flexural tension side, ϵ_x :

$$\begin{aligned}\varepsilon_x &= \frac{M_u / d_v + 0.5N_u + V_u - V_p - A_{ps}f_{po}}{2(E_s A_s + E_p A_{ps})} \leq 0.002 \\ &= \frac{1,125.0(12) / 45.20 + 0 + 265.0 - 17.17 - (40)(0.153)(189)}{2[0 + 28,500(40)(0.153)]} = -1.749 \times 10^{-3}\end{aligned}$$

Since the value of ε_x is negative, a different equation must be used:

$$\varepsilon_x = \frac{M_u / d_v + 0.5N_u + V_u - V_p - A_{ps}f_{po}}{2(E_c A_c + E_s A_s + E_p A_{ps})} \leq 0.002$$

where A_c = area of concrete on the flexural tension side = 473 in^2 .

$$\varepsilon_x = \frac{1,125.0(12) / 45.20 + 0 + 265.0 - 17.17 - (40)(0.153)(189)}{2[4,888(473) + 28,500(40)(0.153)]} = -0.123 \times 10^{-3}$$

b) Evaluation of β and θ

Calculate θ from the longitudinal strain, ε_x .

$$\begin{aligned}\theta &= 29 + 7,000\varepsilon_x \\ &= 29 + 7,000(-0.123 \times 10^{-3}) = 28.1^\circ\end{aligned}$$

Assume that at least the minimum amount of shear reinforcement required is provided. Then, the coefficient, β , is:

$$\begin{aligned}\beta &= \frac{4.8}{(1 + 1,500\varepsilon_x)} \\ &= \frac{4.8}{[1 + 1,500(-0.123 \times 10^{-3})]} = 5.88\end{aligned}$$

c) Evaluation of Concrete Contribution

The contribution of the concrete to the nominal shear resistance is:

$$\begin{aligned}V_c &= 0.0316\beta\sqrt{f'_c}b_v d_v \\ &= 0.0316(5.88)\sqrt{6.5}(8.0)(45.20) = 171.4 \text{ kips}\end{aligned}$$

d) Evaluation of Required Transverse Reinforcement

Check if $V_u > 0.5\phi(V_c + V_p)$

$$V_u = 265.0 \text{ kips} > 0.5\phi(V_c + V_p) = 0.5(0.9)(171.4 + 17.17) = 84.8 \text{ kips}$$

Therefore, transverse shear reinforcement must be provided.

The shear resistance required for the transverse reinforcement is:

$$V_s = (V_u / \phi) - V_c - V_p = (265.0 / 0.9) - 171.4 - 17.17 = 105.9 \text{ kips}$$

The shear strength provided by the transverse reinforcement is:

$$V_s = \frac{A_v f_y d_v (\cot \theta + \cot \alpha) \sin \alpha}{s} \quad [\text{LRFD Eq. 5.8.3.3-4}]$$

When vertical stirrups are used, $\alpha = 90^\circ$. Then, the required area of transverse reinforcement within a spacing (s) is: (use $f_y = 60$ ksi)

$$A_v / s = V_s / (f_y d_v \cot \theta) = 105.9 / [(60)(45.20) \cot 28.1^\circ] = 0.021 \text{ in.}^2 / \text{in.}$$

Therefore, **use #3 double leg stirrups at 11 in. spacing**

$$A_v / s \text{ provided} = 2(0.11) / 11 = 0.0200 \text{ in.}^2 / \text{in.} > A_v / s \text{ required} = 0.021 \text{ in.}^2 / \text{in.}$$

$$\text{Then, provided } V_s = \frac{0.22(60)(45.20) \cot 28.1^\circ}{11} = 101.6 \text{ kips}$$

e) Checks

Maximum Spacing Limitation of Transverse Reinforcement

Maximum spacing of transverse reinforcement shall not exceed the following:

$$\text{When } v_u / f'_c = 0.118 < 0.125, s_{\max} = 0.8d_v \leq 24.0 \text{ in.} \quad [\text{LRFD Eqs. 5.8.2.7-1}]$$

$$\begin{aligned} s_{\max} &\leq 24 \text{ in. (controls)} \\ &\leq 0.8d_v = (0.8)(45.20) = 36.16 \text{ in.} \end{aligned}$$

Since $s = 11 \text{ in.} < s_{\max} \leq 24 \text{ in.}$ O.K.

Minimum Reinforcement Requirement

The area of transverse reinforcement shall not be less than:

$$A_{v,\min} \geq 0.0316 \sqrt{f'_c} \frac{b_v s}{f_y} = 0.0316 \sqrt{6.5} \frac{(8)(11)}{60} = 0.118 \text{ in.}^2 < \text{provided } A_v = 0.22 \text{ in.}^2$$

O.K.

Maximum Nominal Shear Resistance

In order to ensure that the concrete in the web of the girder will not crush prior to yielding of the transverse reinforcement, the LRFD Specifications specify an upper limit on V_n as follows:

$$\begin{aligned} V_n &\leq 0.25 f'_c b_v d_v + V_p \\ V_n &= 171.4 + 101.6 + 17.17 = 290.1 \text{ kips} \\ &< 0.25 f'_c b_v d_v + V_p = 0.25(6.5)(8)(45.20) + 17.17 = 604.8 \text{ kips} \end{aligned}$$

O.K.

J.7.7 Summary and Conclusions

Shear design in accordance with the Modified STD Approach and the Modified CSA Approach are used to determine the required amount and spacing of the transverse reinforcement at a section of a 100-ft span AASHTO Type IV beam with harped (draped) pretensioned strands. The shear design results are summarized in Table J-22. While the calculated compression strut angle by both approaches is almost same, the required amount of transverse reinforcement is very different, i.e., the Modified STD Approach required about 50% more transverse reinforcement than the Modified CSA Approach due to the differences in the concrete contribution calculated by the two approaches.

Table J-22 Summary of Results

Required or calculated	Proposal 1: Modified STD Approach	Proposal 2: Modified CSA Approach
$(V_c + V_p)$, kips	152.2	188.5
V_s , kips	142.2	105.9
θ , deg.	29.0	28.1
Reinforcement Provided	double leg #4 bars @12 inches	double leg #3 bars @11 inches

Modulus of elasticity, E_p [LRFD Art. 5.4.4.2]	28,500 ksi (197,000MPa)
REINFORCING BARS	
Yield strength, f_y	25M ,60 ksi (400MPa)
Modulus of elasticity, E_s [LRFD Art. 5.4.3.2]	29,000 ksi (200,000MPa)

J.8.4 Sectional Properties and Forces

The design section was located near the interface of second pier as marked in Fig J-29. The sectional properties and forces are given in Table J-24.

Table J-24 Sectional Properties and Forces

OVERALL GEOMETRY AND SECTIONAL PROPERTIES	
Span length, L	196.85 ft(60m)
Overall depth of girder, h	106.3 in.(2700mm)
Width of web, b_w	31.5 in. (800mm)
Area of cross-section of girder, A_g	12,268 in. ²
Moment of inertia, I_g	20,368,314 in. ⁴
Distance from centroid to extreme bottom fiber, y_b	63.82in.
Distance from centroid to extreme top fiber, y_t	42.48 in.
Section modulus for the extreme bottom fiber, S_b	319,154 in ³
Section modulus for the extreme top fiber, S_t	480,562 in ³
Area of non-prestressed tension reinforcement, A_s	0 in ²
Distance from extreme compression fiber to centroid of longitudinal tension reinforcement, d_s	0 in
Area of prestressed tension reinforcement, A_p	51.87 in ² (33464mm ²)
Distance from the bottom fiber to the centroid of prestressed tendons, d_p	101.65in
Weight of beam	11.88kip/ft (520KN/3m)
SECTIONAL FORCES AT DESIGN SECTION*	
Unfactored shear force due to dead load, V_d	998 kips (4440 KN)
Factored shear force, V_u	1803 kips (8022KN)
Unfactored moment due to dead load, M_d	22793 ft-kips (30903KN-m)
Factored moment, M_u	39504 ft-kips (53560KN-m)

*Negative moment, bottom slab is in compression

Calculation of effective depth, d_v :

The compressive block depth, $a = 15.9$ in (403mm)

$$d_e = d_p = 101.65 \text{ in}$$

$$d_v = \max \left\{ \begin{array}{l} d_e - a/2 \\ 0.9d_e \\ 0.72h \end{array} \right\} = \max \left\{ \begin{array}{l} 101.65 - 0.5(15.9) = 93.7 \\ 0.9(101.65) = 91.5 \\ 0.72(106.3) = 76.5 \end{array} \right\} = 93.7 \text{ in}$$

The design shear stress is:

$$v_u = \frac{V_u - \phi V_p}{\phi b_v d_v} = \frac{1803 - 0}{(0.9)(31.5)(93.7)} = 0.679 \text{ ksi}$$

Thus, $v_u / f'_c = 0.679 / 6.1 = 0.111 < 0.18$

J.8.5 Shear Design by Proposal 1: Modified STD Approach

Shear design in accordance with the Modified STD Approach is used to determine the amount and spacing of the required shear reinforcement.

a) Evaluation of Web-Shear Cracking Strength

Compute web-shear cracking strength, V_{cw} :

$$V_{cw} = (0.06\sqrt{f'_c} + 0.3f_{pc})b_v d_v + V_p$$

The effective prestress force is:

$$P_{se} = (51.87)(198.8) = 10311.8 \text{ kips}$$

Compressive stress in concrete at the centroid of cross section due to prestress is:

$$f_{pc} = \frac{P_{se}}{A_g} = \frac{10311.8}{12268} = 0.841 \text{ kips}$$

Therefore,

$$V_{cw} = [0.06\sqrt{6.1} + 0.3(0.841)](31.5)(93.7) + 0 = 1182 \text{ kips}$$

b) Evaluation of Flexure-Shear Cracking Strength

Compute flexure-shear cracking strength, V_{ci} :

$$V_{ci} = 0.02\sqrt{f'_c}b_v d_v + V_d + V_i \frac{M_{cr}}{M_{\max}} \geq 0.06\sqrt{f'_c}b_v d_v$$

$$V_i = V_u - V_d = 1803 - 998 = 805 \text{ kips},$$

$$M_{\max} = M_u - M_d = 39504 - 22793 = 16711 \text{ ft} \cdot \text{kips}.$$

Moment causing flexural cracking at the design section due to externally applied loads:

$$M_{cr} = \frac{I_g}{y_t} (0.2\sqrt{f'_c} + f_{pe} - f_d) \text{ (Negative moment, bottom in compression)}$$

The center of gravity of the strand pattern at the design section is:

$$d_p = 101.65 \text{ in (from bottom fiber)}$$

The eccentricity of the strands at the design section is:

$$e = d_p - y_b = 101.65 - 63.82 = 37.83 \text{ in.}$$

Compressive stress in concrete due to effective prestress forces only:

$$f_{pe} = \frac{P_{se}}{A_g} + \frac{P_{se}e}{S_t} = \frac{10311.8}{12268} + \frac{10311.8(37.83)}{480562} = 1.652 \text{ ksi}$$

Stress due to service dead load:

$$f_d = \frac{M_d}{S_t} = \frac{22793 \times 12}{480562} = 0.569 \text{ ksi}$$

Therefore, $M_{cr} = 480562(0.2\sqrt{6.1} + 1.652 - 0.569) = 63152 \text{ ft} \cdot \text{kips}$

The flexure-shear cracking strength, V_{ci} , is:

$$\begin{aligned} V_{ci} &= 0.02\sqrt{6.1}(31.5)(93.7) + 998 + \frac{805(63152)}{16711} = 4186 \text{ kips} \\ &> 0.06\sqrt{f'_c}b_vd_v = 0.06\sqrt{6.1}(31.5)(93.7) = 437.4 \text{ kips} \end{aligned}$$

c) Evaluation of Concrete Contribution

The nominal shear strength provided by concrete is the lesser of V_{ci} and V_{cw} .

Web-shear cracking strength $V_{cw} = 1182 \text{ kips}$ (Governs)

Flexure-shear cracking strength $V_{ci} = 4186 \text{ kips}$

Thus, the nominal shear strength provided by concrete is:

$$V_c = 1182 \text{ kips}$$

d) Evaluation of Required Transverse Reinforcement

Check if $V_u > 0.5\phi V_c$

$$V_u = 1803 \text{ kips} > 0.5\phi V_c = 0.5(0.9)(1182) = 532 \text{ kips}$$

Therefore, transverse reinforcement must be provided.

The shear force required is

$$V_s = (V_u / \phi) - V_c = (1803 / 0.9) - 1182 = 821.3 \text{ kips}$$

The shear strength provided by the transverse reinforcement is:

$$V_s = \frac{A_v f_y d_v (\cot \theta + \cot \alpha) \sin \alpha}{s} \quad \text{[LRFD Eq. 5.8.3.3-4]}$$

When vertical stirrups are used, $\alpha = 90^\circ$.

Since V_{cw} governs and $M_u = 39,504 \text{ ft} \cdot \text{kips} < M_{cr} = 63,152 \text{ ft} \cdot \text{kips}$, the angle of the compressive strut is obtained as:

$$\cot \theta = 1 + 3f_{pc} / \sqrt{f'_c} \leq 1.80$$

$$\cot \theta = 1 + 3(0.841) / \sqrt{6.1} = 2.02 > 1.80 \text{ (Governs), so } \cot \theta = 1.80.$$

Therefore, the area of the required transverse reinforcement (in^2) within a spacing (s) is: (use $f_y = 60 \text{ ksi}$)

$$A_v / s = V_s / (f_y d_v \cot \theta) = 821.3 / [(60)(93.7)(1.80)] = 0.0812 \text{ in}^2 / \text{in.}$$

Therefore, use **2-25M bars in each web at a spacing of 24 in.**

$$A_v = 4(0.775) = 3.1 \text{ in.}^2 \text{ and } s = 24 \text{ in.}$$

$$\frac{A_v}{s} (\text{provided}) = 3.1 / 24 = 0.129 \text{ in.}^2 / \text{in.} > \frac{A_v}{s} (\text{required}) = 0.0812 \text{ in.}^2 / \text{in.}$$

$$\text{Then, provided } V_s = \frac{3.1 \times 60 \times 93.7 \times 1.8}{24} = 1307 \text{ kips}$$

e) Checks

Maximum Spacing Limitation of Transverse Reinforcement

Maximum spacing of transverse reinforcement must not exceed the following:

When $v_u / f'_c = 0.111 < 0.125$, $s_{\max} = 0.8d_v \leq 24.0 \text{ in.}$ [LRFD Eqs. 5.8.2.7-1]

$$s_{\max} = \min \left\{ \begin{array}{l} 24 \text{ in} \\ 0.8d_v \end{array} \right\} = \min \left\{ \begin{array}{l} 24 \text{ in} \\ 0.8(31.5) = 25.2 \text{ in} \end{array} \right\} = 24 \text{ in}$$

Since $s = 24 \text{ in.} \leq s_{\max} = 24 \text{ in.}$ O.K.

Minimum Reinforcement Requirement

The area of transverse reinforcement shall not be less than:

$$A_{v,\min} \geq 0.0316 \sqrt{f'_c} \frac{b_v s}{f_y} = 0.0316 \sqrt{6.1} \frac{(31.5)(24)}{60} = 0.983 \text{ in.}^2 < \text{provided } A_v = 3.1 \text{ in.}^2$$

O.K.

Maximum Nominal Shear Resistance

In order to ensure that the concrete in the web of the girder will not crush prior to yielding of the transverse reinforcement, the LRFD Specifications specify an upper limit on V_n as follows:

$$V_n \leq 0.18 f'_c b_v d_v + V_p$$

$$V_n = 1182 + 1307 = 2489 \text{ kips} < 0.18 f'_c b_v d_v + 0 = 0.18(6.1)(31.5)(93.7) = 3241 \text{ kips}$$

O.K.

J.8.6 Shear Design by Proposal 2: Modified CSA Approach

Shear design in accordance with the Modified CSA Approach is used to determine the amount and spacing of the shear reinforcement required at the selected section.

a) Evaluation of ε_x

Calculate the strain in the reinforcement on the flexural tension side, ε_x :

$$\begin{aligned} \varepsilon_x &= \frac{M_u / d_v + 0.5N_u + V_u - V_p - A_{ps} f_{po}}{2(E_s A_s + E_p A_{ps})} \leq 0.002 \\ &= \frac{39504(12) / 93.7 + 0 + 1803 - 0 - 51.87(198.8)}{2[(0 + 28,500(51.87))]} = -1.167 \times 10^{-3} \end{aligned}$$

Since the value of ε_x is negative, a different equation must be used:

$$\varepsilon_x = \frac{M_u / d_v + 0.5N_u + V_u - V_p - A_{ps}f_{po}}{2(E_c A_c + E_s A_s + E_p A_{ps})} \leq 0.003$$

where A_c = area of concrete on the flexural tension side (top half of beam) = 6170 in^2

$$\varepsilon_x = \frac{39504(12)/93.7 + 0 + 1803 - 0 - 51.87(198.8)}{2[(4510)(6172) + 28,500(51.87)]} = -0.059 \times 10^{-3}$$

b) Evaluation of β and θ

Calculate θ from the longitudinal strain, ε_x .

$$\begin{aligned}\theta &= 29 + 7000\varepsilon_x \\ &= 29 + 7,000(-0.059 \times 10^{-3}) = 28.6^\circ \\ \cot \theta &= 1.834\end{aligned}$$

Assume that at least the minimum amount of shear reinforcement required is provided. Then, the coefficient, β , is:

$$\beta = \frac{4.8}{(1 + 1500\varepsilon_x)} = \frac{4.8}{(1 + (1500)(-0.059 \times 10^{-3}))} = 5.27$$

c) Evaluation of Concrete Contribution

The contribution of the concrete to the nominal shear resistance is:

$$\begin{aligned}V_c &= 0.0316\beta\sqrt{f'_c}b_v d_v \\ &= 0.0316(5.27)\sqrt{6.1}(31.5)(93.7) = 1214 \text{ kips}\end{aligned}$$

d) Evaluation of Required Transverse Reinforcement

Check if $V_u > 0.5\phi(V_c + V_p)$

$$V_u = 1803 \text{ kips} > 0.5\phi(V_c + V_p) = 0.5(0.9)(1214 + 0) = 546.3 \text{ kips}$$

Therefore, transverse shear reinforcement must be provided.

The shear resistance to be provided by the transverse reinforcement is:

$$V_s = (V_u / \phi) - V_c - V_p = (1803 / 0.9) - 1214 - 0 = 789 \text{ kips}$$

The shear strength provided by the transverse reinforcement is:

$$V_s = \frac{A_v f_y d_v (\cot \theta + \cot \alpha) \sin \alpha}{s} \quad [\text{LRFD Eq. 5.8.3.3-4}]$$

By using $f_y = 60 \text{ ksi}$, $\alpha = 90^\circ$, $\cot \theta = 1.834$, and:

$$A_v / s = V_s / (f_y d_v \cot \theta) = 789 / [(60)(93.7) \cot 28.6^\circ] = 0.0765 \text{ in}^2 / \text{in.}$$

Therefore, use **2-25M bars in each web at a spacing of 24 in.**

$$A_v = 4(0.775) = 3.1 \text{ in.}^2 \text{ and } s = 24 \text{ in.}$$

$$\frac{A_v}{s} (\text{provided}) = 3.1/24 = 0.129 \text{ in.}^2 / \text{in.} > \frac{A_v}{s} (\text{required}) = 0.0765 \text{ in.}^2 / \text{in.}$$

$$\text{Then, provided } V_s = \frac{3.1 \times 60 \times 93.7 \times 1.834}{24} = 1332 \text{ kips}$$

e) Checks

Maximum Spacing Limitation of Transverse Reinforcement

Maximum spacing of transverse reinforcement shall not exceed the following:

$$\text{When } v_u / f'_c = 0.111 < 0.125, s_{\max} = 0.8d_v \leq 24.0 \text{ in.} \quad [\text{LRFD Eqs. 5.8.2.7-1}]$$

$$s_{\max} = \min \left\{ \begin{array}{l} 24 \text{ in} \\ 0.8d_v \end{array} \right\} = \min \left\{ \begin{array}{l} 24 \text{ in} \\ 0.8(31.5) = 25.2 \text{ in} \end{array} \right\} = 24 \text{ in}$$

Since $s = 24 \text{ in.} \leq s_{\max} = 24 \text{ in.}$ O.K.

Minimum Reinforcement Requirement

The area of transverse reinforcement shall not be less than:

$$A_{v,\min} \geq 0.0316 \sqrt{f'_c} \frac{b_v s}{f_y} = 0.0316 \sqrt{6.1} \frac{(31.5)(24)}{60} = 0.983 \text{ in.}^2 < \text{provided } A_v = 3.1 \text{ in.}^2$$

O.K.

Maximum Nominal Shear Resistance

In order to ensure that the concrete in the web of the girder will not crush prior to yielding of the transverse reinforcement, the LRFD Specifications specify an upper limit on V_n as follows:

$$V_n \leq 0.18 f'_c b_v d_v + V_p$$

$$V_c + V_s = 1214 + 1332 = 2546 \text{ kips} < 0.18 f'_c b_v d_v = 0.18(6.1)(31.5)(93.7) = 3241 \text{ kips}$$

O.K.

J.8.7 Summary and Conclusions

Shear design in accordance with the Modified STD Approach and the Modified CSA Approach are used to determine the amount and spacing of the required transverse reinforcement at a section of a 5-span Precast Balanced Cantilever Bridge constructed using AASHTO-PCI-ASBI Segmental Box Girders. The design results are summarized in Table J-25. The required amount of transverse reinforcement by those two approaches is very similar.

Table J-25 Summary of Results

Required or calculated	Proposal 1: Modified STD Approach	Proposal 2: Modified CSA Approach
$(V_c + V_p), \text{ kips}$	1182	1214

$V_s, kips$	821	789
$\theta, deg.$	29.0	28.6
Reinforcement Provided	4- 25M bars @24 inches	4- 25M bars @24 inches